

Expanding the droplet microfluidic community – towards a modular active platform

by

Marie Hébert

A thesis
presented to the University of Waterloo
in fulfilment of the
thesis requirement for the degree of
Doctor of Philosophy
in
Mechanical and Mechatronics Engineering

Waterloo, Ontario, Canada, 2020

© Marie Hébert 2020

Examining Committee Membership

The following served on the Examining Committee for this thesis. The decision of the Examining Committee is by majority vote.

External Examiner: Steve Shih
Associate Professor
Dept. of Electrical and Computer Engineering
Concordia University

Supervisors: Carolyn L. Ren
Professor
Jan P. Huissoon
Professor and Chair
Dept. of Mechanical and Mechatronics Engineering
University of Waterloo

Internal Members: Soo Jeon
Associate Professor
Sean Peterson
Associate Professor
Dept. of Mechanical and Mechatronics Engineering
University of Waterloo

Internal-External Member: Frank Gu
Associate Professor
Dept. of Chemical Engineering
University of Waterloo

Author's Declaration

I hereby declare that I am the sole author of this thesis. This is a true copy of the thesis, including any required final revisions, as accepted by my examiners.

I understand that my thesis may be made electronically available to the public.

Abstract

Microfluidics has progressed tremendously as a field over the last two decades. Various areas of microfluidics developed in fully-fledged domains of their own such as organ-on-a-chip, digital and paper microfluidics. Nevertheless, the technological advancement of microfluidics as a field has not yet reached end-users such as chemists and biologists for independent use. A modular automated platform is envisioned to provide the stacking and modularity required to lower the knowledge barrier for end-users; hence, microfluidics will simply be considered as a tool for the application-focused researchers. The numerous advantages of droplet microfluidics—self-contained reactions, shorter reaction times, lower reagent consumption—will be leveraged by non-microfluidic researchers. However, the technological and knowledge gaps between the current state of the field and the modular automated platform is prohibitively large. This thesis aims to significantly advance the automated technology and to target key issues restricting droplet microfluidic accessibility. The main advancements are separated into two categories: technological and knowledge-focused. The technology-focused advancements (semi-automated droplet control, open-source pressure pump, critical system overview) are necessary stepping stones towards the development of a fully automated modular microfluidic platform. The knowledge-focused contribution (air tubing dynamics, droplet resistance, microfluidic chip compliance) enable the smarter development of the technology; better understanding and modelling the system is of special importance for active control. Furthermore, a deeper understanding of the system can be leveraged for other active platforms and passive microfluidic devices.

The semi-automated droplet manipulations are implemented in an additional layer of the control algorithm. The functionality enables a user to set the droplet length or split ratio before automatically performing the manipulation. The droplet generation accuracy is $\pm 10\%$ of the length and a monodispersity of $\pm 1.3\%$ for 500- μm -long droplets. The splitting ratio resolution is limited by the channel width for the daughter droplet length; the accuracy is $\pm 4\%$ of the initial length. The droplets are merged on-demand. Finally, the effective mixing of the droplet is demonstrated. The manipulations are leveraged in a qualitative drug screening assay that showcases the potential of the platform.

μPump is an open-source pressure pump that targets microfluidic users. Researchers focusing on either passive or active microfluidics can benefit from this system. A similar application performance (i.e. consistency in droplet volume) is achieved for a lesser price tag than comparable commercial systems. Furthermore,

the open-source nature of the system enables a better understanding of the actuation limitation and the communication protocol.

The air tubing connecting the pressure pump outlet to the reservoir holder is generally neglected. The dynamics of the tubing are investigated. For 1/16" inner diameter, the dynamic effects are negligible for a length up to 60 cm and a pressure resolution of 2 mbar. For the 1 mm inner diameter tubing, the dynamic effects are significant. The dynamics are modelled as a first-order system. The performance difference between the nonlinear and linear first-order model is found to be negligible. Therefore, a simple first-order model with a time constant depending on tubing length is deemed adequate. Passive and active microfluidic devices benefit from a better understanding of the air tubing dynamics.

Droplet resistance affects the micro-channel network behaviour as they move through the channels. The uncertainties of their impact lengthen the iterative design process. Numerous studies investigated droplet resistance. However, a consensus is still pending. Most methods rely on passive principles. Oppositely, the method herein introduced relies on the active droplet control platform and grey-box system identification. The preliminary results are promising and in agreement with the literature. Process improvement is envisioned to better the resolution and to enable apply the technique to many more conditions such as non-Newtonian fluids.

The model of the microfluidic chip compliance is improved and justified using experimental results. The better understanding of the dynamics is especially impactful for active microfluidics but also for passive microfluidics. A fitting parameter (ϕ) is required to adjust for the difference in geometry and viscosity. The capacitance is on the order of 10^{-15} . The previous formula predicted values around 10^{-20} whereas the other formula (without considering the fitting parameter) predicts around 10^{-16} . Moreover, the relationship of the fitting parameter is unintuitively stronger with respect to the height-to-length ratio than with the width-to-length ratio. The length is related to the flow rate. Shorter lengths mean larger flow rates, and consequently, larger volume per unit pressure (i.e. capacitance).

The path towards an automated modular platform that can easily be adopted by end-users as a tool relies on a shift towards a standalone system. The most important components to focus on are the actuation, feedback system, and the automation algorithm. The actuation through the current pressure pump is limiting due to its dependence on a pressured airline. The bulky and expensive microscope prohibits users from easily adopting the platform. Finally, the algorithm must be further developed to handle the procedure automatically such that minimal user input is required.

Acknowledgements

I would like to firstly thank my two supervisors—Prof. Carolyn Ren and Prof. Jan Huissoon—for their support and guidance during the completion of my degree. Their expertise and their advice enabled me to immensely grow as a researcher and also, as a person. I am thankful for their expertise and advice.

I would also like to thank the members of my comprehensive exam committee and my Ph.D. defence committee: Dr. Sean Peterson, Dr. Soo Jeon, Dr. Frank Gu, and Dr. Steve Shih. Their insights from a different perspective are greatly appreciated.

The other members of the Waterloo Microfluidics Laboratory have been instrumental in the completion of my Ph.D. First of all, I would like to thank David Wong that laid the foundations for the active droplet control platform. His patience and thoroughness when transferring me the project started me on the right track. I also want to thank Anna Nguyen for training me in the lab. Your knowledge and insight were more than useful. I am also grateful for your support during the perilous times encountered along the way. Finally, I want to thank other members of the Waterloo Microfluidic Laboratory: William Baxter, Matthew Courtney, Weijia Cui, Jeff Farnese, Runze Gao, and Pei Zhao.

In the end, I want to express my deepest gratitude to my friends and family who supported me through my Ph.D. journey. A special thanks to Élise for her love and encouragement during my periods of doubt.

Table of Contents

| | |
|------------------------------------------------------------|----------|
| List of Figures | xvi |
| List of Tables | xxvi |
| 1 Introduction | 1 |
| 1.1 Background and motivation ¹ | 1 |
| 1.2 Research focus | 3 |
| 1.3 Thesis overview | 4 |
| 2 Literature review and background | 6 |
| 2.1 Fundamentals of microfluidics | 6 |
| 2.1.1 Dimensionless numbers | 6 |
| 2.1.2 Interfacial tension: Fluid-fluid interface | 7 |
| 2.1.3 Surface wetting: Surface-fluid interface | 8 |
| 2.1.4 Droplet flow in microchannels | 8 |
| 2.1.5 Chip fabrication | 10 |
| 2.2 Droplet manipulations | 10 |
| 2.3 Enabling platform technologies ¹ | 13 |
| 2.3.1 Applications in many fields | 13 |
| 2.3.2 Modular platforms | 17 |
| 2.3.3 Active control platforms | 19 |

| | | |
|----------|------------------------------------------------------------------------------------|-----------|
| 2.3.4 | Summary | 28 |
| 2.4 | Modelling for microfluidic systems | 29 |
| 2.4.1 | Assumptions | 29 |
| 2.4.2 | Electric circuit analogy | 31 |
| 2.4.3 | Modular system for building the channel network | 32 |
| 2.5 | Control system theory | 33 |
| 2.5.1 | Single-input-single-output (SISO) versus multi-input-multi-output (MIMO) | 35 |
| 2.5.2 | State feedback | 36 |
| 2.5.3 | State observer | 38 |
| 2.5.4 | Principle of separation | 39 |
| 2.5.5 | Kalman Filter | 40 |
| 3 | Methodology | 42 |
| 3.1 | Microfluidics | 42 |
| 3.1.1 | Chip fabrication | 42 |
| 3.1.2 | Active control platform setup | 44 |
| 3.1.3 | Flow sensors | 46 |
| 3.2 | Control system | 48 |
| 3.2.1 | Image processing | 48 |
| 3.2.2 | C++ implementation | 49 |
| 3.2.3 | Modelling modularity | 49 |
| 3.2.4 | Controller topology | 50 |
| 4 | Semi-automated droplet control | 52 |
| 4.1 | Overview | 52 |
| 4.2 | Introduction | 53 |
| 4.2.1 | Passive droplet manipulation | 53 |
| 4.2.2 | Active droplet manipulation | 54 |

| | | |
|-------|---------------------------------------------------------------------------------------------------|----|
| 4.2.3 | Active control of individual droplet through pressure-driven flow using visual feedback | 55 |
| 4.3 | Working principle | 57 |
| 4.3.1 | Manual control: modelling and controller design | 57 |
| 4.3.2 | Semi-automatic droplet control | 58 |
| 4.4 | Experimental setup and methods | 60 |
| 4.4.1 | Materials and chip fabrication | 60 |
| 4.4.2 | System overview | 62 |
| 4.5 | Result and discussion | 63 |
| 4.5.1 | Automated on-demand individual manipulations | 63 |
| 4.5.2 | Limitations and uncertainties | 68 |
| 4.6 | Application to a drug screening assay | 70 |
| 4.6.1 | Context and motivation | 70 |
| 4.6.2 | Methodology | 71 |
| 4.6.3 | Results and discussion | 72 |
| 4.6.4 | Challenges and further direction | 73 |
| 4.7 | Conclusion | 76 |
| 4.8 | Electronic Supplementary Information: ESI 1 – Software logic | 76 |
| 4.8.1 | General definitions | 77 |
| 4.8.2 | Flow chart legend | 77 |
| 4.8.3 | General to all flow charts | 78 |
| 4.8.4 | Specific to the droplet generation flow chart | 79 |
| 4.8.5 | Specific to the droplet merging flow chart | 79 |
| 4.8.6 | Specific to the droplet splitting flow chart | 80 |
| 4.8.7 | Flow charts | 81 |
| 4.9 | Electronic Supplementary Information: ESI 2 – Drug screening | 84 |
| 4.9.1 | Image processing and data acquisition | 84 |
| 4.9.2 | Screenshot artificial intensity increase | 89 |
| 4.9.3 | Length variations between the two droplets | 89 |
| 4.10 | Electronic Supplementary Information: ESI 3 to 6 – Videos | 90 |

| | | |
|----------|------------------------------------------------------------------|------------|
| 5 | An open-source pressure pump system: μPump | 92 |
| 5.1 | Introduction: Hardware in context | 92 |
| 5.2 | Hardware description | 94 |
| 5.2.1 | System overview | 94 |
| 5.2.2 | Required performance | 96 |
| 5.2.3 | Active pressure actuator characterisation | 96 |
| 5.3 | Software and graphical user interface | 97 |
| 5.3.1 | Open-source benefits and concerns | 97 |
| 5.3.2 | Software architecture: Computer | 98 |
| 5.3.3 | Communication between the computer and Arduino | 101 |
| 5.3.4 | Software architecture: Arduino | 104 |
| 5.3.5 | Software operation | 110 |
| 5.4 | System validation and characterisation | 110 |
| 5.4.1 | Pressure output | 113 |
| 5.4.2 | Droplet volume validation | 115 |
| 5.5 | Summary | 123 |
| 6 | Tubing dynamics | 125 |
| 6.1 | Overview | 125 |
| 6.2 | Introduction | 126 |
| 6.2.1 | Microfluidics context | 126 |
| 6.2.2 | Motivation | 127 |
| 6.2.3 | Literature overview | 128 |
| 6.2.4 | Pressure-driven flow actuation dynamics | 131 |
| 6.2.5 | Overview of this study | 132 |
| 6.3 | Experimental methods and materials | 132 |
| 6.3.1 | First order model fit | 133 |
| 6.3.2 | Pressure sensors | 133 |

| | | |
|----------|------------------------------------------------------------------------|------------|
| 6.3.3 | Tubing materials and dimensions | 134 |
| 6.4 | Results and discussion | 135 |
| 6.4.1 | Pump dynamics | 136 |
| 6.4.2 | Tubing dynamics | 138 |
| 6.4.3 | Validation | 143 |
| 6.4.4 | Limitations | 147 |
| 6.5 | Conclusion | 148 |
| 6.5.1 | Summary | 148 |
| 6.5.2 | Future work | 148 |
| 6.6 | Pressure sensor junction minimum time resolution | 150 |
| 6.7 | Elastic modulus of the different tubing materials | 152 |
| 6.8 | Pump software output compared to pressure sensor measurement | 152 |
| 7 | Droplet hydrodynamic resistance | 155 |
| 7.1 | Introduction | 155 |
| 7.1.1 | Motivation | 155 |
| 7.1.2 | Literature overview | 156 |
| 7.1.3 | A novel approach using active control and system identification | 158 |
| 7.2 | Working principle | 159 |
| 7.2.1 | Active control of droplets using visual feedback | 159 |
| 7.2.2 | System identification | 159 |
| 7.2.3 | Identifiability analysis | 160 |
| 7.3 | Experimental setup for droplet control | 162 |
| 7.3.1 | Materials and chip fabrication | 162 |
| 7.3.2 | Overview for experiment design | 163 |
| 7.3.3 | Active control system implementation | 163 |
| 7.4 | System identification methodology | 165 |
| 7.4.1 | Data separation | 165 |

| | | |
|----------|---------------------------------------------------------------------------------|------------|
| 7.4.2 | Data pre-filtering | 166 |
| 7.4.3 | <code>greyest</code> algorithm | 166 |
| 7.4.4 | Parameter subset used for identification | 167 |
| 7.4.5 | Parameter set validation | 172 |
| 7.4.6 | How to calculate droplet resistance from the total channel resistance | 173 |
| 7.4.7 | Resistance ratio | 173 |
| 7.4.8 | Statistical significance of the results | 174 |
| 7.5 | Results and discussion | 175 |
| 7.5.1 | Experimental droplet hydrodynamic resistance | 175 |
| 7.5.2 | Comparison with literature results | 177 |
| 7.5.3 | Limitations | 179 |
| 7.6 | Conclusion | 179 |
| 7.6.1 | Summary | 179 |
| 7.6.2 | Future work | 180 |
| 7.7 | State-space model structure | 181 |
| 8 | Microfluidic chip compliance | 182 |
| 8.1 | Introduction | 182 |
| 8.1.1 | Microfluidic context | 182 |
| 8.1.2 | Motivation | 182 |
| 8.1.3 | Literature overview | 183 |
| 8.2 | Methodology | 184 |
| 8.2.1 | Microfluidic chip fabrication | 184 |
| 8.2.2 | Pressure and flow rate measurements | 184 |
| 8.2.3 | Flow sensor calibration | 185 |
| 8.2.4 | Sample tubing dynamics | 185 |
| 8.2.5 | Inlet design | 188 |

| | | |
|----------|---------------------------------------------------------------------|------------|
| 8.2.6 | Experimental setup for data collection | 192 |
| 8.2.7 | Assumptions for the time constant | 194 |
| 8.2.8 | Data processing | 195 |
| 8.3 | Results and discussion | 196 |
| 8.3.1 | Comparison with previous models | 197 |
| 8.3.2 | Fitting parameter (ϕ) | 199 |
| 8.3.3 | Limitations and uncertainties | 201 |
| 8.4 | Concluding remarks | 202 |
| 8.4.1 | Conclusion | 202 |
| 8.4.2 | Future work | 203 |
| 9 | A critical system analysis | 204 |
| 9.1 | Objective | 204 |
| 9.1.1 | Why a faster platform? | 204 |
| 9.1.2 | Why a modular platform? | 205 |
| 9.1.3 | Overview | 205 |
| 9.2 | Controller (1) | 206 |
| 9.2.1 | Performance | 206 |
| 9.2.2 | Order minimization | 208 |
| 9.2.3 | Actuation saturation | 209 |
| 9.2.4 | Delays | 209 |
| 9.2.5 | Control strategies | 211 |
| 9.3 | Actuation (2) | 215 |
| 9.3.1 | Limitation from commercial systems | 215 |
| 9.3.2 | Open-source system from off-the-shelf pressure regulators | 217 |
| 9.3.3 | Other approaches | 217 |
| 9.4 | Air transport and reservoir holder (3) | 220 |
| 9.5 | Sample transport (4) | 223 |

| | | |
|-----------|-----------------------------------------------------------|------------|
| 9.5.1 | Dead volume | 223 |
| 9.5.2 | Dynamics | 223 |
| 9.6 | Microfluidic chip (5) | 228 |
| 9.7 | Feedback (6) | 229 |
| 9.7.1 | Visual feedback | 230 |
| 9.7.2 | Capacitive sensors | 230 |
| 9.7.3 | Microwave sensor | 231 |
| 9.7.4 | CMOS arrays for lensless systems | 231 |
| 9.7.5 | Microscope (6.a) | 233 |
| 9.7.6 | Camera (6.b) | 234 |
| 9.7.7 | Image processing (6.c) | 239 |
| 9.8 | Summary | 243 |
| 10 | Conclusion | 246 |
| 10.1 | Summary | 246 |
| 10.2 | Original contribution | 248 |
| 10.3 | Future work | 249 |
| | Copyright permissions | 250 |
| | References | 331 |
| | APPENDICES | 364 |
| A | Operating procedure: flow sensor calibration | 365 |
| B | State-space matrices – Symmetric model | 380 |
| B.1 | Analogy between fluid and electrical principles | 381 |
| B.2 | Overview | 383 |
| B.3 | States, inputs, and outputs | 383 |

| | | |
|----------|----------------------------------------------------------|------------|
| B.4 | Circuit and derivation at the channel junction | 385 |
| B.5 | Circuit and derivation for \dot{U}_{tubeX} | 385 |
| B.6 | Circuit and derivation for \dot{U}_{chX} | 385 |
| B.7 | Circuit and derivation for \dot{I}_{tubeXa} | 386 |
| B.8 | Circuit and derivation for \dot{I}_{chXb} | 386 |
| B.9 | Circuit and derivation for \dot{I}_{tubeXb} | 389 |
| B.10 | State-space matrices | 390 |
| B.10.1 | $A \in \mathbb{R}^{14 \times 14}$ | 390 |
| B.10.2 | $B \in \mathbb{R}^{14 \times 3}$ | 393 |
| B.10.3 | $C \in \mathbb{R}^{1 \times 14}$ | 393 |
| B.10.4 | $D \in \mathbb{R}^{3 \times 3}$ | 393 |
| C | Flexible strain sensor | 394 |
| C.1 | Relation to other work in this thesis | 394 |
| C.2 | Overview | 395 |
| C.3 | Introduction | 395 |
| C.3.1 | Microfluidics context | 395 |
| C.3.2 | Motivation | 397 |
| C.3.3 | Literature overview | 398 |
| C.3.4 | Thick-wall compliant tubing dynamics | 398 |
| C.4 | Materials and experimental methods | 399 |
| C.4.1 | Materials | 399 |
| C.4.2 | Experimental setup | 400 |
| C.5 | Results and discussion | 401 |
| C.5.1 | Step input | 402 |
| C.5.2 | Ramp input | 402 |
| C.5.3 | Potential impact | 405 |
| C.6 | Summary | 406 |

List of Figures

| | | |
|-----|--------------------------------------------------------------------------------------------------------------------------------------------------------------------------------------------------------------------------------------------------------------------------------------------------------------------------------------------------------------------|----|
| 1.1 | Schematic overview of the relationship between the chapters of the thesis. | 5 |
| 2.1 | Surface wetting of the droplet, continuous phase, and solid substrate. Reproduced from Ref. [162] with permission from Wiley & Sons. . . | 8 |
| 2.2 | Squeezing regime flow in circular and rectangular channels. The thin film between the dispersed phase and the wall is indicated by (e). The gutter region is indicated by dashed-line arrows for the rectangular cross-section channel. Reproduced from Ref. [21] with permission from The Royal Society of Chemistry. | 9 |
| 2.3 | Schematic of fluid flow for a low dispersed phase relative viscosity. Flow pattern for all viscosity ratios in [116]. Reproduced from Ref. [21] with permission from The Royal Society of Chemistry. | 10 |
| 2.4 | Stackable modular platform structure and vision for easy control of individual droplets by end-users. Structure of a stackable modular platform. The vertical arrow shows the stacking while the horizontal arrow shows modularity. Each manipulation is a module that leverages stacking such that only high-level information from the user is required. | 18 |
| 2.5 | Working principle of multi-layer devices with a sample and a control layer. The zone at the intersection between the two layers acts as an on-chip solenoid valve. | 24 |
| 2.6 | Working principle of in-line solenoid valve. The rotating solenoid valve aligns and blocks the gate pathway for the sample to flow. | 26 |

| | | |
|------|----------------------------------------------------------------------------------------------------------------------------------------------------------------------------------------------------------------------------------------------------------------------------------------------------------------------|----|
| 2.7 | Working principle of the combined active and passive platform. The controller calculates the required pressure to apply at each microfluidic chip inlet based on the feedback provided by the microscope, camera, and on-line image processing. | 27 |
| 2.8 | Building block of the electric circuit analogy with symmetric RLC components. | 33 |
| 2.9 | Simple T junction assembled building block with 3 channels, 3 tubes, and 3 inlets. | 34 |
| 2.10 | Homogeneous system response according to pole location (shown with triangles) in the s-plane [70]. The desirable pole location is in the negative real plane (i.e. left-hand side) for an exponential decay envelope. | 37 |
| 3.1 | Soft lithography fabrication procedure for PDMS chips (cross-sectional view). | 43 |
| 3.2 | Schematic overview of the system with flow of information indicated by the arrow direction. (a) Pressure pump (Fluigent MFCS-EZ) (b) PDMS microfluidic chip (typical single T junction design) (c) Microscope (Nikon Eclipse Ti-E) with 4X objective (d) Camera (Andor Zyla 5.5 sCMOS) (e) Desktop computer. | 44 |
| 3.3 | Schematic of the reservoir holder used to interface between the pressurized air and the fluid contained in the vials. | 45 |
| 3.4 | Image processing workflow overview. Reproduced with permission from Ref. [311]. | 49 |
| 3.5 | Controller topology overview with the integral state feedback (z), the state observer (\hat{x}), and the Kalman Filter (KF) for disturbance cancellation. | 50 |
| 4.1 | Flowchart representation of software logic for merging two droplets. | 61 |
| 4.2 | System overview for active control of droplet in microchannels through pressure-driven flow. (a) Nikon Inverted Microscope ECLIPSE Ti-E, (b) Andor Zyla 5.5 sCMOS camera, (c) personal computer, (d) Fluigent MFCS-8c pressure pump, (e) microfluidic chip. | 62 |
| 4.3 | On-demand droplet generation distribution using semi-automatic control. | 64 |

| | | |
|------|-------------------------------------------------------------------------------------------------------------------------------------------------------------------------------------------------------------------------------------------------------------------------------------------------------------------------------------------------------------------------------------------------------------------------------------------------------------------------------------------------------------------------------------------------------------------------------------|----|
| 4.4 | Droplet generation process (a) Source channel setup completed and ready to generate droplet (b) Filling of the source channel and overflow in other channels at the T junction (c) Manual selection of the new marker in the destination channel (d) Adjustment of the droplet length with respect to the junction (e) Droplet sectioning (f) Final stage with both interfaces stabilized. | 65 |
| 4.5 | On-demand droplet splitting distribution using semi-automatic control. | 66 |
| 4.6 | Successive droplet splitting process (a) Setup of the initial droplet (b) Adjusting the distance of markers with respect to the junction and the desired split ratio (c) Sectioning the droplet (d) First split completed for the 150 μm channel width (e) Sorting of the desired droplet to be split again (f) Transition to the 75 μm channel width region (g) Manual setup of the droplet (h) Adjusting the distance with respect to the second junction (i) Sectioning the daughter droplet (j) Final product of the double splitting with greater precision. | 67 |
| 4.7 | Droplet merging process (a) Initial manual setup of the two droplets on either side of the T junction (b) Both droplets reach the T junction simultaneously (c) The interface breaks and the two droplets merge (d) Merging is complete. | 68 |
| 4.8 | On-demand droplet mixing index according to resulting droplet total length. | 69 |
| 4.9 | Droplet mixing process (a) Initial manual setup of the two droplets on either side of the T junction (b) Merging of the two droplets (c) Initial position after merging before mixing manipulations (d) Mixing on one side of the T junction with part of the droplet in each of the three channel (e) Transition to the destination channel with once again a part of the droplet in the third channel to break the symmetry of flow within the droplet (f) Final droplet fully mixed. | 70 |
| 4.10 | Fluorescent intensity change of Thioflavine T corresponding to the aggregation of AcPHF6 over time with and without the Orange G inhibitor. Error bars show standard deviation for 3 sets of experiments. Qualitative assessment showing the reduced fluorescent aggregation from the inhibitor. | 73 |

| | | |
|------|----------------------------------------------------------------------------------------------------------------------------------------------------------------------------------------------------------------------------------------------------|-----|
| 4.11 | Artificially brighter screenshots of fluorescent intensity change of Thioflavine T corresponding to the aggregation of AcPHF6 over time with and without the Orange G inhibitor. Original image comparison shown in ESI 2 (Section 4.9.2). | 74 |
| 4.12 | Definitions of elements to understand active droplet control. | 77 |
| 4.13 | Flow chart for generation of a droplet of a specified length. | 81 |
| 4.14 | Flow chart for merging of two droplets. | 82 |
| 4.15 | Flow chart for splitting of a droplet at a specified ratio. | 83 |
| 4.16 | Image processing before droplet merging. Uniform intensity confirms the dye did not self aggregate. | 85 |
| 4.17 | Image processing after droplet merging. Correlation along the channel to locate the droplet and apply the mask. | 86 |
| 4.18 | Image processing after droplet merging. Correlation along the channel to locate the droplet and apply the mask. | 88 |
| 4.19 | Side by side comparison of the drug screening screenshots: before and after increasing the brightness. The purpose is for better readability and visual representation of the assay. The data is extracted from the untouched images. | 89 |
| 4.20 | Schematic representation of the merging of the two droplets and the simplified distribution of the solutions in the resulting single droplet. | 90 |
| 5.1 | System schematic. | 94 |
| 5.2 | Microfluidic pump (μ Pump) with four independently controlled pressure output channels. | 95 |
| 5.3 | Pneumatic actuator time response. | 97 |
| 5.4 | Pneumatic actuator frequency response: magnitude and phase shift. | 98 |
| 5.5 | Definitions of the Unified Modeling Language (UML) symbols. | 99 |
| 5.6 | UML class diagram providing an overview of the windows and their relationships. | 100 |
| 5.7 | UML class diagram for pump control. | 101 |
| 5.8 | Signals and slots relationships between the objects. Solid lines (-) indicates explicit signal to slot link. Dashed line (- -) shows relationship within a same object from slot to signal. | 102 |

| | | |
|------|---------------------------------------------------------------------------------------------------------------------------------------------------------------------------------------------------------------------------------------------------------------------------------------------------|-----|
| 5.9 | Finite State Machine (FSM) diagram for PumpThread. | 103 |
| 5.10 | Communication setup between PC and Arduino. | 105 |
| 5.11 | Communication loop between PC and Arduino. | 106 |
| 5.12 | Software operation overview. | 112 |
| 5.13 | Pressure step response. | 113 |
| 5.14 | Flow step response. | 114 |
| 5.15 | Hysteresis comparison between μ Pump and Fluigent MFCS-EZ. | 115 |
| 5.16 | Stability comparison between μ Pump and Fluigent MFCS-EZ under load. | 116 |
| 5.17 | Experimental setup to experimental measure the channel height based on pressure and flow rate. The pressure pump is either a commercial or open-source system. The pressure sensor is TE Connectivity U536D-H00015-001BG. The flow sensor is Sensirion SLG-1430. | 117 |
| 5.18 | Representative frame recorded with the <i>Zyla 5.5 sCMOS</i> camera with 4 ms exposure time. Multiple droplets of nominally equal volume are captured simultaneously. | 119 |
| 5.19 | Automated droplet outline extraction using <i>ImageJ</i> macro scripts. | 120 |
| 5.20 | Automated droplet area and perimeter extraction using <i>Matlab</i> scripts. | 121 |
| 5.21 | Graphical representation of the outlier rejection based on a $\pm 15\%$ variation from an identified acceptable data point. | 122 |
| 5.22 | Comparison of droplet volume data. (a) Previously published data from [100]. (b) New data collected under similar conditions to compare the performance of the μ Pump system with the Fluigent MFCS-EZ. | 122 |
| 6.1 | Overview of the typical setup for pressure-driven flow. The focus of this study is on the difference in pressure for the air tubing (ΔP_{air}). The tubing carrying the liquid sample is already considered in the model (ΔP_{sample}) from previous work [308, 111]. | 127 |
| 6.2 | Separation between pump and tubing dynamics. | 132 |
| 6.3 | Experimental setup to measure the impact of the air tubing dynamics (ΔP_{air}). Two pressure sensors are strategically located to measure the pressure at either end of the air tubing with minimal impact. | 134 |

| | | |
|------|--------------------------------------------------------------------------------------------------------------------------------------------------------------------------------------------------------------------------------------------------------------------------------------------------------------------------------------------------------------------------------------------------------------------------------|-----|
| 6.4 | Time constant (τ) variations with pressure for the <i>Fluigent MFCS-EZ</i> pump. The error bars represent ± 1 standard deviation from the overall mean time constant. | 137 |
| 6.5 | Time constant (τ) variations with pressure for $\mu Pump$. The error bars represent ± 1 standard deviation from the overall mean time constant. | 138 |
| 6.6 | Experimental quantification of first order dynamics over the pressure range for the 1X3 mm medium silicone tubing of 66.5 cm length and 2 ml vial volume. The trend of the decreasing and increasing data shows the hysteresis effects. The time constant is consistently smaller for decreasing pressure compared to increasing pressure. The error bars represent ± 1 standard deviation from the overall mean constant. | 139 |
| 6.7 | Experimental quantification of first order dynamics over the pressure range for the 1/16"X1/8" medium silicone tubing of 66.5 cm length and 2 ml vial volume. Similar results are obtained for all three materials (Table 6.2). The time constant is too small to accurately quantify with the current experimental setup. The error bars represent ± 1 standard deviation from the overall mean constant. | 140 |
| 6.8 | Summary of the time constant (τ) fit for different lengths. Tubing dimensions of 1X3 mm. The detailed data is presented in Table 6.3. | 141 |
| 6.9 | Summary of the time constant (τ) fit for different volumes (ml). Tubing dimensions of 1X3 mm. The detailed data is presented in Table 6.3. | 142 |
| 6.10 | Model validation and comparison between no model, the nonlinear model and the simple linear model simulations. The similar MSEs show that there is not significant prediction error improvement for the more complex nonlinear model compared to the simpler linear model. (1X3 mm tubing, 66.5 cm long, 2 ml vial). Either model significantly improves upon the no-model prediction. | 146 |
| 6.11 | Experimental setup to determine the pressure sensor junction time resolution. The pressure regulator is manually operated to inflate the balloon. After the regulator is closed, the balloon is burst using a sharp scalpel. | 150 |
| 6.12 | Typical response from bursting a balloon to assess the time resolution of the pressure sensor junctions. | 151 |
| 6.13 | Experimental quantification of the elastic modulus for the three different tubing materials (soft silicone, medium silicone, hard Tygon). . | 153 |

| | | |
|------|----------------------------------------------------------------------------------------------------------------------------------------------------------------------------------------------------------------------------------------------------------------------------------------------------------------------------------------------------------------------------------------------------------------------------------------------------------------------------------------------------------------------------------------------------------------------------------------------------------------------------------------------------------------------------------------------------------------------------------------------------------------------------------------------------------------------------------------------------------------------------------------------------------------------------------------------------------|-----|
| 6.14 | Difference between the pressure pump output and pressure measured by the external pressure sensor (P1). | 154 |
| 7.1 | Overview of the control loop implemented for the active platform. | 159 |
| 7.2 | A general workflow for system identification. (1) System actuation is necessary to excite the frequencies of interest. Without the proper choice of the arbitrary path to follow, the information provided by the system will not be informative enough (See Figure 7.3 for more details). (2) The input and output to the system (in this case, each inlet pressure and the droplet position) are simultaneously recorded while the system is actuated. (3) The recorded input-output data is post-processed using the Matlab <code>greyest</code> algorithm from the System Identification toolbox. (4) The system identification algorithm returns the set of parameters that best fit the input-output data provided. The parameter of interest is the resistance of channel 3 that contains a single droplet and is otherwise filled with the continuous phase. The subset of parameters is selected based on the identifiability analysis. | 161 |
| 7.3 | Arbitrary reference position signal for the droplet interface in the channel of interest (Ch3). | 165 |
| 7.4 | Relationship between the number of parameters and the fit to a single input-output data set. Over-parametrization lead to poor fit to other datasets from the same system. A validation data set is used to verify adequate fit to another input-output dataset. | 168 |
| 7.5 | Identifiability analysis of the RLC state-space model with 18 parameters. (a) parameter sensitivity. (b) largest identifiable subgroup. (c) highly collinear parameter groups. (d) identifiable parameters. | 170 |
| 7.6 | Figure 1.5 (continued): Identifiability analysis of the RLC state-space model with 18 parameters. (a) parameter sensitivity. (b) largest identifiable subgroup. (c) highly collinear parameter groups. (d) identifiable parameters. | 171 |
| 7.7 | Schematic representation of the total channel resistance ($R_{channel}$) as the sum of the droplet resistance ($R_{droplet}$) and the rest of the channel filled with the continuous phase ($R_{continuous}$). | 174 |

| | | |
|------|----------------------------------------------------------------------------------------------------------------------------------------------------------------------------------------------------------------------------------------------------------------------------------------------------------------------------------------------------------------------------------------|-----|
| 7.8 | Model simulation of nominal and identified model compared to the actual recorded system output. Dashed red rectangle shows oscillations too fast for the physical system indicating potential over-parametrization. | 176 |
| 7.9 | Percent fit variations and the corresponding identified channel resistance (Rch3). Selected threshold is 50%. Model fit defined as per the Matlab <code>compare</code> function. | 177 |
| 7.10 | Experimental droplet resistance results. | 178 |
| 8.1 | Calibration curves for water and silicone oil using the <i>Sensirion SLI-430</i> flow sensor. Scaling limits from $-100 \mu L/min$ to $120 \mu L/min$ | 186 |
| 8.2 | Experimental setup schematic to test sample tubing resistance and dynamics. | 187 |
| 8.3 | Resistance of the sample tubing for different lengths. The fluid is silicone oil 50 cst. The data for 0.76 m uses a #10-32 to #10-32 union to link two tubing segments. The error bars represent one standard deviation for $n = 3$ | 188 |
| 8.4 | Time constant for different tubing inner diameters. The larger 0.030" tubing has a smaller time constant, but the resulting large flow rates are undesirable for the limited sample vial volume and the flow sensor range. The error bars represents one standard deviation for $n = 21$ | 189 |
| 8.5 | Time constant for different tubing lengths with inner diameters of 0.020". A shorter tubing is desirable, but the physical layout of the components requires a minimum length for proper assembly. The error bars represents one standard deviation for $n = 21$ | 190 |
| 8.6 | Time constant for different fluids through a tubing of 0.020" inner diameters and 0.769 meters. The time constant for silicone 5 cst and water are considered negligible. The data for silicone oil 20 cst and 50 cst will be compensated for when processing the data for the microfluidic chip time constant. The error bars represent one standard deviation for $n = 21$ | 191 |
| 8.7 | Experimental setup schematic for data collection with the microfluidic chip before the flow sensor. | 192 |
| 8.8 | First-order fit of the flow rate based on the measured pressure. | 197 |

| | | |
|------|-------------------------------------------------------------------------------------------------------------------------------------------------------------------------------------------------------------------------------------------------------------------------------------------------------------------------------------------------------------------------------------------------------------------------------------------------------------|-----|
| 8.9 | Capacitance results for the different fluids (water, and silicone oil 5 cst, 20 cst, and 50 cst) according to the height-to-width ratio. | 198 |
| 8.10 | Fitting parameter (ϕ) relationship with geometric ratios for all fluids. | 200 |
| 8.11 | Assessment of fit for the fitting parameter (ϕ) as a function of the chip only. This does not consider variations in width-to-height ratio; the smallest ϕ value for each chip is used. | 201 |
| 9.1 | System overview separated into independent components. | 207 |
| 9.2 | Speed limitation test for <i>Fluigent EZ-MFCS</i> . Unresponsive below 100 ms. Sampling shown is every 40 ms. | 216 |
| 9.3 | Bode plot for the pressure regulator (<i>ControlAir T900-CIM</i>) included in μ Pump. Natural frequency (ω_n) around 6 Hz. Reproduced from Ref. [90]. | 218 |
| 9.4 | Pressure fluctuations between the pressure pump output and the reservoir holder connected by a 1-mm inner diameter soft tubing of 65 cm length. | 221 |
| 9.5 | Schematic representation of the combination of air and hydro-static pressure transmitted to the liquid sample. | 222 |
| 9.6 | Graphical representation of the constraints to minimize the resistance ratio and time constant associated with the capacitance and inductance. The 3 common inner diameters for 1/16" outer diameter tubing are denoted by the grey vertical lines. Not to scale. | 227 |
| 9.7 | Schematic representation of the suggestion division of the image processing workflow. Each channel and junction region is separated to reduce the matrix size to process. The regions on either side of CH1 are ignored. | 241 |
| 9.8 | Overview of a proposed modular platform architecture. | 244 |
| B.1 | Symmetric RLC block element. | 381 |
| B.2 | Analogy between fluid and electrical principles. Where μ is the dynamic viscosity [$kg/m \cdot s$], l is the channel length [m], and d_h is the hydraulic diameter [m], ρ is density [kg/m^3] and l is channel length [m], A is the cross sectional area [m^2], κ is the substrate stiffness [$Pa \cdot m$], l is the channel length [m], and β is the adiabatic bulk modulus [Pa]. | 382 |

| | | |
|-----|-----------------------------------------------------------------------------------------------------------------------------------------------------------------------------------------------------------------------------------------------------------------------------------------------------------------------------------|-----|
| B.3 | Overview of the T-junction circuit. Each element has the internal RLC components illustrated in Figure B.1 with their value associated with the system properties. | 383 |
| B.4 | Circuit for derivation of equations for \dot{U}_{tubeX} states (8, 11, and 14). | 386 |
| B.5 | Circuit for derivation of equations for \dot{U}_{chX} states (1, 3, and 5). | 387 |
| B.6 | Circuit for derivation of equations for \dot{I}_{tubeXa} states (6, 9, and 12). | 388 |
| B.7 | Circuit for derivation of equations for \dot{I}_{chXb} states (2, and 4). | 389 |
| B.8 | Circuit for derivation of equations for \dot{I}_{tubeXb} states (7, 10, and 13). | 390 |
| C.1 | Setup of the air tubing between the pressure pump and the reservoir holder. | 396 |
| C.2 | Overview of the circuit: V_{DC} is the power supply voltage, V_{REG} provides a precision reference and supply voltage, $1X$ represents the voltage follower, and DAC is the digital-to-analog converter | 401 |
| C.3 | Successive step input response with strain sensor measurement. The intrinsic nanocomposite strain sensor properties dominates the response at steady pressure. The sharp pressure increase and corresponding sharp change in the sensor resistance nonetheless indicates responsiveness for the small scale deformations. | 403 |
| C.4 | Ramp input response. The similar response between the milder and steeper pressure ramp inputs suggests a constant relationship with the strain time derivative. | 404 |

List of Tables

| | | |
|-----|-----------------------------------------------------------------------------------------------------------------------------------------------------------|-----|
| 2.1 | Dimensionless number definition and relative importance [162]. | 7 |
| 2.2 | Droplet manipulation methods | 12 |
| 2.3 | Kalman Filter algorithm for disturbance estimation. | 41 |
| 4.1 | Statistical analysis for droplet generation performance. | 64 |
| 4.2 | Final concentration after droplet merging for each compound. | 72 |
| 5.1 | Minimum performance criteria for microfluidic applications | 96 |
| 5.2 | PumpArduino – Important member variables and functions. | 108 |
| 5.3 | Configuration – Variable description. | 111 |
| 5.4 | Summary of pressure specifications for μ Pump. | 124 |
| 6.1 | Specification summary for the pressure sensors (<i>TE Connectivity U536D-H00015-001BG</i>). | 135 |
| 6.2 | Details of the materials and dimensions of the various tubing. | 135 |
| 6.3 | Summary of the variations in the time constant (τ) depending on tubing length (Figure 6.8) and vial volume (Figure 6.9) for 1X3 mm tubing. | 143 |
| 6.4 | Repeatability summary for 100 mbar pressure set point. | 144 |
| 6.5 | Repeatability summary for 200 mbar pressure setpoint. | 144 |
| 6.6 | Performance for each first order linear model for the mean parameter values based on length compared against the no-model performance. | 147 |
| 8.1 | Length-to-height ratios with corresponding dimensions. | 194 |

| | | |
|-----|-----------------------------------------------------------------------------------------------------------------|-----|
| 8.2 | Specification of the length-to-height ratio considered for each fluid. . . | 194 |
| 9.1 | Sample vial O-ring for better seal (McMaster product number: 9559K18). | 210 |
| 9.2 | Typical distribution of delays [ms] for the software (maximum total delay allowed: 100 ms). | 211 |
| 9.3 | Summary of available tubing dimensions in imperial and metric units. | 227 |
| 9.4 | Summary of specifications of CCD and CMOS cameras | 237 |
| 9.5 | Summary of specifications of Machine Vision and CMOS cameras . . | 238 |
| 9.6 | Summary of the recommendations for a faster modular active droplet control platform for each component. | 245 |
| C.1 | Specification summary for the pressure sensors (<i>TE Connectivity U536D-H00015-001BG</i>). | 402 |

Chapter 1

Introduction

1.1 Background and motivation¹

As a field, microfluidics evolved and progressed over the decades of research supported by contributors from around the globe and from varied backgrounds. The state of the field with respect to its overarching vision is herein considered through the lens of active microfluidic platforms that are used as a tool for applications in other fields.

Although multiple early studies undoubtedly contributed to the emergence of the microfluidics field, most articles trace back the infancy of microfluidics to the 1990s [203, 147]. The initial microfluidics studies leveraged the mature manufacturing processes from the semiconductor industry (i.e. lithography) [292]. The vision was to miniaturize the Total Analysis System (TAS) into a single miniature device that takes the sample in and provides the answer [203]. The evolution of such innovative vision is still ongoing. As per one of the former presidents of Bell Labs, Mervin Kelly, innovation progresses from fundamental scientific discovery to product development before reaching the market [95]. Many studies established strong fundamentals both through theoretical [309] and experimental [147] work. The focus of the publications is now increasingly on product development for various applications. However, the translation from academic studies to market products is challenging; fundraising many millions and spending years are necessary to bring a microfluidic product to market for the end-users [325].

¹Excerpt from submitted manuscript: **Marie Hébert**, Jan P. Huissoon, and Carolyn L. Ren. “A perspective of active microfluidic platforms as an enabling tool for applications in other fields.” (2020).

The initial vision of μ TAS persists through the more recent microfluidic developments; the field nevertheless expanded into multiple branches with diversified objectives and scopes. The ambitious goal of achieving μ TAS involves processing a sample to perform a series of chemical analyses from preparation to detection; a generally more manageable scope is to only consider one or a few steps at a time using a Lab-On-a-Chip (LOC). Some LOC microfluidic devices are not only developed in academic laboratories [200] but also as commercially viable products. There are numerous companies with products in the market, but due to the cost and operational training required, the benefits of switching from standard protocols to a microfluidic approach do not often outweigh the hurdles [294]. Hence, the impact of microfluidic products in other fields such as chemistry and biology is still somewhat limited. Ideally, end-users such as biologists and chemists would view microfluidics simply as a tool [306].

The path to achieving the vision of microfluidic as a tool is unclear, but Prof. Whitesides proposed progress similar to that of our modern-day computers [305]. The key feature is stacking; the basic building blocks are reliable, predictable, and repeatable. The analogy of how μ TAS relates to the component level aspects relates to how people use websites. The user does not need to understand how the Internet works, or how the different components of their computer interact, or how integrated circuits (IC) operate, or how transistors constitute the different ICs. The building blocks of each previous level are reliable, predictable, and repeatable enough to allow stacking. Hence, the users do not need a thorough electronics understanding to obtain the results of a Google search. Another analogy is how a chemist or a biologist can disregard the inner workings of an electronic balance when they wish to weigh a sample. They simply place their sample and the weight is displayed: sample in, answer out. A similar development in microfluidics would allow application-focused researchers to use these stackable blocks to build systems with new capabilities and fully leverage the potential of microfluidics.

Microfluidics-focused studies typically motivate their device through applications in numerous fields such as water treatment [235], life biology [33], and material synthesis [198, 262]; however, the impact of application-focused studies has mainly been restricted within the microfluidics community. Thus, the field is still searching for pivotal applications that will propel microfluidics from academic development research to end-users' applications. Microfluidic tools have the potential to get at the forefront of impactful discoveries in related fields.

1.2 Research focus

The previous section put into perspective the background and motivation for microfluidic systems as tools for end-users. But how can this be achieved? When considering the different options, one must keep in mind the stacking principle. The selected path should enable the user to work with the microfluidic platform without requiring an in-depth understanding of the underlying principles.

The first layer of the categorization of microfluidic devices, and thus, the first separation of the solution is passive versus active microfluidic devices. Passive microfluidic is characterized by a constant driving mechanism or actuation; the geometry dictates the flow behaviour. Passive devices inherently rely on the user's microfluidic expertise to adjust for the operational and manufacturing uncertainties. Moreover, the design process tailors the device for the specific application. Thus, re-design is required for different applications. In contrast, active microfluidics uses non-constant actuation that often introduces an external force to the system. Active devices enable the user to set parameters without necessarily understanding microfluidic physics to its full extent. The active layer interfaces between the microfluidic device and the user such that the knowledge required to use the devices is lessened. Oppositely, passive microfluidic devices do not provide the user with such an interface; the user must directly understand and interact with the microfluidic principles. Consequently, the active microfluidic approach is deemed more appropriate to move towards microfluidic tools that are more accessible for end-users. The added control provided by the active method relies either on external forces or on a fluctuating driving force. Forces that are external to the microfluidic channel typically require a more complex manufacturing process. For example, electrodes and surface acoustic waves (SAW) necessitate a layer close to the micro-channel with a conductive material. A passivation layer is required to prevent contamination. Therefore, device fabrication requires multiple layers and different materials. The multi-layer device approach is simpler by only requiring one flexible polymer. For example, a control layer actuated with air is superimposed on top of the micro-channels. A thin layer separating the two creates valves. However, this approach still requires relatively complex device fabrication in addition to external equipment for the control layer. Another option is for the control valves to be in-line, but this raises issues with contamination and control capabilities.

Active methods enable the user to interface with the microfluidic device using less knowledge. However, the simple device fabrication and required hardware should be maintained to promote accessibility. Therefore, a combined passive and active

approach is privileged. The added control is provided by visual feedback that is non-intrusive and that does not require any complex device fabrication. The interface with the user is provided through the software and a controller. The controller adjusts the driving forces provided by the pressure pump. This is envisioned to be the most promising approach that minimizes the user burden of microfluidic knowledge, fabrication, and hardware. The following two research questions are used to guide our research within the context of the combined active and passive microfluidic platform:

- How can we make droplet microfluidics more accessible to end-users?
- What are the issues restricting the accessibility and better control of droplet microfluidics?

1.3 Thesis overview

Our approach to making microfluidic more accessible as a tool for end-users is separated into different projects. As shown in Figure 1.1, there are two main categories of projects: working “towards a modular platform” that are more technology-based, and “better understanding the system” that are more knowledge-based. The contribution of this work is beneficial for both passive and active microfluidic devices. For example, the open-source pressure pump is suitable for pressure-drive approach whether passive or active. Furthermore, the knowledge-based projects develop a better understanding of the dynamics of the system. Passive and active microfluidic have different trade offs. Nevertheless, the knowledge and modelling enable to optimize for different objectives; for example, the tubing dynamics should be minimized for active approaches whereas the damping effect is beneficial for the actuation stability of passive microfluidic systems.

The automation of droplet manipulations (Chapter 4) aims to perform more accurate and repeatable procedures independently of the user’s skills. The added algorithm layer further separates the user from the microfluidic knowledge to make microfluidic devices more accessible to end-users such as chemists and biologists. The open-source pressure pump μ Pump (Chapter 5) lowers the financial burden associated with microfluidic-specific equipment. Moreover, an open-source system provides more customizability and control. The tubing dynamics (Chapter 6) is a previously neglected part of the model. Experimentally quantifying the air tubing dynamics enables us to build a more complete model to better understand droplets

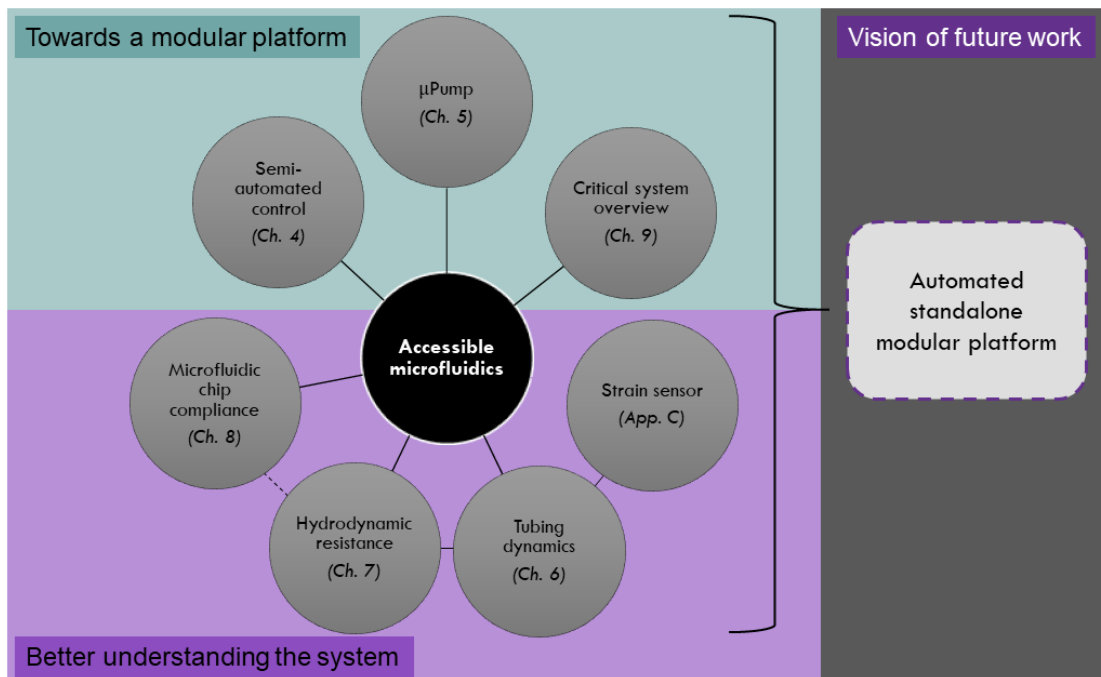


Figure 1.1: Schematic overview of the relationship between the chapters of the thesis.

in microchannels. The droplet resistance (Chapter 7) is another part of the system that must be better understood. The uncertainties in the droplet resistance cause reliability and robustness issues that inhibit accessibility. The active droplet control platform enables a new approach that leverages system identification techniques. The compliance of the microfluidic chip (Chapter 8) is another part of the system—similarly to the air tubing dynamics—that must be better understood through experiments. Finally, a critical system overview (Chapter 9) informs the next steps to continue the work for accessible microfluidics. Each chapter targets a different part of the microfluidic system to make it more accessible for end-users either through technological and knowledge-based progress.

Chapter 2

Literature review and background

The literature review will first cover the fundamentals of microfluidics; then, it will continue with the different manipulations achieved using various methods and the platform technologies implementing multiple of these manipulations. The modelling of the microfluidic system will bridge the microfluidics to the control systems background. Finally, the relevant topics briefly covering state-feedback, observer, and Kalman Filter (KF) will be presented.

2.1 Fundamentals of microfluidics

2.1.1 Dimensionless numbers

Dimensionless numbers are used to represent the relative importance of forces according to the suitable variables. The most important characteristic of microfluidic systems with respect to dimensionless numbers is the characteristic length that is on the order of $\sim 10^{-6}$ m. Consequently, any quantities scaled by the length (at any power other than zero) will be disproportionally large or small. This is reflected by the relative importance column in Table 2.1. The Capillary number is used to characterize microfluidic flow, which is laminar since the Reynolds number is much less than 1. Other forces such as inertia, gravity, and buoyancy are generally neglected as justified by the small values of the corresponding dimensionless numbers, namely the Weber, Bond, and Grashoff numbers, respectively.

Table 2.1: Dimensionless number definition and relative importance [162].

| Dimensionless number | Qualitative description | Quantitative description | Relative importance |
|----------------------|-------------------------------------------------------|------------------------------------------------------------|--------------------------------------|
| Capillary | $\frac{\textit{viscous}}{\textit{interfacial}}$ | $Ca = \frac{\mu U}{\gamma} \propto l^0$ | 1 st (most important) |
| Reynolds | $\frac{\textit{inertia}}{\textit{viscous}}$ | $Re = \frac{\rho U l}{\mu} \propto l^1$ | 2 nd |
| Weber | $\frac{\textit{inertia}}{\textit{interfacial}}$ | $We = \frac{\rho U^2 l}{\gamma} \propto l^1$ | 2 nd |
| Bond | $\frac{\textit{gravitational}}{\textit{interfacial}}$ | $Bo = \frac{l^2(\rho_1 - \rho_2)g}{\gamma} \propto l^2$ | 3 rd |
| Grashoff | $\frac{\textit{buoyancy}}{\textit{viscous}}$ | $Gr = \frac{l^3 \rho^2 \beta \Delta T}{\mu^2} \propto l^3$ | 4 th (least important) |

where \propto is the symbol for proportional to, μ is dynamic viscosity [$Pa \cdot s$], U is characteristic velocity [m/s], γ is interfacial tension [N/m], ρ is density [kg/m^3], l is characteristic length [m], g is the gravitational acceleration [m/s^2], β is coefficient of thermal expansion [$1/K$], ΔT is temperature difference [K].

2.1.2 Interfacial tension: Fluid-fluid interface

For the two-phase flow of immiscible fluids, the interfacial tension (γ) is the force acting at the interface between the two fluids. Typically, the dispersed phase is an aqueous solution while the continuous phase is oil. The existence of a surface inherently requires energy due to the molecules closest to the surface not forming as many bonds with the neighbouring molecules. Consequently, the surface molecules have more energy than the bulk molecules [31].

The interfacial tension between the two phases is modified by adding surfactants; these chemicals are “surface-active agents” [250] that have different groups of molecules with different affinities with the immiscible phases (i.e. amphiphilic molecules). The groups composing the surfactant and hence, the surfactant itself must be selected to match the pair of immiscible fluids [162]. Surfactant dynamics are complex due to the coupling between the interface and the bulk flow as well as other effects such as Marangoni stresses simultaneously occurring [18]. Nevertheless, the main effect of surfactant leveraged is the reduction of droplet merging that is particularly useful in the study with long storage time with a biological focus. The commercial availability of surfactants is limited as the field is still evolving and undergoing major developments. Examples of commercially available surfactants are Triton X-100, Span80, and Tween 20/80[18].

2.1.3 Surface wetting: Surface-fluid interface

For typical droplet microfluidics systems, there are three components: the dispersed phase (usually an aqueous solution), the continuous phase (usually oil), and the solid surface composing the wall of the channels (usually polydimethylsiloxane (PDMS)). In such systems, the continuous phase should preferably wet the wall for droplet formation; the dispersed phase is then contained within the droplet without contacting the wall. The competition between the interfacial tension of the three components is summarized by Equation 2.1 where the two components between which the interfacial tension applies are described in the subscripts [162]. The corresponding schematic is shown in Figure 2.1.

$$\gamma_{solid-continuous} = \gamma_{solid-dispersed} + \gamma_{dispersed-continuous} \cos(\theta) \quad (2.1)$$

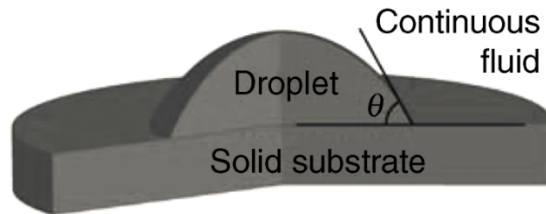


Figure 2.1: Surface wetting of the droplet, continuous phase, and solid substrate. Reproduced from Ref. [162] with permission from Wiley & Sons.

Within the context of microfluidics, the dispersed aqueous phase must not wet the wall. Such a situation occurs for $\gamma_{solid-dispersed}$ larger than $\gamma_{solid-continuous}$ and $\gamma_{dispersed-continuous}$. Consequently, the surface property of the wall should be hydrophobic such that the continuous phase preferably wets the surface. Moreover, the interaction between the fluids and the solid is limited to the surface; surface treatment is performed to alter the properties as desired [310].

2.1.4 Droplet flow in microchannels

Thin film and gutter region

For droplets contained and flowing in the continuous phase, there exist different regimes characterized by the space occupied by the droplet compared to the size of

the channel. The regime of interest throughout is the squeezing regime for which the droplet is bigger than the channel width; consequently, the droplet cannot form a circular or disk shape and rather adopts a slug shape as shown in Figure 2.2.

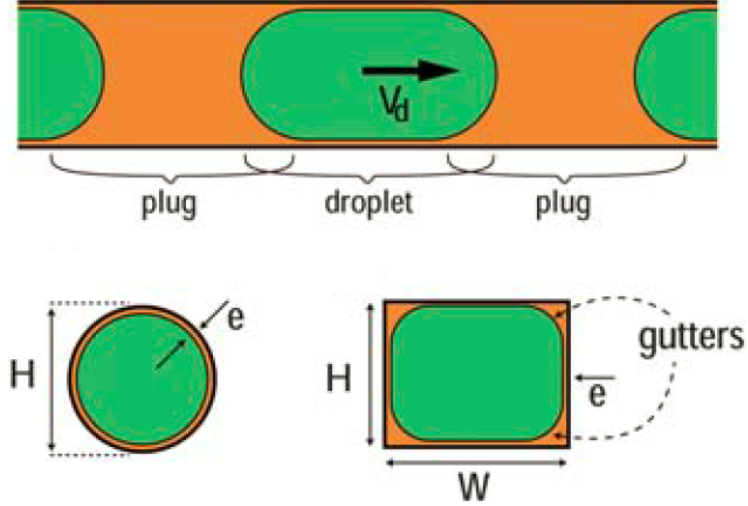


Figure 2.2: Squeezing regime flow in circular and rectangular channels. The thin film between the dispersed phase and the wall is indicated by (e). The gutter region is indicated by dashed-line arrows for the rectangular cross-section channel. Reproduced from Ref. [21] with permission from The Royal Society of Chemistry.

The thin film separating the dispersed phase from the container wall has a thickness scaling with $Ca^{2/3}$ for a small Capillary number ($Ca < 0.01$). Thus, the film thickness corresponds approximately to 1-5% of the half channel height [21]. For the rectangular cross-section, the thin film is not constant along the droplet length as the continuous phase enters and leaves the film surrounding the droplet [309].

Fluid flow and vortices

For a dispersed phase much less viscous than the continuous phase (e.g. water in oil), the flow field is represented schematically as shown in Figure 2.3. The flow field is a complex function of many factors: the viscosity ratio, the geometry of the channel, and the channel aspect ratio. Other studies have considered the 3D flow field in rectangular microchannels both experimentally [107, 156] and through simulations [254, 63]. One important feature of the flow field is the symmetric vortices about

the flow direction that prohibit convective mixing across the two droplet halves. Consequently, achieving mixing within droplets in microchannels is not trivial.

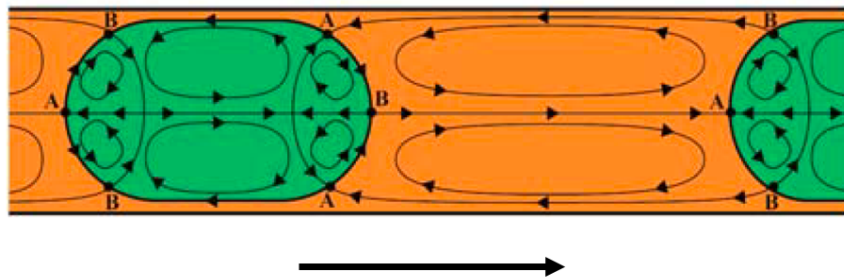


Figure 2.3: Schematic of fluid flow for a low dispersed phase relative viscosity. Flow pattern for all viscosity ratios in [116]. Reproduced from Ref. [21] with permission from The Royal Society of Chemistry.

2.1.5 Chip fabrication

Photolithography for micro-fabrication has its roots in the semiconductor industry for electronic component manufacturing [218]. Although initially used in biochemical applications [83], the disadvantages of the technique led to the development of the more appropriate soft-lithography procedure with faster production and reduced cost [245]. Although lithography is still used to manufacture glass microfluidic chips as provided by Dolomites (T-junction glass chip: Part number 3000453), the fast prototyping of polydimethylsiloxane (PDMS) chips is more appropriate for multiple quick design iterations.

Other alternative manufacturing approaches for microfluidic chips include thermoplastics (e.g. polycarbonate [231], PMMA [117]) and 3D printing [115]. However, these methods generally do not allow resolutions as small as PDMS soft-lithography techniques can achieve.

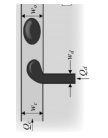

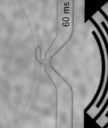

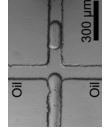
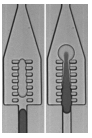
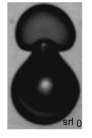
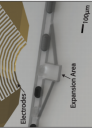


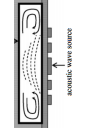
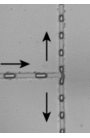


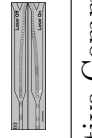
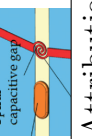
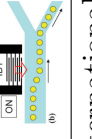
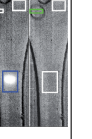
2.2 Droplet manipulations

Droplet manipulations such as: generation, merging, mixing, splitting, and sorting, are classified by the function achieved and the means used. The techniques are generally separated between passive (relying on flow and channel geometry) and

active methods (utilizing an external force through electrodes for instance) [341]. Table 2.2 presents an overview of the diverse ways of achieving the manipulations listed above. The row categorization by manipulation is intended to act as a shopping list if one function is desired while the column categorization focuses on the method used such as the external energy provided.

Generally, passive methods are designed to perform one manipulation well at high-throughput. For example, highly-monodispersed droplet generation is achieved with a coefficient of variation (CV) of 0.2% [141]. However, integrating multiple manipulations in series on a chip is challenging due to the flow field coupling effects, and the small margin of design and operational errors. On the other hand, active methods require more complex manufacturing [333, 76, 216] due to the necessary electrodes (microwave, surface acoustic wave), complex optical alignment (laser), the use of particles not compatible with biological applications (magnetic), or is limited to the tuning of only one function (visual feedback).

Table 2.2: Droplet manipulation methods

| Method Function | Passive | Active | | | | Visual feedback |
|-------------------|---------------------------------------------------------------------------------------------------------|--------------------------------------------------------------------------------------------------------|-------------------------------------------------------------------------------------------------------|-------------------------------------------------------------------------------------------|------------------------------------------------------------------------------------------|-----------------------------------------------------------------------------------------------------|
| | | Laser | Microwave | Surface Acoustic Wave (SAW) | Magnetic | |
| Generation | [42]  | [234]  | N/A | [50]  | [191]  | [55] ¹  |
| Merging | [228]  | [186]  | N/A | [258]  | N/A | N/A |
| Mixing | [28]  | [324] ²  | | [284]  | N/A | N/A |
| Splitting | [189] ³  | N/A | N/A | [139]  | [313]  | N/A |
| Sorting | N/A | [249]  | [323] (sensing)  | [85]  | N/A | [19]  |

¹ Licensed under the Creative Commons Attribution 4.0 International License.

<http://creativecommons.org/licenses/by/4.0/>

² Adapted with permission from Yesiloz, Gurkan, Muhammed S. Boybay, and Carolyn L. Ren. "Effective thermo-capillary mixing in droplet microfluidics integrated with a microwave heater." *Analytical Chemistry* 89.3 (2017): 1978-1984. Copyright 2017 American Chemical Society.

³ Reprinted figure with permission from D. R. Link, S. L. Anna, D. A. Weitz, and H. A. Stone, *Physical review letters*, 92, 054503, 2004. Copyright 2004 by the American Physical Society.

<http://dx.doi.org/10.1103/PhysRevLett.92.054503>

2.3 Enabling platform technologies¹

Generally, the development of enabling platform technologies focus on using microfluidic principles for applications in other fields such as cells, biochemistry, material science, and environmental factor monitoring. The applications motivate the design choices of the platform. Hence, it is useful to understand the various applications to better comprehend the objective of microfluidic devices.

2.3.1 Applications in many fields

A few categories of applications are selected to highlight the potential of microfluidics for end-users, namely: cells, biochemistry, materials, and environmental factor monitoring. Furthermore, impactful studies are singled out in a separate section; their impact is not quantified through publishing analytic but rather by providing unique capabilities impossible without microfluidic methods.

The early motivation arising from the total analysis system vision focuses on obtaining answers from samples through chemical analysis. Microfluidics is applied to many different fields with different objectives. The purpose of each application is generally classified as either information-focused or production-focused. The small volume involved in microfluidic reactions provides key advantages [64] for reagent consumption and reaction time to information-focused applications. Nonetheless, production-focused applications provide valuable contributions through efforts of parallelization to increase yield and synthesis of high-value-added compounds.

Cells

The similar scale of microfluidic devices and single-cells are leveraged in many studies [204, 237, 242, 122, 171, 188, 253]. For example, circulating tumour cells (CTC) are localized in the height direction of a channel using dielectrophoresis electrodes; the CTCs pass through a localized lethal zone that eliminates them without affecting the healthy blood cells [155].

On a multi-cell scale, organs-on-a-chip is a collection of cells mimicking whole organs or organ systems to model *in vitro* processes [240]. For example, a model of

¹ Excerpt from submitted manuscript: **Marie Hébert**, Jan P. Huissoon, and Carolyn L. Ren. “A perspective of active microfluidic platforms as an enabling tool for applications in other fields.” (2020).

the transport of sodium-coupled glucose of the renal proximal tubule is studied using a microfluidic device to understand the effects of administrating a sodium-transport inhibiting drug [291]. The microfluidic *in vitro* models are not restricted to humans; the long-term flow through human intestinal organoids [266] and the fish intestinal barrier [71] are studied using organs-on-a-chip. Micro-tumours are another multi-cell environment; flow conditions control diffusive and conductive mass transport of anti-cancer drug delivery to perform drug screening studies [119].

On an even larger scale, whole organisms are studied using microfluidic devices. *Caenorhabditis elegans* organisms offer a platform for *in vivo* drug screening that is physiologically relevant to humans [142, 53]. Their adult size of 1.3 mm is larger than the micrometre scale, but microfluidic devices provide added control and throughput to study Parkinson's disease for example [327].

A conspicuous challenge of biology-focus μ TAS is the non-Newtonian behaviour of whole blood and other biological fluids with its misunderstood impact for flow in microfluidic devices [283]. Blood is a significant source of information for biological assays and is a key sample to process through μ TAS. In addition to its non-Newtonian behaviour, blood coagulation causes issues. Remediation strategies include chemical or pharmaceutical approaches but the depletion of the active components and the potential for interference cause problems. Dielectrophoresis is explored as a potential solution, but there is still no widely accepted and used solution [154]. There are nevertheless promising advances in the microfluidics field that can handle whole blood through the enrichment of extracellular vesicles by using a magnetic bead-based approach [38]. Furthermore, a digital microfluidic platform incorporated a blood-plasma separation membrane; the blood sample is easily obtained from a finger and the device avoids any sample pre-processing by filtering to deal only with the plasma [66]. More fundamental work is necessary to establish a solid understanding of the complex behaviour of non-Newtonian fluids in microchannels. This is especially important for whole blood considering the dependence of its behaviour on its content among other factors.

Biochemistry

Chemical reactions for biochemistry purposes do not necessarily involve cells; drug screening and protein crystallization are two examples. The microfluidic devices are information-focused. The combination of the different samples and the analysis of their response is the output.

The small volume involved in the reaction at the micro-scale saves reagent. The

impact is particularly significant for sparse samples such as the cerebrospinal fluid from mice [210] or expensive samples such as those used for drug screening assays [224]. Multiple droplet manipulations are required for drug screening assays; droplets containing each solution are generated in parallel, then, they are trapped, merged and monitored [51, 37]. Although the complex manipulations are achieved passively, translating the microfluidic device to a commercial product or device suitable for end-user independent use is a complex endeavour. The structure of microfluidic also enables greater control over the drug delivery mechanisms [338].

The rapidity and lower consumption of reagents are advantageous to probe vast parameter spaces. The search for chemical conditions for the crystallization of proteins enables the study of their structure mainly for medicinal purposes. Microfluidic tools enable the crystallization of otherwise recalcitrant proteins when subjected to traditional larger-scale approaches [181, 80, 190, 185].

Materials

Complex emulsions and nanoparticle synthesis are achieved using microfluidic devices. The capabilities of manipulating fluid at such a small scale with better uniformity than bulk methods are promising [126, 206, 74, 197, 92, 223, 322]. However, achieving significant yield with microfluidic devices is challenging. Thus, most applications focus on using microfluidics as an analytical tool to provide information rather than to yield a product. Nevertheless, microfluidics is leveraged to achieve a narrower size distribution through better control of nanoprecipitation using an acoustically-driven micromixer for example [247]. As for complex emulsions, microfluidic devices allow a higher level of control over the number, size, and type of internal droplets that is not achievable with non-microfluidic approaches [72, 293, 183].

Environmental factors monitoring

The application of microfluidic tools to monitor environmental factors is focused on gathering information that is critical for safety. Various approaches involve microfluidic tools for their small sample volume required, fast response, and low cost. The small size of microfluidic platforms enables portability and point-of-care decentralized testing. Selectivity is important to target the desired compound within the complex chemical profile of water samples. Sensitivity is essential to detect low concentrations of harmful chemicals that are detrimental to health and the environment.

The distinct approaches developed have different requirements and performance. Mercury and arsenic are among the species of interest that are detected. Mercury ions are sensed with concentrations from 2 to 12 nM and only require a 2.8 μL sample [144]. Another electromechanical method enables the detection of arsenic in the range of 1 to 150 $\mu\text{g/L}$ concentration [98]. Although another study requires a larger sample of 40 μL , its operating principle does not involve valves and is thus compact and portable [271]. A simple approach that does not require moving parts is paper-based microfluidics that is used to target copper ions for example [106]. Specificity is challenged for certain platforms. Detecting different ions is impactful and is achieved visually for mercury, lead and copper using DNA-nanoparticle probes; the detection limit for all three ions is on the order of 1 nM [193]. Furthermore, certain micro-organisms present in water are detrimental similarly to heavy metal ions, and the detection of the micro-organisms is thus also important [232].

Focused review articles provide a targeted point of view about environmental factor monitoring. The combination of microfluidics with a smartphone is particularly potent for portable solutions [319]. Furthermore, image-based colourimetric sensing techniques are ideal for portability and low-cost [130]. As for electro-mechanical techniques, nanomaterial-based modification of the electrodes increases the performance through enhanced specificity and sensitivity for different metal ions [184, 296]. Finally, samples are targeted at various points in the water cycle such as wastewater monitoring with biosensors [75] and various approaches to detect metal cations in drinking water [60].

Impactful applications

The most impactful applications of microfluidic devices are the ones providing key advantages and possibilities compared to bulk methods. The high-throughput, low reagent consumption, short reaction times, and reaction compartmentalization are interesting advantages. However, they do not always justify the switch from a more familiar method to microfluidics. Microfluidic devices are more easily adopted when providing new capabilities or definitive advantages [326, 73].

The laminar nature of flow at the micron scale is challenging to thoroughly mix the sample. Nonetheless, it is also leveraged to control the diffusion. Hence, using a simple approach with a syringe pump, denaturalized proteins and the buffer are passed through a chip side by side. The resulting refolding of the proteins is more effective and does not require a post-processing purification step compared to other non-microfluidic-based approaches [317].

The strength of microfluidics more commonly lies in the information it provides rather than the yield it produces. High-value products such as drugs can nevertheless be pertinent applications. Parallelization of micro-reactors yields higher throughput by increasing the production 25 fold to achieve 31 g/hr [5]. The miniaturization and implementation of the instrumentation on the microfluidic device enable in-situ measurement. These are particularly useful for transient measurements. For example, a by-product of the oil industry is deposited on porous media and its temperature properties are examined [36]. Microfluidics enables extensive control over the arrangement and the complexity of the microstructure. Researchers leverage these capabilities and the small scale of microfluidic tools to work towards the generation of artificial cells [207]. Micro-droplets provide a platform with better frequency control of Belousov-Zhabotinsky reactions. Thus, further insights enable a better understanding of the phenomenon [108].

2.3.2 Modular platforms

Framework overview

The development of microfluidic tools that are easy to use in other fields requires reliable, predictable, and repeatable building blocks as formulated by Prof. Whitesides [305]. The stacking principle enables the usage of higher-level functionalities without requiring an understanding of the lower-level building blocks. For microfluidic devices more specifically, stacking signifies that end-users perform manipulations without requiring an in-depth understanding of fluid mechanics at the micro-scale. As illustrated in Figure 2.4, vertically, the building blocks must exhibit reliability, predictability, and repeatability—that is stackability—for the users to depend on them. Horizontally, the modules must operate independently to avoid influencing each other, but appropriate exchange channels must be established between them. In the envisioned modular system, each module is responsible for one droplet manipulation that corresponds to one step of the assay. The operation of the modules is controlled by the supervisory control layer that interprets the user input as instructions for each module. Moreover, progress in the natural language processing field has the potential to simplify user input. A potentially cumbersome user interface is replaced by the direct interpretation of a user’s directives [339].

The value of modular design has already been leveraged in several studies. However, generally, the lack of either independence or stackability of the modules compromises the potential of the platform. Thus, the literature covers various aspects required to achieve an impactful modular platform but separately.

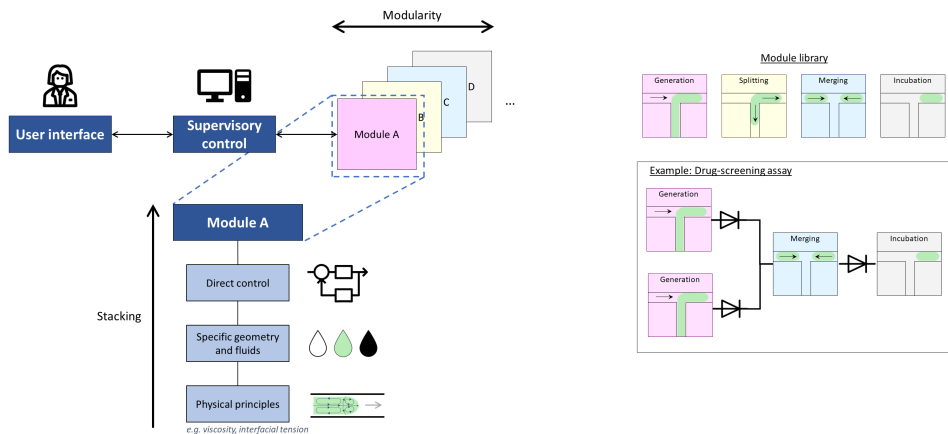


Figure 2.4: Stackable modular platform structure and vision for easy control of individual droplets by end-users. Structure of a stackable modular platform. The vertical arrow shows the stacking while the horizontal arrow shows modularity. Each manipulation is a module that leverages stacking such that only high-level information from the user is required.

Modules

Certain studies focus on developing modules that the user assembles for their specific use; the approach involves either single-phase or droplet flow. Single-phase flow modules behave more independently from each other than droplet flow modules. The dynamic effects of droplets travelling through channels that are coupled through the pressure field easily compromise the independence of each module [8].

Therefore, influence between the modules is circumvented by using single-phase flow for an automated modular approach [257, 273]. However, droplet microfluidics provides key advantages such as compartmentalization that are essential to many applications. A critical issue that modular microfluidic systems must address is the connection of the different modules. The focus on the mechanical assembly of the different modules is essential but usually fails to address the issue of dependability [329, 236, 268, 44, 238, 202, 39, 195]. The coupling of adjacent modules through the pressure field can result in undesirable dynamics compromising the operation of the device. Nevertheless, a reliable connection between the modules is primordial to the success of modular systems. The component with the flow-driving capabilities is a prime candidate for modularity [332]. However, without applying the principles

to the rest of the microfluidic system, the independent usage by end-users is still compromised. Similarly, a heat-exchange module embodies the modularity principle but is limited to the component rather than the whole microfluidic system [340]. The handling of single-cells is automated using a vision-based system. However, the cells are transferred to passive microfluidic channels, and thus, the system is modular and adheres to the stacking principle only for the cell-handling module [286].

Stacking components

Generally, the studies proposing the stacking of components either focus on peripheral components to the chip or the chip itself but not both simultaneously. The modularity of the peripheral equipment to the microfluidic chip is essential to the versatility of the whole system; the stacking of the microfluidic chip function is deemed a critical factor that should also be addressed, but that usually is not. For example, a suspended-microchannel-resonator-focused study demonstrates the potential of modular equipment, but the application as a general microfluidic platform is limited [202]. Similarly, modularity is also demonstrated but is limited to the actuation [179].

The devices that allow the sample as the input and provides the answer as the output embody the principle of stacking. The user of the device does not need to thoroughly understand how the device works. However, the devices are sometimes overly tailored to specific applications, for example, detection and quantification of infectious pathogens using dRPA [318].

2.3.3 Active control platforms

The historical perspective and key applications of microfluidic devices motivate the vision and need for an automated active microfluidic platform that is used as a tool. A sub-field of microfluidics that concentrates on achieving such objectives are active control platforms. Diverse avenues to achieve the envisioned μ TAS are herein included.

The two main objectives achieved are: (1) the integration of chemical and physical sensors for continuous monitoring, and (2) logic and feedback algorithms for automated screening, process control, and optimization [208]. The challenges identified by McMullen *et al.* extend beyond the scope of their article that is focused on analytical chemistry but are nevertheless pertinent to this day.

- Translating the thinking and decision-making skills of a researcher into an automated tool.
- Detecting failures such as clogging to avoid introducing erroneous data into the results.
- Handling the complications that compound as the microchannel network grows.
- Developing algorithms that provide stability, and fast dynamics.
- Collaborating between multiple experts in chemistry, engineering, micro-fabrication, and software development.

The integration of chemical and physical sensors are crucial to monitor the parameters of interest. The two main categories of studies are: (1) screening a vast parameter space for various reactions [91, 104, 103, 157, 272, 270], and (2) real-time optimization and change through online feedback [161, 209]. Implementing sensors for the varied parameters that are monitored on the microfluidic chip is complex and focused review articles provide more details [269, 296, 187]. This section will concentrate on the logic and feedback for process control. The active control is categorized into single-manipulation, single-application, and platform studies.

Single-manipulation focus for droplets

The automation of droplet manipulations is achieved using various methods typically introducing an external force. The common connection between the studies is their objective to automate one single manipulation of droplets. Examples of target manipulations are generation, merging, mixing and sorting. The single manipulation focus signifies that these studies are not platform technologies that would be promising for the μ TAS system vision. The main inhibition in developing a platform from these techniques is the localized effect that cannot easily be extended or multiplexed for multiple manipulations. Nonetheless, the variety of external forces used to control the droplet shows the assortment of approaches.

Although an external force is introduced, and thus, the method is active, the studies focusing on a single-manipulation typically layer the external force on top of passive methods. Most commonly, a passive generation of droplets is the first step of these active single-manipulations. Thus, although the active control enables stacking to some extent, the dependence of the approach on passive microfluidic severely inhibits modularity potential.

Generation Certain review articles focus specifically on the different external forces introduced to actively control the droplet generation process [41]. The introduction of a force such as an alternative current using on-chip electrodes enables the tuning of the droplet size. The generated droplets contain a sodium chloride solution. Moreover, the study demonstrated a negligible difference in the actively controlled generation process using a non-Newtonian fluid, more specifically, xanthan gum [279].

An alternative to introducing an additional external force is to adjust the flow-driving mechanism based on feedback. An approach only requiring the typical equipment without any additional components uses the pressure pump or syringe pump as the force, and a camera to acquire the appropriate feedback. Thus, parameters (e.g. length-to-width ratio) are tuned using a controller (e.g. PID controller) to adjust the flow rate of the syringe pump to achieve the desired outcome [331, 55].

Droplet-on-demand implements active methods without the high-throughput and lack of modularity of layering the external force on top of passive droplet generation [330, 105, 118, 277, 251, 99]. Although the droplets are generated one at a time, they typically enter a passive network. Thus, the control is increased over single droplets rather than multiple droplets. However, the active control is localized at the generation site. Thus, the modularity potential of this approach is limited similar to the active droplet generation techniques that are layered on top of passive generation. The reliance on the passive network is troublesome for users without in-depth knowledge to adjust for operational and manufacturing uncertainties.

Merging and mixing Microfluidic applications involving multiple on-chip reagents require merging and mixing. Review articles provide an overview of the different approaches as well as techniques to achieve merging [79] and mixing [173, 4] passively and actively. For example, an on-chip microwave sensor enables the selective heating of the aqueous droplets; the non-uniform heating pattern causes effective mixing between the two droplet halves [324]. A mixing module is integrated on-chip with Tesla valves to thoroughly mix samples; the concentration is digitally controlled [169]. The intermittent pulse-width-modulated signal is leveraged to control the concentration of up to 6 different reagents using multi-layer valves [312]. Moreover, complex flow profiles are achieved, real-time control is enabled for potential feedback mechanisms, and the necessary design files are provided to replicate the apparatus.

Sorting Sorting droplets inherently requires an active component to deviate the droplets between at least two paths. Moreover, a sensing method must be imple-

mented to detect which droplet to deviate. The need for sorting emerged from leveraging high-throughput encapsulation using microfluidic devices with heterogeneous cell populations. Fluorescence-activated cell sorters (FACS) is an established tool in the biochemistry field [158, 221]; the fluorescent probes enables the sorting of the cells according to targeted characteristics. The feedback system is generally vision-based such as for fluorescent signals of FACS systems. The study object is not restricted to cells and can be organisms such as *C. Elegans* [69]. More complex identification techniques leverage deep learning to identify the element to actively sort using a pulse [227, 6, 128]. Alternatively, the sorting elements span a wider area of unrestricted flow controlled through dielectrophoresis for example [102]. Dielectrophoresis is also leveraged to form a sequentially addressable dielectrophoretic array (SADA) to achieve large-droplet sorting [129].

Single application: Point-of-care platforms

Point-of-care (POC) platforms are prime examples of the potential impact of microfluidics in other fields, often linked to medical applications. Multiple functions are integrated on a microfluidic device to achieve a specifically targeted application [290]. However, the developed microfluidic solutions are highly specific to the target application and lack versatility. Consequently, the end-users cannot adapt the platform to their various need without prior microfluidic knowledge to adapt the design. Nevertheless, the application focus they fulfill demonstrates the potential of microfluidic platforms as tools in other fields.

Paper-based devices are particularly suitable for POC due to their simple operation, compactness, and low-cost. Although the core of paper-based microfluidics relies on passive flow [230], certain active approaches are developed such as thermally activated gates [86].

More generally, point-of-care devices cover a wide range of applications. For example, HIV is detected from whole blood samples [239]. Microfluidic tools are developed and used for iron deficiency anemia [320] and other diagnostics [134, 150, 174]. The detection of micro-organisms is also achieved using microfluidic approaches [222].

The great advantage of point-of-care microfluidic devices is their ability to take the sample as the input, and then, provide the answer as the output [114]. The stacking principle is leveraged such that the user does not need to understand the inner workings of the microfluidic device. However, the researchers developing such devices are certainly required to understand microfluidics.

The potential for automation and great versatility of the platform led to many applications regrouped in pertinent review articles [20, 213]. For example, a commercially available digital microfluidic device is used to efficiently prepare samples for liquid chromatography-mass spectroscopy [177]. Previously, sample losses and manual manipulations challenged the measurement of low cell number samples.

The high automation and modularity potential are key advantages of EWOD platforms. Multiple companies developed products for main application areas: liquid lenses, reflective displays, and biomedical assays [180]. The potential of the platform is demonstrated for sample preparation. A procedure requiring 4 to 5 hours of manual labour is achieved in about 30 minutes using an automated EWOD platform. Nonetheless, typical drawbacks of digital microfluidics include sample evaporation, degradation of the samples from the electric field, and detrimental large droplet volume for single-cell analysis. Moreover, non-adherent surface coating properties are essential when using particularly sticky components such as proteins that easily cross-contaminate. In brief, the digital microfluidic technology is promising in terms of its modularity and automation potential, but inherent drawbacks inhibit its independent use by end-users. The continued development of commercial platforms is nevertheless promising. Any reliability issues must however be first resolved.

Another approach that relies on electrodes is surface acoustic waves (SAW). The principle is fundamentally different; an overview is provided in this review article [65]. A platform for selective cell encapsulation, lysis, and pico-injection was recently developed [219]. The platform also achieves various droplet diameters based on the pulse length and power level.

Multi-layer devices for parallel control channels

Working principle The micro-channel network containing the samples are enclosed within one layer; there is at least one other layer that is used for control purposes. On-off valves commanded by a computer provide control over the sample flow within the micro-channel network. Figure 2.5 schematically illustrates the working principle.

Quake's valves The pioneer of this novel approach—often accordingly labelled as “Quake's valves”—developed the idea in the early 2000s when microfluidics was still in its infancy [285]. The soft nature of polydimethylsiloxane (PDMS) that has been commonly used for rapid prototyping of microfluidic devices is leveraged to create

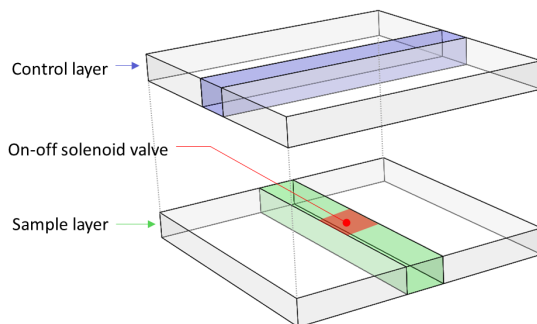


Figure 2.5: Working principle of multi-layer devices with a sample and a control layer. The zone at the intersection between the two layers acts as an on-chip solenoid valve.

on-chip valves. A thin membrane between the sample and control channel is expanded to block flow in the sample channel using pressurized air. The valves create micro-reactors containing the samples similarly to droplets, although the approach fundamentally operates using single-phase flow.

High-throughput applications require numerous on-chip valves to isolate and to control each micro-reactor. A multiplexing technique reduces the number of off-chip solenoid valves to lessen the burden of the external hardware [282]. Although the microfluidic device footprint is small, the required supporting hardware is substantial. Another drawback is the required more complex fabrication of multi-layer devices that is more demanding than simpler single-layer chips. Finally, single-phase flow is susceptible to cross-contamination; accordingly, special care must be taken to avoid undermining the results. Even considering the aforementioned drawbacks, the Quake’s valve platform and similar devices with an air control layer have been applied to numerous studies focusing on applications. They are too numerous to comprehensively list here [172, 9, 170, 178, 121, 233, 321, 328, 192, 120].

Although end-users cannot purchase an off-the-shelf commercial product, numerous journal articles detail the chip fabrication process. The multi-layer microfluidic chip fabrication is detailed both for a regular procedure [167] and a 3D-printer-based procedure [175]. Moreover, the supporting hardware required to operate the multiple solenoid valves is accessible through an open-source project [29].

The multi-layer platform is promising due to its demonstrated capabilities with numerous applications and the overall high impact of this research direction within the microfluidic community. Nevertheless, the independent use of the platform by end-users is still not widespread due to the challenges in using the platform and the knowledge barrier; the numerous articles about the process help lower the barrier, but

the stacking capabilities are not yet developed enough to the level of a commercial product. The air control layer approach nonetheless occupies an important and promising direction of active microfluidic platforms.

Other approaches Quake’s valves specifically leverage the softness of PDMS to deform and block the sample channels using pressurized air. Similar approaches with the parallel multi-layer control layer relying on different principles have been investigated to integrate valves in microfluidic devices. An electroactive polymer-based valve is triggered by applying a $50 \text{ V}/\mu\text{m}$ electric field [276]. The valve provides enough displacement to close the sample channel and is compact. However, the pressure is limited to 4.0 kPa (40 mbar). The response time is about 0.7 seconds.

Alternatively, certain valves are pH activated [17]. The power consumption is low and the thermal risk for the bio-samples is avoided. The valves are hydrogel-based and respond to specific pH solutions to expand and close the channel. The response time is about 10 seconds. The pH-enabled hydrogel valve footprint is about $500 \mu\text{m}$.

Wax valves are melted using heat applied at the desired time [300]. The valves are integrated on a centrifugal disk platform to allow better control of the flow and introduce an active control component. The deformable polymer valves are also integrated within a centrifugal disk platform to control the capillary flow using on-off solenoid valves to an external pressure source [48].

The common objective of adding valves as another layer to microfluidic devices is to supplement the microflow with an active control component. Active control inherently has the potential for stacking of the components. However, a more targeted design solution would enable end-users to more easily and independently leverage the powerful tool that multi-layer microfluidic devices present.

In-line solenoid valves

Similar to Quake’s valve approach, Garstecki’s research group developed an active control method using solenoid valves but in-line as opposed to in parallel [59]. The valves are directly integrated in series with the flow source as shown in Figure 2.6. Hence, the complex multi-layer chip fabrication is avoided. Furthermore, the microflow involved is two-phase flow (i.e. droplet microfluidics) instead of single-phase flow.

The control capabilities are greatly increased without sacrificing manufacturing simplicity and robustness. Moreover, droplet microfluidics has many advantages over

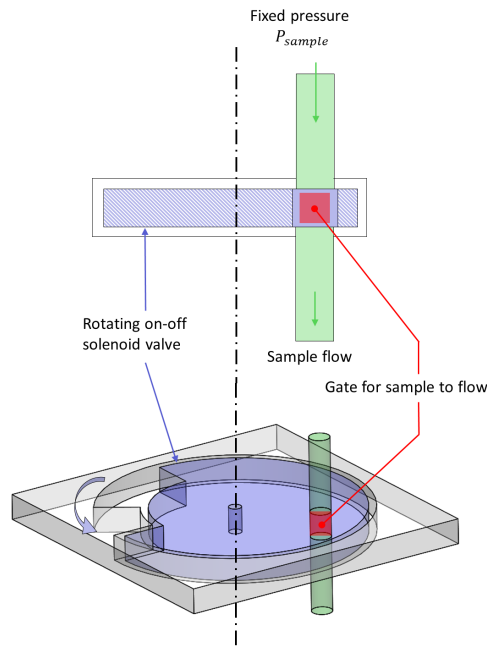


Figure 2.6: Working principle of in-line solenoid valve. The rotating solenoid valve aligns and blocks the gate pathway for the sample to flow.

single-phase microfluidics. The reactions are compartmentalized and thus, largely minimize cross-contamination. Multi-phase flow enables high-throughput without compromising uniformity. However, the in-line solenoid valve system still requires involved user interaction to operate the system, and microfluidics knowledge to setup and operate the actuation pressure behind each of the solenoid valves [46]. A combination of this platform with passive traps allowed for more robust operation without knowledge [241]. Nonetheless, the possible manipulations were limited and required more complex microfluidic chip fabrication.

Overall, the in-line solenoid valve offers added control without extensively complicating the manufacturing process. Thus, modularity potential is high. However, the current control approach heavily relies on knowledge of microfluidics and consequently, would require further development to achieve significant stacking capabilities.

Combining passive and active principles

The control of individual droplets is achieved without introducing an additional force or hardware; the pressure actuation is adjusted based on visual feedback [308, 311, 111, 307]. The controller enables the droplets to be manipulated similarly to passive approaches but with a much greater control directly associated with the varying pressure. Thus, this method combines principles both from passive—the use of the geometry to achieve manipulations—and active—varying forces—methods to control *individual* droplets.

The working principle of the active droplet control platform is illustrated in Figure 2.7. The computer hosts the controller that is at the core of the control of the individual droplets. The communication with the other components of the system is also established through the computer. The pressure pump individually applies pressure to the inlets of the microfluidic chip. The image analysis is also hosted on the computer to provide feedback to the controller in the form of a droplet location.

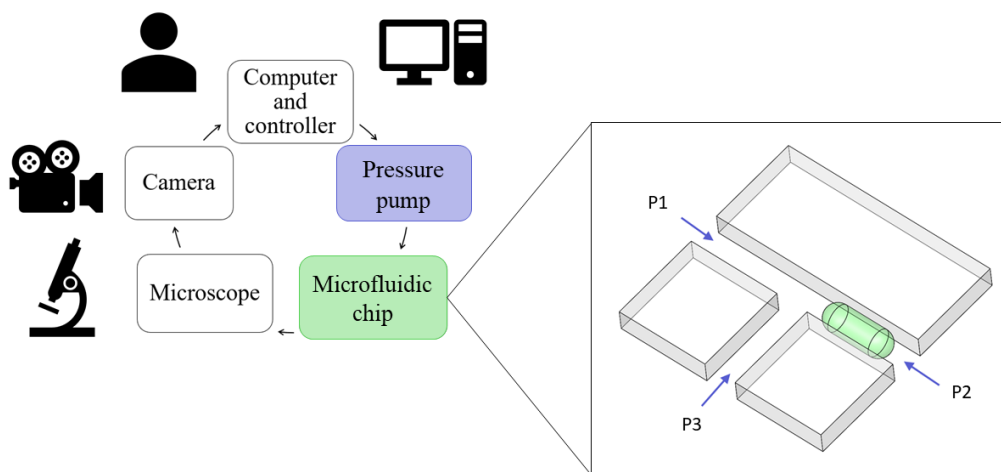


Figure 2.7: Working principle of the combined active and passive platform. The controller calculates the required pressure to apply at each microfluidic chip inlet based on the feedback provided by the microscope, camera, and on-line image processing.

A similar approach that uses visual feedback to locate flow has been implemented in the past [297]. However, the controlled localization is not of a droplet, but an interface. Thus, the potential for applications is much less significant. Another similar approach that incorporates visual feedback and droplet microfluidics is closer

to the platform schematically illustrated in Figure 2.7 from Wong *et al.*. However, the control is over multiple droplets as opposed to single droplets [55]. Consequently, the rest of the microfluidic device relies on passive droplet manipulations that cannot easily be used by end-users.

The simple manufacturing processes and standard microfluidic equipment required for this platform enhances its potential for independent use by end-users. Moreover, stacking is enabled by the controller which removes the microflow knowledge from end-users. Modularity is not addressed yet but is envisioned to have high potential because of the more simple components required.

Future outlook

The impact of microfluidic devices depends on their usage by end-users. The developments that are envisioned to be impactful target the knowledge barrier and the financial cost.

The controller at the core of the active platform should balance simplicity and performance. A simpler approach promotes better accessibility for end-users without significantly sacrificing performance.

Commercial pressure pumps provide a turnkey solution. However, their cost can be prohibitive and limit their accessibility to some researchers. An open-source pressure system provides more flexibility through customization of the different parts. Moreover, the lower cost enables greater accessibility. A minimum understanding of the system is required to properly assemble and maintain the system. Open-source approaches such as μ Pump [90] provide guidance to lessen the burden of a custom system and reduces cost.

The reliance of microfluidic platforms on microscopes and cameras poses a challenge both for accessibility and versatility. The acquisition of high-performance visualization equipment is expensive. Simpler and less expensive imaging solutions are important to develop less costly systems. Moreover, the dependence of microfluidic platforms on bulky systems such as microscopes limits the portability of the devices.

2.3.4 Summary

Microfluidics has tremendous potential to miniaturize total analysis systems (μ TAS) for impactful applications. Applications in the fields of cell studies, biochemistry,

materials, and environmental factors monitoring motivated the development of numerous microfluidic platforms. However, the adoption of microfluidic tools outside of the developers' field by end-users is limited. A modular platform is envisioned to enable end-users to consider microfluidic as a tool to achieve their goal. Active control removes the microfluidic flow knowledge required of the user. Thus, the knowledge barrier is lower by the stacking of reliable, predictable, and repeatable components.

Certain microfluidic platforms demonstrate stacking capabilities while others focus more on modularity. However, both are needed to achieve a platform that can be used independently by end-users. Similarly, many different active approaches to microfluidics enable the user to by-pass the knowledge barrier typically required by passive microfluidic devices. Therefore, many elements of the envisioned platform are present in various studies. However, they need to be regrouped and optimized in one platform that end users can independently leverage in studies in the various fields benefiting from the advantages provided by microfluidics.

2.4 Modelling for microfluidic systems

The fundamentals of microfluidics, its ability to manipulate droplets, and the physics of the system were discussed up to this point. In order to design the controller and simulate the system, a model of the physical system must be defined, albeit based on assumptions. This modelling approach was previously developed and used in [311, 307].

2.4.1 Assumptions

The model must rely on assumptions to be simple enough to be useful in controller design and system simulations.

Linearity

The system is assumed to behave linearly and is described using a set of first order differential equations. A generic example of such first order differential equation is shown in Equation 2.2.

$$\dot{x} = a \cdot x + b \cdot u \tag{2.2}$$

where a is a system property affecting how the system behaves (e.g. mass, stiffness/compliance, damping/viscosity), and b is a system property relating the effect of the input u on the system (e.g. gear ratio, inductance).

The state-space representation formats the system of first-order linear differential equations in a compact arrangement; the matrices (A, B, C, D) describe the physical properties of the system such as mass and damping, while the state-vector (x) characterizes the status of the system through position and velocity for instance. The linearity assumption allows the use of the state-space representation. The different components (tube, channels) are simply connected in series or parallel according to the channel network configuration. The effect of the transition between the tube connected to the chip and going to the channel is neglected as the geometry, and hence the flow is too complex.

Channel properties

The model is based on the channel material properties and on whether the channel contains the dispersed or continuous phase. However, during manipulations and as droplets are generated, the channel composition changes and does not remain static. The changes are assumed to be small enough such that the controller performance is not significantly affected. Similarly, all physical properties of the fluids and materials used are taken nominally without an in-depth analysis of the channel deformation under the applied pressure for instance.

Actuation

The applied pressure is measured at the pump outlet and it is assumed equal to the pressure at the entrance of the tubing containing the fluid in the vial. Any dynamic response from the air tubes, biases from the vial hydrodynamic pressure, and Laplace pressure are disregarded for this model. The effects are nonetheless compensated using a Kalman Filter (details are included further) to estimate the static offset for each pressure input.

Droplet behaviour

The droplets are assumed to be generated in the squeezing regime. Consequently, the discrepancy between the droplet and the continuous phase speed is assumed insignificant. Moreover, the surface properties of the chip enabling the preferable wetting

of the wall by the continuous phase are assumed uniform and constant through time for proper operation of the microfluidic chip. Finally, although the bulk fluid and droplet do not move exactly at the same velocity, the difference is assumed negligible for the performance of the controller.

2.4.2 Electric circuit analogy

The physics-based approach to modelling is preferred to provide information for a variety of system configurations. Various micro-channel network configurations (with varying lengths and varying fluid viscosity in different channels) are used. A physics-based approach to the model enables the quick and simple adjustment of the parameters from their nominal values. Oppositely, a system identification approach would be cumbersome and time-consuming to define the model for each case. Finally, the physics-based approach is proven in previous work by David Wong to provide adequate control performance.

The electric circuit analogy is built by drawing links between analogous physical phenomenon and electric circuit elements [308, 84]. The driving force for the flow is pressure and correspondingly, voltage drives the current. The flow rate, which is taken equivalently to the droplet velocity for a constant cross-section, is then analogous to current. It follows that the droplet position is analogous to charge. Correspondingly, the resistance (R), inductance (L), and capacitance (C) elements describe the system's physical properties.

Resistance

In the electric circuit analogy, resistance accounts for viscous forces as per Equation 2.3.

$$R = \frac{32\mu l}{d_h^2} \quad (2.3)$$

where μ is the dynamic viscosity [$kg/m \cdot s$], l is the channel length [m], and d_h is the hydraulic diameter [m]

Inductance

The inductance encapsulates inertia effects in Equation 2.4.

$$L = \rho l \tag{2.4}$$

where ρ is density [kg/m^3] and l is channel length [m]

Capacitance

The material compliance and the fluid compressibility acts like springs in the physical system and are represented by the capacitance in the electric circuit analogy as described by Equation 2.5.

$$C = \frac{A}{\kappa} + \frac{l}{\beta} \tag{2.5}$$

where A is the cross sectional area [m^2], κ is the substrate stiffness [$Pa \cdot m$], l is the channel length [m], and β is the adiabatic bulk modulus [Pa].

2.4.3 Modular system for building the channel network

The assumed linear behaviour of the system enables the connection of the building blocks in different configurations corresponding to the channel network.

Building blocks

Each element of the network is represented by a block with the corresponding RLC elements. A different block is required if any of the following is varied: channel dimensions, material or fluid physical properties. The resistance and inductance values are split in half on either side of the capacitor to maintain the symmetry of the response as shown in Figure 2.8. The symmetry in each element stems from the behaviour of the droplet that is symmetric for the travel direction within the channel. A droplet travelling towards or away from the pressure inlet of any channel should behave identically as per the assumptions previously stated. Analogously, the block response should be the same for current going from input to output or from output to input. A simpler asymmetric building block regroups the resistance and inductance on the left side of the capacitance.

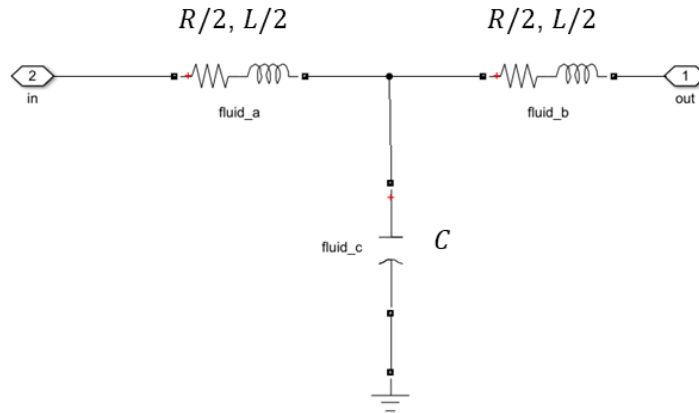


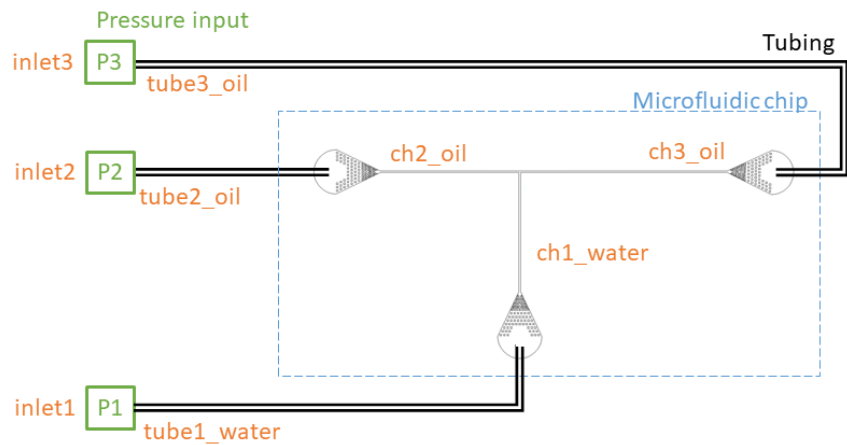
Figure 2.8: Building block of the electric circuit analogy with symmetric RLC components.

Assembly

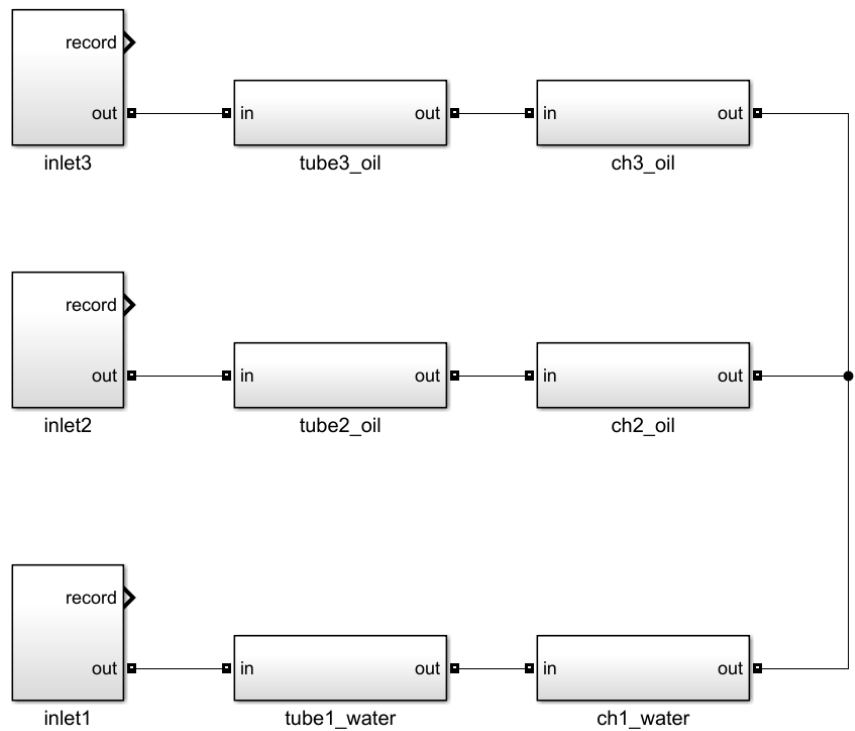
From the assumed linearity of the system, the tubes and channels are similarly connected in series and joined as they are in the physical system. For instance, a simple T junction chip with 3 channels and the corresponding 3 tubes and inlets is shown in Figure 2.9. The state-space model describing the system is obtained automatically through Matlab functions. Although the 3 pressure inputs to the system are designated as inlets, they effectively are a combination of sources and sinks depending on the flow direction in each channel to respect the conservation of mass principle.

2.5 Control system theory

The methods and techniques described in this section are provided as background information. David Wong implemented and reported on using these techniques; he used visual feedback and pressure actuation to form the closed-loop LQR-based controller WongThesis, wong2020robodrop.



(a) Schematic representation of the physical system.



(b) Simulink blocks connected according to the physical system channel configuration.

Figure 2.9: Simple T junction assembled building block with 3 channels, 3 tubes, and 3 inlets.

$$\begin{aligned}
\dot{x}_1 &= a_{11}x_1 + \dots + a_{1n}x_n + \\
&\quad b_{11}u_1 + \dots + b_{1m}u_m \\
&\quad \vdots \\
\dot{x}_n &= a_{n1}x_1 + \dots + a_{nn}x_n + \\
&\quad b_{n1}u_1 + \dots + b_{nm}u_m
\end{aligned}
\quad \rightarrow \quad
\begin{array}{c}
\overbrace{\begin{bmatrix} \dot{x}_1 \\ \vdots \\ \dot{x}_n \end{bmatrix}}^{\dot{X}} = \overbrace{\begin{bmatrix} a_{11} & \cdots & a_{1n} \\ \vdots & \ddots & \vdots \\ a_{n1} & \cdots & a_{nn} \end{bmatrix}}^A \overbrace{\begin{bmatrix} x_1 \\ \vdots \\ x_n \end{bmatrix}}^X + \overbrace{\begin{bmatrix} b_{11} & \cdots & b_{1m} \\ \vdots & \ddots & \vdots \\ b_{m1} & \cdots & b_{mm} \end{bmatrix}}^B \overbrace{\begin{bmatrix} u_1 \\ \vdots \\ u_n \end{bmatrix}}^U
\end{array}$$

$$\begin{aligned}
y_1 &= c_{11}x_1 + \dots + c_{1n}x_n \\
&\quad \vdots \\
y_p &= c_{p1}x_1 + \dots + c_{pn}x_n
\end{aligned}
\quad \rightarrow \quad
\begin{array}{c}
\overbrace{\begin{bmatrix} y_1 \\ \vdots \\ y_p \end{bmatrix}}^{\dot{Y}} = \overbrace{\begin{bmatrix} c_{11} & \cdots & c_{1n} \\ \vdots & \ddots & \vdots \\ c_{p1} & \cdots & c_{pn} \end{bmatrix}}^C \overbrace{\begin{bmatrix} x_1 \\ \vdots \\ x_n \end{bmatrix}}^X
\end{array} \quad (2.6)$$

where $\dot{X} \in \mathbb{R}^{n \times 1}$ is the derivative of the state vector, $X \in \mathbb{R}^{n \times 1}$ is the state vector, $U \in \mathbb{R}^{m \times 1}$ is the input vector, $Y \in \mathbb{R}^{p \times 1}$ is the output vector, and $A \in \mathbb{R}^{n \times n}$, $B \in \mathbb{R}^{n \times m}$, $C \in \mathbb{R}^{p \times n}$ characterises the system response. Notice that the initial conditions are not specified and assumed to be zero (or negligible) for all states $x_i(0) = 0$, $i = 1, \dots, n$.

2.5.1 Single-input-single-output (SISO) versus multi-input-multi-output (MIMO)

Feedback systems are generally classified into two categories: single-input-single-output (SISO) or multi-input-multi-output (MIMO) systems. The MIMO approach is not simply an arrangement of SISO systems in parallel; the complex nature of the multi-variable system is taken into account, including the interrelationship (or coupling) between the different parts [70]. The state-space representation is adequate for MIMO system representation and controller design. The structure is based on stacking into a matrix form the first-order ordinary differential equations (ODE) describing the system. Then, the states (x) are used to represent the status of the system while the A matrix describes the system's intrinsic behaviour, the B matrix relates the input to the states, and the C matrix encapsulates the relationship between the states and the outputs of the system. An overview is shown in Equation 2.6 for the system: $\dot{X} = A \cdot X + B \cdot U$; $Y = C \cdot X$.

2.5.2 State feedback

Control law and system response

State feedback commonly uses pole-placement to design the response of the closed-loop system; in other words, the gain K_S is selected such that the behaviour of the system with the control law $U = -K_S X$, where U is the control input and X is the state vector, is satisfactory. By replacing the control law in the system equations (Equation 2.6), the closed-loop system behaviour is characterised as per Equation 2.7.

$$\dot{X} = A \cdot X + B \cdot \overbrace{(-K_S X)}^U \rightarrow \dot{X} = (A - B \cdot K_S)X \quad (2.7)$$

The behaviour of the closed loop system represented by Equation 2.7 is characterized by the location of the poles (i.e. the roots of the characteristic equation) in the s-plane (horizontal axis: R, vertical axis: C). The poles ($s_i \in \mathbb{C}$) are the roots of the characteristic equation defined using the determinant as per Equation 2.8. The system response is stable only for poles with negative real parts ($Re(s_i) < 0 \forall i$). Note that the state feedback controller leads to the states eventually converging to zero (for stable closed-loop cases) as shown in Figure 2.10.

$$\det(sI - (A - BK_S)) = 0 \quad (2.8)$$

Controllability

The closed-loop system response is determined by the location of the poles as per Equation 2.8. Considering that the control gain K_S is arbitrarily selected, then the response of the system is tuned according to the desired performance. However, whether the poles can be placed arbitrarily on the s-plane relies on the controllability of the system. There are multiple equivalent ways of determining whether a linear time-invariant system (A, B) is controllable or not. The selected method is shown in Equation 2.9 where λ_i represents each eigenvalue of A.

$$\forall \lambda_i, i = 1, \dots, n : \text{rank}([\lambda_i I - A|B]) = n \quad (2.9)$$

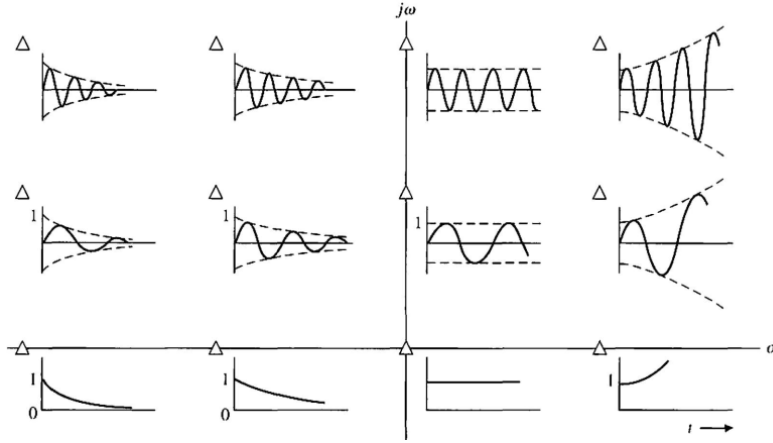


Figure 2.10: Homogeneous system response according to pole location (shown with triangles) in the s -plane [70]. The desirable pole location is in the negative real plane (i.e. left-hand side) for an exponential decay envelope.

Pole-placement and optimal pole-placement using LQR

Given that a system is controllable, the poles of the closed-loop system are arbitrarily placed in the s -plane according to the desired performance. This is done by equating the characteristic equation (Equation 2.8) to the desired characteristic equation built from the desired poles as the roots. Then, the values of the components of the state feedback gain are algebraically solved. Note that the number of poles to be placed corresponds to the order of the system (i.e. n).

The simple and widespread PID controller is not preferred for this system. Although a PID controller can achieve stable closed-loop control of droplets, the LQR approach is preferable. The system is inherently coupled from the pressure field across the different channels. Therefore, a MIMO approach enables the consideration of the impact of one channel on another channel. Moreover, as outlined below, the tuning of the controller parameters is more intuitive for LQR than for PID controllers.

For a large system, the number of poles to place is large; the relationship between each pole location and the performance of the system is not as intuitive as for smaller order systems. Consequently, the tuning of the control gains for the satisfactory performance of the closed-loop system is challenging. The optimal control technique Linear Quadratic Regulator (LQR) allows for tuning of the response using the weighting matrices Q and R [70]. The calculations are executed through the

Matlab `lqr` command; the details will only be outlined. The algorithm minimizes the performance index J given by Equation 2.10. The first part of the equation applies the weighting matrix Q to the states x thus penalizing the value of the states before they converge to zero. The second part associating the weighting matrix R with the inputs U penalizes the effort required to push the states to zero.

$$J = \int_0^{\infty} (x^T Q x + u^T R u) dt; Q \in \mathbb{R}^{n \times n}, R \in \mathbb{R}^{m \times m} \quad (2.10)$$

Note that because the algorithm objective is to minimize the performance index, the absolute value of the weighting matrix entries is not important; the relative magnitude between the entries is the key tuning parameter. The performance index is minimized for K_S according to Equation 2.11 for which P satisfies the so-called Riccati equation as per Equation 2.12.

$$K_S = R^{-1} B^T P \quad (2.11)$$

$$A^T P + P A - P B R^{-1} B^T P + Q = 0 \quad (2.12)$$

Integral state-feedback

The state-feedback controller previously described is used to maintain stability (even of some unstable systems) by driving all the states to zero. However, the tracking of a particular reference point is desirable in many situations. The addition of the integral term eliminates steady-state error for better tracking. The equations describing the system are augmented and the control design procedure is similarly applied to the new augmented system. The calculated gain through the LQR algorithm is then split between the different parts of the controller for implementation.

2.5.3 State observer

Governing equations

The state-feedback control approach described above requires the value of the states to calculate the control input. However, not all states of a system are generally available for measurement; only a subset is measured as per the output equations and the appropriate C matrix. Consequently, a state estimate vector \hat{x} is used in the control law instead. The estimation of the states is governed by the gain L in the first order ODEs shown in Equation 2.13.

$$\dot{\hat{x}} = A\hat{x} + Bu + L(y - C\hat{x}), L \in \mathbb{R}^{n \times p} \quad (2.13)$$

Observability

Similarly to the controllability property of the system previously described, the system must be observable for the state estimates to be reconstructed from the output. The test to determine whether a linear time-invariant system (A, C) is observable is given by Equation 2.14 where λ_i represents each eigenvalue of A .

$$\forall \lambda_i \ i = 1, \dots, n : \text{rank} \left(\begin{bmatrix} \lambda_i I - A \\ C \end{bmatrix} \right) = n \quad (2.14)$$

Observer pole-placement and behaviour

The duality of the controllable and observable properties of a system (not shown herein, see [280]) implies that for a controllable system (A^T, C^T) , the poles are arbitrarily placed using the gain L^T from Equation 2.13. Thus, the LQR algorithm can similarly be used to tune the response of the closed-loop system for the observer; the location of the poles will determine how fast the state estimates converge to the actual state value, or alternatively, how the error between state values and estimates converge to zero.

2.5.4 Principle of separation

The principle of separation guarantees that for a controllable (A, B) and observable (A, C) system, the poles of the state-feedback and observer are placed independently of each other. The matrix describing both the system behaviour (including feedback control), and the error between the actual value and estimate of the states are shown to be upper triangular. Therefore, the eigenvalues of the full matrix are the union of the eigenvalues of the submatrices on the diagonal. The first matrix eigenvalues are from the state-feedback design while the second matrix eigenvalues are from the observer design. The two sets of eigenvalues are designed independently using K_S and L respectively.

As a rule of thumb, the poles of the observer should be faster (> 5 -10 times) than the poles of the state-feedback to allow the estimates to converge to the actual value rapidly.

2.5.5 Kalman Filter

The Kalman Filter is used as a state observer taking into account the characteristics of the noise present in the system similarly to the state observer described in Section 2.5.3. The Kalman Filter in its simplest form is herein presented without the extensive theoretical framework that can be consulted as required [94, 54]. The typical assumption is made that all noise follows a white Gaussian distribution (i.e. $v \sim N(\mu = 0, \sigma^2 = R)$).

Disturbance estimation

An additional state is added to the discrete system to model a static offset disturbance. The state is also assumed to have white noise as shown in Equation 2.15.

$$d(k+1) = d(k) + w_k; \text{ where } w_k \sim N(0, R_w) \quad (2.15)$$

Noise characterization

The output noise (R_v) is characterized by the hardware while the system state noise (R_w) is used as a tuning knob. The resolution of the output, which is from the localization of the interface with ± 0.5 pixel precision, provides the uncertainties in the measurement at the hardware level. By assuming a constant probability across the ± 0.5 pixel interval where the true value lies, the output noise is characterized using the corresponding variance of $(\Delta px)^2/12$.

Algorithm overview

The discrete equations describing the Kalman filter implementations are shown in Table 2.3 starting with an initial arbitrary $P_{0|0}$ and calculating from state prediction to state estimation at each time step.

Table 2.3: Kalman Filter algorithm for disturbance estimation.

| | | |
|------------|---------------------------------------------------------------------------------------|---------------------------------------------------|
| Prediction | 1. State prediction | $\hat{x}_{k k-1} = A\hat{x}_{k-1 k-1} + Bu_{k-1}$ |
| | 2. Output prediction | $\hat{y}_{k k-1} = C\hat{x}_{k k-1}$ |
| | 3. Error | $e_k = y_k - \hat{y}_{k k-1}$ |
| | 4. State prediction error covariance | $P_{k k-1} = AP_{k-1 k-1}A^T + WR_wW^T$ |
| Estimation | 5. Kalman gain | $K_k = P_{k k-1}C^T(CP_{k k-1}C^T + R_v)^{-1}$ |
| | 6. State estimation covariance | $P_{k k} = (I - K_kC)P_{k k-1}$ |
| | 7. State estimation | $\hat{x}_{k k} = \hat{x}_{k k-1} + K_k e_k$ |
| | The estimated states $\hat{x}_{k k}$ will be $\hat{x}_{k-1 k-1}$ for the next sample. | |

Chapter 3

Methodology

The methodology chapter is separated into two main sections: microfluidics and control systems. The content of this chapter generally applies to all projects, and details pertaining to specific projects are described in the appropriate corresponding subsection in subsequent chapters.

3.1 Microfluidics

3.1.1 Chip fabrication

The chip fabrication follows a standard soft photolithography procedure [245]. The two main parts of the fabrication procedure are: the master and the polydimethylsiloxane (PDMS) chip.

The master is used to mould many instances of the same design. Heating the silicon wafer at 170°C for at least 10 minutes reduces moisture and promotes adherence of the SU8 on the surface. An initial ~ 5 nm layer of negative photoresist (SU-8 2005, MicroChem) is spin-coated on the silicon wafer to enhance the adherence of the second SU-8 layer. Exposure to UV light is used to cross-link the whole surface. The second layer of photoresist is spin-coated at the appropriate speed to obtain the desired layer thickness corresponding to the microchannel height (typically 50 μm using SU-8 2025, MicroChem). The photoresist is then selectively exposed using a photomask of the desired channel network design. Finally, the excess unexposed SU-8 is removed using a photo-developer.

The PDMS chip is fabricated by pouring a 10:1 mixture of the elastomer base and curing agent (Sylgard 184) onto the silicon wafer. The curing is performed at 95°C for 1 hour. After careful demolding of the PDMS from the silicon wafer, the channels are formed by bonding the mould to a PDMS coated glass chip using oxygen plasma. The chip must be heated for at least 24 hours at 150°C to retrieve its hydrophobic surface property. The overview of the procedure to fabricate PDMS chips from the silicon wafer master is shown in Figure 3.1.

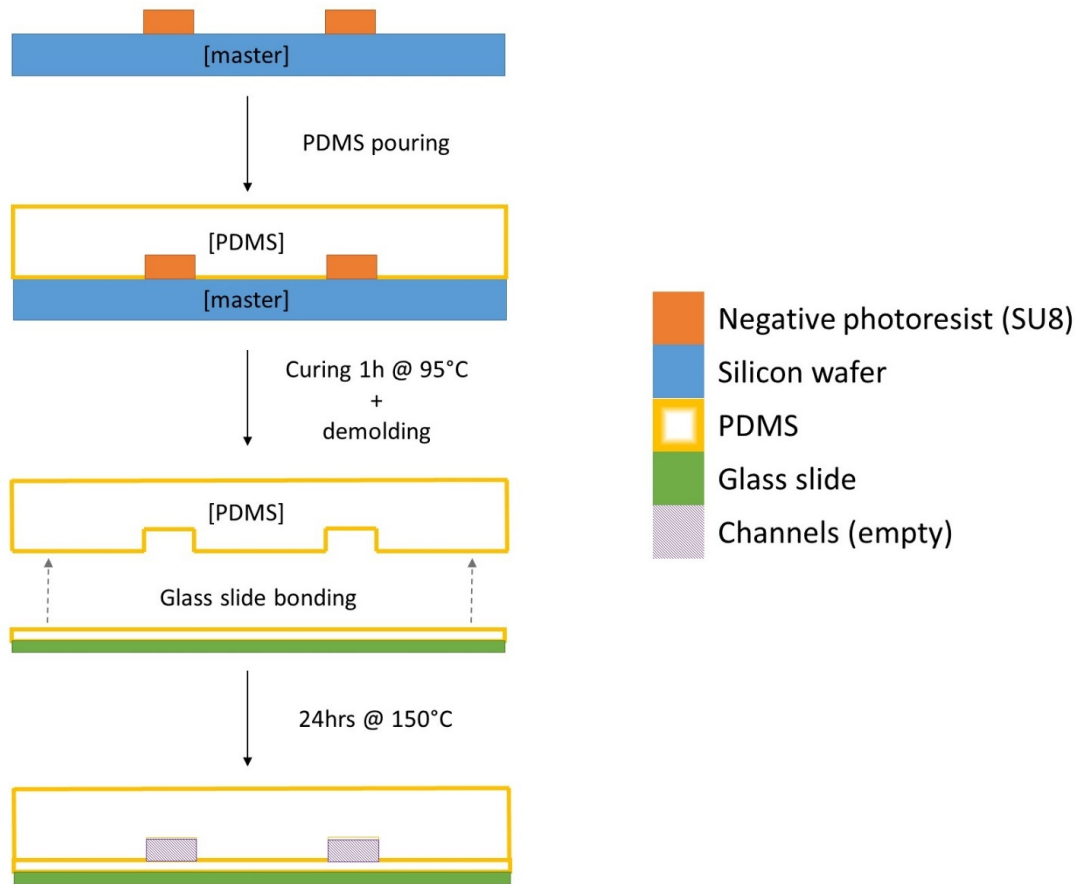


Figure 3.1: Soft lithography fabrication procedure for PDMS chips (cross-sectional view).

3.1.2 Active control platform setup

The active control platform is partitioned into 5 main subsystems: the pressure pump, the microfluidic chip, the microscope, the camera, and the computer. The schematic overview of the flow of information is shown in Figure 3.2.

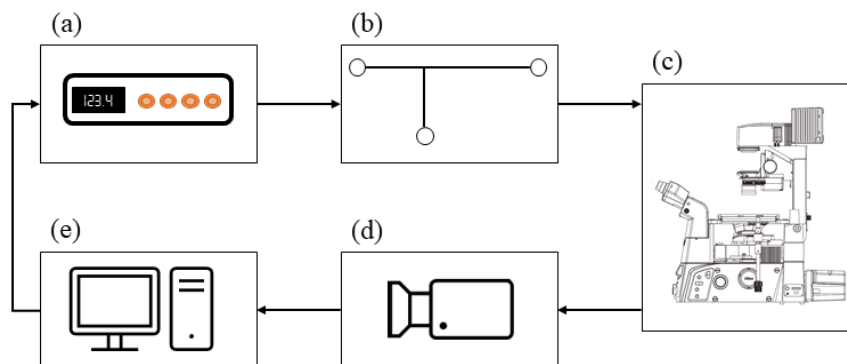


Figure 3.2: Schematic overview of the system with flow of information indicated by the arrow direction. (a) Pressure pump (Fluigent MFCS-EZ) (b) PDMS microfluidic chip (typical single T junction design) (c) Microscope (Nikon Eclipse Ti-E) with 4X objective (d) Camera (Andor Zyla 5.5 sCMOS) (e) Desktop computer.

Actuation – Pressure pump

Generally, the pressure pump used is the Fluigent MFCS-EZ pump [82, 149]. The 4 outlets provide independent pressures applied at the microchannel inlets through the reservoir holder and a connecting perfluoroalkoxy (PFA) tube. The reservoir holder interfacing between the pressurized air and the fluid contained in the vials enables fluids with different physical properties to be driven without calibration or adjustment of the pump. The schematic of the reservoir holder is shown in Figure 3.3. The response time is much faster than a syringe pump. Furthermore, using a pressure pump does not require complex chip manufacturing such as electrodes or multiple layers.

System – Chip with microchannel network

The fabrication procedure for the microfluidic chip using PDMS is described in Section 3.1.1. The soft-lithography fabrication of PDMS chips is well established, rela-

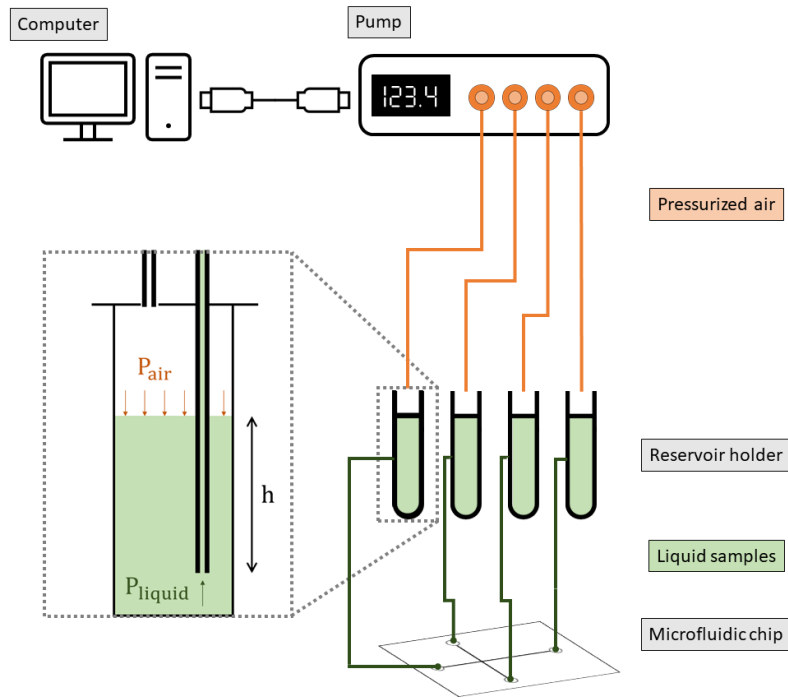


Figure 3.3: Schematic of the reservoir holder used to interface between the pressurized air and the fluid contained in the vials.

tively fast to prototype new designs, and a comparatively low-cost solution. These advantages are prioritized in a research setting when multiple iterations are required for the same design. However, the drawback is the tendency of the chip channels to get obstructed by PDMS debris and the unstable surface property over time.

The transparent property of PDMS and glass to visible light is essential to the imaging that provides the feedback for the controller.

Magnification – Inverted microscope

Considering the small scale of the microchannels used (usually, on the order of $\sim 100 \mu\text{m}$), a microscope is required for the imaging at the proper resolution. The Nikon Eclipse Ti-E inverted microscope is equipped with a 4X magnification objective [226]. The field of view must be stationary for image processing. Consequently, the im-

portant section of the channel network where the T junction(s) is located must be fully visible within the field of view. Higher magnification objectives provide better micron per pixel resolution at the expense of the field of view size.

Imaging – Camera

The microscope is equipped with a camera attached to a C-mount (Andor Zyla 5.5 sCMOS [7]). The field of view previously discussed is also a function of the sensor size that determines the area where light is sensed. The resolution (i.e. the number of pixels in one image) is limited by the sensor size; if pixels get too small, this leads to a problem with light diffraction. Consequently, the current camera setup is optimized for the microscope aperture size with respect to the camera sensor size. The data from the camera is transferred to the computer at a maximum rate of 40 frames per second through a USB 3.0 connection.

Processing – Desktop computer

The desktop computer provides the interface between the different subsystems as well as the computational power required by the controller and the Graphical User Interface (GUI). The custom system is developed in C++ on Windows 7 using the open-source libraries Qt for the GUI and OpenCV for image processing. The communication with the pressure pump and the camera is established using the software development kits (SDK) provided by Fluigent and Andor respectively.

3.1.3 Flow sensors

The flow sensors are not required for the operation of the active control platform. Nonetheless, measurements of the flow are useful for certain experiments.

Sensirion's flow sensors accurately measure small flows using heat transfer principles. A small heating element warms the fluid through the inner capillary wall. Further down the capillary, a temperature measurement is used to determine the flow.

Calibration

A variety of flow sensors from *Sensirion* are used; they are all aimed for microfluidic applications. Thus, the measurement of small flow rates from nL/min to $\mu\text{L}/\text{min}$ is

precise. However, the factory calibration for water is not accurate enough. Moreover, other fluids with other thermal properties are used. Hence, a calibration curve for each fluid must be determined. The overall procedure is outlined below, but a more detailed document is included in Appendix A.

The flow sensor allows us to record the raw data in bits; different sampling rates enable different bit resolution. The smallest resolution is desired to measure the constant flow rate; thus, a slow sample rate is selected. The syringe pump provides a flow rate based on the inner diameter of a glass syringe. However, inherent oscillations in the syringe pump output require numerous data points to average the uncertainties. Another important factor to reduce the oscillations is to ensure no air bubble is present within the syringe and the tubing when recording data. The flow must stabilize for 5 minutes before recording. Then, the raw flow sensor output in bits is recorded for 1 minute for each selected flow rate of the syringe pump. Moreover, three repetitions of all set points are collected: one in increasing order, one in decreasing order, and one randomly. Note that care must be taken when refilling the syringe to limit and to evacuate to the waste air bubbles before starting to record the data; the oscillations will be reduced. Sometimes, air bubbles stick to the piston of the syringe. Filling the syringe and firmly emptying it with the tip still submerged in the liquid will help evacuate the unwanted bubbles. Refilling the syringe should then be without any bubble.

Micro-channel height measurement

The nominal height of the channels on the master is determined based on the SU8 viscosity and the rotation speed of the spin coater. However, the swelling of the PDMS chip leads to significant changes in channel dimensions. Therefore, experimentally determining the channel height is required.

The resistance of a channel network is retrieved by applying constant pressure at one inlet and measuring the flow rate. The resistance is then the ratio of both measurements averaged over a few minutes, and for a rectangular cross-section, the expression is given as per Equation 3.1 [31]. For a network of channels, an equivalent resistance expression is built in combination with a numerical tool to find function zeroes, and solve implicitly for the channel height (h).

$$R_{hyd} = \frac{\Delta P}{Q} = \frac{12\mu L}{w \cdot h^3} \left[1 - 0.63(h/w) \right]^{-1} \quad (3.1)$$

where R_{hyd} is the hydraulic resistance [$Pa \cdot s/m^3$], ΔP is the pressure difference [Pa], Q is the flow rate [m^3/s], μ is the dynamic viscosity [$Pa \cdot s$], L is the channel length [m], h is the channel height [m] and w is the channel width [m].

The PDMS swelling is a dynamic process that requires time to achieve steady-state. Consequently, a chip priming period is required to ensure the dimensions stay the same during and after the channel height measurement. Moreover, the resistance of the system components—except the microfluidic chip—must be considered and compensated for from the global resistance. The first option is to use the nominal dimensions as per the manufacturer’s specifications and calculate the resistance of the tubing and flow sensor. Although this method is relatively accurate and sufficient in some cases, experimentally determining the resistance of the components is more accurate. Hence, the second option requires experimental measurements of the pressure and flow rate without a microfluidic chip. A simple solution to replace the microfluidic chip and use the same tubing is a #10-32 to #10-32 union with minimal dead volume in lieu of the chip.

3.2 Control system

3.2.1 Image processing

The feedback to the control system is provided through the location of the interface between the two phases. The identification is performed using the camera in bright field view; the glass slide and PDMS chip are transparent to visible light. After the initial setup fixing the background and identifying the channels, the field of view must remain static to properly identify the interface within the channels. Therefore, the workspace available to manipulate the droplets is limited to the field of view as dictated by the objective magnification and camera specifications. The image processing steps are outlined in Figure 3.4. The raw image is first acquired at each sampling period (step 1). The background is subtracted to remove the channel outline; a threshold is applied to identify the edges of the objects (step 2). The centre channel mask prepared during the setup phase is then applied to identify the interfaces within the channels (step 3). The markers are the output used by the controller. The droplets must be identified; in other words, that is determining whether two markers are connected by the dispersed phase. The floodfill function isolates the inside of the shapes (step 4). The edges and the internal are combined to create droplets (step 5). Finally, the full channel mask is applied to exclude any background noise, and obtain the full droplets (step 6).

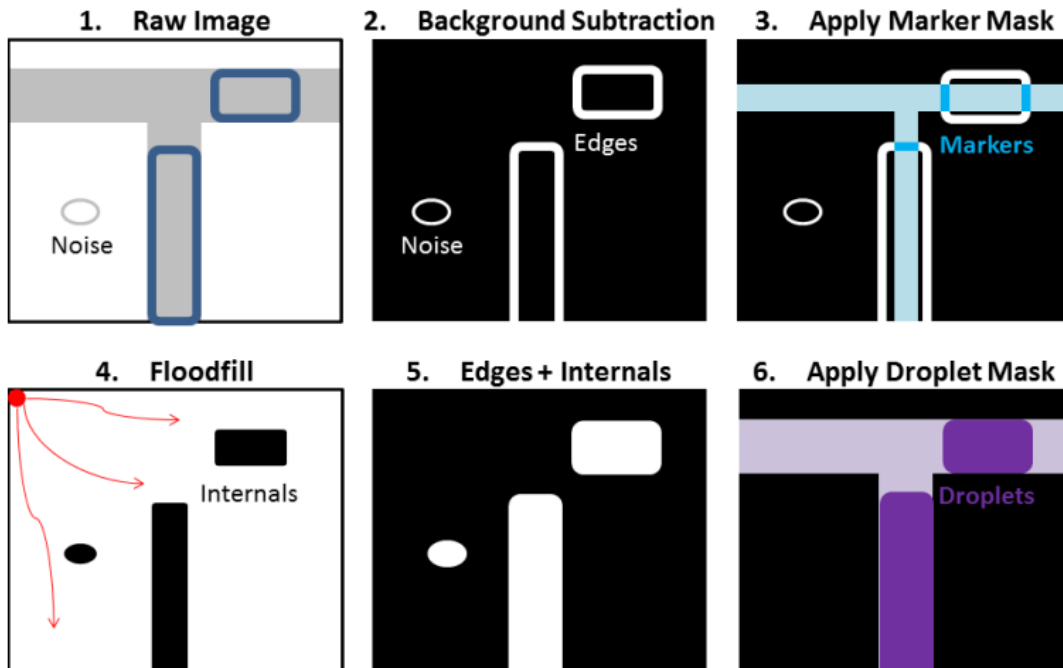


Figure 3.4: Image processing workflow overview. Reproduced with permission from Ref. [311].

3.2.2 C++ implementation

The implementation of the system is in C++ using Visual Studio. The open-libraries Qt and OpenCV are used for the graphical user interface (GUI) and image processing respectively. This allows us to operate the system independently of licensed software such as Matlab and Labview. The software development kits (SDK) are available for both the Fluigent pressure pump and the Andor camera to control via custom C++ code. The implementation of the controller using C++ is digital and consequently, takes into account the 100 ms sampling in converting the continuous-time equations to discrete-time.

3.2.3 Modelling modularity

The model of the channel network is used for controller design and simulations. The state-space model characterizing the physical system is built using modular blocks representing the tubing or the channels; the properties of each block is assigned

based on its dimensions, the materials, and the nominal properties of the dispersed or continuous phase as described in Section 2.4. The modularity allows different channel networks to be built quickly by using Simulink to retrieve the state-space (A, B, C) equations. The state-space representation and MIMO approach is used to capture the coupling between the channels through the pressure field.

3.2.4 Controller topology

The overall topology of the controller is shown in Figure 3.5 and the details of the different components are explained in the following subsections. This controller topology was initially designed and implemented by David Wong (a previous member of the research group) [308, 311, 307]. The corresponding control law to the controller topology is given in Equation 3.2.

$$u = -K_P z_P - K_I z_I - K_s \hat{x} \quad (3.2)$$

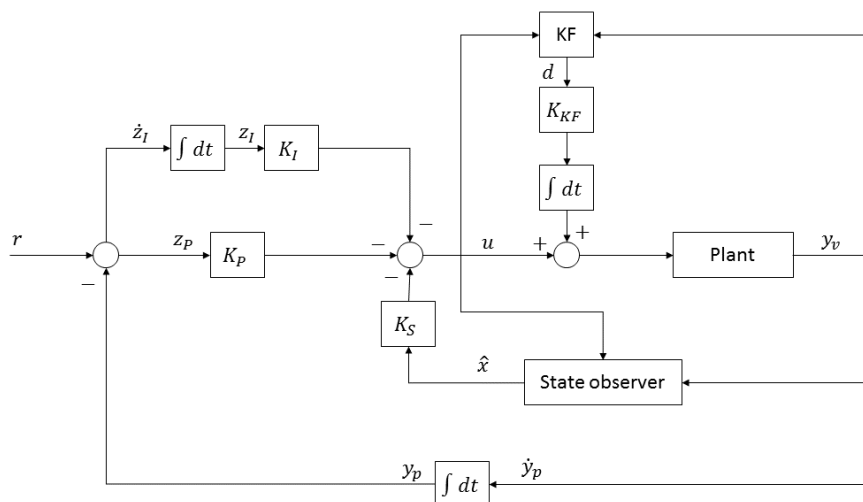


Figure 3.5: Controller topology overview with the integral state feedback (z), the state observer (\hat{x}), and the Kalman Filter (KF) for disturbance cancellation.

Integral state feedback

The state feedback (K_S) is used to drive the states to zero (e.g. the velocity of each channel) while the integral (K_I) and proportional (K_P) gains are used for tracking purposes with respect to the reference signal (r). Considering the size of the system with at least 14 poles (for the simple single T junction), the poles are located optimally using the Matlab Linear Quadratic Regulator (LQR) algorithm rather than manual pole placement.

State observer

The states of the system are composed of a combination of current (analogous to velocity) both in the tubes and in the channels, and of voltage (analogous to pressure). Most states are not measured by the system; the only output available is the position when an interface is present within a channel. Consequently, a state observer is necessary in order to estimate the states and implement the state feedback as per Equation 3.3.

$$\dot{\hat{x}} = A\hat{x} + Bu + L(y - C\hat{x}) \quad (3.3)$$

Kalman filter

The physical system is expected to include constant offsets due to the applied pressure from the pressure pump not being equal to the pressure at the PFA tube inlet, and because of the Laplace pressure across the water-oil interface. The Kalman Filter is used to estimate the disturbance, and then, accordingly modify the input to cancel it. Moreover, any uncertainties and noise present in the system are also compensated for. Hence, the performance of the system is improved, and robustness is increased.

Chapter 4

Semi-automated droplet control

The work included in this chapter is published: **M. Hébert**, M. Courtney, and C. L. Ren, Semi-automated on-demand control of individual droplets with a sample application to a drug screening assay, *Lab on a Chip*, 19 (2019), pp. 1490-1501 [111].

DOI: 10.1039/C9LC00128J

M. Courtney (Ph.D. candidate in the Waterloo Microfluidic Laboratory(WML) at the University of Waterloo) provided expertise for the drug screening assay. Their contribution is included assistance for the laboratory experiments, and editing of the pertinent sections of the manuscript.

M. Hébert designed and performed the experiments in addition to writing and editing the manuscript.

David Wong published work related to the technological advancement reported in this chapter. Wong designed and implemented the closed-loop LQR-based controller based on the circuit element analogy [308, 311, 307] (Section 4.3.1). My contribution from this chapter is the additional algorithm for the so-called semi-automated droplet manipulations (Section 4.3.2).

4.1 Overview

Automated control of individual droplets in microfluidic channels offers tremendous potential for applications requiring high accuracy and minimal user involvement. The

feasibility of active droplet control has been previously demonstrated with pressure-driven flow control and visual feedback, but the manual operation required to perform droplet manipulations limited the accuracy, repeatability, and throughput. The present study improves upon the aforementioned challenges with a higher-level algorithm capturing the dynamics of droplet motion for a semi-automated control system. With a simple T junction geometry, droplets can now be automatically and precisely controlled on-demand. Specifically, there is $\pm 10\%$ accuracy for droplet generation, $\pm 1.3\%$ monodispersity for 500 m long droplets and $\pm 4\%$ accuracy for splitting ratios. On-demand merging, mixing, and sorting are also demonstrated as well as the application of a drug screening assay related to neurodegenerative disorders. Overall, this system serves as a foundation for a fully automated system that does not require valves, embedded electrodes, or complex multi-layer fabrication.

4.2 Introduction

Droplet microfluidics has been envisioned as an enabling technology for quantitative analysis using monodispersed picoliter- to nanoliter-sized droplets as reaction vesicles; they can be generated by injecting one fluid (i.e. water) into another immiscible fluid (i.e. oil) within a network of microchannels. Applications range across various fields including biological assays [337, 23], material synthesis [265, 143], water quality assessment [176] and many more. The key advantages of using droplet microfluidics lie in the low reagent consumption, shorter reaction time, and isolation of individual reactions from each other.

From a mechanical engineering perspective, the different needs of various applications can be simplified to a series of droplet manipulations performed in a desired order using droplet microfluidics as a platform. The manipulations include but are not limited to: generating, splitting, merging, trapping, mixing, and sorting droplets. The approaches to performing them can be categorized into passive or active methods. Notwithstanding the method selected, the challenge hindering most applications pertains to the robust integration of the various functions on a unique platform.

4.2.1 Passive droplet manipulation

The extensive literature about passive droplet manipulations relies on the channel geometry and inherent physical properties of two-phase flow (e.g. interfacial tension) [336]. Manipulations such as generation [93], splitting [189] [113], merging [228],

trapping[15], and sorting [109] have been reported but with minimal integration of multiple functions sequentially on the same chip. Attempts at integrating multiple steps on a passive platform have been successfully achieved but incorporate only a limited number of functionalities [37, 125].

Although passive methods are widely used and studied, their robustness is challenged by manufacturing variations and defects, coupled dynamics, and operational uncertainties that require extensive experience in the microfluidic field to mitigate. Consequently, the passive microfluidic platforms are cumbersome to use for end-users in the biological or chemical engineering field for instance. Furthermore, the design of a microchannel network is application specific; thus, each change in the application (such as changes in droplet volumes or channel width) requires a revision of the design.

4.2.2 Active droplet manipulation

In contrast to passive methods, active methods allow more control over droplets. While some methods focus on tuning the size of droplets generated passively for instance [151, 35], other techniques allow gaining control over individual droplets, for example, generating them on-demand [234, 140]. Splitting has also been achieved through active methods such as those using magnetic force, but the platform deals with relatively large volume on the order of microliters [127], or using surface acoustic waves (SAW), which requires more difficult manufacturing techniques for electrodes; although, Park *et al.* successfully demonstrated a reusable SAW substrate [234]. The ability to actively manipulate individual droplets is appealing to many applications, especially single particle or single cell analysis [11]. More control enables on-demand encapsulation of single cell or particle into individual droplets, removal of wastes after reactions by splitting droplets, perfusion of droplets with fresh media for continuous reactions by merging droplets, and long reaction time by trapping and storing droplets at the desired location. Such control can be achieved through the implementation of feedback control.

Controllers using feedback have been implemented in the context of microfluidics before to regulate: the size of the droplet generated [212], [331], droplet sorting [201], hydrodynamic trapping [264], and particle steering [10] amongst other applications. Nevertheless, direct control of droplets is more sparingly studied. Electrowetting-on-dielectric (EWOD) allows dispensing, mixing, and splitting [78]. The limitations associated with this platform include: direct contact between droplets and air making them susceptible to evaporation; potential cross-contamination from path crossing;

relatively large droplet volume ill-suited for single-cell analysis due to the consequent low concentration; and limited applied voltage to prevent damage from the electric field to the biological compounds for certain applications [316].

Active control of individual reaction vesicles has also been achieved using Quake’s valves by controlling fluid flows in microchannel networks. This technique, however, requires more complex multilayer chip fabrication and bulky external equipment for the numerous solenoid valves [282]. Garstecki’s group also used solenoid valves to generate droplets on-demand; the size of the input reagents can be independently tuned [47], [46]. In their study, only one function (i.e. generation) is actively and precisely implemented while other functions such as merging rely on passive techniques. Improved control over multiple step processes such as dilution is achieved with high precision [241] as well as multiple manipulations [132]. However, the use of external valves is deemed more complicated and unnecessary with their fundamentally different approach. Hence, the approach with direct modulation of the inlet pressure (without additional hardware) is used.

4.2.3 Active control of individual droplet through pressure-driven flow using visual feedback

To ensure robust performance without compromising functionality, an ideal system should employ a simple channel network design and already-in-use hardware components to multiplex performance. Such a proof-of-concept platform has been demonstrated using a simple T junction to perform an unrestrictedly long sequence of manipulations by leveraging the transparent properties of the chip materials with the quick pressure pump response. By using visual feedback to identify droplet location, the pressure can be adjusted to manipulate the droplets according to the user input as implemented in real-time using the computer mouse [308]. This strategy does not require complex multilayers, surface properties or electrode implementation. The geometry can be tuned to accommodate the specifications of a particular application; the number of inlets providing the different reagents can also be adjusted. In addition, the overall platform and principle can be reused without going through the lengthy design process and optimization typical of passive microfluidics.

Nonetheless, the caveat to the greater control is the loss of precision, speed, and repeatability of manipulations due to the lack of human operational accuracy. This becomes more challenging to end users with limited microfluidics experience. In order to increase the robustness and speed of the series of manipulations carried out to enable such a platform for practical applications, a higher-level of control is required

so that users can set up their desired droplet manipulations via a graphic user interface (GUI) rather than manually moving a computer mouse. For example, users can set a specific droplet length to generate or a specific ratio the droplet should be split at by simply inputting these numbers in the GUI. The controller assisted with the camera visual feedback will take care of the rest. This automatic approach marks the beginning of the path leading to modular systems that can be widely adopted by end users.

The advancement from a manual movement of a computer mouse to such an automatic operation is very challenging. It requires: i) translation from intuitive human decisions to a sequential workflow that is executed by an algorithm implemented into the controller. For instance, an end user with minimal microfluidics experience can easily identify when two droplets have been successfully merged; however, translating this situation to a condition understood by the algorithm is not straightforward; and ii) the implementation of the logic must ensure a maximal robustness in order to minimize human interaction in case errors occur during the execution of the workflow. Considering merging of two droplets as an example, the workflow could stop operation when the identification of one droplet is momentarily unsuccessful due to image processing. This study aims to develop technologies to address these challenges towards the development of a fully automated platform that can be widely adopted for various applications and can be easily used without considerable microfluidics experience.

The end goal of a fully automated modular platform must be reached through stepping stones; the first one achieved was the manual control [308]; before the automated manipulations can be implemented, the semi-automatic procedure is an intermediate, yet large stepping stone. The functionalities developed with the semi-automatic manipulations will be at the core of the fully automated platform. In addition, the implementation of different semi-automatic manipulations is not trivial at all due to the complexity of translating the human thought process to a robust algorithm. Succeeding the semi-automatic platform, the automated platform will integrate multiple semi-automatic manipulations as well as further intermediate functionalities such as moving a droplet across different channels. But most importantly, the automated platform will need to deal with the feasibility of the procedure. Hence, the semi-automatic mode is critical as a stepping stone considering that the fundamentals of the automated mode must be firmly established before moving on to the procedure logic. Finally, the modulated platform will need another algorithm layer to synchronize the modular automated platform modules between each other and with respect to the desired sequence.

4.3 Working principle

4.3.1 Manual control: modelling and controller design

The semi-automatic controller is built upon the controller developed for manual operation with the novelty lying in the largely eliminated human interaction during the procedure, and thus, the largely improved accuracy, repeatability and speed. All details concerning the basic modelling of the channel network and the design of the controller can be found in the previous study [311]. Briefly, manipulation of individual droplets in a channel network under pneumatic control is a complex dynamic system requiring the understanding of the dynamic coupling effects between the droplets, carrier fluid and applied pressures. The coupling effects are influenced by the channel geometry, interfacial tension, fluid properties and applied pressures, and governed by the mass conservation and law of motion. To model such a dynamic system for manipulation of individual droplets is very challenging involving coupled first- or higher-order differential equations. An alternative approach to the complex fluid mechanics equations is to develop a state-space model method through an analogy between the fluid system and an electrical circuit where: pressure is analogous to potential and velocity to current. A state-space model is a convenient matrix representation of first-order differential equations describing a physical system (including the coupled relationships) that leverages linear algebra for controller design.

The state of the dynamical system is fully represented by the state variable vector that includes: channel and tubing current (velocity), voltage (pressure) at the interface between channels and tubing, and voltage (pressure) at the chip junction where all three channels meet. Each channel within the network has an associated resistance (Equation 4.1), inductance (Equation 4.2), and capacitance (Equation 4.3) corresponding to viscous, inertia and compliance effects respectively.

$$R = \frac{32\mu l}{d_h^2} \quad (4.1)$$

where μ is the dynamic viscosity [$kg/m \cdot s$], l is the channel length [m], and d_h is the hydraulic diameter [m]

$$L = \rho l \quad (4.2)$$

where ρ is density [kg/m^3] and l is channel length [m]

$$C = \frac{A}{\kappa} + \frac{l}{\beta} \quad (4.3)$$

where A is the cross sectional area [m^2], κ is the substrate stiffness [$Pa \cdot m$], l is the channel length [m], and β is the adiabatic bulk modulus [Pa].

The interaction and coupling between the channels can be modelled by assembling the different individual *RLC* channel elements into a network. The state-space model is obtained through *Simulink* analysis with the standard format $\dot{x} = Ax + Bu$, $y = Cx$ where A, B, C completely characterizes the channel network configuration but also its dimensions and fluids used.

From the state-space model, a Linear Quadratic Regulator (LQR) controller with integral state feedback, and Kalman filter disturbance estimation and cancellation is designed as per [311]. The LQR is used to stabilize the marginally stable system; the integral of the states allow for zero steady error; the Kalman filter cancels the offset due to the Laplace pressure and other disturbances.

The inputs to the controller are the pressure applied at each of the inlets while its outputs are the displacement within each channel. The output is compared to a reference value for which the error asymptotically reaches zero through the controller.

4.3.2 Semi-automatic droplet control

Fundamental functionality

The user can request droplet motion to the controller (e.g. adjusting the length of the droplet to be generated) by pulling the interface in so-called manual mode; however, precision, repeatability and speed vary between different manipulations of the same user, and from one user to the other. In this semi-automatic mode, the higher-level demands are inputted at the beginning through the GUI; leaving the rest to the algorithm and the controller.

The building blocks of the semi-automatic procedures are the measure, wait and move functions.

Measure The implementation of a relatively large feature with a nominal size of $500 \mu\text{m}$ next to all channel network designs allows users to scale pixels to actual lengths. Image processing yields markers that indicate the interface between the continuous (carrier fluid) and dispersed (drop) phase. The distance between markers or from a marker to a junction can be measured using the calibration with the scaling factor.

The accuracy of such measurements depends on the resolution of the camera, the magnification of the microscope objective, and the calibration obtained from the 500 μm feature. The typical resolution for the experiments carried with the 4X objective is $3.302 \pm 0.007 \mu\text{m}/\text{pixel}$ (95%).

Wait The wait procedure is first initialized by resetting all internal variables, and setting the desired time delay as requested by the user input. Then, once the timer is started, the elapsed time is periodically compared to the desired delay. As long as the timer is smaller than the delay, the change in reference for the specified channel is set to 0, meaning that the droplet remains at the same position. Once the timer exceeds the delay, the procedure can move on to the next step or standby for further manipulations.

The comparison of the timer occurs at each loop of the software. The rate is dictated by the hardware and response time. The current system samples at 10 Hz and consequently, the accuracy is limited to ± 0.1 s.

Move Moving can be achieved either relative to the current position or to an absolute distance from the junction. The difference in implementation is only in setting the target position as the first step of the manoeuvre. Then, a proportional controller is applied and is characterized by a gain (K_{gain}) and tolerance (ϵ). The gain represents the speed of moving the interface and the tolerance describes the acceptable difference between the objective ($y_{objective}$) and current position ($y_{current}$). The reference for the specified channel is then changed (dr) until meeting the tolerance (ϵ). Note that the tolerance should be larger than the precision provided per pixel. A more complex controller is not implemented here considering that the change in reference is handled by a LQR controller with integral state feedback that already eliminates steady state error for tracking purposes.

$$dr = K_{gain}(y_{objective} - y_{current}) \quad (4.4)$$

The accuracy achieved is related to the calibration of micron per pixel that sets the lower limit. Nonetheless, due to the dynamic changes of the system and the limited actuating (i.e. pressure) power available, the achieved accuracy is generally larger than the calibration value.

Software implementation

The details of the logic behind the software implementation are included in ESI 1 (Section 4.8) for the generation, merging and splitting of droplets with brief descriptions of every step.

The logic of the semi-automatic controller mimics the steps a user would perform in manual mode. Every step is performed as per the flowchart, for instance, for merging two droplets as shown in Figure 4.1. Each block type is defined in the legend as: user input, condition, semi-automatic control or data. The nomenclature concerning the chip itself is defined in the top right corner of the figure. The channels are arbitrarily separated at the junction. The interface between the water and oil phase is indicated for both the source channel (one interface) and a droplet (two interfaces, one at each end). The position of the interface can be defined from the junction point as the current position y . The image processing identifies the interface from the contrast between the two phases.

4.4 Experimental setup and methods

4.4.1 Materials and chip fabrication

The continuous phase used throughout all experiment is silicone oil with a viscosity of 50cst while ultrapure water is used as the dispersed phase unless otherwise indicated. If other fluids are required such as water-glycerol mixtures and oils of different viscosity, the changes in physical properties are reflected in the controller design (*Feedback Controls in Droplet Microfluidics* [311]) through the RLC parameters as per Equations 4.1 to 4.3. Note that no surfactant is used for any of the experiments as the focus of this study is to develop a semi-automatic platform. Adding surfactants would change the interfacial tension which could be considered in the controller later.

The master of the microchannel network design is manufactured using a silicone wafer for its low surface roughness properties. SU8-2025 (MICROCHEM) is spin coated in order to obtain a thickness of 50 μm after which it is exposed to UV light through the photomask. Then, the unexposed region is developed using SU8 developer. The chip is fabricated using polydimethylsiloxane (PDMS) and a standard soft-lithography procedure [245].

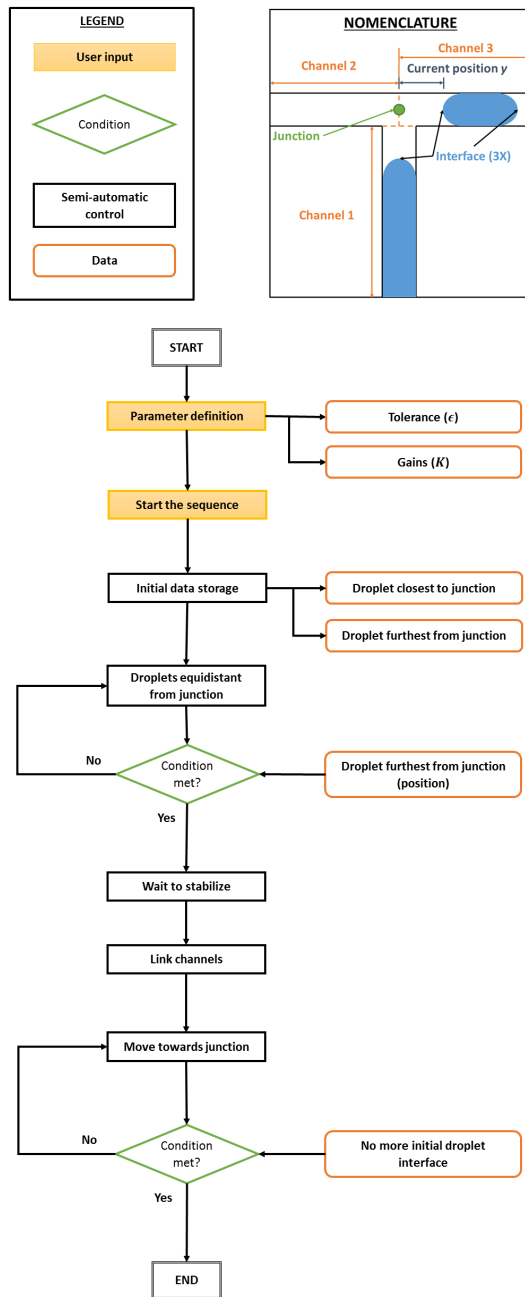


Figure 4.1: Flowchart representation of software logic for merging two droplets.

4.4.2 System overview

The microfluidic chip manufactured as per section 4.4.1 is central to the system that is composed of four other components: camera, microscope, computer, and pressure pump shown in Figure 4.2. The arrows represent the flow of information. The time required to complete the loop is of crucial importance to the system stability. The current setup allows sampling at 10 Hz which is mainly limited by the pressure pump.

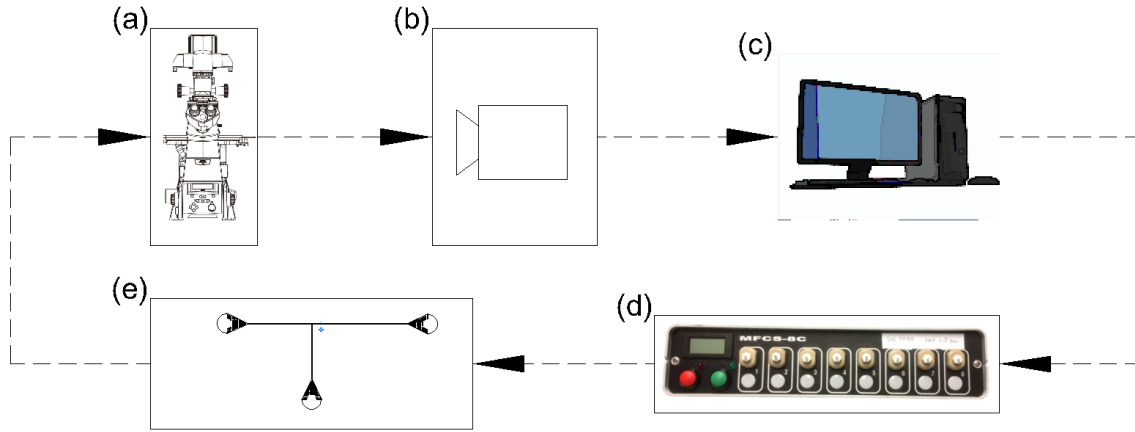


Figure 4.2: System overview for active control of droplet in microchannels through pressure-driven flow. (a) Nikon Inverted Microscope ECLIPSE Ti-E, (b) Andor Zyla 5.5 sCMOS camera, (c) personal computer, (d) Fluigent MFCS-8c pressure pump, (e) microfluidic chip.

Visual feedback is provided by the camera and microscope, and is used to image the chip in real-time. Note that for this system, the field of view must be stationary and cannot be modified. Consequently, the microscope objective magnification is a trade-off between the size of the field of view and resolution (micron per pixel); the magnification used is 4X. The image is relayed to the computer through USB 3.0 communication and analyzed using image processing to extract the location of the two-phase interface. Then, the controller calculates the necessary actuation based on the current and desired positions. Finally, the pressure pump is instructed to apply the various pressure independently to each inlet of the chip.

4.5 Result and discussion

4.5.1 Automated on-demand individual manipulations

Each manipulation can be executed in an arbitrary order according to the desired application. Furthermore, if the results such as droplet length or splitting ratio are deemed unsatisfactory, the procedure can be repeated. The high versatility and multiplexing are key characteristics of this technique.

Generation

Generating a droplet on-demand can be achieved through four main stages: filling the source channel, droplet adjustment in the destination channel, sectioning at the desired length with respect to the T junction, and stabilization. The performance achieved is $\pm 10\%$ on the resulting droplet length for the requested droplet length ranging from 150 - 750 μm as shown in Figure 4.3. The accuracy improves to $\pm 5\%$ for longer requested droplet length because of the relatively smaller errors and the more stable junction region. The uncertainties are related to the resolution (micrometres per pixel) and the dynamic pressure variations (See Section 4.5.2 for more details). A smaller channel width of 50 μm as compared to 100 μm allows more robust generation of smaller droplets in the squeezing regime.

Furthermore, the monodispersity of the generated droplets is assessed through the standard deviation of a sample size of 43 for which a droplet length of 500 μm was requested in a 50 μm wide channel (see Table 4.1). The resulting monodispersity of the generated droplets (i.e. standard deviation divided by mean: σ/\bar{x}) is 1.3%. Comparatively, monodispersity of droplets generated passively at a T junction has been reported as 2% [314]. The sequence of steps to generate a droplet is shown in Figure 4.4 as well as in ESI.S3[†].

Splitting

The ratio at which a droplet is split into two daughter droplets can be selected with an accuracy of $\pm 4\%$. The droplet must first be manually positioned overlapping the two side channels across a T junction. Then, the distance from one end of the droplet to the junction is adjusted automatically before sectioning and stabilizing the two daughter droplets. The limitation of the smallest splitting ratio depends on

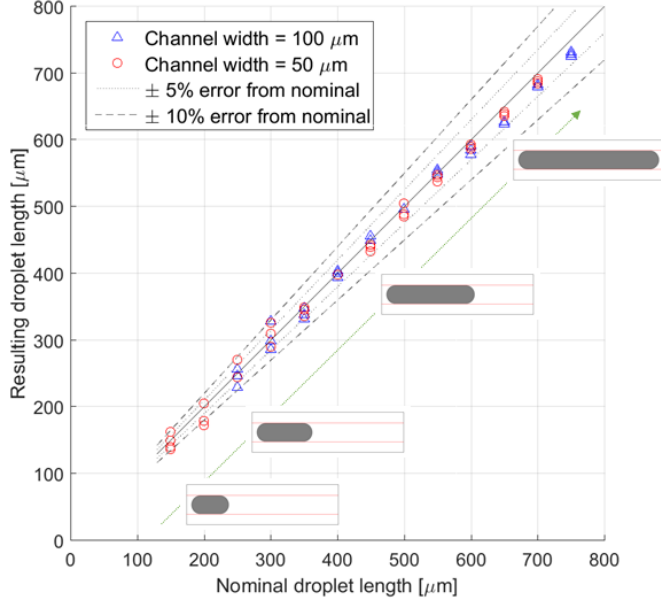


Figure 4.3: On-demand droplet generation distribution using semi-automatic control.

Table 4.1: Statistical analysis for droplet generation performance.

| Description | Value |
|-------------------------------------------------|--------------|
| Requested length [μm] | 500 |
| Sample mean \bar{x} [μm] | 490 |
| Sample standard deviation σ [μm] | 6.5 |
| Sample size | 43 |
| Monodispersity (σ/μ) | 1.3 % |

the channel width (w); a droplet of less than $\sim 1.5w$ cannot be requested in order to stay within the squeezing regime as shown in Figure 4.5.

The control over individual droplet movement allows one of the daughter droplets from a first split to be moved to a section with a smaller channel width in order to split a second time. Hence, higher precision can be achieved if, for instance, the original droplet would be too large to fit within the field of view at the smaller width due to its consequent increased length. The control over the splitting procedure is foreseen to have potential in applications requiring a wash operation. The sequence of steps to successively split a droplet is shown in Figure 4.6 as well as in ESI.S4[†].

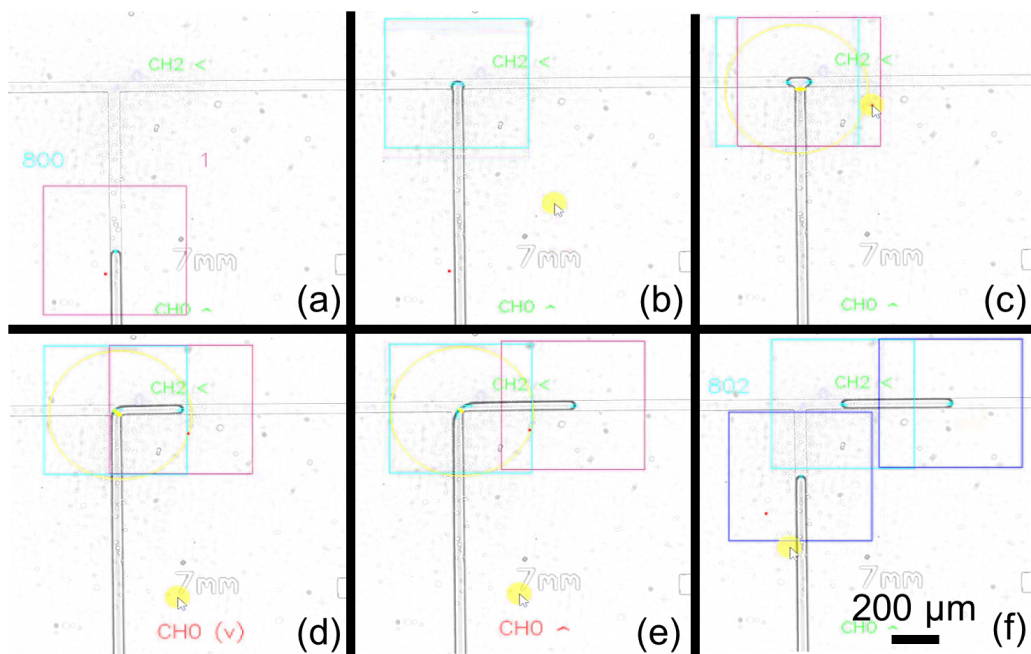


Figure 4.4: Droplet generation process (a) Source channel setup completed and ready to generate droplet (b) Filling of the source channel and overflow in other channels at the T junction (c) Manual selection of the new marker in the destination channel (d) Adjustment of the droplet length with respect to the junction (e) Droplet sectioning (f) Final stage with both interfaces stabilized.

Merging

Merging of two droplets can be achieved by ensuring that the droplets, especially those of uneven length, reach the T junction simultaneously and with enough momentum to break their interface. The sequence of steps to merge two droplets is shown in Figure 4.7 as well as in ESI.S5[†].

Mixing

When two droplets containing different content are merged, mixing can be enhanced through active motion. Mixing in the droplet microfluidic context is challenging due to the inherent laminar nature of the flow. However, the T junction allows motion perpendicular to the two main vortices flowing symmetrically along the channel axis in a droplet. Hence, cross-flow is induced and significantly enhances mixing.

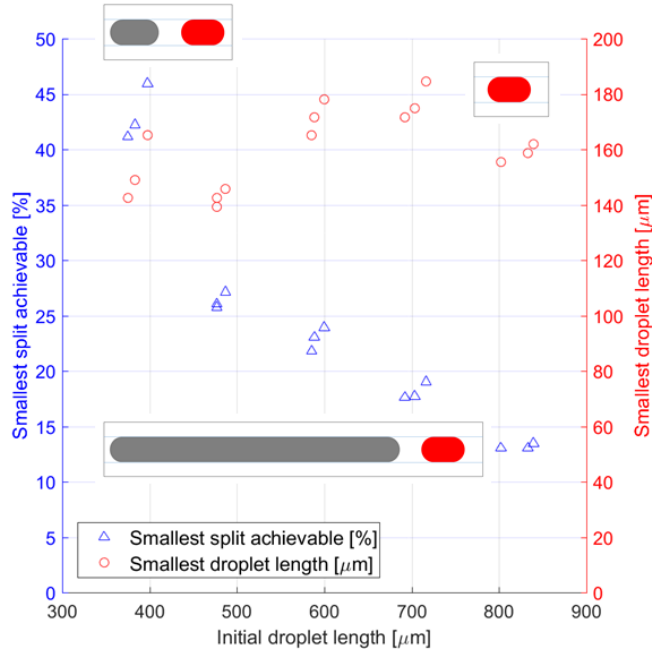


Figure 4.5: On-demand droplet splitting distribution using semi-automatic control.

Mixing is quantified using the mixing index as defined by Danckwerts [61] where $\langle \rangle$ denotes an average over all pixel values within the droplet boundary.

$$MI = 1 - \frac{\langle (N - \langle N \rangle)^2 \rangle}{\langle N \rangle (N_{max} - \langle N \rangle)} \quad (4.5)$$

In Figure 4.8, a mixing index threshold of 0.85 is deemed satisfactory. Moreover, the mixing index before merging considers the pixel values of both the water and dye droplets and is initially low. Hence, the large increase of the mixing index shows the successful mixing through active control of the droplet. The active mixing is completed under 30 seconds. The manipulations could be improved and performed faster through higher actuation gains (although at the expense of stability) and automated steps.

The sequence of steps to mix two droplets is shown in Figure 4.9 as well as in ESI.S6[†]. Note that Figure 4.9 uses methylene blue dye to show the contrast between the two droplets while 100 μ M Thioflavine S fluorescent dye was used to gather the data for mixing index calculations during separate experiments.

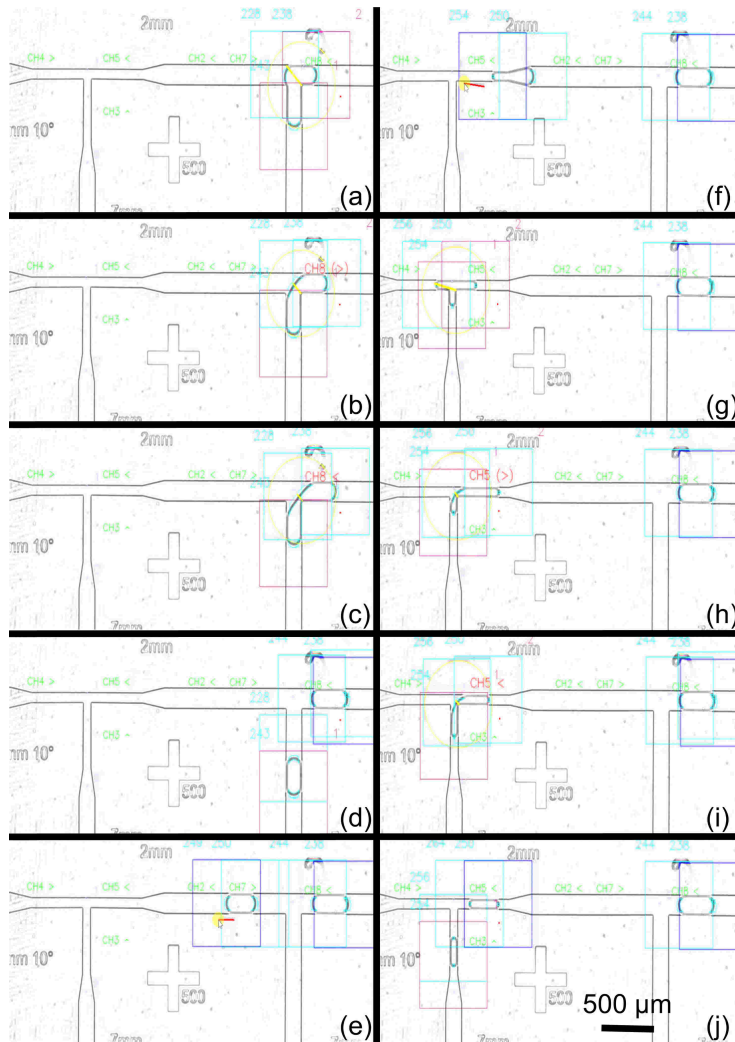


Figure 4.6: Successive droplet splitting process (a) Setup of the initial droplet (b) Adjusting the distance of markers with respect to the junction and the desired split ratio (c) Sectioning the droplet (d) First split completed for the $150 \mu\text{m}$ channel width (e) Sorting of the desired droplet to be split again (f) Transition to the $75 \mu\text{m}$ channel width region (g) Manual setup of the droplet (h) Adjusting the distance with respect to the second junction (i) Sectioning the daughter droplet (j) Final product of the double splitting with greater precision.

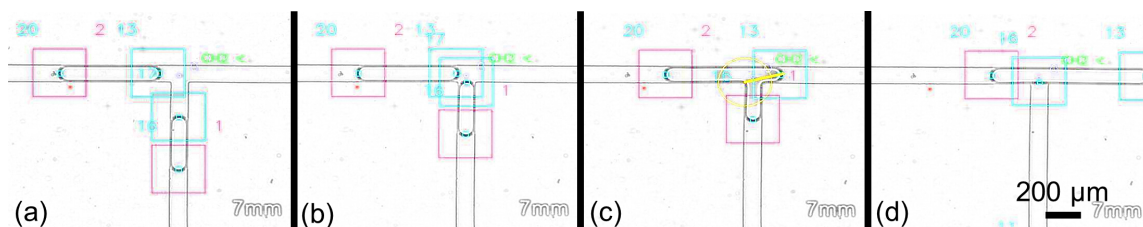


Figure 4.7: Droplet merging process (a) Initial manual setup of the two droplets on either side of the T junction (b) Both droplets reach the T junction simultaneously (c) The interface breaks and the two droplets merge (d) Merging is complete.

Sorting

Sorting can be implemented by discarding the undesirable droplet. When performing manipulations on a droplet, an unwanted daughter droplet of a split, for instance, can be moved in a continuous phase channel and discarded while the droplet of interest is retained and can be further processed.

The sorting capability is shown during the double splitting procedure in Figure 4.6; after the first split, one of the two daughter droplets is selected as desired for the second split procedure while the other is discarded hence effectively sorting the droplets.

The ability to arbitrarily select desired droplets is of particular interests for example following the result of an assay. Depending on the result, the droplet can be further processed or discarded. Furthermore, the combination with the immobilization capabilities is promising for applications requiring incubation.

4.5.2 Limitations and uncertainties

Generation and splitting precision

The limitations in terms of performance are determined by the width of the channel. Smaller channel width permits the generation and splitting into shorter length droplets.

The accuracy of generating and splitting droplets is established as $\pm 10\%$ and $\pm 4\%$ respectively; one of the limiting factors is the resolution of microns per pixel determined by the camera specifications. However, the main source of uncertainties

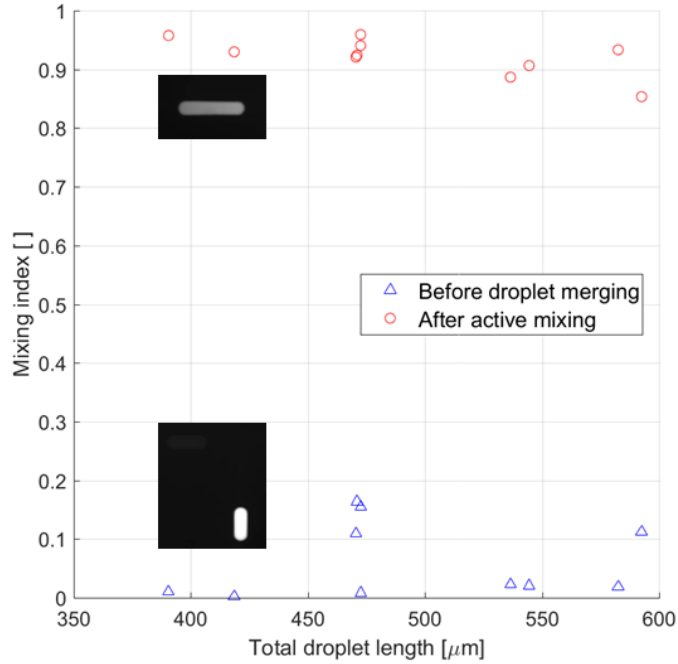


Figure 4.8: On-demand droplet mixing index according to resulting droplet total length.

is from the dynamic pressure changes. The main sources of short-term pressure oscillations are: the response of the pressure pump, PDMS compliance, and the sampling period. The most effective mitigation would be to improve the pressure actuation rate (currently, 10 Hz) because, within these 100 ms intervals, the pressure cannot be changed. Hence, the sampling rate represents a hard limit on the reduction of the short-term oscillations. Considering the current system, the two most significant delays limiting the sampling rate are the pump communication and image processing.

Throughput

One important drawback of this technique is the limited throughput that is traded off for the increased control on droplet manipulations. The currently limited sampling of 10 Hz for the hardware is a hard limit on the throughput. Furthermore, the manual manipulations currently required between the semi-automatic manipulations result in a throughput that cannot be pertinently calculated in Hertz. Nonetheless, the potential to fully automate the sequence of manipulations is foreseen to significantly improve the throughput compared to the semi-automatic mode.

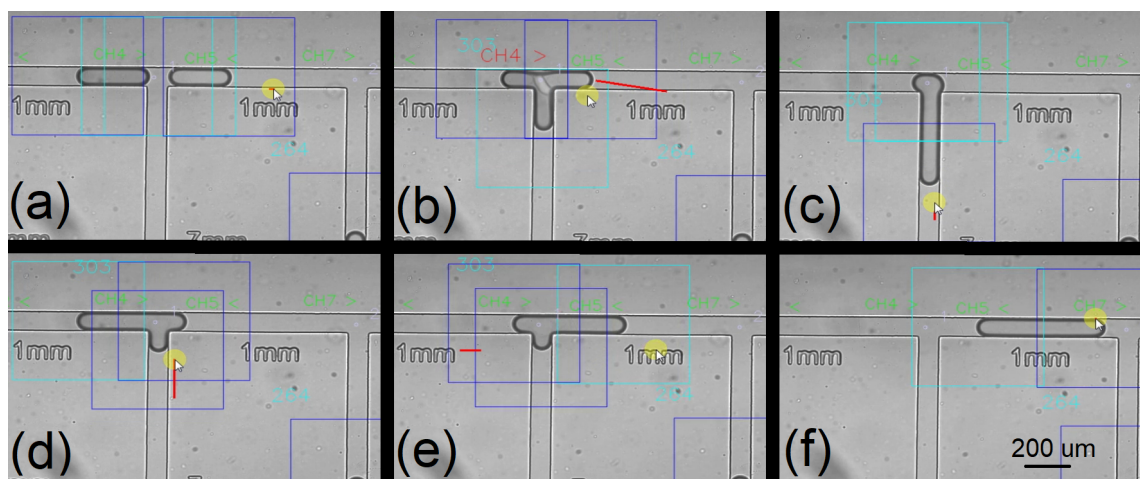


Figure 4.9: Droplet mixing process (a) Initial manual setup of the two droplets on either side of the T junction (b) Merging of the two droplets (c) Initial position after merging before mixing manipulations (d) Mixing on one side of the T junction with part of the droplet in each of the three channel (e) Transition to the destination channel with once again a part of the droplet in the third channel to break the symmetry of flow within the droplet (f) Final droplet fully mixed.

4.6 Application to a drug screening assay

4.6.1 Context and motivation

Neurodegenerative disorders (e.g. Alzheimer’s disease, Parkinson’s disease) can be related to tau-protein aggregation [215]. The assay used herein aims to quantify the efficacy of an inhibitor (Orange G) in the presence of a peptide (Ac-VQIVYK-NH₂ (AcPHF6)), which is derived from a full-length tau protein. To quantify the aggregation, a fluorescent indicator dye (Thioflavine T (ThT)) is used [267]. The aggregation is triggered by the PBS buffer upon merging of the droplets: droplet A contains the peptide dissolved in ultrapure water while droplet B contains the fluorescent indicator with the inhibitor dissolved in buffer. The excitation and emission peaks of the fluorescent dye (ThT) shift upon physically binding the tau-aggregate, and therefore it can be used to track aggregation over time.

Microfluidics approaches to drug screening [51] have two main advantages over traditional 96-well plate assays [123]: reduced reaction time from the smaller length scales, and also, a lower cost associated with the reduced consumption of the expen-

sive reagents.

4.6.2 Methodology

The following chemicals were obtained from *Sigma-Aldrich*: Orange G (for NA electrophoresis), Thioflavine T, solid Phosphate-buffered saline (PBS), and dimethyl sulfoxide (DMSO). The AcPHF6 peptide was acquired from *Celtek Peptides*. The DMSO was used to help dissolve the Orange G in the PBS buffer solution.

The microscope camera is used to record the fluorescent images (16-bit depth) and the data is extracted using post-image processing. The camera (Andor Zyla 5.5 sCMOS) is set to an exposure time of 2 seconds. The excitation wavelength is 440 nm while the emission wavelength is 490 nm using a fluorescence filter (CFP-HQ) with the inverted microscope (Nikon Ti-E).

While the fluorescent data is recorded for a period of more than 6 min (every 2 seconds) after merging of droplet A and B, the controller must be turned off because it is only operational for bright field view. Although the droplets mainly remain stationary, there can be slight movement along the channel. In order to track the droplet motion, a correlation along the channel is used with a mask of the droplet shape. Assuming that the background is dark (pixel value near 0), the fluorescence from the droplet will be taken into account in order to locate the droplet. After the mask is applied at the proper position, the average of all pixels value is simply taken. Further details are included in ESI 2 (Section 4.9.1).

Whether the dye self-aggregates or not is verified by taking a fluorescent image of the droplets and confirming that there is no significant fluorescent intensity compared to the background before merging.

The concentration of each compound after droplet merging is presented in Table 4.2. The two droplets merged are, nominally, of equal length beforehand. Consequently, the solutions prepared are twice (i.e. $32\mu\text{M}$) the concentration indicated in the table (i.e. $16\mu\text{M}$ after merging).

Three trials were performed for each droplet composition. The first and second data set are collected from the same chip, on the same day for repeatability purposes. The third data set is from a different chip on a different day for reproducibility purposes. Figure 4.10 shows the average pixel intensity of the three data sets with the corresponding standard deviation.

The ThT fluorescent indicator photobleaches due to its photosensitivity. Consequently, the initial intensity of the merged droplet decreases over time. In order

Table 4.2: Final concentration after droplet merging for each compound.

| Experiment | Positive control | Orange G | Negative control |
|---------------------|------------------|----------|------------------|
| AcPHF6 [mg/ml] | 0.06 | 0.06 | — |
| ThT [μ M] | 3.0 | 3.0 | 3.0 |
| Orange G [μ M] | — | 16.0 | — |
| PBS buffer [mM] | 16.0 | 16.0 | 16.0 |
| DMSO (% v/v) | < 1 % | < 1 % | < 1 % |

to compare the data between different trials, the intensity is offset from the initial value to only analyze the difference (or increase) in fluorescent intensity. A negative control is also used to help confirm that the dye does not self-aggregate or increase with intensity over time.

4.6.3 Results and discussion

The results for the positive and negative experiments are presented in Figure 4.10 along with the results using the aggregation inhibitor Orange G. Figure 4.11 shows the images of the fluorescent intensity at several time steps for all three cases.

If the dye self-aggregates, there will be a fluorescent signal unrelated to the protein aggregation. Therefore, it is important to verify. The negative control confirms that this is not the case, as there is no significant increase in intensity. Furthermore to the negative control, the images (both bright field and fluorescent view) captured before the droplets merging are used to confirm that the dye is not emitting a fluorescent signal before the aggregation is triggered for all cases.

The positive control does not involve the Orange G chemical. The peptide (AcPHF6) aggregation is triggered by the PBS buffer upon merging. The fluorescent dye (ThT) is used to track the reaction as the intensity increases over time. Eventually, a plateau is reached and sets the intensity baseline that is compared to the experiments involving the aggregation inhibitor (Orange G). For those experiments, the 32 μ M Orange G solution is added to the droplet containing buffer and fluorescent dye. Orange G reduces aggregation which can clearly be seen with the lower fluorescent plateau in Figures 4.10 and 4.11.

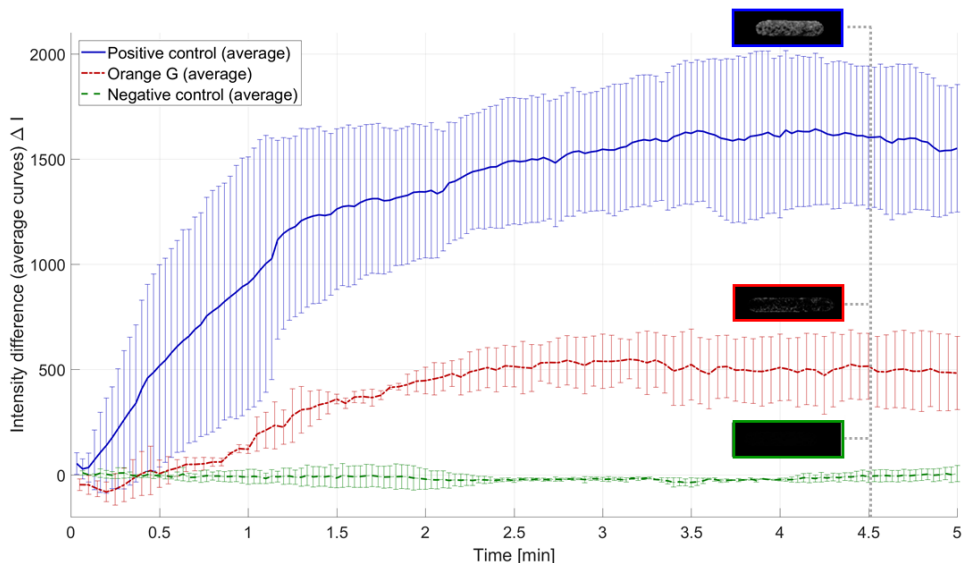


Figure 4.10: Fluorescent intensity change of Thioflavine T corresponding to the aggregation of AcPHF6 over time with and without the Orange G inhibitor. Error bars show standard deviation for 3 sets of experiments. Qualitative assessment showing the reduced fluorescent aggregation from the inhibitor.

4.6.4 Challenges and further direction

As previously mentioned, neurodegenerative disorders are linked to protein aggregation. While the fluorescent dye allows the aggregation to be tracked, analyzing how the aggregation is impacted by the addition of other chemicals is useful to develop drugs. The platform is applied to this particular assay as a proof of concept rather than a thorough study of the influence of Orange G on AcPHF6 protein aggregation. Certain challenges were encountered and are addressed in this subsection.

As noted for certain figures, the intensity of the screenshots is uniformly artificially increased for better readability while retaining the same trend. The overall weak fluorescent signal is attributed to photobleaching of the Thioflavine T dye. The illumination of the dye occurs during the setup (after the filled tubes are connected) as well as on-chip from the microscope light. Considering the slow flow rates (even often immobilized solutions), the photobleaching effects are significant and should be mitigated to study the protein aggregation more thoroughly.

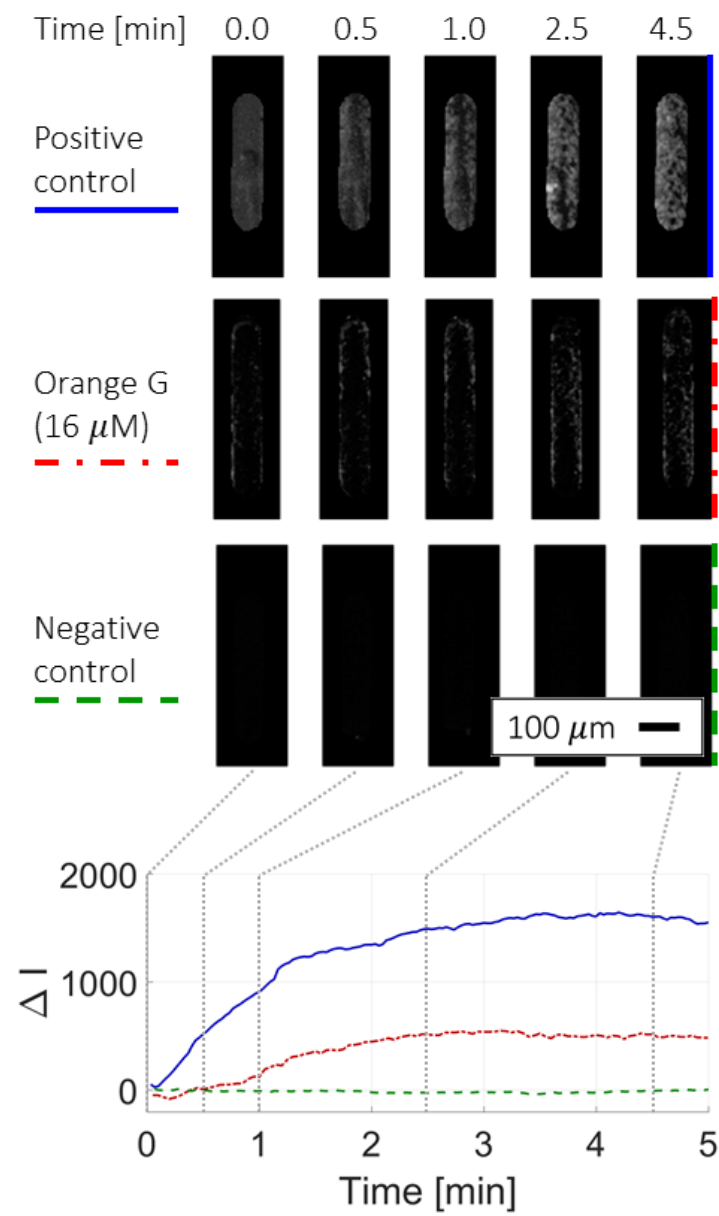


Figure 4.11: Artificially brighter screenshots of fluorescent intensity change of Thioflavine T corresponding to the aggregation of AcPHF6 over time with and without the Orange G inhibitor. Original image comparison shown in ESI 2 (Section 4.9.2).

Another main challenge is that the surface properties of PDMS chips degrade over time, limiting the amount of data that can be collected per chip. Moreover, PDMS is porous and will absorb the dye, leading to an overall increase in background intensity over time.

The chemical solutions used are temperature sensitive; warmer temperatures promote self-aggregation. The peptides can self-aggregate (without the PBS buffer) that is highly undesirable. Although the dye self-aggregation is controlled for by the screenshots before merging and the negative control, this caused problems on other trials not herein included. The reservoir holder with the vials is kept in an ice bath to maintain a low temperature. However, the small dimensions of the tubing connecting to the chip as well as the small channel dimensions lead to a quick thermal exchange with the room temperature. Once again, similarly to photobleaching, this negative factor is exacerbated by the slow flows used with this platform.

Finally, the impact of droplet length on concentration should be more thoroughly analyzed to better quantify the variations. This is further discussed in ESI 2 (Section 4.9.3). Nevertheless, the use of the active control platform to perform drug screening assays has advantages albeit requiring further work to address the challenges mentioned above.

The trapping mechanism is leveraged (albeit not perfectly due to the necessity of fluorescent images), and as demonstrated in ESI 2 (Section 4.9.1), the small displacement can be compensated for. Passive methods, on the other hand, face many more challenges to trap droplets. The solutions are tailored to a particular droplet volume for instance and would require different designs for different droplet lengths.

Moreover, the active platform has the potential to perform multiple tests on the same chip by adding more inlets with the solution for the negative control, Orange G concentration, and positive control. The Orange G concentration could also be varied by using two droplets of different length ratios before proceeding with the other steps. Different inhibitors at different concentrations could also be combined, and then, tested in parallel that is very beneficial and highly desirable for high-throughput screening.

The development of a controller operational also during fluorescent imaging would be useful to limit the displacement of droplets consistently and automatically for more efficient testing.

Another potential solution to the issues raised is to change the PDMS-based chip for a glass chip. The surface properties can similarly be maintained hydrophobic with potentially more stability and there would be no issue with porosity.

4.7 Conclusion

The work performed by Wong *et al.* was a proof-of-concept study in demonstrating active control of individual droplets through the actuation of the pressures as per the information extracted from the visual feedback. The caveat to the additional control was the loss of precision due to poor human repeatability and performance. Hence, a higher-level algorithm is developed and implemented to achieve automated droplet generation on-demand of varying size, droplet splitting at specific ratios, merging, mixing, and sorting. Repeatability and robustness are of particular importance to use this platform for applications. Furthermore, the implementation does not require complex manufacturing techniques and although multiple functions are implemented, the footprint of the chip remain small due to the multiplexed functionality of the T junction.

A further advantage to this active droplet manipulation is the reduction in reagent consumption. Comparatively, passive droplet microfluidics requires a setup and stabilization phase that significantly increases reagent consumption as droplets are processed but not fit to be analyzed yet.

A natural extension of this work would be to further develop the semi-automatic algorithm to a fully automated mode. A procedure would be customized by the end user with minimal interaction required as it is automatically executed and data is collected. Hence, the platform would be more accessible to people in the biological or material science field as a tool without requiring in-depth knowledge about droplet microfluidics.

The application of the active control technology to a drug screening assay successfully demonstrated the potential impact of this microfluidics tool in another field. The positive and negative control curves for the kinetics of the tau-protein aggregation were obtained alongside a concentration of inhibitor (Orange G). The results demonstrated qualitatively the reduction of fluorescent aggregation by the inhibitor.

4.8 Electronic Supplementary Information: ESI 1 – Software logic

The objective of the following sections is to present the logic implemented in the software for each semi-automatic manipulation. First of all, some terms and intermediate steps will be defined. Then, the semi-automatic procedure for generating, merging and splitting droplet will be outlined in flow charts.

4.8.1 General definitions

Channel The channel network is divided in arbitrary channels that are numbered and controlled independently, the positive direction is always towards the nearest junction.

Interface Identifies the droplet limit at the interface between oil and water.

Junction Defines the point at the intersection of three channels that is used for measurement.

Current position Defines the position $y_{current}$ where the interface is located within the channel with respect to the junction.

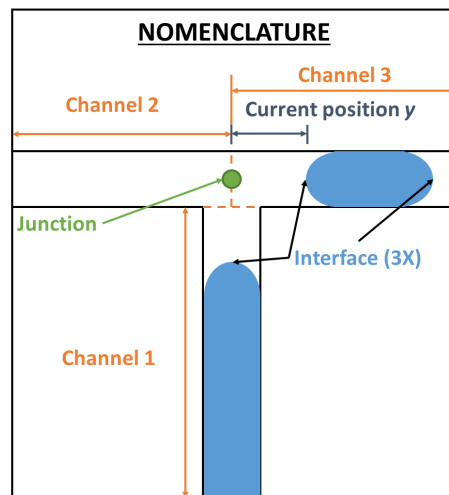


Figure 4.12: Definitions of elements to understand active droplet control.

4.8.2 Flow chart legend

User input Includes any action that requires human intervention from the user through the graphical user interface (GUI).

Condition Defines a state for which specific condition(s) must be met (for instance, the position with respect to the tolerance) in order to progress to the next step.

Semi-automatic control Specifies a step implemented in the software with its general description.

Data Shows the flow of information (depending on the arrow direction), usually represents variables stored in memory that can also be displayed to the user.

4.8.3 General to all flow charts

Parameter definition The user must define key parameter values (if different from default values) using the graphical user interface (GUI).

Tolerance (ϵ) Defines how close to the objective the current position must be before moving to the next step, limited by the resolution of microns per pixel.

Gains (K) Influences the dynamic response of how “fast” the interface reaches the objective position, e.g. K_{gain} in Equation 4.

Start the sequence Debut of the takeover of the semi-automatic algorithm over manual control initiated by the user.

Initial data storage Calculated and measured quantities based on the initial stage of the system when the sequence is initiated.

Link channels Synchronizes two channels such that they move in unison.

Reverse link channels Links the displacement in two channels such that they move in opposite directions.

Split and move away From reverse link of the two appropriate channels, moving in opposite direction leads to the formation of two new interface; the motion away from the junction is implemented to prevent the accidental merging back of the two new interfaces.

Wait to stabilize A delay is implemented such that the droplet(s) can stabilize at their respective location.

Stabilized result droplet(s) No change in the desired droplet position, immobilization of the droplet(s) of interest for accurate measurement.

4.8.4 Specific to the droplet generation flow chart

Desired droplet length [μm] User-specified droplet length to be generated.

Distance to junction Scaled measurement between the interface and the junction point.

Move towards junction The interface is moved towards the junction such that the dispersed phase overflows in the adjacent channels to the junction.

Interface selection in new channel The user must select (using the mouse) the interface in either of the adjacent channels for which the length will be adjusted.

Adjust droplet length The distance between the interface and the junction is matched to the desired droplet length within the specified tolerance.

Droplet length Output of the length of the droplet generated as per the micron per pixel scaling.

4.8.5 Specific to the droplet merging flow chart

Droplet closest to junction The interface of one of the two droplet that is measured closest to the point defining the junction.

Droplet furthest from junction As opposed to the droplet closest to junction, the interface that is furthest from the junction as per the initial measurements.

Droplets equidistant from junction The interface of both droplets at an equal distance from the junction in their respective channel.

No more initial droplet interface The two initial interface have merged and as such do not exist anymore.

4.8.6 Specific to the droplet splitting flow chart

Desired droplet ratio [%] User-specified droplet ratio to be obtained from the two resulting droplets.

Initial ratio Calculated from the initial state of the system.

Distance to move Calculated based on the desired ratio and current state of the system.

Adjust droplet ratio The distance between one of the interface and the objective position is matched within the specified tolerance.

Droplet ratio [%] Ratio based on the measurements of the two droplets obtained at the end of the procedure.

4.8.7 Flow charts

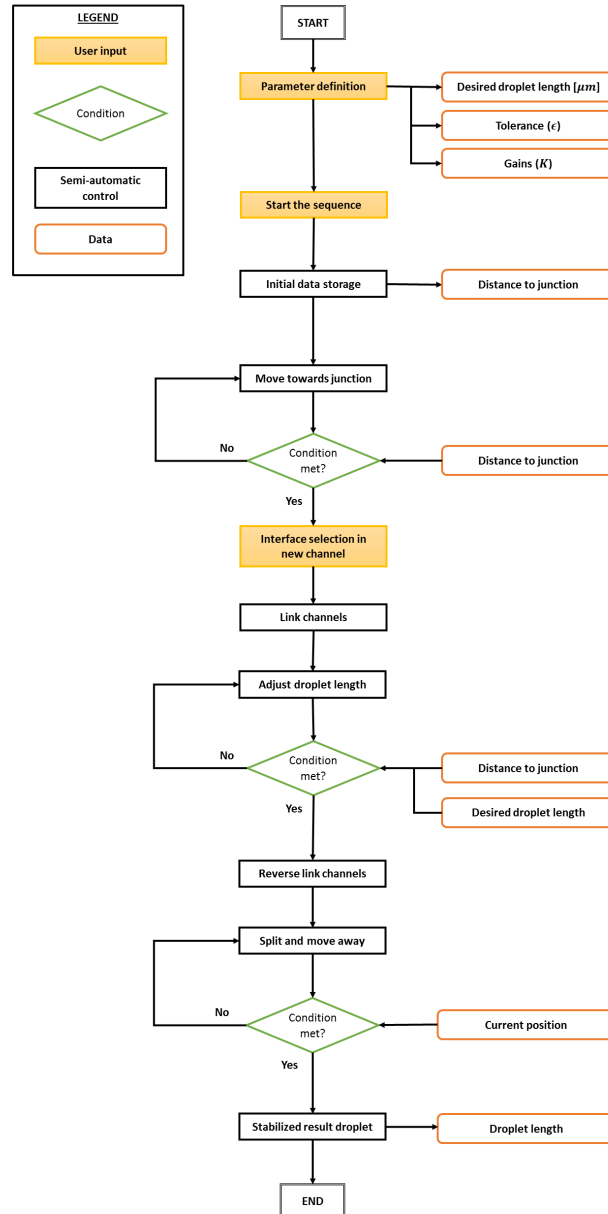


Figure 4.13: Flow chart for generation of a droplet of a specified length.

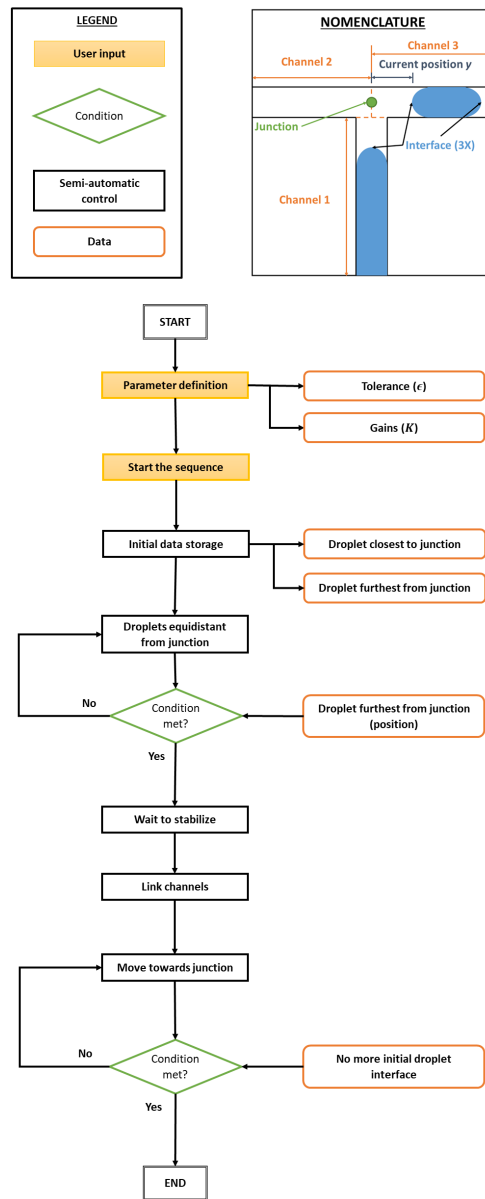


Figure 4.14: Flow chart for merging of two droplets.

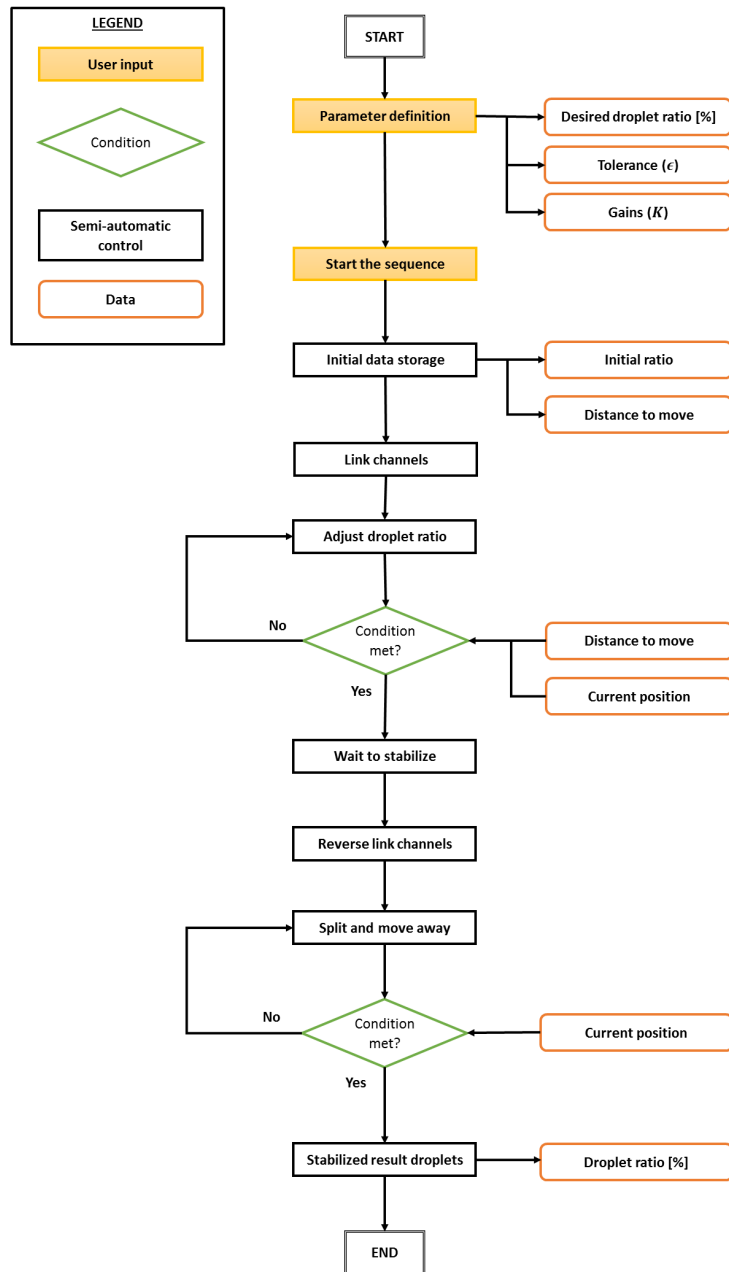


Figure 4.15: Flow chart for splitting of a droplet at a specified ratio.

4.9 Electronic Supplementary Information: ESI 2 – Drug screening

4.9.1 Image processing and data acquisition

This section explains the relevant details pertaining to the application of the platform to drug screening experiments. Some images have their brightness artificially increased to improve contrast for better visualization. All modified images are clearly indicated as such. Note that the images analyzed to collect the data are the original ones without exception.

Image acquisition

The images are acquired using a 4X objective attached to a *Nikon Inverted Microscope ECLIPSE Ti-E*. Using the fluorescent filter *CFP-HQ*, the excitation wavelength is 440 nm while the emission wavelength is 490 nm. The images are then recorded using an *Andor Zyla 5.5 sCMOS* camera attached to the microscope side-mount.

The exposure time is set to 2 seconds, and correspondingly, the camera 16-bit depth image is saved every 2 seconds for at least 6 minutes. Afterwards, a bright field image is saved to obtain the droplet contour. Finally, the fluorescence of the background is recorded at the end for each set of experiments.

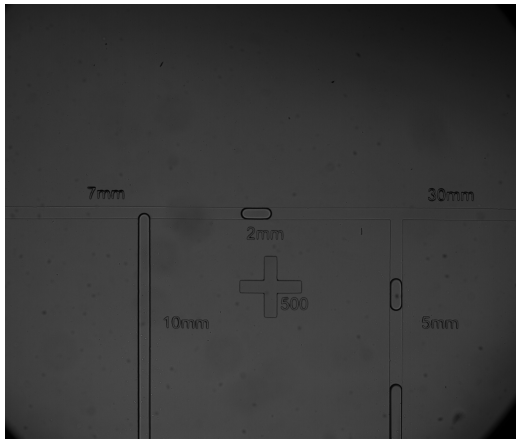
The 6 minutes of recording is of the droplets after merging to assess the aggregation triggered by the buffer. Beforehand, while the solutions are still in the two separate droplets, the bright field and fluorescent image are recorded in quick succession (< 5 seconds) as a baseline and to ensure the dye did not self aggregate.

Image processing

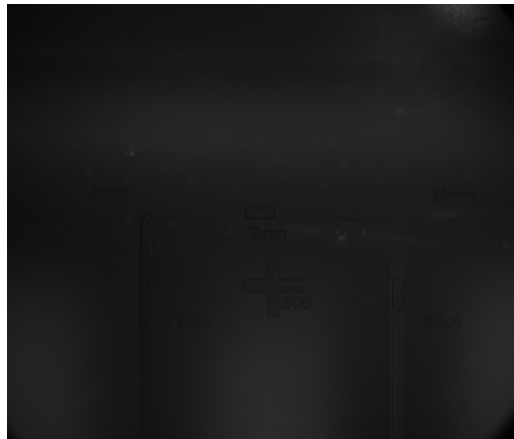
The images are processed using macro scripts in the open-source software *ImageJ*. Most of the processing steps are automated. For each new data set, the appropriate region of interest (ROI), which limits the scope of image processing to the portion of the channel containing the droplet, is manually selected. Also, the processing of the bright field image required varying originating points for the *floodFill* function. The rest of the steps were automated for consistency and efficiency purposes.

The processing steps before and after merging are illustrated in Figures 4.16 and 4.17 respectively. Note that the image processing is performed using *ImageJ* up to

the cropping and background subtraction (Figure 4.17(c)). Afterwards, the images are exported as text files containing the greyscale value for each pixel in a matrix. The text files are then imported into *Matlab* for further processing and plotting as explained in the following section.



(a) Initial bright field image.



(b) Initial fluorescence before droplet merging.



(c) Mask obtained from thresholding, flood-Fill, and erode of region of interest (ROI).



(d) Fluorescent image (b) after background subtraction and the mask is applied.

Figure 4.16: Image processing before droplet merging. Uniform intensity confirms the dye did not self aggregate.



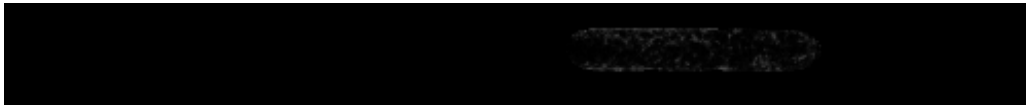
(a) Bright field image of the droplet (after merging of the two solutions).



(b) Mask from the bright field image using thresholding, floodFill, and erode functions in ImageJ.



(c) Cropped frame for each interval (after background subtraction). Intensity artificially increased for better contrast.



(d) Mask applied with displacement from the correlation along the channel (59 pixels displacement) to eliminate background noise and only have fluorescent intensity from the pixels contained in the droplet. Intensity artificially increased for better contrast.

Figure 4.17: Image processing after droplet merging. Correlation along the channel to locate the droplet and apply the mask.

Data acquisition

The droplet mask and cropped fluorescent image (as seen in Figure 4.17(b) and 4.17(c) respectively) are imported in *Matlab* as a 2D array containing the greyscale intensity for each pixel.

The overall fluorescence of any droplet is calculated by averaging over all pixel values contained in the droplet. For the two droplets before merging, the bright field (for the mask) and fluorescent images are taken few seconds apart without the droplets having the time to move significantly. Consequently, the mask can be directly applied to eliminate background noise.

After the droplets are merged, the images are recorded over a longer period of time. Although the displacement is carefully monitored and minimized through

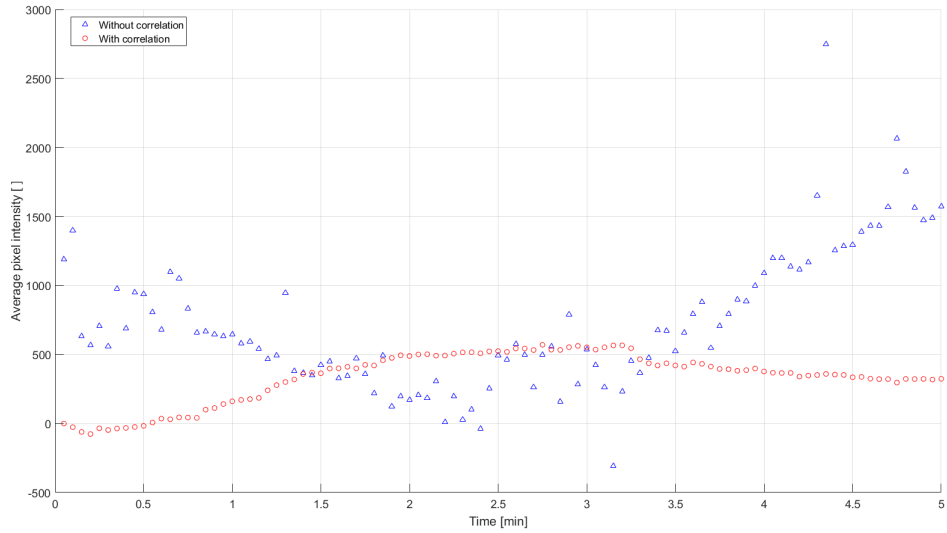
minute manual pressure adjustments, the fluorescent droplet travels along the channel. Thus, the droplet must first be located in order to apply the mask. Correlation in the direction of the channel is used to establish the displacement yielding the highest sum over the mask pixels. The assumption is that any of the background noise would be less bright than the fluorescence of the droplet. This can quickly be confirmed through quick visual inspection of the images such as 4.17(c). Then, the mask is applied with the calculated offset to only keep the fluorescent intensity within the droplet as shown in Figure 4.17(d). An example of the data with and without correlation with the displacement over time is given in Figure 4.18.

Negative control For negative control, due to the low pixel intensity, the correlation algorithm fails to accurately locate the droplet. Nonetheless, the interface location can (barely) be identified visually. In order to circumvent the limitations of the image processing without requiring more complex algorithms, a *Matlab* script was used to record the manually identified location for each frame. For each frame for the duration of the recording, the picture is displayed and the user can identify the interface by clicking on the appropriate location. The corresponding displacement is recorded, and the next image is displayed. This is performed for all frames to obtain the displacement curve in order to properly offset the mask. The human error introduced by this procedure is deemed negligible.

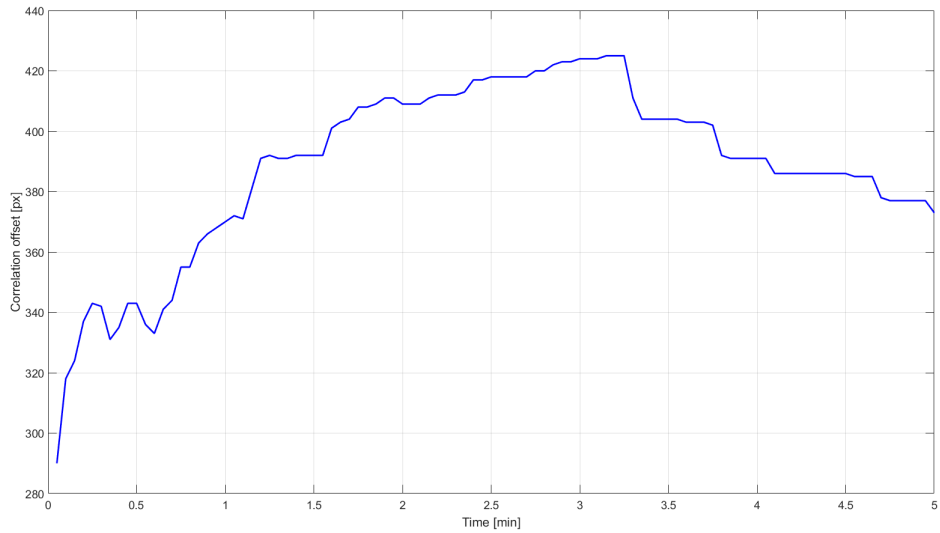
Moreover, for the negative control, the overall background intensity had a slow drift that is believed to be artificially induced by light variations. To compensate for such slow drift, an area further down the channel not containing any droplet was selected. The average of all pixels over time were used to subtract the background intensity drift that affected the whole image.

Data treatment

The curves obtained for the average intensity of the droplet over the 5 minute interval differed in their absolute value. The difference is attributed to the photo sensitivity of the ThS dye. The photo bleaching is not constant due to varying amount of illumination before the data is recorded. The variations in time are due to changing setup time required and the time location of the data for a specific chip (i.e. multiple data points were collected for each chip with the overall intensity decreasing for the later data collected). In order to compare the data, the change in fluorescent intensity is considered by offsetting all points using the first averaged intensity. This method also compensates for any changes in background intensity.



(a) Comparison between the averaged pixel intensity with and without correlation for the mask location from the Orange G (01) curve.



(b) Corresponding displacement obtained with the correlation along the channel.

Figure 4.18: Image processing after droplet merging. Correlation along the channel to locate the droplet and apply the mask.

4.9.2 Screenshot artificial intensity increase

As noted in the article, the screenshots of the fluorescent intensity are artificially and uniformly increased for better visualization and understanding. The trend in fluorescent intensity depending whether peptide and orange G are present is hence clearer. Figure 4.19 shows the original image and brighter image side by side.

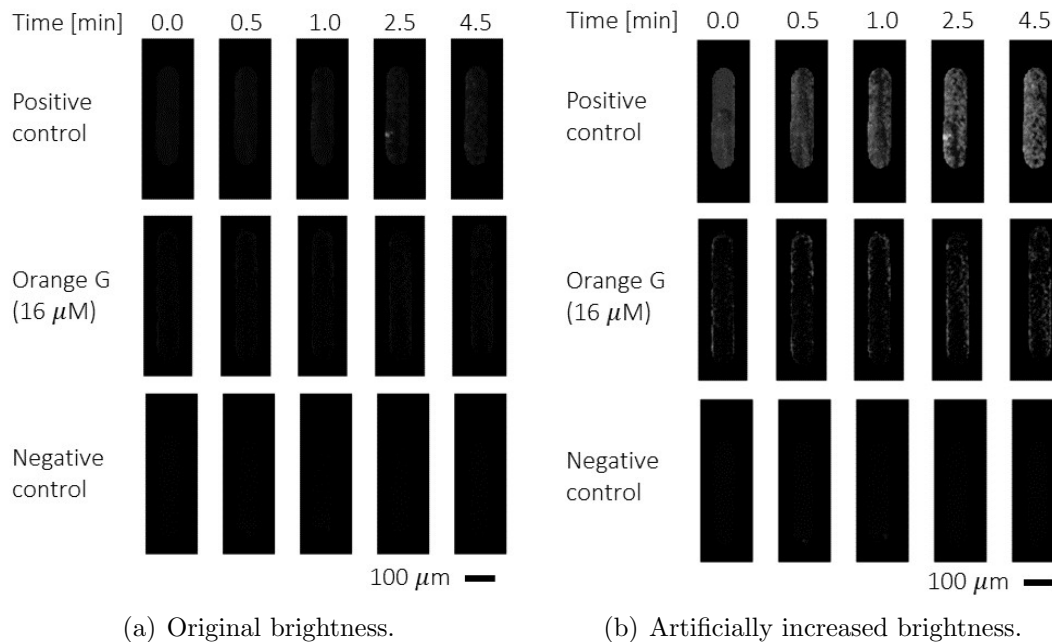


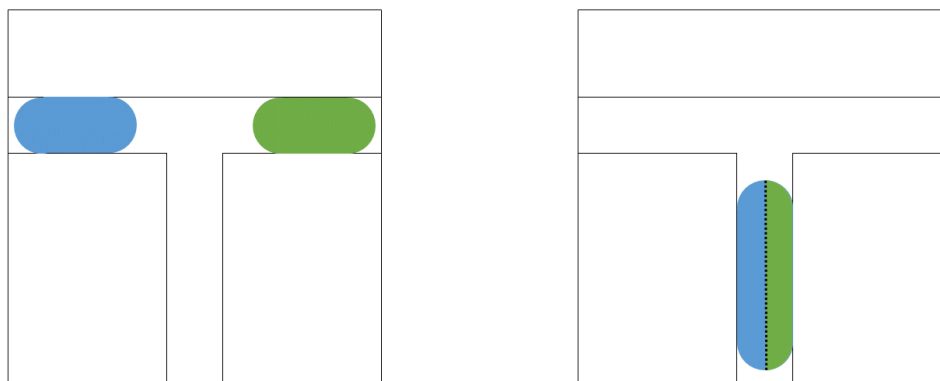
Figure 4.19: Side by side comparison of the drug screening screenshots: before and after increasing the brightness. The purpose is for better readability and visual representation of the assay. The data is extracted from the untouched images.

4.9.3 Length variations between the two droplets

The variations in the length of the two droplets before merging affect the drug screening results. However, the impact is deemed insignificant for the purpose of this study that aims at showing the potential use of the platform rather than a standalone drug screening study.

The effect on the kinetic in terms of time for the reaction is deemed negligible. Figure 4.20 shows schematically (albeit simplified) the resulting droplet after merg-

ing. The principal diffusion length between the two solutions is then the channel width (that is independent of droplet length) rather than the droplet lengths. The bigger impact is on the final concentration of each solution that assumes the merging of 2 droplets of exactly the same length.



(a) Two droplets before merging.

(b) Single droplet after merging.

Figure 4.20: Schematic representation of the merging of the two droplets and the simplified distribution of the solutions in the resulting single droplet.

4.10 Electronic Supplementary Information: ESI 3 to 6 – Videos

The videos of the semi-automated manipulations are available on the publisher website.

DOI: 10.1039/C9LC00128J

Acknowledgements

This work was carried out thanks to grants from NSERC and OCE provided to Prof. Carolyn Ren. Other funding includes NSERC CGS-D scholarship and the Nanofellowship from the Waterloo Institute for Nanotechnology (WIN).

Marie would like to acknowledge the previous work carried out by David Wong setting the foundation for the work presented here as well as Anna Nguyen for the help provided in the laboratory.

Chapter 5

An open-source pressure pump system: μ Pump

The work included in this chapter is published: R. Z. Gao, **M. Hébert**, J. Huissoon, and C. L. Ren, *pump: An open-source pressure pump for precision fluid handling in microfluidics*, *HardwareX*,7 (2020), p. e00096 [90].

DOI: 10.1016/j.ohx.2020.e00096

R. Z. Gao (Ph.D. candidate in the Waterloo Microfluidics Laboratory (WML) at the University of Waterloo) equally contributed to the work. Their contribution started as an intern student and continued into their graduate studies in the WML. The bulk of their contribution focuses on hardware design with the corresponding assembly instructions and other documentation. They participated in writing the manuscript draft.

M. Hébert provided supervision throughout the project. Their other major contribution is the software design, implementation, and documentation. They also completed the image processing for validation of droplet volume. For the manuscript, they contributed to the sections pertinent to the focus of their work and also to the edition of the manuscript drafts.

5.1 Introduction: Hardware in context

Microfluidics deals with the study of fluids at the micron scale. The small scale provides key advantages including lower reagent consumption, shorter reaction time,

and lower cost. Applications range across a variety of fields, including material synthesis [260], biological assays such as PCR [153] and drug development [261], organs-on-a-chip [243] and fuel cells [163]. Most microfluidics platforms use either a syringe pump or a pressure pump to drive the fluids.

In the context of droplet microfluidics, syringe pumps are commonly used when a pressurized air source is unavailable. However, their long and persistent transient is undesirable for high-performance applications [159, 149]. Harvard Apparatus is one of the common providers of commercial syringe pumps. The syringe pump technology is relatively simple and relies on a stepper motor linearly driving the piston of a syringe; hence, building such a prototype is fairly straight forward and has been documented in the literature [168].

Pressure pumps reduce both long and short term oscillations. Commercial systems typically cost more than syringe pumps and are made by companies such as Elveflow and Fluigent. Although some commercial systems have software development kits (SDKs) available, the pump is effectively a black box, and customization is limited.

Open-source pressure-driven options are quite limited. Information for the so-called Quakes valves is available to build a system to control multi-layer microfluidic chips [29, 303], but the operating principle is inherently different from a pressure pump system such as the MFCS-EZ sold by Fluigent. Essentially, pressure pumps are microcontroller-based systems that generate a continuously variable pressure signal (albeit in tiny discrete increments); multi-layer devices, on the other hand, are controlled by solenoid valves that switch port pressures on or off, and are thus discrete (or binary) as opposed to continuous. Recent work has also produced a low cost open-source microfluidic control system that focuses on miniaturization and control of a large array of solenoid valves while incorporating a mini air compressor within the build [302]. However, such a system trades precision and accuracy for portability. μ Pump, on the other hand, is the opposite, it is a high precision benchtop fluidic control system that has the performance on par with much more expensive commercial systems.

An open-source pressure pump system offers not only the higher performance in terms of short response time and improved stability, but also the ability to customize and tailor the design to individual requirements, and at a significantly lower cost than commercially available systems. The lower cost is envisioned to help microfluidics become more accessible to researchers in a broad range of fields, including chemistry, biology, material science, etc. As an open-source system with full access to, and understanding of, the detailed construction and operation, it also shows promise

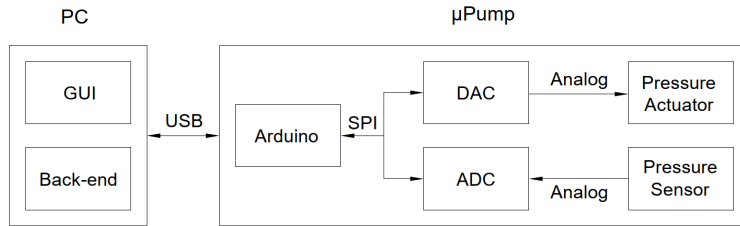


Figure 5.1: System schematic.

in less developed areas of microfluidics such as active control of individual droplets [308, 111].

5.2 Hardware description

5.2.1 System overview

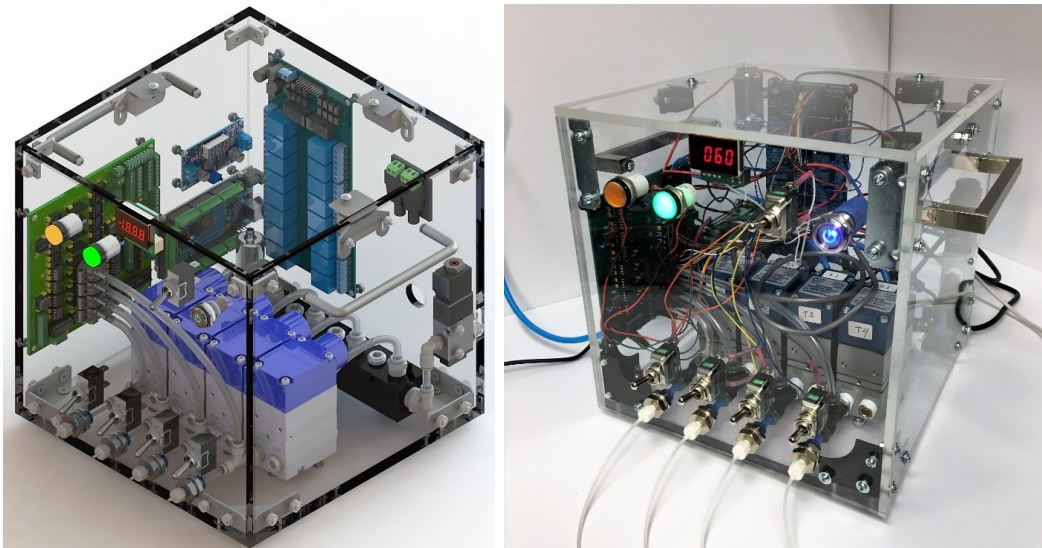
The pressure pump core component is the actuator (i.e. the E/P transducer) providing regulated air according to the electrical signal. Multiple peripheral components to the actuator are required to build the system. As shown in Figure 5.1, the graphical user interface (GUI) is hosted on a computer separated from the pump. The back-end of the software interfaces through USB to the microcontroller-based microfluidic pressure pump: μ Pump.

The Arduino provides the processing power and communication interface through USB and serial peripheral interface (SPI). The SPI protocol connects the Arduino with the digital-to-analog converters (DAC) and analog-to-digital converters (ADC). The DAC sends the signal to the actuator to set the pressure point. The ADC translates the voltage signal from the pressure sensor (i.e. P/E transducer) to a digital signal that the Arduino then transmits to the computer. Although the pressure sensors provide feedback, the actuators operate in a self-contained close loop. The signal from the DAC sets the reference from which the transducer internally measures and regulates the output pressure. Nevertheless, the measurement of the output pressure by the pressure sensor provides useful feedback to the user.

The complete system is shown in Figure 5.2 as a CAD model and a picture of the built system. The open-source journal article provides all necessary documentation and instructions for the reader to replicate μ Pump. The CAD enables the visualization of the complete system. The bill of material lists each component and potential

suppliers with the price. The assembly instructions include the pneumatic subsystem and the housing that holds everything together. The files required for PCB manufacturing are paired with wiring instructions to assemble the electronic assembly. The software source code grants flexibility for modification and integration; executable versions are also provided to use the standalone system as-is. Finally, operation instructions enable the users to easily work with the pressure pump.

The extensive documentation provided with the journal article aligns with the open-source objective of the project. In contrast, commercial pressure pumps refrain from sharing the details; thus, flexibility and customization are limited. Moreover, the cost of commercial systems can be prohibitive to researchers wanting to use microfluidic as a tool; the open-source nature of μ Pump shares the knowledge with the community with the objective of lowering the barriers for the adoption of microfluidic by end-users.



(a) 3D rendering.

(b) Built system.

Figure 5.2: Microfluidic pump (μ Pump) with four independently controlled pressure output channels.

Table 5.1: Minimum performance criteria for microfluidic applications

| | |
|-----------------------------|--------------------------|
| Pressure output accuracy | ± 2 mbar |
| Pressure sensing resolution | ± 1 mbar |
| Sampling rate | 10 Hz (~ 63 rad/s) |

5.2.2 Required performance

The open-source pressure pump should exhibit similar performance to the commercial product (i.e. Fluigent MFCS-EZ). The performance criteria guided the design of the open-source system and the benchmark tests. Table 5.1 summarizes the main performance criteria.

5.2.3 Active pressure actuator characterisation

The actuator performance is significant to the overall system performance. As an off-the-shelf component, the flexibility is limited. Moreover, the setpoint operates in a closed-loop with its integrated feedback system. Therefore, the performance of the pressure output accuracy and sampling rate relies on the performance of the actuator. Both the time and frequency response are investigated to build a complete overview.

The selection of the actuator is based on the performance criterion from Table 5.1. The selected model—*Control Air T900-CIM*—provides the pressure output accuracy for a range of 0 to 2 bar.

The characterization of the actuator uses an oscilloscope (*Tektronix TDS5034B*) to measure voltages, and a function generator to directly drive and measure the voltages for minimal signal latency. The control voltage is provided by a function generator (*Keysight 33210A*) with a high impedance setting due to the attached oscilloscope voltage probes (*Tek P5050 500 MHz 11.1 pF 10 M Ω 10X*) at the common point. Two oscilloscope probes, one attached to the function generator at the signal input of the E/P transducer (*ControlAir T900-CIM*) and the other one at the voltage output pin of the pressure sensor (*MPX4250DP*).

A step input as the control signal is used for the time response. The oscillations indicate an underdamped system. Figure 5.3(a) shows the system settling time of about 0.2 seconds. The increasing and decreasing step of 0.5 V reveals the hysteresis behaviour; the response is asymmetric depending on the step direction. The response

is nevertheless similar in shape and settling time. The actuator response to a larger step of 2 V shown in Figure 5.3(b) exhibits the maximum slew rate of 8 bar/s.

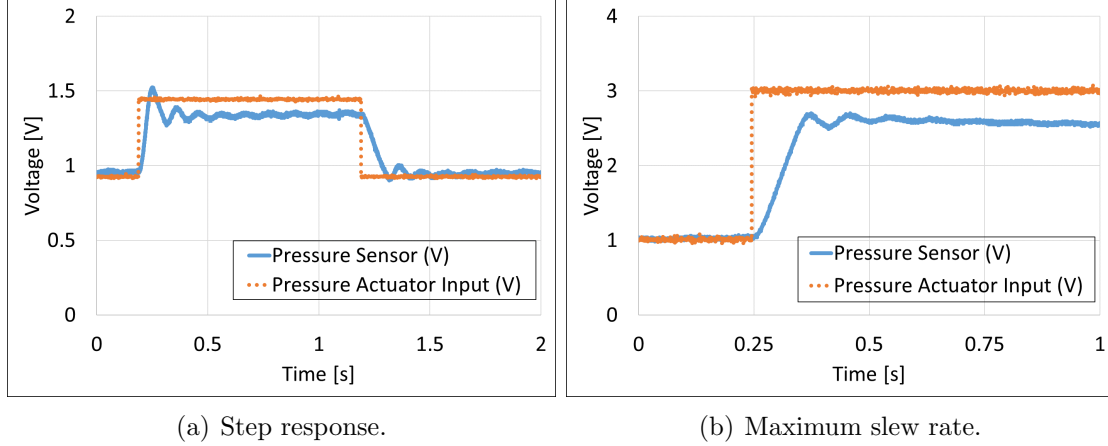


Figure 5.3: Pneumatic actuator time response.

The frequency response of the E/P transducer provides insight into the natural frequency, the amplitude ratio and the phase response for a selected range of frequencies. The actuator bandwidth must meet the sampling rate criterion from Table 5.1. The Bode plot in Figure 5.4 shows a typical 2nd order system frequency response. The natural frequency is estimated at 40.8 rad/s (6.5 Hz).

5.3 Software and graphical user interface

The software and graphical user interface (GUI) are based on open-source libraries, more specifically, *Arduino* and *Qt*. The programming language for the source code is C++ for its object-oriented capabilities. First, open-source benefits and concerns are discussed. Second, software architecture details are presented. Finally, the software operation using the GUI is explained.

5.3.1 Open-source benefits and concerns

The open-source nature of μ Pump democratizes its use, particularly for microfluidic applications. The objective is to lower the cost associated with using pressure

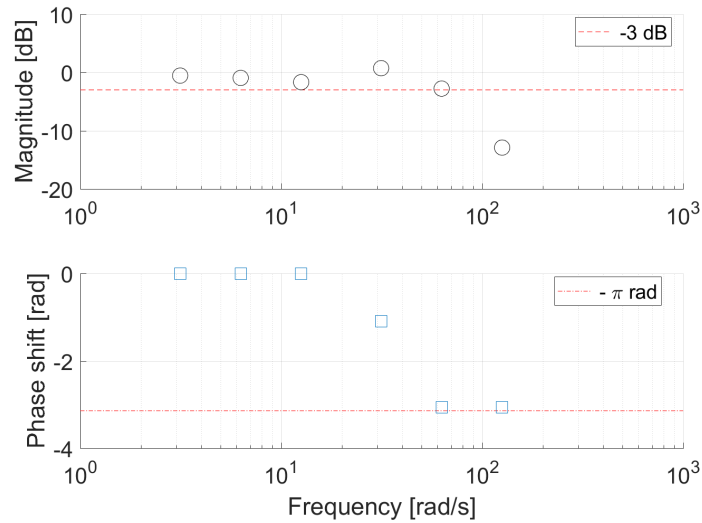


Figure 5.4: Pneumatic actuator frequency response: magnitude and phase shift.

pumps. Similarly to hardware, the software is open-source. The two main libraries are *Arduino* for the microcontroller and *Qt* for the graphical user interface. Both the microcontroller and GUI software are written in C++ for its power and prevalence. Hence, only one coding language is required.

The open-source software enables the users to implement the code “as-is” but also to modify it. The customizability allows us to meet the various requirements within the microfluidic community. The users can thus tailor the system to their needs and integrate it within other systems.

However, in order to modify and integrate μ Pump within another system, the user must be familiar with C++ coding. Moreover, in case of any issue, the support of open-source systems is less than commercial systems. Therefore, for a moderately knowledgeable user, the open-source microfluidic pump enables a cost-saving and flexible solution.

5.3.2 Software architecture: Computer

The following documentation explains the structure of the software running on the computer. The front-end and the back-end are included.



| | |
|-----------------------------------------------------------------------------------|------------------------------------------------------------------------------------------------------------------------------------------------------------------------------------------------------------------------------|
|  | <p>Composition: Indicates that one class contains instances of another class. The filled diamond specifies that when the container class is deleted, the instances of the other classes are also deleted.</p> |
|  | <p>One way: indicates that only one class knows about the other</p> |
| <p>1..*</p> | <p>Multiplicity: indicates how many classes are related to the other. When omitted, a one-to-one relationship is implied. Otherwise, 1..* indicates one or more (unspecified maximum number, but minimum is one).</p> |
| <p>name: type</p> | <p>Member variable: specifies the name and type of the member variable belonging to the class.</p> |
| <p>method name (parameter list): return value type</p> | <p>Member function: specifies the name, parameter list and return value of the method belonging to the class.</p> |
| <p>+ public - private # protected</p> | <p>Visibility: the symbol in front of the member variable or function specifies its visibility outside of the class.</p> |

Figure 5.5: Definitions of the Unified Modeling Language (UML) symbols.

Unified Modeling Language (UML) class diagrams

The standard UML notation is loosely followed in the following UML diagrams. The objective is to provide an overview of the software that is not meant to be comprehensive. The important member variables and functions are listed. But first, the components are defined in the following way in Figure 5.5.

GUI overview

The overview of the software is provided by the class diagram of the windows; their relationships between each other are established and shown in Figure 5.6. The

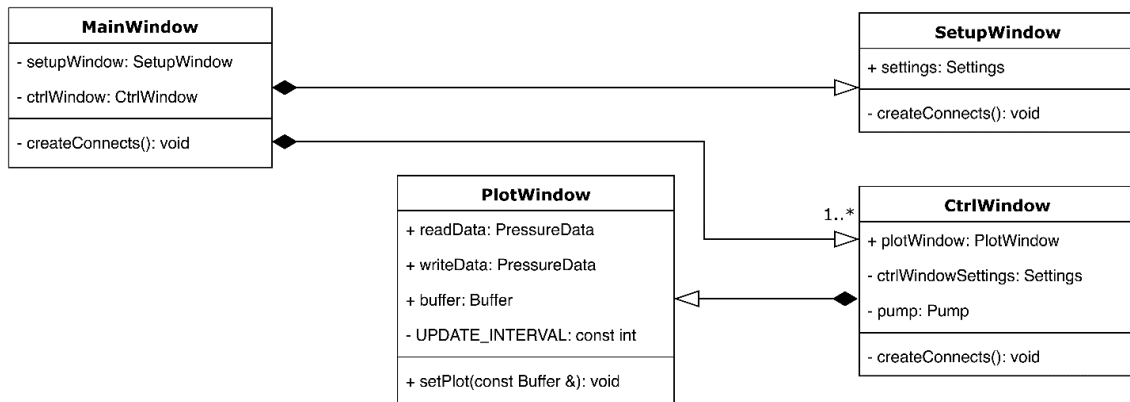


Figure 5.6: UML class diagram providing an overview of the windows and their relationships.

`createConnects()` member function of each of the window is called within the respective constructor of the window and associates the **SIGNALS** and **SLOTS**.

The **SetupWindow** is used to select the settings used to generate the **CtrlWindow** and is stored in an instance of the **Settings** class.

Multiple **CtrlWindow** can be declared to control each of its associated pumps. Correspondingly, the instance of the class will be initiated with the specified settings. Note that multiple instances connecting to the same serial port cannot be created.

Pump control

After the settings are specified in the **SetupWindow**, a corresponding **CtrlWindow** is created with the parameters indicated in the task bar for the users benefit. The **PumpThread** instance belonging to the **Pump** class is private. The **Pump** object acts as the handler for the **PumpThread**; additionally, **PumpThread** is the handler for **serialComm**. This is to better control and restrict access to sensitive variables.

Signals and slots

The *Qt* software package uses signals and slots to communicate between objects as a defining feature. The resources they provide contains all the details [Qt Signals Slots]. The following diagram is meant as a guideline to understand how the different objects communicate together. Note that as per the class diagrams above, certain

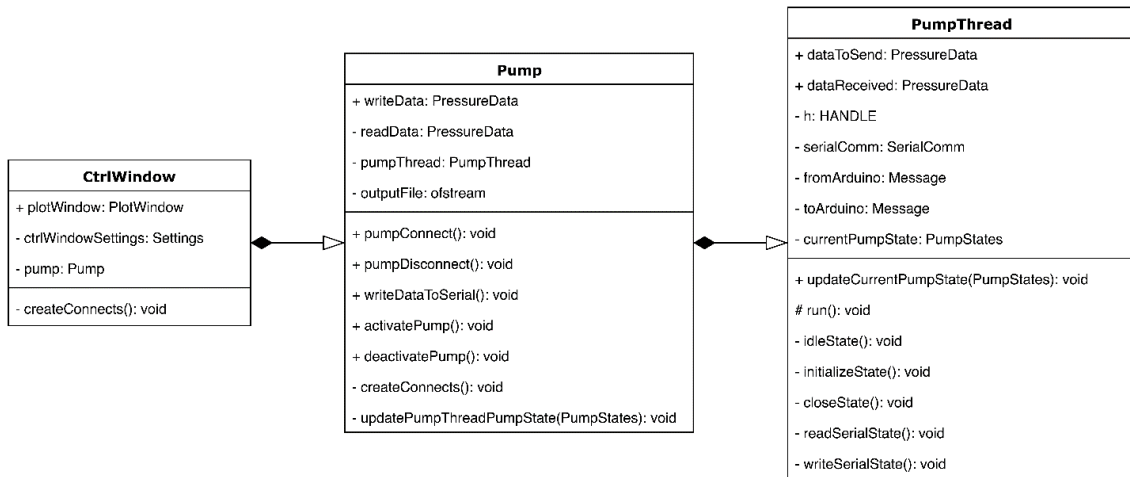


Figure 5.7: UML class diagram for pump control.

instances of classes (i.e. `PumpThread`) are private and thus, cannot be accessed from the higher-level classes (i.e. `CtrlWindow`). Hence, the signals and slots must pass through the intermediate (i.e. `Pump`). The restricted access is to ensure safer handling of the classes at the lower levels.

The connect statements linking the signals to the slots are grouped in each class under the `createConnects()` function.

5.3.3 Communication between the computer and Arduino

The serial communication operates on its separate thread to not interfere with the GUI. The objective of the communication protocol in the context of the pump control is to minimize the delay between a change in requested pressure made by the user in the GUI, and the actuators adjusting their output accordingly. The feedback provided by the pressure sensors is unused by the actuators that have their internal feedback. Consequently, although the pressure feedback is useful to detect leaks, for instance, the priority is less than the command instructions in the context of serial communication.

The reimplement of `run()` in `PumpThread` executes a different function based on a switch statement of the current pump state. Correspondingly, certain instructions will be executed before advancing to the next appropriate state as per the diagram in Figure 5.9. The states are controlled by the `Pump` object and the

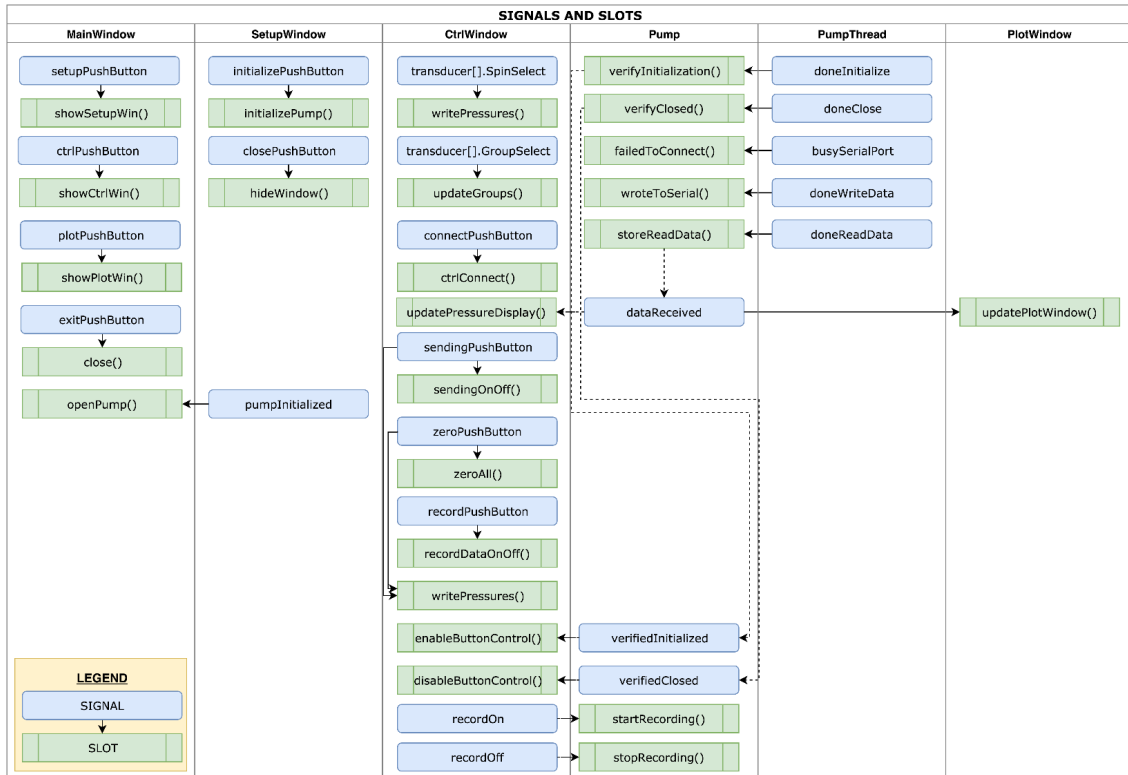


Figure 5.8: Signals and slots relationships between the objects. Solid lines (-) indicates explicit signal to slot link. Dashed line (- -) shows relationship within a same object from slot to signal.

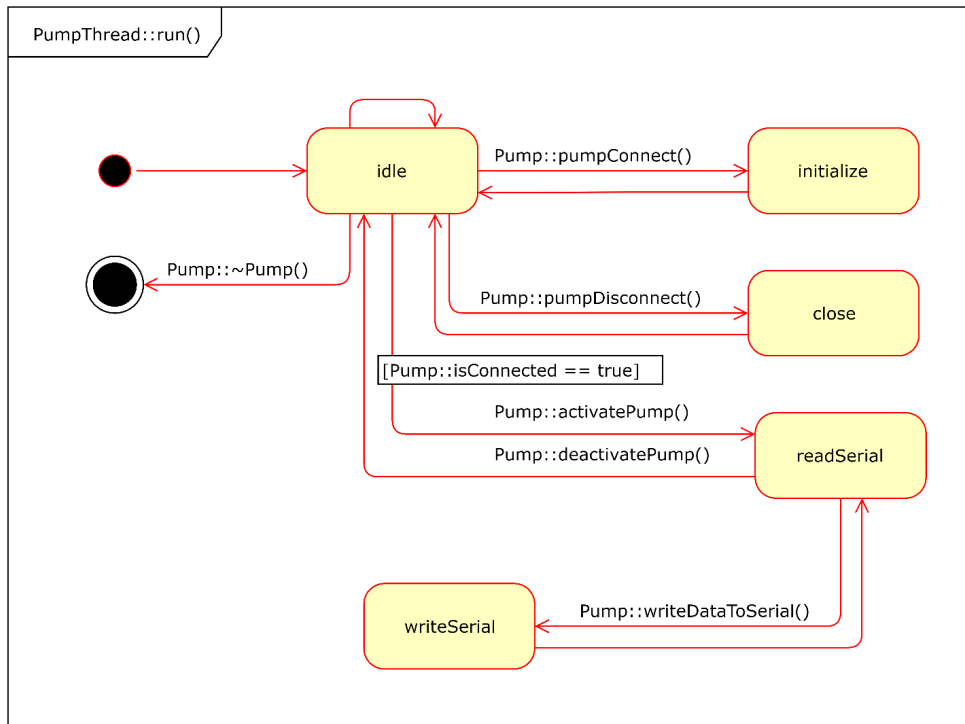


Figure 5.9: Finite State Machine (FSM) diagram for PumpThread.

`updatePumpThreadPumpState()` private member function based on the events. The events are triggered with the corresponding push buttons of the graphical user interface.

Moreover, the `Message` class and `CommCtrl` enum class are used for serial communication purposes with the following details.

Message class The message class is used to receive data one character at a time and to extract the pressure for each transducer after the checksum and end character are received. The checksum is a simple verification of the message integrity. If the value is not as expected, an error is thrown, and the message is not further processed.

'RXSTART' 'P1' 'SEP' 'P2' 'SEP' 'P3' 'SEP' 'P4' 'SEP' 'CKS' 'RXEND'

e.g < P1 & P2 & P3 & P4 & CKS >

The checksum on the PC side is calculated by simply adding the value of all characters composing the message up to the separation character just before the

checksum. The value can overflow but it does not compromise the checksum verification process because it happens identically on the Arduino and on the computer.

For the simplicity of calculations, the checksum on the Arduino side is calculated by adding the values of all non-pressure characters while the pressure values themselves are also added. This is due to the numbers of pressure being processed differently. The asymmetry of the calculations is reflected on the PC and Arduino code accordingly.

`enum class CommCtrl : unsigned char` This enum class is used to better control the scope of the control characters used for communication. The enumeration contains the key control characters used to process the incoming and outgoing message. It is identical both on the PC and Arduino side. From `OtherClasses.h`:

```
//// Serial Communication control characters
enum class CommCtrl : unsigned char
{
    SYN = '@', // Synchronization
    TXSTART = '<', // Start of transmitted message
    TXEND = '>', // End of transmitted message
    RXSTART = '<', // Start of received message
    RXEND = '>', // End of transmitted message
    OK = '!', // Positive acknowledgement
    NOTOK = '?', // Negative acknowledgement
    SEP = '&', // Group separator
    ERR = '^', // Error flag form the PC side (to distinguish from
    NOTOK from Arduino)
};
```

5.3.4 Software architecture: Arduino

Main Arduino script

The main Arduino script is separated into two parts: `setup()` and `loop()`. The former is executed once anytime the Arduino is reset while the latter is subsequently executed as an infinite loop. The `Communication.h` header file is used for the serial communication with the computer and is the only external file required (in addition to the Arduino sketch) for the `testMode`. The classes declared in the other files

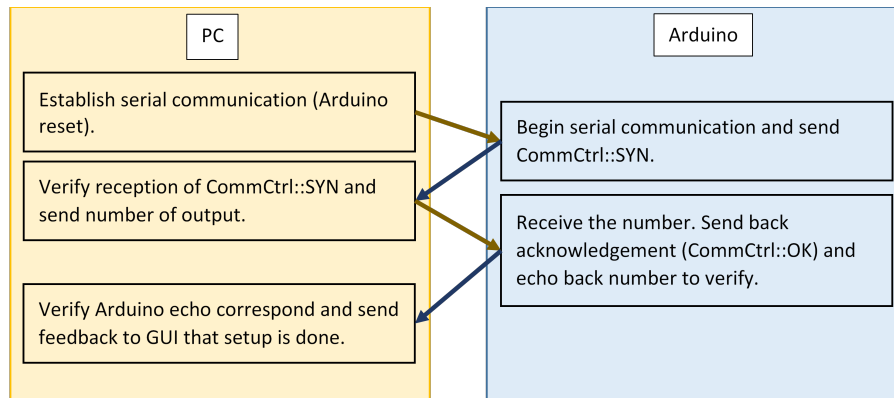


Figure 5.10: Communication setup between PC and Arduino.

(`Configuration.h`, `PumpArduino.h`, etc.) are designed in a modular way. The configuration file contains the variables that can be easily changed to fit the specific build such as pin numbers.

setup() The first step in the setup is the initialization of the serial communication with the default baud rate of 9600 bits/seconds (`Serial.begin(9600)`). This step is analogous to the serial communication setup on the PC side. The baud rate *must* match for all software. If the verification of the synchronization character (`CommCtrl::SYN`) fails, the software automatically reattempts to synchronize with the Arduino.

loop() The logic of the loop is analogous to the one on the computer side; whenever there is information (i.e. pressure command data) in the serial buffer, the data is processed and the set voltage of the actuators correspondingly changed. If the serial communication is available, the feedback pressure is formatted and sent to the computer.

Communication

The communication header and source files are the only ones required for the Arduino test mode when no hardware is connected to the Arduino. The test mode only enables to verify the communication with the computer.

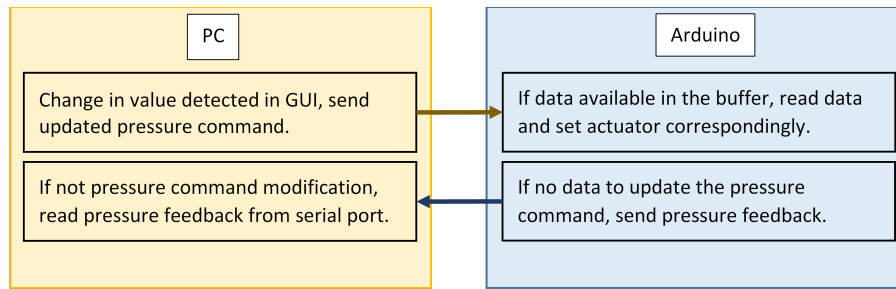


Figure 5.11: Communication loop between PC and Arduino.

The `sendPressure` function is used to properly format and send the pressure feedback in accordance with the communication protocol.

The `PressureData` structure is analogous to the one on the computer side and organizes the pressure for each channel in a vector.

Similarly to `PressureData`, `Message` is analogous to the class on the computer side and is used to handle the reception of the serial data one character at a time.

PumpArduino class

The `PumpArduino` class is the highest level class and includes both the `Sensor` and `Actuator` class instances amongst other member variables. It represents the μ Pump as a whole and is used in the main Arduino script (`uPump_Arduino.ino`) to interact with the pump. Its most important member variables and member functions are summarized in Table 5.2 below.

The sensor and actuator arrays are declared as arrays of pointers of `Sensor` and `Actuator` that are the base classes. This allows to simply point to their respective derived class instances in the configuration file. Hence, all parameters that need to be changed depending on the pump design (sensor model, pin assignment, etc.) are all contained within the `Configuration` file.

Sensor class

The **Sensor** class is the base class used to derive the classes of specific sensor types and ranges. Note that this includes the Analog-to-Digital converter (ADC) chip; thus, two separate derived classes must be defined for the exact same sensor type if they are interfaced with the Arduino using different ADC.

In order to setup a new derived **Sensor** class, the following must be defined:

- ***chipADC**: external ADC chip class instance (e.g. MCP3208)
- **chipChannel**: corresponding ADC chip channel (for chips with multiple channels)
- **pressureFromV(float V)**: the conversion from voltage to pressure in mbar.
- **setupChip()**: the setup of the external ADC class instance with the slave select pin and voltage reference.
- **readVolt()**: the call to the ADC chip function to obtain the voltage reading from the specified channel.

Actuator class

The **Actuator** class is the base class used to derive the classes of specific actuator types and ranges. Note that this includes the Digital-to-Analog converter (DAC) chip; thus, two separate derived classes must be defined for the exact same actuator type if they are interfaced with the Arduino using different DAC.

In order to setup a new derived **Actuator** class, the following must be defined:

- ***chipDAC**: external DAC chip class instance (e.g. MCP4922)
- **chipChannel**: corresponding DAC chip channel (for chips with multiple channels)
- **setupChip()**: the setup of the external DAC class instance with the slave select pin and voltage reference.
- **sendPressure()**: verifies whether the pressure command is outside of the actuator deadband before requesting the voltage output corresponding to the pressure command.

Table 5.2: PumpArduino – Important member variables and functions.

| Member variables | |
|-----------------------------------------------|-----------------------------------------------------------------------------------------------------------------------------------------------------------------------------------------|
| <code>static Configuration cfg</code> | Pin numbers corresponding to the hardware, the sensor types, and actuator types. |
| <code>Sensor *sensors[]</code> | Pointer to reference the derived sensor class in <code>cfg</code> that specifies the sensor type and properties for each channel. |
| <code>Actuator *actuators[]</code> | Pointer to reference the derived actuator class in <code>cfg</code> that specifies the actuator type and properties for each channel. |
| <code>Actuator inputSolenoidValve</code> | Simple actuator with on/off capabilities to control the input solenoid valve. |
| <code>Sensor *inputPressureSensor</code> | Similarly to <code>sensors[]</code> , pointer to reference the derived sensor class in <code>cfg</code> that specifies the sensor type and properties for the inlet pressure sensor. |
| Member functions | |
| <code>void calibrateSensors()</code> | Calibration procedure upon powering on to set the zero gauge pressure as atmospheric (i.e. when the actuators are powered off). |
| <code>void verifyInletPressure()</code> | Used at the beginning of the loop to verify the inlet pressure is within acceptable range and to trigger the warning light sequence as required. Note that this is a blocking function. |
| <code>void actuatorsTurnOn()</code> | Power on all the actuators (when the pressure is within acceptable range). |
| <code>void actuatorsTurnOff()</code> | Power off all the actuators (to prevent damage to the actuators that should not be powered if insufficient inlet pressure). |
| <code>void applyPressure(PressureData)</code> | Instructs the pump to apply the pressure command for each actuator. |
| <code>PressureData getPressure()</code> | Obtains from the sensors the feedback pressure for each channel. |

- `sendDigitalSignal()`: sends the raw (integer) command voltage to the specified DAC chip channel.

Configuration class

The configuration file defines key variables for the association of the hardware with the software. This includes pins for the sensors, actuators, and logic control for the relay. `Configuration.h` contains all the variables that must be changed to match the specific pump built. Hence, it is the only required modification to the Arduino software to operate any pump type that you build. Note that the arrays are declared with size `N_MAX`; if fewer channels are required, use a dummy pin number for any unused parts of the array (suggestion: pin 13). Table 5.3 below contains a brief description of the different variables.

The pin numbers specified in the configuration class file must match the wiring of the Arduino. This is primordial to the proper function of the pressure pump.

5.3.5 Software operation

An overview of the GUI is provided in Figure 5.12. The complete folder containing the executable file—`uPump_PC.exe`—is required to properly operate the software. Opening the executable file will launch the GUI main window in addition to a command prompt window; the command prompt can be disregarded and minimized.

The “Setup” button from the main window opens a window to select parameters: the COM port, the number of pump outputs, and the maximum pressure between 1 and 10 000 mbar. After properly selecting these parameters, the user clicks “Initialize” to hide the setup window and to open the control window.

The control window is used to connect and disconnect the communication with the pump. Furthermore, the pressure of each outlet is set independently. Three input methods are supported for each pressure: numerical input, arrow increase and decrease, and slider. The “ON/Send Data” button must be activated for the pump to respond to the input. The “Zero All” button enables the quick closure of all output pressure by setting the required pressure to zero for all. Finally, the “Record” button and the text field underneath save the data in a comma-separated value (CSV) format. The file is located in the same folder as the executable file.

From the main window, a plotter window is shown using the “Plotter” button. The requested and measured pressure are graphically shown in real-time for information purposes. The channels to be displayed must be selected using the control key to select multiple items from the left panel.

We recommend setting all output to zero to properly close the μ Pump system. The pump is disconnected with the “Disconnect” button. Finally, the main window is closed either using the “Exit” button or the “x” in the corner.

5.4 System validation and characterisation

The μ Pump system is validated in two ways: pressure and droplet volume. The pressure output comparison to the commercial system aims to quantify the potential difference in performance. The droplet volume comparison to the commercial system evaluates the difference in a targeted application.

Table 5.3: Configuration – Variable description.

| Variable name | Description and information |
|-----------------------------------------|-------------------------------------------------------------------------------------------------------------------------------------------------------|
| <code>static const int N_MAX</code> | Variable used to set the size of any array needed for all channels. Currently restricted to only one digit (i.e. up to 9). |
| <code>T900X actuators[N_MAX]</code> | The derived class type (e.g. T900X) specifies the actuator type and chip used as defined in <code>Actuator.h/.cpp</code> . |
| <code>actuatorRelayPin[N_MAX]</code> | Pins used to control the power to the actuators. |
| <code>MPX4250 sensors[N_MAX]</code> | The derived class type (e.g. MPX4250) specifies the sensor type and chip used as defined in <code>Sensor.h/.cpp</code> . |
| <code>MSP300 inputPressureSensor</code> | The derived class type (e.g. MSP300) specifies the sensor type and chip used to monitor the inlet pressure as defined in <code>Sensor.h/.cpp</code> . |
| <code>MCP3208_SS</code> | ADC slave select pin used in the constructor (<code>Configuration()</code>) to set <code>pinSPISlave_ADC</code> . |
| <code>pinSPISlave_ADC[N_MAX]</code> | Slave select pins for the ADC of each pump channel. |
| <code>channelADCSPI[N_MAX]</code> | ADC chip channel for each pump channel. |
| <code>MCP4922_SS</code> | DAC slave select pin used in the constructor (<code>Configuration()</code>) to set <code>pinSPISlave_DAC</code> . |
| <code>pinSPISlave_DAC[N_MAX]</code> | Slave select pins for the DAC of each pump channel. |
| <code>channelDACSPI[N_MAX]</code> | DAC chip channel for each pump channel. |
| <code>SPI_CLK</code> | Clock speed for SPI communication to external ADC and DAC. |
| <code>VREF</code> | Voltage reference (in mV) for ADC and DAC. |
| <code>pinInletPressure</code> | Pin to read voltage from inlet pressure sensor without an external ADC. |
| <code>pinInletSolenoid</code> | Pin to control the inlet pressure solenoid valve. |
| <code>pinLEDgreen</code> | Pin to control the green LED indicator. |
| <code>pinLEDyellow</code> | Pin to control the yellow LED indicator. |

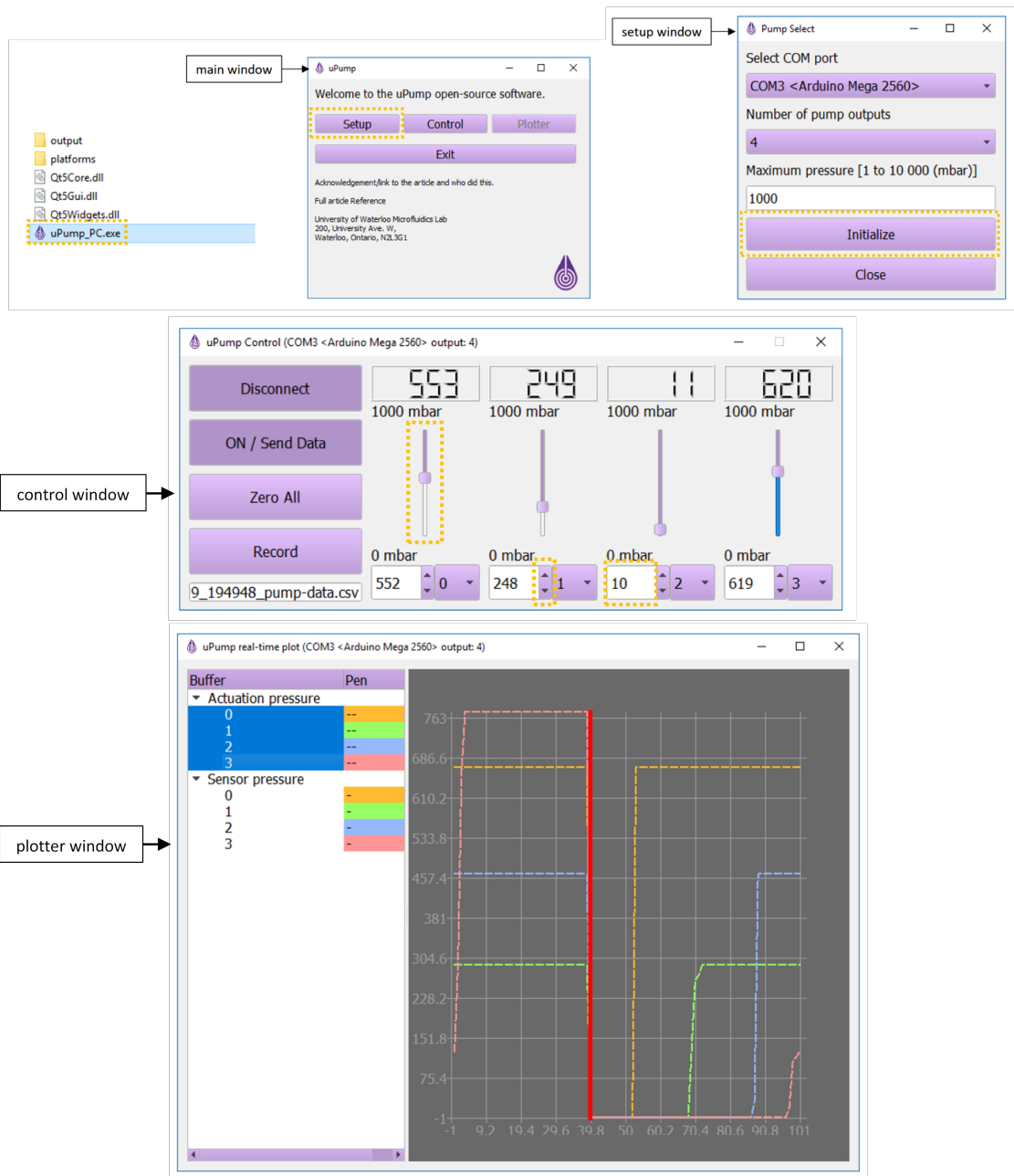


Figure 5.12: Software operation overview.

5.4.1 Pressure output

The μ Pump system is validated using the pressure output because outputting pressurized air is its primary purpose. A commercial system—Fluigent MFCS-EZ—is used as the standard that μ Pump is compared against. For all data, the response of one of the output channels is represented for better clarity; all outputs performed similarly. Four criteria are used to compare the two systems: pressure response, flow rate response, hysteresis, and stability. The key specifications for μ Pump are summarized in Table 5.4 and are comparable to the specifications of the commercial system that correspond to the minimum performance criteria (Table 5.1).

Pressure response

Figure 5.13 shows a greater peak for an increasing step change for μ Pump comparatively to Fluigent MFCS-EZ. For decreasing step changes, the difference between the two systems is less significant. Nonetheless, the stabilization to the constant pressure is fast in all cases.

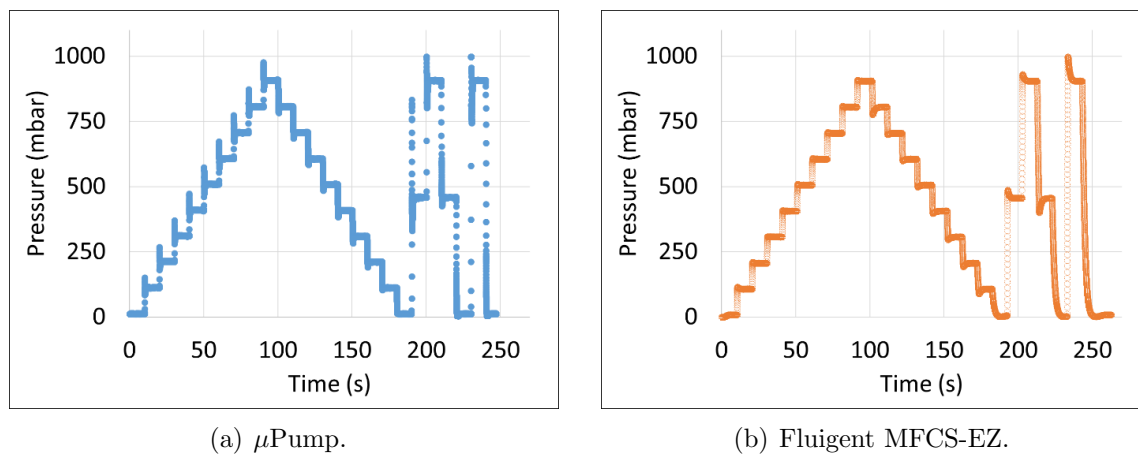


Figure 5.13: Pressure step response.

Flow rate response

The flow rate response shown in Figure 5.14 follows the same conclusion as for the pressure response. However, the difference between the two systems is lesser.

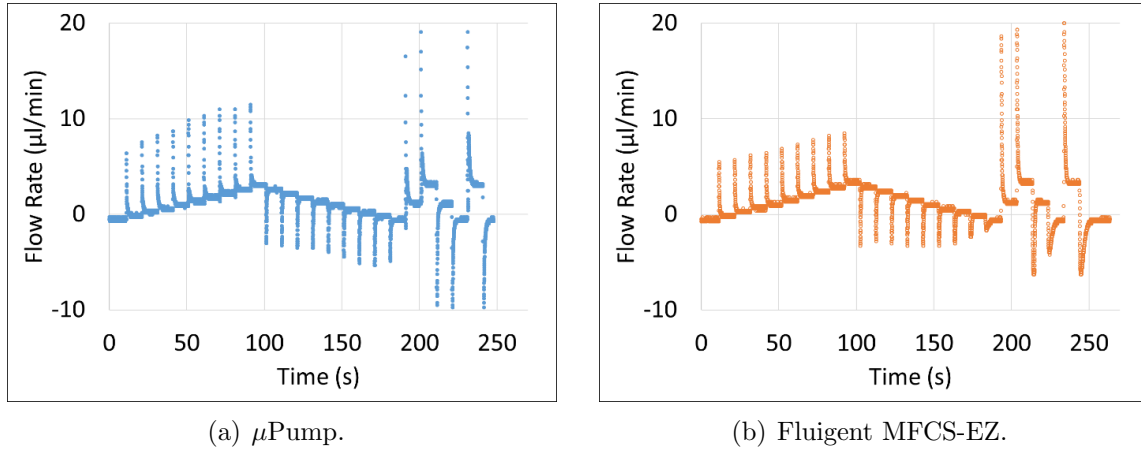


Figure 5.14: Flow step response.

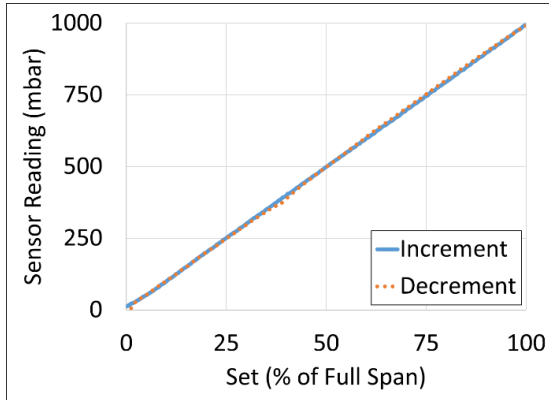
Hysteresis

The hysteresis of both systems is evaluated for pressure and for flow rate response as shown in Figure 5.15. The flow rate exhibits greater hysteresis than pressure data for both μ Pump and Fluigent MFCS-EZ. However, μ Pump performs significantly better than Fluigent MFCS-EZ for the pressure hysteresis. Ideally, the increasing and decreasing curves would overlap on top of each other to form a straight line.

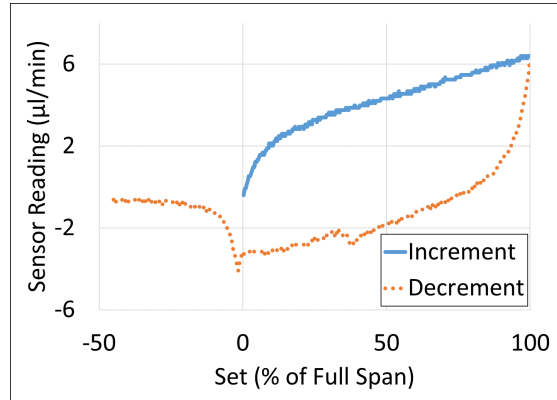
The more important hysteresis from the flow is attributed to the elasticity of the additional components added to the experimental setup. Moreover, the more significant hysteresis of the Fluigent MFCS-EZ pump is associated with the inner workings of the system. The details are not available, but a lack of exhaust for more efficient air usage—as praised in their promotional material—and elastic components are potentially responsible.

Stability

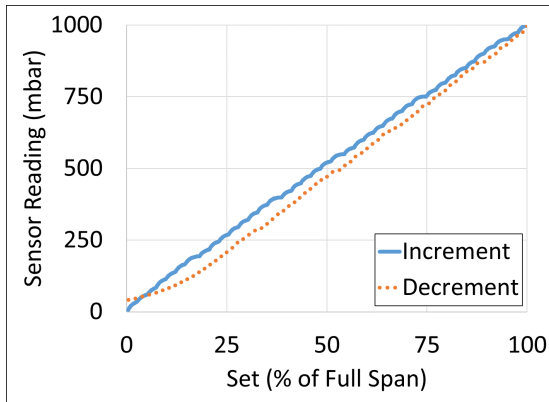
The pressure and flow rate stability are evaluated over a six minutes period; Figure 5.16 shows the graphical results. Although the pressure stability for μ Pump differs from Fluigent MFCS-EZ as shown in Figure 5.16(a), the flow rate stability is comparable for both systems (Figure 5.16(b)). This is attributed to the added compliance to the system by the additional components that dampen the oscillations.



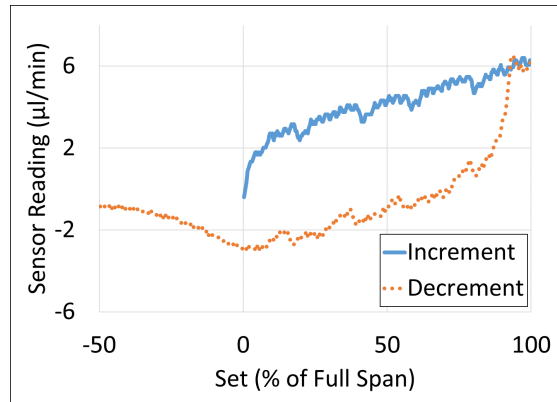
(a) Pressure hysteresis for μ Pump.



(b) Flow hysteresis for μ Pump.



(c) Pressure hysteresis for Fluigent MFCS-EZ.

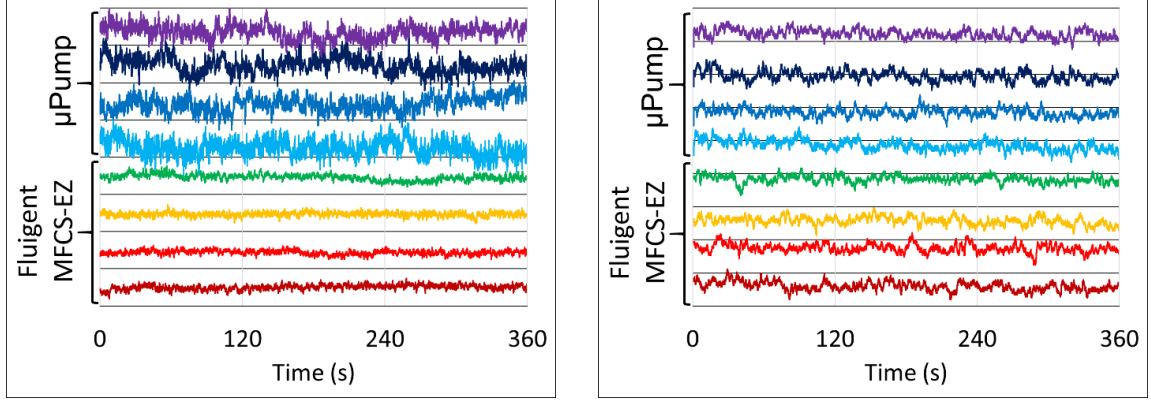


(d) Flow hysteresis for Fluigent MFCS-EZ.

Figure 5.15: Hysteresis comparison between μ Pump and Fluigent MFCS-EZ.

5.4.2 Droplet volume validation

As opposed to the pressure tests, the droplet volume validation examines the performance of the open-source system for its targeted application. For passive droplet generation, droplet volume is a standard measure of uniformity and stability. The importance of channel height for the volume equation requires accurate experimental measurements using a pressure sensor and a flow sensor.



(a) Pressure stability. Horizontal grid spacing is 1 mbar.

(b) Flow rate stability. Horizontal grid spacing is 0.1 $\mu\text{L}/\text{min}$.

Figure 5.16: Stability comparison between μPump and Fluigent MFCS-EZ under load.

Microfluidic channel height

The height of the microchannel greatly influences the resistance (h^{-3}). Therefore, the channel height is experimentally determined rather than assuming the nominal value.

The sensitivity of resistance on channel height is leveraged to experimentally determine the height. A priming phase mitigates significant change in channel height due to swelling. The pressure is applied to an inlet and the flow rate is measured using a flow sensor (Sensirion SLG-1430). The pressure is measured externally by a high accuracy pressure sensor (TE Connectivity U536D-H00015-001BG). For single-phase flow, the resistance is given by an established formula based on the liquid physical properties and the geometry of the channel as per Equation 5.1 [31]. For a network of channels of the same height, an equivalent resistance is formulated based on circuit rules for series and parallel connections. Then, the zeros of the function of height (h) are found using a numerical tool such as the Matlab function `fzero`.

$$R_{hyd} = \frac{12\mu L}{w \cdot h^3} \left[1 - 0.63(h/w) \right]^{-1} \quad (5.1)$$

where R_{hyd} is the hydraulic resistance [$\text{Pa} \cdot \text{s}/\text{m}^3$], μ is the dynamic viscosity [$\text{Pa} \cdot \text{s}$], L is the channel length [m], h is the channel height [m] and w is the channel width [m].

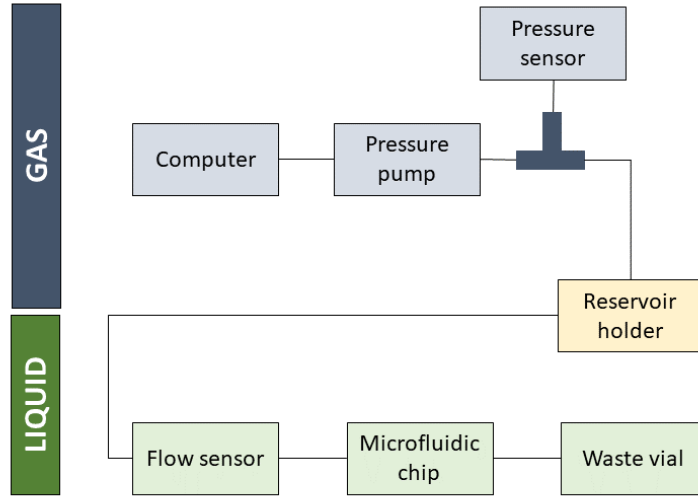


Figure 5.17: Experimental setup to experimental measure the channel height based on pressure and flow rate. The pressure pump is either a commercial or open-source system. The pressure sensor is TE Connectivity U536D-H00015-001BG. The flow sensor is Sensirion SLG-1430.

The resistance is calculated using the measured pressure and flow rate as per Equation 5.2. The values are averaged over a period of long period to reduce uncertainties. When the outlet is at atmospheric pressure, the pressure difference is then the pressure applied at the inlet.

$$\Delta P = R_{hyd} \cdot Q \quad (5.2)$$

where ΔP is the pressure difference [Pa], R_{hyd} is the hydraulic resistance [$Pa \cdot s/m^3$], and Q is the flow rate [m^3/s].

The experimental setup for the experimental measurement of the channel height is illustrated in Figure 5.17. The combination of the pressure sensor and flow sensor measurements, and Equation 5.2 determines the measured resistance. Then, the height is retrieved through the established analytical equation for the hydraulic resistance of a single liquid flowing through micro-channels. The tubing for the liquid between the reservoir holder and the waste bottle contributes negligibly to the resistance of the network; the inner diameter of 0.030" is comparatively much larger than the microfluidic chip channel.

Image processing

The stability of the pressure pump for microfluidic applications is evaluated based on the consistency of the volume of the generated droplets. The individual droplet volume is calculated from the top-down area and perimeter as per Equation 5.3 [287]. This equation takes into account the gutter region filled with the continuous phase surrounding the droplet and the curvature of the interface.

$$V_{droplet} = h \cdot A_{2D} - 2\left(\frac{h}{2}\right)^2 \left(1 - \frac{\pi}{4}\right) l_p \quad (5.3)$$

where $V_{droplet}$ is the volume occupied by the droplet in the squeezing regime [m^3], h is the channel height [m], A_{2D} is the top-view area of the droplet [m^2], and l_p is the perimeter of the A_{2D} area [m].

For the image acquisition, the camera used is the *Zyla 5.5 sCMOS* camera from *Andor*. The *Nikon Ti-E* inverted microscope has the camera installed on the side-mount and a 4X objective for visualization.

The computer saves the image every 2 seconds with an exposure time of 4 milliseconds. The recording period for each series of settings is approximately three minutes for a total of 90 images. The field of view is maintained at the same position throughout the test in order to maintain a static background for post-processing. The exact overlap of the background with each frame allows removing the static elements. An example of a recorded frame is shown in Figure 5.18.

Each frame is processed in two steps first using *ImageJ* and then, *Matlab*. A macro script in *ImageJ*—an open-source image processing software—prepares the images by removing the background and by extracting solely the droplet outline. The process is broken down in steps in Figure 5.19. Then, the binary image is imported in *Matlab* for further processing to obtain the top-down area and perimeter.

The *Matlab* processing takes the binary image output from the *ImageJ* script (see Figure 5.19(f)), and generates the associated droplet area and perimeter. The steps are illustrated in Figure 5.20 for a typical droplet. For the microscope and camera setup with a magnification of 4X, each pixel corresponds to $3.3 \mu\text{m}$. This calibration value is used to convert the pixel measurements into meters for the calculation of the droplet volume in meters cubed.

Although Figures 5.18 to 5.20 demonstrate the process starting from a suitable starting image, not all screenshots collected during the 3 minutes interval are appropriate. Nonetheless, the regularity of the droplet size and space makes the automation of the process easier. One strategy to avoid outliers would be to adapt the

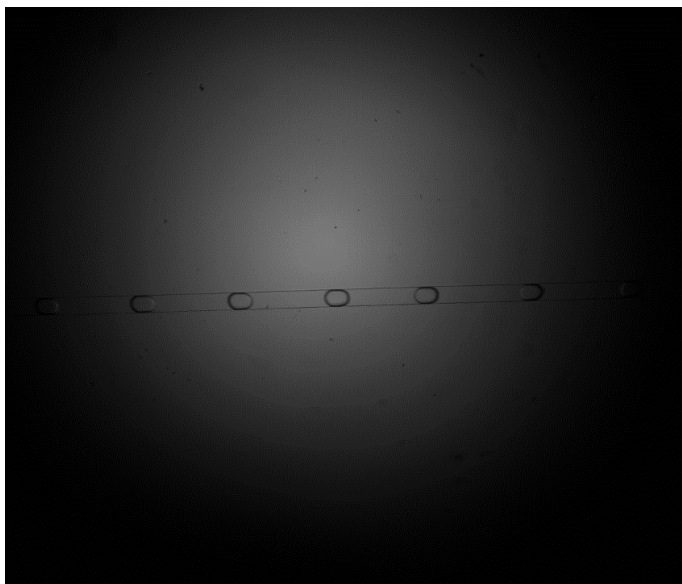
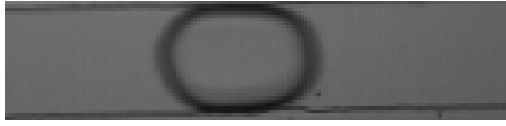


Figure 5.18: Representative frame recorded with the *Zyla 5.5 sCMOS* camera with 4 ms exposure time. Multiple droplets of nominally equal volume are captured simultaneously.

region of interest (ROI) location to each frame. However, the generation frequency and frame rate can difficultly be combined to reliably centre the (ROI) on a single droplet without any other droplets partially in the frame. Thus, the strategy adopted rather relies on the rejection of the outliers; the large data set provided by the rapid generation of droplets enables the size of the filtered data to be satisfactory. The data is selected based on the combination of perimeter and area values. A valid data point is manually selected; then, a $\pm 15\%$ variation on the area and perimeter is considered as the acceptable region. Figure 5.21 illustrates graphically the filtering process that discards the outliers.

Droplet volume comparison

The droplet volume methodology is validated through comparison to a previous dataset. The design of the experiment purposely emulates the conditions of the previously published data [100]. The difference between μ Pump and the commercial pressure pump–Fluigent MFCS-EZ–is assessed to evaluate the performance discrepancy between the open-source and commercial systems.



(a) Initial raw image, cropped (in center of the most luminous region of the field of view) and slightly rotated for a more horizontal channel.



(b) Background image rotated and cropped exactly in the same way for each frame.



(c) Background subtraction to remove channel outline and retain the droplet shape (albeit not perfectly). The contrast between the droplet contour and everything else is enhanced.



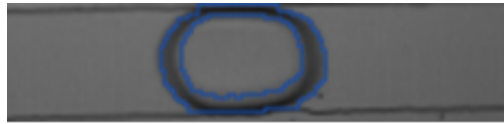
(d) Inversion of the previous image in (c) for better visibility purposes (only for documentation).



(e) Application of a threshold to retain only dark values (i.e. the droplet shape).



(f) **Erode** and **Dilate** functions to remove the noise and imperfections. This is the binary image that is further processed in Matlab.



(g) Coloured overlay of the initial cropped frame and the resulting mask (only outline shown for validation and documentation).

Figure 5.19: Automated droplet outline extraction using *ImageJ* macro scripts.

The data is presented using the dimensionless droplet volume ($V_{d,exp}^*$) and the flow rate ratio (ϕ_{exp}) calculated as per Equations 5.4 and 5.5.

$$V_{d,exp}^* = \frac{V_{drop}}{w_c^2 \cdot h} \quad (5.4)$$

where $V_{d,exp}^*$ is the dimensionless droplet volume [], V_{drop} is the dimensional droplet



(a) Filling the binary image to obtain a solid droplet with `imfill(I,'holes')`.



(b) Using the filled and outline images to extract the perimeter (`bwperim(I,8)`) and area (`bwarea(I)`) of the droplet.

Figure 5.20: Automated droplet area and perimeter extraction using *Matlab* scripts.

volume obtained from image processing and Equation 5.3 [m^3], w_c is the width of the continuous phase inlet (all inlets have the same width for this chip design) [m], and h is the channel height [m].

$$\phi_{exp} = \frac{Q_d}{Q_c} \quad (5.5)$$

where ϕ_{exp} is the experimental flow rate ratio [], Q_d is the flow rate of the dispersed phase inlet [nL/min], and Q_c is the flow rate of the continuous phase inlet [nL/min].

Moreover, the geometrical conditions, the continuous and dispersed phase, the chip material, and the squeezing regime ($Ca < 0.002$) are the same as for the previously published dataset [100]. The similar conditions ensure that the comparison is meaningful. Figure 5.22 shows a similar linear trend between the previous data, and the new data collected for both the Fluigent and μ Pump systems. The day-to-day variations are expected due to the discrepancy of the manufactured chips, and oil absorption during the priming phase. Thus, the method is validated in accordance with the previously published data.

The variations shown in Figure 5.22(b) are larger between different days than between the two systems. In other words, the data for the same day for the two systems agree well with each other. Consequently, μ Pump is validated as a pressure pump that provides similar performance to the commercial system for droplet generation in the squeezing regime.

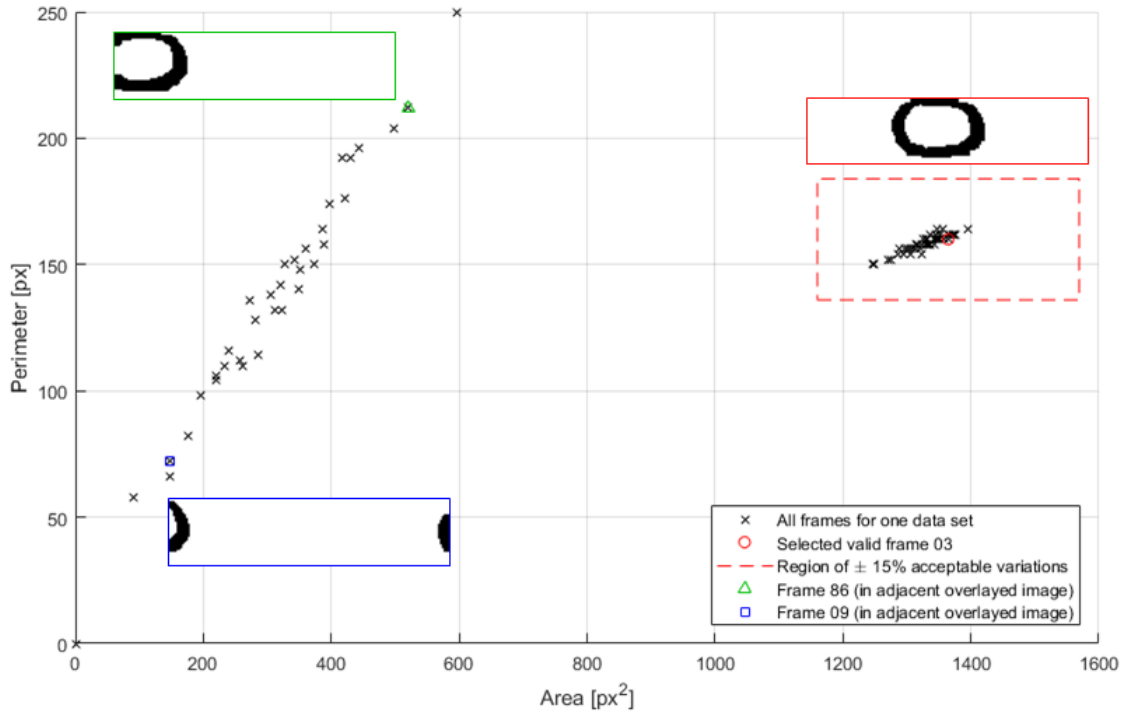


Figure 5.21: Graphical representation of the outlier rejection based on a $\pm 15\%$ variation from an identified acceptable data point.

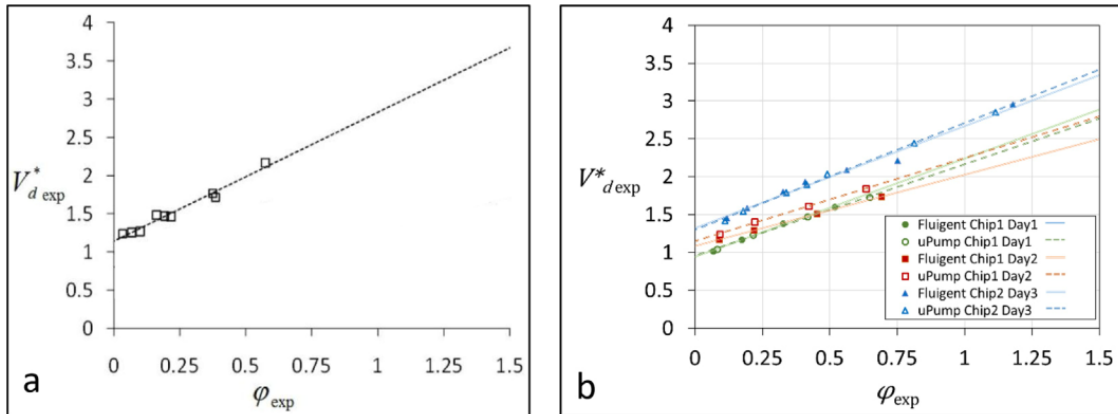


Figure 5.22: Comparison of droplet volume data. (a) Previously published data from [100]. (b) New data collected under similar conditions to compare the performance of the μ Pump system with the Fluigent MFCS-EZ.

5.5 Summary

Comparatively to syringe pumps, pressure pumps reduce both long and short term oscillations. In the microfluidic context, this is especially important to generate droplets of uniform volume. However, the cost of commercial pressure pumps is prohibitively high, especially compared to the less expensive syringe pump. Furthermore, microfluidic devices hold their greatest potential as a tool applied in a variety of other fields. Consequently, the accessibility of microfluidics influences its global impact in fields such as drug development, personalized medicine, and biochemistry. This open-source pressure pump aims to lower the financial cost and provide more flexibility for integration.

The hardware overview presented a synopsis of the system; the details including the bill of materials and assembly instructions are included with the published open-access journal article [90]. The required specifications and the characterization of the actuator are at the core of the pump design. Furthermore, the software documentation is included; the computer and *Arduino* software are explained in addition to the communication protocol between them.

The system validation experimentally determined the specifications of the μ Pump to confirm that the criteria from Table 5.1 are met. These criteria from Table 5.1 are from the Fluigent pump performance. Table 5.4 summarises the achieved specifications. The μ Pump system was furthermore validated using the volume of generated droplets. The methodology was confirmed by comparing it to a previously published dataset [101]. The comparison between the commercial system and the μ Pump open-source system (Figure 5.22) showed an insignificant difference between the droplet volume generated using either system. Thus, a similar performance than the commercial system is achieved by the open-source system. The cost of the pressure pump for microfluidic applications is reduced without compromising performance. Although the technical support from companies is sacrificed, customizability and financial accessibility are gained.

Table 5.4: Summary of pressure specifications for μ Pump.

| Pressure parameter | Value | Units¹ | Description |
|---------------------------|--------------|--------------------------|---------------------------------------------------|
| Accuracy | 0.09 | % F.S. | 1 standard deviation |
| Stability | 0.09 | % F.S. | 1 standard deviation |
| Resolution | 0.02 | % F.S. | from the 12-bit Digital-to-Analog converter |
| Settling time | < 2 | s | time to reach maximum pressure starting from 0 |

¹ % F.S. \equiv % full span

Chapter 6

Tubing dynamics

The work included in this chapter is published: **M. Hébert**, W. Baxter, J. P. Huissoon, and C. L. Ren, A quantitative study of the dynamic response of soft tubing for pressure-driven flow in a microfluidics context, *Microfluidics and Nanofluidics*, 24 (2020), pp. 113 [110].

DOI: 10.1007/s10404-020-02396-6

W. Baxter (Intern in the Waterloo Microfluidics Laboratory (WML) at the University of Waterloo) worked on this project under the supervision of M. Hébert for one semester. They contributed to the software and resources used for the experiments. More specifically, they designed and put together the pressure measurement apparatus and custom reservoir holder.

M. Hébert provided supervision throughout the project. Their other major contribution is conceptualization, data curation, formal analysis, investigation (performing the experiments), methodology, project administration, software development, validation, and writing (at all stages).

6.1 Overview

Microfluidics typically uses either a syringe pump that regulates the flow rate in microchannels or a pressure pump that controls the inlet pressures to drive the flow. In the context of pressure-driven flow, a reservoir holder containing liquid samples is normally used to interface the pressure pump with the microfluidic chip via soft tubing. The tubing connecting the pump and holder transports the pressurized

air while the tubing connecting the holder and chip transports the liquid samples. The pressure output from the pump is usually assumed to be stable and the same as that applied to the liquid in the chip; however, in practice, this assumption is often incorrect and may negatively impact chip performance. This assumption is critically challenged when applied to microfluidic chips involving dynamic control of fluids since the pressures are constantly varied (at > 10 Hz). This study presents a method for investigating, quantifying and modelling the pump stability and the dynamics of the air tubing using two pressure sensors. The relationship between the pressure output from the pump and the reservoir holder pressure is generalized as a first-order linear system. This relationship allows the software that controls the pressure pump to output the required pressure to the reservoir holder and thus to the microfluidic chip. These results should significantly improve the performance of microfluidic chips using active fluid control, and may also benefit passive fluid control applications.

Microfluidics, Active control, Tubing, Dynamic response, Pressure-driven flow

6.2 Introduction

6.2.1 Microfluidics context

Microfluidics deals with fluid flow at the micrometre scale. This enabling technology has been applied in a wide range of fields such as biological assays [52, 12, 13], material synthesis [298, 299], biofuels [25], drug screening [248], and many more. Droplet microfluidics is a subset of microfluidics that considers monodispersed picoliter- to nanoliter-sized droplets as reaction vesicles. The immiscibility of the two phases in combination with good wetting conditions (meaning that one fluid preferably wets the channel surface) allows the isolation of the dispersed phase droplets (typically water) within the continuous phase fluid (typically oil). Hence, the chemical reactions designed to occur in the droplets are confined, minimizing cross-contamination and enhancing mixing. Other major advantages of using microfluidics include reduced reagent consumption and shortened reaction time.

Generally, droplet manipulation methods are categorized as either passive or active. Passive approaches generally rely on microchannel network arrangement, geometry, and applied pressures or flow rates to achieve the desired droplet manipulations. Active methods use external forces to better control the fluid. Although there exists

a wide variety of methods to drive the flow for both passive and active microfluidic solutions, the syringe pump and pressure pump are the most widely utilized.

A syringe pump is generally more lenient than a pressure pump in terms of microfluidic chip design [101]; however, the performance is compromised due to inherently long-term persistent transient behaviour [159]. Additionally, a pressure pump responds much faster than a syringe pump when a change in setpoint is required [149]; thus, pressure pumps exhibit desirable behaviour both on short and long timescales. The short-term dynamics are especially important for active microfluidics that involves frequent adjustment of the applied pressures to the chip.

6.2.2 Motivation

A novel method has been developed for active manipulation of droplets in a microfluidic platform without the use of external components such as electrodes [308, 111]. Central to this method is a controller that calculates the pressures that must be applied to the chip inputs to achieve the desired manipulation of the droplets. This controller design uses a fluid dynamics model to issue pressure pump commands multiple times per second. It requires fast actuation and a pump that can provide rapid pressure adjustments.

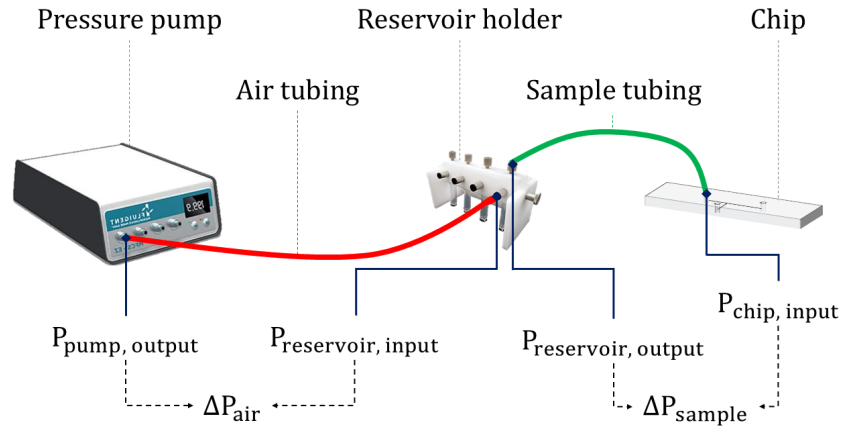


Figure 6.1: Overview of the typical setup for pressure-driven flow. The focus of this study is on the difference in pressure for the air tubing (ΔP_{air}). The tubing carrying the liquid sample is already considered in the model (ΔP_{sample}) from previous work [308, 111].

Although a pressure pump provides key advantages for active manipulation of droplets, the associated setup requires an interface between the pressurized air from the pump and the fluid to be driven in the chip; this is achieved by the so-called reservoir holder. Figure 6.1 schematically represents the setup. Flexible tubing is used to connect the pressure pump outlets to the reservoir inlets to transport the pressurized air. Secondary tubing transports the liquid sample from the reservoir holder outlet to the microfluidic chip. The performance of this active method for droplet manipulation can be challenged due to the dynamic difference between the output pressures specified by the controller and the applied pressures to the chip, $P_{pump,output} \neq P_{chip,input}$. This issue has not been so much of a concern for passive methods, which do not require fast pressure actuation. These dynamic differences in command and actual at-chip pressures are due to a combination of components: the communication between the controller and pump; the response of the pump; the dynamics of the air tubing; and the dynamics of the liquid sample tubing. The communication delay is very small in comparison to the mechanical dynamics, and we assume this is negligible. The liquid sample tubing has a much higher resistance and modulus than the air tubing, and so we assume that this is also negligible. The dynamic response of the pump is typically in the vicinity of 100ms, and the dynamics of the air tubing are unknown. This study thus focuses on investigating the dynamic behaviour of the air tubing and the pressure pump and quantifying the deviations from the requested pressures and the pressures applied to the chip. Understanding these dynamic behaviours is not only useful to improve the performance of the active controller by including these in the controller model, but also highly beneficial to other active microfluidic methods that involve the use of pressure pumps.

6.2.3 Literature overview

While there exists pertinent literature, the context differs sufficiently to justify the investigation of the case under study on its own. The two closest comparable applications are transmission lines for unsteady pressure measurement, and blood flow in arteries; these will be elaborated below.

The system of differential equations that accurately describe the physical system is too complex to have a useful analytical solution. The 1mm thick tubing falls within the thick-walled cylinder classification based on its ratio to the inner diameter: $d_i/t_h = 1 < 40$, [256]. The relationship between inner pressure and radial strain for thick-walled tubing is available in the literature [256]; however, measuring the radial strain of the small tubing (i.e. 1 mm inner diameter and 3 mm outer diameter)

is experimentally challenging. Consequently, the experimental approach with two pressure sensors is favoured; the pressure drop over the air tubing can be accurately measured and incorporates the effects of the radial strain.

Transmission lines for unsteady pressure measurement

The dynamic response of transmission lines for pressure measurement is of interest when considering unsteady phenomena. By using a lumped parameter model, the gas is assumed to move as a unit rather than as a wave. The soundness of this assumption can be gauged by comparing the tubing length to the wavelength based on the speed of sound in the medium. Either way, the finite propagation speed within the tubing entails a time delay. Considering a tubing length of 50 cm and the physical properties of air at room temperature, the corresponding delay from the propagation is on the order of 1 ms. The spring and inertia are represented using a second-order model with the following damping ratio and natural frequency that fully characterizes the system response [67].

$$\zeta = \frac{64\mu L^2}{\pi d_t^4 \sqrt{\gamma P \rho}} \sqrt{0.5 + V/V_t} \quad (6.1)$$

$$\omega_n = \frac{\sqrt{\gamma P / \rho}}{L \sqrt{0.5 + V/V_t}} \quad (6.2)$$

where ζ is the damping ratio [], ω_n is the natural frequency [rad/s], μ is the dynamic viscosity [$kg\ m^{-1}s^{-1}$], L is the tubing length [m], d_t is the internal diameter [m], γ is the heat capacity ratio [], P is the pressure [Pa], ρ is the density [$kg\ m^{-3}$], V is the pressure sensor dead volume [m^3], and V_t is the tubing volume [m^3].

Note that the dependence of the parameters on pressure means that such a lumped parameter model is valid only for small pressure changes. However, the more significant limitation in the application of this model stems from the derivation that hinges upon the rigidity of the walls. Such an assumption fundamentally disagrees with the soft tubing under study.

Blood flow in arteries

The study of the flow of blood through our arteries couples the fluid flow with the wall deformation under pulsatile conditions from the heartbeat. Modelling and an-

alyzing this phenomenon helps to understand the mechanism behind cardiovascular conditions for instance.

The relative scale of the arteries inner and outer diameter allows simplifying the problem by making thin-walled assumptions [32]. However, the dimensions of the air tubing do not allow such simplifications; the inner diameter and wall thickness are of the same order of magnitude. Therefore, thin-wall assumptions are deemed unreasonable.

System of differential equations

The air tubing can be described using a system of differential equations. The coupling between the fluid flow and the wall deformation can hence be represented [14]. Although the equations accurately characterize the physics, the lack of simple analytical solutions renders them impractical.

$$\frac{-\partial Q}{\partial x} = \frac{\partial A}{\partial t} \quad (6.3)$$

$$-\frac{1}{\rho} \frac{\partial P}{\partial x} = \frac{\partial u}{\partial t} + \frac{8\pi\nu}{\rho A} u \quad (6.4)$$

$$P = P_{ext} + \frac{1}{C_0} \left(V - V_0 + \frac{D}{E} \frac{dV}{dt} \right) \quad (6.5)$$

where

$$C_0 = \frac{2\pi L r_0^3}{E h_0}, \quad (6.6)$$

and Q is the volumetric flow rate [$m^3 s^{-1}$], x is the coordinate axis along the longitudinal direction [m], A is the tubing cross-section area (circular) [m^2], t is time [s], ρ is the density [$kg m^{-3}$], P is the internal pressure [Pa], u is the velocity along the x direction [$m s^{-1}$], ν is the dynamic viscosity [$kg m^{-1} s^{-1}$], P_{ext} is the external (atmospheric) pressure [Pa], V is the volume [m^3], V_0 is the initial volume [m^3], D is the material damping modulus [Pa], E is the material elastic modulus [Pa], L is the tubing length [m], r_0 is the initial outer radius [m], h_0 is the initial wall thickness [m].

Thick-walled tubing deformation

The radial strain without considering the viscoelastic behaviour of the tubing (i.e. constant elastic modulus) is given in a textbook (e.g. [256]).

$$\epsilon_r = \frac{P}{E} \left(\frac{r_o^2 + r_i^2}{r_o^2 - r_i^2} + \nu \right) \quad (6.7)$$

where ϵ_r is the radial strain [], P is the internal tubing pressure [Pa], E is the tubing elastic modulus [Pa], r_o is the outside tubing radius [m], r_i is the inner tubing radius, and ν is the tubing material Poisson ratio [].

While a relationship between the radial strain and the inner pressure is available, the measurement of the tubing expansion is challenging with off-the-shelf strain sensors; the outer tubing diameter is only a few millimetres. A novel approach to measure strain using dispersed graphene in a soft silicone matrix was investigated ([26], goophene technical note). The results were unfortunately not promising enough to further the efforts in implementing such a novel strain sensor. The signal noise and intrinsic strain sensor dynamics were the main obstacles. Furthermore, as the results will show, the tubing dynamics are of first-order rather than second order. The two pressure sensors used are deemed to be sufficient for the experimental approach.

6.2.4 Pressure-driven flow actuation dynamics

The dynamics of the actuation system can be separated into two parts: the pump dynamics and tubing dynamics. As conceptually illustrated in Figure 6.2, the pump dynamics characterizes the time response from the requested pressure (P_{req}) to the pump output ($P1$) while the tubing dynamics occurs from the pump output ($P1$) to the reservoir holder ($P2$). The reservoir holder pressure quantifies more faithfully the pressure applied to the fluid tubing inlet than the pressure at the output of the pump. Nonetheless, using the pressure pump output as the intermediary point allows analyzing the pump and tubing dynamics independently.

The tubing dynamics are investigated systematically by varying inner and outer diameters, length, material, and reservoir holder vial volume. The pump dynamics is considered for the commercial system *MFCS-EZ* available from *Fluigent* and the custom in-house pressure pump, μ Pump [90].

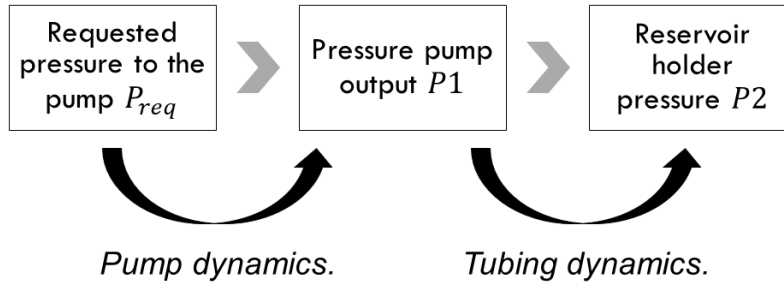


Figure 6.2: Separation between pump and tubing dynamics.

6.2.5 Overview of this study

The objective of this study is to experimentally quantify the dynamics of the soft tubing and develop the associated models. These models can be used to predict the actual pressure applied to the microfluidic chip for fluid pumping. The availability of such models is impactful on microfluidic studies under pressure-driven flow where soft air tubing is often used to connect the pump output to the reservoir holder input (see Figure 6.1); the actual pressure applied to the chip is often assumed to be the pump output that is incorrect. First, a simple, yet practically useful method is presented for identifying the pressure change over the soft tubing using two pressure sensors at either end of the tubing of interest. Then, the pressure change over the soft tubing is measured under different operating conditions such as varying tubing length, material and vial volume. Following the experimental studies, a simple linear model and a nonlinear model are developed and validated to predict the system response. Finally, the performance of the models is compared and their limitations are discussed.

6.3 Experimental methods and materials

The *MFCS-EZ* and $\mu Pump$ can arbitrarily and independently control the pressure output at each of their outlets via a desktop computer software. The sampling rate is about 10 Hz (i.e. 100 ms period). The two pressure sensors at the two ends of the tubing respectively record simultaneously with 1 mbar accuracy every 1 ms. The data is post-processed using *Matlab* to fit a first-order model.

6.3.1 First order model fit

The pressure data recorded provides the information about the system in the time-domain; however, the dynamics of a system is rather characterized in the frequency domain ($s \in \mathbb{C}$) and expressed as a transfer function ($G(s)$). The transfer function is the ratio of the output ($Y(s)$) over the input ($U(s)$). A general model of the first order can be fully characterized by the scaling constant (k) and the time constant (τ). In response to a step input, the output is about 63% of the steady value after one time constant and about 98% of the steady-state value after four time constants [49].

$$G(s) = \frac{Y(s)}{U(s)} = \frac{k}{\tau \cdot s + 1} \quad (6.8)$$

The *Matlab* function `tfest` is used to find the transfer function with no zeros and one pole (i.e. first order as per Equation 6.8) that best fits the data. The first order is selected because of the minimal response overshoot and to keep it simple for easier integration within control designs for instance.

6.3.2 Pressure sensors

Pressure sensor specification

The specifications for the two identical pressure sensors used are summarized in Table C.1. The manufacturer datasheet accuracy is $\pm 0.1\%$ F.S. Therefore, in order to match the ± 1 mbar accuracy of the *Fluigent* pump output, the range is limited to 1 bar although the pressure pump has a range up to 2 bars. Note that each pressure sensor is provided with a factory calibration to accurately convert its voltage output to gauge pressure.

The resolution of the measurements is determined by the smallest voltage increments and should be less than the targeted accuracy level. The *Arduino* communicates via a SPI protocol to an external analog-to-digital converter (ADC) with 12-bit resolution (*Microchip MCP3202*). An accurate voltage reference provides the constant 5 V supplied to the ADC (*Maxim Integrated MAX6250*). The sampling is achieved at 1 ms intervals (i.e. 1 kHz) through the use of interrupts on the *Arduino* to ensure proper and consistent data collection while continuously sending the data to the computer via USB. The 1 ms interval is selected based on the propagation of a pressure wave at the speed of sound through the media.

Pressure sensor location

The choice of location for the two pressure sensors aims to accurately measure the pressure at either end of the tubing. The additional components are shown in green in Figure 6.3. The junctions connecting the pressure sensors to the normal setup are rigid (i.e. steel). Note that a custom reservoir holder had to be manufactured to add the fourth port to measure P2. This approach was preferred than inserting a junction at one of the other reservoir holder port because of its lesser impact on the flow.

The minimum time resolutions of the junctions added to the system are thoroughly assessed. Details are presented in the supplementary material S1. Based on the results of the assessment, the minimum time constant that can confidently be investigated using the junctions is 10 ms.

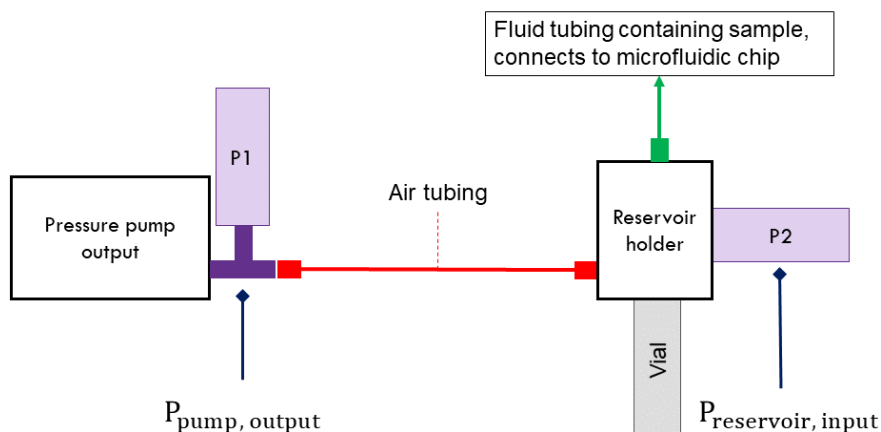


Figure 6.3: Experimental setup to measure the impact of the air tubing dynamics (ΔP_{air}). Two pressure sensors are strategically located to measure the pressure at either end of the air tubing with minimal impact.

6.3.3 Tubing materials and dimensions

The various tubing materials and dimensions investigated are summarized in Table 6.2. The microfluidic pressure pumps and reservoir holder typically use barbed connections. The *MFCS-EZ* from *Fluigent* comes equipped with 1 X 3 mm tubing. Nonetheless, the barbed connections are also functional for the closest imperial

Table 6.1: Specification summary for the pressure sensors (*TE Connectivity U536D-H00015-001BG*).

| | |
|-------------------|--------------|
| Range | 0 to 1 bar |
| Accuracy | ± 1 mbar |
| Resolution | 0.24 mbar |
| Sampling | 1 kHz |

equivalent that has an inner diameter of 1/16" (~ 1.59 mm). The variety of materials for the metric size is more restricted. Hence, the different materials are investigated in the imperial size only.

The elastic modulus of each material is experimentally determined using a straightforward approach with a ruler and suspended weights. The details and the plot are presented in the supplementary material S2.

Table 6.2: Details of the materials and dimensions of the various tubing.

| ID X OD | Wall thickness | Material label | $E^{(1)}$ [MPa] |
|-------------------------------------------------|-----------------------|-----------------------|-----------------------------------|
| 1 X 3 mm ⁽²⁾ | 1 mm | Medium silicone | 4 |
| 1/16" X 1/8" ⁽³⁾ (1.59 X 3.18 mm) | 1/32" (0.79 mm) | Soft silicone | 1 |
| | | Medium silicone | 4 |
| | | Hard Tygon | 7 |

⁽¹⁾ Elastic modulus. See Figure 6.13 for experimental strain-stress curve with linear fit. Uncertainties: ± 0.5 MPa.

⁽²⁾ Length [cm]: 20.4, 30.2, 30.1, 50.3, 66.5

⁽³⁾ Length [cm]: 66.5

6.4 Results and discussion

As shown in Figure 6.2, the system dynamics is separated into the pump dynamics and the tubing dynamics. The results supporting this separation are presented in the supplementary material. The rest of the results is separated into these two main sections before addressing model validation, and finally, limitations.

6.4.1 Pump dynamics

The control strategy previously implemented neglects the dynamics introduced by the soft tubing and the actuation when adjusting the requested pressure [308]. The controller design relied solely on the model of the plant (i.e. the microfluidic chip and fluid tubing), hence excluding the pump and air tubing. The requested pressure to the pump was assumed to instantly correspond to the pressure at the fluid tubing inlet in the vial at the reservoir holder. These dynamics were shown to be reasonably neglected for the current running rate of the system at 10 Hz. Nevertheless, better understanding the short-term actuation dynamics is critical to increasing the controller performance; furthermore, increasing the system sampling rate would magnify the impact of the short-term actuation dynamics and challenge the controller performance.

Note that there are limitations due to the “black-box” nature of commercial products such as *Fluigent’s MFCS-EZ*. Moreover, the implementation of such active control platform on regular desktop computers limits the consistency of the actuation delay due to scheduling handled by the operating system (*Windows*). The pump dynamics is determined as per Equation 6.8. The input is the requested pressure and the output is the pump output pressure ($P1$).

Fluigent

The commercial nature of the *Fluigent MFCS-EZ* pump restricts the information available concerning both the internal components as well as the controller. Consequently, it is treated as a black-box for which the requested pressure is the input and the provided pressure is the output.

The first-order model is observed to match the response fairly well for certain pressures. However, the time constant varies with respect to the pressure and displays significant hysteresis effects in the lower pressure range (see Figure 6.4). Moreover, at high pressures, the first-order model (or even a second-order model) differs significantly from the response. Note that as the pressure output will eventually match the requested pressure, the scaling constant (k) is set to one.

μ Pump

In contrast to the lack of information available for black-box commercial systems such as the *Fluigent* pump, μ Pump is a customized system designed and built in-

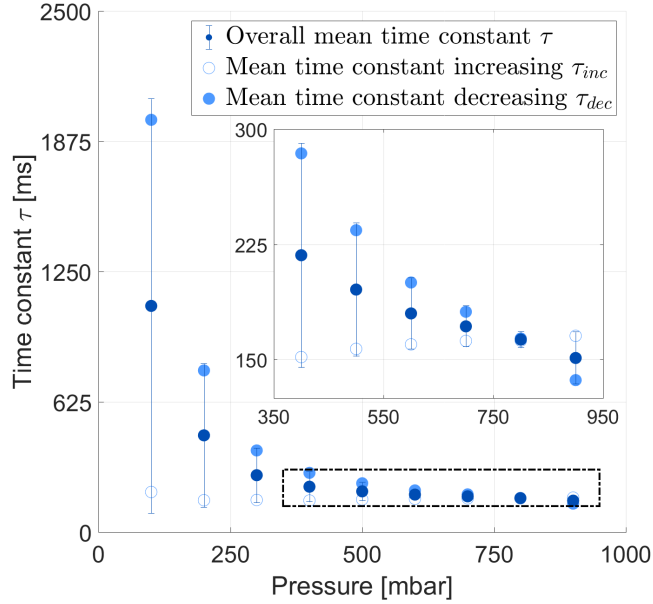


Figure 6.4: Time constant (τ) variations with pressure for the *Fluigent MFCS-EZ* pump. The error bars represent ± 1 standard deviation from the overall mean time constant.

house. All details pertaining to the hardware and the software are available [90]. The pressure output is controlled by the internal circuit of the *ControlAir* E/P transducer (*T900-CIM*).

The response follows more closely a second-order system than a first-order system due to the better-defined oscillations. Nonetheless, there appears to be a relatively slow integral component for the closed-loop controller. Thus, although the output pressure rapidly approaches the requested pressure, there is a noticeable period where the steady-state error is slowly eliminated through the integral component. Hence, the second-order model somewhat differs from the μ Pump dynamics. A crude simplification can be made to simply represent the delay in achieving the requested pressure using a first-order model. Considering that the pump will achieve its target output pressure, the scaling constant value is set to one while the time constant is shown in Figure 6.5. Similarly to the *Fluigent* pump, there are significant hysteresis effects present. However, the overall behaviour is much more constant over the pressure range. Moreover, the time constant is also generally smaller for μ Pump compared to *Fluigent*.

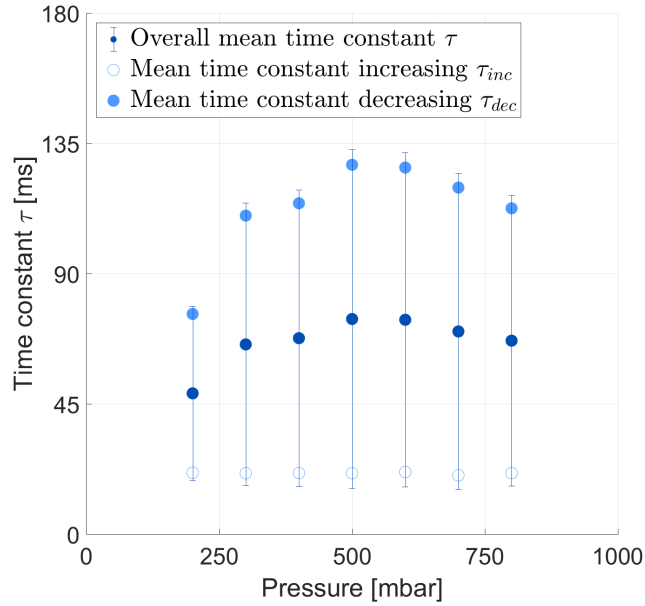


Figure 6.5: Time constant (τ) variations with pressure for $\mu Pump$. The error bars represent ± 1 standard deviation from the overall mean time constant.

6.4.2 Tubing dynamics

The previous section concerning the pump dynamics is mainly pertinent within the context of active microfluidics. The tubing dynamics, on the other hand, is relevant to both passive and active microfluidics. The tubing dynamics is determined as per Equation 6.8. The input is the pump output pressure ($P1$), and the output is the tubing end at the reservoir holder inlet ($P2$).

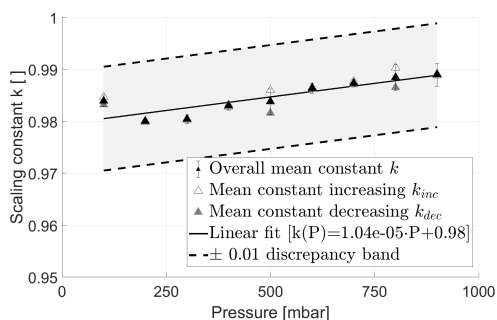
Pressure variations

As previously indicated by the literature about unsteady pressure measurement, the dynamic behaviour of the tubing is expected to depend on pressure.

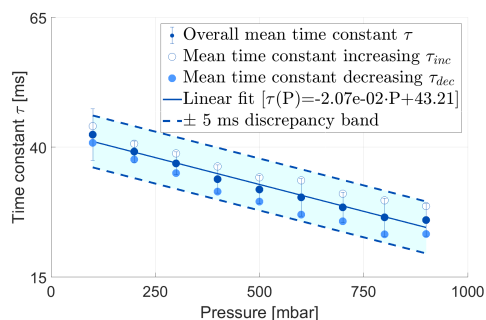
The scaling constant (k) exhibits dependence on the pressure as shown in Figure 6.6(a); however, there is no significant difference whether the pressure is increasing or decreasing. As opposed to the time constant that considers short term transients, the scaling constant characterizes the steady-state that is less prone to hysteresis effects. The value is close to but slightly less than one. This is attributed to the pressure

difference between the tubing ends that is required to drive the flow. Considering that the difference in pressure is proportional to flow rate [31], the value of the scaling constant (k) is expected to decrease with increasing flow.

For the metric 1X3 mm tubing, the time constant variations with pressure are shown in Figure 6.6(b) for both increasing and decreasing pressure. The time constant for increasing pressure is consistently larger than the one for decreasing pressure. This is attributed to the compliance of the tubing. When the pressure is increased, part of the air flows in the outward radial direction to rationalize the increase in diameter. Moreover, from an energy analysis perspective, the expansion of the tubing requires some energy that is then stored as elastic energy in the expanded tubing. When the pressure is decreased, the tubing contracts back to a smaller diameter. The elastic energy that was stored in the wall is transferred back to the flow. Thus, the energy exchange from the flow to the wall elasticity and vice versa results in hysteresis effects for the time constant (τ).



(a) Scaling constant k .



(b) Time constant τ .

Figure 6.6: Experimental quantification of first order dynamics over the pressure range for the 1X3 mm medium silicone tubing of 66.5 cm length and 2 ml vial volume. The trend of the decreasing and increasing data shows the hysteresis effects. The time constant is consistently smaller for decreasing pressure compared to increasing pressure. The error bars represent ± 1 standard deviation from the overall mean constant.

For the imperial tubing, different tubing materials are investigated. However, the dynamics are too fast to be captured accurately by the experimental setup, as shown in Figure 6.7. All materials exhibited a behaviour with time constants less than 10 ms. Compared to the metric tubing, both the inner diameter and wall thickness vary due to the restricted availability of sizes; nonetheless, the faster

dynamics is attributed to the larger inner diameter rather than the thinner wall. The wall thickness influences the tubing expansion and hence, the change with respect to pressure; the nominal starting inner diameter at zero pressure determines the time constant scale. Figure 6.6 shows such decreasing time constant value with increasing diameter (i.e from the increased expanded tubing diameter).

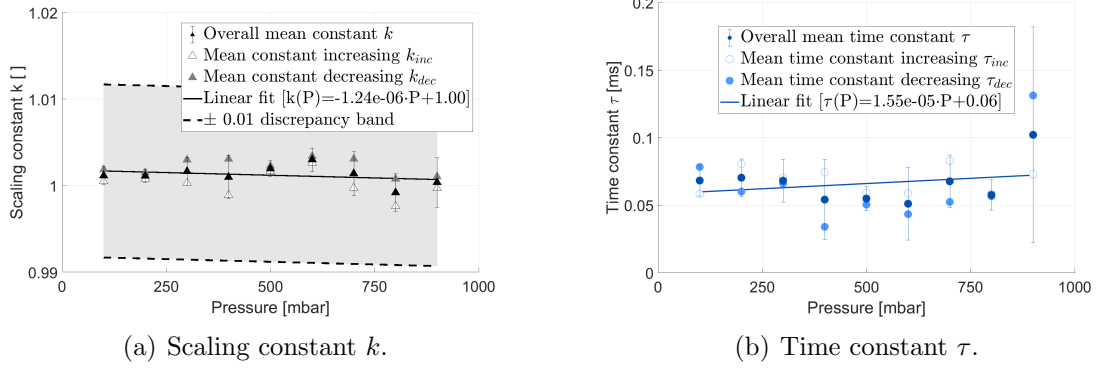


Figure 6.7: Experimental quantification of first order dynamics over the pressure range for the 1/16" X 1/8" medium silicone tubing of 66.5 cm length and 2 ml vial volume. Similar results are obtained for all three materials (Table 6.2). The time constant is too small to accurately quantify with the current experimental setup. The error bars represent ± 1 standard deviation from the overall mean constant.

Length variations

The time constant is expected to get smaller with the tubing length. The longest length of 66.5 cm for the imperial tubing has a time constant already too small to accurately quantify; thus, only the metric tubing is considered henceforth. The results of the linear fit for the tubing time constant for different lengths are presented in Figure 6.8. The scaling constant is not significantly affected by the change in length and thus is omitted.

The details of the linear fit are included in Table 6.3. The general trend is for the time constant to increase with increasing length as expected.

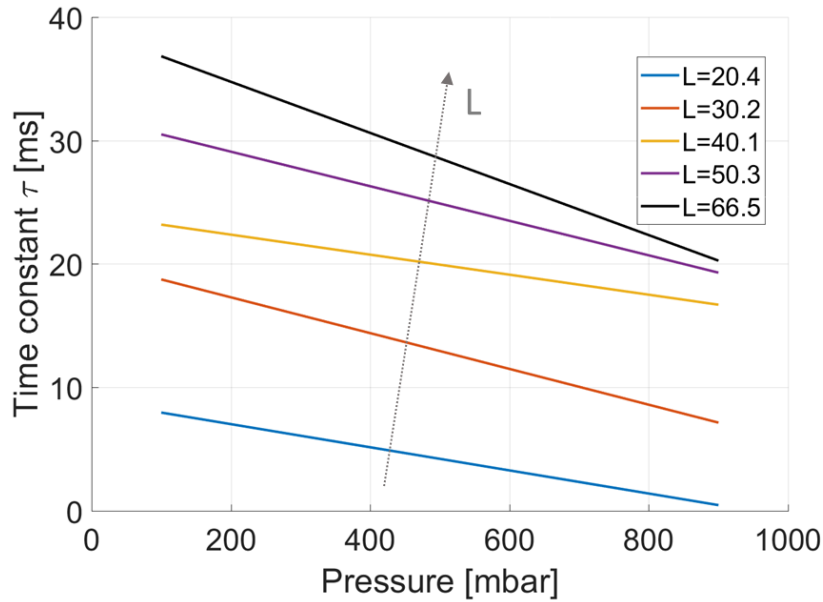


Figure 6.8: Summary of the time constant (τ) fit for different lengths. Tubing dimensions of 1X3 mm. The detailed data is presented in Table 6.3.

Vial volume variations

Similar to the length variations, the vial volume variations only take into account the metric tubing. The vial attached to the reservoir holder contains the sample to be injected into the microfluidic chip. The small quantities required to perform the manipulations at the microfluidic scale entails small changes of the sample volume in the vial. However, variations over long periods of time as well as in the initial volume when filling the vial can potentially lead to changes in the dynamics. The significance of these changes is herein assessed.

The different volumes investigated for the vial are approximately: 0.3 ml, 1 ml, and 2 ml. The results for length variations previously presented all considered the 2 ml vial volume (i.e. empty vial). The relationship for the scaling constant (k) does not vary significantly with volume. However, the time constant relationship does change more significantly depending on the volume of the vial. Nevertheless, the change of the time constant over the full volume and pressure range is reasonably small. The linear fit is mainly at the same time constant scale as shown in Figure

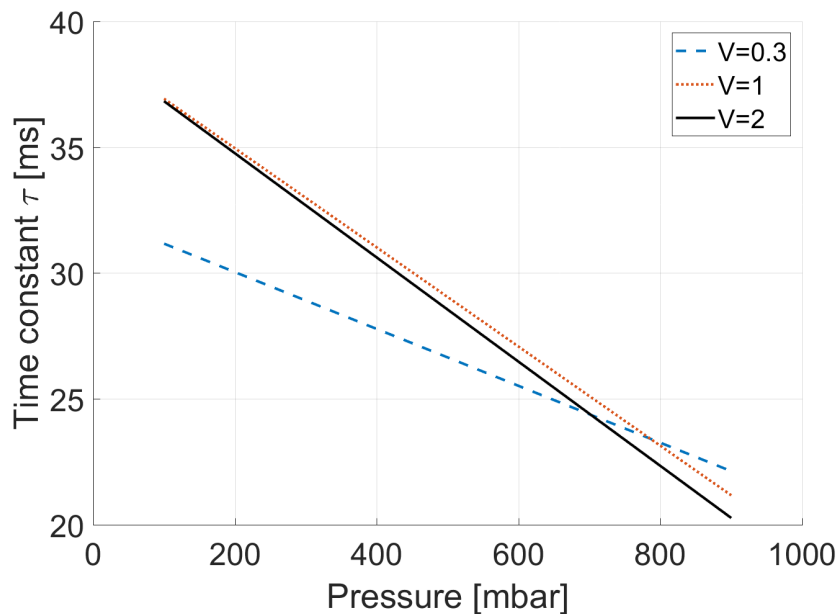


Figure 6.9: Summary of the time constant (τ) fit for different volumes (ml). Tubing dimensions of 1X3 mm. The detailed data is presented in Table 6.3.

6.9. Hence, volume variations are neglected.

Tubing dynamics results summary

The experimental setup can only confidently quantify tubing dynamics with a time constant larger than 10 ms. All results for the 1/16"X1/8" tubing are faster; hence, they are not quantified. Nonetheless, such fast dynamics is considered to be negligible within the microfluidic pump context. Consequently, only the dynamics for the 1X3 mm tubing are herein summarized. Generally, the value for the scaling constant (k) is considered constant as it weakly depends on pressure.

As for the time constant (τ), the results for the different lengths and volumes are summarized in Table 6.3. As previously mentioned, although there are some variations for different vial volumes (over the 1.7 ml range), they are deemed negligible. The overall tubing length affects much more significantly the time constant. Furthermore, the tubing length can easily be measured and maintained constant whereas the vial volume is expected to vary while the experiments are performed.

Table 6.3: Summary of the variations in the time constant (τ) depending on tubing length (Figure 6.8) and vial volume (Figure 6.9) for 1X3 mm tubing.

| Tubing length [cm] | Vial volume [ml] | Time constant $\tau(P)$ [ms] | |
|---------------------|------------------|--------------------------------------------------------------|---------------------|
| | | $a_\tau^{(1)}$ [ms · mbar ⁻¹ × 10 ⁻³] | $b_\tau^{(2)}$ [ms] |
| 20.4 ⁽³⁾ | 2 | -9.37 | 8.9 |
| 30.2 | 2 | -14.5 | 20.2 |
| 40.1 | 2 | -8.11 | 24.0 |
| 50.3 | 2 | -14.0 | 31.9 |
| 66.5 | 2 | -20.7 | 43.2 |
| 66.5 | 1 | -19.7 | 38.9 |
| 66.5 | 0.3 | -11.3 | 32.3 |

⁽¹⁾ a_τ is the slope of the linear fit.

⁽²⁾ b_τ is the intercept of the linear fit.

⁽³⁾ The associated dynamics are too fast to reliably quantify.

6.4.3 Validation

Repeatability for k and τ

The repeatability of the experimental quantification of the scaling and time constants is assessed by alternating between two pressures. The data is averaged over three datasets each consisting of 10 increasing steps and 10 decreasing step responses. The repeated results are summarized in Tables 6.4 and 6.5.

The data obtained from the successive steps (previously in Figure 6.6, the first two data points) is compared against the results of the repeated test. The time constants all match within the time resolution of the system (i.e. 1 ms). The scaling constant shows more variations between the single and repeated data for the 200 mbar setpoint. However, the discrepancy is within 3%; therefore, it is not considered significant.

Model verification

Two models are used for verification: linear and nonlinear.

Table 6.4: Repeatability summary for 100 mbar pressure set point.

| | Scaling constant (k) [] | | | Time constant (τ) [ms] | | |
|----------------------|------------------------------|-------------|-------------|-------------------------------|-------------|-------------|
| | <i>mean</i> | <i>inc.</i> | <i>dec.</i> | <i>mean</i> | <i>inc.</i> | <i>dec.</i> |
| Single data | 0.9755 | 0.9754 | 0.9755 | 41 | 44 | 38 |
| Repeated data | 0.9760 | 0.9760 | 0.9759 | 42 | 44 | 39 |

Table 6.5: Repeatability summary for 200 mbar pressure setpoint.

| | Scaling constant (k) [] | | | Time constant (τ) [ms] | | |
|----------------------|------------------------------|-------------|-------------|-------------------------------|-------------|-------------|
| | <i>mean</i> | <i>inc.</i> | <i>dec.</i> | <i>mean</i> | <i>inc.</i> | <i>dec.</i> |
| Single data | 0.9593 | 0.9595 | 0.9592 | 40 | 41 | 38 |
| Repeated data | 0.9834 | 0.9835 | 0.9833 | 41 | 42 | 39 |

The linear model (Equation 6.8) depends solely on two parameters: the scaling constant (k) and the time constant (τ). The two values are constants determined by averaging over the pressure range. The nonlinear model uses the linear fit to determine the value of the two parameters (k and τ) based on the pressure. The sensitivity of the scaling constant (k) to pressure changes is weak while the sensitivity of the time constant (τ) is more significant. The difference between the input and output pressure is fairly small at all times; furthermore, the linear relationship is fairly shallow. Therefore, the pressure used for the nonlinear model is taken as the mean of the input and output pressure ($P1$ and $P2$). This average pressure is used to calculate the time constant based on the linear fit from Table 6.3. The scaling constant is considered constant at its mean value. Equation 6.9 shows how the linear equation for the time constant ($\tau(x, u)$) is included in the linear model structure.

$$\dot{x} = \left[\frac{-1}{\tau(x, u)} \right] x + \left[\frac{k}{\tau(x, u)} \right] u$$

$$\dot{x} = f(x, u) = \left(\frac{-1}{a_\tau \cdot \bar{P} + b_\tau} \right) x + \left(\frac{k}{a_\tau \cdot \bar{P} + b_\tau} \right) u \quad (6.9)$$

where \dot{x} is the derivative of the state vector, $x = [P2]$ is the state vector, $u = [P1]$ is the input, $\tau(x, u) = a_\tau \cdot \bar{P} + b_\tau$ is obtained from the linear fit parameters from Table 6.3, \bar{P} is the mean of u and x (i.e. $P1$ and $P2$), and k is the scaling constant.

Simulink is used to simulate the nonlinear system (Equation 6.9). However, expressing such a nonlinear system concisely within the context of controller design is challenging. Hence, a pragmatic approach instead uses the simple linear first order with constant parameters for controller design.

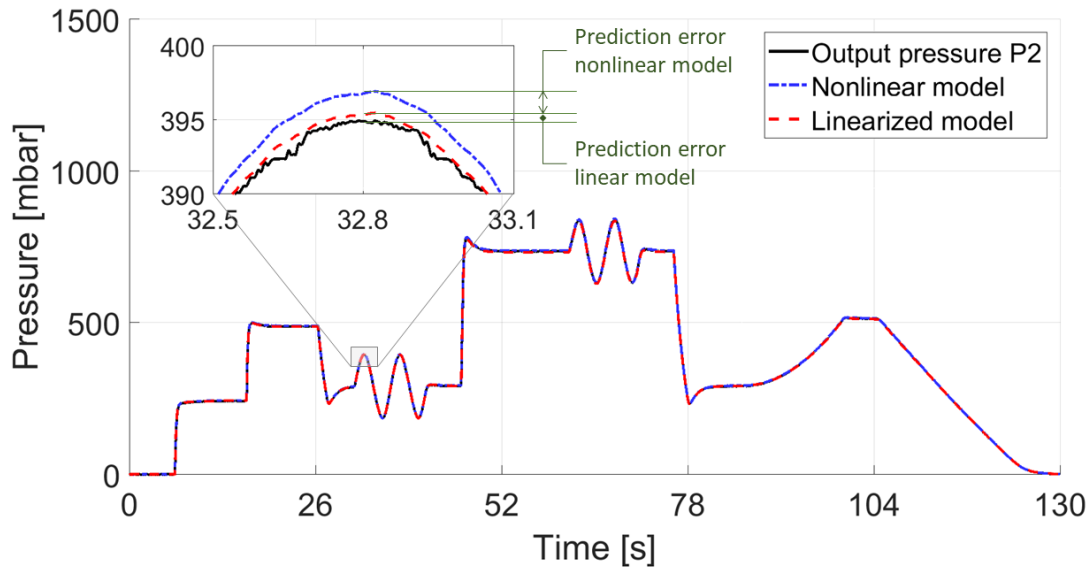
A different and more diverse pressure signal is used to assess model validity. The prediction of the full nonlinear relationship is compared to the simpler first-order linear model. The performance for the prediction is assessed using the mean square error (MSE) and the maximum error between the predicted and actual pressure output ($P2$).

$$MSE = \frac{1}{n} \sum_{i=1}^n (P2_i - \hat{P}2_i)^2 \quad (6.10)$$

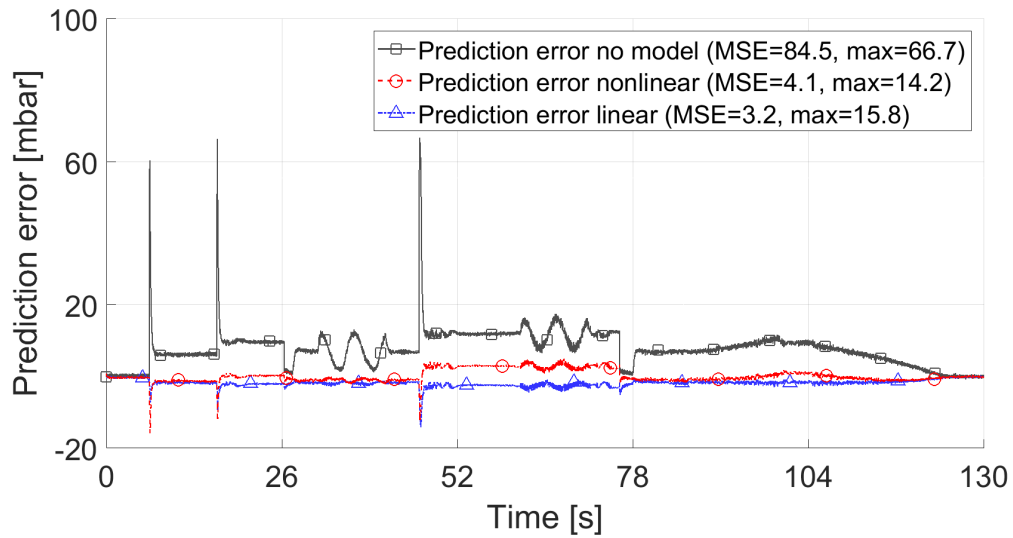
where MSE is the mean square error [$mbar^2$], n is the number of data points [], $P2_i$ is the measured pressure at the reservoir holder for the i^{th} datapoint [$mbar$], and $\hat{P}2_i$ is the predicted pressure at the reservoir holder for the i^{th} datapoint based on the measured $P1$ [$mbar$].

Figure 6.10 shows the validation signal as well as the prediction for both the linear and nonlinear models with their corresponding error. This is specifically for the 1X3 mm tubing that is 66.5 cm long and with the 2 ml vial. The slightly larger MSE and maximum error for the linear model compared to the nonlinear model demonstrates the small performance decrease that must be conceded for the simpler model. Furthermore, the difference between the two pressure sensor measurements represents the assumption that the pressure instantly propagates without any modelling involved; the MSE and maximum error are both much more significant than either of the models. Therefore, the use of the model, albeit with some assumptions and simplifications, still nevertheless improves the accuracy of the reservoir holder pressure prediction.

The first-order linear model performance for each case is summarized in Table 6.6. Their respective parameter taken as the mean are also included. Note that for the various volumes for the 66.5 cm long tubing, the same parameters are used. Nevertheless, the prediction from the model still outperforms the absence of model. Hence, this confirms the validity of the model even with varying volume, only the tubing length should be considered when determining the scaling and time constant parameter values.



(a) Output pressure P2 from the measurement, nonlinear model, and linear model.



(b) Prediction error for the output pressure P2 without a model ($P_2 = P_1$), with the nonlinear model, and with the linear model.

Figure 6.10: Model validation and comparison between no model, the nonlinear model and the simple linear model simulations. The similar MSEs show that there is not significant prediction error improvement for the more complex nonlinear model compared to the simpler linear model. (1X3 mm tubing, 66.5 cm long, 2 ml vial). Either model significantly improves upon the no-model prediction.

Table 6.6: Performance for each first order linear model for the mean parameter values based on length compared against the no-model performance.

| Tubing length [cm] | Vial volume [ml] | Linear model | | Performance criteria | |
|---------------------|------------------|--------------|--------|----------------------------------|------------------------|
| | | k | τ | $MSE^{(1)}$ [mbar ²] | $e_{max}^{(2)}$ [mbar] |
| 20.4 ⁽³⁾ | 2 | 0.99 | 4 | 1.6 | 17.9 |
| 30.2 | 2 | 0.99 | 13 | 2.3 | 12.6 |
| 40.1 | 2 | 0.98 | 20 | 3.0 | 12.4 |
| 50.3 | 2 | 0.99 | 25 | 3.8 | 15.9 |
| 66.5 | 2 | 0.98 | 33 | 3.2 | 15.8 |
| 66.5 | 1 | 0.98 | 33 | 18.2 | 11.4 |
| 66.5 | 0.3 | 0.98 | 33 | 21.0 | 11.2 |
| 66.5 ⁽⁴⁾ | 2 | – | – | 84.5 | 66.7 |

⁽¹⁾ MSE is mean squared error as per Equation 6.10.

⁽²⁾ e_{max} is the maximum error over the validation data.

⁽³⁾ The associated dynamics are too fast to reliably quantify.

⁽⁴⁾ No-model performance. (i.e. $\hat{P}2 = P1$).

6.4.4 Limitations

In general, models do not aim to fully and exactly describe a system with 100% accuracy in all circumstances. The objective is rather to develop a mathematical representation of the system with *sufficient* accuracy under certain operating conditions. In this study, the linear model is validated for pressures between 0 and 1 bar; the linear model is hence meant to be used for a pressure range from 0 to 1 bar. The pressure from the pump is changed every 100 ms (10 Hz).

The maximum actuation frequency of 10 Hz is of special note because of its larger value than the time constant range identified. The variations in time constant with pressure are likely to impact more the prediction error for a faster pressure actuation. However, the current setup frequency is mainly limited by the *Fluigent* pump proprietary software and the μ Pump E/P transducer.

The tubing length is limited between 20.4 cm and 66.5 cm as this corresponds to the range investigated. Moreover, the vial volume is varied only between 0.3 ml to 2 ml. The only tubing dimensions are 1X3 mm although other conclusions are

drawn for the larger 1/16" X 1/8" tubing that exhibited a response too fast for the measuring apparatus. Finally, although different tubing materials were investigated for the 1/16" X 1/8" tubing, no conclusive quantification could be extracted from the results. Only the soft silicone tubing was considered for the 1X3 mm as it is the most widely available materials for these tubing dimensions.

6.5 Conclusion

6.5.1 Summary

The dynamics investigation is mainly pertinent within the context of active microfluidics; short-term oscillations are much less important than long-term behaviour and stability for passive microfluidics. Nonetheless, examining the dynamics of the pump and the tubing is beneficial for both active and passive microfluidics.

On one hand, passive microfluidics aims for stability and dampened short-term oscillations that can be provided by a longer, smaller inner diameter tubing. On the other hand, active microfluidics benefits from shorter delays for the propagation of the pressure from the pump output to the reservoir holder provided by shorter and slightly bigger tubing that is the imperial tubing with 1/16" inner diameter. The dynamics of the 1X3 mm tubing for various lengths operated between pressures of 0 bar to 1 bar and volumes from 0.3 ml to 2 ml can be approximated using a first-order model; the parameters are summarized in Table 6.6. Such a first-order linear model is shown to improve the prediction error compared to the absence of any model. Moreover, the complexity of the nonlinear model only marginally improved the performance and hence, is deemed unnecessary.

6.5.2 Future work

The relationship between the pump output and reservoir holder pressure can be included within the previous control design strategy [308] to enhance performance. The addition of the dynamics introduced by the pump response time as well as the pressure propagation through the tubing hence would eliminate the previously built-in assumption that the pressure requested is applied instantaneously to the sample tubing inlet. The consideration of the pump and air tubing dynamics can be achieved by arranging the subsystems in series: pump, air tubing, and microfluidic chip. For the state-space modelling, this results in matrix concatenation.

The improved model that considers the air tubing can be leveraged in a grey-box system identification study. Briefly, the grey-box system identification fixes the model structure—including the air tubing—to maintain physical meaning of the identified parameters. The system identification algorithm requires the input (pressure) and output (droplet position) to be recorded while a droplet moves within the channel. The model structure used is essential to the quality of the results obtained. The inclusion of the tubing dynamics within the model is envisioned to enable a better description of the physical system. Thus, the results obtained from the system identification algorithm would be more narrowly distributed.

Furthermore, a more detailed analysis of the behaviour of the two different pumps would help to determine a model describing their behaviour better than the crude first-order linear model herein presented. The behaviour could be better represented by a second-order system for instance. Increasing the complexity would enable a more accurate model. Moreover, the significant hysteresis could be taken into account rather than averaged out.

Author contributions

MH participated in the conceptualization, data curation, formal analysis, investigation (performing the experiments), methodology, project administration, supervision of WB, software development, validation, and writing (at all stages).

WB contributed to the software and resources used for the experiments, more specifically, the pressure measurement apparatus and custom reservoir holder manufacturing.

JPH participated in the conceptualization, methodology, and the review and editing of the manuscript.

CLR participated in the manuscript review and editing, conceptualization, project administration, and supervision of both MH and WB. CLR also led the funding acquisition.

Supplemental material

6.6 Pressure sensor junction minimum time resolution

The pressure sensors added to the setup are connected via rigid junctions. The propagation of the pressure through these junctions is important to determine the minimum time resolution of all subsequent measurements. The measurement of the change in pressure can be approximated with a first-order model. A balloon and a pressure regulator are attached on either end of the junction at the inlet and outlet where the flow would get in and out as shown in Figure 6.11. Bursting the balloon with a sharp scalpel provides a very sharp (approximately within 0.25 ms (Tavoularis 2005) step input.

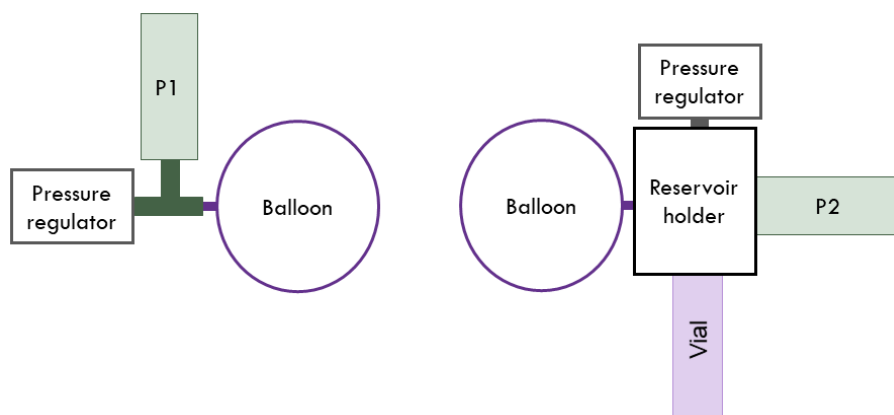
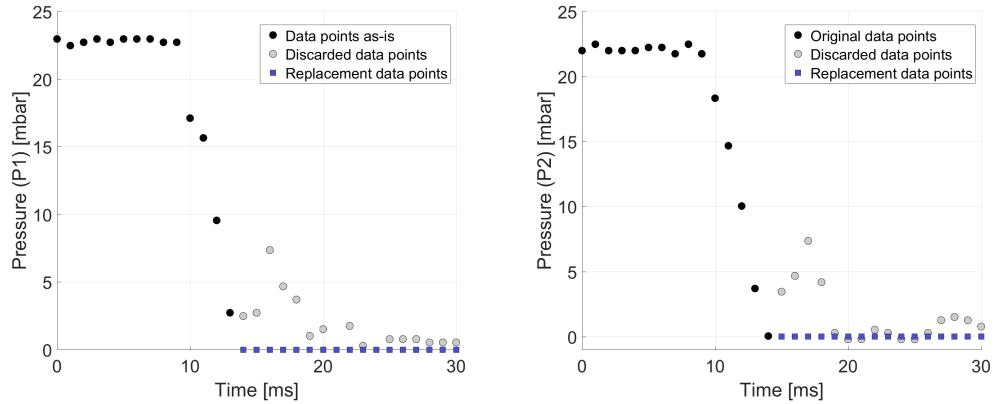


Figure 6.11: Experimental setup to determine the pressure sensor junction time resolution. The pressure regulator is manually operated to inflate the balloon. After the regulator is closed, the balloon is burst using a sharp scalpel.

The typical time response for each junction (P1 and P2) are shown in Figure 6.12. The measurements exhibit an unexpected single *rebound* after the initial drop in pressure. The source of that rise and then subsequent fall in pressure is unknown but could potentially be attributed to a pressure shock wave bouncing back or some internal dynamics of the pressure transducers themselves. For the analysis and quantification of the time constant, any points after the initial drop in pressure are treated as outliers and set to zero.



(a) T-junction at the pump output to connect the pressure sensor measuring $P1$; $\tau_{P1} = 3 \text{ ms}$.
 (b) 4-way junction at the reservoir holder to connect the pressure sensor measuring $P2$; $\tau_{P2} = 4 \text{ ms}$.

Figure 6.12: Typical response from bursting a balloon to assess the time resolution of the pressure sensor junctions.

The experimentally determined time constants are 3 ms and 4 ms for P1 and P2 respectively. Note that these values are close to the time resolution of the measuring apparatus (1 ms) and thus, they should only be considered in terms of order of magnitude. The quantification of the value aims to understand the limiting factor with respect to the time scale. Thus, any dynamic effects occurring at a timescale smaller than ~ 4 ms cannot be accurately measured with the current experimental setup. The junctions could be further optimized to reduce these delays such as by mounting the pressure sensors flush with the flow or reducing the length-to-diameter aspect ratio of the channels. Nonetheless, the current performance is deemed satisfactory as it is close to the limit of the measurement setup (i.e. 1 ms). The smallest time constant that can be measured is 4 ms; however, the threshold is rather established at 10 ms or more to ensure good confidence in the experimental results. In conclusion, any dynamics faster than this lower limit are deemed negligible.

References

S. Tavoularis. Measurement in fluid mechanics. Cambridge University Press, 2005.

6.7 Elastic modulus of the different tubing materials

The elastic modulus of the three different tubing materials is experimentally quantified using a straightforward approach. Weights are suspended from the tubing end, and the deformation is measured using a ruler and camera. The stress is calculated from the suspended mass, the *nominal* tubing inner and outer diameter. The reduction in dimensions from the Poisson ratio is deemed negligible. The strain is determined from the images captured using the camera. A ruler next to the suspended tubing is used to manually determine the elongation. The camera and tripod provide a fixed point of view. The resulting elastic modulus are summarized in Table 2 in the manuscript and the respective strain-stress curves are shown in Figure 6.13.

The measured longitudinal elastic modulus is assumed to be the same as that in the radial direction. Please note that the manufacturing process of the tubing could indeed lead to a difference between longitudinal and radial modulus of elasticity, which is reasonably considered to be less than 5%. For 1 MPa resolution and stiffer material ($E = 7$ MPa) considered in this study, 0.5 MPa then corresponds to 7.1%. Therefore, any anisotropic effects are assumed to be within the uncertainties of our experimental measurement.

6.8 Pump software output compared to pressure sensor measurement

Generally, the pressure pump output (whether from *Fluigent* or *uPump*) agrees well with the pressure as measured by the external pressure sensor (P1). Two examples of the difference between the pump pressure output and the pressure as measured by the pressure sensor (P1) are shown in Figure 6.14.

The data available from the pump software is too restricted in terms of the sampling rate to provide the required information to properly quantify the tubing dynamics. The pressure output from the pump and the pressure sensor measurement are within ± 2 mbar of each other. Consequently, it is reasonable to consider them equal. Thus, referring back to Figure 2 in the manuscript, the middle point–Pressure pump output P1–can be equivalently obtained either from the pump software output or the pressure sensor measurement.

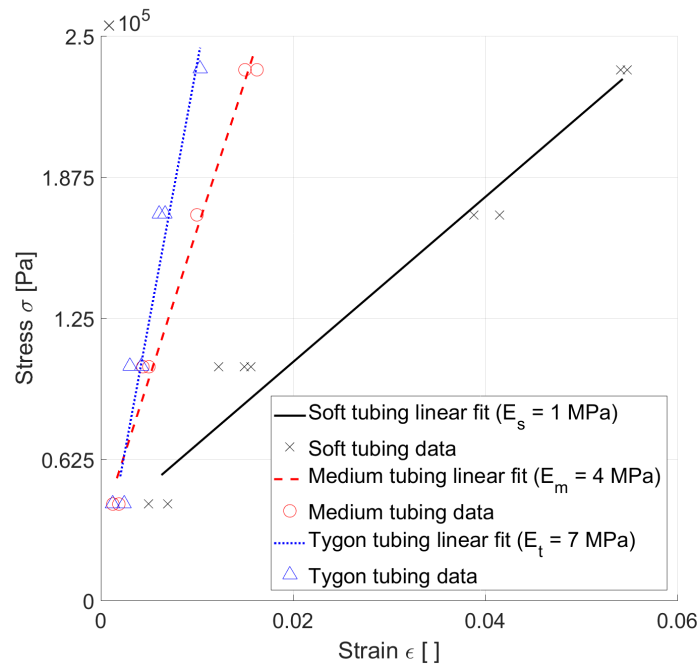
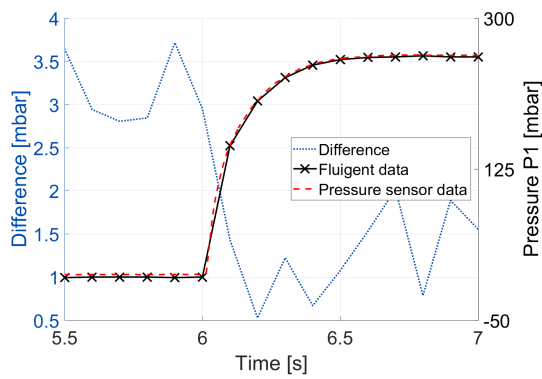
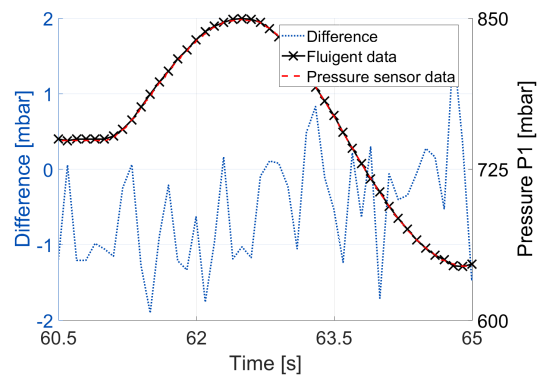


Figure 6.13: Experimental quantification of the elastic modulus for the three different tubing materials (soft silicone, medium silicone, hard Tygon).

The confidence in the match between the pressure pump output and the external pressure sensor output is especially impactful financially; accurately and rapidly monitoring the pressure using an external sensor for *each* pump output is expensive ($\sim 400\$$ per output). Thus, the model developed using the costly pressure sensors can be utilized while requiring nothing more than the usual pressure output as provided by the pump subsequently.



(a) Step change.



(b) Sinusoidal change.

Figure 6.14: Difference between the pressure pump output and pressure measured by the external pressure sensor (P1).

Chapter 7

Droplet hydrodynamic resistance

7.1 Introduction

7.1.1 Motivation

Microfluidics has a wide range of applications in various fields such as water treatment [235], life biology [33], and material synthesis [198]. An expansive literature covers the different manipulations that are achieved individually using passive microfluidics (e.g. droplet generation, merging, synchronization, trapping) [8]. However, most—if not all—applications require multiple manipulations implemented in series.

For example, a drug screening assay performed on a single microfluidic chip includes: two droplet generators in parallel followed by traps immobilizing the droplets to mix their content by the overlapping interface [37]. Multiple iterations of the design must be tested to eventually obtain the final functional device. The iteration process is time and resource-intensive even with relatively short prototyping processes such as polydimethylsiloxane (PDMS)-based soft lithography [245]. The main factors contributing to the design difficulties are the operational uncertainties (short time pressure pump variations), manufacturing uncertainties (PDMS swelling affecting height and width dimensions, manufacturing defects), and most importantly, the unclear *quantitative* effect of droplets on flow rate from their resistance.

The Hagen-Poiseuille law (Equation 7.1) relates the pressure drop and flow rate using the so-called hydraulic resistance [31]. For pressure-driven flow (i.e. for a fixed user-defined pressure drop between inlets), the flow rate of a single-phase liquid is proportional to the resistance. The flow rate quantifies the behaviour of the flow in

the channel given the input (applied pressure) and system (resistance). Although the Hagen-Poiseuille law is a simple equation, the response of micro-channel networks is complex due to the coupling between the channels through pressure fields, but most importantly, because of the time-varying resistance as droplets are formed, enter, and exit channels.

$$\Delta P = RQ \tag{7.1}$$

where ΔP is the pressure drop [Pa], R is the resistance across the channel [$Pa \cdot s/m^3$], and Q is the flow rate [m^3/s].

In addition to generally faster and more robust passive micro-channel networks, a better understanding of droplet resistance favours better droplet trapping designs [24]. For example, immobilizing droplets enables the study of encapsulated cells over a period spanning hours of incubation [124, 16].

7.1.2 Literature overview

The current literature includes a variety of studies aiming to better understand how droplets affect flow in micro-channels. Although individual studies successfully demonstrate the validity of their data, a far-reaching consensus across the microfluidic community is still lacking. Hence, the design of complex passive microfluidic networks primarily relies on a rule of thumbs, iterative design, and previous experience; for example, the droplet length is estimated to increase the resistance 2 to 5 times more than it would be expected by an equivalent single-phase flow. Better droplet resistance quantification is envisioned to enable newcomers to the field to reach their final device design quicker and more easily.

An overview of the various methods follows. Agreement and comparison between the various studies are burdensome due to the different approaches to droplet resistance quantification, range of Capillary number covered, dimensions, and flow-driving methods. Nonetheless, the approaches are separated into three broad categories: pressure sensors, loops, and interface comparison (flow-rate based). Numerical simulations and heat-transfer-oriented studies are omitted for the sake of conciseness but similarly to the studies herein included, the literature generally does not widely agree [275, 1].

Pressure sensors

The pressure tap method essentially uses pressure sensors to measure the pressure drop across a channel section containing one or multiple droplets. This approach is

arguably the more intuitive one and has been applied to both circular [145, 138, 315, 165] and rectangular [57, 3, 252, 58, 152, 166] cross-sections.

Albeit the numerous studies, the variety of chip materials, geometry, continuous phase, and range of Capillary number make a consensus or even a comparison cumbersome. The studies involving circular capillaries appear to concord better with a $\pm \sim 20\%$ discrepancy with previous models [165]. There is nonetheless no clear agreement in the literature for the rectangular cross-section that is more typically used for complex microchannel networks made of polydimethylsiloxane (PDMS) devices for example. The flow physics differ between the circular and rectangular cross-section as a result of the complex gutter flow in the channel corners [21, 133, 160].

All these studies suffered from the same lack of pressure accuracy and time resolution arising inherently from the pressure tap approach. Thus, methods adopting an in-situ approach are deemed more promising.

Comparative loops

Observing the behaviour and traffic of droplets in a loop network minimizes the intrusiveness of the resistance measurement. The droplet resistance is derived from the comparison of the droplets in different sections of the network [88, 255, 164, 259] or in a different calibrated chip [131].

This method relies on assumptions about the flow and the uniformity of the droplets resistance. Once again, the variety of channel dimensions, viscosity ratio, flow rate and even phase of the dispersed fluid (i.e. gas vs. liquid) makes an overarching relationship difficult to define. Another important factor is the presence and concentration of surfactants; their effects on flow are complex. Surfactants impact surface tension, and hence the Capillary number. Moreover, the Marangoni stresses from the surfactant concentration gradient alters the flow [199]. Consequently, whether surfactant is present or not in either the dispersed or continuous phase, this hinders the comparison of the results of multiple studies.

Interface comparison

An interface between two fluids contrasted using a dye quantifies flow rate differences; the droplet resistance is determined based on the calibrated relationship between the interface displacement and corresponding excess flow rate [289, 40]. Thus, the interface essentially provides a localized flow sensor.

Another similar method instead uses a small particle trapped using optical tweezers to quantify the changes in a channel adjacent to the one containing the droplet [136].

The following technique requires furthermore investigation to better assess the validity of the quantification of the droplet resistance. Nevertheless, the results using the resistance of single-phase flow through complex geometry are promising [274]. However, there is not a clear consensus with the results from other methods.

Detailed models

Another approach to understand droplet resistance relies on detailed theory-oriented models. Previous works include both rectangular [309, 246] and circular [116] cross-sections.

However, the complexity of the equations prohibits a straightforward understanding of the factors determining droplet resistance. The complexity would only increase for additional consideration of factors such as cells or micro-particle concentration within the droplet and non-Newtonian behaviour of the fluids. These studies can nonetheless provide *qualitative* insights.

7.1.3 A novel approach using active control and system identification

A majority of the previous methods relied on a syringe pump to drive the flow. However, the persisting short-term and long-term oscillations of the syringe pump are well documented from previous studies [159]. In contrast, the present approach rather uses a pressure pump with fast response and better long term stability [149]. The quick pressure adjustment is a key consideration in the implementation of an active control platform [311, 111]. For this novel approach, the ability of the active control platform to impose an individual droplet movement according to an arbitrary path is leveraged to apply system identification techniques.

7.2 Working principle

7.2.1 Active control of droplets using visual feedback

The active control platform uses a desktop computer to implement the controller and to establish communication with the different parts of the system. Figure 7.1 shows an overview of the flow of information for each sampling period of 100 ms. More details are included in previous work [311, 111]. Essentially, an image analysis algorithm identifies the droplet location based on the interface between the two phases. This feedback is taken by the controller that then calculates the required pressure at each inlet of the microfluidic chip. The pressure pump provides quick actuation adjustments every sampling period.

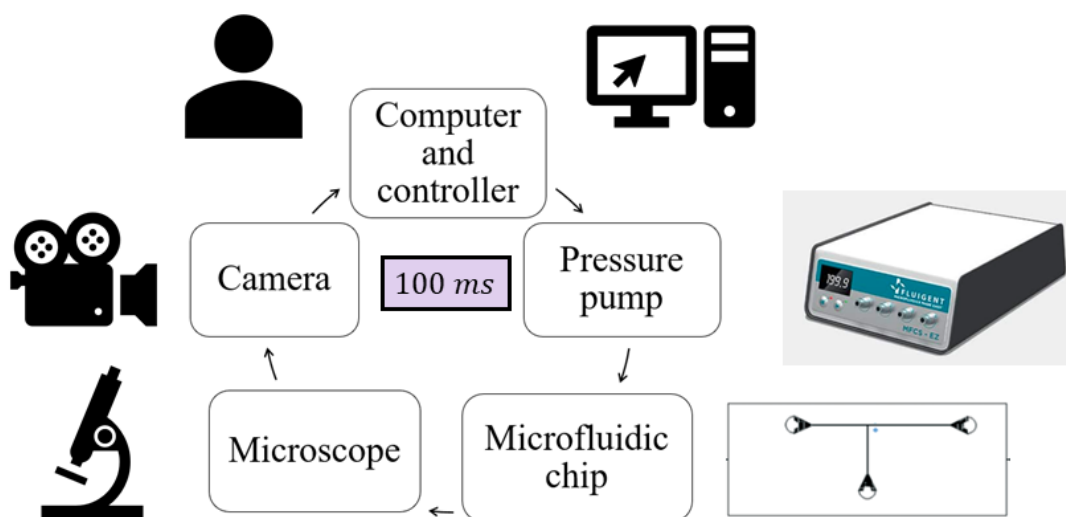


Figure 7.1: Overview of the control loop implemented for the active platform.

7.2.2 System identification

The implementation of active control alone is not sufficient to provide further insight into droplet hydrodynamic resistance. However, its ability to make a droplet follow an arbitrary position reference signal is key to the application of system identification principles. The general workflow for system identification is shown in Figure 7.2. The first step is system actuation; the path the droplet follows is designed to retrieve data providing information about the system. The input and output data are

simultaneously recorded as the active control operate. The *Matlab greyest* system identification algorithm generates a set of parameters that best fits the input-output data provided based on the imposed model structure.

7.2.3 Identifiability analysis

For grey-box system identification, the number of parameters and model structure are rooted in physical principles expressed mathematically using differential equations. The identifiability analysis aims to decide whether the value of the parameters can be confidently determined from the input-output data or not. The overall identifiability property is a combination of the informativity of the experimental data and the identifiability of the model structure [194]. The mathematical definitions are of little insight here; hence, qualitative descriptions are included [22].

Experimental data informativity The input-output data collected experimentally are informative if no other model could generate the same response.

Model structure identifiability A model identifiability is resolved by the existence (or the lack thereof) of two different parameter sets describing the same system. Or more formally, the mapping from the parameter set to the model is injective.

Sensitivity

Varying an identifiable parameter value is expected to change both the state vector and outputs. The sensitivity quantifies the effects of varying a parameter; the normalized quantity is compared with the other model parameters in terms of order of magnitude. A relatively low sensitivity magnitude for a parameter indicates that it is harder to identify; changing its value does not affect as significantly the system behaviour compared to the other parameters values.

Collinearity of parameters

Highly collinear parameters compromises the model structure identifiability. Groups of collinear parameters can compensate for the change in one parameter by varying other parameters. Therefore, multiple sets of parameters yield the same response.

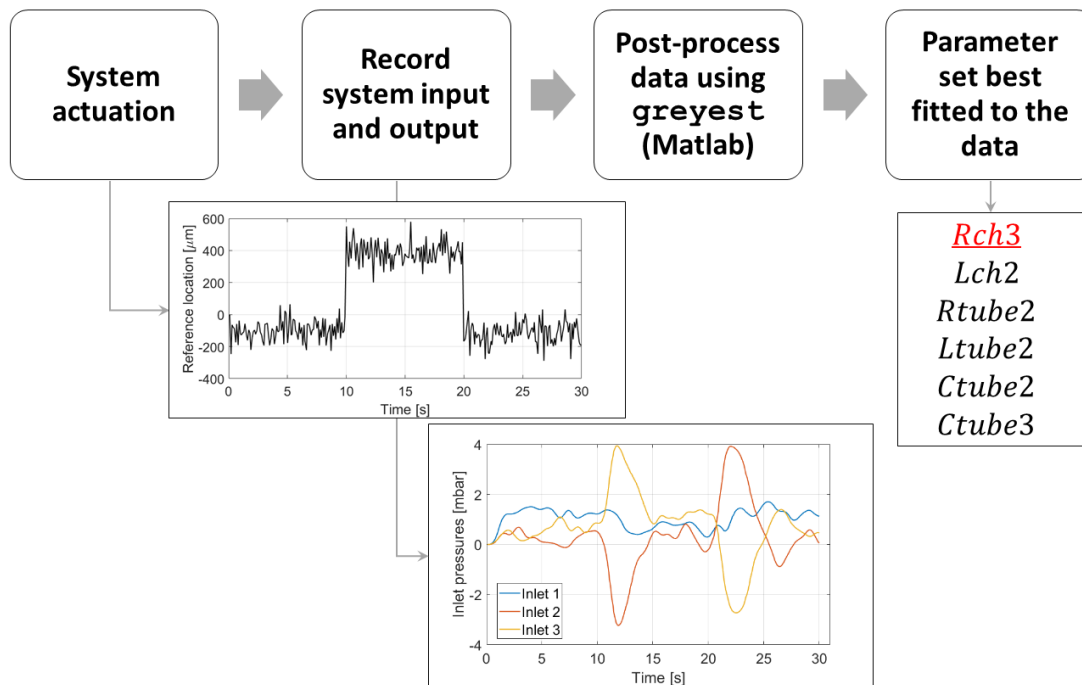


Figure 7.2: A general workflow for system identification. (1) System actuation is necessary to excite the frequencies of interest. Without the proper choice of the arbitrary path to follow, the information provided by the system will not be informative enough (See Figure 7.3 for more details). (2) The input and output to the system (in this case, each inlet pressure and the droplet position) are simultaneously recorded while the system is actuated. (3) The recorded input-output data is post-processed using the Matlab `greyest` algorithm from the System Identification toolbox. (4) The system identification algorithm returns the set of parameters that best fit the input-output data provided. The parameter of interest is the resistance of channel 3 that contains a single droplet and is otherwise filled with the continuous phase. The subset of parameters is selected based on the identifiability analysis.

Through the identifiability analysis, highly collinear parameters are determined and excluded from the subset of parameters to be identified.

The mathematical evaluation of the interplay between the different parameter subsets is implemented and automated in a Matlab-based toolbox [89]. The dependence between parameters is quantified using the collinearity index (CI). A low CI for a subset of parameters means they are *not* significantly collinear; thus, changes in one parameter cannot be compensated by other parameters within that subset. This ensures proper model structure identifiability. The CI quantification is based on the magnitude of the coefficients (α_i) required to make the following linear independence equation zero:

$$\sum_{i=1}^k \alpha_i \cdot \bar{s}_{K,i} = 0 \quad (7.2)$$

where K represents the k -th parameter subset composed of k parameters, α_i are the constants determining linear dependence if there exists a set of $\alpha_i \neq 0$ such that the above equation holds, and $\bar{s}_{K,i}$ is the normalized parameter sensitivity.

Correspondingly, the CI for the specific parameter subset K is defined as:

$$CI_K = \frac{1}{\min_{\|\alpha\|=1} \|\bar{S}_K \alpha\|} \quad (7.3)$$

A group of parameters is deemed identifiable if the CI is less than 20 which corresponds to at least 95% compensation within the collinear parameter group for variations of the parameters outside of the group and at least 5% error for compensation of parameter change within the subset [30].

7.3 Experimental setup for droplet control

7.3.1 Materials and chip fabrication

As previously explained in Section *sec:chip_fabrication*, the microfluidic chip is fabricated using a standard lithography procedure [245]. Briefly, SU-8 is spin-coated on top of a silicon wafer. The micro-channel network is selectively exposed to UV light using a photo-mask. Afterwards, the unexposed SU-8 is washed away using photo-developer. The master is used to create a polydimethylsiloxane (PDMS, Sylgard 184) chip.

A PDMS chip is used to quantify droplet resistance as it is ubiquitous in the microfluidic community and is used in numerous studies. Furthermore, subtle effects

such as the top wall deformation can have substantial importance due to the high power of the height parameter [43]. The difference between the nominal and the actual channel height is the product of multiple factors: variations in the thickness of the spin-coated SU-8 layer, variations in the mould height when transferred from the master, PDMS absorption causing swelling, and deformation from the applied pressure. These small but important circumstances are incorporated in this approach to closely mirror the usual setup with PDMS microfluidic chip for applications.

7.3.2 Overview for experiment design

The continuous phase viscosity and channel length are considered to design an experiment favourable to identifying the changes from a single droplet contained in a microchannel.

The channel resistance is considered as the sum of the length filled with the continuous phase and the dispersed phase droplet. The viscosity contrast between dispersed and continuous phase influences the fluid flow profile within the channels. Typically, the continuous phase such as silicone oil is more viscous than the aqueous dispersed phase. Similarly to numerous other experiments previously summarized in Section 7.1.2, the viscosity ratio is selected fairly low ($2 < \mu_c/\mu_d < 5$). Hence, the changes from the lower viscosity dispersed phase will more significantly affect the overall channel resistance. The selected dispersed phase is DI water while the continuous phase is silicone oil 5 cst.

Likewise, the channel length is selected as short as possible to maximize the influence of the droplet resistance on the overall channel resistance. Channel 3 contains the droplet and is 3 mm long. A shorter channel would increase too much the risk of the droplet overflowing either at the junction with the other channels or in the outlet.

7.3.3 Active control system implementation

System architecture

The active control platform enables the application of system identification methods to the quantification of droplet resistance; Figure 7.1 shows schematically its architecture. The equipment used is more specifically a Fluigent MFCS-EZ pressure pump that pushes the samples to the PDMS microfluidic chip. The Nikon Ti-E

microscope with a 4X magnification objective is used to visualize the droplet in the micro-channel. The information is conveyed to the computer with the Andor Zyla sCMOS 5.5 camera. An image processing algorithm identifies the interface between the dispersed and continuous phase within the channel. The current position is passed on to the controller that compares it against the desired position. The appropriate pressure for each chip inlet is then calculated and communicated to the pressure pump. The complete control loop executes every 100 ms that is a 10 Hz rate.

Arbitrary requested position

The active control platform enables the user to select a droplet interface for which a pre-determined path is followed such as the one shown in Figure 7.3.

Implementation A table containing the desired position at each millisecond is generated offline and loaded into the custom active control platform software. Each time the control loop executes, the elapsed time from the initial timestamp is used to look up in the table the current reference position. The controller calculates the appropriate pressure to apply to each inlet that are then communicated to the pressure pump.

Design justification The reference position that the droplet is following must provide informative experimental data. A single sinusoidal input would allow identifying a couple of parameters [229]. The informativity of the input-output data is ensured by providing a complex reference signal that excite numerous frequencies using white noise. However, the arbitrary reference position signal is not the input data required by the system identification algorithm. The pressure input is determined by the controller based on the reference signal and the current droplet position. Hence, the frequency content of the input provided to the system identification algorithm is filtered from the arbitrary path based on the sampling rate of 10 Hz of the controller. This limits the excitability of the signal; however, extensive modifications to the active control platform are required to accommodate a faster sampling rate.

The sampling rate is limited by the architecture and hence, a time-response approach is selected over the frequency-domain approach. However, simple step responses do not provide enough information about the system. Thus, white noise is added to better excite the system. Furthermore, although the active droplet control

system enables the user to specify an arbitrary path for the droplet to follow within a channel, the model is based on droplet velocity. The white noise is added to a up-and-down step to capture the hysteresis effects and average the behaviour over both cases. The $500\ \mu\text{m}$ step allows for the droplet to reach a greater velocity than with a pseudorandom binary sequence (PBS). Droplet behaviour in micro-channels depends on the droplet velocity generally expressed using the Capillary number. From the peak velocity, the Capillary number for all experiments is less than 10^{-3} .

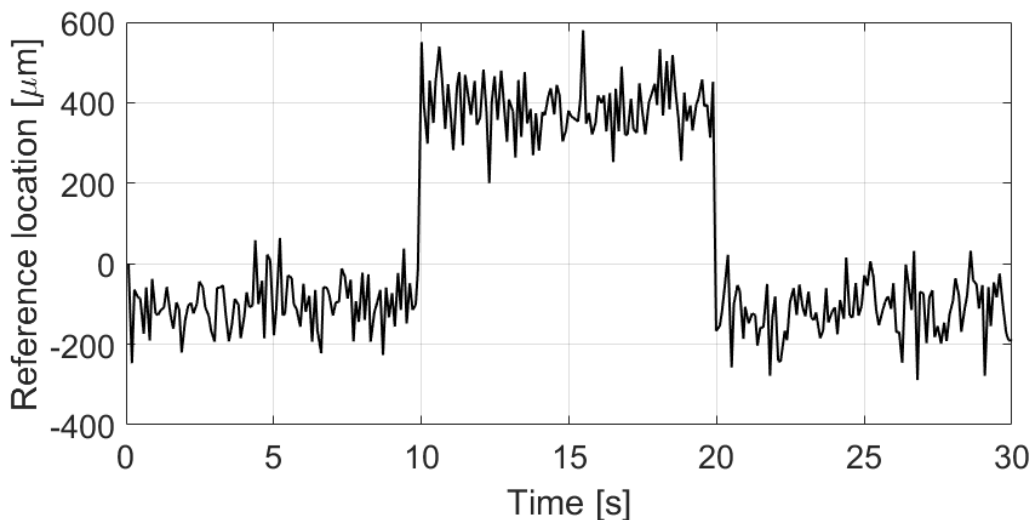


Figure 7.3: Arbitrary reference position signal for the droplet interface in the channel of interest (Ch3).

7.4 System identification methodology

The *Matlab* System Identification toolbox is leveraged with its grey-box system identification algorithm. The `greyest` function from the toolbox developed by L. Ljung is used as-is. The set of parameters to identify are selected based on the identifiability analysis.

7.4.1 Data separation

Three different sets of experiments are carried for each droplet-length-to-channel-width ratio with at least two different chips on two different days. Each set of

experiment is composed of 10 steps up and down (as shown in Figure 7.3) that are subsequently separated into 30 seconds interval for each of the 10 datasets.

7.4.2 Data pre-filtering

To avoid fitting the parameters to noise, both the input and output data are pre-filtered to reject the high-frequency noise. Hence, the analysis concentrates on the frequencies of interest of the model. Briefly, the zero-phase delay filter (`filtfilt`) function from Matlab is used with a low-pass filter frequency of 10 Hz. This ensures no shift or delay.

7.4.3 greyest algorithm

The built-in System Identification Matlab toolbox is used. Grey-box system identification is used in contrast to a black-box approach to retain the physical meaning of the identified model parameters. The resources for grey-box system identification are somewhat limited, especially when considering a multi-input multi-output (MIMO) system. The user-defined model is in the state-space format. The algorithm finds the set of parameters that best fits the provided input-output data.

State-space model structure

The model developed is based on the physical parameters of the system. In this case, these parameters include the channel dimensions, the fluid viscosity, etc. The physical properties are translated to RLC circuit elements similar to the previous design strategy [311]. Differently, the sub-block circuit is a symmetric circuit with the resistance and the inductance equally distributed on either side of the capacitance. Moreover, using *Simulink* to easily obtain the state-space matrices with the *numerical* values is irrelevant; the system equations must be derived analytically to retrieve them in their symbolic form.

The lengthy and cumbersome resulting matrices are included in ESI.S1[†]. The general expression and nomenclature are nevertheless outlined below. This model only encapsulated the physics of the fluid tubing from the reservoir holder to the microfluidic chip and the chip itself; hence the “tc” subscript used.

$$\dot{x}_{tc} = A_{tc} \cdot x_{tc} + B_{tc} \cdot u_{tc} \quad (7.4)$$

$$y = C_{tc} \cdot x_{tc} + D_{tc} \cdot u_{tc} \quad (7.5)$$

where x_{tc} is the state vector composed of currents and potentials, A_{tc} is the state transition matrix and is a function of all the parameters ($RchX$, $LchX$, $CchX$, $RtubeX$, $LtubeX$, $CtubeX$), B_{tc} is the input matrix and is a function of $LtubeX$ only, u_{tc} is the input pressure at each fluid tubing inlet ($P1$, $P2$, $P3$) in the reservoir holder, y is the output vector for the droplet *velocity*, C_{tc} and D_{tc} are the output equation matrices.

Tubing dynamics

The pump software provides the pressure measurement for each of its outlet. However, the pressure at the pump output does not instantaneously and exactly corresponds to the pressure at the fluid tubing inlet ($P1$, $P2$, $P3$). The soft air tubing connecting each pump output to the reservoir holder introduces dynamics of its own that are previously investigated (see Chapter 6). For the air tubing used (1X3 mm diameter and 66.5 cm length), the first-order model (G_{air}) has a scaling constant (k) of 1 and time constant (τ) of 33 ms. The scaling constant is simply one because any static offset is estimated using a Kalman Filter and compensated in the input data.

$$G_{air}(s) = \frac{u_{tc}}{u_{pump}} = \frac{1}{0.033 \cdot s + 1} \quad (7.6)$$

The combination of the air tubing dynamics with the fluid tubing and chip dynamics is straightforwardly implemented using matrix concatenation.

$$\dot{X} = \begin{bmatrix} \dot{x}_{tc} \\ \dot{u}_{tc} \end{bmatrix} = \begin{bmatrix} A_{tc} & B_{tc} \\ 0 & -1/\tau \end{bmatrix} \cdot \begin{bmatrix} x_{tc} \\ u_{tc} \end{bmatrix} + \begin{bmatrix} 0 \\ k/\tau \end{bmatrix} \cdot u_{pump} \quad (7.7)$$

$$y = \begin{bmatrix} C_{tc} & D_{tc} \end{bmatrix} \cdot \begin{bmatrix} x_{tc} \\ u_{tc} \end{bmatrix} + \begin{bmatrix} 0 \end{bmatrix} \cdot u_{pump} \quad (7.8)$$

7.4.4 Parameter subset used for identification

The number of parameters of a model describing a system is a trade-off between the fit to a specific dataset used for identification purposes and the prediction error with another dataset obtained from the same system. Figure 7.4 conceptually represents the trade-off. Ideally, the model is complex enough to capture the dynamics of the

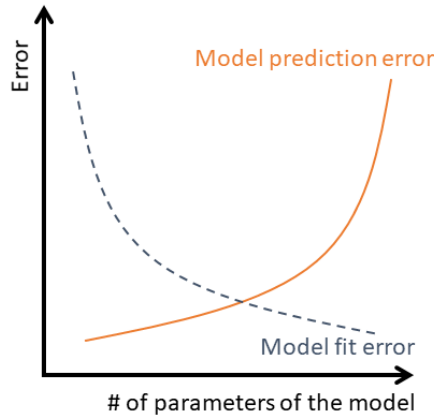


Figure 7.4: Relationship between the number of parameters and the fit to a single input-output data set. Over-parametrization lead to poor fit to other datasets from the same system. A validation data set is used to verify adequate fit to another input-output dataset.

system while retaining a low model prediction error. A validation data set verifies for over-parametrization.

In addition to the number of parameters, the specific subset of parameters to include must be selected. The state-space model of the T junction considers the tubing and channels for the 3 branches and comprises 18 parameters (see ESI.S1[†] for the details of the model). A resistance, an inductance, and a capacitance are associated with each tubing and microchannel. However, as outlined in Section 7.2.3, the mathematical formulation of the model impacts the efficacy of the grey-box system identification algorithm. If subgroups of highly collinear parameters are included in the identification scheme, then, different sets of parameter result in the same output. The compromised model structure identifiability means that changes in one parameter can be compensated by changes in other parameters. Therefore, the parameters included must be carefully selected to provide informative results; the excluded parameters are fixed to their nominal values used for controller design.

The analysis of the numerous parameters would be too cumbersome to complete manually. Hence, a more automated and numerical approach for the identifiability analysis is implemented using a Matlab-based toolbox developed by Gabor *et al.* [89]. There are four components summarized in Figure 7.6: (a) parameter sensitivity,

(b) largest identifiable subgroup, (c) highly collinear parameters, and finally, (d) the identifiable parameters. The key parameter that must be identifiable is Rch3 because this channel contains the single droplet.

(a) Parameter sensitivity The influence of each parameter on the states and the outputs is quantified with a normalized magnitude. The parameters that have an influence several orders of magnitude lower than the maximum magnitude are disregarded as they are not identifiable. Their small influence on the output potentially indicates a model over-parametrization. Nevertheless, eliminating parameters requires the resulting model to also exhibit the desired identifiability behaviour. Hence, although different models are assessed, only the full model with the 18 parameters and the tubing dynamics yields satisfactory results as it will be demonstrated. The parameter of interest (i.e. Rch3) must have a sensitivity around the same order of magnitude as the maximum one to be potentially identifiable as shown in Figure 7.6(a).

(b) Largest identifiable subgroup size The sensitivity analysis eliminates parameters that are more problematic to quantify. Nonetheless, *all* of the other parameters are not necessarily identifiable. Due to the potential collinearity between the parameters, a smaller identifiable subset must be determined. A combinatorial optimization approach is implemented in the toolbox [89] to find the largest group possible for the collinearity index threshold. A threshold of 20 is deemed satisfactory as it means that: (i) variations in the parameters *outside* of the subgroup can be compensated at least to 95%, and (ii) variations to a parameter *within* the subgroup is associated with an error of at least 5% when compensated for.

Multiple subgroups satisfy the collinearity index of 20 with the largest including 6 parameters. The appropriate subgroup K must include the targeted parameter (i.e. Rch3). Furthermore, the analysis of the highly collinear parameter groups must isolate the parameter of interest within a small group. The values of these highly collinear parameters must be reasonably known as further detailed in part (c).

(c) Groups of highly collinear parameters The collinearity between the parameters within the selected subgroup K is further analyzed than using its quantification through the collinearity index (CI_K). Highly collinear parameters are grouped together. These subgroups indicate that any inaccuracy in the nominal values of the non-identifiable parameters will be reflected in the value of the identifiable parameter from the subgroup.

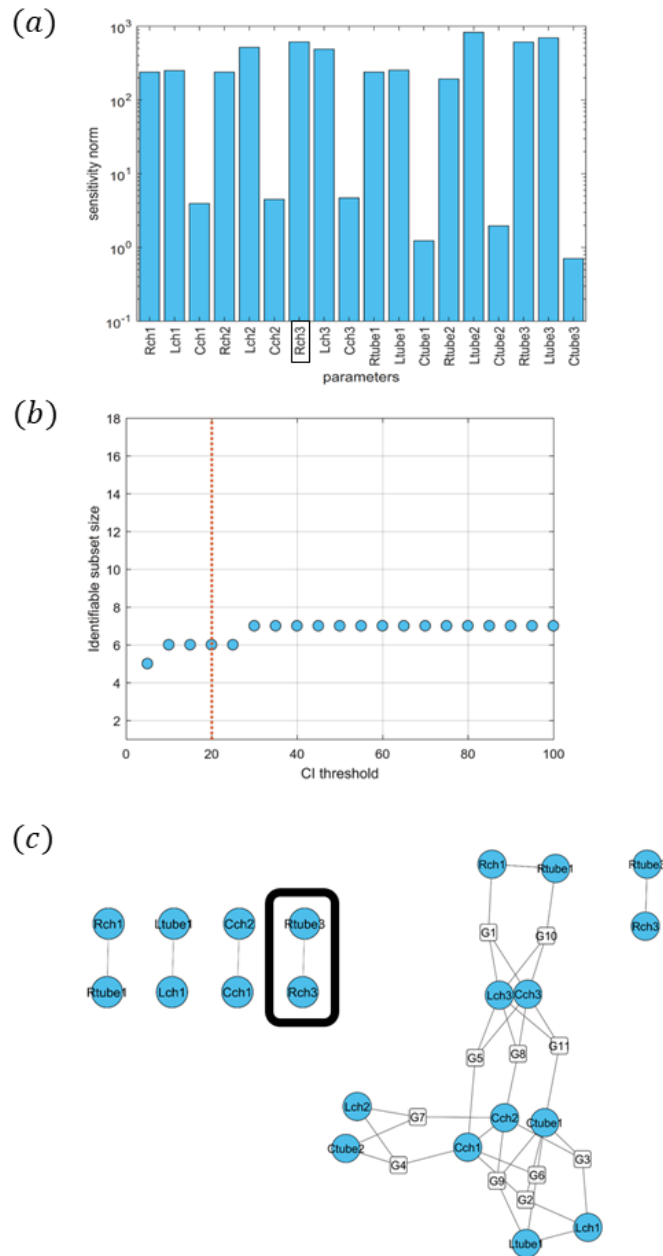


Figure 7.5: Identifiability analysis of the RLC state-space model with 18 parameters. (a) parameter sensitivity. (b) largest identifiable subgroup. (c) highly collinear parameter groups. (d) identifiable parameters.

(d)

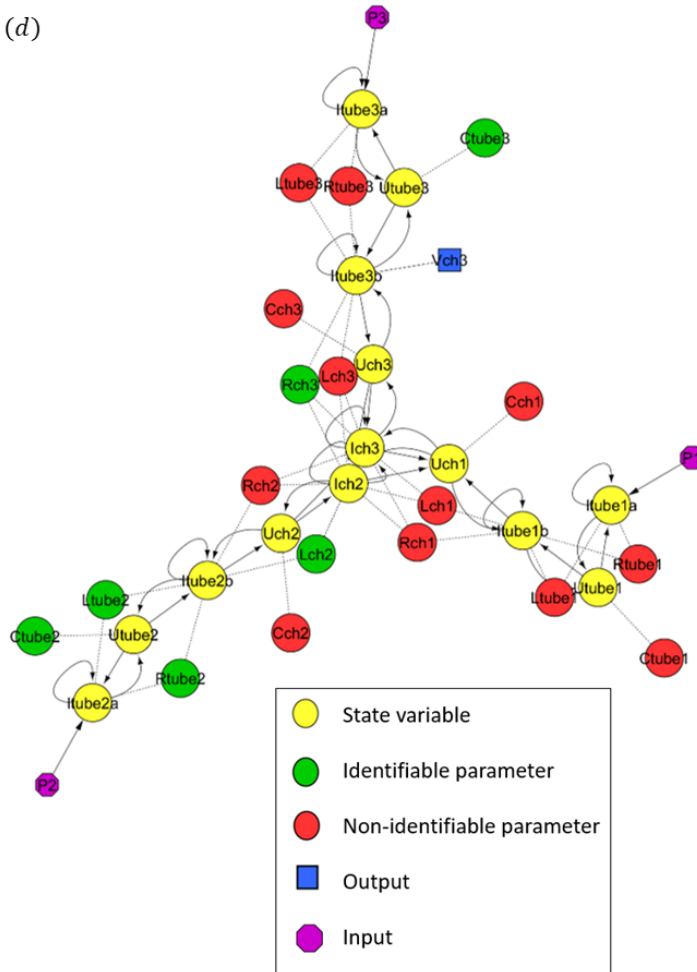


Figure 1.5 (continued): Identifiability analysis of the RLC state-space model with 18 parameters. (a) parameter sensitivity. (b) largest identifiable subgroup. (c) highly collinear parameter groups. (d) identifiable parameters.

Ideally, the parameter of interest—Rch3—would be isolated and have a low collinearity index with all other parameters. However, the structure of the model and the output information available imposes the collinear group relationships. The discrepancy between the nominal values of the parameters excluded from the subgroup will be reflected in the identified values of the other parameters. The best-case scenario, as shown in Figure 7.6(c), is the grouping between Rtube3 and Rch3 only. Thus, any inaccuracy in the nominal value of Rtube3 will be reflected in the identified value of Rch3; however, the value of Rtube3 is experimentally determined with confidence from a separate set of data using a flow sensor. Only Rch3 amongst the identifiable parameters is confidently identified as concluded by this analysis. Nevertheless, Rch3 is the only parameter required to quantify the droplet resistance.

(d) Identifiable parameters The result of the identifiability analysis is visualized graphically in Figure 7.6(d) similarly to a Bond graph. The identifiable parameters are indicated with green circles. The six parameters that are identifiable as concluded by this identifiability analysis are: Rch3, Lch2, Rtube2, Ltube2, Ctube2, and Ctube3. However, as previously mentioned, the uncertainty in the other parameters—except for Rtube3 that is confidently experimentally determined—means that only Rch3 is accurately quantified.

7.4.5 Parameter set validation

Given one set of input-output data, the fit can be arbitrarily increased by increasing the number of parameters. However, the prediction error for an independent input-output dataset increases from over-parametrization as illustrated conceptually in Figure 7.4. Therefore, the model complexity—quantified using the number of parameters—is a trade-off between the fit to the dataset used to determine the parameter, and the model prediction error of an independent dataset.

Moreover, the complexity of the identifiability analysis increases with the number of parameters. The mathematical principles are implemented through *Matlab* toolboxes (i.e. *AMIGO2* and *VisID* [89]) to avoid the overly complex analytical approach.

A straightforward validation of a particular set of parameters is used to simulate the system with another set of input data: the validation data. Then, the measured output is compared with the simulated output to verify that the fit is reasonable. A much lower fit with the validation dataset indicates over-parameterization.

7.4.6 How to calculate droplet resistance from the total channel resistance

The grey-box system identification algorithm determines the set of parameters that best fits the data based on the specified model structure. The parameter of interest within the set is the resistance of the channel containing the droplet that is moved according to the arbitrary path (*Rch3*). The length of the droplet is varied in different sets of experiments, but the channel length is kept constant.

The resistance of single-phase flow is well established compared to the resistance of two-phase flow (i.e. droplet resistance). As per the Hagen-Poiseuille law (Equation 7.1), the dimensions are used to calculate the channel resistance for single-phase flow. Equation 7.9 is for the resistance of a channel for which the height is at least half of the width [31].

$$R_{rectangle} = \frac{12\eta L}{1 - 0.63(h/w)} \frac{1}{h^3 w} \quad (7.9)$$

where R is the resistance [$Pa \cdot s/m^3$], η is the dynamic viscosity [$Pa \cdot s$], L is the channel length [m], h is the channel height [m] and w is the channel width [m].

According to the model structure imposed through the grey-box system identification (see Section 7.4.3), the resistance determined experimentally is for the full channel ($R_{channel}$ as per Figure 7.7). The channel length is maintained constant for all experiments for simplicity. Therefore, in order to calculate the droplet resistance ($R_{droplet}$) from the resistance given by the grey-box system identification algorithm (*Rch3*), the resistance contributed by the continuous phase ($R_{continuous}$) must be compensated for using single-phase theory (Equation 7.9) as shown in Equation 7.10.

$$R_{droplet} = R_{channel} - R_{continuous} \quad (7.10)$$

7.4.7 Resistance ratio

The experimental droplet resistance calculated as per Section 7.4.6 is compared to the equivalent single-phase resistance. The ratio quantifies how much additional resistance the droplet is causing. This additional resistance is attributed to the Laplace pressure from the asymmetric leading and trailing caps, the gutter flow, and the thin film flow. The droplet resistance ratio (DRR) is the quotient of experimental to single-phase resistance; this is the ratio informally estimated as 2 to 5 for passive

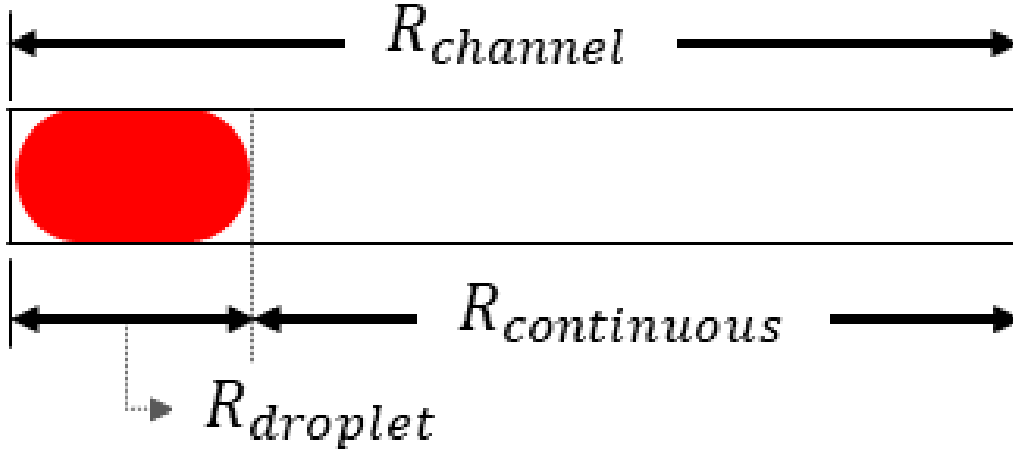


Figure 7.7: Schematic representation of the total channel resistance ($R_{channel}$) as the sum of the droplet resistance ($R_{droplet}$) and the rest of the channel filled with the continuous phase ($R_{continuous}$).

channel network design.

$$DRR = \frac{R_{droplet,exp} \text{ (Eq. 7.10)}}{R_{droplet,single-phase} \text{ (Eq. 7.9)}} \quad (7.11)$$

7.4.8 Statistical significance of the results

The impact of the droplet on the overall channel resistance are expected to be small even with the intentional design as per Section 7.3.2. The challenging quantification partly explains the difficult agreement between the studies summarized in the literature overview.

Graphical representation of the data spread using error bars with their magnitude equal to one standard deviation is deemed inappropriate because of their closeness. Consequently, the statistical significance of the resistance compared to other droplet length ratios is rather determined using a statistic test on the difference of means. The 95% confidence interval of the mean difference is calculated based on the unknown population variances [217]. If the interval includes zero, then, it is concluded

that there is no statistically significant difference between the two sample means.

$$\Delta\bar{x} - t_{\alpha/2,\nu}\sqrt{\frac{s_1^2}{n_1} + \frac{s_2^2}{n_2}} \leq \Delta\mu \leq \Delta\bar{x} + t_{\alpha/2,\nu}\sqrt{\frac{s_1^2}{n_1} + \frac{s_2^2}{n_2}} \quad (7.12)$$

where $\Delta\bar{x}$ is the difference in *sample* means, $t_{\alpha/2,\nu}$ is taken from the student's t distribution with $\alpha = 0.05$ for the 95% confidence interval and ν is the degree of freedom calculated using Equation 7.13 rounded down to the nearest integer, s_1 and s_2 are the standard deviation of the first and second sample respectively, n_1 and n_2 are the number of data points for each sample, and $\Delta\mu$ is the difference in mean of the *population*.

$$\nu = \frac{(s_1^2/n_1 + s_2^2/n_2)^2}{\frac{(s_1^2/n_1)^2}{n_1-1} + \frac{(s_2^2/n_2)^2}{n_2-1}} \quad (7.13)$$

7.5 Results and discussion

7.5.1 Experimental droplet hydrodynamic resistance

The fit of the nominal set of parameters is graphically compared to the one of the identified set of parameters in Figure 7.8. The actual system output shown in grey is the target that the system identification algorithm tries to match by considering the input data and varying the parameters. Fit improvement is observed. The dashed red rectangle shows a region of fast oscillations that are faster than any expected response of the system. Thus, this region indicates an over-parametrization of the model. Nevertheless, the identifiability analysis is suitable to quantify Rch3 using this model structure. By changing the model structure and reducing the number of parameters, a new identifiability analysis yielding similar results would be required and could not be achieved. Hence, the RLC model is retained.

The model fit for each identified set of parameters is plotted in Figure 7.9 against the corresponding Rch3 resistance. The system identification algorithm essentially optimizes the value of the parameters to minimize the discrepancy between the measured and simulated system output. The identifiability analysis aims to select a parameter subgroup that effectively reduces the equivalent local minima that would lead to the algorithm converging to different sets of parameters with the same response. Although the selected set of six parameters reduces the spread of the identified value for Rch3, there is still a considerable range of values. Therefore, the results are selected based on a threshold of 50% model fit for the simulated system

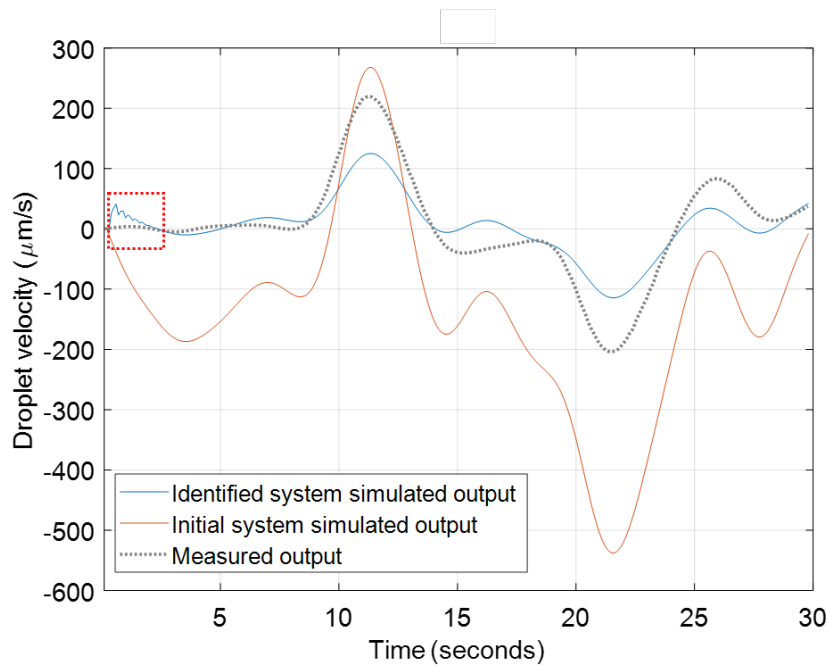


Figure 7.8: Model simulation of nominal and identified model compared to the actual recorded system output. Dashed red rectangle shows oscillations too fast for the physical system indicating potential over-parametrization.

compared with the actual system. Figure 7.9 shows that the values for R_{ch3} are grouped closer at higher percent fit.

The selected data points based on model fit are shown in Figure 7.10(a). The values of the resistance of the channel containing the droplet (R_{ch3}) have a relatively large standard deviation. This is further discussed in Section 7.5.3. The experimental droplet resistance and ratio are calculated as per Equations 7.10 and 7.11 respectively (see Figure 7.10(b)). The error bars are omitted due to their closeness. Instead, a statistical test on the mean is used to determine which data points are statistically significant from the others.

The statistical analysis demonstrates that some points are statistically insignificant from each other. Hence, the method herein presented does not have the resolution to distinguish between the two smaller and the two larger lengths to width ratio. The inclusion of the tubing dynamics is key to obtain statistically meaningful results and supports the significance of this often—if not always—overseen part of the microfluidic system (see Chapter 6).

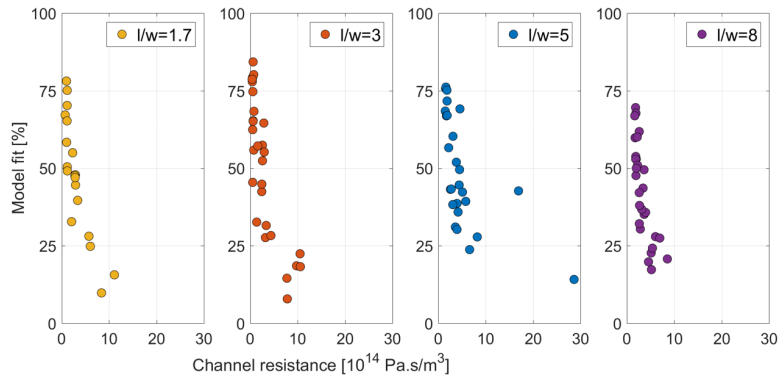
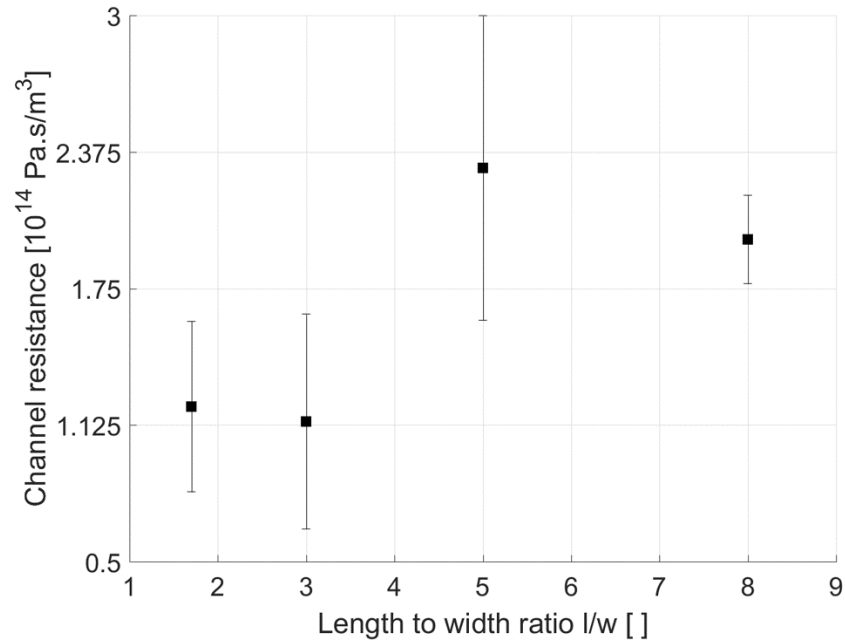


Figure 7.9: Percent fit variations and the corresponding identified channel resistance (Rch3). Selected threshold is 50%. Model fit defined as per the Matlab `compare` function.

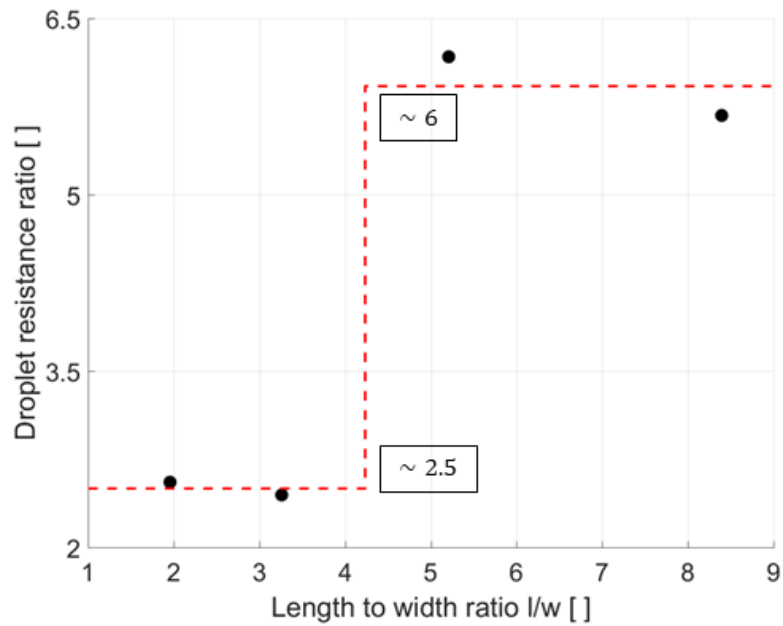
7.5.2 Comparison with literature results

The numerous studies in the literature cover a wide range of parameters with varying chip material, cross-section dimensions and shape, viscosity contrast, surfactant used, Capillary numbers and many more. Nonetheless, a qualitative comparison between the results from Figure 7.10 is useful to assess for the validity of this novel approach to droplet resistance quantification that leverages active droplet control.

The general trend of the additional resistance from droplet is a sharp increase from small to medium length to width ratios after which, a steady linear decrease is observed for larger ratios. The sharp increase to the peak resistance ratio is higher for smaller Capillary numbers and lower dispersed to continuous phase viscosity contrast [289]. For a viscosity contrast around 0.2 and Capillary number less than 10^{-3} , the peak resistance ratio is around 3.5 that is significantly lower than the 6.5 herein quantified [131]. However, the Capillary number is based on the maximum droplet velocity that is only achieved at the step increase and decrease which can potentially contribute to this discrepancy. Nevertheless, the reasonable agreement with the previous literature consolidates this initial investigation that leverages the active droplet control platform to apply system identification techniques to quantify droplet resistance.



(a) Identified channel resistance for droplet-length-to-channel-width ratios with the error bars corresponding to one standard deviation.



(b) Ratio of experimental to theoretical (i.e. single-phase) droplet resistance according to Equation 7.11.

Figure 7.10: Experimental droplet resistance results.

7.5.3 Limitations

The resolution of the droplet resistance ratio is limited as shown in Figure 7.10(b). The results are nonetheless promising for the further development of the technique to improve the resolution. The technique could be applied more readily than the other approaches to a wide variety of channel geometries, and fluid used, even potentially non-Newtonian fluids that still require fundamental research to better understand them. A better resolution is however necessary.

The control sampling rate of 10 Hz or 100 ms intervals limits the frequency content of the input and output data. Although a fast pressure measurement apparatus was developed to quantify the impact of the air tubing connecting the pump output to the reservoir holder (*i.e.* the input), the image processing (*i.e.* the output) is the limiting factor here. Significantly improving the image processing to identify the droplet location is out of the scope of the current work but is envisioned for the future. Moreover, the pressure measurement apparatus would also be required to be further developed to enable three independent pressure sensors, one for each branch of the T junction.

The compounding effects of the sampling frequency and the droplet position to calculate the droplet velocity are not fully analyzed. The velocity must be used as the output rather than the position; the plant to be identified must be strictly stable for the system identification algorithm.

The droplet motion back and forth means a varying velocity, and thus, the Capillary number varies but is bounded by an upper value ($Ca < 10^{-3}$). The comparison with the literature is hindered by the discrepancy in Capillary number in addition to the numerous other experiment parameters.

7.6 Conclusion

7.6.1 Summary

Quantifying droplet resistance attracted research efforts from various angles including pressure taps and interface comparison to quantify flow rate. However, the body of research covers a wide range of conditions. Although each study agrees and draws conclusions in accordance with their data, a consensus has yet to be reached due to the complexity of the phenomenon. The active droplet control platform offers a novel and distinctive approach that uses system identification methods.

The active control enables the user to set an arbitrary path for the droplet. As the droplet moves back and forth following a step with added white noise, the input (i.e. pressure) and output (i.e. droplet position) are recorded. Matlab offers a pre-packaged grey-box identification algorithm that post-processes the input-output data. The model structure is fixed to retain the physical meaning of the parameters. The subset of parameters to identify is carefully selected based on the identifiability analysis to ensure their accuracy and narrower distribution. The system identification algorithm optimizes the parameter value to minimize the difference between the recorded system output and the simulated system output based on the recorded input. The subset of parameters includes the resistance of the channel containing the single droplet. From the known channel length and tubing resistance, the ratio of the experimental droplet resistance to the equivalent single-phase resistance is calculated.

Due to the current limitations of the approach, the resolution of the identified droplet resistance ratio identifies only two levels although four droplet length to channel ratio were tested. Nevertheless, the overall trend is in agreement with previous literature results. A sharp increase in resistance ratio is expected before a steady decrease; the steady decrease region is omitted because of our method's limitation of the droplet length. This proof of concept aligns with the literature but could be further developed to increase its impact and test numerous other conditions.

7.6.2 Future work

The scope of this paper is to present and verify the novel approach to quantify hydrodynamic droplet resistance using active control and system identification. Although the droplet resistance ratio obtained offers a crude resolution, the results are in agreement with previous literature. This is promising as key improvements to this approach could enable droplet resistance ratio quantification for a wide variety of conditions, chip geometry and even, non-Newtonian fluids. There are three main approaches to obtain better resolution for the droplet resistance ratio: upgraded active control platform, targeted system design, and improved identifiability and system identification analysis.

An upgraded active control platform could provide better (i.e. more accurate, more frequent) input-output data. Moreover, additional measurements such as flow rate of the tubing could better quantify R_{tube3} and also help the system identification analysis to compensate for the leaking of the continuous phase through the gutter and thin-film flow.

The identifiability analysis is typically applied to an unknown fixed system for which certain parameters must be quantified. However, in this study, there is some leniency in term of chip design that could be better informed through an in-depth identifiability analysis. This could help the system identification algorithm converge more consistently to the same minima and narrow the data spread.

The grey-box algorithm used is from the Matlab system identification toolbox while the identifiability analysis is performed separately by a toolbox developed by another research group. A better synergy between the identifiability and identification algorithm could enable more reliable convergence to solutions and narrower parameter value spread.

With these improvements and the consequent better quantification resolution, a more thorough study could consider a lot more parameters such as viscosity ratio, channel aspect ratio, a wider variation of droplet length to channel width ratio, different materials, and most importantly, non-Newtonian fluids.

Acknowledgements

Marie would like to acknowledge the help of Attila Gabor in setting up the AMIGO2 [<https://sites.google.com/site/amigo2toolbox/>] and VisID [<https://github.com/gabora/visid>] Matlab toolboxes for the identifiability analysis [89].

Supplemental material

7.7 State-space model structure

See Appendix B.

Chapter 8

Microfluidic chip compliance

8.1 Introduction

8.1.1 Microfluidic context

The study of fluid flow at the micrometre scale enables short reaction times and low reagent consumption. These advantages are leveraged in numerous applications. The applications range across numerous fields such as biomedical assays [87, 263], water quality [176, 235, 295], drug screening [51], materials [198], and many more.

The applications use a variety of microfluidic platforms. The capabilities of both passive and active platforms have been demonstrated in application-based studies. However, the independent use by end-users is still limited. This is attributed to the knowledge barrier faced by users in addition to the robustness of the microfluidic platforms that should be improved.

Active platforms are envisioned to palliate the robustness issues of certain microfluidic platform. Moreover, the active components handle microfluidic-related knowledge. As a result, the end-users are expected to more easily adopt microfluidic platforms to leverage their advantages.

8.1.2 Motivation

The active control of droplets relies on a model for controller design. A better understanding of the dynamics of the microfluidic chip is envisioned to provide better

accuracy. Moreover, better understanding the dynamics of the microfluidic chip can provide insights for chip design.

8.1.3 Literature overview

The dynamic behaviour of the microfluidic chip is seldom studied in the literature. The passive systems that operate at steady state disregard transient behaviours. These transient behaviours inform the dynamic response of the microfluidic chip system. For active control, the actuation is periodically adjusted; small scale dynamics matter.

The relative softness of PDMS-based chips is well known in the field. In addition to change in dimensions due to swelling, the walls of the channel deform under pressure. A study particularly looked at the additional flow rate resulting from the top wall deformation [43]. However, the derivation is restricted to “shallow” microfluidic channels that have a much larger width than height. Furthermore, the comparison with experimental data is for an upper wall thickness of 0.2 mm. Nevertheless, the demonstration of the importance of channel deformation for static flow further motivates the investigation of its dynamic effects.

The previous work carried out by David Wong provided a proof-of-concept system that motivated the further development of the active control platform. The model-based controller relied on a formulation of the capacitance as per Equation 8.1 that proved sufficient for stable operation. However, the formula is not experimentally verified specifically for the capacitance.

$$C = \left(\frac{A}{\kappa} + \frac{l}{\beta} \right) A \quad (8.1)$$

where A is the cross sectional area [m^2], $\kappa(A_{substrate}, E, l) = A_{substrate}E/l$ is the substrate stiffness [$Pa \cdot m$], $A_{substrate}$ is the substrate area [m^2], E is the elastic modulus of the substrate material [Pa], l is the channel length [m], and β is the adiabatic bulk modulus [Pa]. Note that the channel cross-section area (A) is multiplied to the original formula to align with the other references that consider the flow rate rather than the velocity.

Under the assumption of small deformations, the microchannel of rectangular cross-section is approximated as per Equation 8.2 [34]. Although the equations are presented within the context of a manometer design, they are deemed pertinent. This equation is indirectly verified through hydrodynamic resistance experiments.

Nevertheless, the context of the active droplet control platform motivates a deeper and more thorough consideration of the rectangular channel capacitance.

$$C = \frac{\alpha^* w h l(1 + \nu)}{E} \quad (8.2)$$

where C is the rectangular channel capacitance [m^3/Pa], α^* is a scaling factor depending on the width-to-height ratio with maximum value of 1 [], w is the channel width [m], h is the channel height [m], l is the channel length [m], ν is the Poisson's ratio of the material [], and E is the elastic modulus of the material [Pa].

8.2 Methodology

The experiments collect the applied pressure and resulting flow rate at a 1 kHz sampling rate. The objective is to determine the dynamics between the pressure and flow rate using a first-order transfer function fit in *Matlab*.

8.2.1 Microfluidic chip fabrication

The micro-fabrication process follows a standard procedure that is detailed in the literature [245]. The soft lithography procedure requires a master. The fabrication involves the two-step spin coating of SU-8 2005 and SU-8 2025 on a silicon wafer.

The polydimethylsiloxane (PDMS) chip is moulded using the master. Although hydrophobic surface properties are not required because the tests are single-phase, a similar process is followed to ensure similar mechanical properties [137, 301]. The mould is cured at 95°C for 1 hour before bonding to a PDMS-coated glass slide using oxygen plasma. Then, the chip is baked at 170°C for at least 24 hours.

The mechanical properties of the PDMS chip are maintained constant throughout the experiments. Consequently, the weight ratio of the pre-polymer and cross-linker is maintained at 10 to 1. More specifically, the 95% confidence interval of the weight ratio is (9.95, 10.00).

8.2.2 Pressure and flow rate measurements

The pressure sensor (*TE Connectivity U536D-H00015-001BG*) provides a measurement of the input to the system. The range is from 0 to 1 bar with a ± 1 mbar

accuracy and 0.24 mbar measurement resolution. The flow rate sensor (*Sensirion SLL-430*) provides a measurement of the output of the system. The voltage output is measured and then, converted to flow rate using the calibration curve (see “Flow sensor calibration” below). Both the pressure and flow rate sensors are connected to the same sensing apparatus to ensure proper synchronization between the two signals. The sampling rate is 1 kHz; the details of the Arduino-based apparatus are previously published (See Section 6).

8.2.3 Flow sensor calibration

The calibration of the flow rate sensor is necessary to maximize the accuracy of the measurement. Each fluid used—water or silicone oil of various viscosities—exhibit different thermal properties. The working principle of the flow sensor relies on the heat dissipation from the flowing fluid. Consequently, a calibration curve is required for each fluid.

A syringe pump (*Harvard Apparatus Model 33 Twin*) provides the known flow rate. The short term oscillations of the syringe pump are averaged over 3 minutes during data collection. This promotes a better accuracy of the reference flow rate. The measured voltage is recorded in three separate sets: increasing, decreasing, and random. The flow sensor settings ensure that the output is contained between 0 V and 5 V for the whole pressure range. The flow sensor outputs voltage from 0 V to 10.5 V for the positive and negative flow directions. Thus, the zero flow voltage output is around 5 V. The chosen settings scale the flow between $-100 \mu\text{L}/\text{min}$ to $120 \mu\text{L}/\text{min}$ to ensure the negative flow portion is fully contained within the 0 to 5 V range. Moreover, the voltage output is limited to 5 V to prevent damage to the sensing apparatus. Each calibration curve is obtained using the same flow sensor settings as for the data collection. The data points and fitted polynomial curves are shown in Figure 8.1.

8.2.4 Sample tubing dynamics

The sample tubing connects the pressurized reservoir hold to the microfluidic, the microfluidic chip to the flow sensor, and the flow sensor to the waste vial. The connections are a combination of #10-32 and 1/4-28 fittings that conform to the 1/16” outer diameter of the sample tubing. Figure 8.7 illustrates the location of the components for data collection with the microfluidic chip.

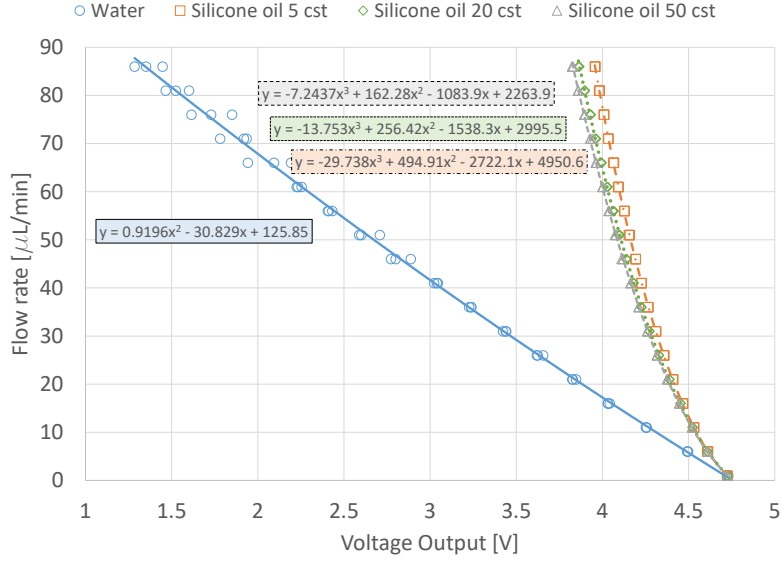


Figure 8.1: Calibration curves for water and silicone oil using the *Sensirion SLI-430* flow sensor. Scaling limits from $-100 \mu\text{L}/\text{min}$ to $120 \mu\text{L}/\text{min}$.

The dynamics associated with the tubing is independently assessed by applying a succession of increasing and decreasing pressure input without a microfluidic chip. The resulting flow rate is fitted with a first-order transfer function to determine the associated time constant. Multiple tubing lengths are evaluated to determine the relationship trend.

Moreover, the resistance of the system is evaluated with a #10-32 union and two #10-32 coned connectors to link two tubings and replace the microfluidic chip. The experimental setup with the chip requires three individual tubing segments. Constant pressure data is collected without the microfluidic chip, but with the three tubing segments to assess the base resistance. The data processing compensates for this resistance. The time constant associated with the use of the #10-32 union is disregarded as only the resistance matters for the later experiments. Figure 8.2 represents schematically the experimental setup to assess the sample tubing dynamics.

For the $0.020'' \times 1/16''$ sample tubing, the resistance is on the order of $10^{13} \frac{\text{Pa}\cdot\text{s}}{\text{m}^3}$ for silicone oil 50 cst. Figure 8.3 shows the resistance according to the total tubing length with the resistance for the flow sensor compensated for. The data for the length of 0.76 meters is for the #10-32 union and is representative of the tubing used for data collection with the microfluidic chip. The resistance with the #10-32

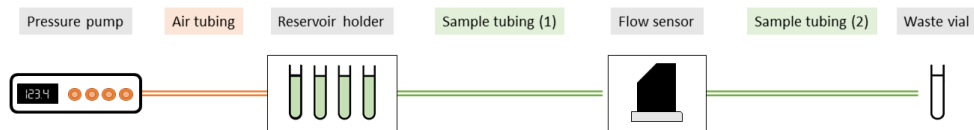


Figure 8.2: Experimental setup schematic to test sample tubing resistance and dynamics.

union is comparable to the one without (i.e. the data point for a length of 0.769 m). Moreover, compared to the resistance of the channel, the variations are negligible. Therefore, it is suitable to use the #10-32 union to initially collect data without the chip to calculate the base resistance.

For the dynamics of the sample tubing, the #10-32 union data is disregarded because it is only required for constant pressure data collection. The sample tubing dynamics are nonetheless required because of its potential impact on the results with the microfluidic chip. Various inner diameters, lengths, and fluid flow are considered. Generally, the tubing time constant should be minimized to avoid interference with the time constant of the microfluidic chip.

Firstly, the time constant associated with tubing of different diameters is assessed. The outer diameter of all tubing is 1/16". Consequently, the wall thickness varies. As shown in Figure 8.4, the smaller diameter tubing corresponds to higher time constants. Although the 0.030" tubing has a much smaller time constant, the large diameter requires a large fluid volume from the sample vial. This is problematic due to the limited volume available for tests before refilling. Moreover, the flow sensor upper flow sensing limit should not be exceeded. The 0.010" exhibits larger time constants than the 0.020" tubing. Consequently, the 0.020" is selected as the most suitable.

Secondly, the length is varied. A shorter length is desirable to minimize the time constant. However, the connection between the reservoir holder, the microfluidic chip, the flow sensor and the waste vial requires a significant tubing length. Consequently, the 0.769 meters tubing is selected to comfortably accommodate the physical layout of the numerous components. Figure 8.5 shows the experimental relationship between the tubing length and time constant.

Thirdly, the time constants associated with the various fluids are assessed. The selected 0.020" tubing that is 0.769 meters long results in a non-negligible time

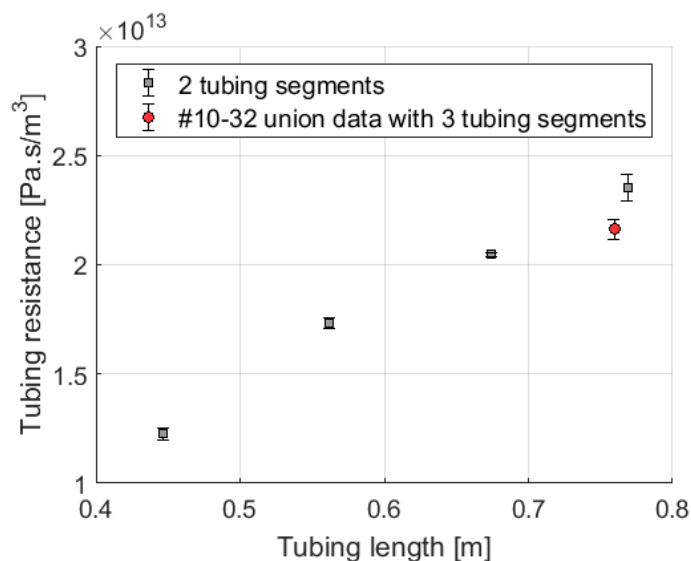


Figure 8.3: Resistance of the sample tubing for different lengths. The fluid is silicone oil 50 cst. The data for 0.76 m uses a #10-32 to #10-32 union to link two tubing segments. The error bars represent one standard deviation for $n = 3$.

constant. Nevertheless, the time constant will be compensated when assessing the time constant of the microfluidic chip. Consequently, the tubing time constant for the different fluids is determined. Figure 8.6 excludes water because the resulting flow rate exceeded the upper flow sensing range of the flow sensor. Nevertheless, the time constant is expected to be proportional to the viscosity of the fluid. Furthermore, the time constant for silicone oil 5 cst is already at the lower limit of the system and is thus considered negligible. Consequently, the time constant for water is also considered negligible.

8.2.5 Inlet design

The tubing is connected through a press fit for the 1/16" outer diameter to the PDMS chip. The inlet then transitions to the micro-channel. The contribution of the inlet to the time constant is not separately considered. However, microfluidic chips require the inlet to easily connect the sample tubing. Therefore, the time constant with the inlet is considered representative of the usual microfluidic chip use.

The time constant associated with the inlet is the product of the resistance and the capacitance. However, the much wider inlet comparatively reduces the contribution

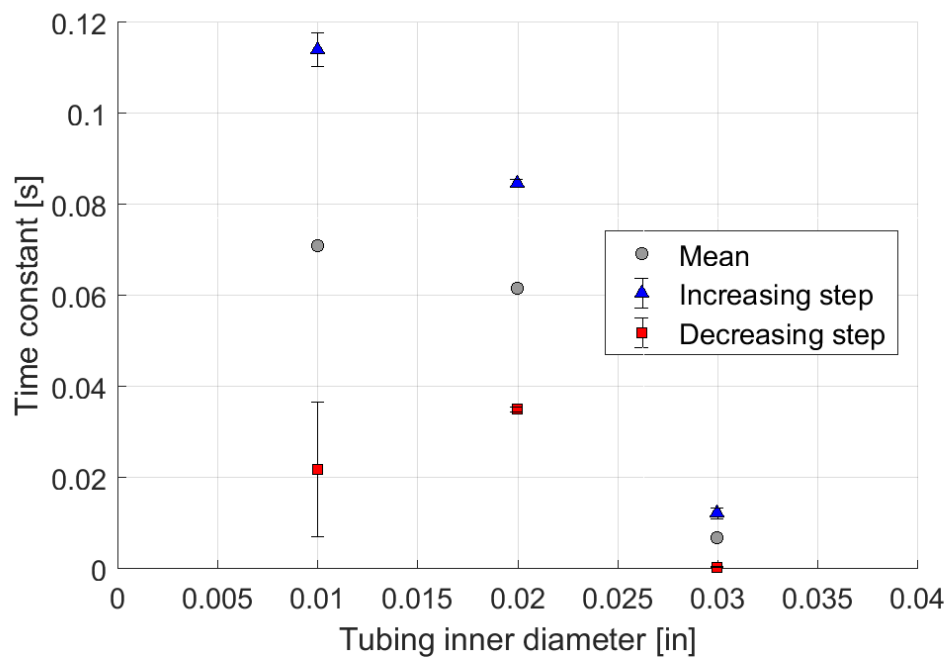


Figure 8.4: Time constant for different tubing inner diameters. The larger 0.030" tubing has a smaller time constant, but the resulting large flow rates are undesirable for the limited sample vial volume and the flow sensor range. The error bars represents one standard deviation for $n = 21$.

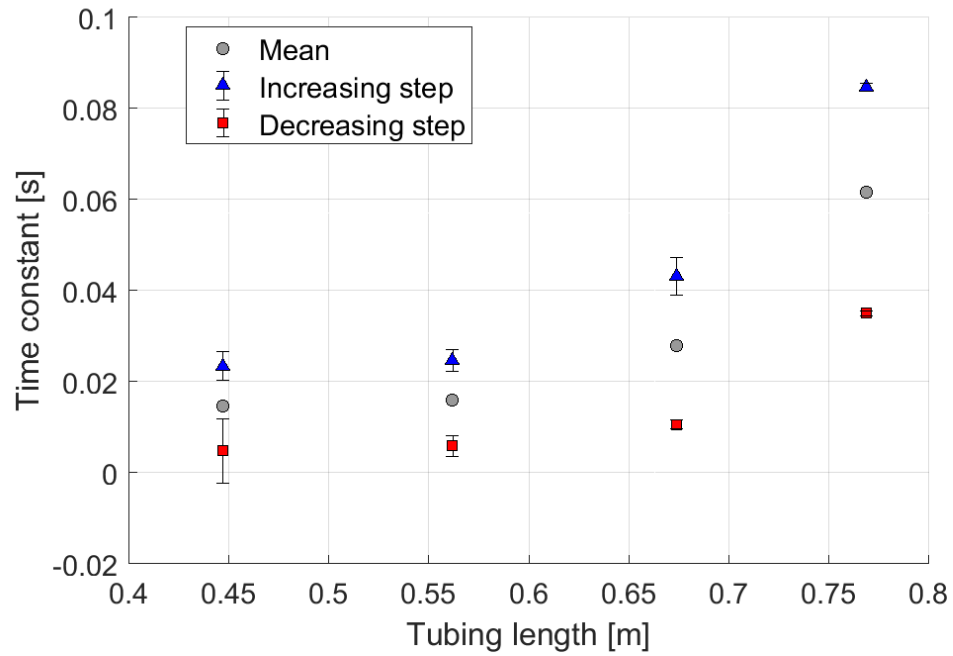


Figure 8.5: Time constant for different tubing lengths with inner diameters of 0.020". A shorter tubing is desirable, but the physical layout of the components requires a minimum length for proper assembly. The error bars represents one standard deviation for $n = 21$.

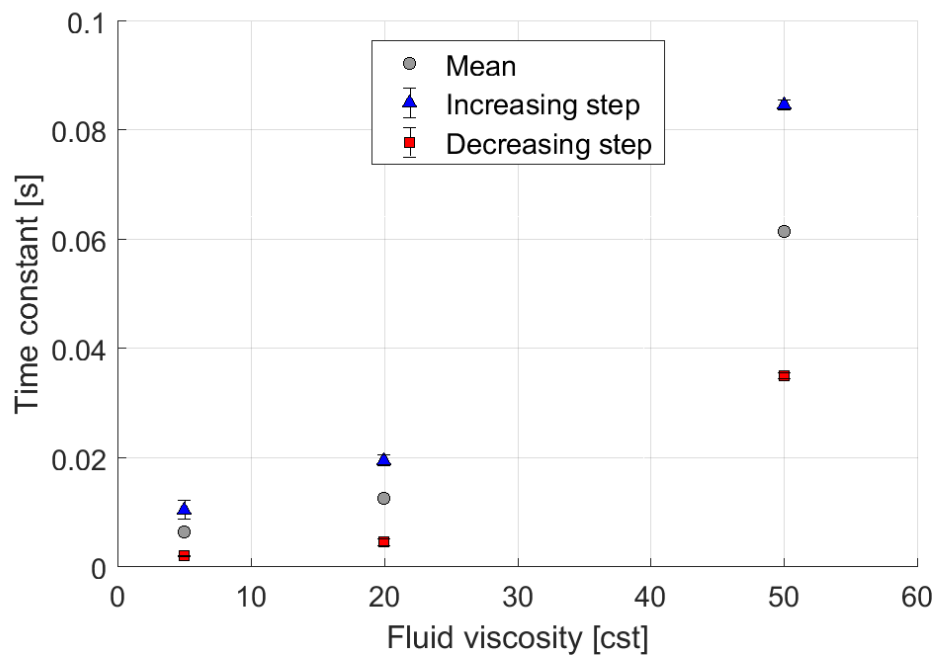


Figure 8.6: Time constant for different fluids through a tubing of 0.020" inner diameters and 0.769 meters. The time constant for silicone 5 cst and water are considered negligible. The data for silicone oil 20 cst and 50 cst will be compensated for when processing the data for the microfluidic chip time constant. The error bars represent one standard deviation for $n = 21$.

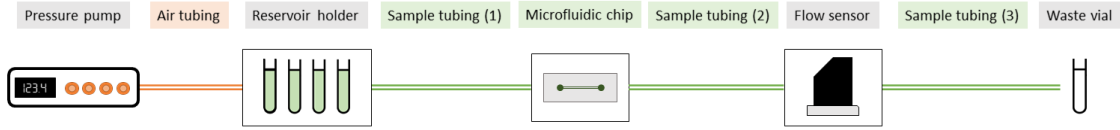


Figure 8.7: Experimental setup schematic for data collection with the microfluidic chip before the flow sensor.

to insignificant levels through a small resistance. Nevertheless, the area is expected to be between 10% and 500% of the channel area depending on the dimensions. The area of the inlet is about $5 \times 10^6 \mu\text{m}^2$. For the smallest channel and the worst case, the width is $100 \mu\text{m}$ and the length is 10 mm for a total area of $1 \times 10^6 \mu\text{m}^2$.

8.2.6 Experimental setup for data collection

The setup to collect data with the microfluidic chip is similar to the one previously shown in Figure 8.2. The microfluidic chip can be located either before or after the flow sensor. If the chip is located after the flow sensor, the shape of the response will have one zero and one pole. Oppositely, when the chip is located before the flow sensor, the response will correspond to the typical first-order system response with no zeros and one pole. For simplicity, the latter setup is selected and is illustrated in Figure 8.7.

The time constant is identified from the experimental data. However, the capacitance of the microfluidic chip is of interest. In order to relate the time constant to the capacitance, the resistance is required. The resistance of the chip itself is isolated from the total system resistance by considering the resistance of the system without the chip. A #10-32 union replaces the chip as per Figure 8.7 to link sample tubing 1 and 2. The base resistance of the system is determined from an applied constant pressure and resulting flow rate as per Equation 8.3 [31].

$$\Delta P = R \cdot Q \quad (8.3)$$

where ΔP is the pressure different [Pa], R is the resistance [$\text{Pa} \cdot \text{s} \cdot \text{m}^{-3}$], and Q is the flow rate [$\text{m}^3 \text{s}^{-1}$].

The microfluidic chip is primed with a constant pressure of at least 250 mbar for 10 minutes before data collection. This allows the PDMS to swell and ensures the

dimension are consistent for the duration of the data collection. After the priming phase, a constant pressure of 200 mbar is applied to record the flow rate. The base resistance of the system—including the sample tubing and flow sensor—is deducted from the overall system resistance to isolate the microfluidic chip resistance. The resistance is later used to get the chip capacitance from the time constant.

A series of 8 increasing and decreasing step functions from 0 to 200 mbar is then applied. The input pressure and output flow rate are recorded with a 1 ms time resolution. Consequently, the smallest time constant that the system can confidently identify is 10 ms. The series of steps is applied to multiple chip designs with repetitions with two different chips on two different days. The time constant is expected to vary based on three main factors: fluid viscosity, height-to-width ratio, and height-to-length ratios. Equation 8.4 combines the resistance [31] for a rectangular cross-section with the capacitance [34] of Equation 8.2.

$$\tau = \left(\frac{12\mu l}{wh^3(1 - \frac{h}{w})} \right) \cdot \left(\frac{\alpha^* w h l(1 + \nu)}{E} \right) \quad (8.4)$$

Simplifying Equation 8.4, rearranging, and assuming that α^* is only a function of the height-to-width ratio ($\alpha^* = \alpha^*(\frac{h}{w})$) yields the following relationship for the time constant. The different parts of the equation are labelled according to the factor determining its value.

$$\tau = 12 \cdot \underbrace{\left(\frac{1 + \nu}{E} \right)}_{\text{material}} \cdot \underbrace{(\mu)}_{\text{fluid}} \cdot \underbrace{\left(\frac{l}{h} \right)^2}_{\text{length}} \cdot \underbrace{\left(\frac{\alpha^*}{1 - 0.63 \frac{h}{w}} \right)}_{\text{width}} \quad (8.5)$$

For this experimental study, only the fluid, length-to-height ratio and height-to-width ratio are investigated. Four different fluids are considered: water, and silicone oil 5 cst, 20 cst and 50 cst. Water and silicone oil are typical dispersed and continuous phases used in microfluidic. Moreover, silicone oil is available with a range of viscosity. The height-to-length ratio ranges from 200 to 3000. The total channel length is restricted by the footprint available on a typical 1" X 3" glass slide. Moreover, typical channel heights of 30 μm and 50 μm are used. Table 8.1 specifies the height and length combinations for the 6 different length-to-height ratios. Furthermore, the height-to-width ratio is varied for each of the length-to-height ratio: $\frac{1}{10}$, $\frac{1}{6}$, $\frac{1}{4}$, and $\frac{1}{2}$.

Only certain fluids are tested with each length-to-height ratio. The expected time constant informs whether the information is useful. For example, for smaller length-

Table 8.1: Length-to-height ratios with corresponding dimensions.

| Length-to-height ratio (l/h) | Length (l) [mm] | Height (h) [μm] |
|-------------------------------------|------------------------|----------------------------------------------|
| 200 | 10 | 50 |
| 300 | 15 | 50 |
| 600 | 30 | 50 |
| 1500 | 45* | 30 |
| 2500 | 75* | 30 |
| 3000 | 90* | 30 |

* Includes one curvature on the standard 1"X3" glass slide

Table 8.2: Specification of the length-to-height ratio considered for each fluid.

| Fluid | Length-to-height ratio | | | | | |
|----------------------------|-------------------------------|------------|------------|-------------|-------------|-------------|
| | 200 | 300 | 600 | 1500 | 2500 | 3000 |
| Silicone oil 50 cst | X | X | X | - | - | - |
| Silicone oil 20 cst | X | X | X | - | - | - |
| Silicone oil 5 cst | X | X | X | - | - | - |
| Water | - | - | - | X | X | X |

to-height ratios, the time constant is expected to decrease. Thus, for water, the higher length-to-height ratios are selected. Table 8.2 summarizes which length-to-height ratios are considered for each fluid. Larger length-to-height ratios for silicone oil results in a flow rate too small to measure with the flow sensor. Smaller length-to-height ratios for water saturates the flow sensor at its maximum flow.

8.2.7 Assumptions for the time constant

The time constant resulting from this methodology is attributed to the compliance of the microfluidic chip. Other factors are disregarded are compensated for as follows.

The input pressure is measured directly at the reservoir holder. Nonetheless, a small pressure offset from the hydrostatic pressure of the fluid in the vial occurs. However, the maximum height variation is 30 mm which corresponds approximately

to 3 mbar. Consequently, this is neglected and lumped with the other system uncertainties.

The time constant associated with the sample tubing was investigated. Hence, the time constant can be compensated for to isolate the contribution from the microfluidic chip itself. Figure 8.6 shows that for a viscosity smaller than 5 cst—thus for water and silicone oil 5 cst—the time constant is negligible compared to the system minimal time constant identifiable of 10 ms. For silicone oil 20 cst and 50 cst, the time constant is accurately identified for increasing and decreasing steps.

As for the other dynamics associated with the microfluidic chip itself, there is inductance and compliance from fluid compressibility. For inductance, the small characteristic length of the micro-channel unsurprisingly means negligible inertial effects. Furthermore, a quick calculation with the worst-case scenario under study confirms the relatively small scale of the associated time constant. Thus, inductance is not considered.

$$\tau_{LR} = \frac{L}{R} = \frac{\rho l}{wh} \cdot \frac{wh^3(1 - 0.63\frac{h}{w})}{12\mu l} = \frac{h^2(1 - 0.63\frac{h}{w})}{12\eta} \quad (8.6)$$

$$\tau_{LR} < \frac{(50 \times 10^{-6})^2(1 - 0.63 \cdot 0.1)}{12 \cdot 1 \times 10^{-6}} < 0.2 \text{ ms} \quad (8.7)$$

As for the compliance contributed by the fluid compressibility comparatively to the material deformation, the adiabatic bulk modulus of the fluids (β) and elastic modulus of PDMS (E) are compared. The order of magnitude of GPa is considered for the adiabatic modulus and a typical value of 2 MPa is used for the PDMS elastic modulus. Thus, the contribution from the fluid compressibility is only about 0.2% of the material deformation. Consequently, the compressibility is neglected, and only the material deformation is considered.

8.2.8 Data processing

The data is processed first by converting the recorded values to pascals (Pa) and meters cubed per second (m^3/s) for the pressure sensor and flow sensor respectively. The series of 8 increasing and decreasing steps is then separated into smaller subsets of input and output data. The output flow rate is offset using the average of the first 1000 data points. Thus, the change in flow rate is considered for the first-order model fit.

Then, the *Matlab* function `tfest` is used to fit a transfer function with no zeros and one pole. The time constant (τ) is obtained from the denominator coefficients. When using silicone oil 20 cst or 50 cst, the time constant of the tubing must be compensated for using the data from Figure 8.6. The time constant of the chip is identified through a lookup table built using a combined system with the time constant of the tubing and an arbitrary time constant covering the desired range. Then, a first-order system is fit to the combined first-order systems. Based on that identified first-order system time constant and the tubing time constant, the time constant of the chip is retrieved.

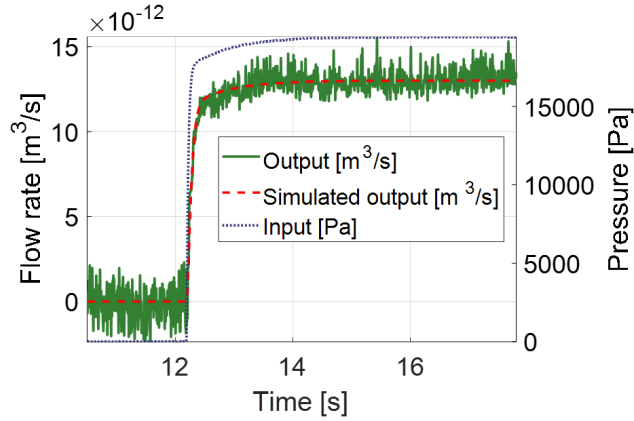
The time constant of the chip (τ_{chip}) considers both its resistance (R_{chip}) and its capacitance (C_{chip}). The resistance is previously determined using constant pressure flow. Thus, the capacitance is calculated from the resistance and the time constant as per Equation 8.8. A symmetric circuit analogy with half of the resistance distributed on either side of the capacitance is used. This is privileged over the simpler RC circuit for the symmetry of the response that corresponds better to the physical system.

$$C_{chip} = 4 \frac{\tau_{chip}}{R_{chip}} \quad (8.8)$$

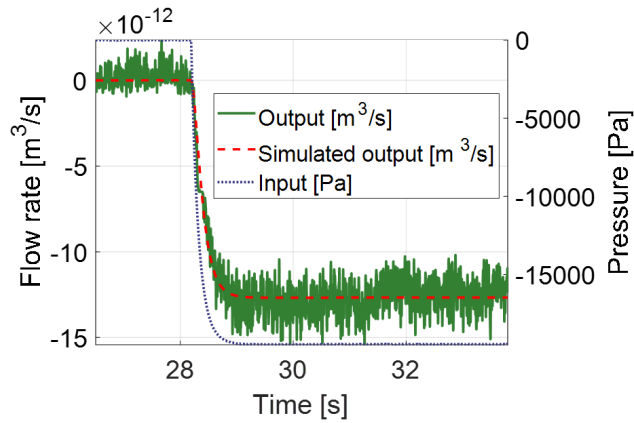
8.3 Results and discussion

The calculation of the capacitance compensates for the variations in resistance from the nominal values. The time constant plots are omitted. Two first-order fit data sets are shown in Figure 8.8. This case is for a smaller flow rate that exhibits a smaller signal-to-noise ratio. However, the first-order function averages the noise and nevertheless provides an acceptable fit.

As expected, the capacitance decreases with an increasing height-to-width ratio; in other words, the more square cross-section has a lesser capacitance than an elongated cross-section. The relationship is more or less inversely proportional ($C \propto \frac{1}{h/w}$). The mean capacitance for the various height-to-width ratios, length-to-height ratio, and fluid used are regrouped in Figure 8.9. Each data point is an average of at least 60 increasing step and 60 decreasing step capacitance. Moreover, the two series for the same nominal length-to-height ratio are from two different chips on two different days. Error bars are omitted due to the relatively large discrepancy between the increasing and decreasing step capacitance.



(a) Increasing step.



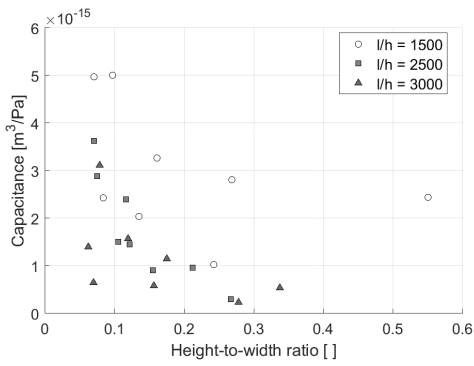
(b) Decreasing step.

Figure 8.8: First-order fit of the flow rate based on the measured pressure.

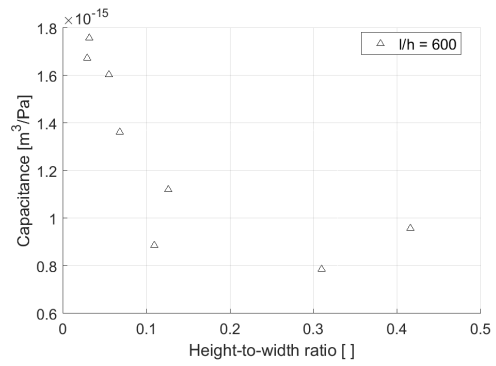
8.3.1 Comparison with previous models

The capacitance of the microfluidic channel considered by previous work is given by Equation 8.1. However, the experimental data significantly disagrees with the previous equation. The difference is 5 orders of magnitude ($O(10^{-20})$ vs. $O(10^{-15})$).

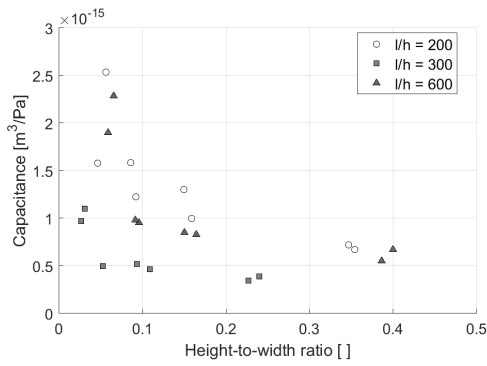
Consequently, an another form for the capacitance equation is considered (Equation 8.2). The fitting parameter (ϕ) allows for the adjustment of the capacitance based on the geometry. Without the fitting parameter, the discrepancy between the experimental values and the capacitance using Equation 8.2 is 1 order of magnitude ($O(10^{-16})$ vs. $O(10^{-15})$). Although the prediction value is in closer agreement with



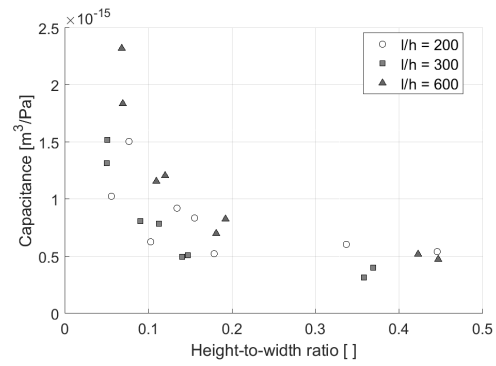
(a) Water



(b) Silicone oil 5 cst



(c) Silicone oil 20 cst



(d) Silicone oil 50 cst

Figure 8.9: Capacitance results for the different fluids (water, and silicone oil 5 cst, 20 cst, and 50 cst) according to the height-to-width ratio.

the experiment value, the fitting parameter enables a more accurate prediction.

8.3.2 Fitting parameter (ϕ)

The fitting parameter (ϕ) compensates for the assumptions and simplifications leading to the discrepancy between the predicted and experimental values. Its value is calculated by dividing the experimental capacitance by all other terms from Equation 8.2.

$$\phi = C_{exp} \cdot \frac{E}{w h l(1 + \nu)} \quad (8.9)$$

The material properties from the PDMS ratio and the chip thickness are maintained constant for all experiments. Consequently, the fitting parameter should only depend on geometric variables. However, other uncertainties increase the spread of the data. The inlet hole location varies as it is manually located and punched before bonding the chip. PDMS debris are present in various quantity and behaves differently from chip to chip; the debris are unavoidable as they arise from the insertion of the tubing in the inlet. Certain chip lengths (for length-to-height ratios of 1500, 2500, and 3000) needed to include a curve to accommodate the full channel length within the glass slide dimensions (1" X 3"). Finally, the viscosity is varied to cover more conditions. However, the resistance compensation effectively negates any influence from the viscosity. Consequently, the only difference should be from geometry (height, width, and length). The correlation between alpha and the normalized width is weaker than for ϕ and the normalized length. The fitting parameter (ϕ), and thus, the capacitance, increases with an increasing height-to-length ratio. Longer channel lengths mean smaller flow rates and smaller additional flow from the deformation. Thus, the volume per pressure unit is also reduced, and hence, the capacitance is smaller.

When considering the capacitance trend per chip and per fluid (see Figure 8.9), the relationship between the capacitance and the height-to-width ratio is clear. For an increased height-to-width ratio (or an increased "squareness"), the capacitance decreases. However, the agglomeration of all results into the fitting parameter plot as a function of the height-to-width ratio (Figure 8.10(a)) does not exhibit any clear trend. Oppositely, the relationship between the fitting parameter and the height-to-length ratio (Figure 8.10(b)) demonstrates an approximately linear trend. Thus, the fitting parameter (ϕ) depends more strongly on the height-to-length ratio than on the height-to-width ratio.

The static deformation of the channel with the corresponding additional flow rate is dependent on the flow rate (and thus, indirectly, to the length) [43]. The

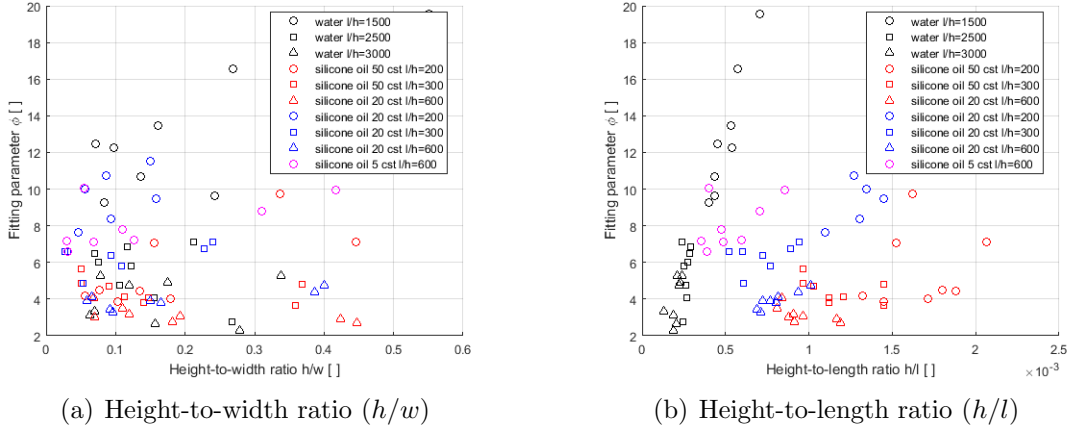


Figure 8.10: Fitting parameter (ϕ) relationship with geometric ratios for all fluids.

additional flow rate from the deformation depends on the second term in the bracket. A large aspect ratio (i.e. wide channel) is assumed. The details of the derivation and assumptions are in the paper.

$$q \approx \frac{h_0^3 w \Delta p}{12 \mu l} \left(1 + \frac{3}{160} (w/t)^3 (w/h_0) (\Delta p/E) \right) \quad (8.10)$$

where h_0 is the initial channel height [m], w is the channel width [m], Δp is the pressure difference across the channel [Pa], μ is the dynamic viscosity [Pa · s], l is the channel length [m], t is the top channel wall thickness [m], and E is the substrate elastic modulus [Pa].

Another study that is in contrast more experiment-based arrives to a similar conclusion [96]. The additional flow rate depends on the initial channel height (h_0) and channel width (W), but not directly on the channel length. However, the dependence on the flow rate dictates a relationship to the channel length.

$$\frac{\Delta Q}{Q} = \frac{Q_{deform} - Q_{rigid}}{Q_{rigid}} \sim \frac{3\alpha}{2} \frac{\Delta p W}{E h_0} \quad (8.11)$$

where Q_i is flow rate [m^3/s], α is a fitting parameter [], Δp is the pressure difference [Pa], W is the channel width [m], E is the substrate elastic modulus [Pa], and h_0 is the initial channel height [m].

The spread of the fitting parameter is too significant to formulate an analytical equation for ϕ that provides an adequate fit for all data. Nevertheless, the use of the

fitting parameter (ϕ) from the plateau at the largest height-to-width ratio for each chip provides an adequate fit. This further reinforces the conclusion that the length-to-width ratio dominates over the height-to-width ratio. Even without considering the height-to-width ratio within the chip-specific data set, a prediction window of $\pm 15\%$ is achieved. However, each fitting parameter used is specific to the chip. A consensus across the various chips could not be achieved.

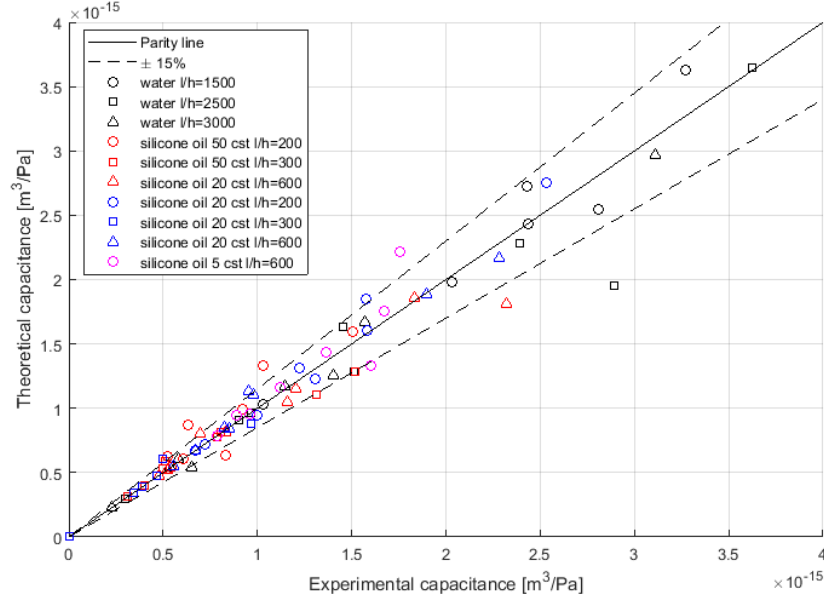


Figure 8.11: Assessment of fit for the fitting parameter (ϕ) as a function of the chip only. This does not consider variations in width-to-height ratio; the smallest ϕ value for each chip is used.

8.3.3 Limitations and uncertainties

The geometric range of conditions is limited to the height, width, and length considered. Any extrapolation cannot be supported. Nevertheless, the dimensions are representative of a wide range of microfluidic chip designs. Moreover, the wide range of viscosity of the fluid used (from 1 cst to 50 cst) covers the usual experimental parameters. Additionally, only PDMS chips are considered. However, the material is ubiquitous in the microfluidic field. The most common ratio of 10 to 1 is selected to ensure a wide extent of the results. Finally, the flow rates and pressures considered

cover a limited range. The step pressure is up to 200 mbar. This is a typical pressure for the active droplet control platform.

There are multiple sources of uncertainties that lead to data scattering. Nevertheless, the scattering is expected to mimic the typical use of microfluidic chip in everyday settings. For a smaller flow rate (as shown in Figure 8.8), the noise is more significant but still adequate. The first-order fit considers an averaged value within the noise. The hysteresis of the system leads to differences between the time constant from increasing and from decreasing steps. However, the time constant is averaged over both increasing and decreasing steps. The inlets are manually punched. Therefore, their location is not well controlled. The variation between the chips of the same nominal dimensions is attributed to that. A more important factor related to the inlet is its effect on the system capacitance and the debris accumulation.

The sample tubing is inserted in the microfluidic chip through a press fit. Although dust and other debris are cleaned during the manufacturing procedure, the insertion of the tubing creates small PDMS debris within the microchannel network. If enough debris accumulate around the inlet, the resistance of the region is significantly increased. Moreover, the height depends on the location of the inlet as the top channel wall deforms with the tubing insertion. The effects on the time constant could be significant. The uncertainties related to the inlet are challenging to control, their variations are expected to similarly impact every day of microfluidic chips.

Finally, the fitting parameter (ϕ) cannot be expressed succinctly as a function of geometric parameters only. In order to do so, the contribution from the inlet would need to be taken into account to limit the data scattering. Moreover, the flow rate also seems to play an important role; the fitting parameter more strongly correlates with the channel length and the fluid viscosity.

8.4 Concluding remarks

8.4.1 Conclusion

The microfluidic chip compliance is considered separately from the sample tubing compliance. The time constant and chip resistance are experimentally determined from measured input pressure and output flow rate. Then, the capacitance is retrieved by assuming a symmetric RC circuit. The height-to-width ratio and height-to-length ratio are varied with different chip designs that are used with various fluids.

The experimental capacitance is compared to a theoretical formula. The accuracy is within one order of magnitude that is much closer than previous approximations. The fitting parameter (ϕ) exhibits a stronger relationship with the height-to-length ratio than for the height-to-width ratio. The purposeful design of the height-to-width ratio enables the minimization of the capacitance; the height-to-width ratio should be larger than 0.2. As for the channel length, the longer channels minimize the fitting parameter, and thus, the capacitance. For the same pressure step, longer channels have smaller flow rates, smaller volume displacement, and thus, smaller capacitance.

8.4.2 Future work

The results herein presented are exploratory. Further work should aim to improve the understanding of the microfluidic chip capacitance. A more extended study with wider pressure and flow rate range would extend the findings to more conditions. Moreover, the material properties should be varied to investigate their effects. Different more rigid materials such as polymethyl methacrylate (PMMA) or polycarbonate might eliminate the compliance effects. However, it would also be beneficial to explore the relationship between the capacitance and the PDMS ratio.

Moreover, further experiments should decouple the inlet and channel capacitance for a more detailed understanding. For the channels only, glued capillaries directly connecting to the channel would avoid the need for inlets.

Finally, the experimental setup with the pressure sensor at the inlet and flow sensor at the outlet could be supplemented by another flow sensor at the inlet. The flow rate difference between the two flow sensors could then be attributed to the deformation of the microfluidic chip. The timing and synchronization between the sensors are crucial.

Chapter 9

A critical system analysis

9.1 Objective

The objective is to examine each component of the active droplet control platform to identify the most impactful improvements to guide future developments towards a faster modular platform.

9.1.1 Why a faster platform?

Improving the droplet control platform to execute its loop at a faster rate provides three main advantages: improved throughput, better control performance, and enhanced information about the system from the input-output data.

The implementation of active feedback for added control in the context of microfluidics comes at the expense of throughput. Active approaches adding a control layer to passive methods as well as traditional passive microfluidics both exhibit significant throughput (i.e. \sim Hz-kHz); arguably, there is potential for the production of high-value products. However, the added control of our active platform is at the expense of the yield. Hence, the focus must be shifted towards obtaining information from the microfluidic platform rather than a product. Although a faster platform could not compete with the throughput of passive microfluidic chips, improved throughput would be beneficial to perform the analysis in shorter-time frames. This could be especially important when handling photosensitive or temperature-sensitive samples.

For the controller, the rate of execution of the control loop limits its performance in terms of the required time to reach the desired position steady state. A faster control loop allows tighter monitoring of the system if actuated more brusquely to ensure the system remains stable and performs adequately.

The control loop rate dictates the frequency information available from the recorded input-output data of the system. Processing the feedback, calculating the required pressure, and applying the pressures more quickly allows obtaining more information from the system. System identification techniques would benefit most from the added information extracted from the system to analyze its behaviour.

9.1.2 Why a modular platform?

The active droplet control platform was initially developed leveraging standard microfluidic apparatus, namely: a microscope with an expensive scientific camera, a commercial pressure system, and PDMS microfluidic chips. Such an approach proved fruitful at the proof-of-concept stage. Nevertheless, the expansion of the platform outside of the microfluidic community requires a more accessible apparatus.

Moving away from the bulky but versatile microscope is envisioned to make the platform easier to use and more accessible. Furthermore, a standalone system could help view the active droplet control platform as a tool to obtain information. Microscopes are expensive pieces of equipment; although versatile, the requirement for the platform under-utilizes their potential that is better suited for other purposes.

Within a modular system, a plug and play approach of each microfluidic function—such as droplet generation, splitting, merging, and incubation—grants researchers outside of the microfluidic field the power to tailor the manipulations to their specific needs. Thus, only high-level instructions would be required to perform their experiments.

9.1.3 Overview

The complete active droplet control platform is divided into its components for convenient analysis. The numbered breakdown is shown in Figure 9.1. Each component is addressed in the subsequent sections. Feedback is further separated into sub-components to address the approach to feedback as a whole (#6 on the figure) but also, each of the components for visual feedback is currently implemented in this iteration of the platform. The core chapters also separately considered many of the

components as shown in Figure 1.1. The semi-automated algorithm (Chapter 4) adds a layer to the controller. The pressure pump (Chapter 5) provides a better understanding and a more flexible actuation. The tubing dynamics (Chapter 6) and microfluidic chip compliance (Chapter 8) are better understood.

The modular platform vision aims to assemble multiple modules, each with the components shown in Figure 9.1. The system is additionally modular in the sense that the actuation, controller, and feedback can be tailored to specific needs relatively independently. The compatibility of the different parts of the system is important, but there are multiple options for each component. For example, the controller calculates the pressure to apply, but different pump models (e.g. commercial such as Fluigent MFCS, open-source such as our μ Pump) can be used to drive the flow; the important aspect is that they are pressure actuators as opposed to flow-driven solutions such as syringe pumps. Notwithstanding their prohibitively slow response, syringe pumps could be used as actuation mean but would require changes in the controller as well. A similar logic is applied to the droplet position feedback. Hence, the variety of options for each of the components is considered relatively independently and are outlined in the subsequent sections.

9.2 Controller (1)

The controller of the active droplet control platform considers the current and required droplet position to calculate each of the pressures to independently apply at the inlets.

9.2.1 Performance

The qualitative performance of the controller is intuitive with criteria such as reasonable settling time for step displacements, avoiding saturation of the pressure, enough force to generate and split droplets, and robustness to disturbances from other channels. However, a quantitative assessment of the performance is required to formally assess different control strategies.

Performance quantification is closely linked to the optimal control field that aims to either minimize or maximize an objective function. A benchmark test (e.g. following a specified representative path for a droplet) would allow the comparison of various control strategies. The quantification of the performance should take into account errors (both steady-state and overshoot), robustness, sensitivity, and whether

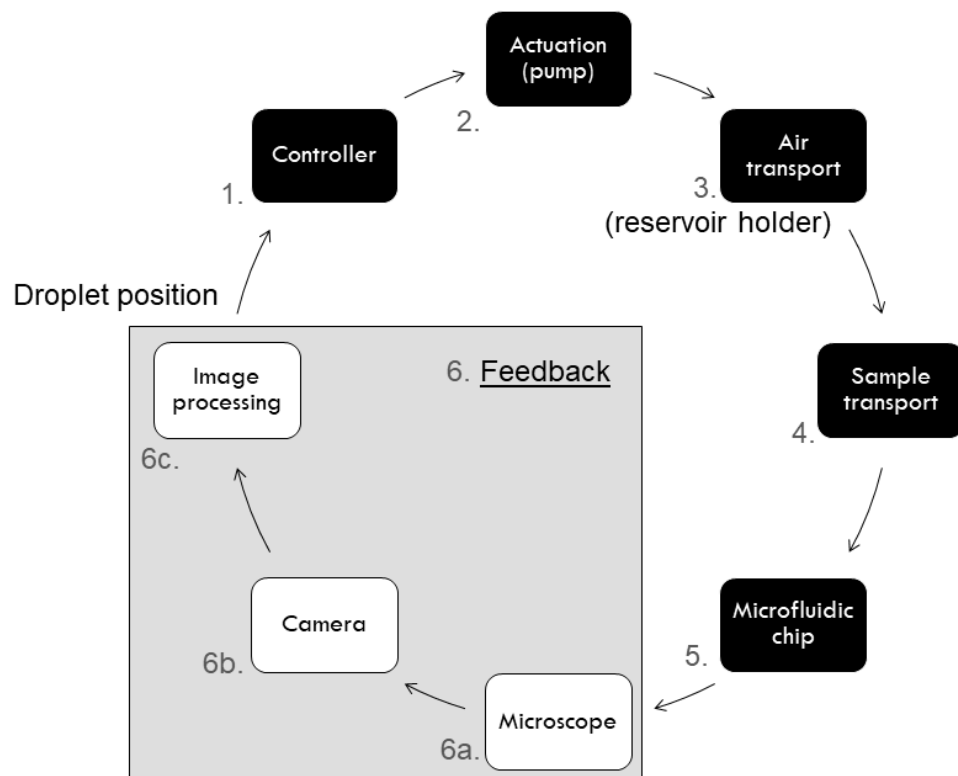


Figure 9.1: System overview separated into independent components.

the minimum requirement is satisfied—or not—taking into account the typical system noise as well as acceptable settling time and overshoot. The proposed benchmark test is a $200\ \mu\text{m}$ step-change for a water droplet that is $\sim 300\ \mu\text{m}$ long in a $50\times 100\ \mu\text{m}$ microchannel with silicone oil 50 cst as the continuous phase. The resulting response should: (i) settle within $6\ \mu\text{m}$ of the objective position, (ii) have a settling time less than 1 second, and (iii) exceed the objective position by no more than 20% (i.e. $40\ \mu\text{m}$).

Moreover, the performance is directly impacted by other components of the system. Saturation of the actuation (either through the limited pressure pump range or air leakage at the reservoir holder) limits the power available as well as introduces non-linearity. The time required to complete each loop that includes the communication with each element and performing all calculations depends generally on each component but image processing and actuation take the most time to complete. The delay can affect system stability if too large.

9.2.2 Order minimization

Reducing the model order generally implies a simplification in the model based on assumptions and neglecting or grouping less influential physics. The trade-off for a smaller order model is typically a loss of accuracy. The negative effects on accuracy can nevertheless be negligible enough to compensate for the gained model simplicity. The two main advantages of reducing the model order are: faster computation and easier controller design.

Arguably, a simpler model will involve smaller matrices. Thus, online computations of the required actuation based on the feedback completes faster. However, considering the computational power provided by the computer in this system architecture, the computational resources are plentiful and the difference in computation time is most likely negligible compared to the other delays required to perform the other steps. Computational power could be more restricted on a modular platform. However, the potential improvements are deemed small enough to not prioritize to achieve a faster control loop.

A simpler model has the potential to simplify the design and the understanding of the controller. Some performance might have to be sacrificed, but the impact could be inconsequential although better quantification tools for the performance are required to accurately assess. The reconfigurable controller design based on each setup is automated and does not require anything more than the information about

the current setup such as channel dimension, properties of fluid used, and inner tubing diameter. However, considering the highly interdisciplinary nature of this approach that combines microfluidics and controls, a more accessible design has the potential to help researchers adopt this platform more readily if they can understand it better.

9.2.3 Actuation saturation

In the context of pressure-driven flow that uses a pressure pump and reservoir holder, the actuation can saturate from two different sources: pressure pump range, and reservoir holder air leakage.

The pressure pump has a maximum pressure that it can apply (1 bar for *Fluigent MFCS* and 2 bar for *Fluigent EZ*). Nevertheless, the pressure should be kept lower to avoid the delamination of the chip from the PDMS covered glass slide. The quality of the bond is affected by uncontrolled factors such as ambient air humidity. Consequently, a conservative maximum of 800 mbar is suggested. Furthermore, the pumps cannot apply vacuum (i.e. negative pressure). The minimum (i.e. 0 mbar) pressure is mitigated through the starting pressure setpoint around 200 mbar. The waste outlet is also connected to a pressure outlet to control the back-pressure.

The reservoir holder provides an interface between the pressurized air from the pump and the liquid samples to be fed to the microfluidic chip. The multiple connections need to be airtight, but for ease of use, they must also be easily removable. Thus, air can typically leak when applying high pressure, effectively saturating the actuation. The usual connections that leak are the top fitting for the sample tubing or the vial connection. Tightening the leaking connection rises the leaking pressure so that it is out of the current operating range. Moreover, an o-ring is added to the vial to help better seal the fairly coarse thread connection (M12X2). McMaster-Carr provides a suitable product that is summarized in Table 9.1. The deformable O-ring is used a few times but needs to be replaced periodically when not effective anymore.

9.2.4 Delays

The total time required to complete the control loop is a delay introduced into the system. The stability of the closed-loop system depends on: the plant, the controller, and the delay. If the delay is too long, an unstable closed-loop system can result.

Table 9.1: Sample vial O-ring for better seal (McMaster product number: 9559K18).

| 9559K18 | |
|----------------|--------------|
| Material | PTFE Plastic |
| Cross-section | Round |
| Dash number | 013 |
| Width | 1/16" |
| Inner diameter | 7/16" |
| Outer diameter | 9/16" |

Furthermore, the delay can limit the performance; although a better quantification is required to assess the significance of the impact.

The current software architecture performs all tasks in series although they are separated on different threads. When one thread completed its task, it idles and the following thread starts. The parallel computing power is not leveraged, but any conflict arising from concurrent access to the same variables is avoided; thus, the software is simpler to write and to maintain. Moreover, a real-time operating system would avoid the Windows sporadic delays from different tasks, but once again, at the expense of simplicity and accessibility. A good resource to handle multi-threading is “C++ Concurrency in Action” by Anthony Williams [304]. Although parallel computations are not implemented, here are some guidelines.

- Concurrency is defined as two or more separate activities happening at the same time.
- Context switching between threads takes time, performance might not be better due to the inherent overhead associated with the threads.
- A race condition occurs when the outcome depends on the relative ordering of the operations of two or more threads (to avoid).
- Mutual exclusion (mutex) tools (e.g. `QMutexLocker`) allow to lock a shared data structure to limit access, but deadlocks must be avoided with proper synchronization between the different access points.
- Conflict arises from multiple threads modifying the same data structure, but reading from multiple access points is ok.

Table 9.2: Typical distribution of delays [ms] for the software (maximum total delay allowed: 100 ms).

| 3 inputs, 1 T junction | |
|--------------------------------|-------|
| Image | 10-30 |
| Controller | < 5 |
| Pressure | 15-30 |
| 5 inputs, 3 T junctions | |
| Image | < 30 |
| Controller | < 5 |
| Pressure | < 50 |
| Δt_{max} | 100 |

- The two main categories of problems arising from concurrency are: unwanted blocking, and race conditions creating instability.
- Good guiding questions to keep in mind when testing and debugging: which data needs to be protected from concurrent access? How do you ensure that the data is protected? Which mutexes does this thread hold? Which mutexes might other threads hold?

Considering the current serial software architecture, the total 100 ms of every loop is distributed between three different tasks summarized in Table 9.2: image acquisition and processing, controller calculations, and pressure actuation. The typical delay for each depends on the number of pressure output as well as the image processing. For the latter, 2X2 binning is used for both cases.

9.2.5 Control strategies

The modularity of each component allows the controller strategy to be considered more or less independently. The assumptions are that a droplet position feedback is obtained, and a pressure output at each of the inlet must be calculated based on the requested droplet position(s).

Single-input single-output (SISO)

The Single-Input Single-Output (SISO) approach considers each channel independently of each other. This proof-of-concept verified the model—to some extent—by successfully stabilizing the marginally stable plant. Without the controller, meaningful data cannot be recorded and analyzed. Hence, the SISO approach was the first step and pioneered the combination of passive and active to launch the active droplet control platform direction by David Wong [308].

Although coupling effects between the channels are not modelled or taken into account, the disturbance from other channels is rejected through the feedback for each individual channel. The pole-placement technique is used while considering only the resistance and inductance portion of the model (2nd order model). The capacitance is included only to assess the performance and compare the response as the higher-order system is not deemed required at this early stage.

The controller performed adequately and stabilized the marginally stable plant. Some disturbance from the motion of droplets in other channels were also successfully rejected. However, the analysis of the performance indicated that this approach would fail for faster systems. More importantly, the selection of the poles although governed by some guidelines requires tuning for a larger system. Thus, a more intuitive tuning technique that takes into account the channel coupling was developed next.

Multi-input multi-output (MIMO)

The Multi-Input Multi-Output (MIMO) controller approach takes into account the inherent coupling of each part of the microchannel network through the pressure field [307]. A state-space representation is well suited for MIMO systems and allows to leverage standard control techniques. In contrast to the arbitrary pole placement from the SISO approach, the Linear Quadratic Regulator (LQR) is a feedback control algorithm that relies on the minimization of an objective function. The objective function has two tuning matrices (Q and R) to weight the states and inputs differently. Furthermore, a Luenberger observer is similarly designed to estimate the states from the output(s). Finally, a static offset is estimated using a Kalman Filter to compensate for any pressure difference such as the hydrostatic pressure and Laplace pressure jumps.

The design of the controller relies on the tuning matrices that contain the relative importance within each matrix as well as between the two matrices. Each value is

assigned depending on the type of quantity the state or input represents and is automated. Therefore, any combination of fluids, microchannel network configuration, and dimensions are easily re-designed with the same procedure. The highly reconfigurable MIMO approach is more suitable than the SISO as it requires essentially no tuning from the user.

Adaptive command generator tracker

The SISO and MIMO approach both relied on the model to design and implement the controller; however, there are model-free approaches. The prominent artificial neural network most probably comes to mind, but they will be subsequently discussed. The direct Model Reference Control (MRC) is herein considered.

Indirect control schemes use the system response to estimate the system parameters periodically. However, for a complex model, the estimation step is too lengthy to efficiently complete online and convergence cannot be guaranteed. Thus, the direct approach is selected. The plant parameter estimation step is bypassed; the adaptive law rather compares the system output and matches it to the reference model output. No plant model is required; therefore, the only restriction on the order is to match the plant and reference model order.

However, the caveat is the restriction from the dimensions of the model and the input. For a command generator tracker, the existence of an inverse relies on the number of controls (i.e. input pressure) being equal to the number of output. Although a pseudoinverse can handle the cases when the number of inputs is larger than the number of output, the opposite case (more outputs than inputs) do not usually have a solution [146]. Therefore, the command generator tracker is only applicable to microchannel networks composed of two T-junctions. This limitation makes it less desirable to implement although it could improve robustness. The multiplexing at the T junction enables the completion of different manipulations. However, the number of reagents would be limited to two.

Other strategies

Other control strategies include artificial neural networks (ANN), model predictive control (MPC), and fuzzy logic.

Artificial Neural Network Another model-free approach different from the command generator tracker is based on Artificial Neural Networks (ANN). The network

ANN relies on a vast training dataset to learn both how the system behaves, and how to control the system [225]. The ANN is a black-box that cannot provide physical insight about the model; hence, this is a model-free approach that uses data rather than knowledge about the system. This is especially purposeful for nonlinear systems that are hard to model and to design a controller for. However, the microfluidic chip behaves “nicely” and does not exhibit acute nonlinear behaviour. Moreover, the current knowledge of the system would not be taken advantage of. Better use of neural networks would be for better image processing or to identify the model better through the grey-box system identification [2].

Model Predictive Control As its name implies, Model Predictive Control (MPC) uses the system’s model to optimize both the current time, but also, for the future. Only the current time step is acted upon; the optimization considering the future time steps is performed again at each time step to take into account the new information. The consideration of the future particularly helps for a higher-order system or systems with longer delays. However, in the case of the microfluidic chip, delays are relatively short. Although the model order is high (> 10) depending on the complexity of the microchannel network, MPC relies on the model of the plant to optimize future time steps. Consequently, the model should be reliable to benefit the most from an MPC algorithm. Moreover, the current model structure does not take into account the varying nature of the model as droplets are created, moved around, and merged. Therefore, the advantage of the MPC would most probably be limited by the inaccuracy of the model.

Fuzzy logic Fuzzy logic is more suited for the control of imprecise or vague numerical quantities. Therefore, this approach is deemed inappropriate for the easily quantified droplet position output and pressure inputs. Nevertheless, a fuzzy logic algorithm could be implemented to determine when the reservoir holder is leaking. A pressure difference between the pressure pump output and reservoir holder pressure is partly attributed to the pressure drop across the soft tubing. However, a “significant” pressure drop can indicate a leakage that saturates the actuation and potentially lead to unstable conditions. The fuzzy logic could detect and alert the user of leakage based on a defuzzification of the pressure difference between the applied and actual pressure output to determine whether it is significant or not.

9.3 Actuation (2)

The two common actuation methods for microfluidic systems are: the pressure pump and the syringe pump. The Hagen-Poiseuille law dictates the relationship between pressure difference, resistance, and flow rate [31].

$$\Delta P = R \cdot Q \quad (9.1)$$

where ΔP is the pressure difference [Pa], R is the resistance [$Pa \cdot s \cdot m^{-3}$], and Q is the flow rate [$m^3 s^{-1}$].

The resistance is determined by the fluid properties and geometry of the channel. While ultimately the flow rate quantifies the flow behaviour, a syringe pump that directly sets the flow rate is not suitable for active control. The response time of a syringe pump is too long (on the order of one minute) and the flow pattern exhibits persistent long-term transient behaviour. On the contrary, the pressure pump provides fast changes in actuation and long-term stability. However, varying resistance of the channel network from droplet manipulations results in fluctuation in flow rate. Nonetheless, designing long channels and using feedback can mitigate these oscillations. Therefore, although a syringe pump provides direct control over the flow rate, pressure-driven flow is favoured for its desirable short- and long-term dynamics.

9.3.1 Limitation from commercial systems

Multiple companies offer pressure pump systems that satisfy the needs of the microfluidic community. Although Dolomites (*Mitos Fluika Pump*) and Elveflow (*AF1*) offer pressure pumps, only the *Fluigent MFCS-EZ* is considered due to the availability restricted by their expensive price.

Commercial systems such as the Fluigent pressure pumps are effectively black-boxes; a pressure is requested, and the pressure output changes accordingly. Although a Software Development Kit (SDK) allows controlling the pump within another custom software, there is no information about the inner workings of the pump or the driver. The documentation explains how to use the functions available through the SDK dynamic link library (DLL) file. However, the capabilities are restricted by the SDK provided by the company.

The major limitation of the Fluigent SDK is the writing and reading speed. As shown in Figure 9.2, the operating speed of the pump is limited to 100 ms.

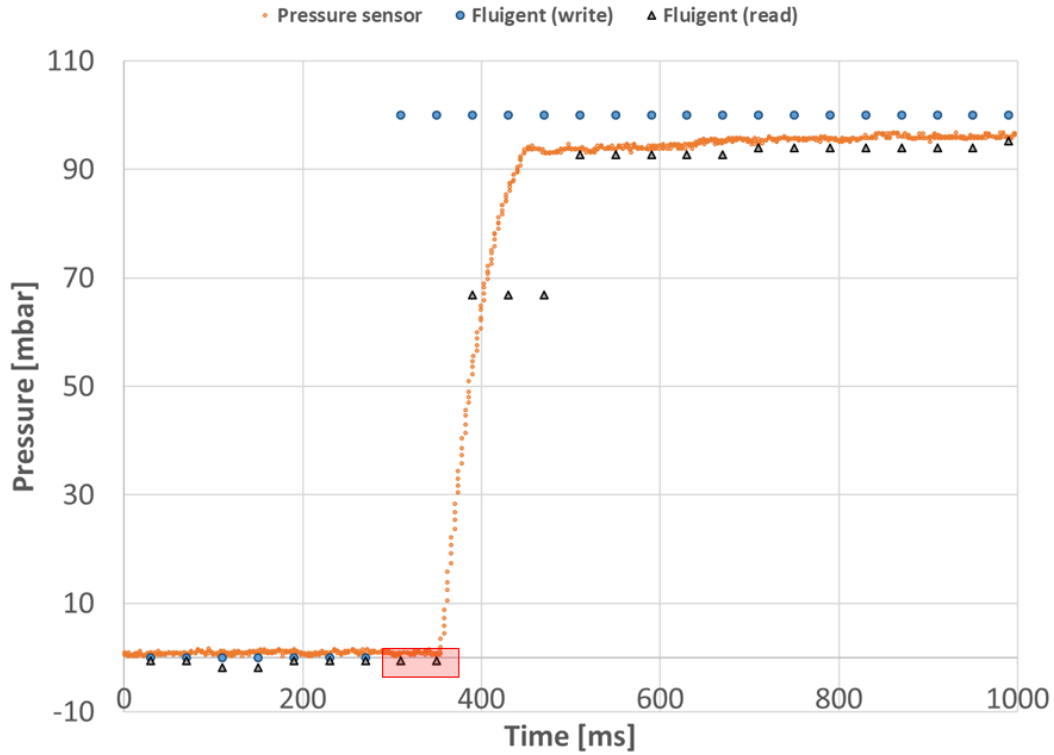


Figure 9.2: Speed limitation test for *Fluigent EZ-MFCS*. Unresponsive below 100 ms. Sampling shown is every 40 ms.

Attempting to operate at 40 ms, for instance, results in repeated data points as the pump updates its state *only* every 100 ms. The feedback from the pump can easily be tested, but to test the pressure command speed, an external pressure sensor is used. The red rectangle in Figure 9.2 highlights the data points for which the command changed—as per the instructions from the software running at a 40 ms sampling loop—but the pressure does not immediately start to change according to either to the pump or external pressure sensor feedback.

The SDK for the Fluigent pump allows setting the proportional term of the controller. Therefore, the responsiveness of the pressure output is tuned. However, there are still some restrictions as the control scheme itself cannot be changed and no information is available other than the one “alpha” parameter that is adjusted

by the user using the `mfcs_set_alpha` function.

9.3.2 Open-source system from off-the-shelf pressure regulators

An open-source system is developed to make microfluidic more accessible to researchers by decreasing the financial burden of important equipment. Contrarily to the commercial system such as the *Fluigent MFCS-EZ* pump, the open-source pump—named μ Pump—allows for customization of each component. Moreover, the details of the communication protocol are available and customizable.

The pressure control is provided by an off-the-shelf pressure regulator (*ControlAir T900-CIM*). Thus, although μ Pump is much more customizable than the comparable commercial systems, the pressure response is dictated by the pressure regulator. Characterization of the response estimated the natural frequency of the actuator around 6 Hz. Therefore, the pressure regulator is the limiting factor for pressure pump response time. A similar natural frequency—within an order of magnitude—is expected from any piezoceramic actuator.

9.3.3 Other approaches

Pressure pumps

Multiple pressure pumps aimed towards microfluidic research are available on the market. Due to their prohibitive cost, only one model (*Fluigent MFCS-EZ*) is thoroughly tested and analyzed as it is the only apparatus purchased.

The accuracy and stability of the *MFCS-EZ* of ± 1 mbar are taken as a baseline against which the other models are compared. The typical operation of the microfluidic pump requires pressures larger than 200 mbar; thus, the error is limited to $< 1\%$. Furthermore, a software development kit (SDK) must be available to integrate the pressure pump control within the custom active droplet control software. *Elveflow* offers a product with a similar performance of 1 mbar accuracy for their 2 bar system [77]. Moreover, they quantify their settling time as 35 ms. An SDK is also available.

The use of a syringe pump is motivated by the unavailability of a pressurized air source typically required to operate pressure pumps. *Dolomite* offers pressure (or vacuum) pumps with more limited pressure ranges (500 mbar) but that does not require a pressurized air source. Moreover, no external power source is required

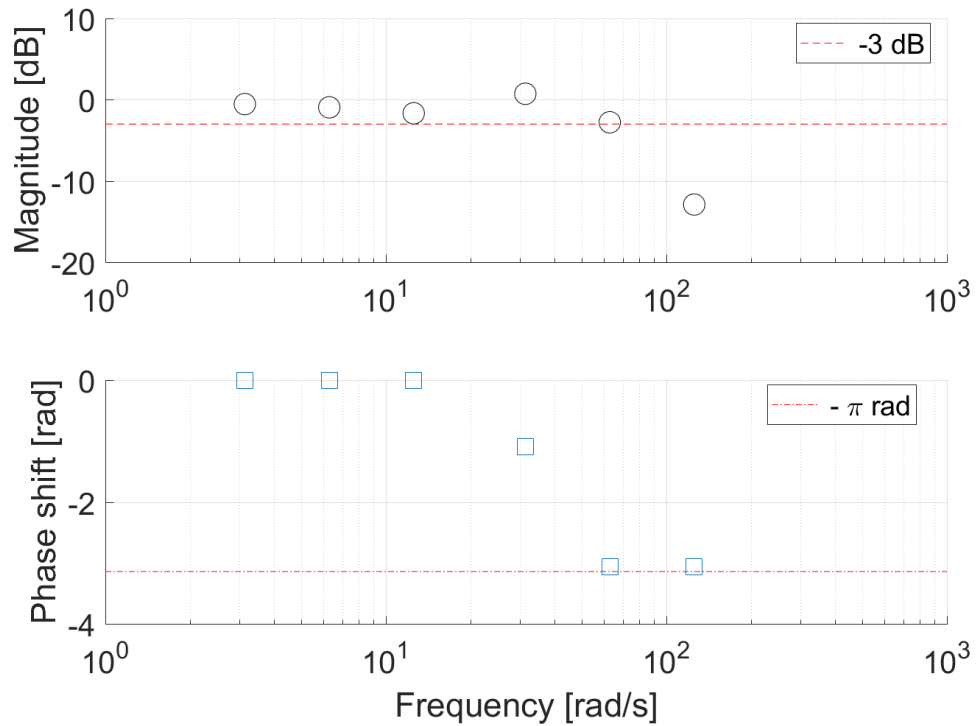


Figure 9.3: Bode plot for the pressure regulator (*ControlAir T900-CIM*) included in μ Pump. Natural frequency (ω_n) around 6 Hz. Reproduced from Ref. [90].

other than the USB connection. Thus, this product is suitable for integration in an environment with more limited resources available. However, some accuracy and stability must be sacrificed with a typical 3 mbar error range [68]. Less demanding applications in terms of accuracy but more demanding because of the environment might benefit. The current active droplet control platform as laboratory equipment has both power and pressurized air available. Nonetheless, in the context of making the requirements less stringent on researchers starting in the field, this product could potentially offer certain advantages.

Servovalves

Considering the limited response time by the type of actuator (i.e. electro-mechanical), a potential solution would be to use another principle to drive the flow. Servovalves typically provide faster actuation due to the mechanical feedback; essentially, an

electric signal is used to modulate the magnetic force retaining the flapper to provide the correct flow rate for which the input pressure is used to drive the valve. A lot of servovalves are developed for large flow rates providing unreasonable accuracy at the required small flow rate (e.g. Moog D941 Series, 8 to 80 L/min with 33 ms response time). Nonetheless, this alternate approach to drive the flow also has a limited selection that handles smaller flow rates.

The *Moog 30 series* range is available down to 0.95 L/min and has a natural frequency of 200 Hz. However, they are rated based on very high input pressure (3000 psi); further characterization of the response under lesser input pressure is required. Moreover, the servovalves handle liquids rather than air. Consequently, either the samples are directly controlled at the expense of contamination and cleaning risks or a novel apparatus similar to the reservoir holder but for liquid-to-liquid interfacing must be developed. Finally, the servovalves output flow rate rather than pressure although they could be combined in a feedback loop with a pressure sensor. *Moog* also have their *E024-LB series* that is for high-performance applications such as aerospace and Formula 1. The specifications go down to 0.4 L/min and a 250 Hz response while maintaining a lightweight and small form factor.

The German origin company *Burkert* offers servovalves specifically for microflows. The volume per stroke is small (5 μL /stroke) but could lead to pulsatile flow, especially for the slower and intermittent flow rate required by the active control to perform droplet manipulations.

The main caveat to servovalve is that they are designed to handle fluids rather than air. Therefore, to avoid cross-contamination, a similar approach as the reservoir holder could be adopted. The servovalve can feed a liquid to pressurize air that is then used to act on the sample. However, such a strategy could significantly reduce the actuation bandwidth.

Sliding mode control pressure pump

The major cost associated with the pressure pump as demonstrated by the open-source μPump is the pressure regulators converting the analog voltage to a pressure output. An alternative approach is to use a combination of solenoid valves [288]. Although some accuracy and stability are sacrificed, the cost is reduced. However, solenoid valves have a limited number of cycles they can perform before failing; hence, minimizing the on-off switching is desirable. A sliding mode control helps to prolong the valve lifetime [334].

On-chip actuation

An on-chip actuation approach could eliminate the air and sample transport while potentially increasing the actuation frequency. However, by eliminating the reservoir holder, the pressure pump actuation would then be dependent on the driven fluid; extensive calibration would most probably be necessary.

Manual actuation approaches are not suitable; the active control approach requires to automatically adjust the actuation according to the calculations from the controller based on the feedback.

A piezoelectric film integrated on-chip is demonstrated to control the flow of water over the range of 0 to 300 $\mu\text{L}/\text{min}$ by tuning the frequency and peak-to-peak voltage of the applied voltage [335].

Another approach uses electro-conjugate fluid pumps that have a 22 X 21 X 1 mm footprint. Oil is driven directly, whereas water is pushed using oil. The relationship between the voltage and resulting flow rate depends on various factors requiring careful calibration, namely: surfactant concentration, viscosity, and wettability [205].

An on-chip micropump developed for organ-on-a-chip applications vibrates a PDMS membrane using a magnet [211]. The frequency and peak voltage of the vibrations are related to the resulting flow rate. However, the pulsating nature of the flow is unsuitable for droplet microfluidics while it is sufficient for single-phase flow. Moreover, the reported accuracy is not satisfactory for the active droplet control platform.

9.4 Air transport and reservoir holder (3)

The pressure from the air output from the pressure pump interfaces with the sample at the reservoir holder, and more specifically, at the surface of the sample in the vial. The additional hardware—that is the reservoir holder with its connections—required to interface between the pressurized air and the samples allows for the pressure pump to be used with any liquid sample without requiring any calibration or any adjustment. The pressure at the sample tubing inlet is the addition of the air pressure to the hydro-static pressure from the liquid contained in the vial. Furthermore, if the surface tension is strong, a non-negligible force could be applied from the curvature with the side of the vial. Nevertheless, only air pressure and hydro-static pressure are herein considered. The impact should be minimized at least within the expected variations from the pressure pump output (± 1 mbar for *Fluigent MFCS-EZ*).

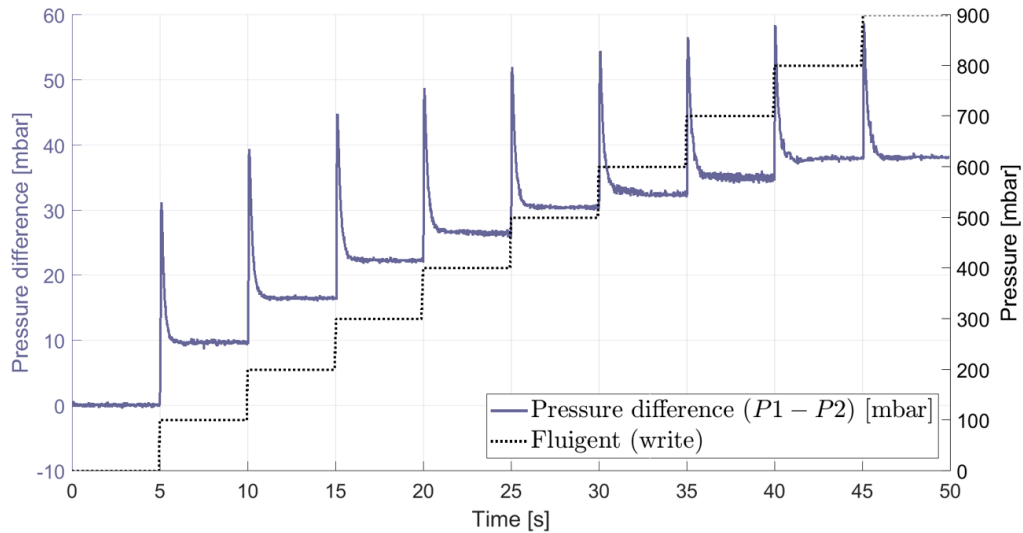


Figure 9.4: Pressure fluctuations between the pressure pump output and the reservoir holder connected by a 1-mm inner diameter soft tubing of 65 cm length.

The soft tubing connecting the pressure pump output to the reservoir holder has two potential inner diameters that fit the standard barbed connection: either 1 mm or 1/16" (1.6 mm). Accurate pressure measurements from external pressure sensors revealed that the larger tubing of 1/16" inner diameter did not exhibit any pressure difference or pressure propagation dynamics. Conversely, the 1 mm inner diameter tubing showed a pressure difference that is approximated using a first-order model (see Chapter 6). Figure 9.4 shows the pressure difference as a step pressure is input over a 1 bar range. Even if the peak occurring at each step change settles after 2 seconds, there is nevertheless a persistent pressure difference between the pump output and the reservoir holder. The difference is attributed to the resistance of the tubing. The resistance is highly dependent—to the fourth power—on the inner diameter of the tubing; thus, the small difference in the inner diameter of 0.6 mm has a high impact on the resistance of the two types of tubing. The resistance of the 1/16" inner diameter tubing is decreased enough for the pressure difference to be negligible. Although for the active droplet control platform such difference is detrimental to its performance, passive microfluidics is more lenient about static offset; pressure stability is more important. The first-order behaviour of the tubing can effectively act as a filter to dampen the oscillations from the pressure pump, and thus, provide a more stable pressure source.

According to the hydrostatic pressure principles, the pressure increases linearly with depth within the vial proportionally to the density of the liquid. The sample tubing tip is usually at the bottom of the vial to prevent introducing air bubbles as the sample level decreases in the vial. However, the height of the liquid above the tubing tip adds pressure in addition to the one provided by the air as illustrated in Figure 9.5. For water, the hydrostatic pressure corresponds to approximately 1 mbar for each centimetre of depth. For shorter experiments or experiments using only a small volume from the vial, the height variations are potentially negligible as they remain within 1 cm throughout the experiments. However, some variations are introduced over longer experiments or between experiments when the level within the sample vial fluctuates.

$$P_{hydrostatic} = \rho \cdot g \cdot h \rightarrow \sim 1 \text{ mbar per 1 cm of water} \quad (9.2)$$

$$P_{liquid} = P_{air} + P_{hydrostatic} \quad (9.3)$$

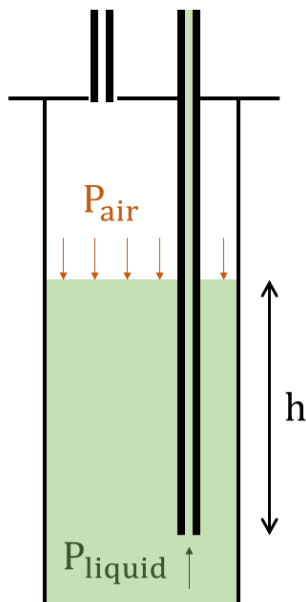


Figure 9.5: Schematic representation of the combination of air and hydro-static pressure transmitted to the liquid sample.

Another potential disadvantage of the reservoir holder is the relatively large volume of sample required to operate. Although the microfluidic experiments use much smaller volumes, the vial should realistically contain at least 100 μL to mitigate the risk of introducing air into the sample tubing. Such high dead volume could ideally be reduced. However, intuitive solutions such as decreasing the volume diameter might lead to more significant capillary forces. Other smarter approaches should be sought to mitigate this issue.

9.5 Sample transport (4)

The reservoir holder provides the interface for the pressure to be applied at the inlet of the sample tubing. Then, the sample is carried to the microfluidic chip inlet.

9.5.1 Dead volume

Similarly to the vial used to contain the sample, the tubing contains a volume significantly larger than the volume required for the droplet manipulations. Hence, the advantage of requiring a smaller volume is reduced. The dead volume is lowered by using a smaller inner diameter and shorter tubing. However, the practical limit of reaching from the reservoir holder to the microfluidic chip restricts how much dead volume is eliminated. Another alternative eliminating the need for the reservoir holder with the sample being loaded directly on the chip might be beneficial but needs to be developed.

Furthermore, the consideration should take into account the difference in scale between the vial and the sample tubing. While the vial can contain ~ 2 ml, the largest tubing diameter with a length of 50 cm corresponds to 0.23 ml that is $\sim 10\%$. As for the smaller tubing, the volume of 0.025 ml is less than 2% of the vial volume.

9.5.2 Dynamics

Considering that tubing is used to transport the sample from the reservoir holder to the microfluidic chip, the dynamics associated with it are minimized. The dynamics are summed by assigning values to RLC circuit elements similarly to how the model is developed. The control loop running at every 100 ms gives an order of magnitude below which any dynamics is deemed negligible. Moreover—and potentially, more

importantly—the relative scale of the dynamics of the tubing compared to the microfluidic chip indicates whether it is appropriate to neglect the dynamics from the tubing.

Resistance

The resistance of the tubing represents the viscous forces involved in moving the sample through the tubing.

$$R_{circ} = \frac{8\mu l_{tubing}}{\pi r^4} \quad (9.4)$$

The sample tubing resistance could be neglected if less than 1 % of the microchannel resistance. For typical rectangular channels of $50 \times 100 \mu\text{m}$, the resistance is calculated as follows [31].

$$R_{rect} = \frac{12\mu l_{channel}}{wh^3(1 - 0.63\frac{h}{w})} \rightarrow R_{50 \times 100} = \frac{12\mu l_{channel}}{8.56 \times 10^{-18}} \quad (9.5)$$

Therefore, for a 1% contribution of the tubing resistance with respect to the microchannel resistance, the diameter should be as follows for a tubing length of 50 cm and a channel length of 5 mm.

$$\frac{R_{circ}}{R_{50 \times 100}} = \frac{8\mu l_{tubing}}{\pi r^4} \cdot \frac{1}{\frac{12\mu l_{channel}}{8.56 \times 10^{-18}}} = 0.01 \rightarrow \frac{5.71 \times 10^{-18} l_{tubing}}{\pi l_{channel} r^4} = 0.01 \quad (9.6)$$

$$\frac{5.71 \times 10^{-18} (0.5)}{\pi (5 \times 10^{-3}) r^4} = 0.01 \rightarrow r = 0.00037 \rightarrow r > 0.37 \text{ mm} \quad (9.7)$$

From the tubing length of 50 cm, and a small channel length of 5 mm, the recommended minimum tubing radius is 0.37 mm. However, if the channel is longer than 5 mm—and thus, has a higher resistance—the tubing can have a smaller diameter. Conversely, if the tubing is longer than 50 cm, the diameter should be smaller. However, considering that the relationship to the radius is to the 4th power, the tubing diameter recommendation is not expected to significantly change. Furthermore, the recommendation is independent of the fluid viscosity because both the tubing and channel contain the same fluid; thus, the viscosity cancels in the ratio.

However, this recommendation does not take into account the reduction of the dead volume contained in the tubing. The length should be minimized, but the reduction is only linear. In contrast, by minimizing the diameter, the volume decreases

to the second-order that is much more impactful, especially for expensive reagents. However, for the more inexpensive samples, then, larger tubing is more desirable with minimal financial impact, but a larger impact on the system's behaviour.

Capacitance

The capacitance effect has two main contributors: the elasticity of the tubing walls and the compressibility of the fluid. Each is considered independently. The elastic modulus of the tubing is lesser than the adiabatic bulk modulus of water; hence, the analysis will first focus on this more important factor. Although the thin-wall assumption is not fully valid in this situation, it can still provide valuable insight concerning the scale of the effects. Furthermore, considering the thick-wall would result in a more conservative (i.e. smaller) time constant estimation for the same outer diameter. The outer diameter is the typical 1/16" compatible with the microfluidic connectors.

$$C_{tubing} = \frac{3\pi r_{inner}^3 l}{2E(r_{outer} - r_{inner})} = \frac{3\pi r_{inner}^3 l}{2E(0.793 \times 10^{-3} - r_{inner})} \quad (9.8)$$

The time constant associated with the capacitance also depends on the resistance of the tubing.

$$\tau_{RC} = R \cdot C = \frac{8\mu l}{\pi r_{inner}^4} \cdot \frac{3\pi r_{inner}^3 l}{2E(r_{outer} - r_{inner})} = \frac{12\mu l^2}{r_{inner}(r_{outer} - r_{inner})E} \quad (9.9)$$

Let's consider the worst-case scenario for a longer tubing of 50 cm, the higher viscosity oil we typically use (silicone oil 50 cst), and the outer radius for the 1/16" tubing. The relationship is quadratic with respect to the inner radius (r). Therefore, the time constant is evaluated for the usual tubing dimensions (0.010", 0.020" and 0.030") rather than calculating the radius range based on the time constant criterion. All standard tubing size results in negligible associated time constants that are less than 5 ms.

$$\tau_{RC1} = \frac{12(0.04815)(0.5)^2}{r(0.00079 - r)500 \times 10^6} \quad (9.10)$$

$$\tau_{0.010"} = 3.4 \text{ ms}; \quad \tau_{0.020"} = 2.1 \text{ ms}; \quad \tau_{0.030"} = 1.8 \text{ ms} \quad (9.11)$$

For the contribution from the adiabatic bulk modulus (i.e. fluid compressibility), the contribution to the time constant is similarly negligible.

$$\tau_{RC2} = \frac{8\mu l}{\pi r^4} \cdot \frac{l\pi r^2}{\beta} = \frac{8\mu l^2}{r^2\beta} \quad (9.12)$$

For a target maximum time constant of 5 ms considering the most viscous sample used and a generously long tubing, the corresponding radius criterion is then.

$$\tau_{RC2} = 5 \times 10^{-3} = \frac{8(0.04815)(0.5)^2}{r^2(2.2 \times 10^9)} \rightarrow r > 0.094 \text{ mm} \quad (9.13)$$

Inductance

As the fluid is accelerated either positively or negatively, the inertial effect of transporting the sample through the tubing contributes to the inductance.

$$L = \frac{\rho l}{A} \quad (9.14)$$

The time constant associated with the inertia effects is the ratio of inductance to resistance. For the recommended tubing diameter, a radius is recommended to minimize the time constant such that it is negligible compared to the control loop time scale.

$$\tau_{LR} = \frac{L}{R} = \frac{\rho l}{\pi r^2} \cdot \frac{1}{\frac{8\mu l}{\pi r^4}} \rightarrow \tau_{LR} = \frac{\rho r^2}{8\mu} = \frac{r^2}{8\nu} \quad (9.15)$$

Typically, the least viscous sample used—which will result in the highest associated time constant—is water-based with a kinematic viscosity about $1 \times 10^{-6} \text{ m}^2/\text{s}$ (or 1 cst). Thus, for a maximum time constant of 5 ms, the maximum diameter is calculated.

$$\tau_{LR} = 5 \times 10^{-3} = \frac{r^2}{8 \cdot 1 \times 10^{-6}} \rightarrow r < 0.2 \text{ mm} \quad (9.16)$$

Table 9.3: Summary of available tubing dimensions in imperial and metric units.

| Imperial inner diameter [<i>in</i>] | Metric inner radius [<i>mm</i>] |
|---------------------------------------|-----------------------------------|
| 0.010 | 0.127 |
| 0.020 | 0.254 |
| 0.030 | 0.381 |

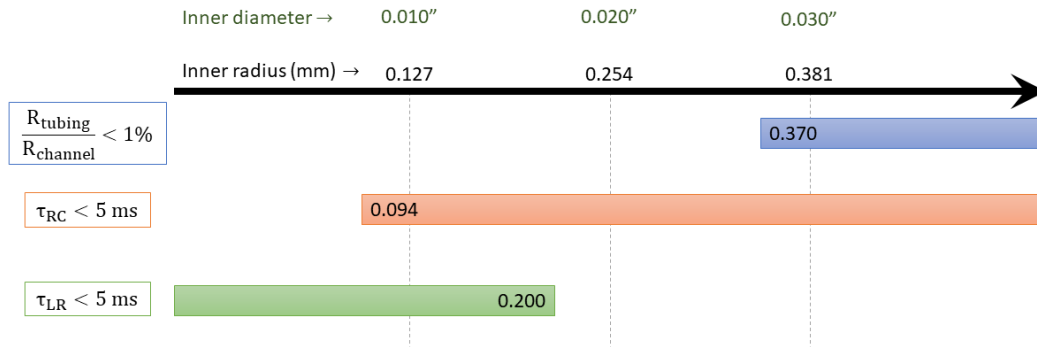


Figure 9.6: Graphical representation of the constraints to minimize the resistance ratio and time constant associated with the capacitance and inductance. The 3 common inner diameters for 1/16" outer diameter tubing are denoted by the grey vertical lines. Not to scale.

Summary

The typical tubing used is a PFA tubing with 1/16" outer diameter available in 3 sizes of inner diameter. The dimensions in imperial and metric units are summarized in Table 9.3. Moreover, a graphical representation of the constraints from each of the elements is shown in Figure 9.6.

Based on the available dimensions, the recommended tubing to simultaneously optimizes the time constant associated with the tubing elasticity, fluid compressibility, and inertial effects is: 0.010" inner diameter. However, the resistance ratio of 1% cannot be satisfied simultaneously. Nonetheless, the resistance of the tubing is more accurately characterized and is taken into account as a pressure drop while the various dynamic effects are much more difficult to quantify confidently and introduces additional complexity with increased model order. The resistance is

a passive element that represents the pressure drop, but that does not involve any time-variations. The corresponding ratio would require microchannels to be at least 349 mm in length to maintain the 1% negligibility that is unreasonable considering the limited footprint available. The resistance ratio could be reduced with a shorter tubing, but that would increase the dynamics associated with the capacitance.

$$\frac{5.71 \times 10^{-18}(0.5)}{\pi(l_{channel})(0.127e - 3)^4} = 0.01 \rightarrow l_{channel} = 0.349 \text{ m} \quad (9.17)$$

For passive microfluidics, the short-term dynamics from the capacitance and inductance are not as important as the resistance ratio. However, channel lengths for passive designs are typically longer. Thus, another guideline should be developed. As for the active design, the contrary applies; short-term dynamics are more detrimental than the resistance ratio between the tubing and the microchannels. The resistance is a passive element that will introduce a pressure drop proportional to the flow rate. For single-phase flow that is present in the sample tubing, the modelling is accurate enough. Comparatively, the dynamic effects of capacitance and inductance have more uncertainty in their modelling and can detrimentally affect the controller performance.

9.6 Microfluidic chip (5)

The dynamic behaviour of the microfluidic chip is considered in two parts: inductance and capacitance. The resistance is a passive element that is related to the flow rate and pressure drop. The time constant associated with the dynamics—either inductance or compliance—is used to assess its importance. The system sampling rate is 100 ms. Therefore, any dynamic with a time constant less than 5 ms is neglected.

For microfluidic channels, the small characteristic length leads to negligible inertial effects. Considering a relatively bad case for which inductance is more prominent yields a negligible time constant. Therefore, the inductance of the microfluidic chip is neglected without significant loss of model accuracy.

$$\tau_{LR} = \frac{L}{R} = \frac{\rho l}{wh} \cdot \frac{wh^3(1 - 0.63\frac{h}{w})}{12\mu l} = \frac{h^2(1 - 0.63\frac{h}{w})}{12\eta} \quad (9.18)$$

$$\tau_{LR} < \frac{(50 \times 10^{-6})^2(1 - 0.63 \cdot 0.1)}{12 \cdot 1 \times 10^{-6}} < 0.2 \text{ ms} \quad (9.19)$$

The capacitance dynamics of the microfluidic chip has two main sources: fluid compressibility and material compliance. Similarly to the sample tubing, the adiabatic bulk modulus of the fluid is much larger than the elastic modulus of PDMS. The relative importance of the fluid compressibility depends on the selected chip material.

$$\tau_{RC1} = \frac{12\mu l}{wh^3(1 - 0.63\frac{h}{w})} \cdot \frac{lwh}{\beta} = \frac{12\mu l^2}{h^2\beta(1 - 0.63\frac{h}{w})} \quad (9.20)$$

$$\tau_{RC1} < \frac{12(0.04815)(100 \times 10^{-3})^2}{(50 \times 10^{-6})^2(2.2 \times 10^9)(1 - 0.63 \cdot 0.5)} < 1.6 \text{ ms} \quad (9.21)$$

Neglecting the inductance and fluid compressibility leaves the compliance from deformation as the principal source of dynamics effects for the microfluidic chip. The experimental data (see Chapter 8) indicates a capacitance on the order of $10^{-15} \text{ m}^3/\text{Pa}$. The capacitance and channel length are inversely proportional. Longer channels increase the resistance, and thus, decrease the flow rate for the same pressure. The channel resistance towards the upper range is on the order of $10^{-15} \text{ Pa} \cdot \text{s}/\text{m}^3$. Therefore, the time constant is significant and should not be neglected. The updated formula from Chapter 8 requires a fitting parameter (ϕ) that is between 2 and 20 depending on geometry and flow rate. Nevertheless, the agreement with the experimental data is much better.

$$C_{chip} = \phi \cdot \frac{h w l (1 + \nu)}{E} \quad [\mathcal{O}(10^{-15}) \text{ m}^3/\text{Pa}] \quad (9.22)$$

9.7 Feedback (6)

The current controller uses the droplet position as feedback. Although velocity could be obtained from the flow rate, the measured flow rate is typically the continuous phase flow rate. Although the difference between the continuous and dispersed phase flow rate is not outrageously significant, the few percent difference can lead to unacceptable performance for the control of the droplets (i.e. the dispersed phase) [133]. Therefore, the potential feedback methods considered will be restricted to droplet position feedback.

The requirements are based on the current characteristics of the system to maintain the current manipulation accuracy. The resolution is about $3 \mu\text{m}/\text{pixel}$, and the maximum frequency achieved is 10 Hz; the impact on computation time and the overall architecture is considered. The main categories of feedback are: optical and

electric feedback. Visual feedback from the camera attached to the microscope as well as the direct implementation of CMOS arrays are considered for optical techniques while capacitive and microwave sensors are considered for potential electrical feedback approaches.

9.7.1 Visual feedback

The current system feedback is provided by a camera attached to the microscope in combination with an image processing algorithm. The phase contrast between the aqueous and oil phase allows for simple identification of the droplet position within the channel under bright field view.

Optical detection can be more advantageous than electrical signal feedback because it is more specific; with electrical signals, multiple situations can yield the same signal while for optical feedback, the signal is more robust. Identifying the droplet position is not jeopardized by the projection of the 3D droplet shape unto the 2D camera sensor when a proper focal plane is used. Moreover, fluorescent dyes are generally selected based on the application and bought off-the-shelf—albeit some are expensive—from a large selection as the field is mature, and fluorescence tagging is common in many bio-applications.

Dyes can be expensive not only because of the price tag of the chemical itself but also, by requiring specific filters to tailor the excitation and emission spectrum. Moreover, the wide-spectrum light source is expensive to acquire but is used for a wide range, and possibly all dyes. Most importantly, the feedback provided by the dyes regarding the assay requires switching from bright field to fluorescent view. This is challenging for the current simple image processing that is stopped such that the system remains stable. However, the controller is not actively maintaining the droplet position; hence, droplet drifts and must be manually maintained in position for the required duration. A peak detection correlation algorithm using the droplet shape is used to post-process the image and extract the fluorescent intensity of the droplet for each frame.

9.7.2 Capacitive sensors

Capacitive sensors utilize the difference in dielectric constant (ϵ) between the dispersed and continuous phases. The capabilities of capacitive sensors have been shown

to provide not only droplet presence but also droplet velocity using inexpensive hardware and software [76]. However, the information provided is localized to the sensor; thus, to acquire a droplet position over the entire channel length, sensors must be located underneath its full length.

Fabrication techniques for capacitive sensors limit their minimal size—and thus, resolution—around $10\ \mu\text{m}$. Furthermore, the microfabrication is significantly complicated and results in a lower yield. Finally, electrodes are prone to fouling. A passivation layer can shield them from the microchannel content; however, decreased sensor sensitivity results.

9.7.3 Microwave sensor

Another type of sensor uses the higher-frequency range (i.e. microwave sensors). Although promising advances have been made by fundamentals studies, the technology is not mature enough yet. Achieving complex position sensing of multiple droplets is currently too challenging.

9.7.4 CMOS arrays for lensless systems

Although individual electrical signal sensors are typically used in microfluidics to obtain localized information, CMOS arrays are used to detect within an *area* of interest. CMOS sensors are ubiquitous for cameras, but they can also be purchased separately and have been utilized within the context of the microfluidic field [214, 97, 62, 45, 148, 182, 220, 196].

The typical size of CMOS array pixels is about $\sim 2\text{-}6\ \mu\text{m}$. Smaller pixel size cause problems with a camera due to the diffraction of light through the aperture; hence, a significant decrease in pixel size is not expected in the future as there is no strong motivation for cameras that is the main target. Nevertheless, a high-end CMOS array (e.g. Canon 120MXSM) has 120 MP for a pixel size of $2.2\ \mu\text{m}$ that is comparable to the current resolution of the visual feedback. However, the rate for full resolution is quite low at 9 fps with the rolling shutter.

Similar to electric signal feedback methods, one of the main advantages of CMOS array is the potential to move away from the traditional microscope. Furthermore, contrary to electrical signal feedback methods, a CMOS array could be integrated into a module with a filter and light source to leverage the wide availability of dyes [214]. This is considered the most promising and versatile option for a modular system

moving away from the traditional microscope setup. Nonetheless, the progress of such a platform still requires development.

9.7.5 Microscope (6.a)

A microscope is a ubiquitous tool in many research laboratories, especially for life science studies. Considering the standard glass-slide size of *microfluidic* devices as well as the many life-science-focused applications, the usage of the microscope is compelling.

The versatility of the microscope comes from its easily interchangeable magnification objectives, and light filters for excitation and emission wavelengths. The camera attachment is also convenient for alignment. However, the size of the attachment (C-mount vs. F-mount) restricts the maximum sensor size, and thus, the field of view. Nikon released a new line of inverted microscopes (Eclipse Ti2 series). The camera F-mount offers more versatility to attach several optical elements as the focal length is longer than for the C-mount. More importantly, the diagonal sensor element is increased from 22 mm to 25 mm; thus, a larger camera sensor is compatible and increases the field of view.

The newer line of product from Nikon (both microscope and camera) has improved specifications, but the improvement is only marginal (25 mm for F-mount vs. 22 mm for C-mount). Nonetheless, a bigger sensor increases the resolution in terms of $\mu\text{m}/\text{pixel}$, and hence, more microchannel elements fit within the field of view. But it also depends on the camera that is discussed in further detail in Section 9.7.6.

Although the microscope is ubiquitous and versatile, it is bulky and expensive. Therefore, in the optic of building a modular system, the disadvantages outweigh the advantages. Each module would require a microscope.

9.7.6 Camera (6.b)

The camera attached to the microscope visualizes the microfluidic chip and provides the information to the computer that then uses image processing to extract the feedback (i.e. droplet position). The specifications of the camera limit the feedback capabilities in multiple ways; the most important are: field of view size, data transmission rate, and fluorescence signal detection.

Field of view size

The camera is attached to the Nikon Eclipse Ti microscope side C-mount. The field of view available as the workspace of the active droplet control platform depends on the sensor size. A bigger sensor allows imaging of a larger area without sacrificing resolution ($\mu\text{m}/\text{pixel}$).

However, the sensor size is limited by the aperture size of the C-mount. An F-mount as a slightly larger opening (25 mm versus 22 mm) that accommodates cameras with correspondingly larger sensors. Furthermore, the number of pixels on a sensor is also limited; light diffraction can result in increased noise and poorly resolved signals. Therefore, the pixels are $\sim 6 \times 6 \mu\text{m}$. Hence, a bigger field of view requires both a camera with a larger sensor and a wider F-mount.

Larger sensor size is desirable.

Data transmission rate

The rate that the camera can transmit the information to the computer depends on: (a) how much information is transmitted, and (b) how fast can the information be read.

The number of pixels—commonly expressed in megapixels (MP)—and the binning determines the number of values that are transmitted. Binning (e.g. 2×2 , 4×4) averages the value over multiple pixels to maintain the size of the region of interest (ROI) but at the expense of resolution. Conversely, the ROI is decreased to diminish the number of pixels while maintaining the resolution. However, for the active droplet platform, both the resolution and ROI must be maximized to encompass a workspace large enough to manipulate droplets and to accurately and robustly identify the droplet interface within the channel. The current setup utilizes 2×2 binning, not because the transmission is too long but rather, because the image processing is

not optimized; thus, too many pixels require too long to process and severely limit the control loop frequency. Moreover, the size of the information transmitted for each pixel depends on the bit-depth that determines how nuanced the images are; a greater bit-depth reduces quantization errors.

The two common transmission modes are either through a standard USB 3.0 connection or using a Camera Link with multiple (e.g. 10) taps. The multiple taps enable to systematically read multiple regions of the sensor simultaneously, and thus, decrease the delay. Therefore, both the frame rate and bit-depth are increased because of the increased transmission capabilities of the additional Camera Link hardware. Furthermore, the shutter operation limits the frame rate per second. A global shutter takes in all the information simultaneously which is slower than the rolling shutter typical of CMOS sensors.

Fluorescence signal detection

Optical detection commonly relies on the detection of fluorescent intensity to quantify the results. A camera sensitivity to fluorescent signal is quantified in electrons (e^-) and is related to the noise from the sensor signal. Photons hitting the sensor will generate a charge (i.e. electrons); for each pixel, an analog voltage is amplified and subsequently converted to a digital signal according to the pixel depth. Additionally, cameras that have vacuum-sealed cooling have better long-term reliability and image darker images with less noise.

Therefore, a lower read noise [e^-] is desirable.

Comparison summary of CCD and CMOS cameras

Table 9.4 summarizes the properties of two CCD cameras and one CMOS camera. Except for the cost, the CMOS camera exhibits better properties for all categories. The most important is the available frame rate that must be high enough, even if restricted by the USB 3.0 connection.

Therefore, the Andor Zyla sCMOS 5.5 is the best choice in this limited selection of camera because of its: (a) larger sensor size, (b) high transmission speed, (c) good bit-depth, and (d) fluorescence signal sensitivity. The cost is higher, but not significantly for the improved specifications.

The current system setup does not fully use the potential of the camera; hence, rather than purchasing another camera, improving the current architecture would

be better. The C-mount restricts the improvement from a larger sensor, and the fluorescence signal sensitivity is already low. However, the transmission rate could be accelerated using a 10-tap Camera Link. Moreover, the bit-depth would also be improved from 12-bit to 16-bit to provide more nuanced information. A frame rate of 100 frames per second (fps) provides visualization every 10 ms that is 2.5 times faster than the current 40 fps provided through the USB 3.0 connection.

Other options

Consumer-grade cameras sometimes have the same sensor as their scientific camera counterparts. However, the integration, support, and SDK are often lacking. The consumer cameras are not designed and built with post-acquisition and linearity as objectives. Thus, accurate quantitative intensity measurements (e.g. fluorescent signals) are compromised due to image compression, colour, and timing accuracy.

A more cost-efficient option is machine vision cameras. For example, *Flir* offers a wide range of products. The 10GigE line leverages the high transmission rate of 10 Gb/s through Ethernet to achieve both high resolution and high frame rate. The selected model is more affordable than the CMOS camera and achieves high frame rates at a satisfactory resolution. The smaller pixel size increases noise, but the degradation in performance cannot be easily quantified without testing the specific conditions. Moreover, although additional hardware is required to connect the camera to a desktop computer, the interface card is relatively inexpensive (~\$310, included in the price in Table 9.5) and uses one PCIe Express 2.0 bus from the motherboard. This additional hardware is much cheaper than the 10-tap camera link required to run the Zyla camera at 100 fps. Furthermore, compliance with the IEEE1588 standard enables accurate synchronization between multiple cameras without user input using a switch. An overview of the characteristics is presented in Table 9.5. *Flir* offers a variety of machine vision cameras with different sensor sizes; the larger the sensor, the slower the frame rate. Thus, there are other options, but the comparable one to the *Andor Zyla* camera is presented in Table 9.5.

Table 9.4: Summary of specifications of CCD and CMOS cameras

| Property | CCD Camera | | CMOS Camera |
|-------------------------------------------|----------------------------------|-----------------------------|----------------------------------------------------------|
| | QImaging Retiga-2000R [244] | ThorLabs 8051M-USB-TE [281] | |
| Model | | | Andor Zyla sCMOS 5.5 [7] (USB 3.0/Camera Link 10-tap) |
| Diagonal sensor size [mm] | 14.8 | 22 | 22 |
| Shutter | Global shutter, progressive scan | | Rolling shutter |
| Data transmission (full-frame) [fps] | 7.5 | 17 (4-tap, 40 MHz) | 40/100 |
| Bit depth | 12 | 14 | 12/16 |
| Fluorescence signal sensitivity [e^-] | 16 | < 10 (20 MHz) | 1 |
| Cost [\sim \$ CAD] | 9 000 | 14 000 | 17 000/24 000 |

Table 9.5: Summary of specifications of Machine Vision and CMOS cameras

| Property | Machine Vision | CMOS Camera |
|-------------------------------------------|----------------------------|----------------------------------------------------------|
| Model | Flir ORX-10G-123S6M-C [81] | Andor Zyla sCMOS 5.5 [7] (USB 3.0/Camera Link 10-tap) |
| Diagonal sensor size [mm] | 17.6 | 22 |
| Shutter | Global shutter | Rolling shutter |
| Data transmission (full-frame) [fps] | 68 | 40/100 |
| Bit depth | 12 | 12/16 |
| Fluorescence signal sensitivity [e^-] | 2.3 | 1 |
| Cost [\sim \$ CAD] | 6 000 | 17 000/24 000 |

9.7.7 Image processing (6.c)

Current image processing work flow

The current platform uses the open-source library *OpenCV* to perform image analysis and extract the feedback required for the controller (i.e. droplet position). There are two main aspects to image processing: setup and online image processing.

The droplet position identification relies on background subtraction. Although the approach of this algorithm is straightforward and sufficient for the proof-of-concept platform, it is the source of many limitations that will be subsequently discussed. The principle is that a static background image is recorded to: identify the channel region, make a mask to only consider the centre of the channel, separate the channel network into individual channels, and identify the channels such that the direction and label correspond to the designed controller.

The background is subtracted from the online images to identify the “new” elements within the field of view. The mask previously setup is applied such that only the interface across the flow direction is identified. Unique markers are assigned to each object, but to maintain continuity, the previous frame is analyzed to track and assign the same marker to the closest object. Furthermore, droplets are identified to recognize the so-called neck region that is used to generate or split droplets. Finally, the feedback is given to the controller from the position of the marker indicated by the user.

Key limitations

Some key limitations hinder the use of the platform: the static background, the processing speed, and the restriction to unfilled droplets under bright field view.

The process of saving a background image to subtract from the online image feed requires the field of view to remain static. Therefore, after the setup, the user is restricted to the same field of view at the same magnification; sometimes you expect the interface to soon appear within the field of view, but for unknown reasons, the interface is not present. If the user decides to change the field of view position to verify if there is debris obstructing the channel for example, then, the background setup must be repeated. The user would otherwise need to return to the *exact* position where the previous setup was completed which cannot be done manually with sufficient accuracy.

The current image processing completes within 30 milliseconds that is the second-highest delay after the pump actuation within the 100 milliseconds sampling rate (see Table 9.2). The resolution of the image is already sacrificed from ~ 1.5 to $3 \mu\text{m}$ per pixel using 2×2 binning to complete within the prescribed time frame. Consequently, the software should be optimized before the hardware (camera sensor size, camera frame rate, aperture size). Upgrading the hardware will be required when the image processing is not the limiting factor, but rather, the information available from the hardware is insufficient. Currently, the software cannot process all the information provided for the hardware; thus, part of the information is discarded through the binning process.

Water in oil appears “unfilled” such that the interface contrast is a line across the channel. Oppositely, a blood droplet would appear “filled” because of the darker colour and insignificant transparency. Consequently, the current image processing recognizes the whole blood droplet as the marker across the channel. Similarly, a droplet filled with fluorescent dye would not be properly recognized by the current algorithm because of the absence of a delimiting line at the edge. This is especially problematic for applications that rely on fluorescent signal for the assay feedback. The image processing and controller must be turned off while fluorescent measurements are recorded; the droplet tends to drift along the channel and must be manually maintained stationary through slight pressure adjustments.

Minor workflow improvements

The current image processing workflow can be marginally modified to improve efficiency without changing the overall structure. The *OpenCV* library is used but with a different processing approach. There are four minor workflow improvements herein suggested: divided workflow per channel, edge detection, automated threshold adjustment, and GPU processing.

Divided workflow The current workflow uses the whole image to subtract the background and apply the mask. All markers are identified, and subsequently, they are assigned to their corresponding channel. This is useful to maintain a global overview allowing to easily compute the neck and to track the marker for the same object across multiple channels. However, the computation is heavier due to the large size of the matrices involved; moreover, the T-junction shape does not allow to easily reduce the dimension in one direction.

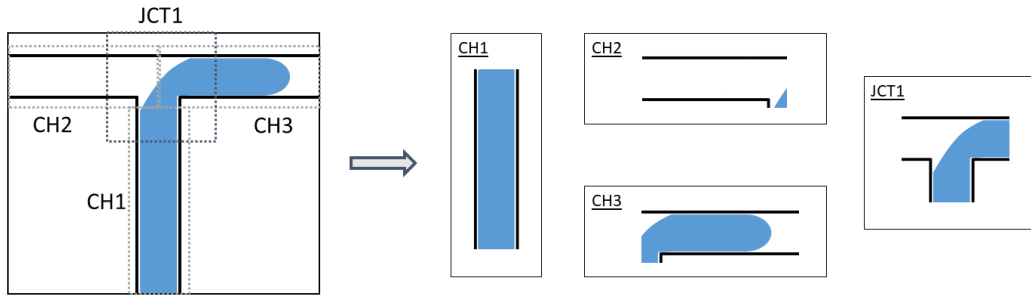


Figure 9.7: Schematic representation of the suggestion division of the image processing workflow. Each channel and junction region is separated to reduce the matrix size to process. The regions on either side of CH1 are ignored.

The background setup and online processing could be modified by sectioning the different regions of interest as the first step to reduce the size of the matrices to process. Moreover, there would be potential to ignore certain regions if they are known to not be of interest at the moment. An additional region for the junction should be setup to identify the so-called neck that is used for feedback during droplet generation and splitting. The overall divided workflow is schematically illustrated in Figure 9.7. One drawback is that tracking the markers of the same object across different channels could be more challenging. Moreover, the overhead cost of separating the full image into regions needs to be tested to ensure faster computation for a wide range of channels and junctions.

Edge detection Microfluidic chips have various applications in the biomedical field. Blood is a bodily sample that provides useful information; yet, its non-Newtonian behaviour is problematic. The active control platform has the potential to adjust to the blood behaviour and compensate for any discrepancy with Newtonian fluid through the feedback. However, the image processing is challenged due to the “filled” appearance of droplets. Similarly, droplets with fluorescent content under fluorescent view lack the distinctive line rather than an area to separate the dispersed from the continuous phase. By introducing an appropriate edge detection step, the algorithm could handle both filled and unfilled droplets by “unfilling” the filled droplets.

Automated threshold adjustment The recognition of both the channel and the droplet interface relies on thresholding to identify the darker lines. The threshold value is manually and dynamically adjusted using the user interface. An automated threshold adjustment could be implemented to reduce setup time and variability between users. Although the lighting conditions are fairly consistent between experiments, the main variability is caused by different focusing that alter the appearance (thickness and darkness) of the channels and droplets.

GPU processing Image processing is performed with all other operations in the main part of the software. Thus, CPU resources are used. The GPU is better suited for image processing. In addition to the faster computational speed, the processing could be done in parallel to other steps. However, this makes the code more complex which means more difficult debugging and maintenance.

Major re-design

Decentralized architecture A standalone system and even more so a modular system would both benefit from decentralized processing of the images through a separated GPU (or CPU). The computation could be performed faster and in parallel to other operations and other modules. However, synchronization and communication could be challenging. Nonetheless, for a modular system, a separated processing platform for each module is envisioned as an efficient way to handle the different modules. Supervisory control would be required to handle synchronization and high-level steps such as collecting the user input from which the steps for each individual module are determined and communicated to each of them.

Neural networks Neural networks have shown tremendous potential especially in the field of image processing. An open-source library such as *TensorFlow* could be implemented to analyze the image and provide the feedback of the droplet position required by the controller. The neural network algorithm could be more robust to handle different situations. However, its performance greatly relies on the nature and quality of the training data. Moreover, obtaining a representation and extensive training data set could be time-consuming, especially if required for new designs that currently are easily handled by standard image processing.

9.8 Summary

Each component of the current active droplet control platform (as per Figure 9.1) is critically analyzed to identify potential improvement to move towards a faster modular platform. The takeaway from each section is summarized in Table 9.6. The envisioned architecture for the modular platform is outlined in Figure 9.8.

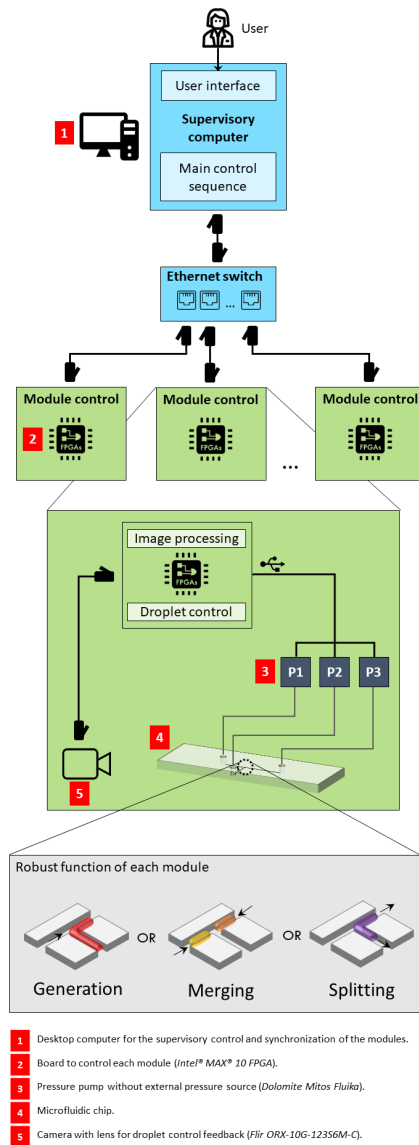


Figure 9.8: Overview of a proposed modular platform architecture.

Table 9.6: Summary of the recommendations for a faster modular active droplet control platform for each component.

| Component | Summary |
|------------------------|-------------------------------------------------------------------------------------------------------------------------------------------------------------------------------------------------------------------------------------------------------------------------|
| 1. Controller | The current MIMO approach is versatile and performs adequately. A simpler model could help make the active droplet control more accessible. |
| 2. Actuation | The limitation of commercial pressure pumps stems from the inflexibility of the software. However, this type of actuator (i.e. piezoelectric E/P transducer) has a limited actuation bandwidth ($\omega_n \approx 6Hz$). |
| 3. Air transport | The dynamics between the pressure pump output and reservoir holder are negligible for the slightly bigger inner tubing diameter of 1/16" versus 1 mm. |
| 4. Sample transport | The smaller tubing with an internal diameter of 0.010" has generally negligible capacitance and inductance dynamics. However, the resistance is significant compared to the microchannel resistance; nonetheless, this is simply a pressure drop for single-phase flow. |
| 5. Microfluidic chip | The most important dynamics is from material compliance. The capacitance is on the order of $10^{-15} m^3/Pa$ for typical dimensions. |
| 6. Feedback | A direct imaging with a CMOS array could replace the camera while providing similar feedback with minimal loss of precision. |
| 6(a). Microscope | The F-mount of the new Nikon inverted microscope line is more advantageous than the C-mount from the previous models. |
| 6(b). Camera | A machine vision camera provides adequate performance at a lower cost, more easily support high frame rates and synchronization between the camera for each module. |
| 6(c). Image processing | An improved workflow separating the different regions of interest can accelerate image processing. A decentralized architecture approach with supervisory control for the modular system is suggested. |

Chapter 10

Conclusion

10.1 Summary

The development of the microfluidic field shows great promise in a wide range of applications. The advantages of flow at the micrometre scale are leveraged in cell studies, biochemistry, environmental factor monitoring, material synthesis, and many more. However, the end-users—researchers in the application fields—do not independently use microfluidic platforms and devices. The lack of accessibility hinders the impact of microfluidics as a field. The active droplet control platform is envisioned to enable end-users to easily leverage microfluidics. The automated portion of a standalone system would interface between the user and the microfluidic flow without requiring the user to fully understand the working principles. The work carried out in this thesis aims towards the development of such an automated standalone modular system for independent use by end-users.

The targeted issues touch upon each part of the system. Moreover, technology and knowledge-based approach are used to make a wider impact. A broad approach is favoured to develop each component in tandem. The components influence each other. Thus, it is preferable to work on the whole system rather than concentrating on components, and subsequently realizing that two subsystems are incompatible or at odds with each other. Achieving the fully automated standalone modular platform is ambitious. This could not reasonably be achieved within the scope of a single thesis. Instead, significant stepping stones are reached for each component to lay a strong foundation for the future development of the modular platform. Each core chapter of this thesis targeted a different part of the system.

The semi-automated algorithm (Chapter 4) targeted the controller to improve manipulation accuracy and repeatability. Moreover, the semi-automated manipulations are important stepping stones towards fully automated procedures involving multiple droplets. The additional layer enabled semi-automated manipulations: generation, splitting, and merging. The droplets are generated with an accuracy of $\pm 10\%$ of the length and a monodispersity of $\pm 1.3\%$ for 500 μm long droplets. The droplets are split with an accuracy of $\pm 4\%$ for the splitting ratio between the two daughter droplets. The automated merging of droplets is demonstrated. Moreover, two droplets with different content are thoroughly mixed as quantified by the mixing index. The potential of the active droplet platform is demonstrated using a drug screening assay. The generation, merging, mixing, and storage of the droplets enable the qualitative assessment of the inhibitor on the aggregation.

The open-source system, μPump (Chapter 5), addresses the lack of transparency and flexibility of commercial actuation systems. Moreover, the financial burden to the users is reduced. The price point of the open-source system is \$3000 USD and \$5000 USD for 4 and 8 independent pressure outputs respectively. The pressure accuracy of 0.1% of full scale (i.e. 2 bar) is suitable for microfluidic applications and is comparable to the commercial systems. Moreover, the application performance is compared between the open-source and commercial pressure pump. The generated droplet volume indicates the system stability. The two systems displayed a similar level of performance, but the open-source system provides more flexibility at a lower cost.

The dynamics associated with the air tubing (Chapter 6) connecting the pressure pump output to the reservoir holder have commonly been neglected. However, active droplet control benefits from a more comprehensive understanding of the system. The 1/16" (~ 1.6 mm) inner diameter tubing is found to have negligible dynamics for various elastic moduli. Nonetheless, the 1 mm inner diameter tubing exhibited significant dynamics. The non-linear relationship is simplified to a linear first-order model without significant accuracy loss. The tubing length is the most important variable in determining the air tubing time constant. A typical time constant value is 33 ms.

The uncertainties about droplet resistance (Chapter 7) lengthen the design process through multiple iterations and requires user intuition to palliate. The studies from the literature agree well each with their own data. However, a consensus has not been established yet. The new approach with the active droplet control platform is promising. The preliminary results agree qualitatively with the literature.

The microfluidic chip compliance (Chapter 8) is more significant than previously

assumed. The order of magnitude of the capacitance for various lengths, aspect ratios, and fluids is $10^{-15} \text{ m}^3/\text{Pa}$. When considering a single chip design, the capacitance decreased with an increasing height-to-width ratio (i.e. for more square cross-sections). However, the overall trend is more significant with respect to the channel length. Longer channel lengths result in decrease capacitance.

A critical overview of the system (Chapter 9) assesses each component to better inform future developments towards an automated standalone platform. The two key components to target for a standalone system are the feedback and the actuation. The microscope and camera are bulky and expensive while a lensless system is small and affordable. Another main obstacle is the pressure pump that requires a pressurized air supply. Instead, smaller pumps that compress the air in addition to regulating the output would be beneficial for a standalone system.

10.2 Original contribution

The original contribution of this thesis is both technological and knowledge-based. The semi-automated control enables more accurate and repeatable droplet manipulations. μ Pump provides users with a cheaper and more flexible actuation alternative that nonetheless performs comparatively as well as premium commercial systems. The open-source system is widely available and is suitable for passive and active microfluidic usage. The critical overview aims to inform the future technological development to achieve a fully automated standalone modular platform.

Issues restricting the accessibility of microfluidics by end-users are better understood as a result of the knowledge-based contributions. The air tubing dynamics are expressed using a simple first-order model. The quantification enables users to assess whether they should neglect the dynamics. Similarly, the microfluidic chip compliance quantification enables users to determine whether they should consider the deformation of the material. The tubing dynamics and microfluidic chip compliance both improve the model accuracy. The droplet resistance investigation using system identification directly benefits from a more accurate model. Moreover, a better understanding of the dynamic behaviour of the pressure-driven microfluidic system is beneficial for all active microfluidics.

The vision is to make microfluidic more accessible for end-users by developing an automated standalone platform. Nonetheless, the major stepping stones promote accessibility by solving financial and knowledge-based issues for end-users. The impact is wider than the development of the modular platform: researchers have access

to more affordable pressure pumps, the dynamics of the air tubing is modelled using a simple and easy-to-understand model, and the microfluidic chip compliance is experimentally quantified to better understand its importance.

10.3 Future work

The concrete next steps for the development of a fully automated standalone modular platform include various parts of the system. The semi-automated manipulation should be linked together through an automated algorithm. A standalone feedback method independent of the expensive and bulky microscope and camera combo should be developed. The droplet resistance study should be furthered with an improved model considering the air tubing, material compliance, sample tubing dynamics, and improved identifiability analysis. These findings should be summarised in a validated and simple model of the system.

From a wider point of view, future work should continue to strive for independent use by end-users. Accessibility should be promoted from multiple angles. First of all, the development should focus on a feedback system independent of the bulk and expensive microscope and scientific camera. Then, the pressure actuation should be moved away from the required pressurized air supply to a standalone unit; for example, miniature pressure pumps pressurize air within the unit. The standalone system could be used by the wider microfluidic community. Moreover, a benchtop system could have the potential for commercialization. The PDMS chips are ubiquitous in the research laboratories for quick iteration. However, unsuitable properties such as unstable surface wetting, porosity, and compliance indicate that an alternative—or at the least, an improvement—to PDMS microfluidic chip is necessary. The microfluidic cartridge should be manufactured cheaply and provide stable wetting conditions. The active droplet control platform is flexible. The T-junction is multiplexed by enabling many different manipulations to occur with the same geometry. Thus, the chip can be universal and would not require frequent iterative design. Finally, the implementation of fully automated droplet procedures would enable end-users to bypass the microfluidic knowledge burden. Once microfluidic tools are in the hands of end-users, the impact of the application would grow significantly while leveraging the advantages of droplet flow at the micrometre scale: shorter reaction times, lower reagent consumption, and containment.

Copyright permissions

**JOHN WILEY AND SONS LICENSE
TERMS AND CONDITIONS**

Sep 29, 2020

This Agreement between University of Waterloo -- Marie Hebert ("You") and John Wiley and Sons ("John Wiley and Sons") consists of your license details and the terms and conditions provided by John Wiley and Sons and Copyright Clearance Center.

| | |
|---------------------------------|---------------------------------------------|
| License Number | 4918230771962 |
| License date | Sep 29, 2020 |
| Licensed Content Publisher | John Wiley and Sons |
| Licensed Content Publication | Wiley Books |
| Licensed Content Title | Microfluidic Reactors for Polymer Particles |
| Licensed Content Author | Eugenia Kumacheva Piotr Garstecki |
| Licensed Content Date | Apr 1, 2011 |
| Licensed Content Pages | 1 |
| Type of use | Dissertation/Thesis |
| Requestor type | University/Academic |
| Format | Print and electronic |
| Portion | Figure/table |

9/29/2020

RightsLink Printable License

Number of figures/tables 1

Will you be translating? No

Title Expanding the droplet microfluidic community – towards a modular active platform

Institution name University of Waterloo

Expected presentation date Jan 2021

Portions Figure 4.6 (b)

Requestor Location
University of Waterloo
200 University Avenue W
Waterloo, ON N2L3G1
Canada
Attn: University of Waterloo

Publisher Tax ID EU826007151

Total 0.00 USD

Terms and Conditions

TERMS AND CONDITIONS

This copyrighted material is owned by or exclusively licensed to John Wiley & Sons, Inc. or one of its group companies (each a "Wiley Company") or handled on behalf of a society with which a Wiley Company has exclusive publishing rights in relation to a particular work (collectively "WILEY"). By clicking "accept" in connection with completing this licensing transaction, you agree that the following terms and conditions apply to this transaction (along with the billing and payment terms and conditions established by the Copyright Clearance Center Inc., ("CCC's Billing and Payment terms and conditions"), at the time that you opened your RightsLink account (these are available at any time at <http://myaccount.copyright.com>).

Terms and Conditions

- The materials you have requested permission to reproduce or reuse (the "Wiley Materials") are protected by copyright.
- You are hereby granted a personal, non-exclusive, non-sub licensable (on a stand-alone basis), non-transferable, worldwide, limited license to reproduce the Wiley Materials for the purpose specified in the licensing process. This license, **and any CONTENT (PDF or image file) purchased as part of your order**, is for a one-time use only and limited to any maximum distribution number specified in the license. The first instance of republication or reuse granted by this license must be completed within two years of the date of the grant of this license (although copies prepared before the end date may be distributed thereafter). The Wiley Materials shall not be used in any other manner or for any other purpose, beyond what is granted in the license. Permission is granted subject to an appropriate acknowledgement given to the author, title of the material/book/journal and the publisher. You shall also duplicate the copyright notice that appears in the Wiley publication in your use of the Wiley Material. Permission is also granted on the understanding that nowhere in the text is a previously published source acknowledged for all or part of this Wiley Material. Any third party content is expressly excluded from this permission.
- With respect to the Wiley Materials, all rights are reserved. Except as expressly granted by the terms of the license, no part of the Wiley Materials may be copied, modified, adapted (except for minor reformatting required by the new Publication), translated, reproduced, transferred or distributed, in any form or by any means, and no derivative works may be made based on the Wiley Materials without the prior permission of the respective copyright owner. **For STM Signatory Publishers clearing permission under the terms of the [STM Permissions Guidelines](#) only, the terms of the license are extended to include subsequent editions and for editions in other languages, provided such editions are for the work as a whole in situ and does not involve the separate exploitation of the permitted figures or extracts**, You may not alter, remove or suppress in any manner any copyright, trademark or other notices displayed by the Wiley Materials. You may not license, rent, sell, loan, lease, pledge, offer as security, transfer or assign the Wiley Materials on a stand-alone basis, or any of the rights granted to you hereunder to any other person.
- The Wiley Materials and all of the intellectual property rights therein shall at all times remain the exclusive property of John Wiley & Sons Inc, the Wiley Companies, or their respective licensors, and your interest therein is only that of having possession of and the right to reproduce the Wiley Materials pursuant to Section 2 herein during the continuance of this Agreement. You agree that you own no right, title or interest in or to the Wiley Materials or any of the intellectual property rights therein. You shall have no rights hereunder other than the license as provided for above in Section 2. No right, license or interest to any trademark, trade name, service mark or other branding ("Marks") of WILEY or its licensors is granted hereunder, and you agree that you shall not assert any such right, license or interest with respect thereto
- NEITHER WILEY NOR ITS LICENSORS MAKES ANY WARRANTY OR REPRESENTATION OF ANY KIND TO YOU OR ANY THIRD PARTY, EXPRESS, IMPLIED OR STATUTORY, WITH RESPECT TO THE MATERIALS OR THE ACCURACY OF ANY INFORMATION CONTAINED IN THE MATERIALS, INCLUDING, WITHOUT LIMITATION, ANY IMPLIED WARRANTY OF MERCHANTABILITY, ACCURACY, SATISFACTORY QUALITY, FITNESS FOR A PARTICULAR PURPOSE, USABILITY, INTEGRATION OR NON-INFRINGEMENT AND ALL SUCH WARRANTIES ARE HEREBY EXCLUDED BY WILEY AND ITS LICENSORS AND WAIVED

BY YOU.

- WILEY shall have the right to terminate this Agreement immediately upon breach of this Agreement by you.
- You shall indemnify, defend and hold harmless WILEY, its Licensors and their respective directors, officers, agents and employees, from and against any actual or threatened claims, demands, causes of action or proceedings arising from any breach of this Agreement by you.
- IN NO EVENT SHALL WILEY OR ITS LICENSORS BE LIABLE TO YOU OR ANY OTHER PARTY OR ANY OTHER PERSON OR ENTITY FOR ANY SPECIAL, CONSEQUENTIAL, INCIDENTAL, INDIRECT, EXEMPLARY OR PUNITIVE DAMAGES, HOWEVER CAUSED, ARISING OUT OF OR IN CONNECTION WITH THE DOWNLOADING, PROVISIONING, VIEWING OR USE OF THE MATERIALS REGARDLESS OF THE FORM OF ACTION, WHETHER FOR BREACH OF CONTRACT, BREACH OF WARRANTY, TORT, NEGLIGENCE, INFRINGEMENT OR OTHERWISE (INCLUDING, WITHOUT LIMITATION, DAMAGES BASED ON LOSS OF PROFITS, DATA, FILES, USE, BUSINESS OPPORTUNITY OR CLAIMS OF THIRD PARTIES), AND WHETHER OR NOT THE PARTY HAS BEEN ADVISED OF THE POSSIBILITY OF SUCH DAMAGES. THIS LIMITATION SHALL APPLY NOTWITHSTANDING ANY FAILURE OF ESSENTIAL PURPOSE OF ANY LIMITED REMEDY PROVIDED HEREIN.
- Should any provision of this Agreement be held by a court of competent jurisdiction to be illegal, invalid, or unenforceable, that provision shall be deemed amended to achieve as nearly as possible the same economic effect as the original provision, and the legality, validity and enforceability of the remaining provisions of this Agreement shall not be affected or impaired thereby.
- The failure of either party to enforce any term or condition of this Agreement shall not constitute a waiver of either party's right to enforce each and every term and condition of this Agreement. No breach under this agreement shall be deemed waived or excused by either party unless such waiver or consent is in writing signed by the party granting such waiver or consent. The waiver by or consent of a party to a breach of any provision of this Agreement shall not operate or be construed as a waiver of or consent to any other or subsequent breach by such other party.
- This Agreement may not be assigned (including by operation of law or otherwise) by you without WILEY's prior written consent.
- Any fee required for this permission shall be non-refundable after thirty (30) days from receipt by the CCC.
- These terms and conditions together with CCC's Billing and Payment terms and conditions (which are incorporated herein) form the entire agreement between you and WILEY concerning this licensing transaction and (in the absence of fraud) supersedes all prior agreements and representations of the parties, oral or written. This Agreement may not be amended except in writing signed by both parties. This Agreement shall be binding upon and inure to the benefit of the parties' successors, legal representatives, and authorized assigns.

- In the event of any conflict between your obligations established by these terms and conditions and those established by CCC's Billing and Payment terms and conditions, these terms and conditions shall prevail.
- WILEY expressly reserves all rights not specifically granted in the combination of (i) the license details provided by you and accepted in the course of this licensing transaction, (ii) these terms and conditions and (iii) CCC's Billing and Payment terms and conditions.
- This Agreement will be void if the Type of Use, Format, Circulation, or Requestor Type was misrepresented during the licensing process.
- This Agreement shall be governed by and construed in accordance with the laws of the State of New York, USA, without regards to such state's conflict of law rules. Any legal action, suit or proceeding arising out of or relating to these Terms and Conditions or the breach thereof shall be instituted in a court of competent jurisdiction in New York County in the State of New York in the United States of America and each party hereby consents and submits to the personal jurisdiction of such court, waives any objection to venue in such court and consents to service of process by registered or certified mail, return receipt requested, at the last known address of such party.

WILEY OPEN ACCESS TERMS AND CONDITIONS

Wiley Publishes Open Access Articles in fully Open Access Journals and in Subscription journals offering Online Open. Although most of the fully Open Access journals publish open access articles under the terms of the Creative Commons Attribution (CC BY) License only, the subscription journals and a few of the Open Access Journals offer a choice of Creative Commons Licenses. The license type is clearly identified on the article.

The Creative Commons Attribution License

The [Creative Commons Attribution License \(CC-BY\)](#) allows users to copy, distribute and transmit an article, adapt the article and make commercial use of the article. The CC-BY license permits commercial and non-

Creative Commons Attribution Non-Commercial License

The [Creative Commons Attribution Non-Commercial \(CC-BY-NC\) License](#) permits use, distribution and reproduction in any medium, provided the original work is properly cited and is not used for commercial purposes.(see below)

Creative Commons Attribution-Non-Commercial-NoDerivs License

The [Creative Commons Attribution Non-Commercial-NoDerivs License \(CC-BY-NC-ND\)](#) permits use, distribution and reproduction in any medium, provided the original work is properly cited, is not used for commercial purposes and no modifications or adaptations are made. (see below)

Use by commercial "for-profit" organizations

Use of Wiley Open Access articles for commercial, promotional, or marketing purposes requires further explicit permission from Wiley and will be subject to a fee.

Further details can be found on Wiley Online Library
<http://olabout.wiley.com/WileyCDA/Section/id-410895.html>

Other Terms and Conditions:

v1.10 Last updated September 2015

Questions? customer care@copyright.com or +1-855-239-3415 (toll free in the US) or +1-978-646-2777.

14/12/2020

<https://marketplace.copyright.com/rs-ui-web/mp/license/2b498d6b-2801-4a7c-a99b-f6a65fc9d8c1/5f9d27c8-9d1e-4ac5-b9c9-799a865d...>Copyright
Clearance
Center

Marketplace™

Royal Society of Chemistry - License Terms and Conditions

This is a License Agreement between Marie Hebert ("You") and Royal Society of Chemistry ("Publisher") provided by Copyright Clearance Center ("CCC"). The license consists of your order details, the terms and conditions provided by Royal Society of Chemistry, and the CCC terms and conditions.

All payments must be made in full to CCC.

| | | | |
|------------------|-------------|-------------|------------------------------------|
| Order Date | 11-Dec-2020 | Type of Use | Republish in a thesis/dissertation |
| Order license ID | 1083493-1 | Publisher | ROYAL SOCIETY OF CHEMISTRY |
| ISSN | 1473-0189 | Portion | Image/photo/illustration |

LICENSED CONTENT

| | | | |
|-------------------|--------------------------------------------|------------------|-------------------------------------------------------------|
| Publication Title | Lab on a chip | Country | United Kingdom of Great Britain and Northern Ireland |
| Author/Editor | Royal Society of Chemistry (Great Britain) | Rightsholder | Royal Society of Chemistry |
| Date | 01/01/2001 | Publication Type | e-Journal |
| Language | English | URL | http://www.rsc.org/loc |

REQUEST DETAILS

| | | | |
|-------------------------------------------|--------------------------|-----------------------------|----------------------------------|
| Portion Type | Image/photo/illustration | Distribution | Worldwide |
| Number of images / photos / illustrations | 2 | Translation | Original language of publication |
| Format (select all that apply) | Print, Electronic | Copies for the disabled? | No |
| Who will republish the content? | Academic institution | Minor editing privileges? | No |
| Duration of Use | Life of current edition | Incidental promotional use? | No |
| Lifetime Unit Quantity | Up to 499 | Currency | USD |
| Rights Requested | Main product | | |

NEW WORK DETAILS

| | | | |
|-----------------|----------------------------------------------------------------------------------|----------------------------|---------------------|
| Title | Expanding the droplet microfluidic community - towards a modular active platform | Institution name | Waterloo University |
| Instructor name | Marie Hebert | Expected presentation date | 2021-01-01 |

ADDITIONAL DETAILS

| | |
|------------------------|-----|
| Order reference number | N/A |
|------------------------|-----|

<https://marketplace.copyright.com/rs-ui-web/mp/license/2b498d6b-2801-4a7c-a99b-f6a65fc9d8c1/5f9d27c8-9d1e-4ac5-b9c9-799a865d50be>

1/4

The requesting person / organization to appear on the license Marie Hebert

REUSE CONTENT DETAILS

| | | | |
|-----------------------------------------------------------|-----------------|--------------------------------------------------|--------------------------------------------|
| Title, description or numeric reference of the portion(s) | Figures 4 and 6 | Title of the article/chapter the portion is from | Dynamics of microfluidic droplets |
| Editor of portion(s) | N/A | Author of portion(s) | Royal Society of Chemistry (Great Britain) |
| Volume of serial or monograph | N/A | Issue, if republishing an article from a serial | N/A |
| Page or page range of portion | 2037, 2039 | Publication date of portion | 2010-06-18 |

CCC Republication Terms and Conditions

1. Description of Service; Defined Terms. This Republication License enables the User to obtain licenses for republication of one or more copyrighted works as described in detail on the relevant Order Confirmation (the "Work(s)"). Copyright Clearance Center, Inc. ("CCC") grants licenses through the Service on behalf of the rightsholder identified on the Order Confirmation (the "Rightsholder"). "Republishing", as used herein, generally means the inclusion of a Work, in whole or in part, in a new work or works, also as described on the Order Confirmation. "User", as used herein, means the person or entity making such republication.
2. The terms set forth in the relevant Order Confirmation, and any terms set by the Rightsholder with respect to a particular Work, govern the terms of use of Works in connection with the Service. By using the Service, the person transacting for a republication license on behalf of the User represents and warrants that he/she/it (a) has been duly authorized by the User to accept, and hereby does accept, all such terms and conditions on behalf of User, and (b) shall inform User of all such terms and conditions. In the event such person is a "freelancer" or other third party independent of User and CCC, such party shall be deemed jointly a "User" for purposes of these terms and conditions. In any event, User shall be deemed to have accepted and agreed to all such terms and conditions if User republishes the Work in any fashion.
3. Scope of License; Limitations and Obligations.
 - 3.1. All Works and all rights therein, including copyright rights, remain the sole and exclusive property of the Rightsholder. The license created by the exchange of an Order Confirmation (and/or any invoice) and payment by User of the full amount set forth on that document includes only those rights expressly set forth in the Order Confirmation and in these terms and conditions, and conveys no other rights in the Work(s) to User. All rights not expressly granted are hereby reserved.
 - 3.2. General Payment Terms: You may pay by credit card or through an account with us payable at the end of the month. If you and we agree that you may establish a standing account with CCC, then the following terms apply: Remit Payment to: Copyright Clearance Center, 29118 Network Place, Chicago, IL 60673-1291. Payments Due: Invoices are payable upon their delivery to you (or upon our notice to you that they are available to you for downloading). After 30 days, outstanding amounts will be subject to a service charge of 1-1/2% per month or, if less, the maximum rate allowed by applicable law. Unless otherwise specifically set forth in the Order Confirmation or in a separate written agreement signed by CCC, invoices are due and payable on "net 30" terms. While User may exercise the rights licensed immediately upon issuance of the Order Confirmation, the license is automatically revoked and is null and void, as if it had never been issued, if complete payment for the license is not received on a timely basis either from User directly or through a payment agent, such as a credit card company.
 - 3.3. Unless otherwise provided in the Order Confirmation, any grant of rights to User (i) is "one-time" (including

14/12/2020

<https://marketplace.copyright.com/rs-ui-web/mp/license/2b498d6b-2801-4a7c-a99b-f6a65fc9d8c1/5f9d27c8-9d1e-4ac5-b9c9-799a865d...>

the editions and product family specified in the license), (ii) is non-exclusive and non-transferable and (iii) is subject to any and all limitations and restrictions (such as, but not limited to, limitations on duration of use or circulation) included in the Order Confirmation or invoice and/or in these terms and conditions. Upon completion of the licensed use, User shall either secure a new permission for further use of the Work(s) or immediately cease any new use of the Work(s) and shall render inaccessible (such as by deleting or by removing or severing links or other locators) any further copies of the Work (except for copies printed on paper in accordance with this license and still in User's stock at the end of such period).

3.4. In the event that the material for which a republication license is sought includes third party materials (such as photographs, illustrations, graphs, inserts and similar materials) which are identified in such material as having been used by permission, User is responsible for identifying, and seeking separate licenses (under this Service or otherwise) for, any of such third party materials; without a separate license, such third party materials may not be used.

3.5. Use of proper copyright notice for a Work is required as a condition of any license granted under the Service. Unless otherwise provided in the Order Confirmation, a proper copyright notice will read substantially as follows: "Republished with permission of [Rightsholder's name], from [Work's title, author, volume, edition number and year of copyright]; permission conveyed through Copyright Clearance Center, Inc. " Such notice must be provided in a reasonably legible font size and must be placed either immediately adjacent to the Work as used (for example, as part of a by-line or footnote but not as a separate electronic link) or in the place where substantially all other credits or notices for the new work containing the republished Work are located. Failure to include the required notice results in loss to the Rightsholder and CCC, and the User shall be liable to pay liquidated damages for each such failure equal to twice the use fee specified in the Order Confirmation, in addition to the use fee itself and any other fees and charges specified.

3.6. User may only make alterations to the Work if and as expressly set forth in the Order Confirmation. No Work may be used in any way that is defamatory, violates the rights of third parties (including such third parties' rights of copyright, privacy, publicity, or other tangible or intangible property), or is otherwise illegal, sexually explicit or obscene. In addition, User may not conjoin a Work with any other material that may result in damage to the reputation of the Rightsholder. User agrees to inform CCC if it becomes aware of any infringement of any rights in a Work and to cooperate with any reasonable request of CCC or the Rightsholder in connection therewith.

4. Indemnity. User hereby indemnifies and agrees to defend the Rightsholder and CCC, and their respective employees and directors, against all claims, liability, damages, costs and expenses, including legal fees and expenses, arising out of any use of a Work beyond the scope of the rights granted herein, or any use of a Work which has been altered in any unauthorized way by User, including claims of defamation or infringement of rights of copyright, publicity, privacy or other tangible or intangible property.

5. Limitation of Liability. UNDER NO CIRCUMSTANCES WILL CCC OR THE RIGHTSHOLDER BE LIABLE FOR ANY DIRECT, INDIRECT, CONSEQUENTIAL OR INCIDENTAL DAMAGES (INCLUDING WITHOUT LIMITATION DAMAGES FOR LOSS OF BUSINESS PROFITS OR INFORMATION, OR FOR BUSINESS INTERRUPTION) ARISING OUT OF THE USE OR INABILITY TO USE A WORK, EVEN IF ONE OF THEM HAS BEEN ADVISED OF THE POSSIBILITY OF SUCH DAMAGES. In any event, the total liability of the Rightsholder and CCC (including their respective employees and directors) shall not exceed the total amount actually paid by User for this license. User assumes full liability for the actions and omissions of its principals, employees, agents, affiliates, successors and assigns.

6. Limited Warranties. THE WORK(S) AND RIGHT(S) ARE PROVIDED "AS IS". CCC HAS THE RIGHT TO GRANT TO USER THE RIGHTS GRANTED IN THE ORDER CONFIRMATION DOCUMENT. CCC AND THE RIGHTSHOLDER DISCLAIM ALL OTHER WARRANTIES RELATING TO THE WORK(S) AND RIGHT(S), EITHER EXPRESS OR IMPLIED, INCLUDING WITHOUT LIMITATION IMPLIED WARRANTIES OF MERCHANTABILITY OR FITNESS FOR A PARTICULAR PURPOSE. ADDITIONAL RIGHTS MAY BE REQUIRED TO USE ILLUSTRATIONS, GRAPHS, PHOTOGRAPHS, ABSTRACTS, INSERTS OR OTHER PORTIONS OF THE WORK (AS OPPOSED TO THE ENTIRE WORK) IN A MANNER CONTEMPLATED BY USER; USER UNDERSTANDS AND AGREES THAT NEITHER CCC NOR THE RIGHTSHOLDER MAY HAVE SUCH ADDITIONAL RIGHTS TO GRANT.

<https://marketplace.copyright.com/rs-ui-web/mp/license/2b498d6b-2801-4a7c-a99b-f6a65fc9d8c1/5f9d27c8-9d1e-4ac5-b9c9-799a865d50be>

3/4

7. Effect of Breach. Any failure by User to pay any amount when due, or any use by User of a Work beyond the scope of the license set forth in the Order Confirmation and/or these terms and conditions, shall be a material breach of the license created by the Order Confirmation and these terms and conditions. Any breach not cured within 30 days of written notice thereof shall result in immediate termination of such license without further notice. Any unauthorized (but licensable) use of a Work that is terminated immediately upon notice thereof may be liquidated by payment of the Rightsholder's ordinary license price therefor; any unauthorized (and unlicensable) use that is not terminated immediately for any reason (including, for example, because materials containing the Work cannot reasonably be recalled) will be subject to all remedies available at law or in equity, but in no event to a payment of less than three times the Rightsholder's ordinary license price for the most closely analogous licensable use plus Rightsholder's and/or CCC's costs and expenses incurred in collecting such payment.

8. Miscellaneous.

- 8.1. User acknowledges that CCC may, from time to time, make changes or additions to the Service or to these terms and conditions, and CCC reserves the right to send notice to the User by electronic mail or otherwise for the purposes of notifying User of such changes or additions; provided that any such changes or additions shall not apply to permissions already secured and paid for.
- 8.2. Use of User-related information collected through the Service is governed by CCC's privacy policy, available online here:<https://marketplace.copyright.com/rs-ui-web/mp/privacy-policy>
- 8.3. The licensing transaction described in the Order Confirmation is personal to User. Therefore, User may not assign or transfer to any other person (whether a natural person or an organization of any kind) the license created by the Order Confirmation and these terms and conditions or any rights granted hereunder; provided, however, that User may assign such license in its entirety on written notice to CCC in the event of a transfer of all or substantially all of User's rights in the new material which includes the Work(s) licensed under this Service.
- 8.4. No amendment or waiver of any terms is binding unless set forth in writing and signed by the parties. The Rightsholder and CCC hereby object to any terms contained in any writing prepared by the User or its principals, employees, agents or affiliates and purporting to govern or otherwise relate to the licensing transaction described in the Order Confirmation, which terms are in any way inconsistent with any terms set forth in the Order Confirmation and/or in these terms and conditions or CCC's standard operating procedures, whether such writing is prepared prior to, simultaneously with or subsequent to the Order Confirmation, and whether such writing appears on a copy of the Order Confirmation or in a separate instrument.
- 8.5. The licensing transaction described in the Order Confirmation document shall be governed by and construed under the law of the State of New York, USA, without regard to the principles thereof of conflicts of law. Any case, controversy, suit, action, or proceeding arising out of, in connection with, or related to such licensing transaction shall be brought, at CCC's sole discretion, in any federal or state court located in the County of New York, State of New York, USA, or in any federal or state court whose geographical jurisdiction covers the location of the Rightsholder set forth in the Order Confirmation. The parties expressly submit to the personal jurisdiction and venue of each such federal or state court. If you have any comments or questions about the Service or Copyright Clearance Center, please contact us at 978-750-8400 or send an e-mail to support@copyright.com.

v 1.1



Pearson
221 River St,
Hoboken, NJ 07030, USA
T +1 201 236 700
E info@pearson.com
W pearson.com

PERMISSIONS GRANT LETTER/INVOICE

| | | | |
|---------------------|--------------------------------------|-------------------|--------|
| Correspondence Date | 15-Aug-2020 | Pearson Reference | 137772 |
| Deal Type | Permissions Granting: Educational | | |

| | | | |
|-------------------------------------|--------------------------------------------------|-------------------------------|--|
| Request date | 24-Jun-2020 | Requester Reference Number | |
| Requester Representative Name | Marie Hebert | | |
| Requester Representative Address | 200 University Ave W Waterloo, ON, N2L3G1 Canada | | |

Requested Content:

| | |
|----------------|-----------------------------------|
| Title | Dorf Modern Control Systems 12 US |
| Author | Robert H. Bishop, Richard C. Dorf |
| ISBN | 9780136024583 |
| Edition Number | 12 |
| Copyright Year | 2011 |
| Pearson Entity | Pearson Education, Inc. |

| | |
|-------------------|----------------------|
| Asset Description | page 321 figure 5.17 |
| Requested Use | Thesis |

Pearson hereby grants you permission to use the specified content of the above work, subject to the terms and conditions contained in the attached schedule; and the specified conditions below:

Rights Granted:

| | | | |
|-----------|----------------|----------------------------|-------|
| Formats | Print, Digital | Territory | World |
| Languages | English | Editions/Revisions | |
| Duration | 1 Year | Number of students/ copies | 100 |

Used By:

| | | | |
|------------------------------------------------|------------------------------------------------------------------------|-------------------|--|
| Publisher/institution | University of Waterloo | Tax Number | |
| Publisher Address | 200 University Ave W Waterloo, ON, N2L3G1 Canada | | |
| Details of the Requesters Product/Title | Expanding the microfluidiccommunity ? towards a modularactive platform | | |
| Author/Instructor | Marie Hebert | | |

Fees:

| | |
|------------------------|-------|
| Fee | 0 USD |
| GST, VAT or HST | 0 USD |
| Total Fee | 0 USD |

Attribution:

DORF, RICHARD C., MODERN CONTROL SYTEMS, 12TH ED,2011

Reprinted by permission of **Pearson Education, Inc.**

(for crediting figures and diagrams, the acknowledgement must appear below each figure and/or diagram).

Please Note:

By accepting the terms and conditions of this license, the signatory agrees to make payment on or before the date of your publication.

Please make payment by check or wire transfer.

To cancel a grant of permission, contact the Pearson Representative indicated below, prior to remit of payment.

Failure to make payment by **[N/A]** may result in an automatic cancellation of this license.

Subsequent use of Pearson Asset(s) without timely payment shall be considered use without permission and may result in assertion of a claim of copyright infringement by Pearson.

Permitted Use of Pearson Asset(s):

The Pearson Asset(s) are being provided to you for your use in connection with your aforementioned use ("Used By" section above).

The rights granted must not deviate from or exceed those right specified in the "Rights Granted" section above. Any expansion beyond these specified terms require a new permission request.

You may only use the Pearson Asset(s) as provided and are prohibited from modifying or otherwise changing the Pearson Asset(s) to create derivatives or other products.

Any assignment, amendment or transfer of this license is not permitted without the prior written consent of Pearson.

| | | | |
|-------------------------------|-----------------|-----------------|--|
| Pearson Representative | Julia Alexander | Capacity | |
| Signature | | Date | |

| | | | |
|-----------------------|--|-----------------|--|
| Requestor Name | | Capacity | |
| Signature | | Date | |

V3.2 APRIL 29, 2020

| | | | |
|--|--|--|--|
| | | | |
|--|--|--|--|

Signature: Marie Hébert
Marie Hébert (Aug 20, 2020 08:41 EDT)

Email: marie.hebert@uwaterloo.ca

Signature: Julia Alexander
Julia Alexander (Aug 21, 2020 13:19 GMT+2)

Email: Julia.Alexander@pearson.com

**SPRINGER NATURE LICENSE
TERMS AND CONDITIONS**

Dec 11, 2020

This Agreement between University of Waterloo -- Marie Hebert ("You") and Springer Nature ("Springer Nature") consists of your license details and the terms and conditions provided by Springer Nature and Copyright Clearance Center.

License Number 4966080623325

License date Dec 11, 2020

Licensed Content Publisher Springer Nature

Licensed Content Publication Microfluids and Nanofluids

Licensed Content Title Numerical and experimental investigations of the formation process of ferrofluid droplets

Licensed Content Author Jing Liu et al

Licensed Content Date Mar 5, 2011

Type of Use Thesis/Dissertation

Requestor type academic/university or research institute

Format print and electronic

Portion figures/tables/illustrations

Number of figures/tables/illustrations 1

11/12/2020

RightsLink Printable License

Will you be translating? no

Circulation/distribution 200 - 499

Author of this Springer Nature content no

Title Expanding the droplet microfluidic community – towards a modular active platform

Institution name University of Waterloo

Expected presentation date Jan 2021

Portions Figure 3 on page 180

University of Waterloo
200 University Avenue W

Requestor Location
Waterloo, ON N2L3G1
Canada
Attn: University of Waterloo

Total 0.00 USD

Terms and Conditions

**Springer Nature Customer Service Centre GmbH
Terms and Conditions**

This agreement sets out the terms and conditions of the licence (the **Licence**) between you and **Springer Nature Customer Service Centre GmbH** (the **Licensor**). By clicking 'accept' and completing the transaction for the material (**Licensed Material**), you also confirm your acceptance of these terms and conditions.

1. Grant of License

1.1. The Licensor grants you a personal, non-exclusive, non-transferable, world-wide licence to reproduce the Licensed Material for the purpose specified in your order only. Licences are granted for the specific use requested in the order and for no other use, subject to the conditions below.

1. 2. The Licensor warrants that it has, to the best of its knowledge, the rights to license reuse of the Licensed Material. However, you should ensure that the material you are requesting is original to the Licensor and does not carry the copyright of another entity (as credited in the published version).

1. 3. If the credit line on any part of the material you have requested indicates that it was reprinted or adapted with permission from another source, then you should also seek permission from that source to reuse the material.

2. Scope of Licence

2. 1. You may only use the Licensed Content in the manner and to the extent permitted by these Ts&Cs and any applicable laws.

2. 2. A separate licence may be required for any additional use of the Licensed Material, e.g. where a licence has been purchased for print only use, separate permission must be obtained for electronic re-use. Similarly, a licence is only valid in the language selected and does not apply for editions in other languages unless additional translation rights have been granted separately in the licence. Any content owned by third parties are expressly excluded from the licence.

2. 3. Similarly, rights for additional components such as custom editions and derivatives require additional permission and may be subject to an additional fee. Please apply to Journalpermissions@springernature.com/bookpermissions@springernature.com for these rights.

2. 4. Where permission has been granted **free of charge** for material in print, permission may also be granted for any electronic version of that work, provided that the material is incidental to your work as a whole and that the electronic version is essentially equivalent to, or substitutes for, the print version.

2. 5. An alternative scope of licence may apply to signatories of the [STM Permissions Guidelines](#), as amended from time to time.

3. Duration of Licence

3. 1. A licence for is valid from the date of purchase ('Licence Date') at the end of the relevant period in the below table:

| Scope of Licence | Duration of Licence |
|--------------------|---------------------------------------------------|
| Post on a website | 12 months |
| Presentations | 12 months |
| Books and journals | Lifetime of the edition in the language purchased |

4. Acknowledgement

4. 1. The Licensor's permission must be acknowledged next to the Licensed Material in print. In electronic form, this acknowledgement must be visible at the same time as the figures/tables/illustrations or abstract, and must be hyperlinked to the journal/book's

homepage. Our required acknowledgement format is in the Appendix below.

5. Restrictions on use

5. 1. Use of the Licensed Material may be permitted for incidental promotional use and minor editing privileges e.g. minor adaptations of single figures, changes of format, colour and/or style where the adaptation is credited as set out in Appendix 1 below. Any other changes including but not limited to, cropping, adapting, omitting material that affect the meaning, intention or moral rights of the author are strictly prohibited.

5. 2. You must not use any Licensed Material as part of any design or trademark.

5. 3. Licensed Material may be used in Open Access Publications (OAP) before publication by Springer Nature, but any Licensed Material must be removed from OAP sites prior to final publication.

6. Ownership of Rights

6. 1. Licensed Material remains the property of either Licensor or the relevant third party and any rights not explicitly granted herein are expressly reserved.

7. Warranty

IN NO EVENT SHALL LICENSOR BE LIABLE TO YOU OR ANY OTHER PARTY OR ANY OTHER PERSON OR FOR ANY SPECIAL, CONSEQUENTIAL, INCIDENTAL OR INDIRECT DAMAGES, HOWEVER CAUSED, ARISING OUT OF OR IN CONNECTION WITH THE DOWNLOADING, VIEWING OR USE OF THE MATERIALS REGARDLESS OF THE FORM OF ACTION, WHETHER FOR BREACH OF CONTRACT, BREACH OF WARRANTY, TORT, NEGLIGENCE, INFRINGEMENT OR OTHERWISE (INCLUDING, WITHOUT LIMITATION, DAMAGES BASED ON LOSS OF PROFITS, DATA, FILES, USE, BUSINESS OPPORTUNITY OR CLAIMS OF THIRD PARTIES), AND WHETHER OR NOT THE PARTY HAS BEEN ADVISED OF THE POSSIBILITY OF SUCH DAMAGES. THIS LIMITATION SHALL APPLY NOTWITHSTANDING ANY FAILURE OF ESSENTIAL PURPOSE OF ANY LIMITED REMEDY PROVIDED HEREIN.

8. Limitations

8. 1. **BOOKS ONLY:** Where 'reuse in a dissertation/thesis' has been selected the following terms apply: Print rights of the final author's accepted manuscript (for clarity, NOT the published version) for up to 100 copies, electronic rights for use only on a personal website or institutional repository as defined by the Sherpa guideline (www.sherpa.ac.uk/romeo/).

9. Termination and Cancellation

9. 1. Licences will expire after the period shown in Clause 3 (above).

9. 2. Licensee reserves the right to terminate the Licence in the event that payment is not received in full or if there has been a breach of this agreement by you.

Appendix 1 — Acknowledgements:

For Journal Content:

Reprinted by permission from [the Licensor]: [Journal Publisher (e.g. Nature/Springer/Palgrave)] [JOURNAL NAME] [REFERENCE CITATION (Article name, Author(s) Name), [COPYRIGHT] (year of publication)

For Advance Online Publication papers:

Reprinted by permission from [the Licensor]: [Journal Publisher (e.g. Nature/Springer/Palgrave)] [JOURNAL NAME] [REFERENCE CITATION (Article name, Author(s) Name), [COPYRIGHT] (year of publication), advance online publication, day month year (doi: 10.1038/sj.[JOURNAL ACRONYM].)

For Adaptations/Translations:

Adapted/Translated by permission from [the Licensor]: [Journal Publisher (e.g. Nature/Springer/Palgrave)] [JOURNAL NAME] [REFERENCE CITATION (Article name, Author(s) Name), [COPYRIGHT] (year of publication)

Note: For any republication from the British Journal of Cancer, the following credit line style applies:

Reprinted/adapted/translated by permission from [the Licensor]: on behalf of Cancer Research UK: : [Journal Publisher (e.g. Nature/Springer/Palgrave)] [JOURNAL NAME] [REFERENCE CITATION (Article name, Author(s) Name), [COPYRIGHT] (year of publication)

For Advance Online Publication papers:

Reprinted by permission from The [the Licensor]: on behalf of Cancer Research UK: [Journal Publisher (e.g. Nature/Springer/Palgrave)] [JOURNAL NAME] [REFERENCE CITATION (Article name, Author(s) Name), [COPYRIGHT] (year of publication), advance online publication, day month year (doi: 10.1038/sj.[JOURNAL ACRONYM])

For Book content:

Reprinted/adapted by permission from [the Licensor]: [Book Publisher (e.g. Palgrave Macmillan, Springer etc) [Book Title] by [Book author(s)] [COPYRIGHT] (year of publication)

Other Conditions:

Version 1.2

11/12/2020

RightsLink Printable License

Questions? customercare@copyright.com or +1-855-239-3415 (toll free in the US) or +1-978-646-2777.



RightsLink®



Home



Help



Email Support



Marie Hebert ▾

Effective Thermo-Capillary Mixing in Droplet Microfluidics Integrated with a Microwave Heater



Author: Gurkan Yesiloz, Muhammed S. Boybay, Carolyn L. Ren

Publication: Analytical Chemistry

Publisher: American Chemical Society

Date: Feb 1, 2017

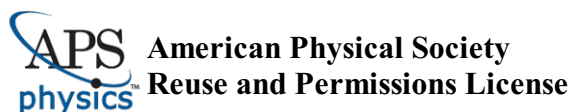
Copyright © 2017, American Chemical Society

PERMISSION/LICENSE IS GRANTED FOR YOUR ORDER AT NO CHARGE

This type of permission/license, instead of the standard Terms & Conditions, is sent to you because no fee is being charged for your order. Please note the following:

- Permission is granted for your request in both print and electronic formats, and translations.
 - If figures and/or tables were requested, they may be adapted or used in part.
 - Please print this page for your records and send a copy of it to your publisher/graduate school.
 - Appropriate credit for the requested material should be given as follows: "Reprinted (adapted) with permission from (COMPLETE REFERENCE CITATION). Copyright (YEAR) American Chemical Society." Insert appropriate information in place of the capitalized words.
 - One-time permission is granted only for the use specified in your request. No additional uses are granted (such as derivative works or other editions). For any other uses, please submit a new request.
- If credit is given to another source for the material you requested, permission must be obtained from that source.

[BACK](#)[CLOSE WINDOW](#)



09-Jul-2020

This license agreement between the American Physical Society ("APS") and Marie Hébert ("You") consists of your license details and the terms and conditions provided by the American Physical Society and SciPris.

Licensed Content Information

License Number: RNP/20/JUL/028015
License date: 09-Jul-2020
DOI: 10.1103/PhysRevLett.92.054503
Title: Geometrically Mediated Breakup of Drops in Microfluidic Devices
Author: D. R. Link et al.
Publication: Physical Review Letters
Publisher: American Physical Society
Cost: USD \$ 0.00

Request Details

Does your reuse require significant modifications: No
Specify intended distribution locations: Worldwide
Reuse Category: Reuse in a thesis/dissertation
Requestor Type: Academic Institution
Items for Reuse: Figures/Tables
Number of Figure/Tables: 1
Figure/Tables Details: FIG. 1. Passive breakup at T junctions. Droplets flow into a T junction, sketched in (a), where the flow is split into two sidearms. The narrow portion of the two side arms, of lengths l_1 and l_2 , contain
Format for Reuse: Print and Electronic
Total number of print copies: Up to 1000

Information about New Publication:

University/Publisher: University of Waterloo
Title of dissertation/thesis: Expanding the microfluidic community – towards a modular active platform
Author(s): Marie Hébert
Expected completion date: Dec. 2020

License Requestor Information

Name: Marie Hébert
Affiliation: Individual
Email Id: marie.hebert@uwaterloo.ca
Country: Canada



TERMS AND CONDITIONS

The American Physical Society (APS) is pleased to grant the Requestor of this license a non-exclusive, non-transferable permission, limited to Print and Electronic format, provided all criteria outlined below are followed.

1. You must also obtain permission from at least one of the lead authors for each separate work, if you haven't done so already. The author's name and affiliation can be found on the first page of the published Article.
2. For electronic format permissions, Requestor agrees to provide a hyperlink from the reprinted APS material using the source material's DOI on the web page where the work appears. The hyperlink should use the standard DOI resolution URL, <http://dx.doi.org/{DOI}>. The hyperlink may be embedded in the copyright credit line.
3. For print format permissions, Requestor agrees to print the required copyright credit line on the first page where the material appears: "Reprinted (abstract/excerpt/figure) with permission from [(FULL REFERENCE CITATION) as follows: Author's Names, APS Journal Title, Volume Number, Page Number and Year of Publication.] Copyright (YEAR) by the American Physical Society."
4. Permission granted in this license is for a one-time use and does not include permission for any future editions, updates, databases, formats or other matters. Permission must be sought for any additional use.
5. Use of the material does not and must not imply any endorsement by APS.
6. APS does not imply, purport or intend to grant permission to reuse materials to which it does not hold copyright. It is the requestor's sole responsibility to ensure the licensed material is original to APS and does not contain the copyright of another entity, and that the copyright notice of the figure, photograph, cover or table does not indicate it was reprinted by APS with permission from another source.
7. The permission granted herein is personal to the Requestor for the use specified and is not transferable or assignable without express written permission of APS. This license may not be amended except in writing by APS.
8. You may not alter, edit or modify the material in any manner.
9. You may translate the materials only when translation rights have been granted.
10. APS is not responsible for any errors or omissions due to translation.
11. You may not use the material for promotional, sales, advertising or marketing purposes.
12. The foregoing license shall not take effect unless and until APS or its agent, Aptara, receives payment in full in accordance with Aptara Billing and Payment Terms and Conditions, which are incorporated herein by reference.
13. Should the terms of this license be violated at any time, APS or Aptara may revoke the license with no refund to you and seek relief to the fullest extent of the laws of the USA. Official written notice will be made using the contact information provided with the permission request. Failure to receive such notice will not nullify revocation of the permission.
14. APS reserves all rights not specifically granted herein.
15. This document, including the Aptara Billing and Payment Terms and Conditions, shall be the entire agreement between the parties relating to the subject matter hereof.

**AIP PUBLISHING LICENSE
TERMS AND CONDITIONS**

Dec 14, 2020

This Agreement between University of Waterloo -- Marie Hebert ("You") and AIP Publishing ("AIP Publishing") consists of your license details and the terms and conditions provided by AIP Publishing and Copyright Clearance Center.

License Number 4967641015921

License date Dec 14, 2020

Licensed Content
Publisher AIP PublishingLicensed Content
Publication Applied Physics Letters

Licensed Content Title Laser switching and sorting for high speed digital microfluidics

Licensed Content
Author Matthieu Robert de Saint Vincent, Régis Wunenburger, Jean-Pierre Delville

Licensed Content Date Apr 14, 2008

Licensed Content
Volume 92

Licensed Content Issue 15

Type of Use Thesis/Dissertation

Requestor type Student

Format Print and electronic

| | |
|----------------------------|--------------------------------------------------------------------------------------------------------------------|
| Portion | Figure/Table |
| Number of figures/tables | 1 |
| Title | Expanding the droplet microfluidic community – towards a modular active platform |
| Institution name | University of Waterloo |
| Expected presentation date | Jan 2021 |
| Portions | Figure 1 (c) |
| Requestor Location | University of Waterloo 200 University Avenue W Waterloo, ON N2L3G1 Canada Attn: University of Waterloo |
| Total | 0.00 USD |

Terms and Conditions

AIP Publishing -- Terms and Conditions: Permissions Uses

AIP Publishing hereby grants to you the non-exclusive right and license to use and/or distribute the Material according to the use specified in your order, on a one-time basis, for the specified term, with a maximum distribution equal to the number that you have ordered. Any links or other content accompanying the Material are not the subject of this license.

1. You agree to include the following copyright and permission notice with the reproduction of the Material: "Reprinted from [FULL CITATION], with the permission of AIP Publishing." For an article, the credit line and permission notice must be printed on the first page of the article or book chapter. For photographs, covers, or tables, the notice may appear with the Material, in a footnote, or in the reference list.
2. If you have licensed reuse of a figure, photograph, cover, or table, it is your responsibility to ensure that the material is original to AIP Publishing and does not contain the copyright of another entity, and that the copyright notice of the figure, photograph, cover, or table does not indicate that it was reprinted by AIP Publishing, with permission, from another source. Under no circumstances does AIP Publishing

purport or intend to grant permission to reuse material to which it does not hold appropriate rights.

You may not alter or modify the Material in any manner. You may translate the Material into another language only if you have licensed translation rights. You may not use the Material for promotional purposes.

3. The foregoing license shall not take effect unless and until AIP Publishing or its agent, Copyright Clearance Center, receives the Payment in accordance with Copyright Clearance Center Billing and Payment Terms and Conditions, which are incorporated herein by reference.
4. AIP Publishing or Copyright Clearance Center may, within two business days of granting this license, revoke the license for any reason whatsoever, with a full refund payable to you. Should you violate the terms of this license at any time, AIP Publishing, or Copyright Clearance Center may revoke the license with no refund to you. Notice of such revocation will be made using the contact information provided by you. Failure to receive such notice will not nullify the revocation.
5. AIP Publishing makes no representations or warranties with respect to the Material. You agree to indemnify and hold harmless AIP Publishing, and their officers, directors, employees or agents from and against any and all claims arising out of your use of the Material other than as specifically authorized herein.
6. The permission granted herein is personal to you and is not transferable or assignable without the prior written permission of AIP Publishing. This license may not be amended except in a writing signed by the party to be charged.
7. If purchase orders, acknowledgments or check endorsements are issued on any forms containing terms and conditions which are inconsistent with these provisions, such inconsistent terms and conditions shall be of no force and effect. This document, including the CCC Billing and Payment Terms and Conditions, shall be the entire agreement between the parties relating to the subject matter hereof.

This Agreement shall be governed by and construed in accordance with the laws of the State of New York. Both parties hereby submit to the jurisdiction of the courts of New York County for purposes of resolving any disputes that may arise hereunder.

V1.2

Questions? customer care@copyright.com or +1-855-239-3415 (toll free in the US) or +1-978-646-2777.



IOP Publishing, Ltd - License Terms and Conditions

This is a License Agreement between Marie Hebert ("You") and IOP Publishing, Ltd ("Publisher") provided by Copyright Clearance Center ("CCC"). The license consists of your order details, the terms and conditions provided by IOP Publishing, Ltd, and the CCC terms and conditions.

All payments must be made in full to CCC.

| | | | |
|------------------|-------------|-------------------|--------------------------------------------|
| Order Date | 11-Dec-2020 | Type of Use | Republish in a thesis/dissertation |
| Order license ID | 1083544-1 | Publisher Portion | IOP Publishing Image/photo/illustration |
| ISSN | 0022-3727 | | |

LICENSED CONTENT

| | | | |
|-------------------|--------------------------------------------------------------------------------------|------------------|------------------------------------------------------|
| Publication Title | Journal of Physics D : Applied Physics | Country | United Kingdom of Great Britain and Northern Ireland |
| Author/Editor | Institute of Physics (Great Britain), Institute of Physics and the Physical Society. | Rightsholder | IOP Publishing, Ltd |
| Date | 01/01/1970 | Publication Type | Journal |
| Language | English | | |

REQUEST DETAILS

| | | | |
|-------------------------------------------|-----------------------------------------|-----------------------------|----------------------------------|
| Portion Type | Image/photo/illustration | Distribution | Worldwide |
| Number of images / photos / illustrations | 1 | Translation | Original language of publication |
| Format (select all that apply) | Print, Electronic | Copies for the disabled? | No |
| Who will republish the content? | Academic institution | Minor editing privileges? | No |
| Duration of Use | Life of current and all future editions | Incidental promotional use? | No |
| Lifetime Unit Quantity | Up to 499 | Currency | USD |
| Rights Requested | Main product | | |

NEW WORK DETAILS

| | | | |
|-----------------|----------------------------------------------------------------------------------|----------------------------|---------------------|
| Title | Expanding the droplet microfluidic community - towards a modular active platform | Institution name | Waterloo University |
| Instructor name | Marie Hebert | Expected presentation date | 2021-01-01 |

ADDITIONAL DETAILS

| | | | |
|------------------------|-----|---------------------------------------------------------------|--------------|
| Order reference number | N/A | The requesting person / organization to appear on the license | Marie Hebert |
|------------------------|-----|---------------------------------------------------------------|--------------|

REUSE CONTENT DETAILS

| | | | |
|-----------------------------------------------------------|--------------|--------------------------------------------------|--------------------------------------------------------------------------------------|
| Title, description or numeric reference of the portion(s) | Figure 1 (b) | Title of the article/chapter the portion is from | Microfluidic methods for generating continuous droplet streams |
| Editor of portion(s) | N/A | Author of portion(s) | Institute of Physics (Great Britain); Institute of Physics and the Physical Society. |
| Volume of serial or monograph | N/A | | |
| Page or page range of portion | R320 | Issue, if republishing an article from a serial | N/A |
| | | Publication date of portion | 2007-09-27 |

PUBLISHER TERMS AND CONDITIONS

These special terms and conditions are in addition to the standard terms and conditions for CCC's Republication Service and, together with those standard terms and conditions, govern the use of the Works. As the User you will make all reasonable efforts to contact the author(s) of the article which the Work is to be reused from, to seek consent for your intended use. Contacting one author who is acting expressly as authorised agent for their co-author(s) is acceptable. User will reproduce the following wording prominently alongside the Work: the source of the Work, including author, article title, title of journal, volume number, issue number (if relevant), page range (or first page if this is the only information available) and date of first publication. This information can be contained in a footnote or reference note; and a link back to the article (via DOI); and if practicable, and IN ALL CASES for new works published under any of the Creative Commons licences, the words "© IOP Publishing. Reproduced with permission. All rights reserved" Without the express permission of the author(s) and the Rightsholder of the article from which the Work is to be reused, User shall not use it in any way which, in the opinion of the Rightsholder, could: (i) distort or alter the author(s)' original intention(s) and meaning; (ii) be prejudicial to the honour or reputation of the author(s); and/or (iii) imply endorsement by the author(s) and/or the Rightsholder. This licence does not apply to any article which is credited to another source and which does not have the copyright line '© IOP Publishing Ltd'. User must check the copyright line of the article from which the Work is to be reused to check that IOP Publishing Ltd has all the necessary rights to be able to grant permission. User is solely responsible for identifying and obtaining separate licences and permissions from the copyright owner for reuse of any such third party material/figures which the Rightsholder is not the copyright owner of. The Rightsholder shall not reimburse any fees which User pays for a republication license for such third party content. This licence does not apply to any material/figure which is credited to another source in the Rightsholder's publication or has been obtained from a third party. User must check the Version of Record of the article from which the Work is to be reused, to check whether any of the material in the Work is third party material. Third party citations and/or copyright notices and/or permissions statements may not be included in any other version of the article from which the Work is to be reused and so cannot be relied upon by the User. User is solely responsible for identifying and obtaining separate licences and permissions from the copyright owner for reuse of any such third party material/figures where the Rightsholder is not the copyright owner. The Rightsholder shall not reimburse any fees which User pays for a republication license for such third party content. User and CCC acknowledge that the Rightsholder may, from time to time, make changes or additions to these special terms and conditions without express notification, provided that these shall not apply to permissions already secured and paid for by User prior to such change or addition. User acknowledges that the Rightsholder (which includes companies within its group and third parties for whom it publishes its titles) may make use of personal data collected through the service in the course of their business. If User is the author of the Work, User may automatically have the right to reuse it under the rights granted back when User transferred the copyright in the article to the Rightsholder. User should check the copyright form and the relevant author rights policy to check whether permission is required. If User is the author of the Work and does require permission for proposed reuse of the Work, User should select 'Author of requested content' as the Requestor Type. The Rightsholder shall not reimburse any fees which User pays for a republication license. If User is the author of the article which User wishes to reuse in User's thesis or dissertation, the republication licence covers the right to include the Accepted Manuscript version (not the Version of Record) of the article. User must include citation details and, for online use, a link to the Version of Record of the article on the Rightsholder's website. User may need to

obtain separate permission for any third party content included within the article. User must check this with the copyright owner of such third party content. User may not include the article in a thesis or dissertation which is published by ProQuest. Any other commercial use of User's thesis or dissertation containing the article would also need to be expressly notified in writing to the Rightsholder at the time of request and would require separate written permission from the Rightsholder. User does not need to request permission for Work which has been published under a CC BY licence. User must check the Version of Record of the CC BY article from which the Work is to be reused, to check whether any of the material in the Work is third party material and so not published under the CC BY licence. User is solely responsible for identifying and obtaining separate licences and permissions from the copyright owner for reuse of any such third party material/figures. The Rightsholder shall not reimburse any fees which User pays for such licences and permissions. As well as CCC, the Rightsholder shall have the right to bring any legal action that it deems necessary to enforce its rights should it consider that the Work infringes those rights in any way. For STM Signatories ONLY (as agreed as part of the STM Guidelines) Any licence granted for a particular edition of a Work will apply also to subsequent editions of it and for editions in other languages, provided such editions are for the Work as a whole in situ and do not involve the separate exploitation of the permitted illustrations or excerpts.

CCC Republication Terms and Conditions

1. Description of Service; Defined Terms. This Republication License enables the User to obtain licenses for republication of one or more copyrighted works as described in detail on the relevant Order Confirmation (the "Work(s)"). Copyright Clearance Center, Inc. ("CCC") grants licenses through the Service on behalf of the rightsholder identified on the Order Confirmation (the "Rightsholder"). "Republication", as used herein, generally means the inclusion of a Work, in whole or in part, in a new work or works, also as described on the Order Confirmation. "User", as used herein, means the person or entity making such republication.
2. The terms set forth in the relevant Order Confirmation, and any terms set by the Rightsholder with respect to a particular Work, govern the terms of use of Works in connection with the Service. By using the Service, the person transacting for a republication license on behalf of the User represents and warrants that he/she/it (a) has been duly authorized by the User to accept, and hereby does accept, all such terms and conditions on behalf of User, and (b) shall inform User of all such terms and conditions. In the event such person is a "freelancer" or other third party independent of User and CCC, such party shall be deemed jointly a "User" for purposes of these terms and conditions. In any event, User shall be deemed to have accepted and agreed to all such terms and conditions if User republishes the Work in any fashion.
3. Scope of License; Limitations and Obligations.
 - 3.1. All Works and all rights therein, including copyright rights, remain the sole and exclusive property of the Rightsholder. The license created by the exchange of an Order Confirmation (and/or any invoice) and payment by User of the full amount set forth on that document includes only those rights expressly set forth in the Order Confirmation and in these terms and conditions, and conveys no other rights in the Work(s) to User. All rights not expressly granted are hereby reserved.
 - 3.2. General Payment Terms: You may pay by credit card or through an account with us payable at the end of the month. If you and we agree that you may establish a standing account with CCC, then the following terms apply: Remit Payment to: Copyright Clearance Center, 29118 Network Place, Chicago, IL 60673-1291. Payments Due: Invoices are payable upon their delivery to you (or upon our notice to you that they are available to you for downloading). After 30 days, outstanding amounts will be subject to a service charge of 1-1/2% per month or, if less, the maximum rate allowed by applicable law. Unless otherwise specifically set forth in the Order Confirmation or in a separate written agreement signed by CCC, invoices are due and payable on "net 30" terms. While User may exercise the rights licensed immediately upon issuance of the Order Confirmation, the license is automatically revoked and is null and void, as if it had never been issued, if complete payment for the license is not received on a timely basis either from User directly or through a payment agent, such as a credit card company.
 - 3.3. Unless otherwise provided in the Order Confirmation, any grant of rights to User (i) is "one-time" (including the editions and product family specified in the license), (ii) is non-exclusive and non-transferable and (iii) is subject to any and all limitations and restrictions (such as, but not limited to, limitations on duration of use or circulation) included in the Order Confirmation or invoice and/or in these terms and conditions.

14/12/2020

<https://marketplace.copyright.com/rs-ui-web/mp/license/6f05c0bc-4e21-4cba-b9ea-242a3df45a24/398ba52c-fa7f-4f9f-80a2-c15cc9f320b4>

Upon completion of the licensed use, User shall either secure a new permission for further use of the Work(s) or immediately cease any new use of the Work(s) and shall render inaccessible (such as by deleting or by removing or severing links or other locators) any further copies of the Work (except for copies printed on paper in accordance with this license and still in User's stock at the end of such period).

- 3.4. In the event that the material for which a republication license is sought includes third party materials (such as photographs, illustrations, graphs, inserts and similar materials) which are identified in such material as having been used by permission, User is responsible for identifying, and seeking separate licenses (under this Service or otherwise) for, any of such third party materials; without a separate license, such third party materials may not be used.
- 3.5. Use of proper copyright notice for a Work is required as a condition of any license granted under the Service. Unless otherwise provided in the Order Confirmation, a proper copyright notice will read substantially as follows: "Republished with permission of [Rightsholder's name], from [Work's title, author, volume, edition number and year of copyright]; permission conveyed through Copyright Clearance Center, Inc. " Such notice must be provided in a reasonably legible font size and must be placed either immediately adjacent to the Work as used (for example, as part of a by-line or footnote but not as a separate electronic link) or in the place where substantially all other credits or notices for the new work containing the republished Work are located. Failure to include the required notice results in loss to the Rightsholder and CCC, and the User shall be liable to pay liquidated damages for each such failure equal to twice the use fee specified in the Order Confirmation, in addition to the use fee itself and any other fees and charges specified.
- 3.6. User may only make alterations to the Work if and as expressly set forth in the Order Confirmation. No Work may be used in any way that is defamatory, violates the rights of third parties (including such third parties' rights of copyright, privacy, publicity, or other tangible or intangible property), or is otherwise illegal, sexually explicit or obscene. In addition, User may not conjoin a Work with any other material that may result in damage to the reputation of the Rightsholder. User agrees to inform CCC if it becomes aware of any infringement of any rights in a Work and to cooperate with any reasonable request of CCC or the Rightsholder in connection therewith.
4. Indemnity. User hereby indemnifies and agrees to defend the Rightsholder and CCC, and their respective employees and directors, against all claims, liability, damages, costs and expenses, including legal fees and expenses, arising out of any use of a Work beyond the scope of the rights granted herein, or any use of a Work which has been altered in any unauthorized way by User, including claims of defamation or infringement of rights of copyright, publicity, privacy or other tangible or intangible property.
5. Limitation of Liability. UNDER NO CIRCUMSTANCES WILL CCC OR THE RIGHTSHOLDER BE LIABLE FOR ANY DIRECT, INDIRECT, CONSEQUENTIAL OR INCIDENTAL DAMAGES (INCLUDING WITHOUT LIMITATION DAMAGES FOR LOSS OF BUSINESS PROFITS OR INFORMATION, OR FOR BUSINESS INTERRUPTION) ARISING OUT OF THE USE OR INABILITY TO USE A WORK, EVEN IF ONE OF THEM HAS BEEN ADVISED OF THE POSSIBILITY OF SUCH DAMAGES. In any event, the total liability of the Rightsholder and CCC (including their respective employees and directors) shall not exceed the total amount actually paid by User for this license. User assumes full liability for the actions and omissions of its principals, employees, agents, affiliates, successors and assigns.
6. Limited Warranties. THE WORK(S) AND RIGHT(S) ARE PROVIDED "AS IS". CCC HAS THE RIGHT TO GRANT TO USER THE RIGHTS GRANTED IN THE ORDER CONFIRMATION DOCUMENT. CCC AND THE RIGHTSHOLDER DISCLAIM ALL OTHER WARRANTIES RELATING TO THE WORK(S) AND RIGHT(S), EITHER EXPRESS OR IMPLIED, INCLUDING WITHOUT LIMITATION IMPLIED WARRANTIES OF MERCHANTABILITY OR FITNESS FOR A PARTICULAR PURPOSE. ADDITIONAL RIGHTS MAY BE REQUIRED TO USE ILLUSTRATIONS, GRAPHS, PHOTOGRAPHS, ABSTRACTS, INSERTS OR OTHER PORTIONS OF THE WORK (AS OPPOSED TO THE ENTIRE WORK) IN A MANNER CONTEMPLATED BY USER; USER UNDERSTANDS AND AGREES THAT NEITHER CCC NOR THE RIGHTSHOLDER MAY HAVE SUCH ADDITIONAL RIGHTS TO GRANT.
7. Effect of Breach. Any failure by User to pay any amount when due, or any use by User of a Work beyond the scope

<https://marketplace.copyright.com/rs-ui-web/mp/license/6f05c0bc-4e21-4cba-b9ea-242a3df45a24/398ba52c-fa7f-4f9f-80a2-c15cc9f320b4>

4/5

14/12/2020

<https://marketplace.copyright.com/rs-ui-web/mp/license/6f05c0bc-4e21-4cba-b9ea-242a3df45a24/398ba52c-fa7f-4f9f-80a2-c15cc9f320b4>

of the license set forth in the Order Confirmation and/or these terms and conditions, shall be a material breach of the license created by the Order Confirmation and these terms and conditions. Any breach not cured within 30 days of written notice thereof shall result in immediate termination of such license without further notice. Any unauthorized (but licensable) use of a Work that is terminated immediately upon notice thereof may be liquidated by payment of the Rightsholder's ordinary license price therefor; any unauthorized (and unlicensable) use that is not terminated immediately for any reason (including, for example, because materials containing the Work cannot reasonably be recalled) will be subject to all remedies available at law or in equity, but in no event to a payment of less than three times the Rightsholder's ordinary license price for the most closely analogous licensable use plus Rightsholder's and/or CCC's costs and expenses incurred in collecting such payment.

8. Miscellaneous.

- 8.1. User acknowledges that CCC may, from time to time, make changes or additions to the Service or to these terms and conditions, and CCC reserves the right to send notice to the User by electronic mail or otherwise for the purposes of notifying User of such changes or additions; provided that any such changes or additions shall not apply to permissions already secured and paid for.
- 8.2. Use of User-related information collected through the Service is governed by CCC's privacy policy, available online here:<https://marketplace.copyright.com/rs-ui-web/mp/privacy-policy>
- 8.3. The licensing transaction described in the Order Confirmation is personal to User. Therefore, User may not assign or transfer to any other person (whether a natural person or an organization of any kind) the license created by the Order Confirmation and these terms and conditions or any rights granted hereunder; provided, however, that User may assign such license in its entirety on written notice to CCC in the event of a transfer of all or substantially all of User's rights in the new material which includes the Work(s) licensed under this Service.
- 8.4. No amendment or waiver of any terms is binding unless set forth in writing and signed by the parties. The Rightsholder and CCC hereby object to any terms contained in any writing prepared by the User or its principals, employees, agents or affiliates and purporting to govern or otherwise relate to the licensing transaction described in the Order Confirmation, which terms are in any way inconsistent with any terms set forth in the Order Confirmation and/or in these terms and conditions or CCC's standard operating procedures, whether such writing is prepared prior to, simultaneously with or subsequent to the Order Confirmation, and whether such writing appears on a copy of the Order Confirmation or in a separate instrument.
- 8.5. The licensing transaction described in the Order Confirmation document shall be governed by and construed under the law of the State of New York, USA, without regard to the principles thereof of conflicts of law. Any case, controversy, suit, action, or proceeding arising out of, in connection with, or related to such licensing transaction shall be brought, at CCC's sole discretion, in any federal or state court located in the County of New York, State of New York, USA, or in any federal or state court whose geographical jurisdiction covers the location of the Rightsholder set forth in the Order Confirmation. The parties expressly submit to the personal jurisdiction and venue of each such federal or state court. If you have any comments or questions about the Service or Copyright Clearance Center, please contact us at 978-750-8400 or send an e-mail to support@copyright.com.

v 1.1

<https://marketplace.copyright.com/rs-ui-web/mp/license/6f05c0bc-4e21-4cba-b9ea-242a3df45a24/398ba52c-fa7f-4f9f-80a2-c15cc9f320b4>

5/5

14/12/2020

<https://marketplace.copyright.com/rs-ui-web/mp/license/66e33542-b460-4a43-894c-26555115564a/7e377971-26b4-4824-aace-350faaa...>Copyright
Clearance
Center

Marketplace™

Royal Society of Chemistry - License Terms and Conditions

This is a License Agreement between Marie Hebert ("You") and Royal Society of Chemistry ("Publisher") provided by Copyright Clearance Center ("CCC"). The license consists of your order details, the terms and conditions provided by Royal Society of Chemistry, and the CCC terms and conditions.

All payments must be made in full to CCC.

| | | | |
|------------------|-------------|-------------|------------------------------------|
| Order Date | 11-Dec-2020 | Type of Use | Republish in a thesis/dissertation |
| Order license ID | 1083552-1 | Publisher | ROYAL SOCIETY OF CHEMISTRY |
| ISSN | 1473-0189 | Portion | Image/photo/illustration |

LICENSED CONTENT

| | | | |
|-------------------|--------------------------------------------|------------------|-------------------------------------------------------------|
| Publication Title | Lab on a chip | Country | United Kingdom of Great Britain and Northern Ireland |
| Author/Editor | Royal Society of Chemistry (Great Britain) | Rightsholder | Royal Society of Chemistry |
| Date | 01/01/2001 | Publication Type | e-Journal |
| Language | English | URL | http://www.rsc.org/loc |

REQUEST DETAILS

| | | | |
|-------------------------------------------|--------------------------|-----------------------------|----------------------------------|
| Portion Type | Image/photo/illustration | Distribution | Worldwide |
| Number of images / photos / illustrations | 1 | Translation | Original language of publication |
| Format (select all that apply) | Print, Electronic | Copies for the disabled? | No |
| Who will republish the content? | Academic institution | Minor editing privileges? | No |
| Duration of Use | Life of current edition | Incidental promotional use? | No |
| Lifetime Unit Quantity | Up to 499 | Currency | USD |
| Rights Requested | Main product | | |

NEW WORK DETAILS

| | | | |
|-----------------|----------------------------------------------------------------------------------|----------------------------|---------------------|
| Title | Expanding the droplet microfluidic community - towards a modular active platform | Institution name | Waterloo University |
| Instructor name | Marie Hebert | Expected presentation date | 2021-01-01 |

ADDITIONAL DETAILS

| | |
|------------------------|-----|
| Order reference number | N/A |
|------------------------|-----|

<https://marketplace.copyright.com/rs-ui-web/mp/license/66e33542-b460-4a43-894c-26555115564a/7e377971-26b4-4824-aace-350faaa3cf83>

1/4

The requesting person / organization to appear on the license Marie Hebert

REUSE CONTENT DETAILS

| | | | |
|-----------------------------------------------------------|--------------|--------------------------------------------------|----------------------------------------------------------------------------------|
| Title, description or numeric reference of the portion(s) | Figure 2 (i) | Title of the article/chapter the portion is from | High-speed droplet generation on demand driven by pulse laser-induced cavitation |
| Editor of portion(s) | N/A | Author of portion(s) | Royal Society of Chemistry (Great Britain) |
| Volume of serial or monograph | N/A | Issue, if republishing an article from a serial | N/A |
| Page or page range of portion | 1011 | Publication date of portion | 2011-02-02 |

CCC Republication Terms and Conditions

1. Description of Service; Defined Terms. This Republication License enables the User to obtain licenses for republication of one or more copyrighted works as described in detail on the relevant Order Confirmation (the "Work(s)"). Copyright Clearance Center, Inc. ("CCC") grants licenses through the Service on behalf of the rights holder identified on the Order Confirmation (the "Rights holder"). "Republishing", as used herein, generally means the inclusion of a Work, in whole or in part, in a new work or works, also as described on the Order Confirmation. "User", as used herein, means the person or entity making such republication.
2. The terms set forth in the relevant Order Confirmation, and any terms set by the Rights holder with respect to a particular Work, govern the terms of use of Works in connection with the Service. By using the Service, the person transacting for a republication license on behalf of the User represents and warrants that he/she/it (a) has been duly authorized by the User to accept, and hereby does accept, all such terms and conditions on behalf of User, and (b) shall inform User of all such terms and conditions. In the event such person is a "freelancer" or other third party independent of User and CCC, such party shall be deemed jointly a "User" for purposes of these terms and conditions. In any event, User shall be deemed to have accepted and agreed to all such terms and conditions if User republishes the Work in any fashion.
3. Scope of License; Limitations and Obligations.
 - 3.1. All Works and all rights therein, including copyright rights, remain the sole and exclusive property of the Rights holder. The license created by the exchange of an Order Confirmation (and/or any invoice) and payment by User of the full amount set forth on that document includes only those rights expressly set forth in the Order Confirmation and in these terms and conditions, and conveys no other rights in the Work(s) to User. All rights not expressly granted are hereby reserved.
 - 3.2. General Payment Terms: You may pay by credit card or through an account with us payable at the end of the month. If you and we agree that you may establish a standing account with CCC, then the following terms apply: Remit Payment to: Copyright Clearance Center, 29118 Network Place, Chicago, IL 60673-1291. Payments Due: Invoices are payable upon their delivery to you (or upon our notice to you that they are available to you for downloading). After 30 days, outstanding amounts will be subject to a service charge of 1-1/2% per month or, if less, the maximum rate allowed by applicable law. Unless otherwise specifically set forth in the Order Confirmation or in a separate written agreement signed by CCC, invoices are due and payable on "net 30" terms. While User may exercise the rights licensed immediately upon issuance of the Order Confirmation, the license is automatically revoked and is null and void, as if it had never been issued, if complete payment for the license is not received on a timely basis either from User directly or through a payment agent, such as a credit card company.

14/12/2020

<https://marketplace.copyright.com/rs-ui-web/mp/license/66e33542-b460-4a43-894c-26555115564a/7e377971-26b4-4824-aace-350faaa...>

- 3.3. Unless otherwise provided in the Order Confirmation, any grant of rights to User (i) is "one-time" (including the editions and product family specified in the license), (ii) is non-exclusive and non-transferable and (iii) is subject to any and all limitations and restrictions (such as, but not limited to, limitations on duration of use or circulation) included in the Order Confirmation or invoice and/or in these terms and conditions. Upon completion of the licensed use, User shall either secure a new permission for further use of the Work(s) or immediately cease any new use of the Work(s) and shall render inaccessible (such as by deleting or by removing or severing links or other locators) any further copies of the Work (except for copies printed on paper in accordance with this license and still in User's stock at the end of such period).
- 3.4. In the event that the material for which a republication license is sought includes third party materials (such as photographs, illustrations, graphs, inserts and similar materials) which are identified in such material as having been used by permission, User is responsible for identifying, and seeking separate licenses (under this Service or otherwise) for, any of such third party materials; without a separate license, such third party materials may not be used.
- 3.5. Use of proper copyright notice for a Work is required as a condition of any license granted under the Service. Unless otherwise provided in the Order Confirmation, a proper copyright notice will read substantially as follows: "Republished with permission of [Rightsholder's name], from [Work's title, author, volume, edition number and year of copyright]; permission conveyed through Copyright Clearance Center, Inc. " Such notice must be provided in a reasonably legible font size and must be placed either immediately adjacent to the Work as used (for example, as part of a by-line or footnote but not as a separate electronic link) or in the place where substantially all other credits or notices for the new work containing the republished Work are located. Failure to include the required notice results in loss to the Rightsholder and CCC, and the User shall be liable to pay liquidated damages for each such failure equal to twice the use fee specified in the Order Confirmation, in addition to the use fee itself and any other fees and charges specified.
- 3.6. User may only make alterations to the Work if and as expressly set forth in the Order Confirmation. No Work may be used in any way that is defamatory, violates the rights of third parties (including such third parties' rights of copyright, privacy, publicity, or other tangible or intangible property), or is otherwise illegal, sexually explicit or obscene. In addition, User may not conjoin a Work with any other material that may result in damage to the reputation of the Rightsholder. User agrees to inform CCC if it becomes aware of any infringement of any rights in a Work and to cooperate with any reasonable request of CCC or the Rightsholder in connection therewith.
4. Indemnity. User hereby indemnifies and agrees to defend the Rightsholder and CCC, and their respective employees and directors, against all claims, liability, damages, costs and expenses, including legal fees and expenses, arising out of any use of a Work beyond the scope of the rights granted herein, or any use of a Work which has been altered in any unauthorized way by User, including claims of defamation or infringement of rights of copyright, publicity, privacy or other tangible or intangible property.
5. Limitation of Liability. UNDER NO CIRCUMSTANCES WILL CCC OR THE RIGHTSHOLDER BE LIABLE FOR ANY DIRECT, INDIRECT, CONSEQUENTIAL OR INCIDENTAL DAMAGES (INCLUDING WITHOUT LIMITATION DAMAGES FOR LOSS OF BUSINESS PROFITS OR INFORMATION, OR FOR BUSINESS INTERRUPTION) ARISING OUT OF THE USE OR INABILITY TO USE A WORK, EVEN IF ONE OF THEM HAS BEEN ADVISED OF THE POSSIBILITY OF SUCH DAMAGES. In any event, the total liability of the Rightsholder and CCC (including their respective employees and directors) shall not exceed the total amount actually paid by User for this license. User assumes full liability for the actions and omissions of its principals, employees, agents, affiliates, successors and assigns.
6. Limited Warranties. THE WORK(S) AND RIGHT(S) ARE PROVIDED "AS IS". CCC HAS THE RIGHT TO GRANT TO USER THE RIGHTS GRANTED IN THE ORDER CONFIRMATION DOCUMENT. CCC AND THE RIGHTSHOLDER DISCLAIM ALL OTHER WARRANTIES RELATING TO THE WORK(S) AND RIGHT(S), EITHER EXPRESS OR IMPLIED, INCLUDING WITHOUT LIMITATION IMPLIED WARRANTIES OF MERCHANTABILITY OR FITNESS FOR A PARTICULAR PURPOSE. ADDITIONAL RIGHTS MAY BE REQUIRED TO USE ILLUSTRATIONS, GRAPHS, PHOTOGRAPHS, ABSTRACTS, INSERTS OR OTHER PORTIONS OF THE WORK (AS OPPOSED TO THE ENTIRE WORK) IN A MANNER CONTEMPLATED BY USER;

<https://marketplace.copyright.com/rs-ui-web/mp/license/66e33542-b460-4a43-894c-26555115564a/7e377971-26b4-4824-aace-350faaa3cf83>

3/4

USER UNDERSTANDS AND AGREES THAT NEITHER CCC NOR THE RIGHTSHOLDER MAY HAVE SUCH ADDITIONAL RIGHTS TO GRANT.

7. Effect of Breach. Any failure by User to pay any amount when due, or any use by User of a Work beyond the scope of the license set forth in the Order Confirmation and/or these terms and conditions, shall be a material breach of the license created by the Order Confirmation and these terms and conditions. Any breach not cured within 30 days of written notice thereof shall result in immediate termination of such license without further notice. Any unauthorized (but licensable) use of a Work that is terminated immediately upon notice thereof may be liquidated by payment of the Rightsholder's ordinary license price therefor; any unauthorized (and unlicensable) use that is not terminated immediately for any reason (including, for example, because materials containing the Work cannot reasonably be recalled) will be subject to all remedies available at law or in equity, but in no event to a payment of less than three times the Rightsholder's ordinary license price for the most closely analogous licensable use plus Rightsholder's and/or CCC's costs and expenses incurred in collecting such payment.

8. Miscellaneous.

8.1. User acknowledges that CCC may, from time to time, make changes or additions to the Service or to these terms and conditions, and CCC reserves the right to send notice to the User by electronic mail or otherwise for the purposes of notifying User of such changes or additions; provided that any such changes or additions shall not apply to permissions already secured and paid for.

8.2. Use of User-related information collected through the Service is governed by CCC's privacy policy, available online here:<https://marketplace.copyright.com/rs-ui-web/mp/privacy-policy>

8.3. The licensing transaction described in the Order Confirmation is personal to User. Therefore, User may not assign or transfer to any other person (whether a natural person or an organization of any kind) the license created by the Order Confirmation and these terms and conditions or any rights granted hereunder; provided, however, that User may assign such license in its entirety on written notice to CCC in the event of a transfer of all or substantially all of User's rights in the new material which includes the Work(s) licensed under this Service.

8.4. No amendment or waiver of any terms is binding unless set forth in writing and signed by the parties. The Rightsholder and CCC hereby object to any terms contained in any writing prepared by the User or its principals, employees, agents or affiliates and purporting to govern or otherwise relate to the licensing transaction described in the Order Confirmation, which terms are in any way inconsistent with any terms set forth in the Order Confirmation and/or in these terms and conditions or CCC's standard operating procedures, whether such writing is prepared prior to, simultaneously with or subsequent to the Order Confirmation, and whether such writing appears on a copy of the Order Confirmation or in a separate instrument.

8.5. The licensing transaction described in the Order Confirmation document shall be governed by and construed under the law of the State of New York, USA, without regard to the principles thereof of conflicts of law. Any case, controversy, suit, action, or proceeding arising out of, in connection with, or related to such licensing transaction shall be brought, at CCC's sole discretion, in any federal or state court located in the County of New York, State of New York, USA, or in any federal or state court whose geographical jurisdiction covers the location of the Rightsholder set forth in the Order Confirmation. The parties expressly submit to the personal jurisdiction and venue of each such federal or state court. If you have any comments or questions about the Service or Copyright Clearance Center, please contact us at 978-750-8400 or send an e-mail to support@copyright.com.

v 1.1

14/12/2020

<https://marketplace.copyright.com/rs-ui-web/mp/license/0a73d5ce-3dc7-4dba-876b-d0a9d2cf29eb/1b7437ba-4709-4786-98f1-37888b2...>Copyright
Clearance
Center

Marketplace™

Royal Society of Chemistry - License Terms and Conditions

This is a License Agreement between Marie Hebert ("You") and Royal Society of Chemistry ("Publisher") provided by Copyright Clearance Center ("CCC"). The license consists of your order details, the terms and conditions provided by Royal Society of Chemistry, and the CCC terms and conditions.

All payments must be made in full to CCC.

| | | | |
|------------------|-------------|-------------|------------------------------------|
| Order Date | 11-Dec-2020 | Type of Use | Republish in a thesis/dissertation |
| Order license ID | 1083553-1 | Publisher | ROYAL SOCIETY OF CHEMISTRY |
| ISSN | 1473-0189 | Portion | Image/photo/illustration |

LICENSED CONTENT

| | | | |
|-------------------|--------------------------------------------|------------------|-------------------------------------------------------------|
| Publication Title | Lab on a chip | Country | United Kingdom of Great Britain and Northern Ireland |
| Author/Editor | Royal Society of Chemistry (Great Britain) | Rightsholder | Royal Society of Chemistry |
| Date | 01/01/2001 | Publication Type | e-Journal |
| Language | English | URL | http://www.rsc.org/loc |

REQUEST DETAILS

| | | | |
|-------------------------------------------|--------------------------|-----------------------------|----------------------------------|
| Portion Type | Image/photo/illustration | Distribution | Worldwide |
| Number of images / photos / illustrations | 1 | Translation | Original language of publication |
| Format (select all that apply) | Print, Electronic | Copies for the disabled? | No |
| Who will republish the content? | Academic institution | Minor editing privileges? | No |
| Duration of Use | Life of current edition | Incidental promotional use? | No |
| Lifetime Unit Quantity | Up to 499 | Currency | USD |
| Rights Requested | Main product | | |

NEW WORK DETAILS

| | | | |
|-----------------|----------------------------------------------------------------------------------|----------------------------|---------------------|
| Title | Expanding the droplet microfluidic community - towards a modular active platform | Institution name | Waterloo University |
| Instructor name | Marie Hebert | Expected presentation date | 2021-01-01 |

ADDITIONAL DETAILS

| | |
|------------------------|-----|
| Order reference number | N/A |
|------------------------|-----|

<https://marketplace.copyright.com/rs-ui-web/mp/license/0a73d5ce-3dc7-4dba-876b-d0a9d2cf29eb/1b7437ba-4709-4786-98f1-37888b26f8a6>

1/4

The requesting person / organization to appear on the license Marie Hebert

REUSE CONTENT DETAILS

| | | | |
|-----------------------------------------------------------|--------------|--------------------------------------------------|--------------------------------------------------------------------------------------------------|
| Title, description or numeric reference of the portion(s) | Figure 2 (a) | Title of the article/chapter the portion is from | Surface acoustic waves for on-demand production of picoliter droplets and particle encapsulation |
| Editor of portion(s) | N/A | Author of portion(s) | Royal Society of Chemistry (Great Britain) |
| Volume of serial or monograph | N/A | Issue, if republishing an article from a serial | N/A |
| Page or page range of portion | 3228 | Publication date of portion | 2013-06-04 |

CCC Republication Terms and Conditions

1. Description of Service; Defined Terms. This Republication License enables the User to obtain licenses for republication of one or more copyrighted works as described in detail on the relevant Order Confirmation (the "Work(s)"). Copyright Clearance Center, Inc. ("CCC") grants licenses through the Service on behalf of the rights holder identified on the Order Confirmation (the "Rights holder"). "Republishing", as used herein, generally means the inclusion of a Work, in whole or in part, in a new work or works, also as described on the Order Confirmation. "User", as used herein, means the person or entity making such republication.
2. The terms set forth in the relevant Order Confirmation, and any terms set by the Rights holder with respect to a particular Work, govern the terms of use of Works in connection with the Service. By using the Service, the person transacting for a republication license on behalf of the User represents and warrants that he/she/it (a) has been duly authorized by the User to accept, and hereby does accept, all such terms and conditions on behalf of User, and (b) shall inform User of all such terms and conditions. In the event such person is a "freelancer" or other third party independent of User and CCC, such party shall be deemed jointly a "User" for purposes of these terms and conditions. In any event, User shall be deemed to have accepted and agreed to all such terms and conditions if User republishes the Work in any fashion.
3. Scope of License; Limitations and Obligations.
 - 3.1. All Works and all rights therein, including copyright rights, remain the sole and exclusive property of the Rights holder. The license created by the exchange of an Order Confirmation (and/or any invoice) and payment by User of the full amount set forth on that document includes only those rights expressly set forth in the Order Confirmation and in these terms and conditions, and conveys no other rights in the Work(s) to User. All rights not expressly granted are hereby reserved.
 - 3.2. General Payment Terms: You may pay by credit card or through an account with us payable at the end of the month. If you and we agree that you may establish a standing account with CCC, then the following terms apply: Remit Payment to: Copyright Clearance Center, 29118 Network Place, Chicago, IL 60673-1291. Payments Due: Invoices are payable upon their delivery to you (or upon our notice to you that they are available to you for downloading). After 30 days, outstanding amounts will be subject to a service charge of 1-1/2% per month or, if less, the maximum rate allowed by applicable law. Unless otherwise specifically set forth in the Order Confirmation or in a separate written agreement signed by CCC, invoices are due and payable on "net 30" terms. While User may exercise the rights licensed immediately upon issuance of the Order Confirmation, the license is automatically revoked and is null and void, as if it had never been issued, if complete payment for the license is not received on a timely basis either from User directly or through a payment agent, such as a credit card company.

14/12/2020

<https://marketplace.copyright.com/rs-ui-web/mp/license/0a73d5ce-3dc7-4dba-876b-d0a9d2cf29eb/1b7437ba-4709-4786-98f1-37888b2...>

- 3.3. Unless otherwise provided in the Order Confirmation, any grant of rights to User (i) is "one-time" (including the editions and product family specified in the license), (ii) is non-exclusive and non-transferable and (iii) is subject to any and all limitations and restrictions (such as, but not limited to, limitations on duration of use or circulation) included in the Order Confirmation or invoice and/or in these terms and conditions. Upon completion of the licensed use, User shall either secure a new permission for further use of the Work(s) or immediately cease any new use of the Work(s) and shall render inaccessible (such as by deleting or by removing or severing links or other locators) any further copies of the Work (except for copies printed on paper in accordance with this license and still in User's stock at the end of such period).
- 3.4. In the event that the material for which a republication license is sought includes third party materials (such as photographs, illustrations, graphs, inserts and similar materials) which are identified in such material as having been used by permission, User is responsible for identifying, and seeking separate licenses (under this Service or otherwise) for, any of such third party materials; without a separate license, such third party materials may not be used.
- 3.5. Use of proper copyright notice for a Work is required as a condition of any license granted under the Service. Unless otherwise provided in the Order Confirmation, a proper copyright notice will read substantially as follows: "Republished with permission of [Rightsholder's name], from [Work's title, author, volume, edition number and year of copyright]; permission conveyed through Copyright Clearance Center, Inc. " Such notice must be provided in a reasonably legible font size and must be placed either immediately adjacent to the Work as used (for example, as part of a by-line or footnote but not as a separate electronic link) or in the place where substantially all other credits or notices for the new work containing the republished Work are located. Failure to include the required notice results in loss to the Rightsholder and CCC, and the User shall be liable to pay liquidated damages for each such failure equal to twice the use fee specified in the Order Confirmation, in addition to the use fee itself and any other fees and charges specified.
- 3.6. User may only make alterations to the Work if and as expressly set forth in the Order Confirmation. No Work may be used in any way that is defamatory, violates the rights of third parties (including such third parties' rights of copyright, privacy, publicity, or other tangible or intangible property), or is otherwise illegal, sexually explicit or obscene. In addition, User may not conjoin a Work with any other material that may result in damage to the reputation of the Rightsholder. User agrees to inform CCC if it becomes aware of any infringement of any rights in a Work and to cooperate with any reasonable request of CCC or the Rightsholder in connection therewith.
4. Indemnity. User hereby indemnifies and agrees to defend the Rightsholder and CCC, and their respective employees and directors, against all claims, liability, damages, costs and expenses, including legal fees and expenses, arising out of any use of a Work beyond the scope of the rights granted herein, or any use of a Work which has been altered in any unauthorized way by User, including claims of defamation or infringement of rights of copyright, publicity, privacy or other tangible or intangible property.
5. Limitation of Liability. UNDER NO CIRCUMSTANCES WILL CCC OR THE RIGHTSHOLDER BE LIABLE FOR ANY DIRECT, INDIRECT, CONSEQUENTIAL OR INCIDENTAL DAMAGES (INCLUDING WITHOUT LIMITATION DAMAGES FOR LOSS OF BUSINESS PROFITS OR INFORMATION, OR FOR BUSINESS INTERRUPTION) ARISING OUT OF THE USE OR INABILITY TO USE A WORK, EVEN IF ONE OF THEM HAS BEEN ADVISED OF THE POSSIBILITY OF SUCH DAMAGES. In any event, the total liability of the Rightsholder and CCC (including their respective employees and directors) shall not exceed the total amount actually paid by User for this license. User assumes full liability for the actions and omissions of its principals, employees, agents, affiliates, successors and assigns.
6. Limited Warranties. THE WORK(S) AND RIGHT(S) ARE PROVIDED "AS IS". CCC HAS THE RIGHT TO GRANT TO USER THE RIGHTS GRANTED IN THE ORDER CONFIRMATION DOCUMENT. CCC AND THE RIGHTSHOLDER DISCLAIM ALL OTHER WARRANTIES RELATING TO THE WORK(S) AND RIGHT(S), EITHER EXPRESS OR IMPLIED, INCLUDING WITHOUT LIMITATION IMPLIED WARRANTIES OF MERCHANTABILITY OR FITNESS FOR A PARTICULAR PURPOSE. ADDITIONAL RIGHTS MAY BE REQUIRED TO USE ILLUSTRATIONS, GRAPHS, PHOTOGRAPHS, ABSTRACTS, INSERTS OR OTHER PORTIONS OF THE WORK (AS OPPOSED TO THE ENTIRE WORK) IN A MANNER CONTEMPLATED BY USER;

<https://marketplace.copyright.com/rs-ui-web/mp/license/0a73d5ce-3dc7-4dba-876b-d0a9d2cf29eb/1b7437ba-4709-4786-98f1-37888b26f8a6>

3/4

USER UNDERSTANDS AND AGREES THAT NEITHER CCC NOR THE RIGHTSHOLDER MAY HAVE SUCH ADDITIONAL RIGHTS TO GRANT.

7. Effect of Breach. Any failure by User to pay any amount when due, or any use by User of a Work beyond the scope of the license set forth in the Order Confirmation and/or these terms and conditions, shall be a material breach of the license created by the Order Confirmation and these terms and conditions. Any breach not cured within 30 days of written notice thereof shall result in immediate termination of such license without further notice. Any unauthorized (but licensable) use of a Work that is terminated immediately upon notice thereof may be liquidated by payment of the Rightsholder's ordinary license price therefor; any unauthorized (and unlicensable) use that is not terminated immediately for any reason (including, for example, because materials containing the Work cannot reasonably be recalled) will be subject to all remedies available at law or in equity, but in no event to a payment of less than three times the Rightsholder's ordinary license price for the most closely analogous licensable use plus Rightsholder's and/or CCC's costs and expenses incurred in collecting such payment.

8. Miscellaneous.

8.1. User acknowledges that CCC may, from time to time, make changes or additions to the Service or to these terms and conditions, and CCC reserves the right to send notice to the User by electronic mail or otherwise for the purposes of notifying User of such changes or additions; provided that any such changes or additions shall not apply to permissions already secured and paid for.

8.2. Use of User-related information collected through the Service is governed by CCC's privacy policy, available online here: <https://marketplace.copyright.com/rs-ui-web/mp/privacy-policy>

8.3. The licensing transaction described in the Order Confirmation is personal to User. Therefore, User may not assign or transfer to any other person (whether a natural person or an organization of any kind) the license created by the Order Confirmation and these terms and conditions or any rights granted hereunder; provided, however, that User may assign such license in its entirety on written notice to CCC in the event of a transfer of all or substantially all of User's rights in the new material which includes the Work(s) licensed under this Service.

8.4. No amendment or waiver of any terms is binding unless set forth in writing and signed by the parties. The Rightsholder and CCC hereby object to any terms contained in any writing prepared by the User or its principals, employees, agents or affiliates and purporting to govern or otherwise relate to the licensing transaction described in the Order Confirmation, which terms are in any way inconsistent with any terms set forth in the Order Confirmation and/or in these terms and conditions or CCC's standard operating procedures, whether such writing is prepared prior to, simultaneously with or subsequent to the Order Confirmation, and whether such writing appears on a copy of the Order Confirmation or in a separate instrument.

8.5. The licensing transaction described in the Order Confirmation document shall be governed by and construed under the law of the State of New York, USA, without regard to the principles thereof of conflicts of law. Any case, controversy, suit, action, or proceeding arising out of, in connection with, or related to such licensing transaction shall be brought, at CCC's sole discretion, in any federal or state court located in the County of New York, State of New York, USA, or in any federal or state court whose geographical jurisdiction covers the location of the Rightsholder set forth in the Order Confirmation. The parties expressly submit to the personal jurisdiction and venue of each such federal or state court. If you have any comments or questions about the Service or Copyright Clearance Center, please contact us at 978-750-8400 or send an e-mail to support@copyright.com.

v 1.1

14/12/2020

<https://marketplace.copyright.com/rs-ui-web/mp/license/616ea563-d56f-474d-8b8c-1f55b5cbec67/95b822af-5a32-48f8-9eaa-2ae06c41...>

Marketplace™

Royal Society of Chemistry - License Terms and Conditions

This is a License Agreement between Marie Hebert ("You") and Royal Society of Chemistry ("Publisher") provided by Copyright Clearance Center ("CCC"). The license consists of your order details, the terms and conditions provided by Royal Society of Chemistry, and the CCC terms and conditions.

All payments must be made in full to CCC.

| | | | |
|------------------|-------------|-------------|------------------------------------|
| Order Date | 11-Dec-2020 | Type of Use | Republish in a thesis/dissertation |
| Order license ID | 1083556-1 | Publisher | ROYAL SOCIETY OF CHEMISTRY |
| ISSN | 1473-0189 | Portion | Image/photo/illustration |

LICENSED CONTENT

| | | | |
|-------------------|--------------------------------------------|------------------|-------------------------------------------------------------|
| Publication Title | Lab on a chip | Country | United Kingdom of Great Britain and Northern Ireland |
| Author/Editor | Royal Society of Chemistry (Great Britain) | Rightsholder | Royal Society of Chemistry |
| Date | 01/01/2001 | Publication Type | e-Journal |
| Language | English | URL | http://www.rsc.org/loc |

REQUEST DETAILS

| | | | |
|-------------------------------------------|--------------------------|-----------------------------|----------------------------------|
| Portion Type | Image/photo/illustration | Distribution | Worldwide |
| Number of images / photos / illustrations | 1 | Translation | Original language of publication |
| Format (select all that apply) | Print, Electronic | Copies for the disabled? | No |
| Who will republish the content? | Academic institution | Minor editing privileges? | No |
| Duration of Use | Life of current edition | Incidental promotional use? | No |
| Lifetime Unit Quantity | Up to 499 | Currency | USD |
| Rights Requested | Main product | | |

NEW WORK DETAILS

| | | | |
|-----------------|----------------------------------------------------------------------------------|----------------------------|---------------------|
| Title | Expanding the droplet microfluidic community - towards a modular active platform | Institution name | Waterloo University |
| Instructor name | Marie Hebert | Expected presentation date | 2021-01-01 |

ADDITIONAL DETAILS

| | |
|------------------------|-----|
| Order reference number | N/A |
|------------------------|-----|

<https://marketplace.copyright.com/rs-ui-web/mp/license/616ea563-d56f-474d-8b8c-1f55b5cbec67/95b822af-5a32-48f8-9eaa-2ae06c41c56a>

1/4

The requesting person / organization to appear on the license Marie Hebert

REUSE CONTENT DETAILS

| | | | |
|-----------------------------------------------------------|--------------|--------------------------------------------------|---------------------------------------------------------|
| Title, description or numeric reference of the portion(s) | Figure 4 (c) | Title of the article/chapter the portion is from | Pillar-induced droplet merging in microfluidic circuits |
| Editor of portion(s) | N/A | Author of portion(s) | Royal Society of Chemistry (Great Britain) |
| Volume of serial or monograph | N/A | Issue, if republishing an article from a serial | N/A |
| Page or page range of portion | 1841 | Publication date of portion | 2008-10-08 |

CCC Republication Terms and Conditions

1. Description of Service; Defined Terms. This Republication License enables the User to obtain licenses for republication of one or more copyrighted works as described in detail on the relevant Order Confirmation (the "Work(s)"). Copyright Clearance Center, Inc. ("CCC") grants licenses through the Service on behalf of the rightsholder identified on the Order Confirmation (the "Rightsholder"). "Republishing", as used herein, generally means the inclusion of a Work, in whole or in part, in a new work or works, also as described on the Order Confirmation. "User", as used herein, means the person or entity making such republication.
2. The terms set forth in the relevant Order Confirmation, and any terms set by the Rightsholder with respect to a particular Work, govern the terms of use of Works in connection with the Service. By using the Service, the person transacting for a republication license on behalf of the User represents and warrants that he/she/it (a) has been duly authorized by the User to accept, and hereby does accept, all such terms and conditions on behalf of User, and (b) shall inform User of all such terms and conditions. In the event such person is a "freelancer" or other third party independent of User and CCC, such party shall be deemed jointly a "User" for purposes of these terms and conditions. In any event, User shall be deemed to have accepted and agreed to all such terms and conditions if User republishes the Work in any fashion.
3. Scope of License; Limitations and Obligations.
 - 3.1. All Works and all rights therein, including copyright rights, remain the sole and exclusive property of the Rightsholder. The license created by the exchange of an Order Confirmation (and/or any invoice) and payment by User of the full amount set forth on that document includes only those rights expressly set forth in the Order Confirmation and in these terms and conditions, and conveys no other rights in the Work(s) to User. All rights not expressly granted are hereby reserved.
 - 3.2. General Payment Terms: You may pay by credit card or through an account with us payable at the end of the month. If you and we agree that you may establish a standing account with CCC, then the following terms apply: Remit Payment to: Copyright Clearance Center, 29118 Network Place, Chicago, IL 60673-1291. Payments Due: Invoices are payable upon their delivery to you (or upon our notice to you that they are available to you for downloading). After 30 days, outstanding amounts will be subject to a service charge of 1-1/2% per month or, if less, the maximum rate allowed by applicable law. Unless otherwise specifically set forth in the Order Confirmation or in a separate written agreement signed by CCC, invoices are due and payable on "net 30" terms. While User may exercise the rights licensed immediately upon issuance of the Order Confirmation, the license is automatically revoked and is null and void, as if it had never been issued, if complete payment for the license is not received on a timely basis either from User directly or through a payment agent, such as a credit card company.
 - 3.3. Unless otherwise provided in the Order Confirmation, any grant of rights to User (i) is "one-time" (including

14/12/2020

<https://marketplace.copyright.com/rs-ui-web/mp/license/616ea563-d56f-474d-8b8c-1f55b5cbec67/95b822af-5a32-48f8-9eaa-2ae06c41...>

the editions and product family specified in the license), (ii) is non-exclusive and non-transferable and (iii) is subject to any and all limitations and restrictions (such as, but not limited to, limitations on duration of use or circulation) included in the Order Confirmation or invoice and/or in these terms and conditions. Upon completion of the licensed use, User shall either secure a new permission for further use of the Work(s) or immediately cease any new use of the Work(s) and shall render inaccessible (such as by deleting or by removing or severing links or other locators) any further copies of the Work (except for copies printed on paper in accordance with this license and still in User's stock at the end of such period).

- 3.4. In the event that the material for which a republication license is sought includes third party materials (such as photographs, illustrations, graphs, inserts and similar materials) which are identified in such material as having been used by permission, User is responsible for identifying, and seeking separate licenses (under this Service or otherwise) for, any of such third party materials; without a separate license, such third party materials may not be used.
- 3.5. Use of proper copyright notice for a Work is required as a condition of any license granted under the Service. Unless otherwise provided in the Order Confirmation, a proper copyright notice will read substantially as follows: "Republished with permission of [Rightsholder's name], from [Work's title, author, volume, edition number and year of copyright]; permission conveyed through Copyright Clearance Center, Inc. " Such notice must be provided in a reasonably legible font size and must be placed either immediately adjacent to the Work as used (for example, as part of a by-line or footnote but not as a separate electronic link) or in the place where substantially all other credits or notices for the new work containing the republished Work are located. Failure to include the required notice results in loss to the Rightsholder and CCC, and the User shall be liable to pay liquidated damages for each such failure equal to twice the use fee specified in the Order Confirmation, in addition to the use fee itself and any other fees and charges specified.
- 3.6. User may only make alterations to the Work if and as expressly set forth in the Order Confirmation. No Work may be used in any way that is defamatory, violates the rights of third parties (including such third parties' rights of copyright, privacy, publicity, or other tangible or intangible property), or is otherwise illegal, sexually explicit or obscene. In addition, User may not conjoin a Work with any other material that may result in damage to the reputation of the Rightsholder. User agrees to inform CCC if it becomes aware of any infringement of any rights in a Work and to cooperate with any reasonable request of CCC or the Rightsholder in connection therewith.
4. Indemnity. User hereby indemnifies and agrees to defend the Rightsholder and CCC, and their respective employees and directors, against all claims, liability, damages, costs and expenses, including legal fees and expenses, arising out of any use of a Work beyond the scope of the rights granted herein, or any use of a Work which has been altered in any unauthorized way by User, including claims of defamation or infringement of rights of copyright, publicity, privacy or other tangible or intangible property.
5. Limitation of Liability. UNDER NO CIRCUMSTANCES WILL CCC OR THE RIGHTSHOLDER BE LIABLE FOR ANY DIRECT, INDIRECT, CONSEQUENTIAL OR INCIDENTAL DAMAGES (INCLUDING WITHOUT LIMITATION DAMAGES FOR LOSS OF BUSINESS PROFITS OR INFORMATION, OR FOR BUSINESS INTERRUPTION) ARISING OUT OF THE USE OR INABILITY TO USE A WORK, EVEN IF ONE OF THEM HAS BEEN ADVISED OF THE POSSIBILITY OF SUCH DAMAGES. In any event, the total liability of the Rightsholder and CCC (including their respective employees and directors) shall not exceed the total amount actually paid by User for this license. User assumes full liability for the actions and omissions of its principals, employees, agents, affiliates, successors and assigns.
6. Limited Warranties. THE WORK(S) AND RIGHT(S) ARE PROVIDED "AS IS". CCC HAS THE RIGHT TO GRANT TO USER THE RIGHTS GRANTED IN THE ORDER CONFIRMATION DOCUMENT. CCC AND THE RIGHTSHOLDER DISCLAIM ALL OTHER WARRANTIES RELATING TO THE WORK(S) AND RIGHT(S), EITHER EXPRESS OR IMPLIED, INCLUDING WITHOUT LIMITATION IMPLIED WARRANTIES OF MERCHANTABILITY OR FITNESS FOR A PARTICULAR PURPOSE. ADDITIONAL RIGHTS MAY BE REQUIRED TO USE ILLUSTRATIONS, GRAPHS, PHOTOGRAPHS, ABSTRACTS, INSERTS OR OTHER PORTIONS OF THE WORK (AS OPPOSED TO THE ENTIRE WORK) IN A MANNER CONTEMPLATED BY USER; USER UNDERSTANDS AND AGREES THAT NEITHER CCC NOR THE RIGHTSHOLDER MAY HAVE SUCH ADDITIONAL RIGHTS TO GRANT.

<https://marketplace.copyright.com/rs-ui-web/mp/license/616ea563-d56f-474d-8b8c-1f55b5cbec67/95b822af-5a32-48f8-9eaa-2ae06c41c56a>

3/4

7. Effect of Breach. Any failure by User to pay any amount when due, or any use by User of a Work beyond the scope of the license set forth in the Order Confirmation and/or these terms and conditions, shall be a material breach of the license created by the Order Confirmation and these terms and conditions. Any breach not cured within 30 days of written notice thereof shall result in immediate termination of such license without further notice. Any unauthorized (but licensable) use of a Work that is terminated immediately upon notice thereof may be liquidated by payment of the Rightsholder's ordinary license price therefor; any unauthorized (and unlicensable) use that is not terminated immediately for any reason (including, for example, because materials containing the Work cannot reasonably be recalled) will be subject to all remedies available at law or in equity, but in no event to a payment of less than three times the Rightsholder's ordinary license price for the most closely analogous licensable use plus Rightsholder's and/or CCC's costs and expenses incurred in collecting such payment.

8. Miscellaneous.

8.1. User acknowledges that CCC may, from time to time, make changes or additions to the Service or to these terms and conditions, and CCC reserves the right to send notice to the User by electronic mail or otherwise for the purposes of notifying User of such changes or additions; provided that any such changes or additions shall not apply to permissions already secured and paid for.

8.2. Use of User-related information collected through the Service is governed by CCC's privacy policy, available online here: <https://marketplace.copyright.com/rs-ui-web/mp/privacy-policy>

8.3. The licensing transaction described in the Order Confirmation is personal to User. Therefore, User may not assign or transfer to any other person (whether a natural person or an organization of any kind) the license created by the Order Confirmation and these terms and conditions or any rights granted hereunder; provided, however, that User may assign such license in its entirety on written notice to CCC in the event of a transfer of all or substantially all of User's rights in the new material which includes the Work(s) licensed under this Service.

8.4. No amendment or waiver of any terms is binding unless set forth in writing and signed by the parties. The Rightsholder and CCC hereby object to any terms contained in any writing prepared by the User or its principals, employees, agents or affiliates and purporting to govern or otherwise relate to the licensing transaction described in the Order Confirmation, which terms are in any way inconsistent with any terms set forth in the Order Confirmation and/or in these terms and conditions or CCC's standard operating procedures, whether such writing is prepared prior to, simultaneously with or subsequent to the Order Confirmation, and whether such writing appears on a copy of the Order Confirmation or in a separate instrument.

8.5. The licensing transaction described in the Order Confirmation document shall be governed by and construed under the law of the State of New York, USA, without regard to the principles thereof of conflicts of law. Any case, controversy, suit, action, or proceeding arising out of, in connection with, or related to such licensing transaction shall be brought, at CCC's sole discretion, in any federal or state court located in the County of New York, State of New York, USA, or in any federal or state court whose geographical jurisdiction covers the location of the Rightsholder set forth in the Order Confirmation. The parties expressly submit to the personal jurisdiction and venue of each such federal or state court. If you have any comments or questions about the Service or Copyright Clearance Center, please contact us at 978-750-8400 or send an e-mail to support@copyright.com.

v 1.1

14/12/2020

<https://marketplace.copyright.com/rs-ui-web/mp/license/9ea51988-53a9-4fa3-b7da-bee76f3d5baf/04c0d42f-2497-453c-8996-01dfa13ee...>Copyright
Clearance
Center

Marketplace™

Royal Society of Chemistry - License Terms and Conditions

This is a License Agreement between Marie Hebert ("You") and Royal Society of Chemistry ("Publisher") provided by Copyright Clearance Center ("CCC"). The license consists of your order details, the terms and conditions provided by Royal Society of Chemistry, and the CCC terms and conditions.

All payments must be made in full to CCC.

| | | | |
|------------------|-------------|-------------|------------------------------------|
| Order Date | 11-Dec-2020 | Type of Use | Republish in a thesis/dissertation |
| Order license ID | 1083557-1 | Publisher | ROYAL SOCIETY OF CHEMISTRY |
| ISSN | 1473-0189 | Portion | Image/photo/illustration |

LICENSED CONTENT

| | | | |
|-------------------|--------------------------------------------|------------------|-------------------------------------------------------------|
| Publication Title | Lab on a chip | Country | United Kingdom of Great Britain and Northern Ireland |
| Author/Editor | Royal Society of Chemistry (Great Britain) | Rightsholder | Royal Society of Chemistry |
| Date | 01/01/2001 | Publication Type | e-Journal |
| Language | English | URL | http://www.rsc.org/loc |

REQUEST DETAILS

| | | | |
|-------------------------------------------|--------------------------|-----------------------------|----------------------------------|
| Portion Type | Image/photo/illustration | Distribution | Worldwide |
| Number of images / photos / illustrations | 1 | Translation | Original language of publication |
| Format (select all that apply) | Print, Electronic | Copies for the disabled? | No |
| Who will republish the content? | Academic institution | Minor editing privileges? | No |
| Duration of Use | Life of current edition | Incidental promotional use? | No |
| Lifetime Unit Quantity | Up to 499 | Currency | USD |
| Rights Requested | Main product | | |

NEW WORK DETAILS

| | | | |
|-----------------|----------------------------------------------------------------------------------|----------------------------|---------------------|
| Title | Expanding the droplet microfluidic community - towards a modular active platform | Institution name | Waterloo University |
| Instructor name | Marie Hebert | Expected presentation date | 2021-01-01 |

ADDITIONAL DETAILS

| | |
|------------------------|-----|
| Order reference number | N/A |
|------------------------|-----|

<https://marketplace.copyright.com/rs-ui-web/mp/license/9ea51988-53a9-4fa3-b7da-bee76f3d5baf/04c0d42f-2497-453c-8996-01dfa13ee35e>

1/4

The requesting person / organization to appear on the license Marie Hebert

REUSE CONTENT DETAILS

| | | | |
|-----------------------------------------------------------|----------|--------------------------------------------------|------------------------------------------------------------------|
| Title, description or numeric reference of the portion(s) | Figure 4 | Title of the article/chapter the portion is from | Fast on-demand droplet fusion using transient cavitation bubbles |
| Editor of portion(s) | N/A | Author of portion(s) | Royal Society of Chemistry (Great Britain) |
| Volume of serial or monograph | N/A | Issue, if republishing an article from a serial | N/A |
| Page or page range of portion | 1882 | Publication date of portion | 2011-04-12 |

CCC Republication Terms and Conditions

1. Description of Service; Defined Terms. This Republication License enables the User to obtain licenses for republication of one or more copyrighted works as described in detail on the relevant Order Confirmation (the "Work(s)"). Copyright Clearance Center, Inc. ("CCC") grants licenses through the Service on behalf of the rightsholder identified on the Order Confirmation (the "Rightsholder"). "Republishing", as used herein, generally means the inclusion of a Work, in whole or in part, in a new work or works, also as described on the Order Confirmation. "User", as used herein, means the person or entity making such republication.
2. The terms set forth in the relevant Order Confirmation, and any terms set by the Rightsholder with respect to a particular Work, govern the terms of use of Works in connection with the Service. By using the Service, the person transacting for a republication license on behalf of the User represents and warrants that he/she/it (a) has been duly authorized by the User to accept, and hereby does accept, all such terms and conditions on behalf of User, and (b) shall inform User of all such terms and conditions. In the event such person is a "freelancer" or other third party independent of User and CCC, such party shall be deemed jointly a "User" for purposes of these terms and conditions. In any event, User shall be deemed to have accepted and agreed to all such terms and conditions if User republishes the Work in any fashion.
3. Scope of License; Limitations and Obligations.
 - 3.1. All Works and all rights therein, including copyright rights, remain the sole and exclusive property of the Rightsholder. The license created by the exchange of an Order Confirmation (and/or any invoice) and payment by User of the full amount set forth on that document includes only those rights expressly set forth in the Order Confirmation and in these terms and conditions, and conveys no other rights in the Work(s) to User. All rights not expressly granted are hereby reserved.
 - 3.2. General Payment Terms: You may pay by credit card or through an account with us payable at the end of the month. If you and we agree that you may establish a standing account with CCC, then the following terms apply: Remit Payment to: Copyright Clearance Center, 29118 Network Place, Chicago, IL 60673-1291. Payments Due: Invoices are payable upon their delivery to you (or upon our notice to you that they are available to you for downloading). After 30 days, outstanding amounts will be subject to a service charge of 1-1/2% per month or, if less, the maximum rate allowed by applicable law. Unless otherwise specifically set forth in the Order Confirmation or in a separate written agreement signed by CCC, invoices are due and payable on "net 30" terms. While User may exercise the rights licensed immediately upon issuance of the Order Confirmation, the license is automatically revoked and is null and void, as if it had never been issued, if complete payment for the license is not received on a timely basis either from User directly or through a payment agent, such as a credit card company.
 - 3.3. Unless otherwise provided in the Order Confirmation, any grant of rights to User (i) is "one-time" (including

14/12/2020

<https://marketplace.copyright.com/rs-ui-web/mp/license/9ea51988-53a9-4fa3-b7da-bee76f3d5baf/04c0d42f-2497-453c-8996-01dfa13ee...>

the editions and product family specified in the license), (ii) is non-exclusive and non-transferable and (iii) is subject to any and all limitations and restrictions (such as, but not limited to, limitations on duration of use or circulation) included in the Order Confirmation or invoice and/or in these terms and conditions. Upon completion of the licensed use, User shall either secure a new permission for further use of the Work(s) or immediately cease any new use of the Work(s) and shall render inaccessible (such as by deleting or by removing or severing links or other locators) any further copies of the Work (except for copies printed on paper in accordance with this license and still in User's stock at the end of such period).

3.4. In the event that the material for which a republication license is sought includes third party materials (such as photographs, illustrations, graphs, inserts and similar materials) which are identified in such material as having been used by permission, User is responsible for identifying, and seeking separate licenses (under this Service or otherwise) for, any of such third party materials; without a separate license, such third party materials may not be used.

3.5. Use of proper copyright notice for a Work is required as a condition of any license granted under the Service. Unless otherwise provided in the Order Confirmation, a proper copyright notice will read substantially as follows: "Republished with permission of [Rightsholder's name], from [Work's title, author, volume, edition number and year of copyright]; permission conveyed through Copyright Clearance Center, Inc. " Such notice must be provided in a reasonably legible font size and must be placed either immediately adjacent to the Work as used (for example, as part of a by-line or footnote but not as a separate electronic link) or in the place where substantially all other credits or notices for the new work containing the republished Work are located. Failure to include the required notice results in loss to the Rightsholder and CCC, and the User shall be liable to pay liquidated damages for each such failure equal to twice the use fee specified in the Order Confirmation, in addition to the use fee itself and any other fees and charges specified.

3.6. User may only make alterations to the Work if and as expressly set forth in the Order Confirmation. No Work may be used in any way that is defamatory, violates the rights of third parties (including such third parties' rights of copyright, privacy, publicity, or other tangible or intangible property), or is otherwise illegal, sexually explicit or obscene. In addition, User may not conjoin a Work with any other material that may result in damage to the reputation of the Rightsholder. User agrees to inform CCC if it becomes aware of any infringement of any rights in a Work and to cooperate with any reasonable request of CCC or the Rightsholder in connection therewith.

4. Indemnity. User hereby indemnifies and agrees to defend the Rightsholder and CCC, and their respective employees and directors, against all claims, liability, damages, costs and expenses, including legal fees and expenses, arising out of any use of a Work beyond the scope of the rights granted herein, or any use of a Work which has been altered in any unauthorized way by User, including claims of defamation or infringement of rights of copyright, publicity, privacy or other tangible or intangible property.

5. Limitation of Liability. UNDER NO CIRCUMSTANCES WILL CCC OR THE RIGHTSHOLDER BE LIABLE FOR ANY DIRECT, INDIRECT, CONSEQUENTIAL OR INCIDENTAL DAMAGES (INCLUDING WITHOUT LIMITATION DAMAGES FOR LOSS OF BUSINESS PROFITS OR INFORMATION, OR FOR BUSINESS INTERRUPTION) ARISING OUT OF THE USE OR INABILITY TO USE A WORK, EVEN IF ONE OF THEM HAS BEEN ADVISED OF THE POSSIBILITY OF SUCH DAMAGES. In any event, the total liability of the Rightsholder and CCC (including their respective employees and directors) shall not exceed the total amount actually paid by User for this license. User assumes full liability for the actions and omissions of its principals, employees, agents, affiliates, successors and assigns.

6. Limited Warranties. THE WORK(S) AND RIGHT(S) ARE PROVIDED "AS IS". CCC HAS THE RIGHT TO GRANT TO USER THE RIGHTS GRANTED IN THE ORDER CONFIRMATION DOCUMENT. CCC AND THE RIGHTSHOLDER DISCLAIM ALL OTHER WARRANTIES RELATING TO THE WORK(S) AND RIGHT(S), EITHER EXPRESS OR IMPLIED, INCLUDING WITHOUT LIMITATION IMPLIED WARRANTIES OF MERCHANTABILITY OR FITNESS FOR A PARTICULAR PURPOSE. ADDITIONAL RIGHTS MAY BE REQUIRED TO USE ILLUSTRATIONS, GRAPHS, PHOTOGRAPHS, ABSTRACTS, INSERTS OR OTHER PORTIONS OF THE WORK (AS OPPOSED TO THE ENTIRE WORK) IN A MANNER CONTEMPLATED BY USER; USER UNDERSTANDS AND AGREES THAT NEITHER CCC NOR THE RIGHTSHOLDER MAY HAVE SUCH ADDITIONAL RIGHTS TO GRANT.

<https://marketplace.copyright.com/rs-ui-web/mp/license/9ea51988-53a9-4fa3-b7da-bee76f3d5baf/04c0d42f-2497-453c-8996-01dfa13ee35e>

3/4

7. Effect of Breach. Any failure by User to pay any amount when due, or any use by User of a Work beyond the scope of the license set forth in the Order Confirmation and/or these terms and conditions, shall be a material breach of the license created by the Order Confirmation and these terms and conditions. Any breach not cured within 30 days of written notice thereof shall result in immediate termination of such license without further notice. Any unauthorized (but licensable) use of a Work that is terminated immediately upon notice thereof may be liquidated by payment of the Rightsholder's ordinary license price therefor; any unauthorized (and unlicensable) use that is not terminated immediately for any reason (including, for example, because materials containing the Work cannot reasonably be recalled) will be subject to all remedies available at law or in equity, but in no event to a payment of less than three times the Rightsholder's ordinary license price for the most closely analogous licensable use plus Rightsholder's and/or CCC's costs and expenses incurred in collecting such payment.

8. Miscellaneous.

8.1. User acknowledges that CCC may, from time to time, make changes or additions to the Service or to these terms and conditions, and CCC reserves the right to send notice to the User by electronic mail or otherwise for the purposes of notifying User of such changes or additions; provided that any such changes or additions shall not apply to permissions already secured and paid for.

8.2. Use of User-related information collected through the Service is governed by CCC's privacy policy, available online here:<https://marketplace.copyright.com/rs-ui-web/mp/privacy-policy>

8.3. The licensing transaction described in the Order Confirmation is personal to User. Therefore, User may not assign or transfer to any other person (whether a natural person or an organization of any kind) the license created by the Order Confirmation and these terms and conditions or any rights granted hereunder; provided, however, that User may assign such license in its entirety on written notice to CCC in the event of a transfer of all or substantially all of User's rights in the new material which includes the Work(s) licensed under this Service.

8.4. No amendment or waiver of any terms is binding unless set forth in writing and signed by the parties. The Rightsholder and CCC hereby object to any terms contained in any writing prepared by the User or its principals, employees, agents or affiliates and purporting to govern or otherwise relate to the licensing transaction described in the Order Confirmation, which terms are in any way inconsistent with any terms set forth in the Order Confirmation and/or in these terms and conditions or CCC's standard operating procedures, whether such writing is prepared prior to, simultaneously with or subsequent to the Order Confirmation, and whether such writing appears on a copy of the Order Confirmation or in a separate instrument.

8.5. The licensing transaction described in the Order Confirmation document shall be governed by and construed under the law of the State of New York, USA, without regard to the principles thereof of conflicts of law. Any case, controversy, suit, action, or proceeding arising out of, in connection with, or related to such licensing transaction shall be brought, at CCC's sole discretion, in any federal or state court located in the County of New York, State of New York, USA, or in any federal or state court whose geographical jurisdiction covers the location of the Rightsholder set forth in the Order Confirmation. The parties expressly submit to the personal jurisdiction and venue of each such federal or state court. If you have any comments or questions about the Service or Copyright Clearance Center, please contact us at 978-750-8400 or send an e-mail to support@copyright.com.

v 1.1

14/12/2020

<https://marketplace.copyright.com/rs-ui-web/mp/license/9e585076-8d98-415b-b6a4-1649abdfa8a4/5ae47617-27da-4b53-b6d3-a7f46ae...>

Marketplace™

Royal Society of Chemistry - License Terms and Conditions

This is a License Agreement between Marie Hebert ("You") and Royal Society of Chemistry ("Publisher") provided by Copyright Clearance Center ("CCC"). The license consists of your order details, the terms and conditions provided by Royal Society of Chemistry, and the CCC terms and conditions.

All payments must be made in full to CCC.

| | | | |
|------------------|-------------|-------------|------------------------------------|
| Order Date | 11-Dec-2020 | Type of Use | Republish in a thesis/dissertation |
| Order license ID | 1083558-1 | Publisher | ROYAL SOCIETY OF CHEMISTRY |
| ISSN | 1473-0189 | Portion | Image/photo/illustration |

LICENSED CONTENT

| | | | |
|-------------------|--------------------------------------------|------------------|-------------------------------------------------------------|
| Publication Title | Lab on a chip | Country | United Kingdom of Great Britain and Northern Ireland |
| Author/Editor | Royal Society of Chemistry (Great Britain) | Rightsholder | Royal Society of Chemistry |
| Date | 01/01/2001 | Publication Type | e-Journal |
| Language | English | URL | http://www.rsc.org/loc |

REQUEST DETAILS

| | | | |
|-------------------------------------------|--------------------------|-----------------------------|----------------------------------|
| Portion Type | Image/photo/illustration | Distribution | Worldwide |
| Number of images / photos / illustrations | 1 | Translation | Original language of publication |
| Format (select all that apply) | Print, Electronic | Copies for the disabled? | No |
| Who will republish the content? | Academic institution | Minor editing privileges? | No |
| Duration of Use | Life of current edition | Incidental promotional use? | No |
| Lifetime Unit Quantity | Up to 499 | Currency | USD |
| Rights Requested | Main product | | |

NEW WORK DETAILS

| | | | |
|-----------------|----------------------------------------------------------------------------------|----------------------------|---------------------|
| Title | Expanding the droplet microfluidic community - towards a modular active platform | Institution name | Waterloo University |
| Instructor name | Marie Hebert | Expected presentation date | 2021-01-01 |

ADDITIONAL DETAILS

| | |
|------------------------|-----|
| Order reference number | N/A |
|------------------------|-----|

<https://marketplace.copyright.com/rs-ui-web/mp/license/9e585076-8d98-415b-b6a4-1649abdfa8a4/5ae47617-27da-4b53-b6d3-a7f46ae2e28d>

1/4

The requesting person / organization to appear on the license Marie Hebert

REUSE CONTENT DETAILS

| | | | |
|-----------------------------------------------------------|----------|--------------------------------------------------|---------------------------------------------------------------------|
| Title, description or numeric reference of the portion(s) | Figure 1 | Title of the article/chapter the portion is from | Microfluidic on-demand droplet merging using surface acoustic waves |
| Editor of portion(s) | N/A | Author of portion(s) | Royal Society of Chemistry (Great Britain) |
| Volume of serial or monograph | N/A | Issue, if republishing an article from a serial | N/A |
| Page or page range of portion | 3326 | Publication date of portion | 2014-06-23 |

CCC Republication Terms and Conditions

1. Description of Service; Defined Terms. This Republication License enables the User to obtain licenses for republication of one or more copyrighted works as described in detail on the relevant Order Confirmation (the "Work(s)"). Copyright Clearance Center, Inc. ("CCC") grants licenses through the Service on behalf of the rightsholder identified on the Order Confirmation (the "Rightsholder"). "Republishing", as used herein, generally means the inclusion of a Work, in whole or in part, in a new work or works, also as described on the Order Confirmation. "User", as used herein, means the person or entity making such republication.
2. The terms set forth in the relevant Order Confirmation, and any terms set by the Rightsholder with respect to a particular Work, govern the terms of use of Works in connection with the Service. By using the Service, the person transacting for a republication license on behalf of the User represents and warrants that he/she/it (a) has been duly authorized by the User to accept, and hereby does accept, all such terms and conditions on behalf of User, and (b) shall inform User of all such terms and conditions. In the event such person is a "freelancer" or other third party independent of User and CCC, such party shall be deemed jointly a "User" for purposes of these terms and conditions. In any event, User shall be deemed to have accepted and agreed to all such terms and conditions if User republishes the Work in any fashion.
3. Scope of License; Limitations and Obligations.
 - 3.1. All Works and all rights therein, including copyright rights, remain the sole and exclusive property of the Rightsholder. The license created by the exchange of an Order Confirmation (and/or any invoice) and payment by User of the full amount set forth on that document includes only those rights expressly set forth in the Order Confirmation and in these terms and conditions, and conveys no other rights in the Work(s) to User. All rights not expressly granted are hereby reserved.
 - 3.2. General Payment Terms: You may pay by credit card or through an account with us payable at the end of the month. If you and we agree that you may establish a standing account with CCC, then the following terms apply: Remit Payment to: Copyright Clearance Center, 29118 Network Place, Chicago, IL 60673-1291. Payments Due: Invoices are payable upon their delivery to you (or upon our notice to you that they are available to you for downloading). After 30 days, outstanding amounts will be subject to a service charge of 1-1/2% per month or, if less, the maximum rate allowed by applicable law. Unless otherwise specifically set forth in the Order Confirmation or in a separate written agreement signed by CCC, invoices are due and payable on "net 30" terms. While User may exercise the rights licensed immediately upon issuance of the Order Confirmation, the license is automatically revoked and is null and void, as if it had never been issued, if complete payment for the license is not received on a timely basis either from User directly or through a payment agent, such as a credit card company.
 - 3.3. Unless otherwise provided in the Order Confirmation, any grant of rights to User (i) is "one-time" (including

14/12/2020

<https://marketplace.copyright.com/rs-ui-web/mp/license/9e585076-8d98-415b-b6a4-1649abdfa8a4/5ae47617-27da-4b53-b6d3-a7f46ae...>

the editions and product family specified in the license), (ii) is non-exclusive and non-transferable and (iii) is subject to any and all limitations and restrictions (such as, but not limited to, limitations on duration of use or circulation) included in the Order Confirmation or invoice and/or in these terms and conditions. Upon completion of the licensed use, User shall either secure a new permission for further use of the Work(s) or immediately cease any new use of the Work(s) and shall render inaccessible (such as by deleting or by removing or severing links or other locators) any further copies of the Work (except for copies printed on paper in accordance with this license and still in User's stock at the end of such period).

3.4. In the event that the material for which a republication license is sought includes third party materials (such as photographs, illustrations, graphs, inserts and similar materials) which are identified in such material as having been used by permission, User is responsible for identifying, and seeking separate licenses (under this Service or otherwise) for, any of such third party materials; without a separate license, such third party materials may not be used.

3.5. Use of proper copyright notice for a Work is required as a condition of any license granted under the Service. Unless otherwise provided in the Order Confirmation, a proper copyright notice will read substantially as follows: "Republished with permission of [Rightsholder's name], from [Work's title, author, volume, edition number and year of copyright]; permission conveyed through Copyright Clearance Center, Inc. " Such notice must be provided in a reasonably legible font size and must be placed either immediately adjacent to the Work as used (for example, as part of a by-line or footnote but not as a separate electronic link) or in the place where substantially all other credits or notices for the new work containing the republished Work are located. Failure to include the required notice results in loss to the Rightsholder and CCC, and the User shall be liable to pay liquidated damages for each such failure equal to twice the use fee specified in the Order Confirmation, in addition to the use fee itself and any other fees and charges specified.

3.6. User may only make alterations to the Work if and as expressly set forth in the Order Confirmation. No Work may be used in any way that is defamatory, violates the rights of third parties (including such third parties' rights of copyright, privacy, publicity, or other tangible or intangible property), or is otherwise illegal, sexually explicit or obscene. In addition, User may not conjoin a Work with any other material that may result in damage to the reputation of the Rightsholder. User agrees to inform CCC if it becomes aware of any infringement of any rights in a Work and to cooperate with any reasonable request of CCC or the Rightsholder in connection therewith.

4. Indemnity. User hereby indemnifies and agrees to defend the Rightsholder and CCC, and their respective employees and directors, against all claims, liability, damages, costs and expenses, including legal fees and expenses, arising out of any use of a Work beyond the scope of the rights granted herein, or any use of a Work which has been altered in any unauthorized way by User, including claims of defamation or infringement of rights of copyright, publicity, privacy or other tangible or intangible property.

5. Limitation of Liability. UNDER NO CIRCUMSTANCES WILL CCC OR THE RIGHTSHOLDER BE LIABLE FOR ANY DIRECT, INDIRECT, CONSEQUENTIAL OR INCIDENTAL DAMAGES (INCLUDING WITHOUT LIMITATION DAMAGES FOR LOSS OF BUSINESS PROFITS OR INFORMATION, OR FOR BUSINESS INTERRUPTION) ARISING OUT OF THE USE OR INABILITY TO USE A WORK, EVEN IF ONE OF THEM HAS BEEN ADVISED OF THE POSSIBILITY OF SUCH DAMAGES. In any event, the total liability of the Rightsholder and CCC (including their respective employees and directors) shall not exceed the total amount actually paid by User for this license. User assumes full liability for the actions and omissions of its principals, employees, agents, affiliates, successors and assigns.

6. Limited Warranties. THE WORK(S) AND RIGHT(S) ARE PROVIDED "AS IS". CCC HAS THE RIGHT TO GRANT TO USER THE RIGHTS GRANTED IN THE ORDER CONFIRMATION DOCUMENT. CCC AND THE RIGHTSHOLDER DISCLAIM ALL OTHER WARRANTIES RELATING TO THE WORK(S) AND RIGHT(S), EITHER EXPRESS OR IMPLIED, INCLUDING WITHOUT LIMITATION IMPLIED WARRANTIES OF MERCHANTABILITY OR FITNESS FOR A PARTICULAR PURPOSE. ADDITIONAL RIGHTS MAY BE REQUIRED TO USE ILLUSTRATIONS, GRAPHS, PHOTOGRAPHS, ABSTRACTS, INSERTS OR OTHER PORTIONS OF THE WORK (AS OPPOSED TO THE ENTIRE WORK) IN A MANNER CONTEMPLATED BY USER; USER UNDERSTANDS AND AGREES THAT NEITHER CCC NOR THE RIGHTSHOLDER MAY HAVE SUCH ADDITIONAL RIGHTS TO GRANT.

<https://marketplace.copyright.com/rs-ui-web/mp/license/9e585076-8d98-415b-b6a4-1649abdfa8a4/5ae47617-27da-4b53-b6d3-a7f46ae2e28d>

3/4

7. Effect of Breach. Any failure by User to pay any amount when due, or any use by User of a Work beyond the scope of the license set forth in the Order Confirmation and/or these terms and conditions, shall be a material breach of the license created by the Order Confirmation and these terms and conditions. Any breach not cured within 30 days of written notice thereof shall result in immediate termination of such license without further notice. Any unauthorized (but licensable) use of a Work that is terminated immediately upon notice thereof may be liquidated by payment of the Rightsholder's ordinary license price therefor; any unauthorized (and unlicensable) use that is not terminated immediately for any reason (including, for example, because materials containing the Work cannot reasonably be recalled) will be subject to all remedies available at law or in equity, but in no event to a payment of less than three times the Rightsholder's ordinary license price for the most closely analogous licensable use plus Rightsholder's and/or CCC's costs and expenses incurred in collecting such payment.

8. Miscellaneous.

- 8.1. User acknowledges that CCC may, from time to time, make changes or additions to the Service or to these terms and conditions, and CCC reserves the right to send notice to the User by electronic mail or otherwise for the purposes of notifying User of such changes or additions; provided that any such changes or additions shall not apply to permissions already secured and paid for.
- 8.2. Use of User-related information collected through the Service is governed by CCC's privacy policy, available online here:<https://marketplace.copyright.com/rs-ui-web/mp/privacy-policy>
- 8.3. The licensing transaction described in the Order Confirmation is personal to User. Therefore, User may not assign or transfer to any other person (whether a natural person or an organization of any kind) the license created by the Order Confirmation and these terms and conditions or any rights granted hereunder; provided, however, that User may assign such license in its entirety on written notice to CCC in the event of a transfer of all or substantially all of User's rights in the new material which includes the Work(s) licensed under this Service.
- 8.4. No amendment or waiver of any terms is binding unless set forth in writing and signed by the parties. The Rightsholder and CCC hereby object to any terms contained in any writing prepared by the User or its principals, employees, agents or affiliates and purporting to govern or otherwise relate to the licensing transaction described in the Order Confirmation, which terms are in any way inconsistent with any terms set forth in the Order Confirmation and/or in these terms and conditions or CCC's standard operating procedures, whether such writing is prepared prior to, simultaneously with or subsequent to the Order Confirmation, and whether such writing appears on a copy of the Order Confirmation or in a separate instrument.
- 8.5. The licensing transaction described in the Order Confirmation document shall be governed by and construed under the law of the State of New York, USA, without regard to the principles thereof of conflicts of law. Any case, controversy, suit, action, or proceeding arising out of, in connection with, or related to such licensing transaction shall be brought, at CCC's sole discretion, in any federal or state court located in the County of New York, State of New York, USA, or in any federal or state court whose geographical jurisdiction covers the location of the Rightsholder set forth in the Order Confirmation. The parties expressly submit to the personal jurisdiction and venue of each such federal or state court. If you have any comments or questions about the Service or Copyright Clearance Center, please contact us at 978-750-8400 or send an e-mail to support@copyright.com.

v 1.1

Copyright
Clearance
Center

Marketplace™

The Royal Society (U.K.) - License Terms and Conditions

This is a License Agreement between Marie Hebert ("You") and The Royal Society (U.K.) ("Publisher") provided by Copyright Clearance Center ("CCC"). The license consists of your order details, the terms and conditions provided by The Royal Society (U.K.), and the CCC terms and conditions.

All payments must be made in full to CCC.

| | | | |
|------------------|-------------|-------------------|----------------------------------------|
| Order Date | 11-Dec-2020 | Type of Use | Republish in a thesis/dissertation |
| Order license ID | 1083559-1 | Publisher Portion | ROYAL SOCIETY Image/photo/illustration |
| ISSN | 1471-2962 | | |

LICENSED CONTENT

| | | | |
|-------------------|----------------------------------------------------------------------------------------------------------------------|------------------|-------------------------------------------------------------------------------------|
| Publication Title | Philosophical Transactions of the Royal Society of London. Series A: Mathematical, Physical and Engineering Sciences | Country | United Kingdom of Great Britain and Northern Ireland |
| Author/Editor | Royal Society | Rightsholder | The Royal Society (U.K.) |
| Date | 01/01/1997 | Publication Type | e-Journal |
| Language | English | URL | https://royalsociety.org/journals/ |

REQUEST DETAILS

| | | | |
|-------------------------------------------|-----------------------------------------|-----------------------------|----------------------------------|
| Portion Type | Image/photo/illustration | Distribution | Worldwide |
| Number of images / photos / illustrations | 1 | Translation | Original language of publication |
| Format (select all that apply) | Print, Electronic | Copies for the disabled? | No |
| Who will republish the content? | Academic institution | Minor editing privileges? | No |
| Duration of Use | Life of current and all future editions | Incidental promotional use? | No |
| Lifetime Unit Quantity | Up to 499 | Currency | USD |
| Rights Requested | Main product | | |

NEW WORK DETAILS

| | | | |
|-----------------|----------------------------------------------------------------------------------|----------------------------|---------------------|
| Title | Expanding the droplet microfluidic community - towards a modular active platform | Institution name | Waterloo University |
| Instructor name | Marie Hebert | Expected presentation date | 2021-01-01 |

ADDITIONAL DETAILS

| | | | |
|------------------------|-----|---------------------------------------------------------------|--------------|
| Order reference number | N/A | The requesting person / organization to appear on the license | Marie Hebert |
|------------------------|-----|---------------------------------------------------------------|--------------|

REUSE CONTENT DETAILS

| | | | |
|-----------------------------------------------------------|--------------|--------------------------------------------------|------------------------------------------------------------------------------------|
| Title, description or numeric reference of the portion(s) | Figure 5 (b) | Title of the article/chapter the portion is from | Microfluidic systems for chemical kinetics that rely on chaotic mixing in droplets |
| Editor of portion(s) | N/A | Author of portion(s) | Royal Society |
| Volume of serial or monograph | N/A | Issue, if republishing an article from a serial | N/A |
| Page or page range of portion | 1095 | Publication date of portion | 2004-03-18 |

PUBLISHER TERMS AND CONDITIONS

Out of Copyright - any journal requested with a Publication date older than 70 years.

CCC Republication Terms and Conditions

1. Description of Service; Defined Terms. This Republication License enables the User to obtain licenses for republication of one or more copyrighted works as described in detail on the relevant Order Confirmation (the "Work(s)"). Copyright Clearance Center, Inc. ("CCC") grants licenses through the Service on behalf of the rightsholder identified on the Order Confirmation (the "Rightsholder"). "Republishing", as used herein, generally means the inclusion of a Work, in whole or in part, in a new work or works, also as described on the Order Confirmation. "User", as used herein, means the person or entity making such republication.
2. The terms set forth in the relevant Order Confirmation, and any terms set by the Rightsholder with respect to a particular Work, govern the terms of use of Works in connection with the Service. By using the Service, the person transacting for a republication license on behalf of the User represents and warrants that he/she/it (a) has been duly authorized by the User to accept, and hereby does accept, all such terms and conditions on behalf of User, and (b) shall inform User of all such terms and conditions. In the event such person is a "freelancer" or other third party independent of User and CCC, such party shall be deemed jointly a "User" for purposes of these terms and conditions. In any event, User shall be deemed to have accepted and agreed to all such terms and conditions if User republishes the Work in any fashion.
3. Scope of License; Limitations and Obligations.
 - 3.1. All Works and all rights therein, including copyright rights, remain the sole and exclusive property of the Rightsholder. The license created by the exchange of an Order Confirmation (and/or any invoice) and payment by User of the full amount set forth on that document includes only those rights expressly set forth in the Order Confirmation and in these terms and conditions, and conveys no other rights in the Work(s) to User. All rights not expressly granted are hereby reserved.
 - 3.2. General Payment Terms: You may pay by credit card or through an account with us payable at the end of the month. If you and we agree that you may establish a standing account with CCC, then the following terms apply: Remit Payment to: Copyright Clearance Center, 29118 Network Place, Chicago, IL 60673-1291. Payments Due: Invoices are payable upon their delivery to you (or upon our notice to you that they are available to you for downloading). After 30 days, outstanding amounts will be subject to a service charge of 1-1/2% per month or, if less, the maximum rate allowed by applicable law. Unless otherwise specifically set forth in the Order Confirmation or in a separate written agreement signed by CCC, invoices are due and payable on "net 30" terms. While User may exercise the rights licensed immediately upon issuance of the Order Confirmation, the license is automatically revoked and is null and void, as if it had never been

14/12/2020

<https://marketplace.copyright.com/rs-ui-web/mp/license/86b394f9-e74f-4fba-8908-2d54d5e52b22/6d1e3a79-5b0b-4981-ab9e-79dcaef...>

issued, if complete payment for the license is not received on a timely basis either from User directly or through a payment agent, such as a credit card company.

- 3.3. Unless otherwise provided in the Order Confirmation, any grant of rights to User (i) is "one-time" (including the editions and product family specified in the license), (ii) is non-exclusive and non-transferable and (iii) is subject to any and all limitations and restrictions (such as, but not limited to, limitations on duration of use or circulation) included in the Order Confirmation or invoice and/or in these terms and conditions. Upon completion of the licensed use, User shall either secure a new permission for further use of the Work(s) or immediately cease any new use of the Work(s) and shall render inaccessible (such as by deleting or by removing or severing links or other locators) any further copies of the Work (except for copies printed on paper in accordance with this license and still in User's stock at the end of such period).
- 3.4. In the event that the material for which a republication license is sought includes third party materials (such as photographs, illustrations, graphs, inserts and similar materials) which are identified in such material as having been used by permission, User is responsible for identifying, and seeking separate licenses (under this Service or otherwise) for, any of such third party materials; without a separate license, such third party materials may not be used.
- 3.5. Use of proper copyright notice for a Work is required as a condition of any license granted under the Service. Unless otherwise provided in the Order Confirmation, a proper copyright notice will read substantially as follows: "Republished with permission of [Rightsholder's name], from [Work's title, author, volume, edition number and year of copyright]; permission conveyed through Copyright Clearance Center, Inc. " Such notice must be provided in a reasonably legible font size and must be placed either immediately adjacent to the Work as used (for example, as part of a by-line or footnote but not as a separate electronic link) or in the place where substantially all other credits or notices for the new work containing the republished Work are located. Failure to include the required notice results in loss to the Rightsholder and CCC, and the User shall be liable to pay liquidated damages for each such failure equal to twice the use fee specified in the Order Confirmation, in addition to the use fee itself and any other fees and charges specified.
- 3.6. User may only make alterations to the Work if and as expressly set forth in the Order Confirmation. No Work may be used in any way that is defamatory, violates the rights of third parties (including such third parties' rights of copyright, privacy, publicity, or other tangible or intangible property), or is otherwise illegal, sexually explicit or obscene. In addition, User may not conjoin a Work with any other material that may result in damage to the reputation of the Rightsholder. User agrees to inform CCC if it becomes aware of any infringement of any rights in a Work and to cooperate with any reasonable request of CCC or the Rightsholder in connection therewith.
4. Indemnity. User hereby indemnifies and agrees to defend the Rightsholder and CCC, and their respective employees and directors, against all claims, liability, damages, costs and expenses, including legal fees and expenses, arising out of any use of a Work beyond the scope of the rights granted herein, or any use of a Work which has been altered in any unauthorized way by User, including claims of defamation or infringement of rights of copyright, publicity, privacy or other tangible or intangible property.
5. Limitation of Liability. UNDER NO CIRCUMSTANCES WILL CCC OR THE RIGHTSHOLDER BE LIABLE FOR ANY DIRECT, INDIRECT, CONSEQUENTIAL OR INCIDENTAL DAMAGES (INCLUDING WITHOUT LIMITATION DAMAGES FOR LOSS OF BUSINESS PROFITS OR INFORMATION, OR FOR BUSINESS INTERRUPTION) ARISING OUT OF THE USE OR INABILITY TO USE A WORK, EVEN IF ONE OF THEM HAS BEEN ADVISED OF THE POSSIBILITY OF SUCH DAMAGES. In any event, the total liability of the Rightsholder and CCC (including their respective employees and directors) shall not exceed the total amount actually paid by User for this license. User assumes full liability for the actions and omissions of its principals, employees, agents, affiliates, successors and assigns.
6. Limited Warranties. THE WORK(S) AND RIGHT(S) ARE PROVIDED "AS IS". CCC HAS THE RIGHT TO GRANT TO USER THE RIGHTS GRANTED IN THE ORDER CONFIRMATION DOCUMENT. CCC AND THE RIGHTSHOLDER DISCLAIM ALL OTHER WARRANTIES RELATING TO THE WORK(S) AND RIGHT(S), EITHER EXPRESS OR IMPLIED, INCLUDING

<https://marketplace.copyright.com/rs-ui-web/mp/license/86b394f9-e74f-4fba-8908-2d54d5e52b22/6d1e3a79-5b0b-4981-ab9e-79dcaefa58d>

3/4

14/12/2020

<https://marketplace.copyright.com/rs-ui-web/mp/license/86b394f9-e74f-4fba-8908-2d54d5e52b22/6d1e3a79-5b0b-4981-ab9e-79dcaef...>

WITHOUT LIMITATION IMPLIED WARRANTIES OF MERCHANTABILITY OR FITNESS FOR A PARTICULAR PURPOSE. ADDITIONAL RIGHTS MAY BE REQUIRED TO USE ILLUSTRATIONS, GRAPHS, PHOTOGRAPHS, ABSTRACTS, INSERTS OR OTHER PORTIONS OF THE WORK (AS OPPOSED TO THE ENTIRE WORK) IN A MANNER CONTEMPLATED BY USER; USER UNDERSTANDS AND AGREES THAT NEITHER CCC NOR THE RIGHTSHOLDER MAY HAVE SUCH ADDITIONAL RIGHTS TO GRANT.

7. Effect of Breach. Any failure by User to pay any amount when due, or any use by User of a Work beyond the scope of the license set forth in the Order Confirmation and/or these terms and conditions, shall be a material breach of the license created by the Order Confirmation and these terms and conditions. Any breach not cured within 30 days of written notice thereof shall result in immediate termination of such license without further notice. Any unauthorized (but licensable) use of a Work that is terminated immediately upon notice thereof may be liquidated by payment of the Rightsholder's ordinary license price therefor; any unauthorized (and unlicensable) use that is not terminated immediately for any reason (including, for example, because materials containing the Work cannot reasonably be recalled) will be subject to all remedies available at law or in equity, but in no event to a payment of less than three times the Rightsholder's ordinary license price for the most closely analogous licensable use plus Rightsholder's and/or CCC's costs and expenses incurred in collecting such payment.

8. Miscellaneous.

8.1. User acknowledges that CCC may, from time to time, make changes or additions to the Service or to these terms and conditions, and CCC reserves the right to send notice to the User by electronic mail or otherwise for the purposes of notifying User of such changes or additions; provided that any such changes or additions shall not apply to permissions already secured and paid for.

8.2. Use of User-related information collected through the Service is governed by CCC's privacy policy, available online here:<https://marketplace.copyright.com/rs-ui-web/mp/privacy-policy>

8.3. The licensing transaction described in the Order Confirmation is personal to User. Therefore, User may not assign or transfer to any other person (whether a natural person or an organization of any kind) the license created by the Order Confirmation and these terms and conditions or any rights granted hereunder; provided, however, that User may assign such license in its entirety on written notice to CCC in the event of a transfer of all or substantially all of User's rights in the new material which includes the Work(s) licensed under this Service.

8.4. No amendment or waiver of any terms is binding unless set forth in writing and signed by the parties. The Rightsholder and CCC hereby object to any terms contained in any writing prepared by the User or its principals, employees, agents or affiliates and purporting to govern or otherwise relate to the licensing transaction described in the Order Confirmation, which terms are in any way inconsistent with any terms set forth in the Order Confirmation and/or in these terms and conditions or CCC's standard operating procedures, whether such writing is prepared prior to, simultaneously with or subsequent to the Order Confirmation, and whether such writing appears on a copy of the Order Confirmation or in a separate instrument.

8.5. The licensing transaction described in the Order Confirmation document shall be governed by and construed under the law of the State of New York, USA, without regard to the principles thereof of conflicts of law. Any case, controversy, suit, action, or proceeding arising out of, in connection with, or related to such licensing transaction shall be brought, at CCC's sole discretion, in any federal or state court located in the County of New York, State of New York, USA, or in any federal or state court whose geographical jurisdiction covers the location of the Rightsholder set forth in the Order Confirmation. The parties expressly submit to the personal jurisdiction and venue of each such federal or state court. If you have any comments or questions about the Service or Copyright Clearance Center, please contact us at 978-750-8400 or send an e-mail to support@copyright.com.

v 1.1

<https://marketplace.copyright.com/rs-ui-web/mp/license/86b394f9-e74f-4fba-8908-2d54d5e52b22/6d1e3a79-5b0b-4981-ab9e-79dcaefa58d>

4/4

14/12/2020

<https://marketplace.copyright.com/rs-ui-web/mp/license/0fa469ab-2038-4cd3-a39d-8425c6355a1e/0b6506b3-4d38-4119-b43d-76b2b23...>

Marketplace™

IOP Publishing, Ltd - License Terms and Conditions

This is a License Agreement between Marie Hebert ("You") and IOP Publishing, Ltd ("Publisher") provided by Copyright Clearance Center ("CCC"). The license consists of your order details, the terms and conditions provided by IOP Publishing, Ltd, and the CCC terms and conditions.

All payments must be made in full to CCC.

| | | | |
|------------------|-------------|-------------|------------------------------------|
| Order Date | 11-Dec-2020 | Type of Use | Republish in a thesis/dissertation |
| Order license ID | 1083562-1 | Publisher | INSTITUTE OF PHYSICS PUBLISHING |
| ISSN | 0960-1317 | Portion | Image/photo/illustration |

LICENSED CONTENT

| | | | |
|-------------------|-----------------------------------------------------------------------------------|------------------|------------------------------------------------------|
| Publication Title | Journal of micromechanics and microengineering : structures, devices, and systems | Country | United Kingdom of Great Britain and Northern Ireland |
| Author/Editor | Institute of Physics (Great Britain) | Rightholder | IOP Publishing, Ltd |
| Date | 01/01/1991 | Publication Type | Journal |
| Language | English | | |

REQUEST DETAILS

| | | | |
|-------------------------------------------|-----------------------------------------|-----------------------------|----------------------------------|
| Portion Type | Image/photo/illustration | Distribution | Worldwide |
| Number of images / photos / illustrations | 1 | Translation | Original language of publication |
| Format (select all that apply) | Print, Electronic | Copies for the disabled? | No |
| Who will republish the content? | Academic institution | Minor editing privileges? | No |
| Duration of Use | Life of current and all future editions | Incidental promotional use? | No |
| Lifetime Unit Quantity | Up to 499 | Currency | USD |
| Rights Requested | Main product | | |

NEW WORK DETAILS

| | | | |
|-----------------|----------------------------------------------------------------------------------|----------------------------|---------------------|
| Title | Expanding the droplet microfluidic community - towards a modular active platform | Institution name | Waterloo University |
| Instructor name | Marie Hebert | Expected presentation date | 2021-01-01 |

ADDITIONAL DETAILS

<https://marketplace.copyright.com/rs-ui-web/mp/license/0fa469ab-2038-4cd3-a39d-8425c6355a1e/0b6506b3-4d38-4119-b43d-76b2b23e475e>

1/5

| | | | |
|------------------------|-----|---------------------------------------------------------------|--------------|
| Order reference number | N/A | The requesting person / organization to appear on the license | Marie Hebert |
|------------------------|-----|---------------------------------------------------------------|--------------|

REUSE CONTENT DETAILS

| | | | |
|-----------------------------------------------------------|--------------|--------------------------------------------------|-----------------------------------------------------------------------|
| Title, description or numeric reference of the portion(s) | Figure 1 (a) | Title of the article/chapter the portion is from | Active micro-mixers using surface acoustic waves on Y-cut 128° LiNbO3 |
| Editor of portion(s) | N/A | Author of portion(s) | Institute of Physics (Great Britain) |
| Volume of serial or monograph | N/A | Issue, if republishing an article from a serial | N/A |
| Page or page range of portion | 540 | Publication date of portion | 2006-02-06 |

PUBLISHER TERMS AND CONDITIONS

These special terms and conditions are in addition to the standard terms and conditions for CCC's Reproduction Service and, together with those standard terms and conditions, govern the use of the Works. As the User you will make all reasonable efforts to contact the author(s) of the article which the Work is to be reused from, to seek consent for your intended use. Contacting one author who is acting expressly as authorised agent for their co-author(s) is acceptable. User will reproduce the following wording prominently alongside the Work: the source of the Work, including author, article title, title of journal, volume number, issue number (if relevant), page range (or first page if this is the only information available) and date of first publication. This information can be contained in a footnote or reference note; and a link back to the article (via DOI); and if practicable, and IN ALL CASES for new works published under any of the Creative Commons licences, the words "© IOP Publishing. Reproduced with permission. All rights reserved" Without the express permission of the author(s) and the Rightsholder of the article from which the Work is to be reused, User shall not use it in any way which, in the opinion of the Rightsholder, could: (i) distort or alter the author(s)' original intention(s) and meaning; (ii) be prejudicial to the honour or reputation of the author(s); and/or (iii) imply endorsement by the author(s) and/or the Rightsholder. This licence does not apply to any article which is credited to another source and which does not have the copyright line '© IOP Publishing Ltd'. User must check the copyright line of the article from which the Work is to be reused to check that IOP Publishing Ltd has all the necessary rights to be able to grant permission. User is solely responsible for identifying and obtaining separate licences and permissions from the copyright owner for reuse of any such third party material/figures which the Rightsholder is not the copyright owner of. The Rightsholder shall not reimburse any fees which User pays for a republication licence for such third party content. This licence does not apply to any material/figure which is credited to another source in the Rightsholder's publication or has been obtained from a third party. User must check the Version of Record of the article from which the Work is to be reused, to check whether any of the material in the Work is third party material. Third party citations and/or copyright notices and/or permissions statements may not be included in any other version of the article from which the Work is to be reused and so cannot be relied upon by the User. User is solely responsible for identifying and obtaining separate licences and permissions from the copyright owner for reuse of any such third party material/figures where the Rightsholder is not the copyright owner. The Rightsholder shall not reimburse any fees which User pays for a republication licence for such third party content. User and CCC acknowledge that the Rightsholder may, from time to time, make changes or additions to these special terms and conditions without express notification, provided that these shall not apply to permissions already secured and paid for by User prior to such change or addition. User acknowledges that the Rightsholder (which includes companies within its group and third parties for whom it publishes its titles) may make use of personal data collected through the service in the course of their business. If User is the author of the Work, User may automatically have the right to reuse it under the rights granted back when User transferred the copyright in the article to the Rightsholder. User should check the copyright form and the relevant author rights policy to check whether permission is required. If User is the author of the Work and does require permission for proposed reuse of the Work, User should select 'Author of requested content' as the Requestor Type. The Rightsholder shall not reimburse any fees which User pays for a republication licence. If User is the author of the article which User wishes to reuse in User's thesis or dissertation, the republication licence covers the right to include the Accepted Manuscript version (not the Version of Record) of the article. User must include citation details and, for online use, a link to the Version of Record of the article on the Rightsholder's website. User may need to obtain separate permission for any third party content included within the article. User must check this with the copyright owner of such third party content. User may not include the article in a thesis or dissertation which is published by

ProQuest. Any other commercial use of User's thesis or dissertation containing the article would also need to be expressly notified in writing to the Rightsholder at the time of request and would require separate written permission from the Rightsholder. User does not need to request permission for Work which has been published under a CC BY licence. User must check the Version of Record of the CC BY article from which the Work is to be reused, to check whether any of the material in the Work is third party material and so not published under the CC BY licence. User is solely responsible for identifying and obtaining separate licences and permissions from the copyright owner for reuse of any such third party material/figures. The Rightsholder shall not reimburse any fees which User pays for such licences and permissions. As well as CCC, the Rightsholder shall have the right to bring any legal action that it deems necessary to enforce its rights should it consider that the Work infringes those rights in any way. For STM Signatories ONLY (as agreed as part of the STM Guidelines) Any licence granted for a particular edition of a Work will apply also to subsequent editions of it and for editions in other languages, provided such editions are for the Work as a whole in situ and do not involve the separate exploitation of the permitted illustrations or excerpts.

CCC Republication Terms and Conditions

1. Description of Service; Defined Terms. This Republication License enables the User to obtain licenses for republication of one or more copyrighted works as described in detail on the relevant Order Confirmation (the "Work(s)"). Copyright Clearance Center, Inc. ("CCC") grants licenses through the Service on behalf of the rightsholder identified on the Order Confirmation (the "Rightsholder"). "Republishing", as used herein, generally means the inclusion of a Work, in whole or in part, in a new work or works, also as described on the Order Confirmation. "User", as used herein, means the person or entity making such republication.
2. The terms set forth in the relevant Order Confirmation, and any terms set by the Rightsholder with respect to a particular Work, govern the terms of use of Works in connection with the Service. By using the Service, the person transacting for a republication license on behalf of the User represents and warrants that he/she/it (a) has been duly authorized by the User to accept, and hereby does accept, all such terms and conditions on behalf of User, and (b) shall inform User of all such terms and conditions. In the event such person is a "freelancer" or other third party independent of User and CCC, such party shall be deemed jointly a "User" for purposes of these terms and conditions. In any event, User shall be deemed to have accepted and agreed to all such terms and conditions if User republishes the Work in any fashion.
3. Scope of License; Limitations and Obligations.
 - 3.1. All Works and all rights therein, including copyright rights, remain the sole and exclusive property of the Rightsholder. The license created by the exchange of an Order Confirmation (and/or any invoice) and payment by User of the full amount set forth on that document includes only those rights expressly set forth in the Order Confirmation and in these terms and conditions, and conveys no other rights in the Work(s) to User. All rights not expressly granted are hereby reserved.
 - 3.2. General Payment Terms: You may pay by credit card or through an account with us payable at the end of the month. If you and we agree that you may establish a standing account with CCC, then the following terms apply: Remit Payment to: Copyright Clearance Center, 29118 Network Place, Chicago, IL 60673-1291. Payments Due: Invoices are payable upon their delivery to you (or upon our notice to you that they are available to you for downloading). After 30 days, outstanding amounts will be subject to a service charge of 1-1/2% per month or, if less, the maximum rate allowed by applicable law. Unless otherwise specifically set forth in the Order Confirmation or in a separate written agreement signed by CCC, invoices are due and payable on "net 30" terms. While User may exercise the rights licensed immediately upon issuance of the Order Confirmation, the license is automatically revoked and is null and void, as if it had never been issued, if complete payment for the license is not received on a timely basis either from User directly or through a payment agent, such as a credit card company.
 - 3.3. Unless otherwise provided in the Order Confirmation, any grant of rights to User (i) is "one-time" (including the editions and product family specified in the license), (ii) is non-exclusive and non-transferable and (iii) is subject to any and all limitations and restrictions (such as, but not limited to, limitations on duration of use or circulation) included in the Order Confirmation or invoice and/or in these terms and conditions. Upon completion of the licensed use, User shall either secure a new permission for further use of the Work(s) or immediately cease any new use of the Work(s) and shall render inaccessible (such as by

14/12/2020

<https://marketplace.copyright.com/rs-ui-web/mp/license/0fa469ab-2038-4cd3-a39d-8425c6355a1e/0b6506b3-4d38-4119-b43d-76b2b3...>

deleting or by removing or severing links or other locators) any further copies of the Work (except for copies printed on paper in accordance with this license and still in User's stock at the end of such period).

- 3.4. In the event that the material for which a republication license is sought includes third party materials (such as photographs, illustrations, graphs, inserts and similar materials) which are identified in such material as having been used by permission, User is responsible for identifying, and seeking separate licenses (under this Service or otherwise) for, any of such third party materials; without a separate license, such third party materials may not be used.
- 3.5. Use of proper copyright notice for a Work is required as a condition of any license granted under the Service. Unless otherwise provided in the Order Confirmation, a proper copyright notice will read substantially as follows: "Republished with permission of [Rightsholder's name], from [Work's title, author, volume, edition number and year of copyright]; permission conveyed through Copyright Clearance Center, Inc. " Such notice must be provided in a reasonably legible font size and must be placed either immediately adjacent to the Work as used (for example, as part of a by-line or footnote but not as a separate electronic link) or in the place where substantially all other credits or notices for the new work containing the republished Work are located. Failure to include the required notice results in loss to the Rightsholder and CCC, and the User shall be liable to pay liquidated damages for each such failure equal to twice the use fee specified in the Order Confirmation, in addition to the use fee itself and any other fees and charges specified.
- 3.6. User may only make alterations to the Work if and as expressly set forth in the Order Confirmation. No Work may be used in any way that is defamatory, violates the rights of third parties (including such third parties' rights of copyright, privacy, publicity, or other tangible or intangible property), or is otherwise illegal, sexually explicit or obscene. In addition, User may not conjoin a Work with any other material that may result in damage to the reputation of the Rightsholder. User agrees to inform CCC if it becomes aware of any infringement of any rights in a Work and to cooperate with any reasonable request of CCC or the Rightsholder in connection therewith.
4. Indemnity. User hereby indemnifies and agrees to defend the Rightsholder and CCC, and their respective employees and directors, against all claims, liability, damages, costs and expenses, including legal fees and expenses, arising out of any use of a Work beyond the scope of the rights granted herein, or any use of a Work which has been altered in any unauthorized way by User, including claims of defamation or infringement of rights of copyright, publicity, privacy or other tangible or intangible property.
5. Limitation of Liability. UNDER NO CIRCUMSTANCES WILL CCC OR THE RIGHTSHOLDER BE LIABLE FOR ANY DIRECT, INDIRECT, CONSEQUENTIAL OR INCIDENTAL DAMAGES (INCLUDING WITHOUT LIMITATION DAMAGES FOR LOSS OF BUSINESS PROFITS OR INFORMATION, OR FOR BUSINESS INTERRUPTION) ARISING OUT OF THE USE OR INABILITY TO USE A WORK, EVEN IF ONE OF THEM HAS BEEN ADVISED OF THE POSSIBILITY OF SUCH DAMAGES. In any event, the total liability of the Rightsholder and CCC (including their respective employees and directors) shall not exceed the total amount actually paid by User for this license. User assumes full liability for the actions and omissions of its principals, employees, agents, affiliates, successors and assigns.
6. Limited Warranties. THE WORK(S) AND RIGHT(S) ARE PROVIDED "AS IS". CCC HAS THE RIGHT TO GRANT TO USER THE RIGHTS GRANTED IN THE ORDER CONFIRMATION DOCUMENT. CCC AND THE RIGHTSHOLDER DISCLAIM ALL OTHER WARRANTIES RELATING TO THE WORK(S) AND RIGHT(S), EITHER EXPRESS OR IMPLIED, INCLUDING WITHOUT LIMITATION IMPLIED WARRANTIES OF MERCHANTABILITY OR FITNESS FOR A PARTICULAR PURPOSE. ADDITIONAL RIGHTS MAY BE REQUIRED TO USE ILLUSTRATIONS, GRAPHS, PHOTOGRAPHS, ABSTRACTS, INSERTS OR OTHER PORTIONS OF THE WORK (AS OPPOSED TO THE ENTIRE WORK) IN A MANNER CONTEMPLATED BY USER; USER UNDERSTANDS AND AGREES THAT NEITHER CCC NOR THE RIGHTSHOLDER MAY HAVE SUCH ADDITIONAL RIGHTS TO GRANT.
7. Effect of Breach. Any failure by User to pay any amount when due, or any use by User of a Work beyond the scope of the license set forth in the Order Confirmation and/or these terms and conditions, shall be a material breach of the license created by the Order Confirmation and these terms and conditions. Any breach not cured within 30

<https://marketplace.copyright.com/rs-ui-web/mp/license/0fa469ab-2038-4cd3-a39d-8425c6355a1e/0b6506b3-4d38-4119-b43d-76b2b3e475e>

4/5

days of written notice thereof shall result in immediate termination of such license without further notice. Any unauthorized (but licensable) use of a Work that is terminated immediately upon notice thereof may be liquidated by payment of the Rightsholder's ordinary license price therefor; any unauthorized (and unlicensable) use that is not terminated immediately for any reason (including, for example, because materials containing the Work cannot reasonably be recalled) will be subject to all remedies available at law or in equity, but in no event to a payment of less than three times the Rightsholder's ordinary license price for the most closely analogous licensable use plus Rightsholder's and/or CCC's costs and expenses incurred in collecting such payment.

8. Miscellaneous.

- 8.1. User acknowledges that CCC may, from time to time, make changes or additions to the Service or to these terms and conditions, and CCC reserves the right to send notice to the User by electronic mail or otherwise for the purposes of notifying User of such changes or additions; provided that any such changes or additions shall not apply to permissions already secured and paid for.
- 8.2. Use of User-related information collected through the Service is governed by CCC's privacy policy, available online here:<https://marketplace.copyright.com/rs-ui-web/mp/privacy-policy>
- 8.3. The licensing transaction described in the Order Confirmation is personal to User. Therefore, User may not assign or transfer to any other person (whether a natural person or an organization of any kind) the license created by the Order Confirmation and these terms and conditions or any rights granted hereunder; provided, however, that User may assign such license in its entirety on written notice to CCC in the event of a transfer of all or substantially all of User's rights in the new material which includes the Work(s) licensed under this Service.
- 8.4. No amendment or waiver of any terms is binding unless set forth in writing and signed by the parties. The Rightsholder and CCC hereby object to any terms contained in any writing prepared by the User or its principals, employees, agents or affiliates and purporting to govern or otherwise relate to the licensing transaction described in the Order Confirmation, which terms are in any way inconsistent with any terms set forth in the Order Confirmation and/or in these terms and conditions or CCC's standard operating procedures, whether such writing is prepared prior to, simultaneously with or subsequent to the Order Confirmation, and whether such writing appears on a copy of the Order Confirmation or in a separate instrument.
- 8.5. The licensing transaction described in the Order Confirmation document shall be governed by and construed under the law of the State of New York, USA, without regard to the principles thereof of conflicts of law. Any case, controversy, suit, action, or proceeding arising out of, in connection with, or related to such licensing transaction shall be brought, at CCC's sole discretion, in any federal or state court located in the County of New York, State of New York, USA, or in any federal or state court whose geographical jurisdiction covers the location of the Rightsholder set forth in the Order Confirmation. The parties expressly submit to the personal jurisdiction and venue of each such federal or state court. If you have any comments or questions about the Service or Copyright Clearance Center, please contact us at 978-750-8400 or send an e-mail to support@copyright.com.

v 1.1

14/12/2020

<https://marketplace.copyright.com/rs-ui-web/mp/license/dc9dfb27-e304-492d-9a6c-178db6cfb091/714da3de-cc66-49cd-b0ba-544578a7...>Copyright
Clearance
Center

Marketplace™

Royal Society of Chemistry - License Terms and Conditions

This is a License Agreement between Marie Hebert ("You") and Royal Society of Chemistry ("Publisher") provided by Copyright Clearance Center ("CCC"). The license consists of your order details, the terms and conditions provided by Royal Society of Chemistry, and the CCC terms and conditions.

All payments must be made in full to CCC.

| | | | |
|------------------|-------------|-------------|------------------------------------|
| Order Date | 14-Dec-2020 | Type of Use | Republish in a thesis/dissertation |
| Order license ID | 1084058-1 | Publisher | ROYAL SOCIETY OF CHEMISTRY |
| ISSN | 1473-0189 | Portion | Image/photo/illustration |

LICENSED CONTENT

| | | | |
|-------------------|--------------------------------------------|------------------|-------------------------------------------------------------|
| Publication Title | Lab on a chip | Country | United Kingdom of Great Britain and Northern Ireland |
| Author/Editor | Royal Society of Chemistry (Great Britain) | Rightsholder | Royal Society of Chemistry |
| Date | 01/01/2001 | Publication Type | e-Journal |
| Language | English | URL | http://www.rsc.org/loc |

REQUEST DETAILS

| | | | |
|-------------------------------------------|--------------------------|-----------------------------|----------------------------------|
| Portion Type | Image/photo/illustration | Distribution | Worldwide |
| Number of images / photos / illustrations | 1 | Translation | Original language of publication |
| Format (select all that apply) | Print, Electronic | Copies for the disabled? | No |
| Who will republish the content? | Academic institution | Minor editing privileges? | No |
| Duration of Use | Life of current edition | Incidental promotional use? | No |
| Lifetime Unit Quantity | Up to 499 | Currency | USD |
| Rights Requested | Main product | | |

NEW WORK DETAILS

| | | | |
|-----------------|----------------------------------------------------------------------------------|----------------------------|---------------------|
| Title | Expanding the droplet microfluidic community - towards a modular active platform | Institution name | Waterloo University |
| Instructor name | Marie Hebert | Expected presentation date | 2021-01-01 |

ADDITIONAL DETAILS

| | |
|------------------------|-----|
| Order reference number | N/A |
|------------------------|-----|

<https://marketplace.copyright.com/rs-ui-web/mp/license/dc9dfb27-e304-492d-9a6c-178db6cfb091/714da3de-cc66-49cd-b0ba-544578a7bc22>

1/4

The requesting person / organization to appear on the license Marie Hebert

REUSE CONTENT DETAILS

| | | | |
|-----------------------------------------------------------|----------|--------------------------------------------------|----------------------------------------------------------|
| Title, description or numeric reference of the portion(s) | Figure 2 | Title of the article/chapter the portion is from | On-demand droplet splitting using surface acoustic waves |
| Editor of portion(s) | N/A | Author of portion(s) | Royal Society of Chemistry (Great Britain) |
| Volume of serial or monograph | N/A | Issue, if republishing an article from a serial | N/A |
| Page or page range of portion | 3239 | Publication date of portion | 2016-07-08 |

CCC Republication Terms and Conditions

1. Description of Service; Defined Terms. This Republication License enables the User to obtain licenses for republication of one or more copyrighted works as described in detail on the relevant Order Confirmation (the "Work(s)"). Copyright Clearance Center, Inc. ("CCC") grants licenses through the Service on behalf of the rightsholder identified on the Order Confirmation (the "Rightsholder"). "Republishing", as used herein, generally means the inclusion of a Work, in whole or in part, in a new work or works, also as described on the Order Confirmation. "User", as used herein, means the person or entity making such republication.
2. The terms set forth in the relevant Order Confirmation, and any terms set by the Rightsholder with respect to a particular Work, govern the terms of use of Works in connection with the Service. By using the Service, the person transacting for a republication license on behalf of the User represents and warrants that he/she/it (a) has been duly authorized by the User to accept, and hereby does accept, all such terms and conditions on behalf of User, and (b) shall inform User of all such terms and conditions. In the event such person is a "freelancer" or other third party independent of User and CCC, such party shall be deemed jointly a "User" for purposes of these terms and conditions. In any event, User shall be deemed to have accepted and agreed to all such terms and conditions if User republishes the Work in any fashion.
3. Scope of License; Limitations and Obligations.
 - 3.1. All Works and all rights therein, including copyright rights, remain the sole and exclusive property of the Rightsholder. The license created by the exchange of an Order Confirmation (and/or any invoice) and payment by User of the full amount set forth on that document includes only those rights expressly set forth in the Order Confirmation and in these terms and conditions, and conveys no other rights in the Work(s) to User. All rights not expressly granted are hereby reserved.
 - 3.2. General Payment Terms: You may pay by credit card or through an account with us payable at the end of the month. If you and we agree that you may establish a standing account with CCC, then the following terms apply: Remit Payment to: Copyright Clearance Center, 29118 Network Place, Chicago, IL 60673-1291. Payments Due: Invoices are payable upon their delivery to you (or upon our notice to you that they are available to you for downloading). After 30 days, outstanding amounts will be subject to a service charge of 1-1/2% per month or, if less, the maximum rate allowed by applicable law. Unless otherwise specifically set forth in the Order Confirmation or in a separate written agreement signed by CCC, invoices are due and payable on "net 30" terms. While User may exercise the rights licensed immediately upon issuance of the Order Confirmation, the license is automatically revoked and is null and void, as if it had never been issued, if complete payment for the license is not received on a timely basis either from User directly or through a payment agent, such as a credit card company.
 - 3.3. Unless otherwise provided in the Order Confirmation, any grant of rights to User (i) is "one-time" (including

14/12/2020

<https://marketplace.copyright.com/rs-ui-web/mp/license/dc9dfb27-e304-492d-9a6c-178db6cfb091/714da3de-cc66-49cd-b0ba-544578a7...>

the editions and product family specified in the license), (ii) is non-exclusive and non-transferable and (iii) is subject to any and all limitations and restrictions (such as, but not limited to, limitations on duration of use or circulation) included in the Order Confirmation or invoice and/or in these terms and conditions. Upon completion of the licensed use, User shall either secure a new permission for further use of the Work(s) or immediately cease any new use of the Work(s) and shall render inaccessible (such as by deleting or by removing or severing links or other locators) any further copies of the Work (except for copies printed on paper in accordance with this license and still in User's stock at the end of such period).

- 3.4. In the event that the material for which a republication license is sought includes third party materials (such as photographs, illustrations, graphs, inserts and similar materials) which are identified in such material as having been used by permission, User is responsible for identifying, and seeking separate licenses (under this Service or otherwise) for, any of such third party materials; without a separate license, such third party materials may not be used.
- 3.5. Use of proper copyright notice for a Work is required as a condition of any license granted under the Service. Unless otherwise provided in the Order Confirmation, a proper copyright notice will read substantially as follows: "Republished with permission of [Rightsholder's name], from [Work's title, author, volume, edition number and year of copyright]; permission conveyed through Copyright Clearance Center, Inc. " Such notice must be provided in a reasonably legible font size and must be placed either immediately adjacent to the Work as used (for example, as part of a by-line or footnote but not as a separate electronic link) or in the place where substantially all other credits or notices for the new work containing the republished Work are located. Failure to include the required notice results in loss to the Rightsholder and CCC, and the User shall be liable to pay liquidated damages for each such failure equal to twice the use fee specified in the Order Confirmation, in addition to the use fee itself and any other fees and charges specified.
- 3.6. User may only make alterations to the Work if and as expressly set forth in the Order Confirmation. No Work may be used in any way that is defamatory, violates the rights of third parties (including such third parties' rights of copyright, privacy, publicity, or other tangible or intangible property), or is otherwise illegal, sexually explicit or obscene. In addition, User may not conjoin a Work with any other material that may result in damage to the reputation of the Rightsholder. User agrees to inform CCC if it becomes aware of any infringement of any rights in a Work and to cooperate with any reasonable request of CCC or the Rightsholder in connection therewith.
4. Indemnity. User hereby indemnifies and agrees to defend the Rightsholder and CCC, and their respective employees and directors, against all claims, liability, damages, costs and expenses, including legal fees and expenses, arising out of any use of a Work beyond the scope of the rights granted herein, or any use of a Work which has been altered in any unauthorized way by User, including claims of defamation or infringement of rights of copyright, publicity, privacy or other tangible or intangible property.
5. Limitation of Liability. UNDER NO CIRCUMSTANCES WILL CCC OR THE RIGHTSHOLDER BE LIABLE FOR ANY DIRECT, INDIRECT, CONSEQUENTIAL OR INCIDENTAL DAMAGES (INCLUDING WITHOUT LIMITATION DAMAGES FOR LOSS OF BUSINESS PROFITS OR INFORMATION, OR FOR BUSINESS INTERRUPTION) ARISING OUT OF THE USE OR INABILITY TO USE A WORK, EVEN IF ONE OF THEM HAS BEEN ADVISED OF THE POSSIBILITY OF SUCH DAMAGES. In any event, the total liability of the Rightsholder and CCC (including their respective employees and directors) shall not exceed the total amount actually paid by User for this license. User assumes full liability for the actions and omissions of its principals, employees, agents, affiliates, successors and assigns.
6. Limited Warranties. THE WORK(S) AND RIGHT(S) ARE PROVIDED "AS IS". CCC HAS THE RIGHT TO GRANT TO USER THE RIGHTS GRANTED IN THE ORDER CONFIRMATION DOCUMENT. CCC AND THE RIGHTSHOLDER DISCLAIM ALL OTHER WARRANTIES RELATING TO THE WORK(S) AND RIGHT(S), EITHER EXPRESS OR IMPLIED, INCLUDING WITHOUT LIMITATION IMPLIED WARRANTIES OF MERCHANTABILITY OR FITNESS FOR A PARTICULAR PURPOSE. ADDITIONAL RIGHTS MAY BE REQUIRED TO USE ILLUSTRATIONS, GRAPHS, PHOTOGRAPHS, ABSTRACTS, INSERTS OR OTHER PORTIONS OF THE WORK (AS OPPOSED TO THE ENTIRE WORK) IN A MANNER CONTEMPLATED BY USER; USER UNDERSTANDS AND AGREES THAT NEITHER CCC NOR THE RIGHTSHOLDER MAY HAVE SUCH ADDITIONAL RIGHTS TO GRANT.

<https://marketplace.copyright.com/rs-ui-web/mp/license/dc9dfb27-e304-492d-9a6c-178db6cfb091/714da3de-cc66-49cd-b0ba-544578a7bc22>

3/4

7. Effect of Breach. Any failure by User to pay any amount when due, or any use by User of a Work beyond the scope of the license set forth in the Order Confirmation and/or these terms and conditions, shall be a material breach of the license created by the Order Confirmation and these terms and conditions. Any breach not cured within 30 days of written notice thereof shall result in immediate termination of such license without further notice. Any unauthorized (but licensable) use of a Work that is terminated immediately upon notice thereof may be liquidated by payment of the Rightsholder's ordinary license price therefor; any unauthorized (and unlicensable) use that is not terminated immediately for any reason (including, for example, because materials containing the Work cannot reasonably be recalled) will be subject to all remedies available at law or in equity, but in no event to a payment of less than three times the Rightsholder's ordinary license price for the most closely analogous licensable use plus Rightsholder's and/or CCC's costs and expenses incurred in collecting such payment.

8. Miscellaneous.

8.1. User acknowledges that CCC may, from time to time, make changes or additions to the Service or to these terms and conditions, and CCC reserves the right to send notice to the User by electronic mail or otherwise for the purposes of notifying User of such changes or additions; provided that any such changes or additions shall not apply to permissions already secured and paid for.

8.2. Use of User-related information collected through the Service is governed by CCC's privacy policy, available online here: <https://marketplace.copyright.com/rs-ui-web/mp/privacy-policy>

8.3. The licensing transaction described in the Order Confirmation is personal to User. Therefore, User may not assign or transfer to any other person (whether a natural person or an organization of any kind) the license created by the Order Confirmation and these terms and conditions or any rights granted hereunder; provided, however, that User may assign such license in its entirety on written notice to CCC in the event of a transfer of all or substantially all of User's rights in the new material which includes the Work(s) licensed under this Service.

8.4. No amendment or waiver of any terms is binding unless set forth in writing and signed by the parties. The Rightsholder and CCC hereby object to any terms contained in any writing prepared by the User or its principals, employees, agents or affiliates and purporting to govern or otherwise relate to the licensing transaction described in the Order Confirmation, which terms are in any way inconsistent with any terms set forth in the Order Confirmation and/or in these terms and conditions or CCC's standard operating procedures, whether such writing is prepared prior to, simultaneously with or subsequent to the Order Confirmation, and whether such writing appears on a copy of the Order Confirmation or in a separate instrument.

8.5. The licensing transaction described in the Order Confirmation document shall be governed by and construed under the law of the State of New York, USA, without regard to the principles thereof of conflicts of law. Any case, controversy, suit, action, or proceeding arising out of, in connection with, or related to such licensing transaction shall be brought, at CCC's sole discretion, in any federal or state court located in the County of New York, State of New York, USA, or in any federal or state court whose geographical jurisdiction covers the location of the Rightsholder set forth in the Order Confirmation. The parties expressly submit to the personal jurisdiction and venue of each such federal or state court. If you have any comments or questions about the Service or Copyright Clearance Center, please contact us at 978-750-8400 or send an e-mail to support@copyright.com.

v 1.1

14/12/2020

<https://marketplace.copyright.com/rs-ui-web/mp/license/ef882f9d-b119-42b1-9bd8-233bbf48295f/edfa4207-a6b0-4603-af37-f8bf40509328>Copyright
Clearance
Center

Marketplace™

Royal Society of Chemistry - License Terms and Conditions

This is a License Agreement between Marie Hebert ("You") and Royal Society of Chemistry ("Publisher") provided by Copyright Clearance Center ("CCC"). The license consists of your order details, the terms and conditions provided by Royal Society of Chemistry, and the CCC terms and conditions.

All payments must be made in full to CCC.

| | | | |
|------------------|-------------|-------------|------------------------------------|
| Order Date | 14-Dec-2020 | Type of Use | Republish in a thesis/dissertation |
| Order license ID | 1084062-1 | Publisher | ROYAL SOCIETY OF CHEMISTRY |
| ISSN | 1473-0189 | Portion | Image/photo/illustration |

LICENSED CONTENT

| | | | |
|-------------------|--------------------------------------------|------------------|-------------------------------------------------------------|
| Publication Title | Lab on a chip | Country | United Kingdom of Great Britain and Northern Ireland |
| Author/Editor | Royal Society of Chemistry (Great Britain) | Rightsholder | Royal Society of Chemistry |
| Date | 01/01/2001 | Publication Type | e-Journal |
| Language | English | URL | http://www.rsc.org/loc |

REQUEST DETAILS

| | | | |
|-------------------------------------------|--------------------------|-----------------------------|----------------------------------|
| Portion Type | Image/photo/illustration | Distribution | Worldwide |
| Number of images / photos / illustrations | 1 | Translation | Original language of publication |
| Format (select all that apply) | Print, Electronic | Copies for the disabled? | No |
| Who will republish the content? | Academic institution | Minor editing privileges? | No |
| Duration of Use | Life of current edition | Incidental promotional use? | No |
| Lifetime Unit Quantity | Up to 499 | Currency | USD |
| Rights Requested | Main product | | |

NEW WORK DETAILS

| | | | |
|-----------------|----------------------------------------------------------------------------------|----------------------------|---------------------|
| Title | Expanding the droplet microfluidic community - towards a modular active platform | Institution name | Waterloo University |
| Instructor name | Marie Hebert | Expected presentation date | 2021-01-01 |

ADDITIONAL DETAILS

| | |
|------------------------|-----|
| Order reference number | N/A |
|------------------------|-----|

<https://marketplace.copyright.com/rs-ui-web/mp/license/ef882f9d-b119-42b1-9bd8-233bbf48295f/edfa4207-a6b0-4603-af37-f8bf40509328>

1/4

The requesting person / organization to appear on the license Marie Hebert

REUSE CONTENT DETAILS

| | | | |
|-----------------------------------------------------------|--------------|--------------------------------------------------|---------------------------------------------------------------------------------------------------------|
| Title, description or numeric reference of the portion(s) | Figure 1 (b) | Title of the article/chapter the portion is from | Label-free high-throughput detection and content sensing of individual droplets in microfluidic systems |
| Editor of portion(s) | N/A | Author of portion(s) | Royal Society of Chemistry (Great Britain) |
| Volume of serial or monograph | N/A | Issue, if republishing an article from a serial | N/A |
| Page or page range of portion | 4009 | Publication date of portion | 2015-08-20 |

CCC Republication Terms and Conditions

1. Description of Service; Defined Terms. This Republication License enables the User to obtain licenses for republication of one or more copyrighted works as described in detail on the relevant Order Confirmation (the "Work(s)"). Copyright Clearance Center, Inc. ("CCC") grants licenses through the Service on behalf of the rightsholder identified on the Order Confirmation (the "Rightsholder"). "Republishing", as used herein, generally means the inclusion of a Work, in whole or in part, in a new work or works, also as described on the Order Confirmation. "User", as used herein, means the person or entity making such republication.
2. The terms set forth in the relevant Order Confirmation, and any terms set by the Rightsholder with respect to a particular Work, govern the terms of use of Works in connection with the Service. By using the Service, the person transacting for a republication license on behalf of the User represents and warrants that he/she/it (a) has been duly authorized by the User to accept, and hereby does accept, all such terms and conditions on behalf of User, and (b) shall inform User of all such terms and conditions. In the event such person is a "freelancer" or other third party independent of User and CCC, such party shall be deemed jointly a "User" for purposes of these terms and conditions. In any event, User shall be deemed to have accepted and agreed to all such terms and conditions if User republishes the Work in any fashion.
3. Scope of License; Limitations and Obligations.
 - 3.1. All Works and all rights therein, including copyright rights, remain the sole and exclusive property of the Rightsholder. The license created by the exchange of an Order Confirmation (and/or any invoice) and payment by User of the full amount set forth on that document includes only those rights expressly set forth in the Order Confirmation and in these terms and conditions, and conveys no other rights in the Work(s) to User. All rights not expressly granted are hereby reserved.
 - 3.2. General Payment Terms: You may pay by credit card or through an account with us payable at the end of the month. If you and we agree that you may establish a standing account with CCC, then the following terms apply: Remit Payment to: Copyright Clearance Center, 29118 Network Place, Chicago, IL 60673-1291. Payments Due: Invoices are payable upon their delivery to you (or upon our notice to you that they are available to you for downloading). After 30 days, outstanding amounts will be subject to a service charge of 1-1/2% per month or, if less, the maximum rate allowed by applicable law. Unless otherwise specifically set forth in the Order Confirmation or in a separate written agreement signed by CCC, invoices are due and payable on "net 30" terms. While User may exercise the rights licensed immediately upon issuance of the Order Confirmation, the license is automatically revoked and is null and void, as if it had never been issued, if complete payment for the license is not received on a timely basis either from User directly or through a payment agent, such as a credit card company.

- 3.3. Unless otherwise provided in the Order Confirmation, any grant of rights to User (i) is "one-time" (including the editions and product family specified in the license), (ii) is non-exclusive and non-transferable and (iii) is subject to any and all limitations and restrictions (such as, but not limited to, limitations on duration of use or circulation) included in the Order Confirmation or invoice and/or in these terms and conditions. Upon completion of the licensed use, User shall either secure a new permission for further use of the Work(s) or immediately cease any new use of the Work(s) and shall render inaccessible (such as by deleting or by removing or severing links or other locators) any further copies of the Work (except for copies printed on paper in accordance with this license and still in User's stock at the end of such period).
- 3.4. In the event that the material for which a republication license is sought includes third party materials (such as photographs, illustrations, graphs, inserts and similar materials) which are identified in such material as having been used by permission, User is responsible for identifying, and seeking separate licenses (under this Service or otherwise) for, any of such third party materials; without a separate license, such third party materials may not be used.
- 3.5. Use of proper copyright notice for a Work is required as a condition of any license granted under the Service. Unless otherwise provided in the Order Confirmation, a proper copyright notice will read substantially as follows: "Republished with permission of [Rightsholder's name], from [Work's title, author, volume, edition number and year of copyright]; permission conveyed through Copyright Clearance Center, Inc. " Such notice must be provided in a reasonably legible font size and must be placed either immediately adjacent to the Work as used (for example, as part of a by-line or footnote but not as a separate electronic link) or in the place where substantially all other credits or notices for the new work containing the republished Work are located. Failure to include the required notice results in loss to the Rightsholder and CCC, and the User shall be liable to pay liquidated damages for each such failure equal to twice the use fee specified in the Order Confirmation, in addition to the use fee itself and any other fees and charges specified.
- 3.6. User may only make alterations to the Work if and as expressly set forth in the Order Confirmation. No Work may be used in any way that is defamatory, violates the rights of third parties (including such third parties' rights of copyright, privacy, publicity, or other tangible or intangible property), or is otherwise illegal, sexually explicit or obscene. In addition, User may not conjoin a Work with any other material that may result in damage to the reputation of the Rightsholder. User agrees to inform CCC if it becomes aware of any infringement of any rights in a Work and to cooperate with any reasonable request of CCC or the Rightsholder in connection therewith.
4. Indemnity. User hereby indemnifies and agrees to defend the Rightsholder and CCC, and their respective employees and directors, against all claims, liability, damages, costs and expenses, including legal fees and expenses, arising out of any use of a Work beyond the scope of the rights granted herein, or any use of a Work which has been altered in any unauthorized way by User, including claims of defamation or infringement of rights of copyright, publicity, privacy or other tangible or intangible property.
5. Limitation of Liability. UNDER NO CIRCUMSTANCES WILL CCC OR THE RIGHTSHOLDER BE LIABLE FOR ANY DIRECT, INDIRECT, CONSEQUENTIAL OR INCIDENTAL DAMAGES (INCLUDING WITHOUT LIMITATION DAMAGES FOR LOSS OF BUSINESS PROFITS OR INFORMATION, OR FOR BUSINESS INTERRUPTION) ARISING OUT OF THE USE OR INABILITY TO USE A WORK, EVEN IF ONE OF THEM HAS BEEN ADVISED OF THE POSSIBILITY OF SUCH DAMAGES. In any event, the total liability of the Rightsholder and CCC (including their respective employees and directors) shall not exceed the total amount actually paid by User for this license. User assumes full liability for the actions and omissions of its principals, employees, agents, affiliates, successors and assigns.
6. Limited Warranties. THE WORK(S) AND RIGHT(S) ARE PROVIDED "AS IS". CCC HAS THE RIGHT TO GRANT TO USER THE RIGHTS GRANTED IN THE ORDER CONFIRMATION DOCUMENT. CCC AND THE RIGHTSHOLDER DISCLAIM ALL OTHER WARRANTIES RELATING TO THE WORK(S) AND RIGHT(S), EITHER EXPRESS OR IMPLIED, INCLUDING WITHOUT LIMITATION IMPLIED WARRANTIES OF MERCHANTABILITY OR FITNESS FOR A PARTICULAR PURPOSE. ADDITIONAL RIGHTS MAY BE REQUIRED TO USE ILLUSTRATIONS, GRAPHS, PHOTOGRAPHS, ABSTRACTS, INSERTS OR OTHER PORTIONS OF THE WORK (AS OPPOSED TO THE ENTIRE WORK) IN A MANNER CONTEMPLATED BY USER;

14/12/2020

<https://marketplace.copyright.com/rs-ui-web/mp/license/ef882f9d-b119-42b1-9bd8-233bbf48295f/edfa4207-a6b0-4603-af37-f8bf40509328>

USER UNDERSTANDS AND AGREES THAT NEITHER CCC NOR THE RIGHTSHOLDER MAY HAVE SUCH ADDITIONAL RIGHTS TO GRANT.

7. Effect of Breach. Any failure by User to pay any amount when due, or any use by User of a Work beyond the scope of the license set forth in the Order Confirmation and/or these terms and conditions, shall be a material breach of the license created by the Order Confirmation and these terms and conditions. Any breach not cured within 30 days of written notice thereof shall result in immediate termination of such license without further notice. Any unauthorized (but licensable) use of a Work that is terminated immediately upon notice thereof may be liquidated by payment of the Rightsholder's ordinary license price therefor; any unauthorized (and unlicensable) use that is not terminated immediately for any reason (including, for example, because materials containing the Work cannot reasonably be recalled) will be subject to all remedies available at law or in equity, but in no event to a payment of less than three times the Rightsholder's ordinary license price for the most closely analogous licensable use plus Rightsholder's and/or CCC's costs and expenses incurred in collecting such payment.

8. Miscellaneous.

8.1. User acknowledges that CCC may, from time to time, make changes or additions to the Service or to these terms and conditions, and CCC reserves the right to send notice to the User by electronic mail or otherwise for the purposes of notifying User of such changes or additions; provided that any such changes or additions shall not apply to permissions already secured and paid for.

8.2. Use of User-related information collected through the Service is governed by CCC's privacy policy, available online here:<https://marketplace.copyright.com/rs-ui-web/mp/privacy-policy>

8.3. The licensing transaction described in the Order Confirmation is personal to User. Therefore, User may not assign or transfer to any other person (whether a natural person or an organization of any kind) the license created by the Order Confirmation and these terms and conditions or any rights granted hereunder; provided, however, that User may assign such license in its entirety on written notice to CCC in the event of a transfer of all or substantially all of User's rights in the new material which includes the Work(s) licensed under this Service.

8.4. No amendment or waiver of any terms is binding unless set forth in writing and signed by the parties. The Rightsholder and CCC hereby object to any terms contained in any writing prepared by the User or its principals, employees, agents or affiliates and purporting to govern or otherwise relate to the licensing transaction described in the Order Confirmation, which terms are in any way inconsistent with any terms set forth in the Order Confirmation and/or in these terms and conditions or CCC's standard operating procedures, whether such writing is prepared prior to, simultaneously with or subsequent to the Order Confirmation, and whether such writing appears on a copy of the Order Confirmation or in a separate instrument.

8.5. The licensing transaction described in the Order Confirmation document shall be governed by and construed under the law of the State of New York, USA, without regard to the principles thereof of conflicts of law. Any case, controversy, suit, action, or proceeding arising out of, in connection with, or related to such licensing transaction shall be brought, at CCC's sole discretion, in any federal or state court located in the County of New York, State of New York, USA, or in any federal or state court whose geographical jurisdiction covers the location of the Rightsholder set forth in the Order Confirmation. The parties expressly submit to the personal jurisdiction and venue of each such federal or state court. If you have any comments or questions about the Service or Copyright Clearance Center, please contact us at 978-750-8400 or send an e-mail to support@copyright.com.

v 1.1

<https://marketplace.copyright.com/rs-ui-web/mp/license/ef882f9d-b119-42b1-9bd8-233bbf48295f/edfa4207-a6b0-4603-af37-f8bf40509328>

4/4

14/12/2020

<https://marketplace.copyright.com/rs-ui-web/mp/license/ef882f9d-b119-42b1-9bd8-233bbf48295f/edfa4207-a6b0-4603-af37-f8bf40509328>Copyright
Clearance
Center

Marketplace™

Royal Society of Chemistry - License Terms and Conditions

This is a License Agreement between Marie Hebert ("You") and Royal Society of Chemistry ("Publisher") provided by Copyright Clearance Center ("CCC"). The license consists of your order details, the terms and conditions provided by Royal Society of Chemistry, and the CCC terms and conditions.

All payments must be made in full to CCC.

| | | | |
|------------------|-------------|-------------|------------------------------------|
| Order Date | 14-Dec-2020 | Type of Use | Republish in a thesis/dissertation |
| Order license ID | 1084062-1 | Publisher | ROYAL SOCIETY OF CHEMISTRY |
| ISSN | 1473-0189 | Portion | Image/photo/illustration |

LICENSED CONTENT

| | | | |
|-------------------|--------------------------------------------|------------------|-------------------------------------------------------------|
| Publication Title | Lab on a chip | Country | United Kingdom of Great Britain and Northern Ireland |
| Author/Editor | Royal Society of Chemistry (Great Britain) | Rightsholder | Royal Society of Chemistry |
| Date | 01/01/2001 | Publication Type | e-Journal |
| Language | English | URL | http://www.rsc.org/loc |

REQUEST DETAILS

| | | | |
|-------------------------------------------|--------------------------|-----------------------------|----------------------------------|
| Portion Type | Image/photo/illustration | Distribution | Worldwide |
| Number of images / photos / illustrations | 1 | Translation | Original language of publication |
| Format (select all that apply) | Print, Electronic | Copies for the disabled? | No |
| Who will republish the content? | Academic institution | Minor editing privileges? | No |
| Duration of Use | Life of current edition | Incidental promotional use? | No |
| Lifetime Unit Quantity | Up to 499 | Currency | USD |
| Rights Requested | Main product | | |

NEW WORK DETAILS

| | | | |
|-----------------|----------------------------------------------------------------------------------|----------------------------|---------------------|
| Title | Expanding the droplet microfluidic community - towards a modular active platform | Institution name | Waterloo University |
| Instructor name | Marie Hebert | Expected presentation date | 2021-01-01 |

ADDITIONAL DETAILS

| | |
|------------------------|-----|
| Order reference number | N/A |
|------------------------|-----|

<https://marketplace.copyright.com/rs-ui-web/mp/license/ef882f9d-b119-42b1-9bd8-233bbf48295f/edfa4207-a6b0-4603-af37-f8bf40509328>

1/4

The requesting person / organization to appear on the license Marie Hebert

REUSE CONTENT DETAILS

| | | | |
|-----------------------------------------------------------|--------------|--------------------------------------------------|---------------------------------------------------------------------------------------------------------|
| Title, description or numeric reference of the portion(s) | Figure 1 (b) | Title of the article/chapter the portion is from | Label-free high-throughput detection and content sensing of individual droplets in microfluidic systems |
| Editor of portion(s) | N/A | Author of portion(s) | Royal Society of Chemistry (Great Britain) |
| Volume of serial or monograph | N/A | Issue, if republishing an article from a serial | N/A |
| Page or page range of portion | 4009 | Publication date of portion | 2015-08-20 |

CCC Republication Terms and Conditions

1. Description of Service; Defined Terms. This Republication License enables the User to obtain licenses for republication of one or more copyrighted works as described in detail on the relevant Order Confirmation (the "Work(s)"). Copyright Clearance Center, Inc. ("CCC") grants licenses through the Service on behalf of the rightsholder identified on the Order Confirmation (the "Rightsholder"). "Republishing", as used herein, generally means the inclusion of a Work, in whole or in part, in a new work or works, also as described on the Order Confirmation. "User", as used herein, means the person or entity making such republication.
2. The terms set forth in the relevant Order Confirmation, and any terms set by the Rightsholder with respect to a particular Work, govern the terms of use of Works in connection with the Service. By using the Service, the person transacting for a republication license on behalf of the User represents and warrants that he/she/it (a) has been duly authorized by the User to accept, and hereby does accept, all such terms and conditions on behalf of User, and (b) shall inform User of all such terms and conditions. In the event such person is a "freelancer" or other third party independent of User and CCC, such party shall be deemed jointly a "User" for purposes of these terms and conditions. In any event, User shall be deemed to have accepted and agreed to all such terms and conditions if User republishes the Work in any fashion.
3. Scope of License; Limitations and Obligations.
 - 3.1. All Works and all rights therein, including copyright rights, remain the sole and exclusive property of the Rightsholder. The license created by the exchange of an Order Confirmation (and/or any invoice) and payment by User of the full amount set forth on that document includes only those rights expressly set forth in the Order Confirmation and in these terms and conditions, and conveys no other rights in the Work(s) to User. All rights not expressly granted are hereby reserved.
 - 3.2. General Payment Terms: You may pay by credit card or through an account with us payable at the end of the month. If you and we agree that you may establish a standing account with CCC, then the following terms apply: Remit Payment to: Copyright Clearance Center, 29118 Network Place, Chicago, IL 60673-1291. Payments Due: Invoices are payable upon their delivery to you (or upon our notice to you that they are available to you for downloading). After 30 days, outstanding amounts will be subject to a service charge of 1-1/2% per month or, if less, the maximum rate allowed by applicable law. Unless otherwise specifically set forth in the Order Confirmation or in a separate written agreement signed by CCC, invoices are due and payable on "net 30" terms. While User may exercise the rights licensed immediately upon issuance of the Order Confirmation, the license is automatically revoked and is null and void, as if it had never been issued, if complete payment for the license is not received on a timely basis either from User directly or through a payment agent, such as a credit card company.

- 3.3. Unless otherwise provided in the Order Confirmation, any grant of rights to User (i) is "one-time" (including the editions and product family specified in the license), (ii) is non-exclusive and non-transferable and (iii) is subject to any and all limitations and restrictions (such as, but not limited to, limitations on duration of use or circulation) included in the Order Confirmation or invoice and/or in these terms and conditions. Upon completion of the licensed use, User shall either secure a new permission for further use of the Work(s) or immediately cease any new use of the Work(s) and shall render inaccessible (such as by deleting or by removing or severing links or other locators) any further copies of the Work (except for copies printed on paper in accordance with this license and still in User's stock at the end of such period).
- 3.4. In the event that the material for which a republication license is sought includes third party materials (such as photographs, illustrations, graphs, inserts and similar materials) which are identified in such material as having been used by permission, User is responsible for identifying, and seeking separate licenses (under this Service or otherwise) for, any of such third party materials; without a separate license, such third party materials may not be used.
- 3.5. Use of proper copyright notice for a Work is required as a condition of any license granted under the Service. Unless otherwise provided in the Order Confirmation, a proper copyright notice will read substantially as follows: "Republished with permission of [Rightsholder's name], from [Work's title, author, volume, edition number and year of copyright]; permission conveyed through Copyright Clearance Center, Inc. " Such notice must be provided in a reasonably legible font size and must be placed either immediately adjacent to the Work as used (for example, as part of a by-line or footnote but not as a separate electronic link) or in the place where substantially all other credits or notices for the new work containing the republished Work are located. Failure to include the required notice results in loss to the Rightsholder and CCC, and the User shall be liable to pay liquidated damages for each such failure equal to twice the use fee specified in the Order Confirmation, in addition to the use fee itself and any other fees and charges specified.
- 3.6. User may only make alterations to the Work if and as expressly set forth in the Order Confirmation. No Work may be used in any way that is defamatory, violates the rights of third parties (including such third parties' rights of copyright, privacy, publicity, or other tangible or intangible property), or is otherwise illegal, sexually explicit or obscene. In addition, User may not conjoin a Work with any other material that may result in damage to the reputation of the Rightsholder. User agrees to inform CCC if it becomes aware of any infringement of any rights in a Work and to cooperate with any reasonable request of CCC or the Rightsholder in connection therewith.
4. Indemnity. User hereby indemnifies and agrees to defend the Rightsholder and CCC, and their respective employees and directors, against all claims, liability, damages, costs and expenses, including legal fees and expenses, arising out of any use of a Work beyond the scope of the rights granted herein, or any use of a Work which has been altered in any unauthorized way by User, including claims of defamation or infringement of rights of copyright, publicity, privacy or other tangible or intangible property.
5. Limitation of Liability. UNDER NO CIRCUMSTANCES WILL CCC OR THE RIGHTSHOLDER BE LIABLE FOR ANY DIRECT, INDIRECT, CONSEQUENTIAL OR INCIDENTAL DAMAGES (INCLUDING WITHOUT LIMITATION DAMAGES FOR LOSS OF BUSINESS PROFITS OR INFORMATION, OR FOR BUSINESS INTERRUPTION) ARISING OUT OF THE USE OR INABILITY TO USE A WORK, EVEN IF ONE OF THEM HAS BEEN ADVISED OF THE POSSIBILITY OF SUCH DAMAGES. In any event, the total liability of the Rightsholder and CCC (including their respective employees and directors) shall not exceed the total amount actually paid by User for this license. User assumes full liability for the actions and omissions of its principals, employees, agents, affiliates, successors and assigns.
6. Limited Warranties. THE WORK(S) AND RIGHT(S) ARE PROVIDED "AS IS". CCC HAS THE RIGHT TO GRANT TO USER THE RIGHTS GRANTED IN THE ORDER CONFIRMATION DOCUMENT. CCC AND THE RIGHTSHOLDER DISCLAIM ALL OTHER WARRANTIES RELATING TO THE WORK(S) AND RIGHT(S), EITHER EXPRESS OR IMPLIED, INCLUDING WITHOUT LIMITATION IMPLIED WARRANTIES OF MERCHANTABILITY OR FITNESS FOR A PARTICULAR PURPOSE. ADDITIONAL RIGHTS MAY BE REQUIRED TO USE ILLUSTRATIONS, GRAPHS, PHOTOGRAPHS, ABSTRACTS, INSERTS OR OTHER PORTIONS OF THE WORK (AS OPPOSED TO THE ENTIRE WORK) IN A MANNER CONTEMPLATED BY USER;

14/12/2020

<https://marketplace.copyright.com/rs-ui-web/mp/license/ef882f9d-b119-42b1-9bd8-233bbf48295f/edfa4207-a6b0-4603-af37-f8bf40509328>

USER UNDERSTANDS AND AGREES THAT NEITHER CCC NOR THE RIGHTSHOLDER MAY HAVE SUCH ADDITIONAL RIGHTS TO GRANT.

7. Effect of Breach. Any failure by User to pay any amount when due, or any use by User of a Work beyond the scope of the license set forth in the Order Confirmation and/or these terms and conditions, shall be a material breach of the license created by the Order Confirmation and these terms and conditions. Any breach not cured within 30 days of written notice thereof shall result in immediate termination of such license without further notice. Any unauthorized (but licensable) use of a Work that is terminated immediately upon notice thereof may be liquidated by payment of the Rightsholder's ordinary license price therefor; any unauthorized (and unlicensable) use that is not terminated immediately for any reason (including, for example, because materials containing the Work cannot reasonably be recalled) will be subject to all remedies available at law or in equity, but in no event to a payment of less than three times the Rightsholder's ordinary license price for the most closely analogous licensable use plus Rightsholder's and/or CCC's costs and expenses incurred in collecting such payment.

8. Miscellaneous.

8.1. User acknowledges that CCC may, from time to time, make changes or additions to the Service or to these terms and conditions, and CCC reserves the right to send notice to the User by electronic mail or otherwise for the purposes of notifying User of such changes or additions; provided that any such changes or additions shall not apply to permissions already secured and paid for.

8.2. Use of User-related information collected through the Service is governed by CCC's privacy policy, available online here:<https://marketplace.copyright.com/rs-ui-web/mp/privacy-policy>

8.3. The licensing transaction described in the Order Confirmation is personal to User. Therefore, User may not assign or transfer to any other person (whether a natural person or an organization of any kind) the license created by the Order Confirmation and these terms and conditions or any rights granted hereunder; provided, however, that User may assign such license in its entirety on written notice to CCC in the event of a transfer of all or substantially all of User's rights in the new material which includes the Work(s) licensed under this Service.

8.4. No amendment or waiver of any terms is binding unless set forth in writing and signed by the parties. The Rightsholder and CCC hereby object to any terms contained in any writing prepared by the User or its principals, employees, agents or affiliates and purporting to govern or otherwise relate to the licensing transaction described in the Order Confirmation, which terms are in any way inconsistent with any terms set forth in the Order Confirmation and/or in these terms and conditions or CCC's standard operating procedures, whether such writing is prepared prior to, simultaneously with or subsequent to the Order Confirmation, and whether such writing appears on a copy of the Order Confirmation or in a separate instrument.

8.5. The licensing transaction described in the Order Confirmation document shall be governed by and construed under the law of the State of New York, USA, without regard to the principles thereof of conflicts of law. Any case, controversy, suit, action, or proceeding arising out of, in connection with, or related to such licensing transaction shall be brought, at CCC's sole discretion, in any federal or state court located in the County of New York, State of New York, USA, or in any federal or state court whose geographical jurisdiction covers the location of the Rightsholder set forth in the Order Confirmation. The parties expressly submit to the personal jurisdiction and venue of each such federal or state court. If you have any comments or questions about the Service or Copyright Clearance Center, please contact us at 978-750-8400 or send an e-mail to support@copyright.com.

v 1.1

<https://marketplace.copyright.com/rs-ui-web/mp/license/ef882f9d-b119-42b1-9bd8-233bbf48295f/edfa4207-a6b0-4603-af37-f8bf40509328>

4/4

14/12/2020

<https://marketplace.copyright.com/rs-ui-web/mp/license/c6fa1b5c-77a3-467f-b44b-d29992d214c2/11c99bd0-3f83-412b-bce2-be3aceafca07>Copyright
Clearance
Center

Marketplace™

Royal Society of Chemistry - License Terms and Conditions

This is a License Agreement between Marie Hebert ("You") and Royal Society of Chemistry ("Publisher") provided by Copyright Clearance Center ("CCC"). The license consists of your order details, the terms and conditions provided by Royal Society of Chemistry, and the CCC terms and conditions.

All payments must be made in full to CCC.

| | | | |
|------------------|-------------|-------------|------------------------------------|
| Order Date | 14-Dec-2020 | Type of Use | Republish in a thesis/dissertation |
| Order license ID | 1084065-1 | Publisher | ROYAL SOCIETY OF CHEMISTRY |
| ISSN | 1473-0189 | Portion | Chart/graph/table/figure |

LICENSED CONTENT

| | | | |
|-------------------|--------------------------------------------|------------------|-------------------------------------------------------------|
| Publication Title | Lab on a chip | Country | United Kingdom of Great Britain and Northern Ireland |
| Author/Editor | Royal Society of Chemistry (Great Britain) | Rightsholder | Royal Society of Chemistry |
| Date | 01/01/2001 | Publication Type | e-Journal |
| Language | English | URL | http://www.rsc.org/loc |

REQUEST DETAILS

| | | | |
|--------------------------------------------------------|--------------------------|-----------------------------|----------------------------------|
| Portion Type | Chart/graph/table/figure | Distribution | Worldwide |
| Number of charts / graphs / tables / figures requested | 1 | Translation | Original language of publication |
| Format (select all that apply) | Print, Electronic | Copies for the disabled? | No |
| Who will republish the content? | Academic institution | Minor editing privileges? | No |
| Duration of Use | Life of current edition | Incidental promotional use? | No |
| Lifetime Unit Quantity | Up to 499 | Currency | USD |
| Rights Requested | Main product | | |

NEW WORK DETAILS

| | | | |
|-----------------|----------------------------------------------------------------------------------|----------------------------|---------------------|
| Title | Expanding the droplet microfluidic community - towards a modular active platform | Institution name | Waterloo University |
| Instructor name | Marie Hebert | Expected presentation date | 2021-01-01 |

ADDITIONAL DETAILS

| | |
|------------------------|-----|
| Order reference number | N/A |
|------------------------|-----|

<https://marketplace.copyright.com/rs-ui-web/mp/license/c6fa1b5c-77a3-467f-b44b-d29992d214c2/11c99bd0-3f83-412b-bce2-be3aceafca07>

1/4

The requesting person / organization to appear on the license Marie Hebert

REUSE CONTENT DETAILS

| | | | |
|-----------------------------------------------------------|--------------|--------------------------------------------------|-------------------------------------------------------------------------------------|
| Title, description or numeric reference of the portion(s) | Figure 1 (b) | Title of the article/chapter the portion is from | Surface acoustic wave (SAW) directed droplet flow in microfluidics for PDMS devices |
| Editor of portion(s) | N/A | Author of portion(s) | Royal Society of Chemistry (Great Britain) |
| Volume of serial or monograph | N/A | Issue, if republishing an article from a serial | N/A |
| Page or page range of portion | 2626 | Publication date of portion | 2009-06-26 |

CCC Replication Terms and Conditions

1. Description of Service; Defined Terms. This Replication License enables the User to obtain licenses for republication of one or more copyrighted works as described in detail on the relevant Order Confirmation (the "Work(s)"). Copyright Clearance Center, Inc. ("CCC") grants licenses through the Service on behalf of the rights holder identified on the Order Confirmation (the "Rights holder"). "Replication", as used herein, generally means the inclusion of a Work, in whole or in part, in a new work or works, also as described on the Order Confirmation. "User", as used herein, means the person or entity making such republication.
2. The terms set forth in the relevant Order Confirmation, and any terms set by the Rights holder with respect to a particular Work, govern the terms of use of Works in connection with the Service. By using the Service, the person transacting for a republication license on behalf of the User represents and warrants that he/she/it (a) has been duly authorized by the User to accept, and hereby does accept, all such terms and conditions on behalf of User, and (b) shall inform User of all such terms and conditions. In the event such person is a "freelancer" or other third party independent of User and CCC, such party shall be deemed jointly a "User" for purposes of these terms and conditions. In any event, User shall be deemed to have accepted and agreed to all such terms and conditions if User republishes the Work in any fashion.
3. Scope of License; Limitations and Obligations.
 - 3.1. All Works and all rights therein, including copyright rights, remain the sole and exclusive property of the Rights holder. The license created by the exchange of an Order Confirmation (and/or any invoice) and payment by User of the full amount set forth on that document includes only those rights expressly set forth in the Order Confirmation and in these terms and conditions, and conveys no other rights in the Work(s) to User. All rights not expressly granted are hereby reserved.
 - 3.2. General Payment Terms: You may pay by credit card or through an account with us payable at the end of the month. If you and we agree that you may establish a standing account with CCC, then the following terms apply: Remit Payment to: Copyright Clearance Center, 29118 Network Place, Chicago, IL 60673-1291. Payments Due: Invoices are payable upon their delivery to you (or upon our notice to you that they are available to you for downloading). After 30 days, outstanding amounts will be subject to a service charge of 1-1/2% per month or, if less, the maximum rate allowed by applicable law. Unless otherwise specifically set forth in the Order Confirmation or in a separate written agreement signed by CCC, invoices are due and payable on "net 30" terms. While User may exercise the rights licensed immediately upon issuance of the Order Confirmation, the license is automatically revoked and is null and void, as if it had never been issued, if complete payment for the license is not received on a timely basis either from User directly or through a payment agent, such as a credit card company.

- 3.3. Unless otherwise provided in the Order Confirmation, any grant of rights to User (i) is "one-time" (including the editions and product family specified in the license), (ii) is non-exclusive and non-transferable and (iii) is subject to any and all limitations and restrictions (such as, but not limited to, limitations on duration of use or circulation) included in the Order Confirmation or invoice and/or in these terms and conditions. Upon completion of the licensed use, User shall either secure a new permission for further use of the Work(s) or immediately cease any new use of the Work(s) and shall render inaccessible (such as by deleting or by removing or severing links or other locators) any further copies of the Work (except for copies printed on paper in accordance with this license and still in User's stock at the end of such period).
- 3.4. In the event that the material for which a republication license is sought includes third party materials (such as photographs, illustrations, graphs, inserts and similar materials) which are identified in such material as having been used by permission, User is responsible for identifying, and seeking separate licenses (under this Service or otherwise) for, any of such third party materials; without a separate license, such third party materials may not be used.
- 3.5. Use of proper copyright notice for a Work is required as a condition of any license granted under the Service. Unless otherwise provided in the Order Confirmation, a proper copyright notice will read substantially as follows: "Republished with permission of [Rightsholder's name], from [Work's title, author, volume, edition number and year of copyright]; permission conveyed through Copyright Clearance Center, Inc. " Such notice must be provided in a reasonably legible font size and must be placed either immediately adjacent to the Work as used (for example, as part of a by-line or footnote but not as a separate electronic link) or in the place where substantially all other credits or notices for the new work containing the republished Work are located. Failure to include the required notice results in loss to the Rightsholder and CCC, and the User shall be liable to pay liquidated damages for each such failure equal to twice the use fee specified in the Order Confirmation, in addition to the use fee itself and any other fees and charges specified.
- 3.6. User may only make alterations to the Work if and as expressly set forth in the Order Confirmation. No Work may be used in any way that is defamatory, violates the rights of third parties (including such third parties' rights of copyright, privacy, publicity, or other tangible or intangible property), or is otherwise illegal, sexually explicit or obscene. In addition, User may not conjoin a Work with any other material that may result in damage to the reputation of the Rightsholder. User agrees to inform CCC if it becomes aware of any infringement of any rights in a Work and to cooperate with any reasonable request of CCC or the Rightsholder in connection therewith.
4. Indemnity. User hereby indemnifies and agrees to defend the Rightsholder and CCC, and their respective employees and directors, against all claims, liability, damages, costs and expenses, including legal fees and expenses, arising out of any use of a Work beyond the scope of the rights granted herein, or any use of a Work which has been altered in any unauthorized way by User, including claims of defamation or infringement of rights of copyright, publicity, privacy or other tangible or intangible property.
5. Limitation of Liability. UNDER NO CIRCUMSTANCES WILL CCC OR THE RIGHTSHOLDER BE LIABLE FOR ANY DIRECT, INDIRECT, CONSEQUENTIAL OR INCIDENTAL DAMAGES (INCLUDING WITHOUT LIMITATION DAMAGES FOR LOSS OF BUSINESS PROFITS OR INFORMATION, OR FOR BUSINESS INTERRUPTION) ARISING OUT OF THE USE OR INABILITY TO USE A WORK, EVEN IF ONE OF THEM HAS BEEN ADVISED OF THE POSSIBILITY OF SUCH DAMAGES. In any event, the total liability of the Rightsholder and CCC (including their respective employees and directors) shall not exceed the total amount actually paid by User for this license. User assumes full liability for the actions and omissions of its principals, employees, agents, affiliates, successors and assigns.
6. Limited Warranties. THE WORK(S) AND RIGHT(S) ARE PROVIDED "AS IS". CCC HAS THE RIGHT TO GRANT TO USER THE RIGHTS GRANTED IN THE ORDER CONFIRMATION DOCUMENT. CCC AND THE RIGHTSHOLDER DISCLAIM ALL OTHER WARRANTIES RELATING TO THE WORK(S) AND RIGHT(S), EITHER EXPRESS OR IMPLIED, INCLUDING WITHOUT LIMITATION IMPLIED WARRANTIES OF MERCHANTABILITY OR FITNESS FOR A PARTICULAR PURPOSE. ADDITIONAL RIGHTS MAY BE REQUIRED TO USE ILLUSTRATIONS, GRAPHS, PHOTOGRAPHS, ABSTRACTS, INSERTS OR OTHER PORTIONS OF THE WORK (AS OPPOSED TO THE ENTIRE WORK) IN A MANNER CONTEMPLATED BY USER;

14/12/2020

<https://marketplace.copyright.com/rs-ui-web/mp/license/c6fa1b5c-77a3-467f-b44b-d29992d214c2/11c99bd0-3f83-412b-bce2-be3aceaafca...>

USER UNDERSTANDS AND AGREES THAT NEITHER CCC NOR THE RIGHTSHOLDER MAY HAVE SUCH ADDITIONAL RIGHTS TO GRANT.

7. Effect of Breach. Any failure by User to pay any amount when due, or any use by User of a Work beyond the scope of the license set forth in the Order Confirmation and/or these terms and conditions, shall be a material breach of the license created by the Order Confirmation and these terms and conditions. Any breach not cured within 30 days of written notice thereof shall result in immediate termination of such license without further notice. Any unauthorized (but licensable) use of a Work that is terminated immediately upon notice thereof may be liquidated by payment of the Rightsholder's ordinary license price therefor; any unauthorized (and unlicensable) use that is not terminated immediately for any reason (including, for example, because materials containing the Work cannot reasonably be recalled) will be subject to all remedies available at law or in equity, but in no event to a payment of less than three times the Rightsholder's ordinary license price for the most closely analogous licensable use plus Rightsholder's and/or CCC's costs and expenses incurred in collecting such payment.

8. Miscellaneous.

8.1. User acknowledges that CCC may, from time to time, make changes or additions to the Service or to these terms and conditions, and CCC reserves the right to send notice to the User by electronic mail or otherwise for the purposes of notifying User of such changes or additions; provided that any such changes or additions shall not apply to permissions already secured and paid for.

8.2. Use of User-related information collected through the Service is governed by CCC's privacy policy, available online here:<https://marketplace.copyright.com/rs-ui-web/mp/privacy-policy>

8.3. The licensing transaction described in the Order Confirmation is personal to User. Therefore, User may not assign or transfer to any other person (whether a natural person or an organization of any kind) the license created by the Order Confirmation and these terms and conditions or any rights granted hereunder; provided, however, that User may assign such license in its entirety on written notice to CCC in the event of a transfer of all or substantially all of User's rights in the new material which includes the Work(s) licensed under this Service.

8.4. No amendment or waiver of any terms is binding unless set forth in writing and signed by the parties. The Rightsholder and CCC hereby object to any terms contained in any writing prepared by the User or its principals, employees, agents or affiliates and purporting to govern or otherwise relate to the licensing transaction described in the Order Confirmation, which terms are in any way inconsistent with any terms set forth in the Order Confirmation and/or in these terms and conditions or CCC's standard operating procedures, whether such writing is prepared prior to, simultaneously with or subsequent to the Order Confirmation, and whether such writing appears on a copy of the Order Confirmation or in a separate instrument.

8.5. The licensing transaction described in the Order Confirmation document shall be governed by and construed under the law of the State of New York, USA, without regard to the principles thereof of conflicts of law. Any case, controversy, suit, action, or proceeding arising out of, in connection with, or related to such licensing transaction shall be brought, at CCC's sole discretion, in any federal or state court located in the County of New York, State of New York, USA, or in any federal or state court whose geographical jurisdiction covers the location of the Rightsholder set forth in the Order Confirmation. The parties expressly submit to the personal jurisdiction and venue of each such federal or state court. If you have any comments or questions about the Service or Copyright Clearance Center, please contact us at 978-750-8400 or send an e-mail to support@copyright.com.

v 1.1

<https://marketplace.copyright.com/rs-ui-web/mp/license/c6fa1b5c-77a3-467f-b44b-d29992d214c2/11c99bd0-3f83-412b-bce2-be3aceaafca07>

4/4

14/12/2020

<https://marketplace.copyright.com/rs-ui-web/mp/license/ea5b3bb9-a0dd-48f2-a860-a7bb39fdaf10/1804a995-921f-42c9-a791-efa0ca60b...>Copyright
Clearance
Center

Marketplace™

Royal Society of Chemistry - License Terms and Conditions

This is a License Agreement between Marie Hebert ("You") and Royal Society of Chemistry ("Publisher") provided by Copyright Clearance Center ("CCC"). The license consists of your order details, the terms and conditions provided by Royal Society of Chemistry, and the CCC terms and conditions.

All payments must be made in full to CCC.

| | | | |
|------------------|-------------|-------------|------------------------------------|
| Order Date | 14-Dec-2020 | Type of Use | Republish in a thesis/dissertation |
| Order license ID | 1084066-1 | Publisher | ROYAL SOCIETY OF CHEMISTRY |
| ISSN | 1473-0189 | Portion | Image/photo/illustration |

LICENSED CONTENT

| | | | |
|-------------------|--------------------------------------------|------------------|-------------------------------------------------------------|
| Publication Title | Lab on a chip | Country | United Kingdom of Great Britain and Northern Ireland |
| Author/Editor | Royal Society of Chemistry (Great Britain) | Rightsholder | Royal Society of Chemistry |
| Date | 01/01/2001 | Publication Type | e-Journal |
| Language | English | URL | http://www.rsc.org/loc |

REQUEST DETAILS

| | | | |
|-------------------------------------------|--------------------------|-----------------------------|----------------------------------|
| Portion Type | Image/photo/illustration | Distribution | Worldwide |
| Number of images / photos / illustrations | 1 | Translation | Original language of publication |
| Format (select all that apply) | Print, Electronic | Copies for the disabled? | No |
| Who will republish the content? | Academic institution | Minor editing privileges? | No |
| Duration of Use | Life of current edition | Incidental promotional use? | No |
| Lifetime Unit Quantity | Up to 499 | Currency | USD |
| Rights Requested | Main product | | |

NEW WORK DETAILS

| | | | |
|-----------------|----------------------------------------------------------------------------------|----------------------------|---------------------|
| Title | Expanding the droplet microfluidic community - towards a modular active platform | Institution name | Waterloo University |
| Instructor name | Marie Hebert | Expected presentation date | 2021-01-01 |

ADDITIONAL DETAILS

| | |
|------------------------|-----|
| Order reference number | N/A |
|------------------------|-----|

<https://marketplace.copyright.com/rs-ui-web/mp/license/ea5b3bb9-a0dd-48f2-a860-a7bb39fdaf10/1804a995-921f-42c9-a791-efa0ca60ba68>

1/4

The requesting person / organization to appear on the license Marie Hebert

REUSE CONTENT DETAILS

| | | | |
|-----------------------------------------------------------|--------------|--------------------------------------------------|----------------------------------------------------------------------------------------------------------------|
| Title, description or numeric reference of the portion(s) | Figure 4 (c) | Title of the article/chapter the portion is from | Fluorescence-activated droplet sorting (FADS): efficient microfluidic cell sorting based on enzymatic activity |
| Editor of portion(s) | N/A | Author of portion(s) | Royal Society of Chemistry (Great Britain) |
| Volume of serial or monograph | N/A | Issue, if republishing an article from a serial | N/A |
| Page or page range of portion | 1853 | Publication date of portion | 2009-04-23 |

CCC Republication Terms and Conditions

1. Description of Service; Defined Terms. This Republication License enables the User to obtain licenses for republication of one or more copyrighted works as described in detail on the relevant Order Confirmation (the "Work(s)"). Copyright Clearance Center, Inc. ("CCC") grants licenses through the Service on behalf of the rightsholder identified on the Order Confirmation (the "Rightsholder"). "Republishing", as used herein, generally means the inclusion of a Work, in whole or in part, in a new work or works, also as described on the Order Confirmation. "User", as used herein, means the person or entity making such republication.
2. The terms set forth in the relevant Order Confirmation, and any terms set by the Rightsholder with respect to a particular Work, govern the terms of use of Works in connection with the Service. By using the Service, the person transacting for a republication license on behalf of the User represents and warrants that he/she/it (a) has been duly authorized by the User to accept, and hereby does accept, all such terms and conditions on behalf of User, and (b) shall inform User of all such terms and conditions. In the event such person is a "freelancer" or other third party independent of User and CCC, such party shall be deemed jointly a "User" for purposes of these terms and conditions. In any event, User shall be deemed to have accepted and agreed to all such terms and conditions if User republishes the Work in any fashion.
3. Scope of License; Limitations and Obligations.
 - 3.1. All Works and all rights therein, including copyright rights, remain the sole and exclusive property of the Rightsholder. The license created by the exchange of an Order Confirmation (and/or any invoice) and payment by User of the full amount set forth on that document includes only those rights expressly set forth in the Order Confirmation and in these terms and conditions, and conveys no other rights in the Work(s) to User. All rights not expressly granted are hereby reserved.
 - 3.2. General Payment Terms: You may pay by credit card or through an account with us payable at the end of the month. If you and we agree that you may establish a standing account with CCC, then the following terms apply: Remit Payment to: Copyright Clearance Center, 29118 Network Place, Chicago, IL 60673-1291. Payments Due: Invoices are payable upon their delivery to you (or upon our notice to you that they are available to you for downloading). After 30 days, outstanding amounts will be subject to a service charge of 1-1/2% per month or, if less, the maximum rate allowed by applicable law. Unless otherwise specifically set forth in the Order Confirmation or in a separate written agreement signed by CCC, invoices are due and payable on "net 30" terms. While User may exercise the rights licensed immediately upon issuance of the Order Confirmation, the license is automatically revoked and is null and void, as if it had never been issued, if complete payment for the license is not received on a timely basis either from User directly or through a payment agent, such as a credit card company.

- 3.3. Unless otherwise provided in the Order Confirmation, any grant of rights to User (i) is "one-time" (including the editions and product family specified in the license), (ii) is non-exclusive and non-transferable and (iii) is subject to any and all limitations and restrictions (such as, but not limited to, limitations on duration of use or circulation) included in the Order Confirmation or invoice and/or in these terms and conditions. Upon completion of the licensed use, User shall either secure a new permission for further use of the Work(s) or immediately cease any new use of the Work(s) and shall render inaccessible (such as by deleting or by removing or severing links or other locators) any further copies of the Work (except for copies printed on paper in accordance with this license and still in User's stock at the end of such period).
- 3.4. In the event that the material for which a republication license is sought includes third party materials (such as photographs, illustrations, graphs, inserts and similar materials) which are identified in such material as having been used by permission, User is responsible for identifying, and seeking separate licenses (under this Service or otherwise) for, any of such third party materials; without a separate license, such third party materials may not be used.
- 3.5. Use of proper copyright notice for a Work is required as a condition of any license granted under the Service. Unless otherwise provided in the Order Confirmation, a proper copyright notice will read substantially as follows: "Republished with permission of [Rightsholder's name], from [Work's title, author, volume, edition number and year of copyright]; permission conveyed through Copyright Clearance Center, Inc. " Such notice must be provided in a reasonably legible font size and must be placed either immediately adjacent to the Work as used (for example, as part of a by-line or footnote but not as a separate electronic link) or in the place where substantially all other credits or notices for the new work containing the republished Work are located. Failure to include the required notice results in loss to the Rightsholder and CCC, and the User shall be liable to pay liquidated damages for each such failure equal to twice the use fee specified in the Order Confirmation, in addition to the use fee itself and any other fees and charges specified.
- 3.6. User may only make alterations to the Work if and as expressly set forth in the Order Confirmation. No Work may be used in any way that is defamatory, violates the rights of third parties (including such third parties' rights of copyright, privacy, publicity, or other tangible or intangible property), or is otherwise illegal, sexually explicit or obscene. In addition, User may not conjoin a Work with any other material that may result in damage to the reputation of the Rightsholder. User agrees to inform CCC if it becomes aware of any infringement of any rights in a Work and to cooperate with any reasonable request of CCC or the Rightsholder in connection therewith.
4. Indemnity. User hereby indemnifies and agrees to defend the Rightsholder and CCC, and their respective employees and directors, against all claims, liability, damages, costs and expenses, including legal fees and expenses, arising out of any use of a Work beyond the scope of the rights granted herein, or any use of a Work which has been altered in any unauthorized way by User, including claims of defamation or infringement of rights of copyright, publicity, privacy or other tangible or intangible property.
5. Limitation of Liability. UNDER NO CIRCUMSTANCES WILL CCC OR THE RIGHTSHOLDER BE LIABLE FOR ANY DIRECT, INDIRECT, CONSEQUENTIAL OR INCIDENTAL DAMAGES (INCLUDING WITHOUT LIMITATION DAMAGES FOR LOSS OF BUSINESS PROFITS OR INFORMATION, OR FOR BUSINESS INTERRUPTION) ARISING OUT OF THE USE OR INABILITY TO USE A WORK, EVEN IF ONE OF THEM HAS BEEN ADVISED OF THE POSSIBILITY OF SUCH DAMAGES. In any event, the total liability of the Rightsholder and CCC (including their respective employees and directors) shall not exceed the total amount actually paid by User for this license. User assumes full liability for the actions and omissions of its principals, employees, agents, affiliates, successors and assigns.
6. Limited Warranties. THE WORK(S) AND RIGHT(S) ARE PROVIDED "AS IS". CCC HAS THE RIGHT TO GRANT TO USER THE RIGHTS GRANTED IN THE ORDER CONFIRMATION DOCUMENT. CCC AND THE RIGHTSHOLDER DISCLAIM ALL OTHER WARRANTIES RELATING TO THE WORK(S) AND RIGHT(S), EITHER EXPRESS OR IMPLIED, INCLUDING WITHOUT LIMITATION IMPLIED WARRANTIES OF MERCHANTABILITY OR FITNESS FOR A PARTICULAR PURPOSE. ADDITIONAL RIGHTS MAY BE REQUIRED TO USE ILLUSTRATIONS, GRAPHS, PHOTOGRAPHS, ABSTRACTS, INSERTS OR OTHER PORTIONS OF THE WORK (AS OPPOSED TO THE ENTIRE WORK) IN A MANNER CONTEMPLATED BY USER;

USER UNDERSTANDS AND AGREES THAT NEITHER CCC NOR THE RIGHTSHOLDER MAY HAVE SUCH ADDITIONAL RIGHTS TO GRANT.

7. Effect of Breach. Any failure by User to pay any amount when due, or any use by User of a Work beyond the scope of the license set forth in the Order Confirmation and/or these terms and conditions, shall be a material breach of the license created by the Order Confirmation and these terms and conditions. Any breach not cured within 30 days of written notice thereof shall result in immediate termination of such license without further notice. Any unauthorized (but licensable) use of a Work that is terminated immediately upon notice thereof may be liquidated by payment of the Rightsholder's ordinary license price therefor; any unauthorized (and unlicensable) use that is not terminated immediately for any reason (including, for example, because materials containing the Work cannot reasonably be recalled) will be subject to all remedies available at law or in equity, but in no event to a payment of less than three times the Rightsholder's ordinary license price for the most closely analogous licensable use plus Rightsholder's and/or CCC's costs and expenses incurred in collecting such payment.

8. Miscellaneous.

8.1. User acknowledges that CCC may, from time to time, make changes or additions to the Service or to these terms and conditions, and CCC reserves the right to send notice to the User by electronic mail or otherwise for the purposes of notifying User of such changes or additions; provided that any such changes or additions shall not apply to permissions already secured and paid for.

8.2. Use of User-related information collected through the Service is governed by CCC's privacy policy, available online here:<https://marketplace.copyright.com/rs-ui-web/mp/privacy-policy>

8.3. The licensing transaction described in the Order Confirmation is personal to User. Therefore, User may not assign or transfer to any other person (whether a natural person or an organization of any kind) the license created by the Order Confirmation and these terms and conditions or any rights granted hereunder; provided, however, that User may assign such license in its entirety on written notice to CCC in the event of a transfer of all or substantially all of User's rights in the new material which includes the Work(s) licensed under this Service.

8.4. No amendment or waiver of any terms is binding unless set forth in writing and signed by the parties. The Rightsholder and CCC hereby object to any terms contained in any writing prepared by the User or its principals, employees, agents or affiliates and purporting to govern or otherwise relate to the licensing transaction described in the Order Confirmation, which terms are in any way inconsistent with any terms set forth in the Order Confirmation and/or in these terms and conditions or CCC's standard operating procedures, whether such writing is prepared prior to, simultaneously with or subsequent to the Order Confirmation, and whether such writing appears on a copy of the Order Confirmation or in a separate instrument.

8.5. The licensing transaction described in the Order Confirmation document shall be governed by and construed under the law of the State of New York, USA, without regard to the principles thereof of conflicts of law. Any case, controversy, suit, action, or proceeding arising out of, in connection with, or related to such licensing transaction shall be brought, at CCC's sole discretion, in any federal or state court located in the County of New York, State of New York, USA, or in any federal or state court whose geographical jurisdiction covers the location of the Rightsholder set forth in the Order Confirmation. The parties expressly submit to the personal jurisdiction and venue of each such federal or state court. If you have any comments or questions about the Service or Copyright Clearance Center, please contact us at 978-750-8400 or send an e-mail to support@copyright.com.

v 1.1

References

- [1] A. ABDOLLAHI, R. N. SHARMA, AND A. VATANI, *Fluid flow and heat transfer of liquid-liquid two phase flow in microchannels: A review*, International Communications in Heat and Mass Transfer, 84 (2017), pp. 66–74.
- [2] G. ACUÑA, F. CUBILLOS, J. THIBAUT, AND E. LATRILLE, *Comparison of methods for training grey-box neural network models*, Computers & Chemical Engineering, 23 (1999), pp. S561–S564.
- [3] B. J. ADZIMA AND S. S. VELANKAR, *Pressure drops for droplet flows in microfluidic channels*, Journal of Micromechanics and Microengineering, 16 (2006), p. 1504.
- [4] H. AHMED, S. RAMESAN, L. LEE, A. R. REZK, AND L. Y. YEO, *On-chip generation of vortical flows for microfluidic centrifugation*, Small, 16 (2020), p. 1903605.
- [5] G.-N. AHN, T. YU, H.-J. LEE, K.-W. GYAK, J.-H. KANG, D. YOU, AND D.-P. KIM, *A numbering-up metal microreactor for the high-throughput production of a commercial drug by copper catalysis*, Lab on a Chip, 19 (2019), pp. 3535–3542.
- [6] V. ANAGNOSTIDIS, B. SHERLOCK, J. METZ, P. MAIR, F. HOLLFELDER, AND F. GIELEN, *Deep learning guided image-based droplet sorting for on-demand selection and analysis of single cells and 3d cell cultures*, Lab on a Chip, 20 (2020), pp. 889–900.
- [7] ANDOR, *Zyla scmos: Speed and sensitivity for physical science imaging and spectroscopy*.
- [8] S. L. ANNA, *Droplets and bubbles in microfluidic devices*, Annual Review of Fluid Mechanics, 48 (2016), pp. 285–309.

- [9] I. E. ARACI, M. ROBLES, AND S. R. QUAKE, *A reusable microfluidic device provides continuous measurement capability and improves the detection limit of digital biology*, *Lab on a Chip*, 16 (2016), pp. 1573–1578.
- [10] M. D. ARMANI, S. V. CHAUDHARY, R. PROBST, AND B. SHAPIRO, *Using feedback control of microflows to independently steer multiple particles*, *Journal of Microelectromechanical systems*, 15 (2006), pp. 945–956.
- [11] L. ARMBRECHT AND P. DITTRICH, *Recent advances in the analysis of single cells*, *Analytical Chemistry*, 89 (2017), pp. 2–21.
- [12] S. ATABAKHSH AND S. J. ASHTIANI, *Thermal actuation and confinement of water droplets on paper-based digital microfluidics devices*, *Microfluidics and Nanofluidics*, 22 (2018), p. 43.
- [13] M. AZIZI, M. ZAFERANI, S. H. CHEONG, AND A. ABBASPOUR-RAD, *Pathogenic bacteria detection using rna-based loop-mediated isothermal-amplification-assisted nucleic acid amplification via droplet microfluidics*, *ACS sensors*, (2019).
- [14] C. F. BABBS, *Behavior of a viscoelastic valveless pump: a simple theory with experimental validation*, *Biomedical engineering online*, 9 (2010), p. 42.
- [15] Y. BAI, X. HE, D. LIU, S. N. PATIL, D. BRATTON, A. HUEBNER, F. HOLLFELDER, C. ABELL, AND W. T. HUCK, *A double droplet trap system for studying mass transport across a droplet-droplet interface*, *Lab on a chip*, 10 (2010), pp. 1281–1285.
- [16] Y. BAI, S. PATIL, S. BOWDEN, S. POULTER, J. PAN, G. SALMOND, M. WELCH, W. HUCK, AND C. ABELL, *Intra-species bacterial quorum sensing studied at single cell level in a double droplet trapping system*, *International journal of molecular sciences*, 14 (2013), pp. 10570–10581.
- [17] A. BALCK, M. MICHALZIK, L. AL-HALABI, S. DÜBEL, AND S. BÜTTGENBACH, *Design and fabrication of a lab-on-a-chip for point-of-care diagnostics*, *Sensors & Transducers*, 127 (2011), p. 102.
- [18] J.-C. BARET, *Surfactants in droplet-based microfluidics*, *Lab on a Chip*, 12 (2012), pp. 422–433.

- [19] J.-C. BARET, O. J. MILLER, V. TALY, M. RYCKELYNCK, A. EL-HARRAK, L. FRENZ, C. RICK, M. L. SAMUELS, J. B. HUTCHISON, J. J. AGRESTI, ET AL., *Fluorescence-activated droplet sorting (fads): efficient microfluidic cell sorting based on enzymatic activity*, *Lab on a Chip*, 9 (2009), pp. 1850–1858.
- [20] J. BARMAN, W. SHAO, B. TANG, D. YUAN, J. GROENEWOLD, AND G. ZHOU, *Wettability manipulation by interface-localized liquid dielectrophoresis: Fundamentals and applications*, *Micromachines*, 10 (2019), p. 329.
- [21] C. N. BAROUD, F. GALLAIRE, AND R. DANGLA, *Dynamics of microfluidic droplets*, *Lab on a Chip*, 10 (2010), pp. 2032–2045.
- [22] A. S. BAZANELLA, M. GEVERS, AND L. MIŠKOVIC, *Closed-loop identification of mimo systems: a new look at identifiability and experiment design*, *European Journal of Control*, 16 (2010), pp. 228–239.
- [23] A. A. S. BHAGAT, H. BOW, H. W. HOU, S. J. TAN, J. HAN, AND C. T. LIM, *Microfluidics for cell separation*, *Medical & biological engineering & computing*, 48 (2010), pp. 999–1014.
- [24] S. S. BITHI, M. NEKOU EI, AND S. A. VANAPALLI, *Bistability in the hydrodynamic resistance of a drop trapped at a microcavity junction*, *Microfluidics and Nanofluidics*, 21 (2017), p. 164.
- [25] P. BODÉNÈS, H.-Y. WANG, T.-H. LEE, H.-Y. CHEN, AND C.-Y. WANG, *Microfluidic techniques for enhancing biofuel and biorefinery industry based on microalgae*, *Biotechnology for biofuels*, 12 (2019), p. 33.
- [26] C. S. BOLAND, U. KHAN, G. RYAN, S. BARWICH, R. CHARIFOU, A. HARVEY, C. BACKES, Z. LI, M. S. FERREIRA, M. E. MÖBIUS, ET AL., *Sensitive electromechanical sensors using viscoelastic graphene-polymer nanocomposites*, *Science*, 354 (2016), pp. 1257–1260.
- [27] G. E. BOX AND N. R. DRAPER, *Response surfaces, mixtures, and ridge analyses*, vol. 649, John Wiley & Sons, 2007.
- [28] M. R. BRINGER, C. J. GERDTS, H. SONG, J. D. TICE, AND R. F. ISMAGILOV, *Microfluidic systems for chemical kinetics that rely on chaotic mixing in droplets*, *Philosophical Transactions of the Royal Society of London A: Mathematical, Physical and Engineering Sciences*, 362 (2004), pp. 1087–1104.

- [29] K. BROWER, R. R. PUCCINELLI, C. J. MARKIN, T. C. SHIMKO, S. A. LONGWELL, B. CRUZ, R. GOMEZ-SJOBERG, AND P. M. FORDYCE, *An open-source, programmable pneumatic setup for operation and automated control of single-and multi-layer microfluidic devices*, HardwareX, 3 (2018), pp. 117–134.
- [30] R. BRUN, P. REICHERT, AND H. R. KÜNSCH, *Practical identifiability analysis of large environmental simulation models*, Water Resources Research, 37 (2001), pp. 1015–1030.
- [31] H. BRUUS, *Theoretical microfluidics*, vol. 18, Oxford university press Oxford, 2008.
- [32] S. ČANIĆ, J. TAMBAČA, G. GUIDOBONI, A. MIKELIĆ, C. J. HARTLEY, AND D. ROSENSTRAUCH, *Modeling viscoelastic behavior of arterial walls and their interaction with pulsatile blood flow*, SIAM Journal on Applied Mathematics, 67 (2006), pp. 164–193.
- [33] H. CAO, X. ZHOU, AND Y. ZENG, *Microfluidic exponential rolling circle amplification for sensitive microrna detection directly from biological samples*, Sensors and Actuators B: Chemical, 279 (2019), pp. 447–457.
- [34] M. A. CARTAS AYALA, *Hydrodynamic resistance and sorting of deformable particles in microfluidic circuits*, PhD thesis, Massachusetts Institute of Technology, 2013.
- [35] E. CASTRO-HERNÁNDEZ, P. GARCÍA-SÁNCHEZ, S. H. TAN, A. M. GAÑÁN-CALVO, J.-C. BARET, AND A. RAMOS, *Breakup length of ac electrified jets in a microfluidic flow-focusing junction*, Microfluidics and Nanofluidics, 19 (2015), pp. 787–794.
- [36] W. CHEN, T. GUO, Y. KAPOOR, C. RUSSELL, P. JUYAL, A. YEN, AND R. L. HARTMAN, *An automated microfluidic system for the investigation of asphaltene deposition and dissolution in porous media*, Lab on a Chip, 19 (2019), pp. 3628–3640.
- [37] X. CHEN AND C. L. REN, *A microfluidic chip integrated with droplet generation, pairing, trapping, merging, mixing and releasing*, RSC Advances, 7 (2017), pp. 16738–16750.

- [38] Y.-S. CHEN, Y.-D. MA, C. CHEN, S.-C. SHIESH, AND G.-B. LEE, *An integrated microfluidic system for on-chip enrichment and quantification of circulating extracellular vesicles from whole blood*, *Lab on a Chip*, 19 (2019), pp. 3305–3315.
- [39] A. CHIADÒ, G. PALMARA, A. CHIAPPONE, C. TANZANU, C. F. PIRRI, I. ROPPOLO, AND F. FRASCELLA, *A modular 3d printed lab-on-a-chip for early cancer detection*, *Lab on a Chip*, 20 (2020), pp. 665–674.
- [40] S. CHOI, M. G. LEE, AND J.-K. PARK, *Microfluidic parallel circuit for measurement of hydraulic resistance*, *Biomicrofluidics*, 4 (2010), p. 034110.
- [41] Z. Z. CHONG, S. H. TAN, A. M. GAÑÁN-CALVO, S. B. TOR, N. H. LOH, AND N.-T. NGUYEN, *Active droplet generation in microfluidics*, *Lab on a Chip*, 16 (2016), pp. 35–58.
- [42] G. F. CHRISTOPHER AND S. L. ANNA, *Microfluidic methods for generating continuous droplet streams*, *Journal of Physics D: Applied Physics*, 40 (2007), p. R319.
- [43] I. C. CHRISTOV, V. COGNET, T. C. SHIDHORE, AND H. A. STONE, *Flow ratepressure drop relation for deformable shallow microfluidic channels*, *Journal of Fluid Mechanics*, 841 (2018), p. 267286.
- [44] L. CHRONOPOULOU, C. SPARAGO, AND C. PALOCCI, *A modular microfluidic platform for the synthesis of biopolymeric nanoparticles entrapping organic actives*, *Journal of nanoparticle research*, 16 (2014), p. 2703.
- [45] J. CHUNG, H. Y. HWANG, Y. CHEN, AND T. Y. LEE, *Microfluidic packaging of high-density cmos electrode array for lab-on-a-chip applications*, *Sensors and Actuators B: Chemical*, 254 (2018), pp. 542–550.
- [46] K. CHURSKI, T. S. KAMINSKI, S. JAKIELA, W. KAMYSZ, W. BARANSKA-RYBAK, D. B. WEIBEL, AND P. GARSTECKI, *Rapid screening of antibiotic toxicity in an automated microdroplet system*, *Lab on a Chip*, 12 (2012), pp. 1629–1637.
- [47] K. CHURSKI, P. KORCZYK, AND P. GARSTECKI, *High-throughput automated droplet microfluidic system for screening of reaction conditions*, *Lab on a Chip*, 10 (2010), pp. 816–818.

- [48] L. CLIME, J. DAOUD, D. BRASSARD, L. MALIC, M. GEISSLER, AND T. VERES, *Active pumping and control of flows in centrifugal microfluidics*, *Microfluidics and Nanofluidics*, 23 (2019), p. 29.
- [49] C. M. CLOSE, D. K. FREDERICK, AND J. C. NEWELL, *Modeling and analysis of dynamic systems*, vol. 3, Wiley New York, NY, 2002.
- [50] D. J. COLLINS, T. ALAN, K. HELMERSON, AND A. NEILD, *Surface acoustic waves for on-demand production of picoliter droplets and particle encapsulation*, *Lab on a Chip*, 13 (2013), pp. 3225–3231.
- [51] M. COURTNEY, X. CHEN, S. CHAN, T. MOHAMED, P. P. RAO, AND C. L. REN, *Droplet microfluidic system with on-demand trapping and releasing of droplet for drug screening applications*, *Analytical chemistry*, 89 (2016), pp. 910–915.
- [52] H. J. CRABTREE, J. LAUZON, Y. C. MORRISSEY, B. J. TAYLOR, T. LIANG, R. W. JOHNSTONE, A. J. STICKEL, D. P. MANAGE, A. ATRAZHEV, C. J. BACKHOUSE, ET AL., *Inhibition of on-chip pcr using pdms–glass hybrid microfluidic chips*, *Microfluidics and nanofluidics*, 13 (2012), pp. 383–398.
- [53] M. M. CRANE, B. SANDS, C. BATTAGLIA, B. JOHNSON, S. YUN, M. KAEBERLEIN, R. BRENT, AND A. MENDENHALL, *In vivo measurements reveal a single 5-intron is sufficient to increase protein expression level in caenorhabditis elegans*, *Scientific Reports*, 9 (2019), p. 9192.
- [54] J. L. CRASSIDIS AND J. L. JUNKINS, *Optimal estimation of dynamic systems*, CRC press, 2011.
- [55] D. CRAWFORD, C. SMITH, AND G. WHYTE, *Image-based closed-loop feedback for highly mono-dispersed microdroplet production*, *Scientific reports*, 7 (2017), p. 10545.
- [56] R. CROSS, *Elastic and viscous properties of silly putty*, *American Journal of Physics*, 80 (2012), pp. 870–875.
- [57] T. CUBAUD AND C.-M. HO, *Transport of bubbles in square microchannels*, *Physics of fluids*, 16 (2004), pp. 4575–4585.
- [58] O. CYBULSKI AND P. GARSTECKI, *Transport of resistance through a long microfluidic channel*, *Physical Review E*, 82 (2010), p. 056301.

- [59] O. CYBULSKI, S. JAKIELA, AND P. GARSTECKI, *Whole teflon valves for handling droplets*, Lab on a Chip, 16 (2016), pp. 2198–2210.
- [60] J. DALMIEDA AND P. KRUSE, *Metal cation detection in drinking water*, Sensors, 19 (2019), p. 5134.
- [61] P. DANCKWERTS, *The definition and measurement of some characteristics of mixtures*, Applied Scientific Research, Section A, 3 (1952), pp. 279–296.
- [62] T. DATTA-CHAUDHURI, E. SMELA, AND P. A. ABSHIRE, *System-on-chip considerations for heterogeneous integration of cmos and fluidic bio-interfaces*, IEEE transactions on biomedical circuits and systems, 10 (2016), pp. 1129–1142.
- [63] A. DE LOZAR, A. HAZEL, AND A. JUEL, *Scaling properties of coating flows in rectangular channels*, Physical review letters, 99 (2007), p. 234501.
- [64] A. J. DEMELLO, *Control and detection of chemical reactions in microfluidic systems*, Nature, 442 (2006), pp. 394–402.
- [65] X. DING, P. LI, S.-C. S. LIN, Z. S. STRATTON, N. NAMA, F. GUO, D. SLOTCAVAGE, X. MAO, J. SHI, F. COSTANZO, ET AL., *Surface acoustic wave microfluidics*, Lab on a Chip, 13 (2013), pp. 3626–3649.
- [66] C. DIXON, J. LAMANNA, AND A. R. WHEELER, *Direct loading of blood for plasma separation and diagnostic assays on a digital microfluidic device*, Lab on a Chip, (2020).
- [67] E. O. DOEBELIN AND D. N. MANIK, *Measurement systems: application and design*, (2007).
- [68] DOLOMITE, *Mitos fluika pressure and vacuum pumps datasheet*.
- [69] X. DONG, P. SONG, AND X. LIU, *An automated microfluidic system for morphological measurement and size-based sorting of c. elegans*, IEEE transactions on nanobioscience, 18 (2019), pp. 373–380.
- [70] R. DORF AND R. BISHOP, *Modern Control Systems*, Pearson Prentice Hall, 2011.
- [71] C. DRIESCHNER, S. KÖNEMANN, P. RENAUD, AND K. SCHIRMER, *Fish-gut-on-chip: development of a microfluidic bioreactor to study the role of the fish intestine in vitro*, Lab on a Chip, 19 (2019), pp. 3268–3276.

- [72] W. J. DUNCANSON, T. LIN, A. R. ABATE, S. SEIFFERT, R. K. SHAH, AND D. A. WEITZ, *Microfluidic synthesis of advanced microparticles for encapsulation and controlled release*, Lab on a Chip, 12 (2012), pp. 2135–2145.
- [73] T. A. DUNCOMBE, A. M. TENTORI, AND A. E. HERR, *Microfluidics: re-framing biological enquiry*, Nature Reviews Molecular Cell Biology, 16 (2015), p. 554.
- [74] S. DURAISWAMY AND S. A. KHAN, *Droplet-based microfluidic synthesis of anisotropic metal nanocrystals*, small, 5 (2009), pp. 2828–2834.
- [75] F. EJEIAN, P. ETEDALI, H.-A. MANSOURI-TEHRANI, A. SOOZANIPOUR, Z.-X. LOW, M. ASADNIA, A. TAHERI-KAFRANI, AND A. RAZMJOU, *Biosensors for wastewater monitoring: A review*, Biosensors and Bioelectronics, 118 (2018), pp. 66–79.
- [76] C. ELBUKEN, T. GLAWDEL, D. CHAN, AND C. L. REN, *Detection of microdroplet size and speed using capacitive sensors*, Sensors and Actuators A: Physical, 171 (2011), pp. 55–62.
- [77] ELVEFLOW, *Product catalog 2019*.
- [78] S.-K. FAN, C. HASHI, AND C.-J. KIM, *Manipulation of multiple droplets on $n \times m$ grid by cross-reference ewod driving scheme and pressure-contact packaging*, Micro Electro Mechanical Systems, 2003. MEMS-03 Kyoto. IEEE the Sixteenth Annual International Conference on, (2003), pp. 694–697.
- [79] S. FENG, L. YI, L. ZHAO-MIAO, C. REN-TUO, AND W. GUI-REN, *Advances in micro-droplets coalescence using microfluidics*, Chinese Journal of Analytical Chemistry, 43 (2015), pp. 1942–1954.
- [80] J. FERREIRA, F. CASTRO, F. ROCHA, AND S. KUHN, *Protein crystallization in a droplet-based microfluidic device: Hydrodynamic analysis and study of the phase behaviour*, Chemical Engineering Science, 191 (2018), pp. 232–244.
- [81] FLIR, *Oryx – p/n: Orx-10g-123s6, ultra-high resolutions*.
- [82] FLUIGENT, *Mfcs-ez microfluidic flow control system user manual*, 2016.
- [83] S. P. FODOR, J. L. READ, M. C. PIRRUNG, L. STRYER, A. T. LU, AND D. SOLAS, *Light-directed, spatially addressable parallel chemical synthesis*, science, 251 (1991), pp. 767–773.

- [84] L. FORMAGGIA AND A. VENEZIANI, *Reduced and multiscale models for the human cardiovascular system*, Lecture notes VKI lecture series, 7 (2003).
- [85] T. FRANKE, A. R. ABATE, D. A. WEITZ, AND A. WIXFORTH, *Surface acoustic wave (saw) directed droplet flow in microfluidics for pdms devices*, Lab on a Chip, 9 (2009), pp. 2625–2627.
- [86] H. FU, P. SONG, Q. WU, C. ZHAO, P. PAN, X. LI, N. Y. LI-JESSEN, AND X. LIU, *A paper-based microfluidic platform with shape-memory-polymer-actuated fluid valves for automated multi-step immunoassays*, Microsystems & nanoengineering, 5 (2019), pp. 1–12.
- [87] Y. FU, C. LI, S. LU, W. ZHOU, F. TANG, X. S. XIE, AND Y. HUANG, *Uniform and accurate single-cell sequencing based on emulsion whole-genome amplification*, Proceedings of the National Academy of Sciences, 112 (2015), pp. 11923–11928.
- [88] M. J. FUERSTMAN, A. LAI, M. E. THURLOW, S. S. SHEVKOPLYAS, H. A. STONE, AND G. M. WHITESIDES, *The pressure drop along rectangular microchannels containing bubbles*, Lab on a Chip, 7 (2007), pp. 1479–1489.
- [89] A. GÁBOR, A. F. VILLAYERDE, AND J. R. BANGA, *Parameter identifiability analysis and visualization in large-scale kinetic models of biosystems*, BMC systems biology, 11 (2017), p. 54.
- [90] R. Z. GAO, M. HÉBERT, J. HUISSOON, AND C. L. REN, *μ pump: An open-source pressure pump for precision fluid handling in microfluidics*, HardwareX, 7 (2020), p. e00096.
- [91] E. GARCIA-EGIDO, V. SPIKMANS, S. Y. WONG, AND B. H. WARRINGTON, *Synthesis and analysis of combinatorial libraries performed in an automated micro reactor system*, Lab on a Chip, 3 (2003), pp. 73–76.
- [92] N. GARG, R. TONA, P. MARTIN, P. MARTIN-SOLADANA, G. WARD, N. DOUILLET, AND D. LAI, *Seeded droplet microfluidic system for small molecule crystallization*, Lab on a Chip, (2020).
- [93] P. GARSTECKI, M. J. FUERSTMAN, H. A. STONE, AND G. M. WHITESIDES, *Formation of droplets and bubbles in a microfluidic t-junctions: scaling and mechanism of break-up*, Lab on a Chip, 6 (2006), pp. 437–446.
- [94] A. GELB, *Applied optimal estimation*, MIT press, 1974.

- [95] J. GERTNER, *The idea factory: Bell Labs and the great age of American innovation*, Penguin, 2012.
- [96] T. GERVAIS, J. EL-ALI, A. GÜNTHER, AND K. F. JENSEN, *Flow-induced deformation of shallow microfluidic channels*, *Lab on a Chip*, 6 (2006), pp. 500–507.
- [97] Y. H. GHALLAB, H. A. EL-HAMID, AND Y. ISMAIL, *Lab on a chip based on cmos technology: system architectures, microfluidic packaging, and challenges*, *IEEE Design & Test*, 32 (2015), pp. 20–31.
- [98] P. GIMÉNEZ-GÓMEZ, A. BALDI, C. AYORA, AND C. FERNÁNDEZ-SÁNCHEZ, *Automated determination of as (iii) in waters with an electrochemical sensor integrated into a modular microfluidic system*, *ACS sensors*, (2019).
- [99] C. GIRABAWA AND S. FRADEN, *An image-driven drop-on-demand system*, *Sensors and Actuators B: Chemical*, 238 (2017), pp. 532–539.
- [100] T. GLAWDEL, C. ELBUKEN, AND C. L. REN, *Droplet formation in microfluidic t-junction generators operating in the transitional regime. i. experimental observations*, *Physical Review E*, 85 (2012), p. 016322.
- [101] T. GLAWDEL AND C. L. REN, *Global network design for robust operation of microfluidic droplet generators with pressure-driven flow*, *Microfluidics and nanofluidics*, 13 (2012), pp. 469–480.
- [102] N. GODINO, F. PFISTERER, T. GERLING, C. GUERNTH-MARSCHNER, C. DUSCHL, AND M. KIRSCHBAUM, *Combining dielectrophoresis and computer vision for precise and fully automated single-cell handling and analysis*, *Lab on a Chip*, 19 (2019), pp. 4016–4020.
- [103] J. R. GOODELL, J. P. MCMULLEN, N. ZABORENKO, J. R. MALONEY, C.-X. HO, K. F. JENSEN, J. A. PORCO JR, AND A. B. BEELER, *Development of an automated microfluidic reaction platform for multidimensional screening: reaction discovery employing bicyclo [3.2. 1] octanoid scaffolds*, *The Journal of organic chemistry*, 74 (2009), pp. 6169–6180.
- [104] C. M. GRIFFITHS-JONES, M. D. HOPKIN, D. JÖNSSON, S. V. LEY, D. J. TAPOLCZAY, E. VICKERSTAFFE, AND M. LADLOW, *Fully automated flow-through synthesis of secondary sulfonamides in a binary reactor system*, *Journal of combinatorial chemistry*, 9 (2007), pp. 422–430.

- [105] H. GU, C. U. MURADE, M. H. DUIJS, AND F. MUGELE, *A microfluidic platform for on-demand formation and merging of microdroplets using electric control*, *Biomicrofluidics*, 5 (2011), p. 011101.
- [106] Y. GUAN AND B. SUN, *Detection and extraction of heavy metal ions using paper-based analytical devices fabricated via atom stamp printing*, *Microsystems & Nanoengineering*, 6 (2020), pp. 1–12.
- [107] A. GÜNTHER, M. JHUNJHUNWALA, M. THALMANN, M. A. SCHMIDT, AND K. F. JENSEN, *Micromixing of miscible liquids in segmented gas-liquid flow*, *Langmuir*, 21 (2005), pp. 1547–1555.
- [108] S.-U. HASSAN, F. GIELEN, X. NIU, AND J. B. EDEL, *Controlled one-dimensional oscillation of the belousov-zhabotinsky reaction confined within microchannels*, *RSC Advances*, 2 (2012), pp. 6408–6410.
- [109] A. C. HATCH, A. PATEL, N. R. BEER, AND A. P. LEE, *Passive droplet sorting using viscoelastic flow focusing*, *Lab on a Chip*, 13 (2013), pp. 1308–1315.
- [110] M. HÉBERT, W. BAXTER, J. P. HUISOON, AND C. L. REN, *A quantitative study of the dynamic response of soft tubing for pressure-driven flow in a microfluidics context*, *Microfluidics and Nanofluidics*, 24 (2020), pp. 1–13.
- [111] M. HÉBERT, M. COURTNEY, AND C. L. REN, *Semi-automated on-demand control of individual droplets with a sample application to a drug screening assay*, *Lab on a Chip*, 19 (2019), pp. 1490–1501.
- [112] M. HÉBERT, J. P. HUISOON, AND C. L. REN, *A silicone-based soft matrix nanocomposite strain-like sensor fabricated using graphene and silly putty®*, *Sensors and Actuators A: Physical*, (2020), p. 111917.
- [113] M. HEIN, M. MOSKOPP, AND R. SEEMANN, *Flow field induced particle accumulation inside droplets in rectangular channels*, *Lab on a Chip*, 15 (2015), pp. 2879–2886.
- [114] E. HEMMIG, Y. TEMIZ, O. GOKCE, R. D. LOVCHIK, AND E. DELAMARCHE, *Transposing lateral flow immunoassays to capillary-driven microfluidics using self-coalescence modules and capillary-assembled receptor carriers*, *Analytical Chemistry*, (2019).

- [115] C. M. B. HO, S. H. NG, K. H. H. LI, AND Y.-J. YOON, *3d printed microfluidics for biological applications*, Lab on a Chip, 15 (2015), pp. 3627–3637.
- [116] S. HODGES, O. JENSEN, AND J. RALLISON, *The motion of a viscous drop through a cylindrical tube*, Journal of fluid mechanics, 501 (2004), pp. 279–301.
- [117] T.-F. HONG, W.-J. JU, M.-C. WU, C.-H. TAI, C.-H. TSAI, AND L.-M. FU, *Rapid prototyping of pmma microfluidic chips utilizing a co 2 laser*, Microfluidics and nanofluidics, 9 (2010), pp. 1125–1133.
- [118] L. HOU, W. ZHANG, L. ZHU, ET AL., *Preparation of paper micro-fluidic devices used in bio-assay based on drop-on-demand wax droplet generation*, Analytical Methods, 6 (2014), pp. 878–885.
- [119] Y.-H. HSU, W.-W. LIU, T.-H. WU, C. J.-T. LEE, Y.-H. CHEN, AND P.-C. LI, *Study of diffusive-and convective-transport mediated microtumor growth in a controlled microchamber*, Biomedical microdevices, 21 (2019), p. 7.
- [120] S.-P. HUANG, Y.-J. CHUANG, W.-B. LEE, Y.-C. TSAI, C.-N. LIN, K.-F. HSU, AND G.-B. LEE, *An integrated microfluidic system for rapid, automatic and high-throughput staining of clinical tissue samples for diagnosis of ovarian cancer*, Lab on a Chip, 20 (2020), pp. 1103–1109.
- [121] W.-Y. HUANG, C.-A. LIU, R.-S. FAN, Z.-D. LIN, K. WANG, AND G.-B. LEE, *Automatic optimization of drug cocktails on an integrated microfluidic system*, Biomicrofluidics, 11 (2017), p. 034109.
- [122] D. HUBER, A. OSKOOEI, X. CASADEVALL I SOLVAS, A. DEMELLO, AND G. V. KAIGALA, *Hydrodynamics in cell studies*, Chemical reviews, 118 (2018), pp. 2042–2079.
- [123] S. A. HUDSON, H. ECROYD, T. W. KEE, AND J. A. CARVER, *The thioflavin t fluorescence assay for amyloid fibril detection can be biased by the presence of exogenous compounds*, The FEBS journal, 276 (2009), pp. 5960–5972.
- [124] A. HUEBNER, D. BRATTON, G. WHYTE, M. YANG, A. J. DEMELLO, C. ABELL, AND F. HOLLFELDER, *Static microdroplet arrays: a microfluidic device for droplet trapping, incubation and release for enzymatic and cell-based assays*, Lab on a Chip, 9 (2009), pp. 692–698.

- [125] L.-H. HUNG, K. M. CHOI, W.-Y. TSENG, Y.-C. TAN, K. J. SHEA, AND A. P. LEE, *Alternating droplet generation and controlled dynamic droplet fusion in microfluidic device for cds nanoparticle synthesis*, *Lab on a Chip*, 6 (2006), pp. 174–178.
- [126] L.-H. HUNG AND A. P. LEE, *Microfluidic devices for the synthesis of nanoparticles and biomaterials*, *Journal of Medical and Biological Engineering*, 27 (2007), p. 1.
- [127] T. HUTAMA AND R. OLESCHUK, *Magnetically manipulated droplet splitting on a 3d-printed device to carry out a complexometric assay*, *Lab on a Chip*, 17 (2017), pp. 2640–2649.
- [128] A. ISOZAKI, H. MIKAMI, H. TEZUKA, H. MATSUMURA, K. HUANG, M. AKAMINE, K. HIRAMATSU, T. IINO, T. ITO, H. KARAKAWA, ET AL., *Intelligent image-activated cell sorting 2.0*, *Lab on a Chip*, (2020).
- [129] A. ISOZAKI, Y. NAKAGAWA, M. LOO, Y. SHIBATA, N. TANAKA, D. SETYANINGRUM, J.-W. PARK, Y. SHIRASAKI, H. MIKAMI, D. HUANG, ET AL., *Sequentially addressable dielectrophoretic array for high-throughput sorting of large-volume biological compartments*, *Science Advances*, 6 (2020), p. eaba6712.
- [130] R. JAIN, A. THAKUR, P. KAUR, K.-H. KIM, AND P. DEVI, *Advances in imaging-assisted sensing techniques for heavy metals in water: Trends, challenges, and opportunities*, *TrAC Trends in Analytical Chemistry*, (2019), p. 115758.
- [131] S. JAKIELA, *Measurement of the hydrodynamic resistance of microdroplets*, *Lab on a Chip*, 16 (2016), pp. 3695–3699.
- [132] S. JAKIELA, T. S. KAMINSKI, O. CYBULSKI, D. B. WEIBEL, AND P. GARSTECKI, *Bacterial growth and adaptation in microdroplet chemostats*, *Angewandte Chemie International Edition*, 52 (2013), pp. 8908–8911.
- [133] S. JAKIELA, S. MAKULSKA, P. M. KORCZYK, AND P. GARSTECKI, *Speed of flow of individual droplets in microfluidic channels as a function of the capillary number, volume of droplets and contrast of viscosities*, *Lab on a Chip*, 11 (2011), pp. 3603–3608.
- [134] G. JENKINS AND C. D. MANSFIELD, *Microfluidic diagnostics: methods and protocols*, Springer, 2013.

- [135] P. JIN, J. LAN, K. WANG, M. S. BAKER, C. HUANG, AND E. C. NICE, *Pathology, proteomics and the pathway to personalised medicine*, Expert review of proteomics, 15 (2018), pp. 231–243.
- [136] Y. JIN, A. ORTH, E. SCHONBRUN, AND K. B. CROZIER, *Measuring the pressures across microfluidic droplets with an optical tweezer*, Optics express, 20 (2012), pp. 24450–24464.
- [137] I. JOHNSTON, D. MCCLUSKEY, C. TAN, AND M. TRACEY, *Mechanical characterization of bulk sylgard 184 for microfluidics and microengineering*, Journal of Micromechanics and Microengineering, 24 (2014), p. 035017.
- [138] J. JOVANOVIĆ, W. ZHOU, E. V. REBROV, T. NIJHUIS, V. HESSEL, AND J. C. SCHOUTEN, *Liquid–liquid slug flow: hydrodynamics and pressure drop*, Chemical Engineering Science, 66 (2011), pp. 42–54.
- [139] J. H. JUNG, G. DESTGEER, B. HA, J. PARK, AND H. J. SUNG, *On-demand droplet splitting using surface acoustic waves*, Lab on a Chip, 16 (2016), pp. 3235–3243.
- [140] S. KAHKESHANI AND D. DI CARLO, *Drop formation using ferrofluids driven magnetically in a step emulsification device*, Lab on a Chip, 16 (2016), pp. 2474–2480.
- [141] A. KALANTARIFARD, E. ALIZADEH-HAGHIGHI, A. SAATEH, AND C. EL-BUKEN, *Theoretical and experimental limits of monodisperse droplet generation*, Chemical Engineering Science, (2020), p. 116093.
- [142] T. KALETTA AND M. O. HENGARTNER, *Finding function in novel targets: C. elegans as a model organism*, Nature reviews Drug discovery, 5 (2006), pp. 387–399.
- [143] R. KARNIK, F. GU, P. BASTO, C. CANNIZZARO, L. DEAN, W. KYEIMANU, R. LANGER, AND O. C. FAROKHZAD, *Microfluidic platform for controlled synthesis of polymeric nanoparticles*, Nano letters, 8 (2008), pp. 2906–2912.
- [144] K. KARTHIKEYAN AND L. SUJATHA, *Fluorometric sensor for mercury ion detection in a fluidic mems device*, IEEE Sensors Journal, 18 (2018), pp. 5225–5231.

- [145] M. N. KASHID AND D. W. AGAR, *Hydrodynamics of liquid–liquid slug flow capillary microreactor: flow regimes, slug size and pressure drop*, Chemical Engineering Journal, 131 (2007), pp. 1–13.
- [146] H. KAUFMAN, I. BARKANA, AND K. SOBEL, *Direct adaptive control algorithms: theory and applications*, Springer Science & Business Media, 2012.
- [147] P. J. KENIS, R. F. ISMAGILOV, AND G. M. WHITESIDES, *Microfabrication inside capillaries using multiphase laminar flow patterning*, Science, 285 (1999), pp. 83–85.
- [148] S. M. KHAN, A. GUMUS, J. M. NASSAR, AND M. M. HUSSAIN, *Cmos enabled microfluidic systems for healthcare based applications*, Advanced Materials, 30 (2018), p. 1705759.
- [149] C.-A. KIEFFER, S. RITTY, T. BOUDOT, N. PETIT, J. WEBER, AND A. LE NEL, *A high-precision fluid handling system based on pressure actuation: multi-inlets flow rate control*, in Proc. 3rd Eur. Conf. Microfluidics, vol. 252, 2012.
- [150] C.-J. KIM, D. Y. KI, J. PARK, V. SUNKARA, T.-H. KIM, Y. MIN, AND Y.-K. CHO, *Fully automated platelet isolation on a centrifugal microfluidic device for molecular diagnostics*, Lab on a Chip, (2020).
- [151] H. KIM, D. LUO, D. LINK, D. A. WEITZ, M. MARQUEZ, AND Z. CHENG, *Controlled production of emulsion drops using an electric field in a flow-focusing microfluidic device*, Applied Physics Letters, 91 (2007), p. 133106.
- [152] N. KIM, M. C. MURPHY, S. A. SOPER, AND D. E. NIKITOPOULOS, *Liquid–liquid segmented flows in polycarbonate microchannels with cross-sectional expansions*, International Journal of Multiphase Flow, 58 (2014), pp. 83–96.
- [153] S. C. KIM, I. C. CLARK, P. SHAHI, AND A. R. ABATE, *Single-cell rt-pcr in microfluidic droplets with integrated chemical lysis*, Analytical chemistry, 90 (2018), pp. 1273–1279.
- [154] S. KINIO AND J. K. MILLS, *Effects of dielectrophoresis on thrombogenesis in human whole blood*, Electrophoresis, 38 (2017), pp. 1755–1763.
- [155] —, *Localized electroporation with dielectrophoretic field flow fractionation: Toward removal of circulating tumour cells from human blood*, IEEE transactions on nanobioscience, 16 (2017), pp. 802–809.

- [156] H. KINOSHITA, S. KANEDA, T. FUJII, AND M. OSHIMA, *Three-dimensional measurement and visualization of internal flow of a moving droplet using confocal micro-piv*, *Lab on a Chip*, 7 (2007), pp. 338–346.
- [157] K. KOCH, B. J. VAN WEERDENBURG, J. M. VERKADE, P. J. NIEUWLAND, F. P. RUTJES, AND J. C. VAN HEST, *Optimizing the deprotection of the amine protecting p-methoxyphenyl group in an automated microreactor platform*, *Organic Process Research & Development*, 13 (2009), pp. 1003–1006.
- [158] T. KOMODA AND T. MATSUNAGA, *Biochemistry for Medical Professionals*, Academic Press, 2015.
- [159] P. M. KORCZYK, O. CYBULSKI, S. MAKULSKA, AND P. GARSTECKI, *Effects of unsteadiness of the rates of flow on the dynamics of formation of droplets in microfluidic systems*, *Lab on a Chip*, 11 (2011), pp. 173–175. 10.1039/c0lc00088d.
- [160] P. M. KORCZYK, V. VAN STEIJN, S. BLONSKI, D. ZAREMBA, D. A. BEATTIE, AND P. GARSTECKI, *Accounting for corner flow unifies the understanding of droplet formation in microfluidic channels*, *Nature communications*, 10 (2019), p. 2528.
- [161] S. KRISHNADASAN, R. BROWN, A. DEMELLO, AND J. DEMELLO, *Intelligent routes to the controlled synthesis of nanoparticles*, *Lab on a Chip*, 7 (2007), pp. 1434–1441.
- [162] E. KUMACHEVA AND P. GARSTECKI, *Microfluidic reactors for polymer particles*, John Wiley & Sons, 2011.
- [163] Y. KWOK, Y. WANG, M. WU, F. LI, Y. ZHANG, H. ZHANG, AND D. LEUNG, *A dual fuel microfluidic fuel cell utilizing solar energy and methanol*, *Journal of Power Sources*, 409 (2019), pp. 58–65.
- [164] V. LABROT, M. SCHINDLER, P. GUILLOT, A. COLIN, AND M. JOANICOT, *Extracting the hydrodynamic resistance of droplets from their behavior in microchannel networks*, *Biomicrofluidics*, 3 (2009), p. 012804.
- [165] A. ŁADOSZ, E. RIGGER, AND P. R. VON ROHR, *Pressure drop of three-phase liquid–liquid–gas slug flow in round microchannels*, *Microfluidics and Nanofluidics*, 20 (2016), p. 49.

- [166] A. LADOSZ AND P. R. VON ROHR, *Pressure drop of two-phase liquid-liquid slug flow in square microchannels*, Chemical Engineering Science, 191 (2018), pp. 398–409.
- [167] A. LAI, N. ALTEMOSE, J. A. WHITE, AND A. M. STREETS, *On-ratio pdms bonding for multilayer microfluidic device fabrication*, Journal of Micromechanics and Microengineering, 29 (2019), p. 107001.
- [168] J. R. LAKE, K. C. HEYDE, AND W. C. RUDER, *Low-cost feedback-controlled syringe pressure pumps for microfluidics applications*, PLoS One, 12 (2017), p. e0175089.
- [169] R. H. LAM AND W. J. LI, *A digitally controllable polymer-based microfluidic mixing module array*, Micromachines, 3 (2012), pp. 279–294.
- [170] C. LAVAL, A. BOUCHAUDY, AND J.-B. SALMON, *Fabrication of microscale materials with programmable composition gradients*, Lab on a Chip, 16 (2016), pp. 1234–1242.
- [171] A. P. LEE, M. AGHAAMOO, T. N. ADAMS, AND L. A. FLANAGAN, *It's electric: when technology gives a boost to stem cell science*, Current Stem Cell Reports, 4 (2018), pp. 116–126.
- [172] C.-C. LEE, G. SUI, A. ELIZAROV, C. J. SHU, Y.-S. SHIN, A. N. DOOLEY, J. HUANG, A. DARIDON, P. WYATT, D. STOUT, ET AL., *Multistep synthesis of a radiolabeled imaging probe using integrated microfluidics*, Science, 310 (2005), pp. 1793–1796.
- [173] C.-Y. LEE, C.-L. CHANG, Y.-N. WANG, AND L.-M. FU, *Microfluidic mixing: a review*, International journal of molecular sciences, 12 (2011), pp. 3263–3287.
- [174] K. LEE, T. YOON, H.-S. YANG, S. CHA, Y.-P. CHEON, L. KASHEFI-KHEYRABADI, AND H.-I. JUNG, *All-in-one platform for salivary cotinine detection integrated with a microfluidic channel and an electrochemical biosensor*, Lab on a Chip, (2020).
- [175] Y.-S. LEE, N. BHATTACHARJEE, AND A. FOLCH, *3d-printed quake-style microvalves and micropumps*, Lab on a Chip, 18 (2018), pp. 1207–1214.

- [176] F. LEFEVRE, A. CHALIFOUR, L. YU, V. CHODAVARAPU, P. JUNEAU, AND R. IZQUIERDO, *Algal fluorescence sensor integrated into a microfluidic chip for water pollutant detection*, *Lab on a Chip*, 12 (2012), pp. 787–793.
- [177] J. LEIPERT AND A. THOLEY, *Miniaturized sample preparation on a digital microfluidics device for sensitive bottom-up microproteomics of mammalian cells using magnetic beads and mass spectrometry-compatible surfactants*, *Lab on a Chip*, 19 (2019), pp. 3490–3498.
- [178] T. LEVI AND T. FUJII, *Microfluidic neurons, a new way in neuromorphic engineering?*, *Micromachines*, 7 (2016), p. 146.
- [179] G. LI, Y. LUO, Q. CHEN, L. LIAO, AND J. ZHAO, *A place n play modular pump for portable microfluidic applications*, *Biomicrofluidics*, 6 (2012), p. 014118.
- [180] J. LI AND C. KIM, *Current commercialization status of electrowetting-on-dielectric (ewod) digital microfluidics.*, *Lab on a Chip*, (2020).
- [181] L. LI AND R. F. ISMAGILOV, *Protein crystallization using microfluidic technologies based on valves, droplets, and slipchip*, *Annual review of biophysics*, 39 (2010), pp. 139–158.
- [182] L. LI, H. YIN, AND A. J. MASON, *Epoxy chip-in-carrier integration and screen-printed metalization for multichannel microfluidic lab-on-cmos microsystems*, *IEEE transactions on biomedical circuits and systems*, 12 (2018), pp. 416–425.
- [183] W. LI, L. ZHANG, X. GE, B. XU, W. ZHANG, L. QU, C.-H. CHOI, J. XU, A. ZHANG, H. LEE, ET AL., *Microfluidic fabrication of microparticles for biomedical applications*, *Chemical Society Reviews*, 47 (2018), pp. 5646–5683.
- [184] Y. LI, Y. CHEN, H. YU, L. TIAN, AND Z. WANG, *Portable and smart devices for monitoring heavy metal ions integrated with nanomaterials*, *TrAC Trends in Analytical Chemistry*, 98 (2018), pp. 190–200.
- [185] Y. LI, J. XUAN, R. HU, P. ZHANG, X. LOU, AND Y. YANG, *Microfluidic triple-gradient generator for efficient screening of chemical space*, *Talanta*, 204 (2019), pp. 569–575.

- [186] Z. LI, K. ANDO, J. YU, A. LIU, J. ZHANG, AND C. OHL, *Fast on-demand droplet fusion using transient cavitation bubbles*, Lab on a Chip, 11 (2011), pp. 1879–1885.
- [187] Z. LIAO, Y. ZHANG, Y. LI, Y. MIAO, S. GAO, F. LIN, Y. DENG, AND L. GENG, *Microfluidic chip coupled with optical biosensors for simultaneous detection of multiple analytes: A review*, Biosensors and Bioelectronics, 126 (2019), pp. 697–706.
- [188] L. LIN, Q. CHEN, AND J. SUN, *Micro/nanofluidics-enabled single-cell biochemical analysis*, TrAC Trends in Analytical Chemistry, 99 (2018), pp. 66–74.
- [189] D. LINK, S. L. ANNA, D. WEITZ, AND H. STONE, *Geometrically mediated breakup of drops in microfluidic devices*, Physical review letters, 92 (2004), p. 054503.
- [190] D. LIU, H. ZHANG, F. FONTANA, J. T. HIRVONEN, AND H. A. SANTOS, *Current developments and applications of microfluidic technology toward clinical translation of nanomedicines*, Advanced drug delivery reviews, 128 (2018), pp. 54–83.
- [191] J. LIU, S.-H. TAN, Y. F. YAP, M. Y. NG, AND N.-T. NGUYEN, *Numerical and experimental investigations of the formation process of ferrofluid droplets*, Microfluidics and nanofluidics, 11 (2011), pp. 177–187.
- [192] W.-T. LIU, W.-B. LEE, Y.-C. TSAI, Y.-J. CHUANG, K.-F. HSU, AND G.-B. LEE, *An automated microfluidic system for selection of aptamer probes against ovarian cancer tissues*, Biomicrofluidics, 13 (2019), p. 014114.
- [193] X. LIU, Y. WANG, AND Y. SONG, *Visually multiplexed quantitation of heavy metal ions in water using volumetric bar-chart chip*, Biosensors and Bioelectronics, 117 (2018), pp. 644–650.
- [194] L. LJUNG, *System Identification: Theory for the User*, Pearson Education, 1998.
- [195] S. A. LONGWELL AND P. M. FORDYCE, *micrio: an open-source autosampler and fraction collector for automated microfluidic input–output*, Lab on a Chip, 20 (2020), pp. 93–106.

- [196] C. H. LU, T.-S. SHIH, P.-C. SHIH, G. P. PENDHARKAR, C.-E. LIU, C.-K. CHEN, L. HSU, H.-Y. CHANG, C.-L. YANG, AND C.-H. LIU, *Finger-powered agglutination lab chip with cmos image sensing for rapid point-of-care diagnosis applications*, Lab on a Chip, (2020).
- [197] G. LUO, L. DU, Y. WANG, AND K. WANG, *Manipulation and control of structure and size of inorganic nanomaterials in microchemical systems*, Chemical Engineering & Technology, 42 (2019), pp. 1996–2008.
- [198] ———, *Recent developments in microfluidic device-based preparation, functionalization, and manipulation of nano-and micro-materials*, Particuology, (2019).
- [199] Z. Y. LUO, X. L. SHANG, AND B. F. BAI, *Marangoni effect on the motion of a droplet covered with insoluble surfactant in a square microchannel*, Physics of Fluids, 30 (2018), p. 077101.
- [200] Y.-D. MA, K.-H. LI, Y.-H. CHEN, Y.-M. LEE, S.-T. CHOU, Y.-Y. LAI, P.-C. HUANG, H.-P. MA, AND G.-B. LEE, *A sample-to-answer, portable platform for rapid detection of pathogens with a smartphone interface*, Lab on a Chip, 19 (2019), pp. 3804–3814.
- [201] J. MADDALA, B. SRINIVASAN, S. S. BITHI, S. A. VANAPALLI, AND R. RENGASWAMY, *Design of a model-based feedback controller for active sorting and synchronization of droplets in a microfluidic loop*, AIChE Journal, 58 (2012), pp. 2120–2130.
- [202] D. MAILLARD, A. DE PASTINA, T. LARSEN, AND L. G. VILLANUEVA, *Modular interface and experimental setup for in-vacuum operation of microfluidic devices*, Review of Scientific Instruments, 90 (2019), p. 045006.
- [203] A. MANZ, N. GRABER, AND H. WIDMER, *Miniaturized total chemical analysis systems: a novel concept for chemical sensing*, Sensors and actuators B: Chemical, 1 (1990), pp. 244–248.
- [204] X. MAO AND T. J. HUANG, *Exploiting mechanical biomarkers in microfluidics*, Lab on a Chip, 12 (2012), pp. 4006–4009.
- [205] Z. MAO, K. YOSHIDA, AND J.-W. KIM, *A droplet-generator-on-a-chip actuated by ecf (electro-conjugate fluid) micropumps*, Microfluidics and Nanofluidics, 23 (2019), p. 130.

- [206] S. MARRE, J. PARK, J. REMPEL, J. GUAN, M. G. BAWENDI, AND K. F. JENSEN, *Supercritical continuous-microflow synthesis of narrow size distribution quantum dots*, *Advanced Materials*, 20 (2008), pp. 4830–4834.
- [207] C. MARTINO AND A. J. DEMELLO, *Droplet-based microfluidics for artificial cell generation: A brief review*, *Interface focus*, 6 (2016), p. 20160011.
- [208] J. P. MCMULLEN AND K. F. JENSEN, *Integrated microreactors for reaction automation: new approaches to reaction development*, *Annual review of analytical chemistry*, 3 (2010), pp. 19–42.
- [209] J. P. MCMULLEN, M. T. STONE, S. L. BUCHWALD, AND K. F. JENSEN, *An integrated microreactor system for self-optimization of a heck reaction: From micro-to mesoscale flow systems*, *Angewandte Chemie International Edition*, 49 (2010), pp. 7076–7080.
- [210] M. MEIER, J. KENNEDY-DARLING, S. H. CHOI, E. M. NORSTROM, S. S. SISODIA, AND R. F. ISMAGILOV, *Plug-based microfluidics with defined surface chemistry to miniaturize and control aggregation of amyloidogenic peptides*, *Angewandte Chemie International Edition*, 48 (2009), pp. 1487–1489.
- [211] S. MI, H. PU, S. XIA, AND W. SUN, *A minimized valveless electromagnetic micropump for microfluidic actuation on organ chips*, *Sensors and Actuators A: Physical*, 301 (2020), p. 111704.
- [212] E. MILLER, M. ROTEA, AND J. P. ROTHSTEIN, *Microfluidic device incorporating closed loop feedback control for uniform and tunable production of micro-droplets*, *Lab on a Chip*, 10 (2010), pp. 1293–1301.
- [213] X. MIN AND W. S. KIM, *Beyond high voltage in the digital microfluidic devices for an integrated portable sensing system*, *Microfluidics and Nanofluidics*, 23 (2019), p. 127.
- [214] N. MISAWA AND S. TAKEUCHI, *Portable imaging system for on-site analysis using cmos imagermicrofluidic analysis and fluorescence imaging*, *IEEJ Transactions on Electrical and Electronic Engineering*, 6 (2011), pp. 97–100.
- [215] T. MOHAMED, T. HOANG, M. JELOKHANI-NIARAKI, AND P. P. RAO, *Tau-derived-hexapeptide 306vqivyk311 aggregation inhibitors: nitrocatechol moiety as a pharmacophore in drug design*, *ACS chemical neuroscience*, 4 (2013), pp. 1559–1570.

- [216] A. MOHAMMADZADEH, A. E. F. ROBICHAUD, AND P. R. SELVAGANAPATHY, *Rapid and inexpensive method for fabrication and integration of electrodes in microfluidic devices*, Journal of Microelectromechanical Systems, 28 (2019), pp. 597–605.
- [217] D. C. MONTGOMERY AND G. C. RUNGER, *Applied statistics and probability for engineers*, John Wiley & Sons, 2010.
- [218] W. M. MOREAU, *Semiconductor lithography: principles, practices, and materials*, Springer Science & Business Media, 2012.
- [219] K. MUTAFOPULOS, P. J. LU, R. GARRY, P. SPINK, AND D. A. WEITZ, *Selective cell encapsulation, lysis, pico-injection and size-controlled droplet generation using traveling surface acoustic waves in a microfluidic device*, Lab on a Chip, (2020).
- [220] G. NABOVATI, E. GHAFAR-ZADEH, A. LETOURNEAU, AND M. SAWAN, *Smart cell culture monitoring and drug test platform using cmos capacitive sensor array*, IEEE Transactions on Biomedical Engineering, 66 (2018), pp. 1094–1104.
- [221] L. NAN, Z. YANG, H. LYU, K. Y. Y. LAU, AND H. C. SHUM, *A microfluidic system for one-chip harvesting of single-cell-laden hydrogels in culture medium*, Advanced Biosystems, 3 (2019), p. 1900076.
- [222] B. NASSERI, N. SOLEIMANI, N. RABIEE, A. KALBASI, M. KARIMI, AND M. R. HAMBLIN, *Point-of-care microfluidic devices for pathogen detection*, Biosensors and Bioelectronics, 117 (2018), pp. 112–128.
- [223] J. NETTE, P. D. HOWES, AND A. J. DEMELLO, *Microfluidic synthesis of luminescent and plasmonic nanoparticles: Fast, efficient, and data-rich*, Advanced Materials Technologies, (2020), p. 2000060.
- [224] P. NEUŽIL, S. GISELBRECHT, K. LÄNGE, T. J. HUANG, AND A. MANZ, *Revisiting lab-on-a-chip technology for drug discovery*, Nature reviews Drug discovery, 11 (2012), pp. 620–632.
- [225] D. H. NGUYEN AND B. WIDROW, *Neural networks for self-learning control systems*, IEEE Control systems magazine, 10 (1990), pp. 18–23.
- [226] NIKON, *Eclipse ti: Inverted research microscope*.

- [227] N. NITTA, T. SUGIMURA, A. ISOZAKI, H. MIKAMI, K. HIRAKI, S. SAKUMA, T. IINO, F. ARAI, T. ENDO, Y. FUJIWAKI, ET AL., *Intelligent image-activated cell sorting*, *Cell*, 175 (2018), pp. 266–276.
- [228] X. NIU, S. GULATI, J. B. EDEL, AND A. J. DEMELLO, *Pillar-induced droplet merging in microfluidic circuits*, *Lab on a Chip*, 8 (2008), pp. 1837–1841.
- [229] J. P. NORTON, *An introduction to identification*, Courier Corporation, 2009.
- [230] E. NOVIANA, C. P. MCCORD, K. M. CLARK, I. JANG, AND C. S. HENRY, *Electrochemical paper-based devices: sensing approaches and progress toward practical applications*, *Lab on a Chip*, 20 (2019), pp. 9–34.
- [231] D. OGONCZYK, J. WEGRZYN, P. JANKOWSKI, B. DABROWSKI, AND P. GARSTECKI, *Bonding of microfluidic devices fabricated in polycarbonate*, *Lab on a Chip*, 10 (2010), pp. 1324–1327.
- [232] R. ORTIZ, J. L. CHEN, D. C. STUCKEY, AND T. W. STEELE, *Rapid serial diluting biomicrofluidic provides ec50 in minutes*, *Micro and Nano Engineering*, 2 (2019), pp. 92–103.
- [233] S. PADMANABHAN, T. MISTELI, AND D. DEVOE, *Controlled droplet discretization and manipulation using membrane displacement traps*, *Lab on a Chip*, 17 (2017), pp. 3717–3724.
- [234] S.-Y. PARK, T.-H. WU, Y. CHEN, M. A. TEITELL, AND P.-Y. CHIOU, *High-speed droplet generation on demand driven by pulse laser-induced cavitation*, *Lab on a Chip*, 11 (2011), pp. 1010–1012.
- [235] L. PATINGLAG, D. SAWTELL, A. ILES, L. M. MELLING, AND K. J. SHAW, *A microfluidic atmospheric-pressure plasma reactor for water treatment*, *Plasma Chemistry and Plasma Processing*, (2019), pp. 1–15.
- [236] G. PEROZZIELLO, G. SIMONE, P. CANDELORO, F. GENTILE, N. MALARA, R. LAROCCA, M. COLUCCIO, S. A. PULLANO, L. TIRINATO, O. GESCHKE, ET AL., *A fluidic motherboard for multiplexed simultaneous and modular detection in microfluidic systems for biological application*, *Micro and Nanosystems*, 2 (2010), pp. 227–238.
- [237] A. PERSAT, C. D. NADELL, M. K. KIM, F. INGREMEAU, A. SIRYAPORN, K. DRESCHER, N. S. WINGREEN, B. L. BASSLER, Z. GITAI, AND H. A. STONE, *The mechanical world of bacteria*, *Cell*, 161 (2015), pp. 988–997.

- [238] A. PFREUNDT, K. B. ANDERSEN, M. DIMAKI, AND W. E. SVENDSEN, *An easy-to-use microfluidic interconnection system to create quick and reversibly interfaced simple microfluidic devices*, Journal of Micromechanics and Micro-engineering, 25 (2015), p. 115010.
- [239] E. A. PHILLIPS, T. J. MOEHLING, K. F. EJENDAL, O. S. HOILETT, K. M. BYERS, L. A. BASING, L. A. JANKOWSKI, J. B. BENNETT, L.-K. LIN, L. A. STANCIU, ET AL., *Microfluidic rapid and autonomous analytical device (microraad) to detect hiv from whole blood samples*, Lab on a Chip, 19 (2019), pp. 3375–3386.
- [240] R. POCEVICIUTE AND R. F. ISMAGILOV, *Human-gut-microbiome on a chip*, Nature biomedical engineering, 3 (2019), p. 500.
- [241] W. POSTEK, T. KAMINSKI, AND P. GARSTECKI, *A precise and accurate microfluidic droplet dilutor*, Analyst, 142 (2017), pp. 2901–2911.
- [242] S. M. PRAKADAN, A. K. SHALEK, AND D. A. WEITZ, *Scaling by shrinking: empowering single-cell’omics’ with microfluidic devices*, Nature Reviews Genetics, 18 (2017), p. 345.
- [243] R. PRANTIL-BAUN, R. NOVAK, D. DAS, M. R. SOMAYAJI, A. PRZEK-WAS, AND D. E. INGBER, *Physiologically based pharmacokinetic and pharmacodynamic analysis enabled by microfluidically linked organs-on-chips*, Annual review of pharmacology and toxicology, 58 (2018), pp. 37–64.
- [244] QIMAGING, *Retiga-2000r: High sensitivity ieee 1394 firewire digital ccd camera*.
- [245] D. QIN, Y. XIA, AND G. M. WHITESIDES, *Soft lithography for micro- and nanoscale patterning*, Nat.Protocols, 5 (2010), pp. 491–502.
- [246] S. S. RAO AND H. WONG, *The motion of long drops in rectangular microchannels at low capillary numbers*, Journal of Fluid Mechanics, 852 (2018), pp. 60–104.
- [247] M. R. RASOULI AND M. TABRIZIAN, *An ultra-rapid acoustic micromixer for synthesis of organic nanoparticles*, Lab on a Chip, 19 (2019), pp. 3316–3325.
- [248] M. RASPONI, A. GAZANEO, A. BONOMI, A. GHIGLIETTI, P. OCCHETTA, G. B. FIORE, A. PESSINA, AND A. REDAELLI, *Lab-on-chip for testing myelotoxic effect of drugs and chemicals*, Microfluidics and Nanofluidics, 19 (2015), pp. 935–940.

- [249] M. ROBERT DE SAINT VINCENT, R. WUNENBURGER, AND J.-P. DELVILLE, *Laser switching and sorting for high speed digital microfluidics*, Applied Physics Letters, 92 (2008), p. 154105.
- [250] M. J. ROSEN AND J. T. KUNJAPPU, *Surfactants and interfacial phenomena*. hoboken, NJ, USA: Wiley. DOI, 10 (2004), p. 561.
- [251] J. SAEZ, J. ETXEBARRIA, M. ANTOÑANA-DIEZ, AND F. BENITO-LOPEZ, *On-demand generation and removal of alginate biocompatible microvalves for flow control in microfluidics*, Sensors and Actuators B: Chemical, 234 (2016), pp. 1–7.
- [252] A. SALIM, M. FOURAR, J. PIRONON, AND J. SAUSSE, *Oil–water two-phase flow in microchannels: Flow patterns and pressure drop measurements*, The Canadian Journal of Chemical Engineering, 86 (2008), pp. 978–988.
- [253] J. E. SANFILIPPO, A. LORESTANI, M. D. KOCH, B. P. BRATTON, A. SIRYAPORN, H. A. STONE, AND Z. GITAI, *Microfluidic-based transcriptomics reveal force-independent bacterial rheosensing*, Nature microbiology, 4 (2019), pp. 1274–1281.
- [254] F. SARRAZIN, T. BONOMETTI, L. PRAT, C. GOURDON, AND J. MAGNAUDET, *Hydrodynamic structures of droplets engineered in rectangular microchannels*, Microfluidics and Nanofluidics, 5 (2008), pp. 131–137.
- [255] M. SCHINDLER AND A. AJDARI, *Droplet traffic in microfluidic networks: A simple model for understanding and designing*, Physical Review Letters, 100 (2008), p. 044501.
- [256] S. R. SCHMID, B. J. HAMROCK, AND B. O. JACOBSON, *Fundamentals of machine elements: SI version*, CRC Press, 2014.
- [257] F. SCHMIEDER, S. SCHMIEDER, R. EGER, S. FRIEDRICH, A. WERNER, N. DANZ, U. MARX, AND F. SONNTAG, *Automated universal chip platform for fluorescence based cellular assays*, Biomedical Engineering/Biomedizinische Technik, 57 (2012), pp. 340–343.
- [258] M. SESEN, T. ALAN, AND A. NEILD, *Microfluidic on-demand droplet merging using surface acoustic waves*, Lab on a Chip, 14 (2014), pp. 3325–3333.

- [259] D. SESSOMS, M. BELLOUL, W. ENGL, M. ROCHE, L. COURBIN, AND P. PANIZZA, *Droplet motion in microfluidic networks: Hydrodynamic interactions and pressure-drop measurements*, *Physical Review E*, 80 (2009), p. 016317.
- [260] S. SEVIM, A. SORRENTI, C. FRANCO, S. FURUKAWA, S. PANÉ, A. DEMELLO, AND J. PUIGMARTÍ-LUIS, *Self-assembled materials and supramolecular chemistry within microfluidic environments: from common thermodynamic states to non-equilibrium structures*, *Chemical Society Reviews*, 47 (2018), pp. 3788–3803.
- [261] M. SHANG, R. H. SOON, C. T. LIM, B. L. KHOO, AND J. HAN, *Microfluidic modelling of the tumor microenvironment for anti-cancer drug development*, *Lab on a Chip*, 19 (2019), pp. 369–386.
- [262] M. SHAO, Q. YU, N. JING, Y. CHENG, D. WANG, Y.-D. WANG, AND J.-H. XU, *Continuous synthesis of carbon dots with full spectrum fluorescence and the mechanism of their multiple color emission*, *Lab on a Chip*, 19 (2019), pp. 3974–3978.
- [263] N. SHEMBEKAR, C. CHAIPAN, R. UTHARALA, AND C. A. MERTEN, *Droplet-based microfluidics in drug discovery, transcriptomics and high-throughput molecular genetics*, *Lab on a Chip*, 16 (2016), pp. 1314–1331.
- [264] A. SHENOY, M. TANYERI, AND C. M. SCHROEDER, *Characterizing the performance of the hydrodynamic trap using a control-based approach*, *Microfluidics and Nanofluidics*, 18 (2015), pp. 1055–1066.
- [265] I. SHESTOPALOV, J. D. TICE, AND R. F. ISMAGILOV, *Multi-step synthesis of nanoparticles performed on millisecond time scale in a microfluidic droplet-based system*, *Lab on a Chip*, 4 (2004), pp. 316–321.
- [266] B. SIDAR, B. R. JENKINS, S. HUANG, J. R. SPENCE, S. T. WALK, AND J. N. WILKING, *Long-term flow through human intestinal organoids with the gut organoid flow chip (goflowchip)*, *Lab on a Chip*, 19 (2019), pp. 3552–3562.
- [267] S. A. SIEVERS, J. KARANICOLAS, H. W. CHANG, A. ZHAO, L. JIANG, O. ZIRAFI, J. T. STEVENS, J. MÜNCH, D. BAKER, AND D. EISENBERG, *Structure-based design of non-natural amino-acid inhibitors of amyloid fibril formation*, *Nature*, 475 (2011), p. 96.

- [268] P. SKAFTE-PEDERSEN, C. G. SIP, A. FOLCH, AND M. DUFVA, *Modular microfluidic systems using reversibly attached pdms fluid control modules*, Journal of Micromechanics and Microengineering, 23 (2013), p. 055011.
- [269] B. SRINIVASAN AND S. TUNG, *Development and applications of portable biosensors*, Journal of laboratory automation, 20 (2015), pp. 365–389.
- [270] Z. SU, J. HE, P. ZHOU, L. HUANG, AND J. ZHOU, *A high-throughput system combining microfluidic hydrogel droplets with deep learning for screening the antisolvent-crystallization conditions of active pharmaceutical ingredient*, Lab on a Chip, (2020).
- [271] V. SUBRAMANIAN, S. LEE, S. JENA, S. K. JANA, D. RAY, S. J. KIM, AND P. THALAPPIL, *Enhancing the sensitivity of point-of-use electrochemical microfluidic sensors by ion concentration polarisation—a case study on arsenic*, Sensors and Actuators B: Chemical, 304 (2020), p. 127340.
- [272] A. SUGIMOTO, T. FUKUYAMA, M. T. RAHMAN, AND I. RYU, *An automated-flow microreactor system for quick optimization and production: application of 10-and 100-gram order productions of a matrix metalloproteinase inhibitor using a sonogashira coupling reaction*, Tetrahedron Letters, 50 (2009), pp. 6364–6367.
- [273] Q. SUN, J. PEI, Q. LI, K. NIU, AND X. WANG, *Reusable standardized universal interface module (rsuim) for generic organ-on-a-chip applications*, Micromachines, 10 (2019), p. 849.
- [274] N. S. SUTERIA, M. NEKOU EI, AND S. A. VANAPALLI, *Microfluidic bypass manometry: highly parallelized measurement of flow resistance of complex channel geometries and trapped droplets*, Lab on a Chip, 18 (2018), pp. 343–355.
- [275] V. TALIMI, Y. MUZYCHKA, AND S. KOCABIYIK, *A review on numerical studies of slug flow hydrodynamics and heat transfer in microtubes and microchannels*, International Journal of Multiphase Flow, 39 (2012), pp. 88–104.
- [276] Y. TANAKA, T. FUJIKAWA, Y. KAZOE, AND T. KITAMORI, *An active valve incorporated into a microchip using a high strain electroactive polymer*, Sensors and Actuators B: Chemical, 184 (2013), pp. 163–169.
- [277] U. TANGEN, A. SHARMA, P. WAGLER, AND J. S. MCCASKILL, *On demand nanoliter-scale microfluidic droplet generation, injection, and mixing using a passive microfluidic device*, Biomicrofluidics, 9 (2015), p. 014119.

- [278] H. TAVAKOLI, W. ZHOU, L. MA, S. PEREZ, A. IBARRA, F. XU, S. ZHAN, AND X. LI, *Recent advances in microfluidic platforms for single-cell analysis in cancer biology, diagnosis and therapy*, TrAC Trends in Analytical Chemistry, (2019).
- [279] A. J. TEO, M. YAN, J. DONG, H.-D. XI, Y. FU, S. H. TAN, AND N.-T. NGUYEN, *Controllable droplet generation at a microfluidic t-junction using ac electric field*, Microfluidics and Nanofluidics, 24 (2020), pp. 1–9.
- [280] W. J. TERRELL, *Some fundamental control theory i: controllability, observability, and duality*, The American mathematical monthly, 106 (1999), pp. 705–719.
- [281] THORLABS, *Scientific-grade digital camera user guide for models 8051, 4070, 1501, and 340*.
- [282] T. THORSEN, S. J. MAERKL, AND S. R. QUAKE, *Microfluidic large-scale integration*, Science, 298 (2002), pp. 580–584.
- [283] F. TIAN, Q. FENG, Q. CHEN, C. LIU, T. LI, AND J. SUN, *Manipulation of bio-micro/nanoparticles in non-newtonian microflows*, Microfluidics and Nanofluidics, 23 (2019), p. 68.
- [284] W.-K. TSENG, J.-L. LIN, W.-C. SUNG, S.-H. CHEN, AND G.-B. LEE, *Active micro-mixers using surface acoustic waves on y-cut 128 linbo₃*, Journal of Micromechanics and Microengineering, 16 (2006), p. 539.
- [285] M. A. UNGER, H.-P. CHOU, T. THORSEN, A. SCHERER, AND S. R. QUAKE, *Monolithic microfabricated valves and pumps by multilayer soft lithography*, Science, 288 (2000), pp. 113–116.
- [286] H. UVET, A. HASEGAWA, K. OHARA, T. TAKUBO, Y. MAE, AND T. ARAI, *Vision-based automated single-cell loading and supply system*, IEEE transactions on nanobioscience, 8 (2009), pp. 332–340.
- [287] V. VAN STEIJN, C. R. KLEIJN, AND M. T. KREUTZER, *Predictive model for the size of bubbles and droplets created in microfluidic t-junctions*, Lab on a Chip, 10 (2010), pp. 2513–2518.
- [288] R. B. VAN VARSEVELD AND G. M. BONE, *Accurate position control of a pneumatic actuator using on/off solenoid valves*, IEEE/ASME Transactions on mechatronics, 2 (1997), pp. 195–204.

- [289] S. A. VANAPALLI, A. G. BANPURKAR, D. VAN DEN ENDE, M. H. DUIJS, AND F. MUGELE, *Hydrodynamic resistance of single confined moving drops in rectangular microchannels*, *Lab on a Chip*, 9 (2009), pp. 982–990.
- [290] S. K. VASHIST, P. B. LUPPA, L. Y. YEO, A. OZCAN, AND J. H. LUONG, *Emerging technologies for next-generation point-of-care testing*, *Trends in biotechnology*, 33 (2015), pp. 692–705.
- [291] E. M. VEDULA, J. L. ALONSO, M. A. ARNAOUT, AND J. L. CHAREST, *A microfluidic renal proximal tubule with active reabsorptive function*, *PLoS One*, 12 (2017), p. e0184330.
- [292] E. VERPOORTE, A. MANZ, H. LÜDI, A. BRUNO, F. MAYSTRE, B. KRATTIGER, H. WIDMER, B. VAN DER SCHOOT, AND N. DE ROOIJ, *A silicon flow cell for optical detection in miniaturized total chemical analysis systems*, *Sensors and Actuators B: Chemical*, 6 (1992), pp. 66–70.
- [293] G. T. VLADISAVLJEVIĆ, *Recent advances in the production of controllable multiple emulsions using microfabricated devices*, *Particuology*, 24 (2016), pp. 1–17.
- [294] L. R. VOLPATTI AND A. K. YETISEN, *Commercialization of microfluidic devices*, *Trends in biotechnology*, 32 (2014), pp. 347–350.
- [295] B. B. WAGHWANI, S. S. ALI, S. C. ANJANKAR, S. S. BALPANDE, P. MONDAL, AND J. P. KALAMBE, *In vitro detection of water contaminants using microfluidic chip and luminescence sensing platform*, *Microfluidics and Nanofluidics*, 24 (2020), pp. 1–12.
- [296] A. WAHEED, M. MANSHA, AND N. ULLAH, *Nanomaterials-based electrochemical detection of heavy metals in water: current status, challenges and future direction*, *TrAC Trends in Analytical Chemistry*, 105 (2018), pp. 37–51.
- [297] C. WANG, N.-T. NGUYEN, T. N. WONG, Z. WU, C. YANG, AND K. T. OOI, *Investigation of active interface control of pressure driven two-fluid flow in microchannels*, *Sensors and Actuators A: Physical*, 133 (2007), pp. 323–328.
- [298] J. WANG, M. JIN, Y. GONG, H. LI, S. WU, Z. ZHANG, G. ZHOU, L. SHUI, J. C. EIJKEL, AND A. VAN DEN BERG, *Continuous fabrication of microcapsules with controllable metal covered nanoparticle arrays using droplet microfluidics for localized surface plasmon resonance*, *Lab on a Chip*, 17 (2017), pp. 1970–1979.

- [299] J. WANG, Y. LI, X. WANG, J. WANG, H. TIAN, P. ZHAO, Y. TIAN, Y. GU, L. WANG, AND C. WANG, *Droplet microfluidics for the production of microparticles and nanoparticles*, *Micromachines*, 8 (2017), p. 22.
- [300] Y. WANG, Z. LI, X. HUANG, W. JI, X. NING, K. LIU, J. TAN, J. YANG, H.-P. HO, AND G. WANG, *On-board control of wax valve on active centrifugal microfluidic chip and its application for plasmid dna extraction*, *Microfluidics and Nanofluidics*, 23 (2019), p. 112.
- [301] Z. WANG, A. A. VOLINSKY, AND N. D. GALLANT, *Crosslinking effect on polydimethylsiloxane elastic modulus measured by custom-built compression instrument*, *Journal of Applied Polymer Science*, 131 (2014).
- [302] C. WATSON AND S. SENYO, *All-in-one automated microfluidics control system*, *HardwareX*, 5 (2019), p. e00063.
- [303] J. A. WHITE AND A. M. STREETS, *Controller for microfluidic large-scale integration*, *HardwareX*, 3 (2018), pp. 135–145.
- [304] A. WILLIAMS, *C++ concurrency in action: practical multithreading*, Manning Publ., 2012.
- [305] J. WILLIAMS, *George whitesides on what’s next for microfluidics – free presentation*, Dec 2017.
- [306] ———, *Technological developments in microfluidics – andrew demello*, Feb 2018.
- [307] D. WONG, K. ERKORKMAZ, AND C. L. REN, *Robodrop: A multi-input multi-output control system for on-demand manipulation of microfluidic droplets based on computer vision feedback*, *IEEE/ASME Transactions on Mechatronics*, 25 (2020), pp. 1129–1137.
- [308] D. WONG AND C. L. REN, *Microfluidic droplet trapping, splitting and merging with feedback controls and state space modelling*, *Lab on a Chip*, 16 (2016), pp. 3317–3329.
- [309] H. WONG, C. RADKE, AND S. MORRIS, *The motion of long bubbles in polygonal capillaries. part 1. thin films*, *Journal of Fluid Mechanics*, 292 (1995), pp. 71–94.
- [310] I. WONG AND C.-M. HO, *Surface molecular property modifications for poly(dimethylsiloxane)(pdms) based microfluidic devices*, *Microfluidics and nanofluidics*, 7 (2009), p. 291.

- [311] Y. H. WONG, *Feedback controls in droplet microfluidics*, Master's thesis, University of Waterloo, 2016.
- [312] K. WOODRUFF AND S. J. MAERKL, *Microfluidic module for real-time generation of complex multimolecule temporal concentration profiles*, *Analytical chemistry*, 90 (2018), pp. 696–701.
- [313] Y. WU, T. FU, Y. MA, AND H. Z. LI, *Active control of ferrofluid droplet breakup dynamics in a microfluidic t-junction*, *Microfluidics and Nanofluidics*, 18 (2015), pp. 19–27.
- [314] J. XU, S. LI, J. TAN, Y. WANG, AND G. LUO, *Preparation of highly monodisperse droplet in a t-junction microfluidic device*, *AIChE journal*, 52 (2006), pp. 3005–3010.
- [315] K. XU, C. P. TOSTADO, J.-H. XU, Y.-C. LU, AND G.-S. LUO, *Direct measurement of the differential pressure during drop formation in a co-flow microfluidic device*, *Lab on a Chip*, 14 (2014), pp. 1357–1366.
- [316] X. XU, L. SUN, L. CHEN, Z. ZHOU, J. XIAO, AND Y. ZHANG, *Electrowetting on dielectric device with crescent electrodes for reliable and low-voltage droplet manipulation*, *Biomicrofluidics*, 8 (2014), p. 064107.
- [317] H. YAMAGUCHI, M. MIYAZAKI, M. P. BRIONES-NAGATA, AND H. MAEDA, *Refolding of difficult-to-fold proteins by a gradual decrease of denaturant using microfluidic chips*, *The journal of biochemistry*, 147 (2010), pp. 895–903.
- [318] H. YANG, Z. CHEN, X. CAO, Z. LI, S. STAVRAKIS, J. CHOO, A. J. DEMELLO, P. D. HOWES, AND N. HE, *A sample-in-digital-answer-out system for rapid detection and quantitation of infectious pathogens in bodily fluids*, *Analytical and bioanalytical chemistry*, 410 (2018), pp. 7019–7030.
- [319] K. YANG, H. PERETZ-SOROKA, Y. LIU, AND F. LIN, *Novel developments in mobile sensing based on the integration of microfluidic devices and smartphones*, *Lab on a Chip*, 16 (2016), pp. 943–958.
- [320] B. K. YAP, M. SOAIR, S. NURARIFAH, N. A. TALIK, W. F. LIM, I. MEI, ET AL., *Potential point-of-care microfluidic devices to diagnose iron deficiency anemia*, *Sensors*, 18 (2018), p. 2625.

- [321] Y. C. YAP, T. C. DICKSON, A. E. KING, M. C. BREADMORE, AND R. M. GUIJT, *Microfluidic device for studying traumatic brain injury*, in *Stem Cell Technologies in Neuroscience*, Springer, 2017, ch. 10, pp. 145–156.
- [322] Z. YE, K. WANG, M. LOU, X. JIA, F. XU, AND G. YE, *Consecutive synthesis of gold nanobipyramids with controllable morphologies using a microfluidic platform*, *Microfluidics and Nanofluidics*, 24 (2020), p. 38.
- [323] G. YESILOZ, M. S. BOYBAY, AND C. L. REN, *Label-free high-throughput detection and content sensing of individual droplets in microfluidic systems*, *Lab on a Chip*, 15 (2015), pp. 4008–4019.
- [324] G. YESILOZ, M. S. BOYBAY, AND C. L. REN, *Effective thermo-capillary mixing in droplet microfluidics integrated with a microwave heater*, *Analytical chemistry*, 89 (2017), pp. 1978–1984.
- [325] YOLE-DÉVELOPEMENT, *Molecular medicine tri-conference: Microfluidic technologies are taking point-of-care testing to the next level*, 2019.
- [326] J.-I. YOSHIDA, A. NAGAKI, AND T. YAMADA, *Flash chemistry: fast chemical synthesis by using microreactors*, *Chemistry—A European Journal*, 14 (2008), pp. 7450–7459.
- [327] K. YOUSSEF, A. TANDON, AND P. REZAI, *Studying parkinsons disease using caenorhabditis elegans models in microfluidic devices*, *Integrative Biology*, 11 (2019), pp. 186–207.
- [328] F. B. YU, L. WILLIS, R. M. W. CHAU, A. ZAMBON, M. HOROWITZ, D. BHAYA, K. C. HUANG, AND S. R. QUAKE, *Long-term microfluidic tracking of coccoid cyanobacterial cells reveals robust control of division timing*, *BMC biology*, 15 (2017), p. 11.
- [329] P. K. YUEN, *Smartbuild—a truly plug-n-play modular microfluidic system*, *Lab on a Chip*, 8 (2008), pp. 1374–1378.
- [330] S. ZENG, B. LI, J. QIN, B. LIN, ET AL., *Microvalve-actuated precise control of individual droplets in microfluidic devices*, *Lab on a Chip*, 9 (2009), pp. 1340–1343.
- [331] W. ZENG, S. LI, AND Z. WANG, *Closed-loop feedback control of droplet formation in a t-junction microdroplet generator*, *Sensors and Actuators A: Physical*, 233 (2015), pp. 542–547.

- [332] H. ZHANG, G. LI, L. LIAO, H. MAO, Q. JIN, AND J. ZHAO, *Direct detection of cancer biomarkers in blood using a place n play modular polydimethylsiloxane pump*, *Biomicrofluidics*, 7 (2013), p. 034105.
- [333] M. ZHANG, J. WU, L. WANG, K. XIAO, AND W. WEN, *A simple method for fabricating multi-layer pdms structures for 3d microfluidic chips*, *Lab on a Chip*, 10 (2010), pp. 1199–1203.
- [334] Y. ZHANG AND G. M. BONE, *Direct switching position control algorithms for pneumatic actuators using on/off solenoid valves*, (2018).
- [335] B. ZHAO, X. CUI, W. REN, F. XU, M. LIU, AND Z.-G. YE, *A controllable and integrated pump-enabled microfluidic chip and its application in droplets generating*, *Scientific reports*, 7 (2017), p. 11319.
- [336] C.-X. ZHAO AND A. P. MIDDELBERG, *Two-phase microfluidic flows*, *Chemical Engineering Science*, 66 (2011), pp. 1394–1411.
- [337] B. ZHENG, C. J. GERDTS, AND R. F. ISMAGILOV, *Using nanoliter plugs in microfluidics to facilitate and understand protein crystallization*, *Current opinion in structural biology*, 15 (2005), pp. 548–555.
- [338] Y. B. ZHENG, B. KIRALY, AND T. J. HUANG, *Molecular machines drive smart drug delivery*, *Nanomedicine*, 5 (2010), pp. 1309–1312.
- [339] J. ZHONG, J. RIORDON, T. WU, H. EDWARDS, A. R. WHEELER, K. PARDEE, A. A. GUZIK, AND D. SINTON, *When robotics met fluidics*, *Lab on a Chip*, (2020).
- [340] J. Y. ZHU, S. A. SUAREZ, P. THURGOOD, N. NGUYEN, M. MOHAMMED, H. ABDELWAHAB, S. NEEDHAM, E. PIROGOVA, K. GHORBANI, S. BARATCHI, ET AL., *Reconfigurable, self-sufficient convective heat exchanger for temperature control of microfluidic systems*, *Analytical chemistry*, 91 (2019), pp. 15784–15790.
- [341] P. ZHU AND L. WANG, *Passive and active droplet generation with microfluidics: a review*, *Lab on a Chip*, 17 (2017), pp. 34–75.

APPENDICES

Appendix A

Operating procedure: flow sensor calibration

Flow sensor calibration





| Revision | Date | Modified by | Notes |
|----------|----------|--------------|----------------------------|
| Rev 1.0 | 20190123 | Marie Hébert | Original released document |
| | | | |




1 Introduction

This document provides instructions for calibrating a flow sensor output for a specific fluid. It includes the data processing using the Excel template [[flow sensor calibration report generator 20180128-02](#)] that is used to generate a standardized report. The instructions to operate the flow sensor [[Flow Sensor SOP](#)] and the syringe pump [[Syringe Pump SOP](#)] are provided elsewhere. Information about the required materials and equipment as well as general guidance are provided in the following sections. The step-by-step procedure is listed at the end of this document.

2 Data collection

2.1 Required materials and equipment

| Qty | Description | Image |
|------------------|-----------------------------------------------------------|---------------------------------------------------------------------------------------|
| <i>Equipment</i> | | |
| 1 | Sensirion SLG-1430 flow sensor | |
| 1 | Flow sensor cable | |
| 1 | Serial-to-usb adapter | |
| 1 | Gas airtight glass syringe (Hamilton) | |
| 1 | Tubing cutter | |
| 1 | Syringe pump | |
| 3 | Disposable Luer syringes | |
| 3 | 20 ml vials for waste collection | |
| 3 | Reservoir holder vials (microwtube) | |
| <i>Fittings</i> | | |
| 3 | Filters (2 μm) | |
| 2 | Capillary 360 μm OD to 1/16" OD tubing adapter |  |
| 1 | Syringe (Luer) to 10-32 adapter |  |
| 3 | 10-32 fitting (1/16" OD) |  |
| 2 | 6-32 fitting (360 μm OD) |  |

| | | |
|-------------------------|-------------------------------------------------------------|-------------------------------------------------------------------------------------|
| 2 | PEEK MicroTight Ferrule 5/16-24 Coned, for 360µm OD [F-152] |  |
| 2 | MicroTight Ferrule Plug [P-116] |  |
| 2 | VHP Female Nut (Micro Fittings), 5/16-24 Coned [P-416] |  |
| <i>Tubing</i> | | |
| 2 | Copper capillary (250 µm ID X 360 µm OD) [> 5 cm length] | |
| 2 | Plastic tubing (0.010"X1/16") [> 30 cm] | |
| <i>Chemicals</i> | | |
| 10 | ml of the fluid of interest | |
| 5 | ml of isopropanol (IPA) | |
| 5 | ml of acetone | |

2.2 Syringe pump

Currently, there are two syringe pumps available in the lab: Harvard Apparatus 33 Twin model and Harvard Apparatus Pico Plus. Consult the appropriate SOP on how to operate them [[Syringe Pump SOP](#)].

The flow rate must be set in $\mu\text{l}/\text{min}$ for the calibration and the internal diameter of the syringe must be entered (in mm). Consult the following datasheet (double-click Adobe icon).

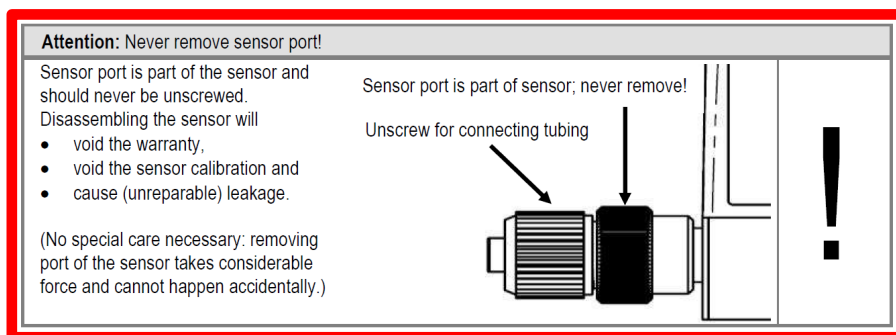
 → [Hamilton Airtight Gas Syringe datasheet](#)
 Adobe Acrobat Document

Care must be taken to watch for the syringe pump emptying and still trying to advance. This will break the wings of the expensive glass syringe.

For faster setup, once all connections are made, it is easier to *manually* push the fluid through the tubing all the way to the waste and ensure there are no air bubbles. Then, the syringe can be driven using the syringe pump.

2.3 Flow sensor

DO NOT TOUCH THE PARTS INDICATED IN THE FIGURE. BY UNTIGHTENING, YOU WILL BREAK THE > \$6000 PIECE OF EQUIPMENT THAT IS THE FLOW SENSOR.



The ferrule for the 360 μm OD capillary can be unusable due to a piece of capillary breaking in them. Care must be taken to not break the capillary by avoiding to bending and torsion at all cost.

The Sensirion SLG-1430 datasheet is included below (double-click Adobe icon).



2.4 Collecting the data

The transient response of the syringe pump is much longer than for the pressure pump. Therefore, after setting the flow rate on the syringe pump, 5 minutes must elapse before data is collected.

The tip of the tubing must be submerged in the waste vial to prevent variations from the formation (and breakage) of droplets at the tip that will affect the flow rate.

Record data for 1 min at lowest frequency (1.56 Hz) in raw mode for better (smaller) resolution. Raw mode records the output in bits [0-32767] rather than applying the default factory water calibration. Note that the header in the recorded file will still specify flow rate in [$\mu\text{l}/\text{min}$] rather than in bits, but the values will be in bits. Simply disregard the header.

The range to cover before the relationship becomes nonlinear is generally from 1.0 $\mu\text{l}/\text{min}$ to 5.0 $\mu\text{l}/\text{min}$ in 0.5 $\mu\text{l}/\text{min}$ increments. Each flow rate must be repeated 3 times under loading (increasing flow rate) and unloading (decreasing flow rate) conditions. The third repetition conditions is up to the user.

All files should be saved in the same folder. The naming convention for the recorded files must follow the convention: *i*.d ul/min *n* dataset → *i_d-n.txt* e.g. 1.5 ul/min 2nd dataset → 1_5-2.txt

2.4.1. SensiView software for data collection.

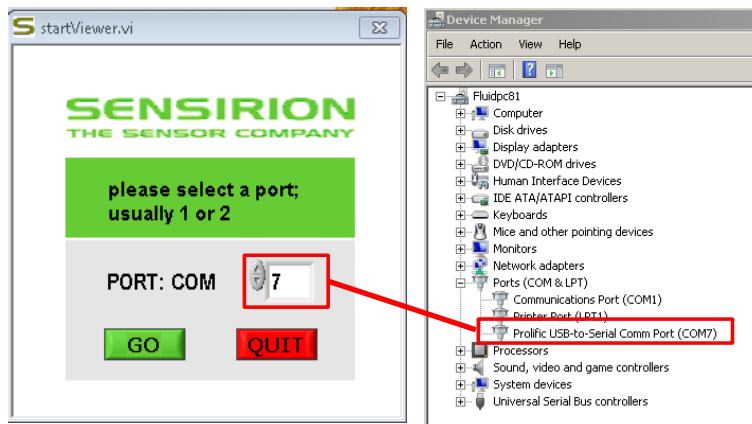


Figure 1. SensiView software screenshot of opening window and device manager to identify the correct COM port.

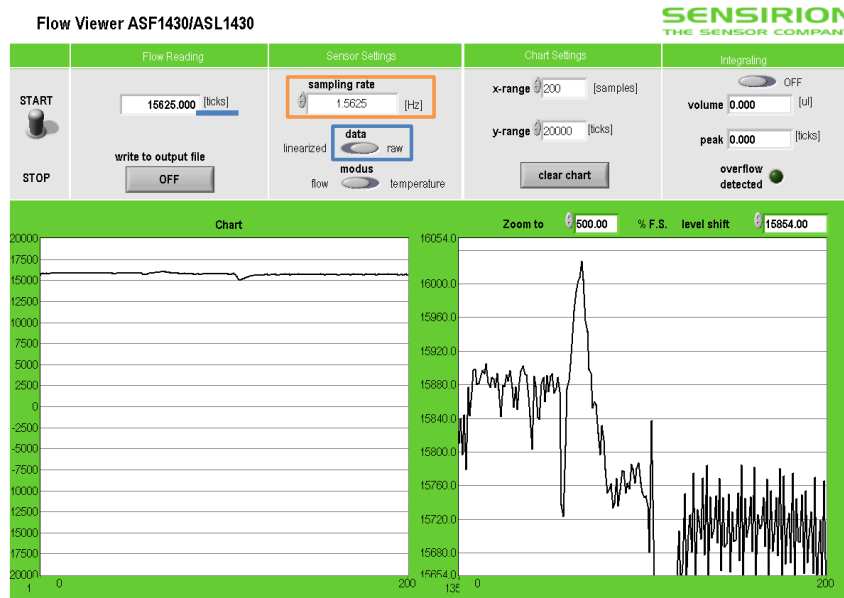


Figure 2. SensiView software screenshot with important settings highlighted.

2.5 Cleaning up

The pressure pump with the reservoir holder can help to clean the setup easily by pushing the appropriate fluid (or air) through the whole tubing.

Prepare one filtered isopropanol solution, one filtered acetone solution and one empty vial in the reservoir holder. All pressures can be set to 250 mbar. It is important to first clean with acetone and then with isopropanol; acetone leaves an undesirable residue after evaporation that isopropanol does not; however, acetone is a better cleaning agent.

In order to connect the input that was initially to the syringe, the 10-32 fitting can be removed from the syringe (Luer) to 10-32 adapter and then, it can be directly connected to the reservoir holder output.

3 Report generation

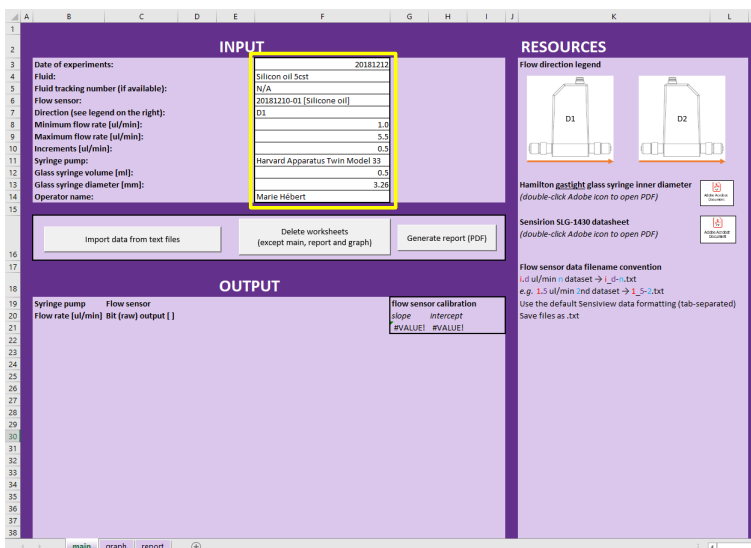
3.1 Data files preparation

All the files of the data collected should be grouped into one folder. Make sure the files follow the following naming convention and are as-is from the SensiView software (i.e. tab-separated files saved as txt).

i.d ul/min n dataset → i_d-n.txt
 e.g. 1.5 ul/min 2nd dataset → 1_5-2.txt

3.2 Using the Excel template

1. Place a copy of the Excel template for report generation [[flow sensor calibration report generator 20180128-02](#)] in the same folder as all your data.
2. Open the file.
3. Enter all information pertaining to the calibration data that was collected in the “Input” section. The range for flow rate is indicated with the minimum, maximum and incremental flow rate. Three repetitions are assumed for all data.



4. Click the “Import data from text files” button. Note this can take some moment to process. All data will now be in its separate tab with the summary (i.e. the average) shown on the main page. The graph tab also updates automatically.

The screenshot shows the software interface with three main sections: INPUT, RESOURCES, and OUTPUT.

INPUT

| | |
|---------------------------------------|---------------------------------|
| Date of experiments: | 20181212 |
| Fluid: | Silicon oil 5cst |
| Fluid tracking number (if available): | N/A |
| Flow sensor: | 20181219-01 (Silicone oil) |
| Direction (see legend on the right): | D1 |
| Minimum flow rate [ul/min]: | 1.0 |
| Maximum flow rate [ul/min]: | 5.5 |
| Increments [ul/min]: | 0.5 |
| Syringe pump: | Harvard Apparatus Twin Model 33 |
| Glass syringe volume [ml]: | 0.5 |
| Glass syringe diameter [mm]: | 3.26 |
| Operator name: | Marie Hébert |

RESOURCES

Flow direction legend

D1: D2:

Hamilton gastight glass syringe inner diameter (double-click Adobe icon to open PDF)

Sensirion SSG-1430 datasheet (double-click Adobe icon to open PDF)

Flow sensor data filename convention
 .i.ul/min - dataset -> i-0-i.txt
 e.g. 1.5 ul/min - md dataset -> 1_5-1.txt
 Use the default Sensiview data formatting (tab-separated)
 Save files as .txt

OUTPUT

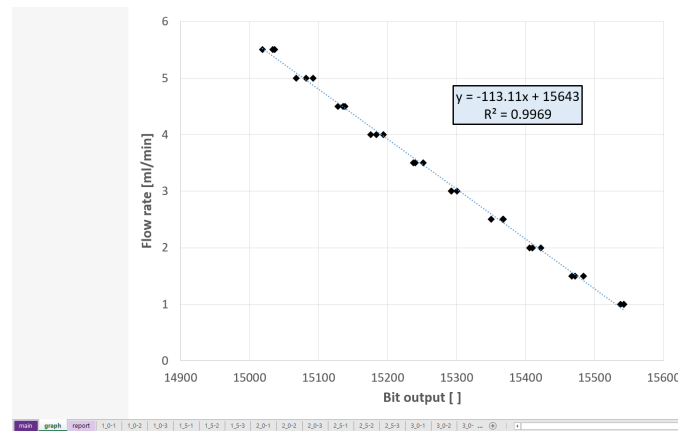
| Syringe pump | Flow sensor | Flow rate [ul/min] | Bit (raw) output [] |
|--------------|-------------|--------------------|----------------------|
| 1 | 1 | 1.5442 | 61905 |
| 1 | 1 | 15537 | 33333 |
| 1 | 1 | 15542 | 31361 |
| 1.5 | 1.5 | 15466 | 85437 |
| 1.5 | 1.5 | 15483 | 85437 |
| 1.5 | 1.5 | 15471 | 56051 |
| 2 | 2 | 15405 | 68462 |
| 2 | 2 | 15422 | 0198 |
| 2 | 2 | 15409 | 80392 |
| 2.5 | 2.5 | 15367 | 55385 |
| 2.5 | 2.5 | 15350 | 40351 |
| 2.5 | 2.5 | 15367 | 38938 |
| 3 | 3 | 15292 | 74436 |
| 3 | 3 | 15292 | 5 |
| 3 | 3 | 15300 | 89381 |
| 3.5 | 3.5 | 15251 | 76471 |
| 3.5 | 3.5 | 15237 | 20492 |
| 4 | 4 | 15398 | 44399 |

Flow sensor calibration

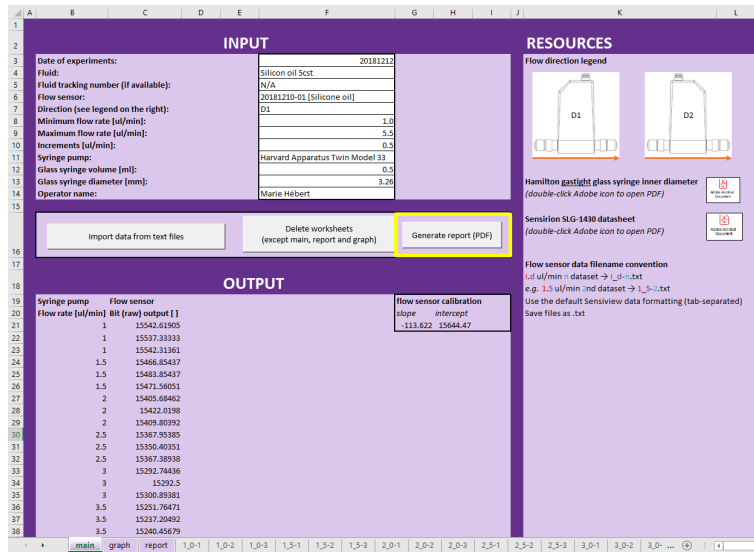
| | |
|-----------|----------|
| slope | -113.622 |
| intercept | 15644.47 |

Buttons: Import data from text files, Delete worksheets (except main, report and graph), Generate report (PDF)

5. Verify that the graph and report are as expected.

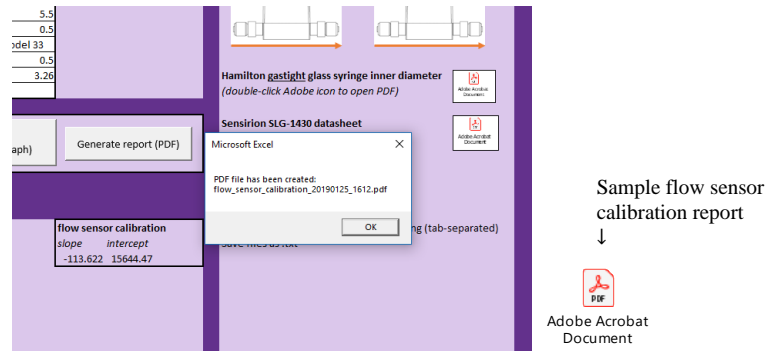


- Automatically generate the report by clicking the “Generate report (PDF)” button on the main tab. This will output a PDF file with all the information entered in the “Input” section and the graph in the same folder.



| Syringe pump | Flow sensor | Flow rate [ul/min] | Bit (raw) output [] | flow sensor calibration |
|--------------|-------------|--------------------|----------------------|-------------------------|
| 1 | 1 | 15542.61905 | | slope intercept |
| 22 | 1 | 15597.33333 | | -113.622 15644.47 |
| 23 | 1 | 15542.31361 | | |
| 24 | 1.5 | 15466.85437 | | |
| 25 | 1.5 | 15483.85437 | | |
| 26 | 1.5 | 15471.56051 | | |
| 27 | 2 | 15405.68462 | | |
| 28 | 2 | 15422.0138 | | |
| 29 | 2 | 15409.80392 | | |
| 30 | 2.5 | 15367.55385 | | |
| 31 | 2.5 | 15350.40351 | | |
| 32 | 2.5 | 15367.38938 | | |
| 33 | 3 | 15292.74436 | | |
| 34 | 3 | 15292.5 | | |
| 35 | 3 | 15300.89381 | | |
| 36 | 3.5 | 15251.76471 | | |
| 37 | 3.5 | 15237.20492 | | |
| 38 | 3.5 | 15240.45679 | | |

- A dialog box will confirm the successful creation of the file. Verify that the PDF file contains the proper information.



Microsoft Excel

PDF file has been created:
flow_sensor_calibration_20190125_1612.pdf

OK

Sample flow sensor calibration report

↓

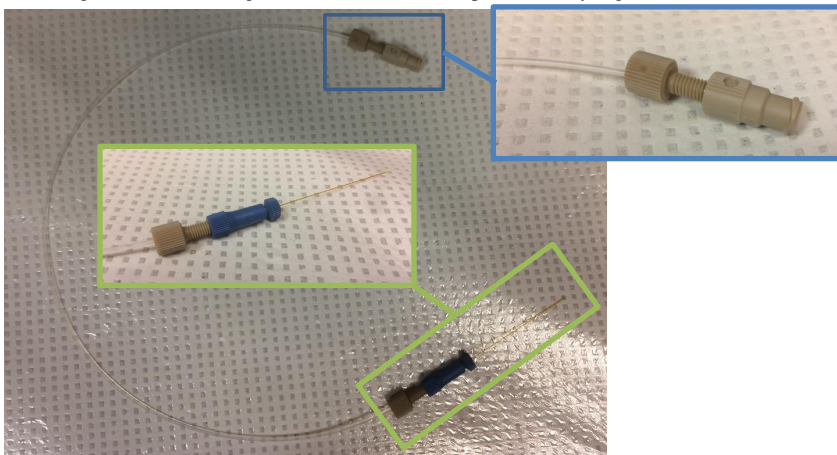
Adobe Acrobat Document

4 Step-by-step procedure

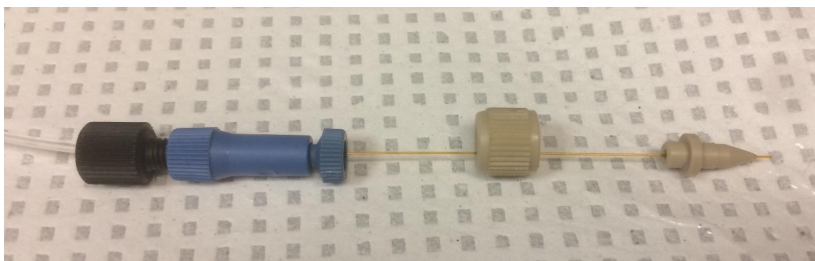
1. Filter the fluid the flow sensor will be calibrated for using a $2\ \mu\text{m}$ filter attached to a Luer syringe into a 20 ml vial. Typically, the total volume that will be required is about 10 ml.
2. Filter acetone and IPA into 2 ml microtube (to use with the reservoir holder and the pressure pump) for the cleaning procedure at the end.
3. Prepare two pieces of capillary (250 ID X 360 OD μm) of at least 5 cm using the tubing cutter.
4. Prepare two pieces of plastic tubing (0.010"X1/16") to connect the syringe pump output to the pressure sensor input (about > 30 cm), and to connect the flow sensor output to the waste vial (about ~20 cm).

Note: The tubing from the flow sensor output to the waste vial should be long enough for the tip to be submerged.

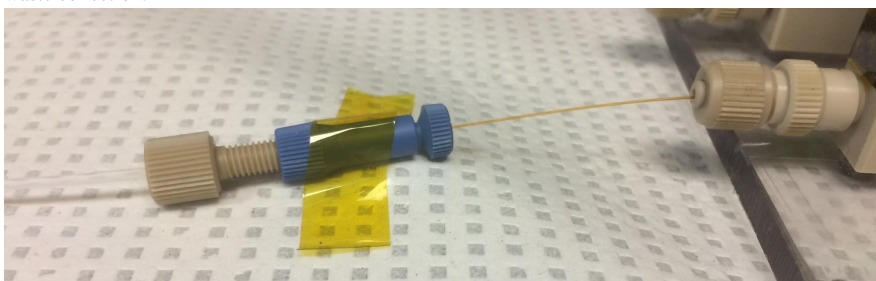
5. Connect the capillary to the 360 μm OD to 1/16" OD tubing adapter with the tubing other end of the tubing to the 10-32 fitting and then, to the Luer adapter for the syringe.



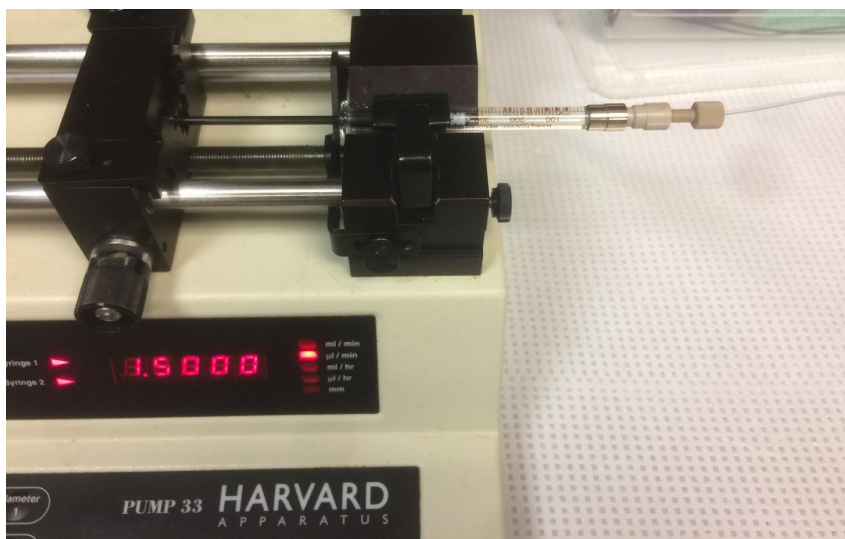
6. Similarly connect the other capillary to the 360 μm OD to 1/16" OD tubing adapter with the tubing other end.



7. Secure the flow sensor on the surface using tape.
8. Connect the flow sensor to the computer (Refer to the flow sensor SOP: [Flow Sensor SOP](#)).
9. Connect the capillaries to the flow sensor input and output. Secure the 360 μm OD to 1/16" OD tubing adapters using tape to prevent the capillary from moving too much and breaking. The input should be close to the syringe pump while the output should be in a 20 ml vial used for waste collection.



10. Fill the glass syringe with the fluid of interest.
11. Connect the syringe to the tubing.
12. Manually fill the entire tubing and fittings. There must be no air bubble.
13. Insert the syringe in the syringe pump (Refer to the syringe pump SOP: [Syringe Pump SOP](#)).



14. Set the desired flow rate and wait 5 minutes for stabilization.
15. Record the raw data for 1 minutes at a sampling frequency of 1.56 Hz following the naming convention: $i.d$ $\mu\text{l}/\text{min}$ n dataset $\rightarrow i_d-n.txt$ e.g. $1.5 \mu\text{l}/\text{min}$ 2nd dataset $\rightarrow 1_5-2.txt$.
16. Repeat steps 14-15 for flow rates from $1.0 \mu\text{l}/\text{min}$ to $5.0 \mu\text{l}/\text{min}$ in $0.5 \mu\text{l}/\text{min}$ increments (3 repetitions for each flow rate).

Note: Be careful of the syringe emptying. The “bottoming” of the syringe will break the glass wings. To replenish the liquid: stop the syringe pump, remove the syringe, disconnect the Luer adapter, fill the syringe, reconnect the Luer adapter, manually push any air bubbles all the way to the waste, reposition in the syringe in the syringe pump, restart the syringe pump, wait 5 min for stabilization before collecting data.

17. To facilitate the cleaning procedure, a pressure pump with an empty microwtube, an acetone microwtube, and an IPA microwtube (pre-filtered solutions) can be used. The Luer lock adapter can be removed, and the 10-32 fitting can be connected to the appropriate output of the reservoir holder.
18. Empty the tubing of the fluid used for calibration by pushing air through.
19. Change the waste bottle to separate the fluid from acetone and IPA. Dispose properly.
20. Rinse with acetone for one minute.
21. Push air through.
22. Rinse with isopropanol for one minute.
→ It is important to do acetone first and then IPA. Acetone leaves a residue when evaporating while IPA does not.
23. Push air through until empty and then for one minute to make sure everything is dry. There should be no liquid in the flow sensor when storing them.
24. Put back the ferrule plugs to seal the flow sensor input and output for storage.

Appendix B

State-space matrices – Symmetric model

The model developed by David Wong ([311]) and subsequently used for controller design relies on the description of the fluid physics using RLC circuit elements. The symmetric model herein described uses a different block element; the resistance and inductance are split in half on either side of the capacitor. Contrarily to the previous simpler RLC circuit, the symmetry leads to a symmetric response whether current flows from in-to-out or out-to-in. The symmetric configuration adds an additional inductor, and hence, the block element is third-order (two inductors and one capacitor) rather than second order. Nonetheless, the connection in series of the tube and the channel combines the resistance and inductor through simple addition. Thus, the overall order—and hence complexity—for the T junction model is only increased from 10th to 14th order.

The assembly of symmetric RLC blocks as shown in Figure B.1 for a T-junction chip and its sample tubing results in a 14th order state-space model. As previously established by the modular design of the controller by Wong, the matrices values can be readily extracted from the *Simulink* graphical representation. However, for resistance identification, the analytical equations rather than numerical matrices are required to use the grey-box algorithm. Although *Matlab* has symbolic variables capabilities, the derivation by-hand is straightforward and preferred. The equations are validated against the numerical matrices calculated using *Matlab*. The symmetry of the network as a whole with respect to the three branches means that certain equations are similar for each channel.

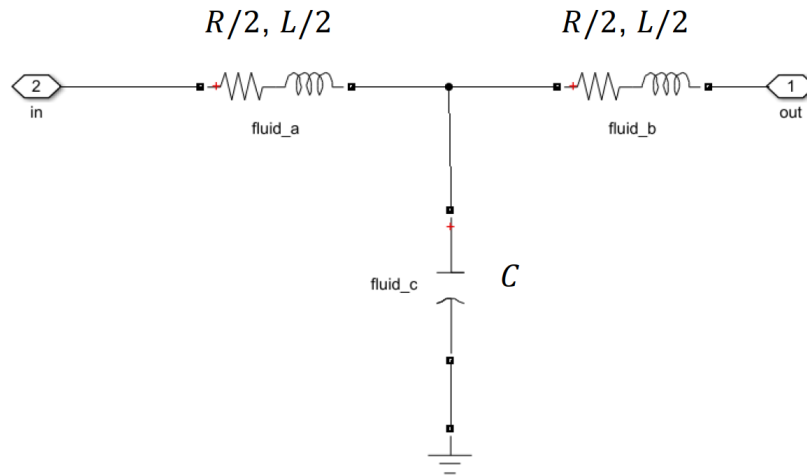


Figure B.1: Symmetric RLC block element.

B.1 Analogy between fluid and electrical principles

The fluid physics involved in two-phase flow in microchannels is complex. Theoretical analytical descriptions are investigated but the complexity is prohibitive to develop a simple mathematical expression ([309, 246]). A simpler model enables controller design and quicker simulation albeit at the cost of accuracy. Nevertheless, it is beneficial to remember that “[...] all models are wrong; the practical question is how wrong do they have to be to not be useful.” ([27, p. 63]). Thus, although a simpler model is less accurate, its usefulness is still significant because if it is not *too* wrong. Therefore, complex fluid flows at the microfluidic chip inlet, two-phase flow, and flow at the T junction where all three channels intersect are neglected.

The analogy between fluid and electrical principles is established. Each section of the system is described by a second-order system that is an RLC circuit. The RLC circuit could be a mass-spring-damper system but *Simulink* allows to more readily extract state-space matrices from a circuit. The details of the equivalence between the fluid and electrical principles are summarized in Figure B.2.

Current is conserved at the junction of element connected in series that is the current in one element is equal to the current in the next element. From a fluid perspective, the flow rate is conserved across the connection between the tube and

channel for example (assuming no leakage). Current is equivalent to flow rate as opposed to velocity because the cross-section of elements in series fluctuates.

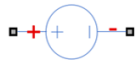
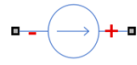



| Fluid principle | Electric circuit element | Units | Circuit element symbol | |
|-----------------------------------------------|--------------------------|---------------------------------------------------------|-------------------------------------------------------------------------------------|-------------------------------------------------------------------------------------|
| Pressure | Potential | Pa |  | |
| Flow rate | Current | m ³ /s |  | |
| Viscous forces | Resistance | $R = \frac{32\mu L}{d_h^2 \cdot A}$ | $\frac{\text{Pa} \cdot \text{s}}{\text{m}^3}$ |  |
| Inertia effects | Inductance | $L = \frac{\rho l}{A}$ | $\frac{\text{Pa} \cdot \text{s}^2}{\text{m}^3}$ |  |
| Material compliance and fluid compressibility | Capacitance | $C = \left(\frac{A}{\kappa} + \frac{1}{\beta}\right) A$ | $\frac{\text{m}^3}{\text{Pa}}$ |  |

Figure B.2: Analogy between fluid and electrical principles. Where μ is the dynamic viscosity [$kg/m \cdot s$], l is the channel length [m], and d_h is the hydraulic diameter [m], ρ is density [kg/m^3] and l is channel length [m], A is the cross sectional area [m^2], κ is the substrate stiffness [$Pa \cdot m$], l is the channel length [m], and β is the adiabatic bulk modulus [Pa].

The dynamics of the passive RLC circuit elements can be expressed using straightforward equations.

$$U_R = R \cdot I_R \tag{B.1}$$

$$I_C = C \cdot \frac{dU_C}{dt} \tag{B.2}$$

$$U_L = L \cdot \frac{dI_L}{dt} \tag{B.3}$$

B.2 Overview

The assembly of the block elements mimics the physical setup with the tube and microchannels. Tubes and channels are connected in series with the source at one end, and the junction at the other as shown in Figure B.3.

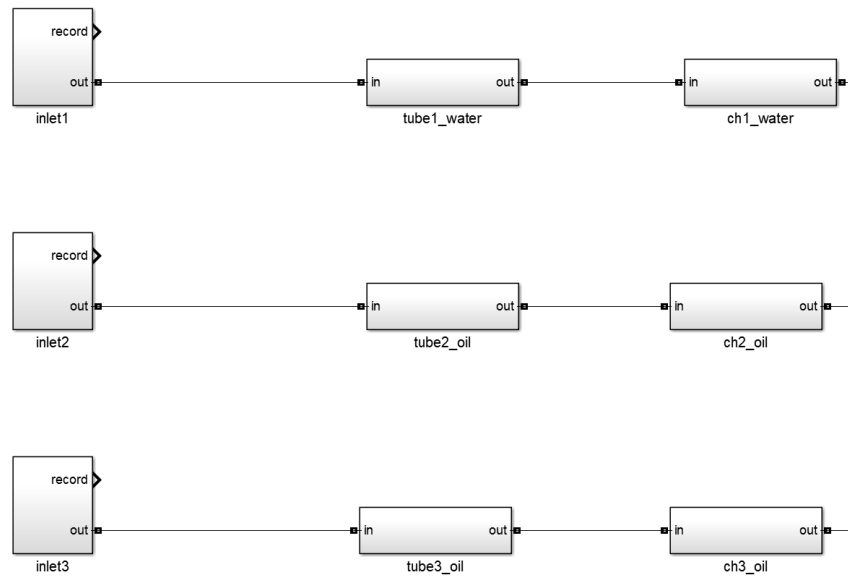


Figure B.3: Overview of the T-junction circuit. Each element has the internal RLC components illustrated in Figure B.1 with their value associated with the system properties.

B.3 States, inputs, and outputs

The states are determined automatically using *Matlab* and can fully described the system's state at any point in time.

$$X = \begin{bmatrix} U_{ch1} & (1) \\ I_{ch2b} & (2) \\ U_{ch2} & (3) \\ I_{ch3b} & (4) \\ U_{ch3b} & (5) \\ I_{tube1a} & (6) \\ I_{tube1b} & (7) \\ U_{tube1} & (8) \\ I_{tube2a} & (9) \\ I_{tube2b} & (10) \\ U_{tube2} & (11) \\ I_{tube3a} & (12) \\ I_{tube3b} & (13) \\ U_{tube3} & (14) \end{bmatrix} \quad (\text{B.4})$$

The actuation is provided by the pressure pump output channels that are independently controlled. Each branch of the T-junction is connected to a tubing transporting the fluid from the reservoir holder. There is also a soft air tubing between the pressure pump and the reservoir holder.

$$U = \begin{bmatrix} P_1 \\ P_2 \\ P_3 \end{bmatrix} \quad (\text{B.5})$$

The output vector is made of the available measurements. The position of the droplet interface in the channel provides the required information. Position, velocity, and flow rate can easily be related to each other ($V = \frac{dx}{dt}$, $Q = V \cdot A$). The system is inherently multi-input-multi-output (MIMO). However, the conservation of mass principle restricts the number of outputs that can simultaneously be tracked. At a T-junction, only two of the three channel flow can be arbitrarily controlled; the third channel flow is algebraically related to the two others, and thus, it cannot be controlled. The appropriate row for the measurement must be removed depending on the request to control which channel.

$$Y = \begin{bmatrix} V_{ch1} \\ V_{ch2} \\ V_{ch3} \end{bmatrix} \quad (\text{B.6})$$

B.4 Circuit and derivation at the channel junction

The three channels meet at the junction where an algebraic relationship between the three currents can easily be established. This is of particular interest for the derivation of the equation for state 1.

$$I_{ch1b} + I_{ch2b} + I_{ch3b} = 0 \rightarrow I_{ch1b} = -I_{ch2b} - I_{ch3b} \quad (\text{B.7})$$

$$\dot{U}_{ch1} = \frac{1}{C_{ch1}}(I_{ch1a} - I_{ch1b}) \quad (\text{B.8})$$

B.5 Circuit and derivation for \dot{U}_{tubeX}

The circuit and derivation for the equations of states 8, 11, and 14 are similar.

$$I_{tube1a} = I_C + I_{tube1b} \rightarrow I_C = I_{tube1a} - I_{tube1b} \quad (\text{B.9})$$

$$\dot{U}_{tube1} = \frac{1}{C_{tube1}}(I_{tube1a} - I_{tube1b}) \quad (\text{B.10})$$

B.6 Circuit and derivation for \dot{U}_{chX}

Equations 3 and 5 are very similarly derived while for Equation 1, the algebraic relationship to the two other branches (Equation B.7) must be used. Moreover, the connection in series between the tube and channel means that the current is conserved.

$$I_{tube2b} = I_{ch2a} \quad (\text{B.11})$$

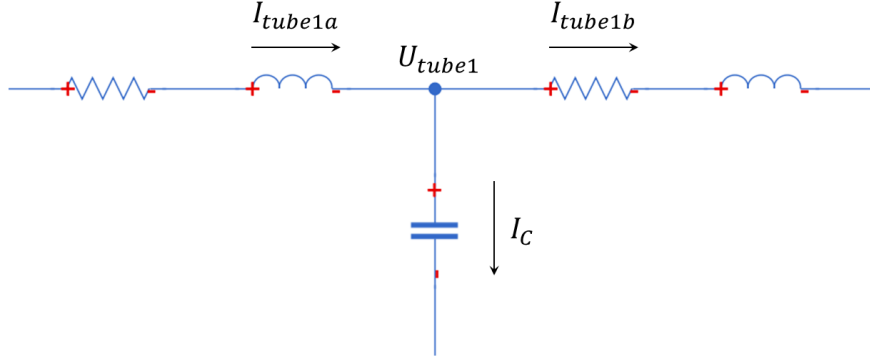


Figure B.4: Circuit for derivation of equations for \dot{U}_{tubeX} states (8, 11, and 14).

$$\dot{U}_{ch2} = \frac{1}{C_{ch2}}(I_{ch2a} - I_{ch2b}) \rightarrow \dot{U}_{ch2} = \frac{1}{C_{ch2}}(I_{tube2b} - I_{ch2b}) \quad (\text{B.12})$$

B.7 Circuit and derivation for \dot{I}_{tubeXa}

The voltage drop between the input (U_1) to the capacitor associated with the tube (U_{tube1}) is expressed in terms of drop across the resistance and inductance.

$$U_1 - U_{tube1} = \frac{L_{tube1}}{2} \dot{I}_{tube1a} + \frac{R_{tube1}}{2} I_{tube1a} \quad (\text{B.13})$$

$$\dot{I}_{tube1a} = \frac{-R_{tube1}}{L_{tube1}} I_{tube1a} + \frac{2}{L_{tube1}} (U_1 - U_{tube1}) \quad (\text{B.14})$$

B.8 Circuit and derivation for \dot{I}_{chXb}

The derivation for Equations 2 and 4 is lengthier and involves combining 3 sub-equations (labeled (i), (ii), and (iii)) to eliminate the intermediary variable U_{jct} . The

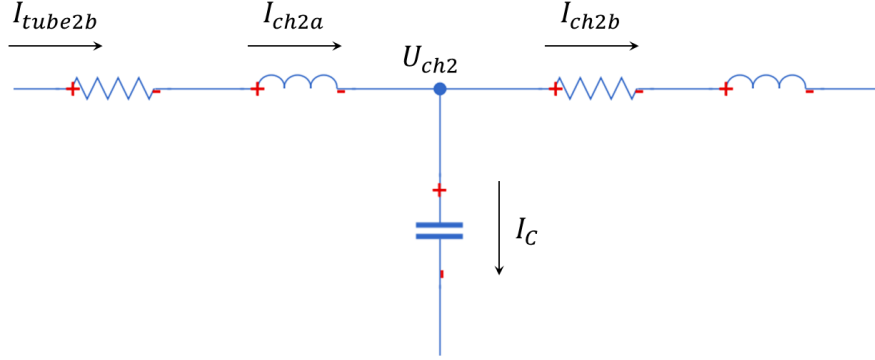


Figure B.5: Circuit for derivation of equations for \dot{U}_{chX} states (1, 3, and 5).

current in CH1 is not a state because there is an algebraic relationship (Equation B.7) with the current in the two other channels that are already states.

$$U_{ch1} - U_{jct} = \frac{L_{ch1}}{2} \dot{I}_{ch1b} + \frac{R_{ch1}}{2} I_{ch1b} \quad (i)$$

$$U_{ch2} - U_{jct} = \frac{L_{ch2}}{2} \dot{I}_{ch2b} + \frac{R_{ch2}}{2} I_{ch2b} \quad (ii)$$

$$U_{ch3} - U_{jct} = \frac{L_{ch3}}{2} \dot{I}_{ch3b} + \frac{R_{ch3}}{2} I_{ch3b} \quad (iii)$$

Combining (ii) and (iii) allows to express \dot{I}_{ch2b} in terms of \dot{I}_{ch3b} and the two states I_{ch2b} and I_{ch3b} .

$$(iii) - (ii) \rightarrow U_{ch3} - U_{ch2} = \frac{L_{ch3}}{2} \dot{I}_{ch3b} + \frac{R_{ch3}}{2} I_{ch3b} - \frac{L_{ch2}}{2} \dot{I}_{ch2b} - \frac{R_{ch2}}{2} I_{ch2b} \quad (B.15)$$

$$(a) \rightarrow \frac{L_{ch2}}{2} \dot{I}_{ch2b} = \frac{L_{ch3}}{2} \dot{I}_{ch3b} + \frac{R_{ch3}}{2} I_{ch3b} - \frac{R_{ch2}}{2} I_{ch2b} + U_{ch2} - U_{ch3} \quad (B.16)$$

For Equation 4:

$$(ii) - (i) \rightarrow U_{ch2} - U_{ch1} = \frac{L_{ch2}}{2} \dot{I}_{ch2b} + \frac{R_{ch2}}{2} I_{ch2b} - \frac{L_{ch1}}{2} \dot{I}_{ch1b} - \frac{R_{ch1}}{2} I_{ch1b} \quad (B.17)$$

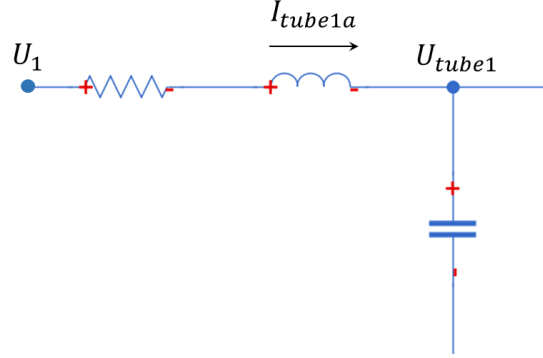


Figure B.6: Circuit for derivation of equations for \dot{I}_{tubeXa} states (6, 9, and 12).

Replace I_{ch1b} using Equation B.7.

$$U_{ch2} - U_{ch1} = \left(\frac{L_{ch2}}{2} + \frac{L_{ch1}}{2} \right) \dot{I}_{ch2b} + \left(\frac{R_{ch2}}{2} + \frac{R_{ch1}}{2} \right) I_{ch2b} + \frac{L_{ch1}}{2} \dot{I}_{ch3b} + \frac{R_{ch1}}{2} I_{ch3b} \quad (\text{B.18})$$

Although I_{ch2b} and I_{ch3b} are both states, their respective derivative is not. Therefore, Equation (a) must be used to eliminate one of the two derivatives.

$$U_{ch2} - U_{ch1} = \underbrace{\left(\frac{L_{ch2}}{2} + \frac{L_{ch1}}{2} \right) \frac{2}{L_{ch2}}}_{(1+L_{ch1}/L_{ch2})} \left(\frac{L_{ch3}}{2} \dot{I}_{ch3b} + \frac{R_{ch3}}{2} I_{ch3b} - \frac{R_{ch2}}{2} I_{ch2b} \right. \\ \left. + U_{ch2} - U_{ch3} \right) + \left(\frac{R_{ch2}}{2} + \frac{R_{ch1}}{2} \right) I_{ch2b} + \frac{L_{ch1}}{2} \dot{I}_{ch3b} + \frac{R_{ch1}}{2} I_{ch3b} \quad (\text{B.19})$$

$$0 = \underbrace{\left(\left(1 + \frac{L_{ch1}}{L_{ch2}} \right) \frac{L_{ch3}}{2} + \frac{L_{ch1}}{2} \right)}_{-d_4} \dot{I}_{ch3b} + \left(\left(1 + \frac{L_{ch1}}{L_{ch2}} \right) \frac{R_{ch3}}{2} + \frac{R_{ch1}}{2} \right) I_{ch3b} \\ + \left(\left(\frac{R_{ch2}}{2} + \frac{R_{ch1}}{2} \right) - \left(1 + \frac{L_{ch1}}{L_{ch2}} \right) \frac{R_{ch2}}{2} \right) I_{ch2b} \\ + U_{ch1} + \left(\frac{L_{ch1}}{L_{ch2}} \right) U_{ch2} - \left(1 + \frac{L_{ch1}}{L_{ch2}} \right) U_{ch3} \quad (\text{B.20})$$

Similarly for Equation 2:

$$\begin{aligned}
0 = & \underbrace{\left(\left(1 + \frac{L_{ch1}}{L_{ch3}} \right) \frac{L_{ch2}}{2} + \frac{L_{ch1}}{2} \right)}_{-d_2} \dot{I}_{ch2b} + \left(\left(1 + \frac{L_{ch1}}{L_{ch3}} \right) \frac{R_{ch2}}{2} + \frac{R_{ch1}}{2} \right) I_{ch2b} \\
& + \left(\left(\frac{R_{ch3}}{2} + \frac{R_{ch1}}{2} \right) - \left(1 + \frac{L_{ch1}}{L_{ch3}} \right) \frac{R_{ch3}}{2} \right) I_{ch3b} \\
& + U_{ch1} - \left(1 + \frac{L_{ch1}}{L_{ch3}} \right) U_{ch2} + \left(\frac{L_{ch1}}{L_{ch3}} \right) U_{ch3} \quad (B.21)
\end{aligned}$$

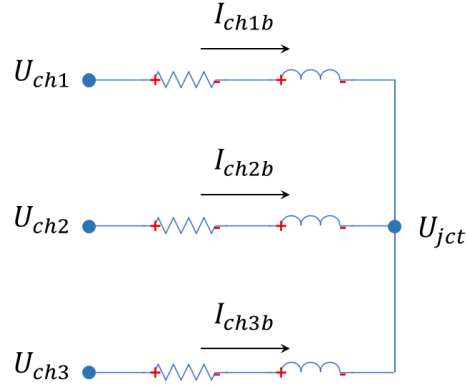


Figure B.7: Circuit for derivation of equations for \dot{I}_{chXb} states (2, and 4).

B.9 Circuit and derivation for \dot{I}_{tubeXb}

The voltage drop from the tube to the channel capacitor potential is expressed in terms of the drop across each components. Similarly to previously, there is a current equivalence (Equation B.11) because the tube and channel are connected in series.

$$U_{tube1} - U_{ch1} = \sum L \dot{I}_{tube1b} + \sum R I_{tube1b} \quad (B.22)$$

where

$$\sum L = \frac{L_{tube}}{2} + \frac{L_{ch}}{2}, \text{ and } \sum R = \frac{R_{tube}}{2} + \frac{R_{ch}}{2}.$$

$$\dot{I}_{tube1b} = \frac{-\sum R}{\sum L} I_{tube1b} + \frac{1}{\sum L} (U_{tube1} - U_{ch1}) \quad (\text{B.23})$$

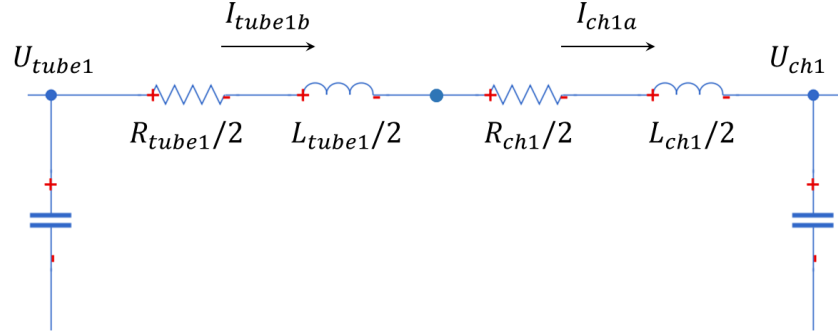


Figure B.8: Circuit for derivation of equations for \dot{I}_{tubeXb} states (7, 10, and 13).

B.10 State-space matrices

The standard state-space format is used to express the MIMO model.

$$\dot{X} = A \cdot X + B \cdot U \quad (\text{B.24})$$

$$Y = C \cdot X + D \cdot U \quad (\text{B.25})$$

For the following matrices, a shorthand is used to keep them more legible. The combination of half the resistance or inductance of the tube and channel is due to their connection in series. For example:

$$\sum R_1 = \frac{R_{tube1}}{2} + \frac{R_{ch1}}{2}$$

$$\sum L_2 = \frac{L_{tube2}}{2} + \frac{L_{ch2}}{2}$$

B.10.1 $A \in \mathbb{R}^{14 \times 14}$

Row 2

$$\begin{aligned}d_2 &= -\left(\frac{Lch1}{2} + \left(1 + \frac{Lch1}{Lch3}\right)\frac{Lch2}{2}\right) \\A_{21} &= \frac{1}{d_2} \\A_{22} &= \left(\frac{Rch1}{2} + \left(1 + \frac{Lch1}{Lch3}\right)\frac{Rch2}{2}\right)/d_2 \\A_{23} &= \left(-\left(1 + \frac{Lch1}{Lch3}\right)\right)/d_2 \\A_{24} &= \left(\frac{Rch3}{2} + \frac{Rch1}{2} - \left(1 + \frac{Lch1}{Lch3}\right)\frac{Rch3}{2}\right)/d_2 \\A_{25} &= \left(\frac{Lch1}{Lch3}\right)/d_2\end{aligned}$$

Row 4

$$\begin{aligned}d_4 &= -\left(\frac{Lch1}{2} + \left(1 + \frac{Lch1}{Lch2}\right)\frac{Lch3}{2}\right) \\A_{41} &= \frac{1}{d_4} \\A_{42} &= \left(\frac{Rch2}{2} + \frac{Rch1}{2} - \left(1 + \frac{Lch1}{Lch2}\right)\frac{Rch2}{2}\right)/d_4 \\A_{43} &= \left(\frac{Lch1}{Lch2}\right)/d_4 \\A_{44} &= \left(\frac{Rch1}{2} + \left(1 + \frac{Lch1}{Lch2}\right)\frac{Rch3}{2}\right)/d_4 \\A_{45} &= \left(-\left(1 + \frac{Lch1}{Lch2}\right)\right)/d_4\end{aligned}$$

B.10.2 $B \in \mathbb{R}^{14 \times 3}$

$$B = \begin{bmatrix} 0 & 0 & 0 & (1) \\ 0 & 0 & 0 & (2) \\ 0 & 0 & 0 & (3) \\ 0 & 0 & 0 & (4) \\ 0 & 0 & 0 & (5) \\ \frac{2}{Ltube1} & 0 & 0 & (6) \\ 0 & 0 & 0 & (7) \\ 0 & 0 & 0 & (8) \\ 0 & \frac{2}{Ltube2} & 0 & (9) \\ 0 & 0 & 0 & (10) \\ 0 & 0 & 0 & (11) \\ 0 & 0 & \frac{2}{Ltube3} & (12) \\ 0 & 0 & 0 & (13) \\ 0 & 0 & 0 & (14) \end{bmatrix}$$

B.10.3 $C \in \mathbb{R}^{1 \times 14}$

$$C = \begin{bmatrix} (1) & (2) & (3) & (4) & (5) & (6) & (7) & (8) & (9) & (10) & (11) & (12) & (13) & (14) \\ 0 & 0 & 0 & 0 & 0 & 0 & 1/A_{x-sect} & 0 & 0 & 0 & 0 & 0 & 0 & 0 \\ 0 & 0 & 0 & 0 & 0 & 0 & 0 & 0 & 0 & 1/A_{x-sect} & 0 & 0 & 0 & 0 \\ 0 & 0 & 0 & 0 & 0 & 0 & 0 & 0 & 0 & 0 & 0 & 0 & 1/A_{x-sect} & 0 \end{bmatrix}$$

B.10.4 $D \in \mathbb{R}^{3 \times 3}$

$$D = \begin{bmatrix} 0 & 0 & 0 \\ 0 & 0 & 0 \\ 0 & 0 & 0 \end{bmatrix}$$

Appendix C

Flexible strain sensor

The work in this chapter was published in the following article:

Hébert, Marie, Jan P. Huissoon, and Carolyn L. Ren. “A Silicone-based Soft Matrix Nanocomposite Strain-like Sensor Fabricated using Graphene and Silly Putty®.” *Sensors and Actuators A: Physical* (2020): 111917. [112]

DOI: 10.1016/j.sna.2020.111917

C.1 Relation to other work in this thesis

The investigation of tubing dynamics presented in Chapter 6 demonstrated the significant impact of the air tubing on the system dynamics; correspondingly, the hydrodynamics resistance project (Chapter 7) considers the tubing dynamics to improve the accuracy of the parameter identification.

C.2 Overview

Off-the-shelf planar strain gauges are ubiquitous and are generally designed for materials with a large elastic modulus such as steel or aluminum. Correspondingly, the strain gauges themselves are stiff and do not deform substantially under applied stress. Pairs of this type of strain gauge are typically used in a Wheatstone bridge circuit allowing the measurement of very small changes in resistance due to the changes in sensing element cross-sectional area to be measured. However, their use with softer low-modulus materials is limited due to the larger elastic deformations involved. The conductive property of graphene is leveraged to produce a different type of strain sensor that is sensitive yet also capable of significant elastic deformation. The graphene is dispersed in a silicone-based polymer matrix such that the deformation induces a change in resistance that can be measured using a voltage divider circuit. The target application for which this sensor is developed is to measure strain in a pressurized length of soft Tygon® tubing which is often used in pumping fluids through microfluidic devices. However, the silicone-based graphene polymer can easily be applied to a variety of other shapes and soft materials.

C.3 Introduction

C.3.1 Microfluidics context

Microfluidics deals with fluid flow at the micrometre scale. This enabling technology has been applied in a wide range of fields such as biological assays [13], material synthesis [298], biofuels [25], and many more. Droplet microfluidics is a subset of microfluidics that considers monodispersed picoliter to nanoliter-sized droplets as reaction vesicles. The immiscibility of the two phases in combination with the microchannel wall surface properties allows the isolation of the dispersed phase droplets (i.e. water) within the continuous phase (i.e. oil). Hence, the chemical reactions occurring in the droplets are confined with high integrity in addition to the other main advantages of using microfluidics, namely, reduced reagent consumption and shorter reaction time.

Generally, microfluidics methods for liquid manipulation can be categorized as either passive or active. Passive approaches rely on the microchannel network geometry and arrangement to achieve the desired manipulations while active methods introduce external forces to better control the fluid. Although there exists a wide

variety of methods used to drive the flow for both passive and active microfluidic solutions, syringe pumps and pressure pumps are most widely utilized.

Syringe pumps are more forgiving than pressure pumps in terms of microfluidic chip design [101]; however, their performance is compromised by the inherent long oscillation period in the flow [159]. Moreover, pressure pumps respond much faster than syringe pumps when a change is requested [149]. Pressure pumps exhibit desirable behaviour both on short and long timescales.

The fast response of pressure pumps is especially important in active control applications. In the case of an image-based closed-loop active control system for droplet manipulation in a microfluidic chip, the droplet location in a channel network is obtained from a microscope camera image. The droplet location is fed back to the controller, which adjusts the pressures applied to the channels to achieve the desired position or motion of the droplet. The required quick adjustment response of the fluid pressures can only be achieved by a pressure pump [111]. Active droplet control platforms such as this offer unique advantage for manipulating individual droplets, and present opportunities to apply microfluidics in other fields such as biochemistry for single-cell analysis.

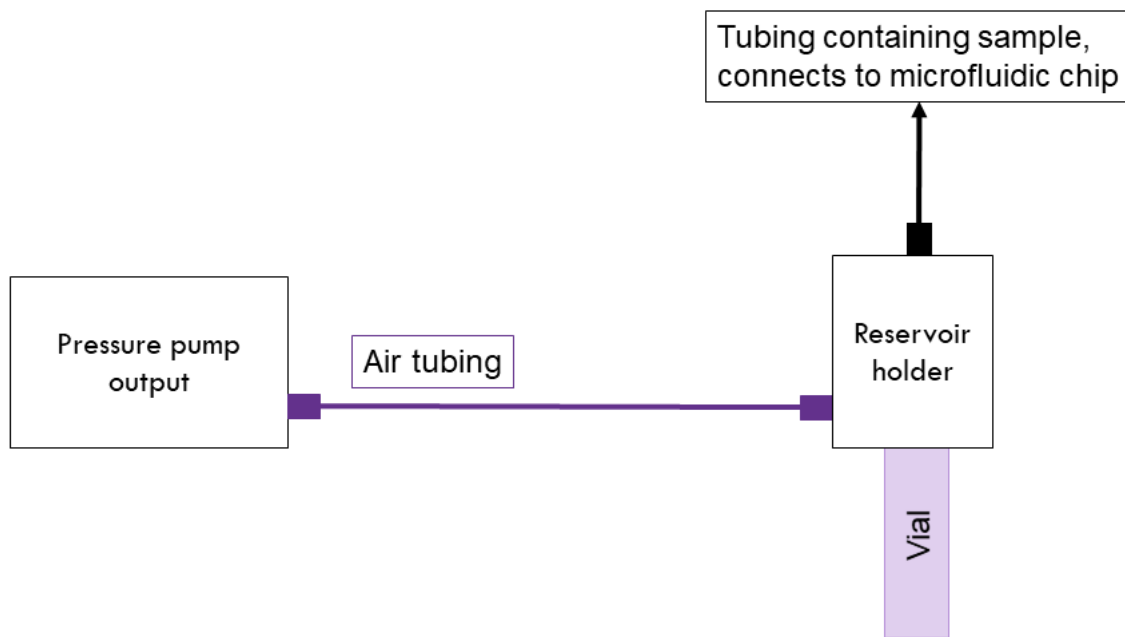


Figure C.1: Setup of the air tubing between the pressure pump and the reservoir holder.

Previous studies concerning the development of this active platform have reported somewhat limited accuracy [308, 111]. Contributing factors include image quality and pressure pump response, but the dynamic response of the tubing connecting the pressure pump and the microfluidic chip is also considered important. The impact of the tubing dynamics is that the pressure at the chip is not the same as the output pressure of the pump. Referring to Figure C.1, the tubing consists of two parts: the first (air tubing) transports air from the pump to the reservoir holder; the second (liquid tubing) transports the liquid sample from the reservoir holder to the microfluidic chip. The recommended air tubing is softer than the liquid tubing, with typically an order of magnitude difference in elastic modulus. Consequently, the fluid dynamics under applied pressures in the liquid tubing can be described by the Hagen-Poiseuille law and are accounted for in the controller. However, the dynamics of the air tubing depends on its material properties and dimensions, and has not yet been accounted for in the model used for controller design. The hypothesis is that neglecting the air tubing dynamics results in lower accuracy in active control for droplet microfluidics. This, in turn, hinders the adoption of droplet microfluidics as an enabling tool for single-cell analysis, high demand in many fields such as disease diagnosis and personalized medicine [278, 135]. To justify the efforts to evaluate and consider tubing dynamics in the active control system, it is important to quantify the impact of tubing dynamics on the performance of the active control system.

C.3.2 Motivation

The active control system for droplet microfluidics uses droplet position feedback provided by analysis of images from a camera attached to a microscope. Together with custom software and appropriate controller parameters, the pressure to be applied at each microfluidic chip inlet is calculated multiple times per second [308, 111]. These pressures are sent to the pressure pump as commands to quickly actuate the fluid. If tubing dynamics are neglected, the set of pressures applied at the reservoir holder is assumed to be the same as the output pressures at the pump. However, in practice, both an offset and delay between the output pressures at the pump and the actual pressures applied at the reservoir holder are observed, which can cause difficulty in achieving the desired droplet manipulation. The net effect is that droplet motions must be slowed which makes the operation less efficient and longer; this is undesirable since some biochemical materials can be time-sensitive due to aggregation.

The better strategy is to account for the dynamic pressure difference, which requires an understanding of the air tubing dynamics. Tubing dynamics are influenced

by multiple factors such as its inner and outer diameter, length, and stiffness. For a given material, the tubing diameter and wall thickness are the key parameters that determine the dynamic response. Incorporating changes in these parameters (or strain) as the internal pressure changes into a dynamic model should enable these effects to be compensated. The motivation is thus to develop a technique whereby the large strains encountered in the relatively soft tubing can be measured in real-time.

C.3.3 Literature overview

Although there exists pertinent previous research, the context and the corresponding assumptions differ sufficiently to justify investigating the specific setup of the pressurized air tubing shown in Figure C.1. The two closest cases in the literature are transmission lines for unsteady pressure measurement and blood flow in arteries.

A remotely localized pressure sensor requires a transmission line to measure the pressure at the location of interest. Concerns with short term variations for the measurement of unsteady pressure can be addressed by describing the dynamics of the transmission line using a 2nd order system [67]. However, the derivation assumes rigid walls as this is the more desirable configuration for remote pressure sensing. Therefore, such modelling would not capture the tubing compliance and its consequent dynamic effects on pressure.

Blood flow through arteries is a typical context studying the pressure propagation through compliant tubing [32]. However, once again, an assumption at the foundation of the derivations threatens the applicability to the air tubing of this study. The typical artery dimensions justify the use of thin-wall assumptions; however, the wall thickness of the air tubing herein under study is of the same order of magnitude as the inner radius. Therefore, thin-wall assumptions made for artery flow seem unreasonable.

C.3.4 Thick-wall compliant tubing dynamics

The dynamics introduced from the thick-wall compliant tubing between the pressure pump output and the reservoir holder are of particular importance for active control within the context of microfluidics. The available literature either does not consider the expansion of the tubing or its thick-walled properties. Hence, an experimental approach is necessary and used here. Nonetheless, the relationship between inner pressure and radial strain is established in the literature [256].

$$\epsilon = \frac{P}{E} \left(\frac{r_o^2 + r_i^2}{r_o^2 - r_i^2} + \nu \right) \quad (\text{C.1})$$

where ϵ is the radial strain [], P is the internal tubing pressure [Pa], E is the tubing elastic modulus [Pa], r_o is the outside tubing radius [m], r_i is the inner tubing radius, and ν is the tubing material Poisson ratio [].

Typical off-the-shelf planar strain gauges are ubiquitous but are generally designed for materials with a large elastic modulus such as steel or aluminum. Correspondingly, the strain gauges themselves are stiff; they are meant to not deform substantially under applied stress. Very small changes in resistance occur due to the changes in the sensing element cross-sectional area. Pairs of this type of strain gauge are used in a Wheatstone bridge circuit to measure such small changes in resistance. However, their use with softer low modulus materials is limited due to the larger elastic deformations involved. Consequently, an alternative approach must be used. The conductive property of graphene is leveraged to produce a different type of strain sensor that is sensitive yet also capable of significant elastic deformation [26]. The graphene is dispersed in a silicone-based polymer matrix such that the deformation induces a change in resistance that can be measured using a voltage divider circuit.

The strain sensor herein developed aims to measure the external radial deformation caused by the pressure within the soft tubing. The strain sensor has a silicone-based polymer matrix for its comparable softness and dispersed graphene for its current conducting properties. The deformation measurement can provide more information about the dynamics of the air tubing as it expands and contracts according to its internal pressure.

C.4 Materials and experimental methods

C.4.1 Materials

The graphene-based strain sensor can simply be fabricated with graphene, Silly Putty®[®], acetone, and silicone oil 5cst.

The graphene has between 5 and 10 layers, a purity of 99.5%, and a lateral size of 5 – 10 μm . The supplier selected for the graphene is accessible for its price range as well as ease to place an order (<https://www.ebay.ca/itm/142264483086>). The Silly Putty®[®] is a brand by Crayola. Although its exact composition is unknown,

its viscoelastic properties have previously been studied [56]. The putty is the soft matrix containing the graphene and is a silicone-based polymer. Acetone is used as the solvent for both the Silly Putty® and to disperse the graphene. The silicone oil 5cst (*Millipore Sigma*) matches the silicone-based chemistry of the Silly Putty® matrix.

Briefly, the fabrication procedure consists of dispersing the graphene and Silly Putty® in acetone in two separate containers. Sonication for 6 hours with intermittent hourly manually shaking contributes to an even dispersion within the solvent. Similarly, after combining the two acetone solutions of graphene and Silly Putty®, sonication for one hour ensures proper mixing. Afterwards, the acetone is left to evaporate at room temperature overnight. Adding a small volume (i.e. 0.1 ml) of 5cst silicone oil helps the dried mixture of Silly Putty® and graphene to regain its original texture as the final step.

Note that the dispersion of graphene within the silicone-based matrix (i.e. Silly Putty®) is named “G-putty” as per [26].

C.4.2 Experimental setup

The G-putty is manually moulded on the tubing to give it a cylindrical shape of minimal thickness ($\sim 500\mu m$) and to establish contact with the tubing. Thus, the tubing deformation is transmitted to the G-putty. The connection to the circuit is established using small stranded wires. Although only contact is required between the wires and the G-putty to transmit the current, a more secure attachment with additional G-putty and tape is used to secure the wires on the tubing. The wires connecting the sensor to the circuit are small stranded wires to minimize interference with the deformation but maximize contact. The strain sensor cover a length of about 1.5 cm located in the middle of the tubing between the two pressure sensors. The Tygon® has a length of $\sim 50cm$, a nominal inner diameter of 1/16”, and an outer diameter of 1/8”.

The electrical measurement relies on a voltage divider circuit that allows to calculate the varying resistance (Z_{sensor}) based on a known precise voltage input (V_{reg}) and resistance (R_1) as per the following equation.

$$Z_{sensor} = \frac{R_1}{\frac{V_{reg}}{V_{out}} - 1} \quad (C.2)$$

This configuration is preferred over the more typical Wheatstone bridge circuits of strain sensors; the G-putty absolute resistance value varies and makes it difficult to

match. The sensor is sensitive enough not to require a more complex circuit. The circuit overview is shown in Figure C.2. Although the sensor would ideally simply behave as a resistor, an impedance is used to represent the sensor due to its more complex behaviour. The high impedance of the strain sensor ($\mathcal{O}(M\Omega)$) and the correspondingly matched resistance of the voltage divider circuit requires a voltage follower (*Texas Instrument TLC2272*) to accurately measure at the desired 1 ms interval. Moreover, an external Digital-to-Analog converter (DAC) with 12-bit resolution (*Microchip MCP3202*) and an accurate voltage reference (*Maxim Integrated MAX6250*) are set up to increase the measurement resolution. An *Arduino Mega2560* is used to communicate with the computer via serial communication.

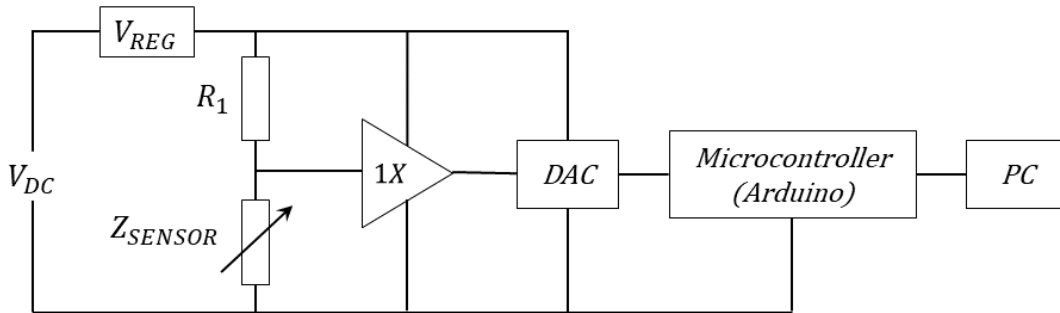


Figure C.2: Overview of the circuit: V_{DC} is the power supply voltage, V_{REG} provides a precision reference and supply voltage, $1X$ represents the voltage follower, and DAC is the digital-to-analog converter

C.5 Results and discussion

The pressure at one end of the soft tubing can be controlled using the pressure pump. The two pressure sensors (TE connectivity U536D-H00015-001BG) at either end of the tubing measure the pressure while the strain sensor measures the tubing radial strain caused by the tubing expansion. The specifications of the pressure sensing apparatus are given in Table C.1.

Table C.1: Specification summary for the pressure sensors (*TE Connectivity U536D-H00015-001BG*).

| | |
|-------------------|--------------|
| Range | 0 to 1 bar |
| Accuracy | ± 1 mbar |
| Resolution | 0.24 mbar |
| Sampling | 1 kHz |

C.5.1 Step input

The input of the pressure pump outlet is successively increased by 100 mbar step changes. Correspondingly, the strain sensor resistance changes. However, as illustrated by Figure C.3, for constant pressure and hence, constant radial strain, the strain resistance diminishes. This is attributed to the intrinsic dynamical behaviour of the nanocomposite strain sensor. The self-healing properties originate from the mobility of the graphene within the matrix [26]. The dynamics can be partly explained by a transfer function with a single zero (i.e. $G(s) = s + a$). Nevertheless, the intrinsic dynamics effects clearly dominate and another approach is sought using the ramp input response.

C.5.2 Ramp input

The step response (Figure C.3) suggests that although the strain sensor is sensitive enough to detect the small radial strain, the intrinsic dynamics introduced dominates. This is clear at constant pressure. Therefore, the ramp input response is investigated as shown in Figure C.4.

Two different rates of change for the ramp are shown in Figure C.4(a) and C.4(b) for the milder and steeper ramp respectively. The pressure spanned is 900 mbar for both but the time required to reach this maximum pressure is 45 seconds and 9 seconds respectively. The subfigures with identical y-axis limits show a similar response trend for the strain sensor measurements.

On one hand, the step response shows that the resistance change is not significant at constant pressures; the peaks at the step change edge are all within about 5% of each other. On the other hand, the ramp response shows a significant change ($\sim 50\%$) over the same 900 mbar pressure range. Moreover, the consistency in response with respect to the rate of both the pressure and strain sensor measurement change

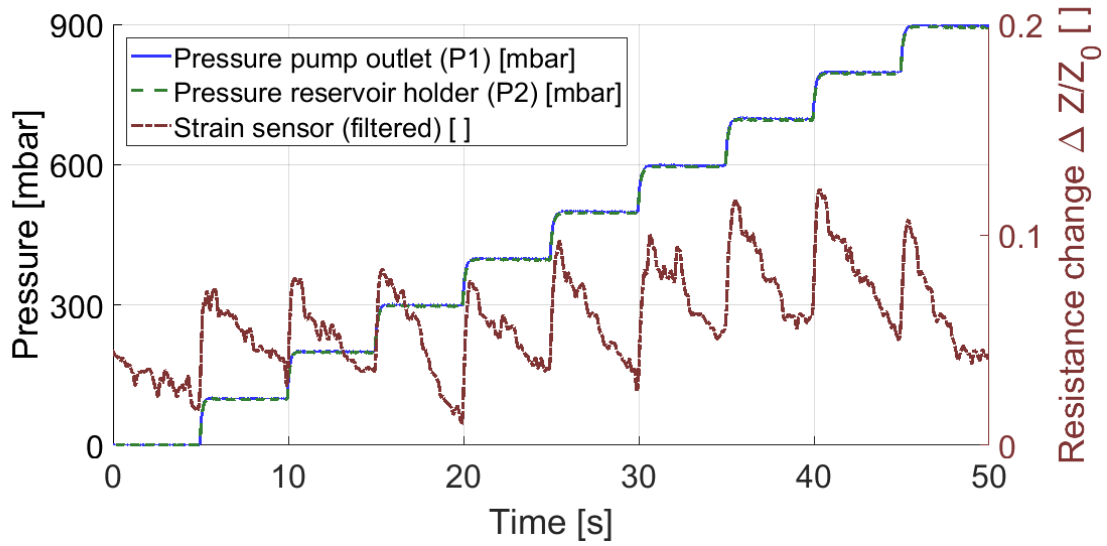
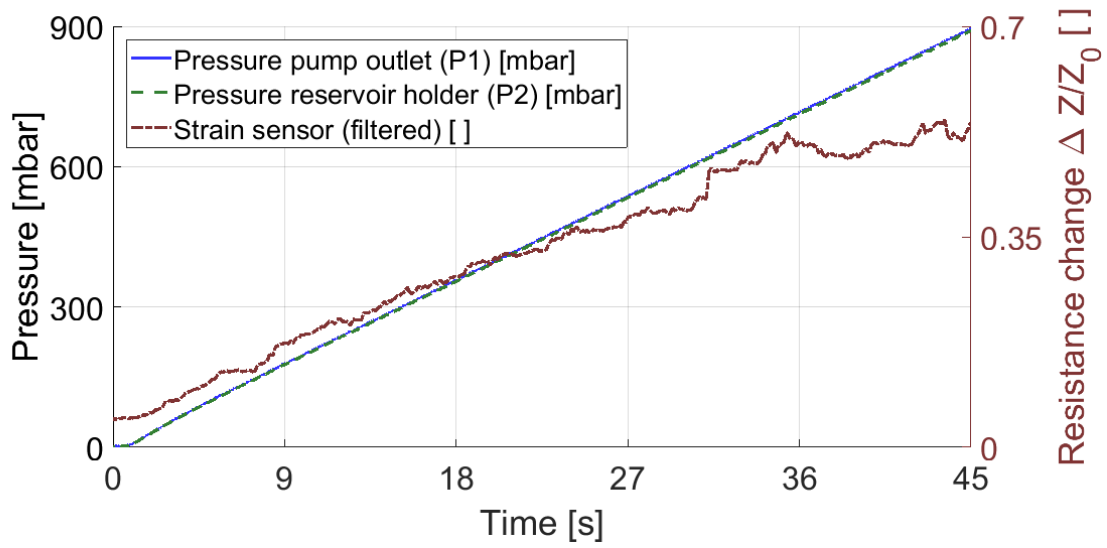


Figure C.3: Successive step input response with strain sensor measurement. The intrinsic nanocomposite strain sensor properties dominates the response at steady pressure. The sharp pressure increase and corresponding sharp change in the sensor resistance nonetheless indicates responsiveness for the small scale deformations.

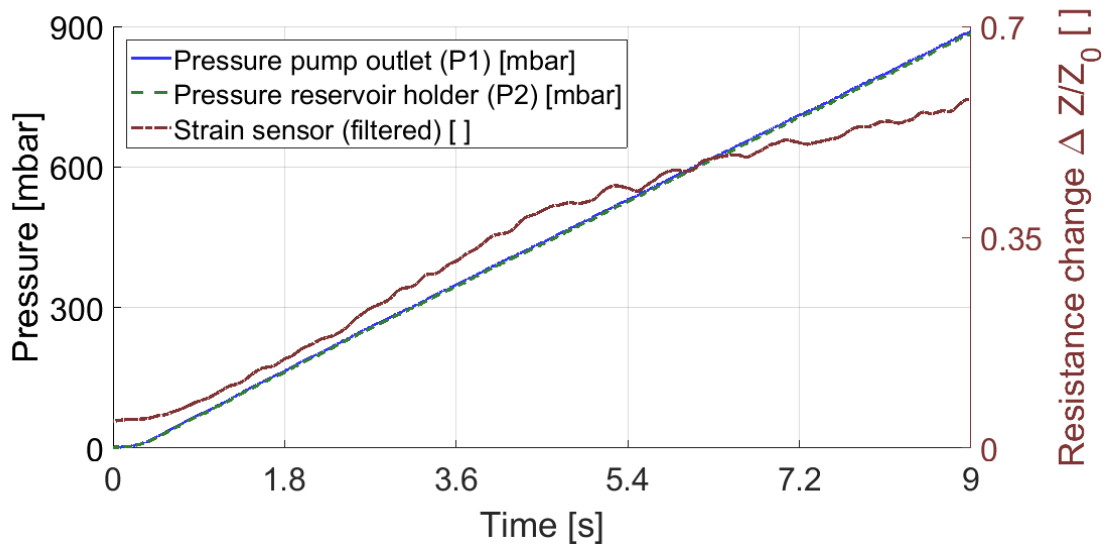
suggests a constant relationship. However, the characterization of that constant is not done in detail here. It is hypothesized that the constant is a function of the volume ratio of graphene to Silly Putty®.

$$\frac{\partial(\Delta R/R_0)/\partial t}{\partial P/\partial t} = k, \text{ where } k \text{ is a constant.} \quad (\text{C.3})$$

Therefore, now revisiting the relationship between inner pressure and radial strain from [256] shown in Equation C.1, the time derivative of the resistance (and hence of the strain) and the pressure time derivative are considered. However, the Silly Putty® and the tubing wall material exhibits viscoelastic behaviour. While the Silly Putty® is characterized in the literature [56], the Tygon® tubing is not; its modulus of elasticity is about 7 MPa. Considering the tubing elastic modulus E as a function rather than a constant would affect the strain rate as part of the change with respect to time. This behaviour could be attributed to the viscoelastic properties of the material rather than to fluctuation in pressures, which is being measured. Therefore, the tubing elastic modulus (E) is considered as a constant in this study.



(a) Milder ramp input response strain sensor measurement.



(b) Steeper ramp input response strain sensor measurement.

Figure C.4: Ramp input response. The similar response between the milder and steeper pressure ramp inputs suggests a constant relationship with the strain time derivative.

Please note that this assumption might not be reasonable for all cases.

$$\frac{\partial \epsilon}{\partial t} = \frac{1}{E} \left(\frac{r_o^2 + r_i^2}{r_o^2 - r_i^2} + \nu \right) \frac{\partial P}{\partial t} \quad (\text{C.4})$$

where ϵ is the radial strain [], t is time [s], P is the internal tubing pressure [Pa], E is the tubing elastic modulus [Pa], r_o is the outside tubing radius [m], r_i is the inner tubing radius, and ν is the tubing material Poisson ratio [].

The relationship from Equation C.4 depends on the mechanical properties of the tubing to establish the proportional relationship between the pressure rate of change and the strain rate of change. The gauge factor (GF) can be estimated from the ramp response (Figure C.4) by averaging the milder and steeper response. Although the data enables the estimation of the gauge factor (GF) as 20, many variables are foreseen to affect the value; the estimation should be verified for specific volume fractions, sensor geometries, and measurement resolution.

C.5.3 Potential impact

As previously specified, the dynamics introduced by the soft tubing in the context of active control in microfluidics is impactful. The deformation of the tubing requires special consideration of the dynamics as opposed to the simpler case of rigid-wall tubing. A strain sensor measuring deformation is particularly insightful.

The usefulness of quantifying deformation is not restricted to microfluidics but could also be extended to other areas for which traditional strain sensors can be inadequate, for example, soft robotics.

Furthermore, the development and understanding of a silicone-based soft matrix nanocomposite strain sensor can be valuable for the materials field. Graphene exhibits various interesting properties that can be leveraged in different ways.

In order to further develop this silicone-based soft matrix nanocomposite strain sensor, its inherent response should be better characterized. Moreover, although the viscoelastic behaviour of Silly Putty® is reported in the literature, the impact of the graphene dispersion should be better assessed. Finally, a pole could be introduced to make an active sensor without requiring to numerically compute the derivative; hence, the response from the zero could be compensated.

C.6 Summary

The fast response of a pressure-driven flow setup can be leveraged in the context of an active microfluidics platform. However, although passive microfluidics can disregard any short-term dynamics and compensate for any static offset, the fast actuation of the pressure (multiple times per second) for active platforms does not allow such leniency. The compliant thick-wall tubing between the pressure pump output and the reservoir holder input is pressurized with air and introduces short-term dynamics. In order to better quantify the intrinsic dynamics of the compliant tubing, the aim is to measure its deformation using a silicone-based soft-matrix nanocomposite strain sensor (i.e. graphene dispersed in a Silly Putty® matrix: G-putty).

The strain sensor itself also introduces inherent dynamics of its own that are not well characterized. Consequently, instead of measuring the absolute value of the strain, its derivative is investigated. The ramp input response for different rates indicates that the ratio between the strain derived with respect to time and the pressure derivative are related through a constant.

Acknowledgements

The authors acknowledge the funding provided by NSERC in the form of grants supplied to Prof. Carolyn Ren and scholarships awarded to Marie Hébert.

Conflict of interest

The authors declare that they have no conflict of interest.